

# Monday

104<sup>th</sup> Scientific Assembly and Annual Meeting November 25–30 | McCormick Place, Chicago





#### SPDL20

You Take the Red Pill-You Stay in Wonderland and I Show You How Deep the Rabbit Hole Goes (Case-based Competition)

Monday, Nov. 26 7:15AM - 8:15AM Room: E451B



AMA PRA Category 1 Credit ™: 1.00 ARRT Category A+ Credit: 1.00

#### Participants

Adam E. Flanders, MD, Philadelphia, PA (*Presenter*) Nothing to Disclose Sandeep P. Deshmukh, MD, Philadelphia, PA (*Presenter*) Nothing to Disclose Vishal Desai, MD, Philadelphia, PA (*Presenter*) Nothing to Disclose Christopher G. Roth, MD,MS, Philadelphia, PA (*Presenter*) Nothing to Disclose

For information about this presentation, contact:

vishal.desai@jefferson.edu

## LEARNING OBJECTIVES

1) Be introduced to a series of radiology case studies via an interactive team game approach designed to encourage 'active' consumption of educational content. 2) Use their mobile wireless device (tablet, phone, laptop) to electronically respond to various imaging case challenges; participants will be able to monitor their individual and team performance in real time. 3) Receive a personalized self-assessment report via email that will review the case material presented during the session, along with individual and team performance. *This interactive session will use RSNA Diagnosis Live*<sup>™</sup>. *Please bring your charged mobile wireless device (phone, tablet or laptop) to participate.* 



#### SPSC20

## Controversy Session: Screening Breast MRI: Abbreviated versus Full Protocol

Monday, Nov. 26 7:15AM - 8:15AM Room: E350



AMA PRA Category 1 Credit ™: 1.00 ARRT Category A+ Credit: 1.00

#### Participants

Margarita L. Zuley, MD, Pittsburgh, PA (Moderator) Investigator, Hologic, Inc

#### For information about this presentation, contact:

zuleyml@upmc.edu

## LEARNING OBJECTIVES

1) Understand the acquisition parameters for full vs abbreviated protocols for screening MRI. 2) Understand the literature surrounding the benefits and limitations of each methodology. 3) Improve your interpretive skills for screening MRI.

#### Sub-Events

## SPSC20A Abbreviated Protocol

Participants Christopher E. Comstock, MD, New York, NY (*Presenter*) Nothing to Disclose

## For information about this presentation, contact:

comstocc@mskcc.org

#### **LEARNING OBJECTIVES**

1) Describe the concept of abbreviated breast MRI (AB-MR) for breast cancer screening. 2) Review the data and current studies evaluating AB-MR. 3) Discuss the possible benefits and future direction of the use of AB-MR.

## SPSC20B Full Protocol

Participants Bonnie N. Joe, MD, PhD, San Francisco, CA (*Presenter*) Nothing to Disclose

For information about this presentation, contact:

bonnie.joe@ucsf.edu

#### **LEARNING OBJECTIVES**

1) Describe the components of a full protocol breast MRI exam. 2) Understand the benefits and limitations of the full protocol breast MRI exam in contrast to an abbreviated protocol.

#### ABSTRACT

This session will review the main components of the full-protocol breast MRI exam, including technical considerations. Benefits and limitations of the full protocol versus an abbreviated protocol for breast cancer screening will be discussed.

## URL

NA



#### SPSH20

## Hot Topic Session: 3D Printing in Urologic Oncology

Monday, Nov. 26 7:15AM - 8:15AM Room: E450A



AMA PRA Category 1 Credit ™: 1.00 ARRT Category A+ Credit: 1.00

#### Participants

Nicole Wake, PhD, New York, NY (Moderator) In-kind support, Stratasys, Ltd

#### For information about this presentation, contact:

nicole.wake@med.nyu.edu

#### Sub-Events

#### SPSH20A **3D Printing Basics: A Primer for the Radiologist**

Participants Frank J. Rybicki III, MD, PhD, Ottawa, ON (Presenter) Medical Director, Imagia Cybernetics Inc

For information about this presentation, contact:

frybicki@toh.ca

#### **LEARNING OBJECTIVES**

1) To introduce imaging and image manipulation required for 3D printing. 2) To outline basic 3D printing lab organization and funding profile, including potential reimbursement. 3) To review indications for 3D printing in urologic oncology.

#### ABSTRACT

This course will provide an overview of 3D printing in radiology and medicine. Requirements from radiology image acquisition will be described, as will methods to use computer aided design to convert imaging datasets into file formats amenable for 3D printing. Commonly used 3D printers will be described, as will aspects of the medical models an how they impact clinical care. Efforts for regulatory and reimbursement strategies will be briefly discussed. Finally, appropriate clinical scenarios for genitourinary oncology will be described. Dr. Rybicki will provide an overview of the field, including the creation and achievements of the RSNA Special Interest Group (SIG) in 3D printing. The disussion will also include strategies and an update on 3D printing reimbursement.

#### **Honored Educators**

Presenters or authors on this event have been recognized as RSNA Honored Educators for participating in multiple qualifying educational activities. Honored Educators are invested in furthering the profession of radiology by delivering high-quality educational content in their field of study. Learn how you can become an honored educator by visiting the website at: https://www.rsna.org/Honored-Educator-Award/ Frank J. Rybicki III, MD, PhD - 2016 Honored Educator

#### SPSH20B Advantages of 3D Printed Models in Renal Sparing Surgery

Participants

Bernard F. King JR, MD, Rochester, MN (Presenter) Nothing to Disclose

For information about this presentation, contact:

bfking@mayo.edu

## **LEARNING OBJECTIVES**

1) To be able to comphrehend the advantages that the urologic surgeon achieves by seeing, handling and better perceiving the complex anatomic relationships that are present in kidneys undergoing nehron sparing surgery. 2) The learner will be able to appy various 3D modeling techniques to best display the actual anatomic relationships of various normal and anomalous renal structures as they relate to the underlying renal tumors in patients with renal tumors undergoing nephron sparing surgery. 3) The learner will be able to understand the key features important in displaying renal tumors in 3D models including proper display of the arterial, venous and collecting system anatomy relative to the renal parenchyma and renal tumor.

#### ABSTRACT

This presentations will review the many advantages of 3D Models to the Urologic surgeon including but not limited to the three dimensional relationships of arteries, veins, collecting system and renal parenchyma to the renal tumor(s). These advantages may lead to safer surgeries with less ischemic time, blood loss and more preservation of renal tissue. This presentation will also review the many potential advantages to urologic residents and medical students. Finally, this presentation will discuss the advatages in patient education that can be valuable in helping the patient understand his/her underlying condition and helping the patient to choose the best treatment approach by seeing and touching the life-like model of their condition

## SPSH20C Impact of 3D Printed Prostate Cancer Models in Pre-Surgical Planning and Patient Care

## Participants

Nicole Wake, PhD, New York, NY (Presenter) In-kind support, Stratasys, Ltd

For information about this presentation, contact:

nicole.wake@med.nyu.edu

## LEARNING OBJECTIVES

1) Understand how to generate patient-specific 3D printed prostate cancer models from multi-parametric magnetic resonance imaging (MRI) datasets. 2) Explain how 3D printed models may help to depict the relationship of dominant tumors to key anatomic structures such as the neurovascular bundles and urethra. 3) Describe how 3D printed prostate cancer models can help in surgical planning and can help patients to better understand their disease.

#### ABSTRACT

Three-dimensional (3D) printing is an adjunctive method of radiological image visualization that may facilitate anatomical understanding and assist with surgical planning. Although 3D printed models are preferred by surgeons over conventional imaging, there is a paucity of data regarding the added value of 3D models and the impact that they can make in patient care. This presentation will provide an overview for how 3D printed prostate cancer models are created from multi-parametric magnetic resonance imaging (MRI) data and will describe how 3D printed prostate cancer models are used for surgical planning and patient education. Case examples will be shown that demonstrate how 3D printing can change the surgical plan and can help patients to better understand their anatomy and disease.

## SPSH20D Panel Discussion and Q&A



#### RCA21

## Prostate MRI (Hands-on)

Monday, Nov. 26 8:00AM - 10:00AM Room: S401AB



AMA PRA Category 1 Credits ™: 2.00 ARRT Category A+ Credits: 2.25

## Participants

Jelle O. Barentsz, MD, PhD, Nijmegen, Netherlands (*Presenter*) Advisor, SPL Medical BV Daniel J. Margolis, MD, Los Angeles, CA (*Presenter*) Consultant, Blue Earth Diagnostics Ltd Roel D. Mus, MD, Groesbeek, Netherlands (*Presenter*) Nothing to Disclose Joyce G. Bomers, Arnhem, Netherlands (*Presenter*) Nothing to Disclose Jurgen J. Futterer, MD, PhD, Nijmegen, Netherlands (*Presenter*) Research Grant, Siemens AG Rianne R. Engels, Nijmegen, Netherlands (*Presenter*) Nothing to Disclose Michiel Sedelaar, MD, PhD, Nijmegen, Netherlands (*Presenter*) Nothing to Disclose Antonio C. Westphalen, MD, Mill Valley, CA (*Presenter*) Nothing to Disclose Leonardo K. Bittencourt, MD, PhD, Rio De Janeiro, Brazil (*Presenter*) Nothing to Disclose Vibeke B. Logager, MD, Herlev, Denmark (*Presenter*) Nothing to Disclose Baris Turkbey, MD, Bethesda, MD (*Presenter*) Nothing to Disclose Joseph J. Busch, MD, Chattanooga, TN (*Presenter*) Nothing to Disclose

#### For information about this presentation, contact:

Renske.vandelft@radboudumc.nl

## LEARNING OBJECTIVES

1) Understand the Pi-RADS v2 Category assessment to detect and localize signifant cancer for both peripheral zone and transitional zone lesions. 2) Recognize benign pathology like inflammation and BPH and to differentiate these from significant prostate cancers.

## ABSTRACT

In this Hands-on Workshop, the participants will able to review up to 47 multi-parametric MRI cases with various prostatic pathology using a dedicated workstation. Focus will be on the overall assessment of PI-RADS v2 category, which enables them to score the probability of the presence of a significant cancer in patients with elevated PSA and/or clinical suspicion. All cases are from daily non-academic practice, and have various levels of difficulty. The cases include: easy and difficult significant peripheral-transition- and central zone cancers, inflammation, BPH, and the most common pitfalls. Internationally renowned teachers will guide the participants during their PI-RADS v2 scoring. The coursebook can be found at http://bit.ly/rsna2018 Please note: To guarantee the best learning expierence, we can only allow 100 people per session. First come first serve.

#### Active Handout:Renske Lian van Delft

http://abstract.rsna.org/uploads/2018/16002001/Workshop RSNA 2018 Coursebook small RCA.pdf



### MSAS21

Evolving Imaging Methods for the Cancer Patient - Part 1 (Sponsored by the Associated Sciences Consortium) (Interactive Session)

Monday, Nov. 26 8:30AM - 10:00AM Room: S105AB



AMA PRA Category 1 Credits ™: 1.50 ARRT Category A+ Credit: 1.75

**FDA** Discussions may include off-label uses.

#### Participants

Kristen Welch, RT, Milwaukee, WI (*Moderator*) Nothing to Disclose William A. Undie, PhD, RT, Houston, TX (*Moderator*) Nothing to Disclose

#### **LEARNING OBJECTIVES**

1. Review evolving procedures within interventional radiology to treat cancer2. Review anatomy involved in evolving procedures utilized to treat cancer patients3. Discuss historical methods utilized in the treatment of various cancers and their evolution

#### ABSTRACT

n/a

Sub-Events

## MSAS21A Advances in Liver Directed Therapy

Participants

Sarah B. White, MD,MS, Philadelphia, PA (*Presenter*) Research support, Guerbet SA; Research support, Siemens AG; Consultant, Guerbet SA; Consultant, BSC; Consultant, Cook Group Incorporated

### LEARNING OBJECTIVES

1) Identify indications, contraindications, and complications of liver directed therapy. 2) Discuss the evolution of treatment options for hepatocellular carcinoma. 3) Identify imaging involved in the care of patients with hepatocellular carcinoma.

## MSAS21B Combination Ablative Therapies

Participants

Alexios Kelekis, MD, PhD, Athens, Greece (*Presenter*) Medical Advisory Board, BTG International Ltd; Medical Advisory Board, Merit Medical Systems, Inc; Research Grant, Mindray Medical

## For information about this presentation, contact:

akelekis@med.uoa.gr

## LEARNING OBJECTIVES

1) Identify options for ablation for patients with cancer. 2) Discuss how ablative therapy combined with other therapies can improve patient outcomes. 3) Review results of current studies in research utilizing combination ablative therapies.

## MSAS21C Introduction to MR-Guided Focused Ultrasound

Participants Sharjeel Sabir, MD, Houston, TX (*Presenter*) Travel support, Johnson & Johnson;

## LEARNING OBJECTIVES

1) Identify indications, contraindications, and complications for MR-Guided Focused Ultrasound. 2) Review procedural details of performing MR-Guided Focused Ultrasound. 3) Review current literature on MR-Guided Focused Ultrasound.



#### MSCM21

Case-based Review of Magnetic Resonance (Interactive Session)

Monday, Nov. 26 8:30AM - 10:00AM Room: S100AB



AMA PRA Category 1 Credits ™: 1.50 ARRT Category A+ Credit: 1.75

#### Participants

Jorge A. Soto, MD, Boston, MA (Director) Royalties, Reed Elsevier

#### Sub-Events

#### MSCM21A MRI of the Spine

Participants Carlos H. Torres, MD,FRCPC, Ottawa, ON (*Presenter*) Nothing to Disclose

#### For information about this presentation, contact:

catorres@toh.ca

#### **LEARNING OBJECTIVES**

1) Review common and infrequent cord and spine pathology using a case-based approach. 2) Highlight key imaging findings in order to narrow the differential diagnosis.

#### **Honored Educators**

Presenters or authors on this event have been recognized as RSNA Honored Educators for participating in multiple qualifying educational activities. Honored Educators are invested in furthering the profession of radiology by delivering high-quality educational content in their field of study. Learn how you can become an honored educator by visiting the website at: https://www.rsna.org/Honored-Educator-Award/ Carlos H. Torres, MD,FRCPC - 2017 Honored Educator

## MSCM21B MRI of the Brain

Participants

Pia C. Maly Sundgren, MD, PhD, Lund, Sweden (Presenter) Nothing to Disclose

#### LEARNING OBJECTIVES

1) Review common and infrequent adult brain pathology using a case-based approach. 2) Highlight key imaging findings that might help to narrow the differential diagnosis.

#### ABSTRACT

In this presentation common and less common adult brain pathologies will be presented. Key imaging features and clinical information will be pointed out to help narrow the differential diagnosis using a case-based approach with the aim to be familiar with normal and abnormal processes in the adult brain using MRI.

## MSCM21C MRI of the Pancreas

Participants Jaroslaw N. Tkacz, MD, Boston, MA (*Presenter*) Nothing to Disclose

#### For information about this presentation, contact:

jaroslaw.tkacz@bmc.org

#### LEARNING OBJECTIVES

1) Become familiar with normal and abnormal appearance of the pancreas on routine MRI sequences. 2) Develop strategies to detect pathology involving the pancreas. 3) Increase confidence in diagnosis of cystic and solid pancreatic neoplasms.

## MSCM21D MRI of the GI System and Liver

Participants Hero K. Hussain, MD, Ann Arbor, MI (*Presenter*) Nothing to Disclose

## For information about this presentation, contact:

hh141@aub.edu.lb

## **LEARNING OBJECTIVES**

1) Describe a range of common and uncommon pathologies of the GI tract and liver. 2) Discuss the role of the various MR sequences in making the diagnosis.

## ABSTRACT

In this presentation, a range of pathologies of the GI tract will be presented, focusing on uncommon presentations of common pathologies using a case-based approach. Pertinent imaging and clinical features will be emphasized, and the value of each MR sequence will be explained to narrow the differential diagnosis and direct clinical management.



#### MSMC21

Cardiac CT Mentored Case Review: Part I (In Conjunction with the North American Society for Cardiovascular Imaging) (Interactive Session)

Monday, Nov. 26 8:30AM - 10:00AM Room: S406A



AMA PRA Category 1 Credits ™: 1.50 ARRT Category A+ Credit: 1.75

#### Participants

Jill E. Jacobs, MD, New York, NY (Moderator) Nothing to Disclose

## For information about this presentation, contact:

jill.jacobs@nyumc.org

## LEARNING OBJECTIVES

1) To be able to identify and understand normal cardiac anatomy. 2) To be able to identify and understand some of the common coronary anomalies.

#### Sub-Events

## MSMC21A Normal Coronary Anatomy

Participants Brian B. Ghoshhajra, MD, Waban, MA (*Presenter*) Research Grant, Siemens Healthcare USA;

## MSMC21B Anomalous Coronary Arteries

Participants

Prachi P. Agarwal, MD, Canton, MI (Presenter) Nothing to Disclose

## LEARNING OBJECTIVES

1) List the various coronary artery anomalies. 2) Identify the CT imaging features and hemodynamics of clinically significant coronary artery anomalies. 3) Apply the knowledge of treatment options to understand normal postoperative appearance and postoperative complications.



## MSMI21

Molecular Imaging Symposium: Basics of Molecular Imaging

Monday, Nov. 26 8:30AM - 10:00AM Room: S405AB



AMA PRA Category 1 Credits ™: 1.50 ARRT Category A+ Credit: 1.75

**FDA** Discussions may include off-label uses.

#### Participants

Zaver M. Bhujwalla, PhD, Baltimore, MD (*Moderator*) Nothing to Disclose Jan Grimm, MD, PhD, New York, NY (*Moderator*) Investor, NortisBio

## Sub-Events

## MSMI21A Molecular Imaging Using Radioactive Tracers

Participants

Jan Grimm, MD, PhD, New York, NY (Presenter) Investor, NortisBio

## LEARNING OBJECTIVES

1) Discuss the various radio tracers and their applications in Molecular Imaging studies. 2) Understand in which situations to use which radio tracers, what to consider when developing the imaging construct and what controls to obtain for nuclear imaging studies. 3) Examples will contain imaging with small molecules, with antibodies and nanoparticles as well as with cells in order to provide the participants with examples how o correctly perform their imaging studies. 4) Most of the examples will be from the oncology field but their underlying principles are universally applicable to other areas as well.

## MSMI21B Molecular Imaging with MRI and MRS

Participants

Zaver M. Bhujwalla, PhD, Baltimore, MD (Presenter) Nothing to Disclose

## LEARNING OBJECTIVES

1) To list the basic principles of magnetic resonance (MR) molecular imaging. 2) To describe the uses of noninvasive multi-nuclear MRI and magnetic resonance spectroscopic imaging (MRSI) for molecular imaging applications that provide spatial and temporal information on vasculature, metabolism and physiology. 3) To identify the applications of targeted MR contrast agents to detect receptor and gene expression. 4) To describe strategies that combine detection with therapy for theranostic imaging and for metabolotheranostics. 5) To provide examples of translational applications of molecular imaging and theranostics.

#### ABSTRACT

Noninvasive multi-nuclear magnetic resonance (MR) imaging and spectroscopic imaging (MRSI) provide a wealth of spatial and temporal information on vasculature, metabolism and physiology. Novel targeted contrast agents have widened the scope of MR techniques for molecular imaging applications to detect receptor and gene expression. In cancer, molecular imaging can be applied to identify targets specific to cancer with imaging, design agents against these targets to visualize their delivery, and monitor response to treatment, with the overall purpose of minimizing collateral damage. Genomic and proteomic profiling can provide an extensive 'fingerprint' of each tumor. With this cancer fingerprint, theranostic agents can be designed to personalize treatment for precision medicine of cancer, and minimize damage to normal tissue.

### MSMI21C Nanoparticles

Participants Heike E. Daldrup-Link, MD, Palo Alto, CA (*Presenter*) Nothing to Disclose

For information about this presentation, contact:

heiked@stanford.edu

#### LEARNING OBJECTIVES

1) To understand important safety aspects of ultrasmall superparamagnetic iron oxide nanoparticles (USPIO). 2) To understand the biodistribution of ferumoxytol nanoparticles and implications for imaging diagnoses. 3) To recognize the value of ferumoxytol nanoparticles for cancer MR imaging and PET/MR imaging.

## ABSTRACT

Gadolinium chelates as contrast agents for MRI have been associated with mounting concerns about nephrogenic sclerosis and gadolinium deposition in the brain. Therefore, a search for safe alternatives is currently underway. In North America, the iron supplement ferumoxytol has gained considerable interest as an MR contrast agent. In Europe, ferumoxtran-10 is re-entering clinical trials. Both ferumoxytol and ferumoxtran-10 provide long-lasting blood pool enhancement, which can be used for MR imaging exams that require detailed and/or long-lasting vessel delineation for MR angiographies, tissue perfusion studies, and whole body tumor staging. Iron oxide nanoparticles are slowly phagocytosed by macrophages in the reticuloendothelial system, making them ideal for

MR imaging detection of tumors in the liver, spleen, lymph nodes, and bone marrow. Similarly, iron oxide nanoparticles are slowly phagocytosed by tumor-associated macrophages in cancers; which can be used to grade tumor-associated inflammation and monitor the efficacy of new cancer immunotherapies. This presentation provides an introduction to the use of iron oxide nanoparticles for clinical MR and PET/MR imaging, including safety data acquired in children thus far, recent insights and mechanisms of rare, but potentially severe adverse reactions, applications that impact patient care and comparisons with gadolinium chelates. New developments for image guided therapy and theranostics are under way.

## MSMI21D Molecular Imaging with Ultrasound

#### Participants

Alexander L. Klibanov, PhD, Charlottesville, VA (*Presenter*) Co-founder, Targeson, Inc; Shareholder, Targeson, Inc; Institutional research collaboration, AstraZeneca PLC; Contract, SoundPipe Therapeutics;

#### For information about this presentation, contact:

sasha@virginia.edu

## LEARNING OBJECTIVES

1) Understand the principles of microbubble design-how to prepare fully biocompatible and safe ultrasound contrast agent particles that are clinically translatable, stable on storage, provide strong acoustic response and high sensitivity of detection by clinical ultrasound imaging systems, and could be targetable. 2) Understand the principles of selection of disease-specific targeting ligands usable for contrast ultrasound imaging, based on receptor levels in the vasculature in the disease issues, as well as vascular biomechanics. 3) Assess the results of early stage clinical trials performed with targeted microbubbles, and opportunities for clinical translation in diagnostic imaging and image-guided interventions.

#### ABSTRACT

Ultrasound is the most widespread clinical imaging modality. Therefore, enabling molecular imaging potential in an ultrasound setting will lead to the expanded and improved clinical diagnostic benefit. Ultrasound contrast microbubbles are already used in clinic as blood pool contrast agents, with excellent detection sensitivity: single particles with sub-picogram mass can be observed with clinical imaging systems in real time, at a depth of several cm. To achieve biomarker-selective molecular imaging, microbubble shell surface is decorated with targeting ligand molecules (antibodies, peptides, carbohydrates) that assure selective binding and retention in the areas of disease. Clinical microbubbles are typically 1-3 um in diameter; they do not extravasate, so target biomarker receptors should be located on the luminal surface of vessel wall, e.g., vascular endothelium. Microbubbles are targeted to the biomarkers in the areas of inflammation and ischemia-reperfusion injury (P- and E-selectin, VCAM-1, ICAM-1) or to tumor neovasculature (VEGFR2). The latter, a heterodimeric peptide-targeted contrast microbubble from industry, has successfully completed Phase 1-2 clinical trials for imaging of ovarian, breast and prostate cancer lesions. Overall, targeted microbubbles empower molecular ultrasound imaging; they could also be used in conjunction with image-guided interventions, such as targeted biopsy and therapy.

## MSMI21E Quantitative Imaging Biomarkers

Participants

Robert J. Gillies, PhD, Tampa, FL (Presenter) Nothing to Disclose

For information about this presentation, contact:

#### robert.gillies@moffitt.org

## LEARNING OBJECTIVES

1) Describe the differences between diagnostic, prognostic, and predictive biomarkers. 2) Describe the analytic pipeline for conventional radiomics. 3) Describe the biological basis and the practice of "habitat imaging" and why it may be useful for prediction and monitoring. 4) Briefly describe the methods and utility of deep learning in radiomics.

## ABSTRACT

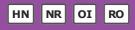
Quantitative Imaging: RadiomicsThe practice of radiology is undergoing revolutionary changes from describing images using a semantic lexicon to one that is increasingly quantitative and data driven, enhanced by machine learning algorithms. The discipline of radiomics grew out CAD systems and has been developing over the last decades to extract quantitative image features and analyze them with an eye to generating diagnostic, prognostic, and predictive models. In conventional radiomics, volumes of interest (VOI) are identified and segmented. In cancer, the VOIs can be the tumor, or the peri-tumor parenchyma. Within these VOI features are extracted describing size, shape, location, texture, and patterns. More than 1,000 of these features are commonly generated from each VOI and this has to be reduced to an smaller informative set using correlation analyses, test-retest data, and then classical statistical methods such as CART, LASSO, or ROC analyses. In the training phase, these can be cross validated by holding out a small sample (1/10 to 1/2) and training on the remaining and testing on the held samples to identify the best multi-variate models. These are then locked down and tested against a completely independent test set, preferably from another institution. Wellpowered studies exceeding 1,000 patients have been published to generate strongly prognostic, diagnostic, and predictive models. An extension of radiomics combines data from multiple imaging modalities (PET+CT, multiparametric MRI) to generate "hypervoxels" that can be clustered using e.g. fuzzy C-means clustering, Gaussian mixture models, Otsu thresholding, identifying spatially contiguous regions with similar phenotypes. These are referred to as "habitats" which can be highly predictive of responses to specific therapeutics, and which can be longitudinally monitored for adaptive therapy dosing. Importantly, habitat imaging obviates the need for explicit segmentation. A further extension of radiomics is the increased use of "deep learning", usually with convolutional neural networks, CNN. The depth of learning is limited by the size of the training set, and many methods are employed to augment the training data by rotating the original data set to generate multiple representations. The depth of the neural network can also be increased trough the use of transfer learning, wherein a network trained on similar data can be used to form the initial layers, and only the final layers are specific to the training data at hand. While CNNs are commonly disparaged because they are "black boxes", newer methods are being deployed that can identify the region of the image that contains the most important diagnostic/prognostic information, making the black box a little more transparent.



#### MSRO21

## BOOST: Head and Neck-Nasopharynx & Perineural Spread (Interactive Session)

Monday, Nov. 26 8:30AM - 10:00AM Room: E450A



AMA PRA Category 1 Credits ™: 1.50 ARRT Category A+ Credit: 1.75

#### Sub-Events

## MSR021A Imaging of the Nasopharynx: Applied Anatomy

Participants Suresh K. Mukherji, MD, Northville, MI (*Presenter*) Nothing to Disclose

#### LEARNING OBJECTIVES

1) Review the normal anatomy of the nasopharynx. 2) Explain common spread patterns of nasopharyngeal carcinoma. 3) Describe the anatomy landmarks that determine staging of nasopharyngeal carcinoma.

#### ABSTRACT

This course will review the normal anatomy of the nasopharyx and common spread patterns of nasopharyngeal carcinoma. The new AJCC 8th edition staging for nasopharyngeal carcinoma will also be reviewed.

#### MSR021B Current Concepts and Controversies in Radiation Planning of the Nasopharynx

Participants Sung Kim, MD, New Brunswick, NJ (*Presenter*) Nothing to Disclose

## LEARNING OBJECTIVES

1) Review important points in contouring nasopharynx cancer based on patterns of spread.

## MSR021C Question & Answer

## MSR021D Anatomy and Imaging of Perineural Spread

Participants

Suresh K. Mukherji, MD, Northville, MI (Presenter) Nothing to Disclose

#### LEARNING OBJECTIVES

1) Describe common pathways of perineural spread. 2) Review the imaging findings of perineural spread. 3) Describe the proper imaging technique for being able to detect perineural spread.

#### ABSTRACT

This lecture will review the common perineural spread patterns of tumprs involving the nasopharynx and skull base. The emphais will be on perineural spread along the cranial nerves and also review how to optimize imagign techniques.

## MSR021E Current Concepts and Controversies in Contouring and Treatment of Perineural Spread

Participants Sung Kim, MD, New Brunswick, NJ (*Presenter*) Nothing to Disclose

## LEARNING OBJECTIVES

1) To identify and discuss some common scenarios when perineural invasion is found in head & neck cancer and how they should be treated with radiation therapy.

## MSR021F Question & Answer



#### MSRO25

## **BOOST: Breast-Oncology Anatomy (Interactive Session)**

Monday, Nov. 26 8:30AM - 10:00AM Room: S103CD



AMA PRA Category 1 Credits ™: 1.50 ARRT Category A+ Credit: 1.75

#### Participants

Stephanie Markovina, MD, PhD, Saint Louis, MO (*Moderator*) Nothing to Disclose Amy M. Fowler, MD, PhD, Madison, WI (*Presenter*) Research support, General Electric Company Maria A. Thomas, MD, PhD, Saint Louis, MO (*Presenter*) Nothing to Disclose

## LEARNING OBJECTIVES

1) Understand breast and regional lymph node anatomy. 2) Become familiar with basic anatomic structures and breast pathology using various imaging modalities. 3) Be familiar with breast and regional lymph node contouring techniques used in radiation treatment planning for breast cancer. 4) Apply contouring knowledge to inform radiation treatment planning for breast cancer.



#### RC201

## The Many Facets of Organizing Pneumonia: A Rad-Path Guide to Understanding and Diagnosis

Monday, Nov. 26 8:30AM - 10:00AM Room: E351



AMA PRA Category 1 Credits ™: 1.50 ARRT Category A+ Credit: 1.75

#### Participants

Jeffrey R. Galvin, MD, Baltimore, MD (Moderator) Nothing to Disclose

#### LEARNING OBJECTIVES

1) Understand the microscopic anatomy of the lung that explains the high resolution CT findings associated with organizing pneumonia. 2) Improve their diagnostic skills related to the imaging recognition of organizing pneumonia. 3) Recognize the range of injuries and inhaled insults that lead to organizing pneumonia. 4) Apply a new knowledge of the pathways to fibrosis that allows for the differentiation of organizing pneumonia, IPF and diffuse alveolar damage. 5) Appreciate the importance of communication between the clinician, radiologist, and pathologist to improve diagnosis.

#### ABSTRACT

This presentation will review the histologic and radiologic findings of organization in lung injury due to diffuse alveolar damage, organizing pneumonia and acute fibrinous and organizing pneumonia. It will clarify the role of organizing pneumonia in the pathway to fibrosis that will sharpen the radiologist's ability to separate the various forms of fibrosis including: idiopathic pulmonary fibrosis, non-specific interstitial pneumonia and diffuse alveolar damage. Finally it will describe the multidisciplinary diagnostic process of which the radiologist is a key member.

## Active Handout:Jeffrey R. Galvin

http://abstract.rsna.org/uploads/2018/17000284/OP Introduction Galvin RC201.pdf

#### Sub-Events

## RC201A Introduction

Participants Jeffrey R. Galvin, MD, Baltimore, MD (*Presenter*) Nothing to Disclose

#### LEARNING OBJECTIVES

View learning objectives under main course title.

## RC201B Pathology of Organizing Pneumonia

Participants

Teri J. Franks, MD, Silver Spring, MD (Presenter) Nothing to Disclose

## LEARNING OBJECTIVES

View learning objectives under main course title.

#### Active Handout:Teri J. Franks

http://abstract.rsna.org/uploads/2018/17000289/OP Pathology FranksRC201B.pdf

## RC201C Imaging of Organizing Pneumonia

Participants Seth J. Kligerman, MD, Denver, CO (*Presenter*) Nothing to Disclose

#### For information about this presentation, contact:

skligerman@ucsd.edu

#### LEARNING OBJECTIVES

View learning objectives under main course title.

#### **Active Handout:Seth Jay Kligerman**

http://abstract.rsna.org/uploads/2018/17000292/OP Imaging KligermanRC201C.pdf

## RC201D Pathways to Fibrosis and Summary

Participants Jeffrey R. Galvin, MD, Baltimore, MD (*Presenter*) Nothing to Disclose

## LEARNING OBJECTIVES

View learning objectives under main course title.



#### RC202

#### **TRaD Talks: Teaching Radiology**

Monday, Nov. 26 8:30AM - 10:00AM Room: S404AB

## ED

AMA PRA Category 1 Credits <sup>™</sup>: 1.50 ARRT Category A+ Credit: 1.75

#### Participants

Petra J. Lewis, MD, Lebanon, NH (Moderator) Nothing to Disclose

#### Sub-Events

## RC202A Cooling the Hot Seat

Participants

Petra J. Lewis, MD, Lebanon, NH (Presenter) Nothing to Disclose

#### For information about this presentation, contact:

petra.lewis@hitchcock.org

#### LEARNING OBJECTIVES

Develop a safe, shame-free environment for learners of all abilities, stages and confidence levels to 'take cases' in conference.
 Individualize instructor interactions according to learner responses.
 Devise means to reinforce and develop learner strengths in this setting.

## RC202B Daily Feedback: Give the Millennials What They Want

Participants

Jonathan O. Swanson, MD, Seattle, WA (Presenter) Nothing to Disclose

#### LEARNING OBJECTIVES

1) Describe the perceived hurdles to in-person feedback. 2) Explain the utility of frequent feedback in the setting of radiology education. 3) Detail strategies to help reluctant faculty buy-in to providing constructive feedback.

## RC202C Overcoming Stagefright

Participants Nancy J. McNulty, MD, Lebanon, NH (*Presenter*) Book contract, Oxford University Press

## For information about this presentation, contact:

Nancy.J.McNulty@hitchcock.org

#### LEARNING OBJECTIVES

1) Describe the scope, cause, and manifestations of public speaking anxiety. 2) Discuss strategies and changes in perception that can be utilized to overcome public speaking anxiety. 3) Apply these strategies before a public speaking engagement.

## RC202D Social and Emotional Intelligence in Education

Participants

Robert B. Percarpio, MD, Lebanon, NH (Presenter) Nothing to Disclose

#### LEARNING OBJECTIVES

1) Define the qualities of social emotional intelligence. 2) Recognize how social emotional intelligence applies to the resident training environment. 3) Develop strategies to improve resident education through the use of social emotional intelligence.

#### RC202E Point-of-Care Ultrasound Procedures: Taming the Wild Wild West

## Participants

Eric J. Monroe, MD, Seattle, WA (Presenter) Advisory Board, Biogen Idec Inc

## For information about this presentation, contact:

eric.monroe@seattlechildrens.org

## LEARNING OBJECTIVES

1) Understand trends in POCUS procedures. 2) Navigate the sensitive politics of non-imaging specialists seeking to perform POCUS procedures. 3) Create value and 'win'.

Participants Aaron P. Kamer, MD, Indianapolis, IN (*Presenter*) Nothing to Disclose

## LEARNING OBJECTIVES

1) Describe how drawing while teaching can solidify concepts for the learner. 2) Illustrate complex radiology topics using widely available tools at the workstation.



#### RC203

#### **Coronary CTA and Calcium Scoring**

Monday, Nov. 26 8:30AM - 10:00AM Room: E263



AMA PRA Category 1 Credits ™: 1.50 ARRT Category A+ Credit: 1.75

#### **Participants**

Gregory Kicska, MD, PhD, Seattle, WA (Moderator) Nothing to Disclose

#### Sub-Events

#### RC203A CT Derived Fractional Flow Reserve (FFR CT): A Sine Qua Non?

Participants

Eric E. Williamson, MD, Rochester, MN (Presenter) Nothing to Disclose

For information about this presentation, contact:

williamson.eric@mayo.edu

#### LEARNING OBJECTIVES

1) Discuss the current evidence for using CT-based fractional flow reserve. 2) Describe a potential role for FFRct in the clinical practice of cardiac CT.

## RC203B Interpreting and Reporting Cardiac CT - CAD-RADS

Participants

Geoffrey D. Rubin, MD, Durham, NC (*Presenter*) Consultant, Fovia, Inc; Consultant, HeartFlow, Inc; Consultant, General Electric Company;

#### LEARNING OBJECTIVES

1) To review the CAD-RADS lexicon, including assessment categories and modifiers, for coronary CT angiography in the evaluation of acute and stable chest pain. 2) To understand how CAD-RADS can improve patient care through standardized reporting and linking management recommendations to actionable information in the radiology report. 3) To apply appropriate CAD-RADS coding for difficult coronary CT angiography cases.

## RC203C Added Value of Myocardial Perfusion Imaging in Cardiac CT

Participants

Ricardo C. Cury, MD, Miami, FL (*Presenter*) Research Grant, General Electric Company; Research Consultant, General Electric Company

## LEARNING OBJECTIVES

1) To review the literature and available evidence of Myocardial CT perfusion. 2) To evaluate the emerging role of Myocardial CTP in the work-up of patients with suspected or known CAD. 3) To describe the incremental value of Myocardial CTP over CT angiography.

## RC203D Cardiac CT in Acute Chest Pain: Critical Review of the Evidence

Participants

Marc Dewey, MD, Berlin, Germany (*Presenter*) Research Grant, General Electric Company; Research Grant, Bracco Group; Research Grant, Guerbet SA; Research Grant, Canon Medical Systems Corporation; Research Grant, European Commission; Research Grant, BIH Digital Health Accelerator; Speakers Bureau, Canon Medical Systems Corporation; Speakers Bureau, Guerbet SA; Speakers Bureau, Bayer AG; Consultant, Guerbet SA; Author, Springer Nature; Editor, Springer Nature; Institutional research agreement, Siemens AG; Institutional research agreement, Koninklijke Philips NV; Institutional research agreement, Canon Medical Systems Corporation; ; ; ; ; ; ; ; ; ; ;

## For information about this presentation, contact:

dewey@charite.de

## LEARNING OBJECTIVES

1) Get to know the evidence for using CT in patients with acute chest pain. 2) Learn about important details from these studies that will show in which patients CT might have greatest clinical value.

#### ABSTRACT

Several clinical trials and smaller studies looked at the advantages and disadvantages of using CT in patients with acute chest pain. This practical talk about the pivotal facts from these clinical studies will provide the information required for informed decision making with referring physicians.

## Active Handout:Marc Dewey

http://abstract.rsna.org/uploads/2018/17001208/dewey 2018 handout RC203D.pdf



#### RC204

#### **Musculoskeletal Series: Knee MRI**

Monday, Nov. 26 8:30AM - 12:00PM Room: E451B



AMA PRA Category 1 Credits ™: 3.50 ARRT Category A+ Credits: 4.00

#### Participants

Naveen Subhas, MD, Shaker Heights, OH (Moderator) Research support, Siemens AG

Kirkland W. Davis, MD, Madison, WI (*Moderator*) Author with royalties, Reed Elsevier; Editor with royalties, Reed Elsevier Thomas M. Link, MD,PhD, San Francisco, CA (*Moderator*) Research Grant, General Electric Company; Research Consultant, General Electric Company; Research Consultant, InSightec Ltd; Research Grant, InSightec Ltd; Royalties, Springer Nature; Consultant, Springer Nature; Research Consultant, Pfizer Inc;

#### For information about this presentation, contact:

thomas.link@ucsf.edu

llenchik@wakehealth.edu

Sub-Events

#### RC204-01 Diagnosis of Meniscus Tears

Monday, Nov. 26 8:30AM - 8:55AM Room: E451B

#### Participants

Kirkland W. Davis, MD, Madison, WI (Presenter) Author with royalties, Reed Elsevier; Editor with royalties, Reed Elsevier

## For information about this presentation, contact:

kdavis@uwhealth.org

#### **LEARNING OBJECTIVES**

1) Demonstrate the imaging appearances of the types of meniscus tears. 2) Describe the most common locations of displaced flap tears of the menisci.3) Determine the best sequences for identifying tears of the meniscal root ligaments. 4) Identify signs that indicate likely presence of flap tears of the menisci.

## RC204-02 Cruciates

Monday, Nov. 26 8:55AM - 9:20AM Room: E451B

Participants Daniel E. Wessell, MD, PhD, Jacksonville, FL (*Presenter*) Nothing to Disclose

## For information about this presentation, contact:

Wessell.Daniel@mayo.edu

## LEARNING OBJECTIVES

Describe the normal imaging appearance of the cruciate ligaments.
 Examine common mechanisms of cruciate ligament injury.
 Describe the imaging appearance of cruciate ligament injuries.
 Identify secondary imaging signs of cruciate ligament injuries.

#### **Honored Educators**

Presenters or authors on this event have been recognized as RSNA Honored Educators for participating in multiple qualifying educational activities. Honored Educators are invested in furthering the profession of radiology by delivering high-quality educational content in their field of study. Learn how you can become an honored educator by visiting the website at: https://www.rsna.org/Honored-Educator-Award/ Daniel E. Wessell, MD, PhD - 2013 Honored Educator

## RC204-03 Quantitative MRI and Biomechanical Characterization of Human Meniscus Pathology

Monday, Nov. 26 9:20AM - 9:30AM Room: E451B

Participants

Tim Finkenstaedt, MD, San Diego, CA (*Presenter*) Nothing to Disclose Reni Biswas, San Diego, CA (*Abstract Co-Author*) Nothing to Disclose Nirusha Abeydeera, BS, La Jolla, CA (*Abstract Co-Author*) Nothing to Disclose Palanan Siriwanarangsun, MD, Bankok, Thailand (*Abstract Co-Author*) Nothing to Disclose Karen C. Chen, MD, Providence, RI (*Abstract Co-Author*) Nothing to Disclose Sheronda Statum, San Diego, CA (*Abstract Co-Author*) Nothing to Disclose Won C. Bae, PhD, La Jolla, CA (*Abstract Co-Author*) Nothing to Disclose Christine B. Chung, MD, La Jolla, CA (*Abstract Co-Author*) Nothing to Disclose

#### For information about this presentation, contact:

#### cbchung@ucsd.edu

#### PURPOSE

Compare the sensitivity of conventional and Ultrashort Time-to-Echo (UTE) MR techniques to indentation biomechanical properties of normal and pathologic human menisci.

### **METHOD AND MATERIALS**

Cadaveric knees (n=10 donors, 80±10 yrs) were dissected to obtain 18 menisci. These were cut radially to obtain three ~5 mm thick triangular pieces from anterior horn, body, and posterior horn regions (n=54 pieces total). Morphologic MRI parallel to the cut plane was performed with proton density weighted spin echo sequence (PDw; TR=2500 ms, TE=15 ms), to classify samples into 3 pathology groups: normal, degenerate and tear. Quantitative MRI was performed with 1) spin echo multi-echo T2 (SE T2; TR=2000 ms, TE=15 to 110 ms) and ultrashort echo time (UTE) T2\* (UTE T2\*; TR=100 ms, TE=0.01 to 20 ms) techniques. After MRI, indentation testing was performed on multiple sites (Figure 1A) on tibial and femoral articular surfaces with a 1-mm diameter plane-ended tip, to a depth of 100  $\mu$ m for 1 s while measuring force, to calculate compressive indentation modulus. At each indentation site, SE T2 and UTE T2\* values were determined using 2-mm circular region of interest (Figure 1B). Correlation between indentation modulus vs. SE T2 (Figure 1C) and UTE T2\* (Figure 1D) was performed for all data, and separately for each group. Additionally, difference in modulus, SE T2, and UTE T2\* values between groups were compared using ANOVA and Tukey posthoc test.

## RESULTS

There was a significant difference in indentation modulus between all 3 groups (Table 1A), stiffest for the normal, and softest for the tear group. While both SE T2 and UTE T2\* showed similar trends, the difference between normal and degenerate groups was far greater for UTE T2\* (Table 1A). Additionally, correlation with modulus was stronger for UTE T2\* than SE T2, regardless of pathology group being considered (Table 1B). Statistically significant correlation was found only for the degenerate group which is interesting and warrants further investigation.

#### CONCLUSION

We found higher sensitivity of UTE T2\* technique to biomechanical alterations of pathologic menisci, compared to SE T2.

## **CLINICAL RELEVANCE/APPLICATION**

Higher sensitivity of UTE MRI to biomechanical meniscus alterations may be useful for early detection of meniscus degeneration and injury, and for follow up after treatment.

RC204-04 Previous Meniscal Surgery is Associated with Higher Cartilage T2 Values Indicating More Advanced Cartilage Deterioration: Data from the Osteoarthritis Initiative

Monday, Nov. 26 9:30AM - 9:40AM Room: E451B

#### Participants

Jan Neumann, MD, San Francisco, CA (*Presenter*) Nothing to Disclose Kai P. Kern, San Francisco, CA (*Abstract Co-Author*) Nothing to Disclose Sarah C. Foreman, MD, San Francisco, CA (*Abstract Co-Author*) Nothing to Disclose Dong Sun, Wuhan, China (*Abstract Co-Author*) Nothing to Disclose Michael C. Nevitt, PhD, San Francisco, CA (*Abstract Co-Author*) Nothing to Disclose Charles E. McCulloch, San Francisco, CA (*Abstract Co-Author*) Nothing to Disclose Gabby B. Joseph, San Francisco, CA (*Abstract Co-Author*) Nothing to Disclose Azien Laqmani, Hamburg, Germany (*Abstract Co-Author*) Nothing to Disclose Thomas M. Link, MD,PhD, San Francisco, CA (*Abstract Co-Author*) Nothing to Disclose Satient, General Electric Company; Research Consultant, InSightec Ltd; Research Grant, InSightec Ltd; Royalties, Springer Nature; Consultant, Springer Nature; Research Consultant, Pfizer Inc;

#### For information about this presentation, contact:

Jan.Neumann@ucsf.edu

#### PURPOSE

To determine if participants with prior meniscal surgery show altered cartilage composition when compared to nonsurgical controls and whether the grade of deterioration is different for non-injury related meniscal surgery or meniscal surgery performed to repair a previous injury.

#### **METHOD AND MATERIALS**

In this cross-sectional study, semi-automatic cartilage segmentation of the right knee of 230 participants from the Osteoarthritis Initiative (OAI) was performed on 2D multi-slice multi-echo sequences, acquired with 3T MRI, and analyzed in a mono-exponential decay model with fitting function for the signal intensity and calculation of T2 maps. Based on the medical history, participants were divided into four groups (i) with meniscal surgery due to an injury (n=79), (ii) meniscal surgery without prior injury (n=36), (iii) controls without meniscal surgery but prior knee injury (n=79) and (iv) controls without meniscal surgery or prior knee injury (n=36). All groups were matched for sex, KL score, age, and BMI. Linear regression analysis was used to compare the T2 values in each compartment, as well as the mean across all compartments.

#### RESULTS

The average age of all study participants was 57.7 years (SD 8.9) with a BMI of 27.9 (SD 4.0) and 76 (33.0%) female participants. Participants with previous meniscal surgery showed significantly higher mean T2 values across all compartments when compared to those without meniscal knee surgery, separately for surgical participants with (p<0.001) and without (p<0.001) previous injury. Similar results were obtained when analyzing the compartments separately: In all weight-bearing compartments (lateral/medial femur and tibia) participants with previous surgery showed significantly higher mean T2 values, when compared to controls without surgery (p<0.05). The subanalysis of

cartilage T2 values between the two surgical groups did not show significant differences.

## CONCLUSION

Participants that underwent meniscal surgery with and without previous meniscal injury exhibited overall higher cartilage mean T2 values when compared to non-surgical controls, while no significant differences were found within the surgical groups. Our results indicate that meniscal surgery contributes to cartilage matrix degeneration, possibly independent of surgical indication.

#### **CLINICAL RELEVANCE/APPLICATION**

Indication for meniscal surgery should be thoroughly considered to prevent early or accelerated cartilage degeneration.

RC204-05 Collagen Meniscal Implant: A Long Term MRI Follow-Up in Asymptomatic Patients

Monday, Nov. 26 9:40AM - 9:50AM Room: E451B

#### Participants

Balazs Krisztian Kovacs, Basel, Switzerland (*Presenter*) Nothing to Disclose Dorothee Harder, Basel, Switzerland (*Abstract Co-Author*) Nothing to Disclose Felix Amsler, Basel, Switzerland (*Abstract Co-Author*) Nothing to Disclose Leonie Keller, Uster, Switzerland (*Abstract Co-Author*) Nothing to Disclose Roger Berbig, Zurich, Switzerland (*Abstract Co-Author*) Nothing to Disclose Michael T. Hirschmann, MD, Bruderholz, Switzerland (*Abstract Co-Author*) Nothing to Disclose Anna Hirschmann, MD, Basel, Switzerland (*Abstract Co-Author*) Nothing to Disclose

For information about this presentation, contact:

#### balazskrisztian.kovacs@usb.ch

## PURPOSE

Long term evaluation of morphology and size of collagen meniscal implants (CMI) and signs of osteoarthritis on MRI in patients with good clinical outcome.

## METHOD AND MATERIALS

79 patients were prospectively included for follow-up (FU) after arthroscopic CMI. Of these, 57 patients (mean age, 44±11 years; gender, 41 male/16 female; side, 48 medial/9 lateral) showed good clinical outcome (Lysholm-score >85; visual analogue satisfaction scale <2) and 79 MRI 1-8 years postoperatively were independently evaluated by two radiologists. CMI morphology, signal intensity (SI), homogeneity and size were assessed and of these results a meniscal score was calculated. Degree of chondral defects and amount of bone marrow edema (BME) were reported as chondral score. Additionally, meniscal extrusion was evaluated. Inter-reader reliability was calculated, Pearson was used to determine correlation between imaging findings and time after operation (P<0.05).

#### RESULTS

One year postoperatively, the CMI varied in size (10% normal, 30% small, 60% hypertroph) and was hyperintense in all patients. During FU (>3 years postoperatively) the size of CMI decreased (6% resorbed, 18% normal, 41% small, 35% hypertroph). CMI was initially hyperintense in all patients and changed to normal SI in only 13% during FU. The meniscal score improved significantly over time (r=0.28). Less meniscal extrusion was present during FU (93% initially, 71% FU; r=0.28). During FU, full-thickness chondral defects were increasingly present at the femoral side (65%; initially 33%). The chondral score was significantly worse during FU (P=0.017). Inter-reader reliability was fair for morphology and SI, moderate for size (0.48), homogeneity (0.41) and meniscal extrusion (0.55) and good for femoral cartilage (0.62) and almost perfect for BME (0.84-0.88).

#### CONCLUSION

In the long-term FU CMI varies in size, is typically hyperintense in SI and appears extruded. Despite asymptomatic knees, full-thickness cartilage defects were present in the majority of knees after CMI.

#### **CLINICAL RELEVANCE/APPLICATION**

Demonstrate the MR-variety of meniscal morphologies after CMI in asymptomatic patients and heighten the awareness of radiologist and referring physicians.

#### RC204-06 Extensor Mechanism

Monday, Nov. 26 9:50AM - 10:10AM Room: E451B

#### Participants

Kirkland W. Davis, MD, Madison, WI (Presenter) Author with royalties, Reed Elsevier; Editor with royalties, Reed Elsevier

#### **LEARNING OBJECTIVES**

1) Identify the anatomic components of the extensor mechanism on XR, CT, and MRI. 2) Assess the extensor mechanism, determine the pathology, and explain mechanism of injury.

## RC204-07 Articular Cartilage

Monday, Nov. 26 10:20AM - 10:40AM Room: E451B

#### Participants

Thomas M. Link, MD, PhD, San Francisco, CA (*Presenter*) Research Grant, General Electric Company; Research Consultant, General Electric Company; Research Consultant, InSightec Ltd; Research Grant, InSightec Ltd; Royalties, Springer Nature; Consultant, Springer Nature; Research Consultant, Pfizer Inc;

#### thomas.link@ucsf.edu

#### **LEARNING OBJECTIVES**

1) To identify abnormalities of the knee cartilage typically found in traumatic and degenerative conditions. 2) To describe MRI findings associated with cartilage repair. 3) To appraise prognostic significance of cartilage abnormalities.

#### RC204-08 Quantitative DCE-MRI Perfusion Imaging of the Subchondral Bone in Knee Osteoarthritis

Monday, Nov. 26 10:40AM - 10:50AM Room: E451B

#### Participants

Bas A. de Vries, MSc, Rotterdam, Netherlands (*Presenter*) Research Grant, Dutch Arthritis Association Joost Verschueren, MD, Rotterdam, Netherlands (*Abstract Co-Author*) Nothing to Disclose Dirk Poot, PhD, Rotterdam, Netherlands (*Abstract Co-Author*) Nothing to Disclose Gabriel P. Krestin, MD, PhD, Rotterdam, Netherlands (*Abstract Co-Author*) Nothing to Disclose Edwin H. Oei, MD, PhD, Palo Alto, CA (*Abstract Co-Author*) Nothing to Disclose

For information about this presentation, contact:

b.devries@erasmusmc.nl

#### PURPOSE

Osteoarthritis (OA) is characterized by articular cartilage degeneration, synovial inflammation and subchondral bone changes. Although subchondral bone changes are believed to have an important role in the progression of OA, the mechanism is insufficiently understood and might be related to locally increased perfusion and inflammation. Perfusion can be visualized and quantified with gadolinium-based dynamic contrast-enhanced MRI (DCE-MRI). The goal of this study was to evaluate subchondral bone perfusion of affected and non-affected compartments in osteoarthritic knees with DCE-MRI.

#### **METHOD AND MATERIALS**

23 patients with unicompartmental knee OA were prospectively included. Multisequence MRI including DCE-MRI was performed at 3T (GE Discovery MR750) using an 8-channel knee coil. Perfusion was measured in subchondral regions of interest (ROI) in both the affected and non-affected knee compartment on three sagittal slices. Perfusion was also measured in ROIs of the bone marrow lesions (BMLs). The main outcome was Ktrans, a measure of capillary permeability. In addition, the flux rate constant Kep was measured. Perfusion parameters of the affected side were compared to the non-affected side. In BMLs these parameters were compared to surrounding subchondral bone without BMLs. Statistical analyses included the Wilcoxon-signed-rank test.

#### RESULTS

The mean Ktrans and Kep were significantly increased (p<0.05) in the affected compared to the non-affected compartment in the subchondral bone of the knee in both the femur and the tibia. Subchondral BMLs detected on fat-saturated T2-weighted images were present in all 23 patients, of which most BMLs close to the articular surface. Ktrans and Kep were significantly (p<0.001) higher within subchondral BMLs compared to surrounding subchondral bone without BMLs.

#### CONCLUSION

Perfusion of the subchondral bone measured with DCE-MRI is significantly increased in the affected compared to the nonaffected side in patients with unicompartmental knee OA. Since subchondral BMLs are highly associated with increased perfusion parameters compared to subchondral bone regions without BMLs, BMLs most likely account for the increased subchondral bone perfusion in knee OA.

## **CLINICAL RELEVANCE/APPLICATION**

Subchondral bone inflammation is suggested to affect cytokine excretion, which accelerates cartilage degeneration. Increased subchondral perfusion, related to inflammation was present in the OA knee.

#### RC204-09 Effects of Foot Strike Pattern on Running Biomechanics and Knee Joint Degeneration

Monday, Nov. 26 10:50AM - 11:00AM Room: E451B

Participants

Richard Kijowski, MD, Madison, WI (*Presenter*) Research support, General Electric Company; Consultant, Boston Imaging Core Lab, LLC

Peter C. Thurlow, MD, Madison, WI (Abstract Co-Author) Nothing to Disclose

Mikel Joachim, Madison, WI (Abstract Co-Author) Nothing to Disclose

Edwin H. Oei, MD, PhD, Palo Alto, CA (Abstract Co-Author) Nothing to Disclose

Joost Verschueren, MD, Rotterdam, Netherlands (Abstract Co-Author) Nothing to Disclose

Joshua M. Farber, MD, Cincinnati, OH (Abstract Co-Author) Research Consultant, Q-Metrics, Inc; Shareholder, Q-Metrics, Inc

Bryan C. Heiderscheit, PhD, Madison, WI (Abstract Co-Author) Nothing to Disclose

#### PURPOSE

To compare running biomechanics and knee joint degeneration between fore-foot and rear-foot runners.

#### **METHOD AND MATERIALS**

Sixteen fore-foot runners and 24 rear-foot runners underwent a running biomechanics gait analysis and 3.0T knee MRI examination consisting of sagittal three-dimensional fast spin-echo (3D-FSE) and T2 mapping sequences. Features of knee joint degeneration on the 3D-FSE images were graded using the standardized MRI Osteoarthritis Knee Scoring

(MOAKS) system. Cartilage thickness and cartilage T2 relaxation time were measured in the patella, trochlea, medial and lateral femoral condyle, and medial and lateral tibia plateau using the 3D-FSE and T2 mapping images respectively. Mann-Whitney-Wilcoxon tests and ANCOVA tests adjusted for age and gender were used to compare biomechanical parameters and MRI parameters respectively between fore-foot and rear-foot runners.

#### RESULTS

Fore-foot runners had a significantly lower foot angle at contact (p<0.001), vertical loading rate (p=0.010), and knee negative work load (p=0.001), but no significant difference in cadence (p=0.439), speed (p=0.090), or external knee adductor moment (p=0.891) when compared to rear-foot runners. Cartilage lesions and bone marrow edema lesions were present in the patella and trochlea of both fore-foot and rear-foot runners, but there was no significant difference (p=0.271-0.512) in MOAKS scores within the patelofemoral compartment. No runner had evidence of morphologic joint degeneration on MRI within the medial or lateral compartments. There was no significant difference (p=0.151-0.854) in cartilage thickness on any articular surface between fore-foot and rear-foot runners. Fore-foot runners had significantly higher cartilage T2 on the medial tibia plateau (p-0.008), but no significant difference (p=0.056-0.930) in cartilage T2 on the remaining articular surfaces when compared to rear-foot runners.

#### CONCLUSION

While fore-foot runners had significantly lower vertical loading rate and knee negative work load than rear-foot runners, morphologic and quantitative MRI showed no benefits of the fore-foot strike pattern on reducing the risk of knee joint degeneration.

#### **CLINICAL RELEVANCE/APPLICATION**

While the fore-foot running pattern has beneficial biomechanical effects, our preliminary cross-sectional study using MRI showed no evidence that the improved biomechanics could reduce the risk of knee joint degeneration.

## RC204-10 Is CT Imaging Necessary for Bone Tunnel Assessment in ACL Revision Surgery? A Comparison of Multi-Planar Reformatting (MPR) Tibial Bone Tunnel Maximum Diameter on Routine MR Imaging versus Dedicated CT Imaging

Monday, Nov. 26 11:00AM - 11:10AM Room: E451B

#### Participants

Ayesha Jameel, MBBS, LONDON, United Kingdom (*Presenter*) Nothing to Disclose Abul Lasker, MBBS, London, United Kingdom (*Abstract Co-Author*) Nothing to Disclose Amandeep Sandhu, MBBS, London, United Kingdom (*Abstract Co-Author*) Nothing to Disclose Muhammad T. Dawood, MBBS, MRCP, London, United Kingdom (*Abstract Co-Author*) Nothing to Disclose Dimitri Amiras, MBBS, FRCR, London, United Kingdom (*Abstract Co-Author*) Nothing to Disclose

#### For information about this presentation, contact:

ayesha.jameel@nhs.net;imran.lasker@nhs.net

#### PURPOSE

ACL revision surgery requires strict preoperative planning to evaluate the existing tibial bone tunnel. If osteolysis has occurred, bone grafting is required intra-operatively. Current practice dictates the use of dedicated preoperative CT imaging for assessment. However all patients considered for ACL revision undergo diagnostic MR study to determine any underlying abnormality and confirm graft failure. We postulate by utilising multi-planar reformatting (MPR), commonly built into PACS, we can accurately and reliably measure the maximum bone tunnel diameter on MRI. This method would reduce cost, patient exposure to radiation and time delay to surgery by obviating the need for dedicated CT.

#### **METHOD AND MATERIALS**

A retrospective review identified 20 ACL revision patients over 10 year period (2008-2018) with both MR and CT studies. These were performed using the department technique with a variety of suppliers and included metal artefact reduction sequences where appropriate. Using Carestream Vue PACS (version 12.1.6) built in MPR capability the maximum diameter of the bone tunnel was measured orthogonally on both MR and CT, >1cm from the tibial intercondylar notch. For MRI the axial proton density fat saturated (PDFS) imaging was realigned to be perpendicular to the sagittal T1 and coronal PDFS. Two musculoskeletal radiologists with up to 5 years experience reviewed each study independently and each modality on separate occasions. The MRI and CT tunnel maximum diameter was compared using a paired T-test. A p-value of <0.05 was taken to be significant.

#### RESULTS

20 patients were reviewed, 1 excluded due to MRI movement artefact. 38 MPR measurements were taken and any metal artefact in the tibial tunnel was documented for further analysis. For both reviewers, there was no statistically significant difference in the MPR measurements on CT and MR (0.7 and 0.2 respectively). The mean tunnel measurements for reviewer 1 were 11.45(CT) and 11.40(MR), for reviewer 2 were 12.25(CT) and 12.6(MR).

#### CONCLUSION

Preoperative MRIs could be used to measure the maximum bone tunnel diameter prior to ACL revision, obviating the need for dedicated CT imaging, for ACL grafts with both metallic and non-metallic interference screws, however more evaluation is required.

#### **CLINICAL RELEVANCE/APPLICATION**

In ACL revision surgery, tibial tunnel osteolysis could be identified and measured accurately on the preoperative MRI, reducing the need for additional CT imaging.

## RC204-11 Extra-articular Knee

## Participants Julia R. Crim, MD, Columbia, MO (*Presenter*) Nothing to Disclose

For information about this presentation, contact:

## crimj@health.missouri.edu

Active Handout:Julia Ruth Crim

http://abstract.rsna.org/uploads/2018/18000780/Crim RSNA handout RC204-11.pdf

## LEARNING OBJECTIVES

1) Analysis of Hoffa fat pad for impingement, synovitis, fibrosis, and mass. 2) Recognition of muscle injury patterns and anatomic variants. 3) Recognition of nerve and vascular abnormalities. 4) Evaluation of the iliotibial band. 5) Recognition of Morel-Lavallee lesion and its distinction from other masses around the knee.

## RC204-12 Post-arthroscopy Knee

Monday, Nov. 26 11:35AM - 12:00PM Room: E451B

### Participants

Naveen Subhas, MD, Shaker Heights, OH (Presenter) Research support, Siemens AG

#### **LEARNING OBJECTIVES**

1) Review the postoperative meniscus: Normal postoperative appearance, postoperative tears, and postoperative complications. 2) Review the postoperative ACL: Normal postoperative appearance, ACL graft tears, and postoperative complications. 3) Review articular cartilage repair: Normal postoperative appearance and postoperative complications.



#### RC205

## **Neuroradiology Series: Brain Tumors**

Monday, Nov. 26 8:30AM - 12:00PM Room: S406B



**FDA** Discussions may include off-label uses.

#### Participants

Soonmee Cha, MD, San Francisco, CA (*Moderator*) Nothing to Disclose Kei Yamada, MD, Kyoto, Japan (*Moderator*) Nothing to Disclose

#### Sub-Events

## RC205-01 Multimodal Molecular Imaging Using Advanced MRI and PET: Applications in Clinical Neuro-Oncology

Monday, Nov. 26 8:30AM - 9:00AM Room: S406B

Participants

Norbert Galldiks, Cologne, Germany (Presenter) Research grant, Wilhelm-Sander Stiftung (Munich, Germany); Advisory board, Abbvie

## LEARNING OBJECTIVES

1) To give an overview on the most relevant advanced MRI techniques (i.e., PWI MRI, 2-hydroxyglutatate MRS) and PET tracers (i.e., amino acid PET tracers, radiolabeled somatostatin receptor ligands) to improve diagnostics in the field of clinical Neuro-Oncology.

#### RC205-02 Robust Pre-Operative Language Mapping in Patients with Brain Tumors: A Feasibility Study

Monday, Nov. 26 9:00AM - 9:10AM Room: S406B

Participants

Mohammad Fakhri, MD, Saint Louis, MO (*Presenter*) Nothing to Disclose Manu S. Goyal, MD, MSc, Saint Louis, MO (*Abstract Co-Author*) Nothing to Disclose Joshua S. Shimony, MD, PhD, Saint Louis, MO (*Abstract Co-Author*) Nothing to Disclose Carl Hacker, Saint Louis, MO (*Abstract Co-Author*) Nothing to Disclose Amrita Hari-Raj, St. Louis, MO (*Abstract Co-Author*) Nothing to Disclose Abraham Z. Snyder, PhD, Saint Louis, MO (*Abstract Co-Author*) Nothing to Disclose

#### For information about this presentation, contact:

fakhri@wustl.edu

#### PURPOSE

We evaluate multilevel perceptron (MLP)-based mapping as a tool for identification of language-related resting-state networks in brain tumor patients. Currently available alternative resting state fMRI analysis methods are either biased (e.g., seed-based correlation) or not robust at the single subject level (e.g., Independent Component Analysis), and therefore, not ideal for use in presurgical planning.

#### **METHOD AND MATERIALS**

Twenty-one patients with a brain tumor in the vicinity of expressive language areas were included (mean age 42 ±16 years; 71% male). The MLP output was compared to seed-based correlation in two different manually defined language regions of nterst (ROIs). The putative language ROIs were defined using meta-analysis of task-fMRI responses, resting state seed based correlation maps, and direct cortical stimulation language maps. MLP performance in patients was also compared to a cohort of 688 normal subjects.

#### RESULTS

Upon presentation, 62% of the patients exhibited expressive aphasia prior to the surgical resection. Thirty-two percent of the patients were positive for IDH-1 mutation and 27% had 1p/11q deletion. The MLP was able to reliably map robust language RSN affiliation in putative language areas in all patients (n=21, 100%). Results were similar to those obtained in a cohort of young, healthy subjects. Fisher z-transformed Pearson correlation maps obtained from seed ROIs were strongly spatially correlated with the MLP score in both evaluation ROIs (Spearman rho=0.74 and 0.62, p<0.0001 and p<0.003 respectively).

#### CONCLUSION

MLP-based language maps are comparable to results obtained using conventional seed-based correlation mapping. MLP-based mapping is reliable in patients with brain tumors. The trained MLP is robust to anatomical shifts owing to mass effects and focal, tumor-related neural dysfunction, hence, is suitable for use in patients with brain tumors.

#### **CLINICAL RELEVANCE/APPLICATION**

A trained machine-learning algorithm can reliably identify resting-state language-related networks on an individual basis in patients

with brain tumors in vicinity of the language cortex.

## RC205-03 Use of Quantitative Blood Oxygen Level Dependent (qBOLD) in Non-Invasively Determining Glioma Grade, with Correlation through Neuropathology

Monday, Nov. 26 9:10AM - 9:20AM Room: S406B

Participants Pejman Jabehdar Maralani, MD, FRCPC, Toronto, ON (*Presenter*) Nothing to Disclose Julia Keith, MD, Toronto, ON (*Abstract Co-Author*) Nothing to Disclose David Munoz, MD, Toronto, ON (*Abstract Co-Author*) Nothing to Disclose Todd Mainprize, MD, Toronto, ON (*Abstract Co-Author*) Nothing to Disclose Arjun Sahgal, Toronto, ON (*Abstract Co-Author*) Speaker, Medtronic plc; Speaker, Elekta AB; Medical Advisory Board, Varian Medical Systems, Inc; Speaker, Accuray Incorporated; Research Grant, Elekta AB Sean P. Symons, MPH, MD, Toronto, ON (*Abstract Co-Author*) Nothing to Disclose Bradley J. Macintosh, PhD, Toronto, ON (*Abstract Co-Author*) Nothing to Disclose Aimee Chan, Toronto, ON (*Abstract Co-Author*) Nothing to Disclose Sunit Das, MD,PhD, Toronto, ON (*Abstract Co-Author*) Nothing to Disclose David J. Mikulis, MD, Toronto, ON (*Abstract Co-Author*) Stockholder, Thornhill Research Inc; Research Grant, General Electric Company;

#### For information about this presentation, contact:

pejman.maralani@utoronto.ca

#### PURPOSE

Quantitative blood oxygen level dependent (qBOLD) magnetic resonance imaging (MRI) has been used as a method to gauge the level of oxygen saturation (SO2) in the tumors of patients with gliomas. We investigated whether there was a difference in the level of oxygenation in different grades of gliomas.

#### **METHOD AND MATERIALS**

10 patients were recruited for this prospective, multi-institutional study. Patients underwent a preoperative Ferumoxytol-based qBOLD MRI. Based on visual inspection of SO2 maps from qBOLD imaging, two volumes of interest (VOIs) from the tumor were chosen. Biopsy samples from the VOIs were taken to correlate histopathological measures of hypoxia against qBOLD, and staining was scored by a neuropathologist. Patients with glioblatoma (GBM; WHO Grade IV) was compared with lower-grade astrocytomas. 1 patients' research samples were inconclusive, and therefore excluded from pathological analysis.

## RESULTS

Pathology reports indicated that: 1 patient had diffuse astrocytoma (WHO Grade II), 3 patients had anaplastic astrocytoma (WHO Grade III), and 6 patients GBM. When comparing low-SO2 samples, non-GBM patients had on average higher SO2 (26.0% vs 10.6%, p=0.07). Pathology staining of low-SO2 samples showed significantly higher levels of staining in HIF1a (p=0.048), VEGF (p=0.04) and CAIX (p<0.01) in GBM compared to lower-grade gliomas. No significant differences were detectable in the high SO2 (mean, 37.4%) tumors.

#### CONCLUSION

Levels of oxygenation appear to decrease with increasing glioma grade, and is detectable by qBOLD MRI. Pathological markers of hypoxia support this notion. The threshold for differentiating GBM from lower-grade gliomas appears to be  $\sim$ 35% SO2. More subjects are required to confirm these results.

#### **CLINICAL RELEVANCE/APPLICATION**

qBOLD MRI can be an alternative method to assess tumor grade when biopsy is not feasible. In light of new hypoxia-targeting therapies, it can also be used to monitor oxygenation state of the tumor during treatment.

## RC205-04 Probabilistic Atlases of Pre-Treatment MRI Reveal Hemispheric and Lobe-Specific Spatial Distributions across Molecular Sub-Types of Diffuse Gliomas

Monday, Nov. 26 9:20AM - 9:30AM Room: S406B

## Awards

## **Trainee Research Prize - Medical Student**

Participants Niha G. Beig, MS, Cleveland, OH (*Presenter*) Nothing to Disclose Marwa Ismail, PhD, Cleveland, OH (*Abstract Co-Author*) Nothing to Disclose Anant Madabhushi, PhD, Cleveland, OH (*Abstract Co-Author*) Research funded, Koninklijke Philips NV Manmeet Ahluwalia, Cleveland, OH (*Abstract Co-Author*) Nothing to Disclose Pallavi Tiwari, PhD, Cleveland, OH (*Abstract Co-Author*) Nothing to Disclose

## For information about this presentation, contact:

niha.beig@case.edu

## PURPOSE

Recent WHO classification of diffuse gliomas defined 3 subtypes based on their molecular status: Isocitrate dehydrogenase wild type (IDH-WT), IDH mutant with 1p/19q intact (IDHmut-noncodel), and IDH mutant with 1p/19q co-deletion (IDHmut-codel). Each category represents different prognosis and chemo-sensitivity thus impacting treatment decisions. Previous studies have linked tumor location with patient outcome. In this feasibility study, we developed population atlases of pre-treatment MRI lesions to evaluate whether IDH-WT, IDHmut-codel, IDHmut-noncodel tumors will have spatial proclivity to hemispheric or lobe-specific locations based on their frequency of occurrence.

#### **METHOD AND MATERIALS**

150 pre-operative MRI sequences (1.5T/3T T1w, T2w, FLAIR scans, multi-center) of patients diagnosed with diffuse gliomas (65 low grade gliomas and 85 glioblastomas) were considered from TCIA, along with their IDH mutation and 1p/19q co-deletion status. Frequency atlases of tumor occurrence in T2/FLAIR hyper-intensity regions were developed for each sub-type, by averaging voxel intensities across all patients. To compute significant differences (p-value<0.05), voxel-based analysis of differential involvement (ADIFFI) based on two-tailed Fisher's exact test was performed on (a) IDH-WT (n= 91) vs IDH-mut (n=59), and (b) IDHmut-codel (n=13) vs IDHmut-noncodel (n=57) atlases. Prominent clusters were identified and mapped to LONI Probabilistic Brain Atlas (LPBA40) parcellations to provide anatomic localization for each sub-type.

#### RESULTS

The ADIFFI analysis revealed that IDHmut tumors were predominant in frontal lobe with a frequency of 52.7% occurrence whereas IDH-WT had a multi-centric distribution across parietal and temporal lobes (p<0.005). Prominent cluster of IDHmut-codel was found to be lateralized to the left hemisphere in the cingulate gyrus region, while IDHmut-noncodel had 60% occurrence in the superior frontal gyrus of the right hemisphere (p<0.05).

#### CONCLUSION

Our analysis suggests spatial proclivity of molecular subtypes to hemispheric and lobe-specific locations in the brain. The spatial localization could serve as an imaging marker for differentiating molecular subtypes of gliomas.

#### **CLINICAL RELEVANCE/APPLICATION**

IDHmut-codel have a favorable response to chemoradiation, while IDHmut-noncodel have improved prognosis versus IDH-WT. Identifying radiogenomic markers of sub-types could enable personalized treatments in Gliomas.

## RC205-05 High-Tumor Mutation Burden (Hypermutation) in Gliomas Exhibit a Unique Predictive Radiomic Signature

Monday, Nov. 26 9:30AM - 9:40AM Room: S406B

Participants

Islam S. Hassan, MD, Houston, TX (*Abstract Co-Author*) Nothing to Disclose Aikaterini Kotrotsou, PhD, MEng, Houston, TX (*Abstract Co-Author*) Nothing to Disclose Carlos M. Kamiya, Houston, TX (*Abstract Co-Author*) Nothing to Disclose Nabil A. Elshafeey, MD, Houston, TX (*Presenter*) Nothing to Disclose Kristin Alfaro-Munoz, MS, Houston, TX (*Abstract Co-Author*) Nothing to Disclose Pascal O. Zinn, MD, Boston, MA (*Abstract Co-Author*) Nothing to Disclose John F. deGroot, MD, Houston, TX (*Abstract Co-Author*) Nothing to Disclose Rivka R. Colen, MD, Houston, TX (*Abstract Co-Author*) Research Grant, General Electric Company;

#### For information about this presentation, contact:

rcolen@mdanderson.org

#### PURPOSE

Increase in tumor mutation burden (TMB) or hypermutation is the excessive accumulation of DNA mutations in cancer cells. Hypermutation was reported in recurrent as well as primary gliomas. Hypermutated gliomas are mostly resistant to alkylating therapies and exhibit a more immunologically reactive microenvironment which makes them a good candidate for immune checkpoint inhibitors. Herein, we sought to use MRI radiomics for prediction of high TMB (hypermutation) in primary and recurrent gliomas.

## METHOD AND MATERIALS

In this IRB-approved retrospective study, we analyzed 101 patients with primary gliomas from the University of Texas MD Anderson Cancer Center. Next generation sequencing (NGS) platforms (T200 and Foundation 1) were used to determine the Mutation burden status in post-biopsy (stereotactic/excisional). Patients were dichotomized based on their mutation burden; 77 Non-hypermutated (<30 mutations) and 24 hypermutated (>=30 mutations or <30 with MMR gene or POLE/POLD gene mutations). Radiomic analysis was performed on the conventional MR images (FLAIR and T1 post-contrast) obtained prior to tumor tissue surgical sampling; and rotation-invariant radiomic features were extracted using: (i) the first-order histogram and (ii) grey level co-occurrence matrix. Then, we performed Logistic regression modelling using LASSO regularization method (Least Absolute Shrinkage and Selection Operator) to select best features from the overall features in the dataset. ROC analysis and a 50-50 split for training and testing, were used to assess the performance of logistic regression classifier and AUC, Sensitivity, Specificity, and p-value were obtained.

#### RESULTS

LASSO regularization (alpha = 1) was performed with all the 4880 features for feature selection and 40 most prominent features were selected for logistic regression modelling. Our 50-50 split ROC analysis showed an accuracy of 94%, sensitivity of 75%, and specificity of 100% and a p-value of 0.0008).

## CONCLUSION

An MRI-radiomic phenotype is predictive of the increase in TMB (Hypermutation) in both primary and recurrent gliomas.

#### **CLINICAL RELEVANCE/APPLICATION**

Hypermutated gliomas are resistant to alkylating therapies but responsive to immune checkpoint inhibitors. Our proposed radiomic biomarker can be used to guide therapy and patient selection for immunotherapy clinical trials.

## RC205-06 Brain Tumor Surveillance Imaging in the Era of Genomics and Personalized Medicine

Monday, Nov. 26 9:40AM - 10:10AM Room: S406B

#### Participants

Rajan Jain, MD, Hartsdale, NY (Presenter) Consultant, Cancer Panels; Royalties, Thieme Medical Publishers, Inc

#### For information about this presentation, contact:

#### rajan.jain@nyumc.org

#### **LEARNING OBJECTIVES**

1) To discuss currently used response assessment criteria in brain tumor surveillance, such as Macdonald and RANO criteria and their limitations. 2) Participants will learn how the emergence of genomic markers has brought a paradigm shift in the management and surveillance of gliomas. 3) Participants will learn about the complexities of post-treatment imaging appearance of brain tumors in the new age of targeted immuno-therapies and what functional imaging techniques can add value to conventional surveillance MRI.

## RC205-07 Update on Pediatric Brain Tumor Imaging

Monday, Nov. 26 10:20AM - 10:50AM Room: S406B

Participants

Zoltan Patay, MD, PhD, Memphis, TN (Presenter) Nothing to Disclose

#### For information about this presentation, contact:

zoltan.patay@stjude.org

#### LEARNING OBJECTIVES

1) Familiarize with new concepts and entities introduced in the 2016 update of the WHO Classification of Tumours of the CNS and pertinent to pediatric brain neoplasms. 2) Review the most recent developments related to the classification of embryonal and ependymal tumors since the publication of the 2016 update. 3) Discuss relevance and implications of the above for the practing radiologist.

## RC205-08 Selection of Imaging-based Surrogate Endpoints Depending on a Specific Target of Test Treatment in Phase III Randomized Controlled Trials of Glioblastoma

Monday, Nov. 26 10:50AM - 11:00AM Room: S406B

Participants

Chong Hyun Suh, MD, Seoul, Korea, Republic Of (*Presenter*) Nothing to Disclose Ho Sung Kim, Seoul, Korea, Republic Of (*Abstract Co-Author*) Nothing to Disclose Sang Joon Kim, MD, Seoul, Korea, Republic Of (*Abstract Co-Author*) Nothing to Disclose

#### PURPOSE

Phase III randomized controlled trials (RCTs) in glioblastoma have used various potential surrogate endpoints with imaging. The surrogacy of imaging-based endpoints remains largely unknown and can be dependent on the type of test treatment. We investigated the surrogacy of imaging-based endpoints as well as their values depending on a specific target of test treatment in patients with glioblastoma.

## METHOD AND MATERIALS

A systematic search of phase III RCTs in glioblastoma was performed. Surrogacy between imaging-based endpoints including progression-free survival (PFS), 6 month PFS (6moPFS), 12 month PFS (12moPFS), median PFS, and objective response rate (ORR) with overall survival (OS) were explored using weighted linear regression for the hazard ratio for OS and the hazard ratios or odds ratios for imaging-based endpoints. Subgroup analyses according to disease entity, a specific target of test treatment, and response assessment criteria were performed. The quality of the reporting of efficacy with these IBEs was also evaluated.

#### RESULTS

Twenty-three RCTs published between 2000 and 2017, covering 8387 patients, met the inclusion criteria. OS showed significant correlations with PFS (standardized ß coefficient [R]=0.719), 6moPFS (R=0.647), and 12moPFS (R=0.638). OS showed nonsignificant correlations with median PFS and ORR. The subgroup analyses consistently showed highly significant correlations between OS and PFS. PFS showed the highest correlations with OS in drugs targeting DNA repair-cell cycle control-epigenetic modifiers (R=0.913) and drugs targeting growth factor receptors-MAPK/PI3K signaling pathways (R=0.962). 12moPFS showed the highest correlations with OS in antiangiogenic therapy, (R=0.821). Trials using RANO criteria showed higher correlation coefficients between OS and PFS, 6moPFS, and 12moPFS than trials using MacDonald criteria. In terms of quality of reporting, there were high proportions of clearly defined primary endpoints (91%) and intent-to-treat analyses (83%). Compared with trials published between 2000 and 2011, those published between 2012 and 2017 were more likely to be supported by industry.

#### CONCLUSION

Imaging-based endpoints can be surrogates in phase III RCTs of glioblastoma.

## **CLINICAL RELEVANCE/APPLICATION**

The specific target of test treatment and response assessment criteria should be considered in selection of imaging-based endpoints as a surrogate endpoint.

## RC205-09 18F-Choline PET/RM in Brain Tumours: Multimodality Imaging in Gliomas Response Assessment

Monday, Nov. 26 11:00AM - 11:10AM Room: S406B

## Awards

Student Travel Stipend Award

Participants Valentina Ferrazzoli, MD, Rome, Italy (*Presenter*) Nothing to Disclose Harpreet K. Hyare, MBBS, London, United Kingdom (*Abstract Co-Author*) Nothing to Disclose Ananth Shankar, London, United Kingdom (*Abstract Co-Author*) Nothing to Disclose Christine Tang, MBBS, London, United Kingdom (*Abstract Co-Author*) Nothing to Disclose Ahmed Al-Khayfawee, MRCP,MD, London, United Kingdom (*Abstract Co-Author*) Nothing to Disclose Roberto Floris, MD, Rome, Italy (*Abstract Co-Author*) Nothing to Disclose Francesco Fraioli, MD, London, United Kingdom (*Abstract Co-Author*) Nothing to Disclose

#### For information about this presentation, contact:

valentinaferrazzoli@hotmail.it

#### PURPOSE

Evaluation of post-treatment glioma burden remains a significant challenge, particularly in Teenage and Young Adult (TYA) population. Although aminoacid PET has impacted on glioma imaging, 18fluoro-Choline Positron Emission Tomography (ChoPET) is currently more widely available. Purpose was to evaluate ChoPET/MR for post-treatment TYA glioma burden.

## **METHOD AND MATERIALS**

27 TYA (mean age 16 years, 8-22 years) in treatment (radiotherapy e/o chemotherapy) for astrocytic brain tumours (14 WHO III/IV; 13 WHO I/II) were evaluated with ChoPET/MR. 59 follow up scans were retrospectively reviewed; maximum standardized uptake values (SUVmax) and MR features (diameters, enhancement) were recorded. In 13 cases dynamic susceptibility contrast perfusion weighted imaging (DSCpwi) was analyzed; relative cerebral blood volume (rCBV) and SUV in enhancing and non-enhancing tumour volumes (Venh, Vne) and in normal appearing white matter (wm) were calculated (rCBVenh, rCBVne, rCBVwm, SUVenh, SUVne, SUVwm). A blinded nuclear medicine and a radiologist scored the images on tumour probability (1:unlikely-5:definitely). Receiver Operating Characteristic (ROC) analysis was used considering as gold standard for diagnosis the histopathology or follow up. Pearson correlation coefficient was used for SUV and rCBV and independent T-Test for differences in ROIs.

#### RESULTS

MR sensitivity for residual tumour was 92.7% (85.7% WHO III/IV,81.5% WHO I/II). PET sensitivity was 78.2% (78.6% WHO III/IV, 63.0% WHO I/II). Discrepancy was of 20% (11/12 non enhancing). Significant positive correlation between SUV and rCBV in all ROIs was found (r=0.051, p=0.0016). Tumour component analysis showed significantly higher SUVenh and SUVne than SUVwm (SUVenh:p<0.001, SUVne: p=0.021) and significantly higher rCBVne than rCBVwm (p=0.005). rCBVenh showed only borderline significance (p=0.053).

#### CONCLUSION

ChoPET is able to detect post-treatment enhancing and non-enhancing tumour but both conventional MR and pwi are superior for evaluating non-enhancing disease. In TYA gliomas follow up a quantitative multimodality evaluation can better identify both enhancing and non-enhancing residual/recurrent disease being promising in the early assessment of tumour response.

## **CLINICAL RELEVANCE/APPLICATION**

In teenage and young-adults gliomas early assessment of tumour response to therapy can be improved by complementary use of PET/MR to evaluate different tumour components.

## RC205-10 Prediction of Genomic Profiles and Survival in Glioblastoma Patients: Feasibility of Qualitative and Quantitative Analyses of Arterial Spin-Labeling Perfusion-Weighted Imaging

Monday, Nov. 26 11:10AM - 11:20AM Room: S406B

Participants Roh-Eul Yoo, MD, Seoul, Korea, Republic Of (*Presenter*) Nothing to Disclose Tae Jin Yun, MD, Seoul, Korea, Republic Of (*Abstract Co-Author*) Nothing to Disclose

For information about this presentation, contact:

roheul7@gmail.com

#### PURPOSE

To explore the feasibility of using arterial spin-labeling perfusion-weighted imaging (ASL-PWI) to predict genomic profiles and survival in glioblastoma (GBM) patients.

### METHOD AND MATERIALS

One hundred thirty-two consecutive GBM patients, who had undergone maximal surgical resection or biopsy followed by concurrent chemo- and radiation therapy and adjuvant chemotherapy using temozolomide between January 2011 and November 2015, were included in this retrospective study. CBF at the contrast-enhancing and T2 hyperintense portions on preoperative ASL-PWI were evaluated both qualitatively (hypo- / iso- / hyperperfusion relative to gray matter) and quantitatively (mean and maximal CBFs of tumors normalized with respect to those of contralateral gray matter [nCBFmean and nCBFmax]). The associations between ASL findings and major genomic profiles or survival were evaluated using Mann-Whitney U-test, Fisher's exact test, Spearman rank correlation, and Kaplan-Meier analysis. Receiver operating characteristics analysis was performed to determine the diagnostic performance of the imaging parameters for prediction of genetic biomarkers.

#### RESULTS

nCBFmean and nCBFmax at contrast-enhancing portions were significantly higher in IDH wild-type group (n = 102) than in IDH mutant (IDH1 or IDH2) group (n = 17) (P = .009 and P = .007, respectively). Sensitivity and specificity for prediction of IDH mutation were 59% and 81% at the optimal cutoff value of 1.13 for nCBFmax. nCBFmax at contrast-enhancing portions tended to be lower in patients with methylated MGMT promoter (n = 65) than in those with unmethylated MGMT promoter (n = 49) (P = .072). No significant associations were found between nCBF and other genetic biomarkers including ATRX, PTEN, p53, and EGFR. Hyperperfusion at contrast-enhancing portions was significantly more common in IDH wild-type group than in IDH mutant group (P = .003). Hyperperfusion was associated with shorter progression-free survival as compared with hypo- or isoperfusion (Median, 6.9 vs. 12.5 vs. 19.3 months; P = .029).

#### CONCLUSION

ACL DWT may halp popinyaciyaly prodict TDH mytation status and progression free survival in diablastama patients

ASE-PWI Hay help nonlinvasively predict 10 minutation status and progression-free survival in gliobidstoria patients.

#### **CLINICAL RELEVANCE/APPLICATION**

ASL-PWI may help noninvasively predict IDH mutation status and progression-free survival in glioblastoma patients and is recommended as part of preoperative tumor evaluation particularly for patients with impaired renal function.

## RC205-11 Clinical Data and Vascular Pattern on MRI to Predict Survival in 'De Novo' Glioblastoma

Monday, Nov. 26 11:20AM - 11:30AM Room: S406B

#### Awards

**Student Travel Stipend Award** 

#### Participants

Blanca Domenech, MD, Barcelona, Spain (*Presenter*) Nothing to Disclose Alfredo Gimeno Cajal, Barcelona, Spain (*Abstract Co-Author*) Nothing to Disclose Gerard Blasco, RT, Girona, Spain (*Abstract Co-Author*) Nothing to Disclose Pepus Daunis-I-Estadella, Girona, Spain (*Abstract Co-Author*) Nothing to Disclose Carmen Balana, Barcelona, Spain (*Abstract Co-Author*) Nothing to Disclose Jaume Capellades, MD, Barcelona, Spain (*Abstract Co-Author*) Nothing to Disclose Angel Alberich-Bayarri, MD, Valencia, Spain (*Abstract Co-Author*) Nothing to Disclose Kambiz Nael, MD, New York, NY (*Abstract Co-Author*) Medical Advisory Board, Canon Medical Systems Corporation Carlos Leiva-Salinas, MD,PhD, Charlottesville, VA (*Abstract Co-Author*) Nothing to Disclose Rajan Jain, MD, Hartsdale, NY (*Abstract Co-Author*) Consultant, Cancer Panels; Royalties, Thieme Medical Publishers, Inc Marco Essig, MD, Erlangen, Germany (*Abstract Co-Author*) Nothing to Disclose Salvador Pedraza, MD, PhD, Girona, Spain (*Abstract Co-Author*) Nothing to Disclose

#### For information about this presentation, contact:

bl.domenech@gmail.com

#### PURPOSE

MRI provides information on the physiologic properties of glioblastomas. In addition to established prognostic markers such as age, performance status, and extent of resection, increased vascularity on contrast-enhanced MRI is associated with shortened survival. We investigated whether glioblastoma vascular pattern (GVP-MRI), combined with clinical variables and other imaging features, could improve the predictive power of survival models.

#### METHOD AND MATERIALS

From January 2012 through December 2016, 97 consecutive patients (62 men; mean age, 58±15 years) with histologically proven glioblastoma (GLIOCAT substudy) underwent 1.5T-MRI including anatomical, diffusion-weighted, first-pass DSC, and T1-weighted sequences after 0.1 mmol/kg gadobutrol (1 mm isometric voxel). We used Olea Sphere V.3.0 software (Olea Medical, La Ciotat, France) to analyze rCBV, rCBF, mean delay time, and apparent diffusion coefficient in volumes of interest for contrast-enhancing lesion (CEL), non-CEL, and contralateral tissue. Glioblastomas with >5 vessels seen within the lesion on postcontrast T1-weighted images were considered hyper-GVP-MRI. Prognostic factors were evaluated by Kaplan-Meier survival, ROC analyses, and hazard ratios (HR).

#### RESULTS

Gioblastomas were considered hyper-GVP-MRI in 58 (60.4%) patients. Patients with hyper-GVP-MRI glioblastomas were older, had higher volumeCEL, increased rCBFCEL and poor survival. Combining Stupp protocol (HR: 0.604; 95% CI: 0.459-0.796), age (HR: 0.163; 95% CI: 0.090-0.297), and GVP-MRI (HR: 1.481; 95% CI: 0.909-2.414) best predicted survival at 1 year (AUC 0.901, 83.3% sensitivity, 93.3% specificity, 96.2% PPV, 73.7% NPV).

## CONCLUSION

Our preliminary data suggest that combining clinical parameters and vascular pattern on MRI improves survival prediction in 'de novo' glioblastoma. Cross-validation studies in other populations are necessary to test the generalizability of our findings.

## **CLINICAL RELEVANCE/APPLICATION**

Information about baseline risk and prognosis is crucial for assigning patients with glioblastomas to optimized treatment regimens in clinical practice or to subgroups in clinical trials.

#### RC205-12 Application of Radiomics & Deep-Learning in Brain Tumor Imaging

Monday, Nov. 26 11:30AM - 12:00PM Room: S406B

## Participants

Philipp Kickingereder, MD, MBA, Heidelberg, Germany (Presenter) Nothing to Disclose

#### For information about this presentation, contact:

philipp.kickingereder@med.uni-heidelberg.de

#### LEARNING OBJECTIVES

1) To understand and critically reflect the impact of radiomics and radiogenomics. 2) To understand the impact of deep-learning for guiding treatment decisions and advancing precision and personalized medicine in neuro-oncology.



#### RC206

Head and Neck Series: There's a New (AJCC 8th Edition) Manual-Updates in Head and Neck Cancer Science and TNM Staging

Monday, Nov. 26 8:30AM - 12:00PM Room: E450B



AMA PRA Category 1 Credits ™: 3.50 ARRT Category A+ Credits: 4.00

**FDA** Discussions may include off-label uses.

#### Participants

Remy R. Lobo, MD, Ann Arbor, MI (*Moderator*) Nothing to Disclose Eugene Yu, MD, FRCPC, Toronto, ON (*Moderator*) Nothing to Disclose

For information about this presentation, contact:

shatzkes@hotmail.com

#### Sub-Events

RC206-01 All About the AJCC and Its 8th Edition

Monday, Nov. 26 8:30AM - 8:55AM Room: E450B

Participants Christine M. Glastonbury, MBBS, San Francisco, CA (*Presenter*) Author with royalties, Reed Elsevier

For information about this presentation, contact:

christine.glastonbury@ucsf.edu

#### **LEARNING OBJECTIVES**

1) To present the rationale for changes in HN cancer staging in the AJCC/UICC 8th edition. 2) To illustrate some specific features that make dramatic changes to the prognostic stage, particularly with regard to HPV; associated OPSCC. 3) To reinforce the necessity of a team approach to cancer management and the utility of the radiologist for aiding staging.

#### ABSTRACT

The 8th edition of the American Joint Committee on Cancer (AJCC) Cancer Staging Manual was published December 2016 but only officially came in to use January 2018. The updates to the head and neck (HN) section, which forms part II of XVIII, were created in collaboration with the Union for International Cancer Control (UICC). The AJCC and UICC cancer staging manuals reflect the current medical understanding of tumor behavior and treatment options. While most of us think of tumor staging as a method to stratify patients into prognostic groups, this system also allows accurate data collection for understanding and refining tumor and treatment protocols and helps determine patient eligibility for clinical trials. Staging is currently an anatomically-based description of the patient's tumor burden: the location and extent of the primary tumor, any evidence of nodal disease and of distant (metastatic) spread. In the AJCC/UICC manuals these tumor descriptors are designated as the T, the N and the M respectively. Oncologists determine a final clinical stage ('cTNM') by combining all available information (physical exam findings, radiology findings, fine needle aspiration, sentinel node biopsy, etc.). The clinical 'c' is replaced with the prefix 'p' when pathological information from surgical tumor resection is included. The cTNM / pTNM determine each patient's overall anatomic stage or prognostic group (O to IV) which in turn influences choice of treatment plans and enables effective communication between care teams. Updates to the staging manual occur periodically, typically every 7-8 years, with analysis of updated knowledge about tumor biology, pathology and patient outcomes. A recognition of better outcomes in specific subsets of patients will thus lead to alteration in previously used staging criteria. The most important example of this in the current AJCC8 is the separation of staging criteria and prognostic stage groupings for HPV-mediated / p16 positive oropharyngeal squamous cell carcinoma [OPSCC] from p16 negative OPSCC. There are now two separate staging tables used for OPSCC with almost matching T criteria, but vastly different nodal criteria and prognostic staging groups when the tumor is HPV+/p16+, reflecting the knowledge that these tumors have a vastly better prognosis with an overall close to 90% 5 year survival. In a similar fashion, changes may be made to the designation of specific imaging findings based on new information as to the prognostic impact of that feature. In the AJCC7 edition, invasion of the lateral pterygoid muscle by a nasopharyngeal carcinoma was designated T4 disease. Publications since then have shown that this is not indicative of a very poor prognosis, so that in AJCC8 lateral pterygoid invasion is designated T2. Invasion beyond the lateral pterygoid muscle however is T4 disease. A new pathologic feature may also alter staging criteria. In the oral cavity SCC section a pathologic feature, depth of invasion, has been added to the T criteria. This has been determined to be an important prognostic feature of oral cavity tumors, and is used in conjunction with the overall tumor size to determine T designation. The imaging feature of extrinsic muscle invasion that has in practice been very difficult to correlate with pathology has been removed from the T criteria. The three features above are part of the substantial changes to the HN section of AJCC8. The Pharynx chapter has been restructured into three chapters: Nasopharyngeal carcinoma, HPV-mediated/p16+ OPSCC, HPV-/p16- OPSCC with Hypopharynx. For the latter two chapters there are substantial changes to the nodal criteria so that there are now 3 separate clinical nodal criteria tables plus two distinct pathologic nodal criteria tables. The cervical nodal chapter added to the AJCC8 also gives guidance as to how to manage the unknown primary tumor. Most of these unknown primary tumors will ultimately be found to be HPV-mediated OPSCC. An important new criterion has been added to the nodal evaluation for HPV-/p16-/EBV- tumors, and this is the clinical designation of extranodal extension [ENEc]. Clinical examination features of skin invasion, infiltration of musculature, dense tethering or fixation or specific nerve invasion with dysfunction [brachial plexus, sympathetic trunk, cranial or phrenic nerve] are required for this designation, but it substantially

modifies the nodal designation to N3 disease. With the restructuring of the pharynx chapter into three plus a new chapter on Cutaneous SCC of the HN there are now 11 HN chapters. Thyroid tumor staging is now located in the Endocrine section of the Manual, and Head and Neck Sarcomas, an entirely new staging system and chapter, is found in the Soft Tissue Sarcomas section of the Manual. It is worth noting that the original published AJCC8 Manual has multiple errors and there are additional updates since publication. The AJCC website lists the errata in addition to having free downloadable staging forms that contain the updated staging tables.

## RC206-02 Monitoring Treatment Response to Chemoradiotherapy in Nasopharyngeal Carcinoma with MR Imaging Features: Value of Diffusion-Weighted Imaging

Monday, Nov. 26 8:55AM - 9:05AM Room: E450B

Participants

Xiangyi Liu, MS, Fuzhou, China (*Presenter*) Nothing to Disclose Yunbin Chen, MD, Fuzhou, China (*Abstract Co-Author*) Nothing to Disclose Dechun Zheng, MS, Fuzhou, China (*Abstract Co-Author*) Nothing to Disclose Ying N. Chen, PhD, Fuzhou, China (*Abstract Co-Author*) Nothing to Disclose

## For information about this presentation, contact:

liuxy8847@hotmail.com

#### PURPOSE

The purpose of this study was to evaluate the monitoring performance of treatment response to chemoradiotherapy (CRT) in Nasopharyngeal Carcinoma (NPC) with Diffusion-weighted imaging (DWI) combining T2-weighted MRI.

## METHOD AND MATERIALS

74 patients with stage III and IV NPC were enrolled and randomly assigned to two groups in this study. DWI sequences were identified and matched with T2-weighted images performed on pretreatment, 3 days, 20 days (group 1 only) /42days (group 2 only) after Neoadjuvant Chemotherapy (NAC) initiated and at the end of chemoradiotherapy initiation (radiotherapy terminated). The tumor size before and after 20/42 days after NAC initiated was measured and classified into responders and non-responders based on treatment response (RECIST 1.1). At the end of CRT, the tumors were regrouped into complete remission (CR) and residual disease. The apparent diffusion coefficient (ADC) values and their changes at each time point were compared between all different outcome groups using dependent-samples t test. The parameters with optimal time point to detect the tumor response to therapy were chosen. Receiver operating characteristics (ROC) analysis and logistic regression model were performed in order to evaluate the feasibility of the chosen parameters in monitoring treatment response.

## RESULTS

The ADCs, ADC changes ( $\Delta$ ADCs) and percentage ADC changes ( $\Delta$ %ADCs) of day 20 in responders were significantly higher than in non-responders (P<0.05) for group 1 (day20). At the end of CRT, responders from group 1 (day20) all achieved CR while responders from group 2 (day42) have two residual lesions. The  $\Delta$ ADCs and  $\Delta$ %ADCs of day 3 in patients with CR were significantly higher than in patients with residual tumor (P=0.007; P=0.005, respectively). When  $\Delta$ ADCs (day3) <=0.099×10-3mm2/s was used for threshold, the sensitivity was 79.6%, with specificity 73.7%. There was a negative correlation between the possibility of residual tumor and  $\Delta$ ADCs (day3) after CRT ( $\beta$ =-8.426, P=0.047).

#### CONCLUSION

DWI with ADCs allows for detecting early treatment response of NPC and provides the opportunity to adjust following CRT regimen. 20 days after NAC initiated might be the optimal time for monitoring NAC response. ADCs on 3 days after NAC initiated was a potential imaging predictor for CRT in NPC.

## **CLINICAL RELEVANCE/APPLICATION**

Accessing the curative effect of chemoradiotherapy in advanced NPC provides the opportunity to adjust following CRT regimen.

## RC206-03 Prognostic Predictive Value of the Primary Lesion Apparent Diffusion Coefficient in Locoregionally Advanced Nasopharyngeal Carcinoma Patients: A Retrospective Cohort Study

Monday, Nov. 26 9:05AM - 9:15AM Room: E450B

Participants

Tao X. Huang, Guangzhou, China (Presenter) Nothing to Disclose

For information about this presentation, contact:

huangtx@sysucc.org.cn

#### PURPOSE

To investigate the prognostic predictive value of the primary lesion apparent diffusion coefficient (PL-ADC) prior treatment in locoregionally advanced nasopharyngeal carcinoma (LA-NPC).

## METHOD AND MATERIALS

A cohort of 919 untreated LA-NPC patients from January 2011 to April 2014 were enrolled, All patients received 3-Tesla MRI examination prior treatment including diffusion weighted imaging(b values:0,1000 sec/ mm2) and the PL-ADC values were calculated. The prognostic value of PL-ADC in LA-NPC patients were analyzed using the Kaplan-Meier method and multivariate analysis.

## RESULTS

The cut-off value of PL-ADC prior treatment was 748.5  $\times$ 10-6 mm2/s(AUC=0.664, 95% CI 0.598-0.729)according to the local relapse. Then patients were divided into PL-ADC-high(>=748.5  $\times$ 10-6 mm2/s) group and PL-ADC-low group(<748.5  $\times$ 10-6 mm2/s). PL-ADC-high group had a significant poor 3-year local relapse-free survival (LRFS) (91.3% vs. 98.3%, P< 0.001) and 3-year

disease-free survival (DFS)(72.1% vs 84.0%, P< 0.001) rates than PL-ADC-low group. However, no significance was found in 3year distant metastasis-free survival(DMFS)and 3-year overall survival (OS) between groups.Results of multivariate analysis showed that high PL-ADC (>=748.5 ×10-6 mm2/s) is an independent risk factor for LRFS (HR 4.80, 95% CI 2.04-11.30, p= 0.0003) and DFS (HR 1.76, 95% CI 1.28-2.41, p= 0.0005) in LA-NPC.

#### CONCLUSION

The PL-ADC prior treatment is an independent prognostic factor for LRFS and DFS in LA-NPC patients, which might be used to select patients at high risk and administrate intense treatment.

#### **CLINICAL RELEVANCE/APPLICATION**

MRI is used for staging and evaluation and parameters obtained from fMR can potentially predict prognosis.

## RC206-04 Prognostic Value of Restaging 18-FDG PET/CT Volumetric Parameters for Post-Index Irradiation Recurrence of Head and Neck Squamous Cell Carcinoma

Monday, Nov. 26 9:15AM - 9:25AM Room: E450B

Participants Burkhan Musaiev, Kiev, Ukraine (*Presenter*) Nothing to Disclose Kateryna O. Musaieva, MD, Vinnitsa, Ukraine (*Abstract Co-Author*) Nothing to Disclose

#### For information about this presentation, contact:

burkhanmusaiev@gmail.com

#### PURPOSE

Statistical image features of tumor metabolism from pretreatment 18F-FDG-PET/CT scans were studied for their potential to predict clinical outcome of the recurrent squamous cell carcinoma of head and neck (HNSCC). The purpose of this study was to define the prognostic value of metabolic and volumetric parameters for recurrent HNSCC and the role of salvage re-irradiation in overall survival in this cohort.

#### **METHOD AND MATERIALS**

Pretreatment PET/CT scans and after treatment PET/CT scans of 69 patients who underwent salvage treatment for recurrent HNSCC, were retrospectively evaluated. Metabolic response was assessed using PET response criteria for solid tumors (PERCIST). Multiple statistical image features related to the standard uptake value (SUV) were computed: metabolic tumor volume, maximum SUV, mean SUV, total lesion glycolysis (TLG). The correlation between the image features and local control and overall survival was calculated.

#### RESULTS

In this study we reported on the utility of PET/CT in survival prognostication for recurrent head and neck cancer. Our analysis indicates that whole body metabolic tumour volume WB MTV has potency in estimating the overall survival. High WB MTV (over 21,5 cc) corresponds with poor prognosis and low one-year survival rate (56,0% of patients will not survive over 12 months); on the other hand, one-year survival at WB MTV < 21,5 cc is estimated as 93,2%. This observation remained robust even after accounting for other known prognostic factors including salvage re-irradiation and recurrence location.

#### CONCLUSION

With this study we established a pre-salvage volumetric cut-off point (whole body metabolic tumour volume WB MTV of 21,5 cc) that predicts one-year survival with high accuracy. A more extensive study is warranted to decide if this cut-off point is acceptable for subgroup of patients who will undergo a salvage re-irradiation.

#### **CLINICAL RELEVANCE/APPLICATION**

18-FDG PET/CT for post-index treatment follow-up is well integrated into the management of HNSCC and a restaging PET/CT is performed to decide the further management, thus, volumetric prognostic parameters can be acquired for each patient without additional expenses. Our experiences herein illustrate the prognostic significance of 18-FDG PET/CT scan in the salvage treatment setting.

## RC206-05 Diffusion Kurtosis Imaging for Characterizing Parotid Gland Tumors: A Preliminary Study

Monday, Nov. 26 9:25AM - 9:35AM Room: E450B

Participants Hao Hu, Nanjing, China (*Presenter*) Nothing to Disclose Wen Qian, Nanjing, China (*Abstract Co-Author*) Nothing to Disclose

#### PURPOSE

Diffusion kurtosis imaging (DKI) has been proven to be potential in diagnosing Sjögren's syndrome; however, no study has explored the usefulness of DKI in differentiating parotid gland tumors. To evaluate the potential of DKI in the characterization of parotid gland tumors.

#### METHOD AND MATERIALS

DKI was performed in 40 patients (33 benign and 7 malignant) with parotid gland tumors. DKI parameters including apparent diffusion coefficient (Dapp) and apparent kurtosis coefficient (Kapp) were obtained using DK model. Independent-samples t test, Steel-Dwass tests and receiver operating characteristic curve analyses were used for statistical analyses.

#### RESULTS

There were no significant differences in Dapp ( $1.283\pm0.443 \times 10-3 \text{ mm2/s vs } 0.937\pm0.250 \times 10-3 \text{ mm2/s}, P=0.055$ ) and Kapp ( $0.575\pm0.323 \text{ vs } 0.589\pm0.235, P=0.915$ ) between benign and malignant group. In the subgroup analyses, pleomorphic adenomas

showed higher Dapp (P=0.001) and lower Kapp (P=0.031) than malignant tumors. Dapp showed better discriminative value (area under curve, 0.889; cutoff value,  $1.319 \times 10-3 \text{ mm2/s}$ ; sensitivity, 77.78%; specificity, 100%). Pleomorphic adenomas also showed higher Dapp (P<0.001) and lower Kapp (P<0.001) than Warthin's tumors. Kapp showed better discriminative value (area under curve, 0.994; cutoff value, 0.663; sensitivity, 94.44%; specificity, 100%). Warthin's tumors demonstrated higher Kapp than malignant tumors (P=0.003), while no significant difference was found on Dapp (P=0.298). The area under curve, sensitivity and specificity of Kapp for discriminating Warthin's tumors from malignant tumors at an optimal threshold of 0.735 were 0.905, 88.89%, and 85.71%, respectively.

## CONCLUSION

DKI may be a promising imaging technique for characterizing parotid gland tumors.

## **CLINICAL RELEVANCE/APPLICATION**

To assist in differentiation of parotid gland tumors.

## RC206-06 Staging Nasopharyngeal Carcinoma

Monday, Nov. 26 9:35AM - 10:00AM Room: E450B

Participants Barton F. Branstetter IV, MD, Pittsburgh, PA (*Presenter*) Nothing to Disclose

## LEARNING OBJECTIVES

1) Define how radiology contributes to the TNM staging of nasopharyngeal carcinoma. 2) Elaborate differences in NPC staging between the 7th and 8th edition of AJCC Staging Manual.

#### ABSTRACT

The 8th edition of the American Joint Committee on Cancer Staging Manual became active in January of 2018. This lecture will delineate the staging scheme for nasopharyngela carcinoma, emphasizing differences between the 7th and 8th editions of the AJCC Manual.

## RC206-07 Staging Oropharyngeal Carcinoma

Monday, Nov. 26 10:05AM - 10:30AM Room: E450B

Participants

Lawrence E. Ginsberg, MD, Houston, TX (Presenter) Nothing to Disclose

#### For information about this presentation, contact:

lginsberg@mdanderson.org

### LEARNING OBJECTIVES

1) Stress the importance of staging in oropharyngeal cancer treatment and research. 2) Review the rationale for revising oropharyngeal cancer staging in the HPV era. 3) Discuss the new features AJCC8 with respect to staging oropharyngeal cancer, emphasizing the differences between HPV +ive and HPV -ive; how to stage if p16 status is unknown.

## RC206-08 The Radiologic Extranodal Extension (ENE) As Imaging Biomarker in Human Papillomavirus (HPV)-Related Oropharyngeal Squamous Cell Carcinoma (OPSCC)

Monday, Nov. 26 10:30AM - 10:40AM Room: E450B

Participants

Boeun Lee, MD, Seoul, Korea, Republic Of (*Presenter*) Nothing to Disclose Young Jun Choi, MD, Seoul, Korea, Republic Of (*Abstract Co-Author*) Nothing to Disclose Jung Hwan Baek, Seoul, Korea, Republic Of (*Abstract Co-Author*) Consultant, STARmed; Consultant, RF Medical Jeong Hyun Lee, MD, PhD, Seoul, Korea, Republic Of (*Abstract Co-Author*) Nothing to Disclose

#### PURPOSE

To determine whether radiologic extranodal extension (ENE) on pretreatment CT and MR could predict prognosis in patients with human papillomavirus (HPV)-related oropharyngeal squamous cell carcinoma (OPSCC).

## METHOD AND MATERIALS

The study population was obtained from a historical cohort who was diagnosed as HPV-related OPSCC between March 2007 and March 2016. We included patients who had metastatic lymph node on pretreatment CT or MR. We analyzed demographic and clinical variables and radiologic ENE. The primary outcome was chosen as progression-free survival (PFS) and secondary outcome was the diagnostic performance of CT of MRI for the diagnosis of ENE among the patients who underwent neck dissection for lymph node. The Cox proportional hazard model identified predictors of PFS.

## RESULTS

A total of 134 patients were included with a mean follow-up of 38 months, among whom 70 patients (52.2%) were ENE-positive. In univariate analysis, the presence of ENE, N-stage, T-stage, overall stage showed statistically significant association with worse PFS. In multivariate analysis, the presence of radiologic ENE was not significantly associated with PFS (P=0.141, hazard ratio [HR], 2.68; 95% CI, 0.72-9.97). The Kaplan-Meier disease-free survival curves showed that PFS was significantly lower in patients with radiologic ENE-positive disease, with a 3-year PFS of 95.3% versus 83.7%, respectively (log-rank P=.023)

#### CONCLUSION

Radiologic ENE in patients with HPV-related OPSCC tend to associate with PFS, but it did not reach statistical significance in our study. Large scale study are needed to determine whether radiologic ENE may be a useful for risk-stratifying patients with HPV-

related OPSCC.

### **CLINICAL RELEVANCE/APPLICATION**

Radiologic ENE in patients with HPV-related OPSCC may serve as an imaging biomarker to tailor individual treatment regimens.

# RC206-09 Detection of Loco-regional Recurrence in Malignant Head and Neck Tumors: A Comparison of CT, MRI, and FDG PET-CT

Monday, Nov. 26 10:40AM - 10:50AM Room: E450B

Participants

Hyungjin Lee, Seoul, Korea, Republic Of (*Presenter*) Nothing to Disclose Eun Soo Kim, Anyang, Korea, Republic Of (*Abstract Co-Author*) Nothing to Disclose Dae Young Yoon, MD, Kangdong-Gu, Korea, Republic Of (*Abstract Co-Author*) Nothing to Disclose You Mie Han, Seoul, Korea, Republic Of (*Abstract Co-Author*) Nothing to Disclose Young Lan Seo, Kangdong-Gu, Korea, Republic Of (*Abstract Co-Author*) Nothing to Disclose Eun Joo Yun, Seoul, Korea, Republic Of (*Abstract Co-Author*) Nothing to Disclose

For information about this presentation, contact:

windbbb@naver.com

# PURPOSE

To compare the diagnostic accuracy of contrast-enhanced computed tomography (CT), contrast-enhanced magnetic resonance imaging (MRI), and fluorodeoxyglucose (FDG) positron emission tomography (PET)-CT, alone and in combination, in detecting the loco-regional recurrence of malignant head and neck tumor.

# METHOD AND MATERIALS

A total of 93 patients with loco-regional recurrence of malignant head and neck tumors underwent CT, MRI, and PET-CT within 30 days before surgery. CT, MRI, and PET-CT for each patient were retrospectively reviewed to determine the presence of recurrent tumors in the primary site on a patient-by-patient basis and that of regional lymph nodes on a level-by-level basis. The diagnostic accuracy of CT, MRI, and PET-CT, alone and combined, were accessed with the postoperative histopathological findings or with 12-months follow-up results as the standard of reference.

### RESULTS

The sensitivity/specificity/accuracy of CT, MRI, and PET-CT for the detection of primary site recurrence was 89.9%/85.7%/89.3%, 94.9%/85.7%/93.6%, and 97.5%/92.9%/96.8%, respectively. The sensitivity/specificity/accuracy of CT, MRI, and PET-CT for the detection of nodal recurrence was 66.3%/99.4%/92.4%, 74.7%/99.4%/94.2%, and 85.5%/94.9%/93.0%, respectively. MRI plus PET-CT achieved the best performance in the receiver operating characteristics curve analysis (Az value=0.958 for primary site recurrence and 0.929 for nodal recurrence)

### CONCLUSION

MRI plus PET-CT offered the highest diagnostic performance in the detection of loco-regional recurrence of malignant head and neck tumor, compared with CT, MRI, PET-CT, and other combinations including CT.

# **CLINICAL RELEVANCE/APPLICATION**

Detecting the loco-regional recurrence of malignant head and neck tumors has important clinical applications because salvage protocols are available.

### RC206-10 Staging Oral Cavity Carcinoma

Monday, Nov. 26 10:50AM - 11:15AM Room: E450B

Participants Kristine M. Mosier, DMD, PhD, Indianapolis, IN (*Presenter*) Nothing to Disclose

# LEARNING OBJECTIVES

1) Know the critical elements for staging oral cavity carcinoma with the 8th Edition of the AJCC. 2) Know the differences in staging between the 7th and 8th Editions, why the changes were made, and the impact on management. 3) Know the differences between tumor thickness and depth of invasion.

# RC206-11 MRI-based Texture Features Serve as the Risk Factors of Cervical Lymph Node Metastases in Early Stage Oral Tongue Cancer

Monday, Nov. 26 11:15AM - 11:25AM Room: E450B

Participants Ying Yuan, shanghai, China (*Presenter*) Nothing to Disclose

Jiliang Ren, Shanghai, China (*Abstract Co-Author*) Nothing to Disclose Yiqian Shi, Shanghai, China (*Abstract Co-Author*) Nothing to Disclose Xiaofeng Tao, Shanghai, China (*Abstract Co-Author*) Nothing to Disclose

For information about this presentation, contact:

yuany83@163.com

### PURPOSE

Lymph node metastases are one of the most important prognostic factor of oral tongue squamous cell carcinoma (OTSCC). However, lymph node metastases are often occult without preoperative signs. It is controversial either to perform elective neck dissection for all early stage (cT1-T2N0) OTSCC patients, because of the disparity in pathologic and clinical lymph node staging in OTSCC. The aim of the study was to assess MRI texture based quantitative imaging biomarkers in the discrimination of cervical lymph node metastases in early OTSCC.

## METHOD AND MATERIALS

This retrospective study enrolled 49 cases of early stage (cT1-T2N0) OTSCC patients. Fifty-three textural parameters were extracted respectively from preoperative T2WI and CE-T1WI, based on histogram, gray-level co-occurrence matrices (GLCM), and gray-level run length matrices (GLRLM). Least absolute shrinkage and selection operator (LASSO) regression model was used for data dimension reduction and feature selection. The receiver operating characteristic (ROC) analyses were conducted to evaluate the ability of each texture model.

## RESULTS

The texture models, which consisted of 5 selected features from T2WI and/or 4 selected features from CE-T1WI, were significantly associated with pathological lymph node metastases, independent of clinical risk factors (P<0.001). The areas under the curve (AUCs) of the T2WI and CE-T1WI based models were 0.84 and 0.747, respectively. The texture model combining T2WI and CE-T1WI showed the best discriminative ability, with AUC value of 0.923. The corresponding accuracy was 89.8%, sensitivity was 90.5% and specificity was 89.3%.

### CONCLUSION

MRI-based texture features could help to preoperatively predict early stage OTSCC with pathological lymph node metastasis. Combined use of features derived from T2WI and CE-T1WI showed the best discriminative power.

# **CLINICAL RELEVANCE/APPLICATION**

It is controversial either to perform elective neck dissection for all early stageOTSCC patients, because of the disparity in pathologic and clinical lymph node staging in OTSCC. Our study provided a new approach for accurate preoperative discrimination of cervical lymph node metastases in early OTSCC, which would be beneficial for clinical treatment selection.

# RC206-12 Discrimination of Human Papillomavirus Status Using CT Texture Analysis in Oral Cavity and Oropharyngeal Squamous Cell Carcinomas

Monday, Nov. 26 11:25AM - 11:35AM Room: E450B

Participants

Miran Han, MD, Suwon, Korea, Republic Of (*Presenter*) Nothing to Disclose Ji Young Lee, MD, Seoul, Korea, Republic Of (*Abstract Co-Author*) Nothing to Disclose Jin Wook Choi, MD, Suwon, Korea, Republic Of (*Abstract Co-Author*) Nothing to Disclose Eun Ju Ha, Suwon, Korea, Republic Of (*Abstract Co-Author*) Nothing to Disclose Taehee Kim, MD, PhD, Suwon, Korea, Republic Of (*Abstract Co-Author*) Nothing to Disclose

For information about this presentation, contact:

miranhanajou@gmail.com

# PURPOSE

To evaluate diagnostic performance of texture analysis for distinguishing HPV-status in oral cavity and oropharyngeal squamous cell carcinoma (OC-OPSCC), separately in primary tumor and metastatic lymph nodes.

# METHOD AND MATERIALS

119 patients with primary tumor and 80 patients with metastatic lymph nodes who have known HPV status and underwent pretreatment contrast-enhanced CT scan were included in the study as discovery population. The CT texture analysis was performed using commercial TexRAD software. The conventional imaging features of primary tumor and metastatic lymph node were also evaluated. Differences between HPV-positive and HPV-negative groups were analyzed using  $\chi^2$  test and independent t-test. For heterogeneity parameters, ROC curve analysis was performed for discrimination of HPV status. Intraclass correlation coefficients (ICC) were estimated to assess intra- and inter-reader measurement reliability. Diagnostic accuracy of texture analysis for HPV status were additionally evaluated in the separated validation-population that comprised of 18 patients obtained from outside hospital.

### RESULTS

The HPV-positivity was 37.0% for the primary tumors and 46.3% for metastatic lymph nodes. HPV-positive groups demonstrated more frequently well-defined border of primary tumor (p<0.001) and cystic nodal metastasis (p=0.015). HPV-negative patients showed extracapsular modal spread more often (p=0.022). Entropy with medium filter (SSF 5) was the best discriminator between HPV-positive and HPV-negative primary tumors (AUC=0.852) and standard deviation (SD) without filter for metastatic lymph nodes (AUC=0.801). Diagnostic accuracy of entropy for primary tumor is 80.6% in discovery and 88.9% in validation group. In case of metastatic lymph nodes, accuracy of SD is 76.3% in discovery and 77.7% in validation groups. Intra and inter-reader measurement reliability for entropy and SD are almost perfect (ICC,  $0.81\sim0.96$ ).

### CONCLUSION

We found significant differences in heterogeneity parameters from texture analysis on pretreatment contrast-enhanced CT, according to HPV status in OC-OPSCC. CT texture analysis can be additional tool for diagnosis of HPV status.

## **CLINICAL RELEVANCE/APPLICATION**

CT texture analysis have possibility of diagnostic tool for discrimination of human papillomavirus status in oral cavity and oropharyngeal squamous cell carcinoma.

# RC206-13 Staging Laryngeal and Hypopharyngeal Carcinoma

Monday, Nov. 26 11:35AM - 12:00PM Room: E450B

Participants Peter M. Som, MD, New York, NY (*Presenter*) Nothing to Disclose

# For information about this presentation, contact:

peter.som@mounjtsinai.org

# LEARNING OBJECTIVES

1) To understand the anatomy of the larynx and hypopharynx and the new Eighth Edition of the AJCC staging for larynx and the hypopharynx as well as the staging of the cervical lymph nodes.



# A Case-based Audience Participation Session (Genitourinary) (Interactive Session)

Monday, Nov. 26 8:30AM - 10:00AM Room: N227B

# GU

AMA PRA Category 1 Credits ™: 1.50 ARRT Category A+ Credit: 1.75

## Participants

Peter S. Liu, MD, Solon, OH (*Moderator*) Nothing to Disclose Peter S. Liu, MD, Solon, OH (*Presenter*) Nothing to Disclose Katherine E. Maturen, MD, Ann Arbor, MI (*Presenter*) Royalties, Reed Elsevier; Royalties, Wolters Kluwer nv; Consultant, Allena Pharmaceuticals, Inc; Tristan Barrett, MBBS, Cambridge, United Kingdom (*Presenter*) Nothing to Disclose

# For information about this presentation, contact:

kmaturen@umich.edu

liup3@ccf.org

# LEARNING OBJECTIVES

1) To be introduced to a series of Genitourinary case studies via an interactive team game approach designed to encourage 'active' consumption of educational content. 2) To be able to use their mobile wireless device (tablet, phone, laptop) to electronically respond to various Genitourinary case challenges; participants will be able to monitor their individual and team performance in real time. 3) To receive a personalized self-assessment report via email that will review the case material presented during the session along with individual and team performance.

### ABSTRACT

The extremely popular audience participation educational experience is back! GU Diagnosis Live is an expert-moderated session featuring a series of interactive Genitourinary case studies that will challenge radiologists' diagnostic skills and knowledge. Building on last year's successful Diagnosis Live premiere, GU Diagnosis Live is a lively, fast-paced game format: participants will be automatically assigned to teams who will then use their personal mobile devices to test their knowledge of GU radiology in a fast-paced session that will be both educational and entertaining. After the session, attendees will receive a personalized self-assessment report via email that will review the case material presented durinig the session, along with individual and team performance.

### **GENERAL INFORMATION**

This interactive session will use RSNA Diagnosis Live<sup>™</sup>. Please bring your charged mobile wireless device (phone, tablet or laptop) to participate.

### **Honored Educators**

Presenters or authors on this event have been recognized as RSNA Honored Educators for participating in multiple qualifying educational activities. Honored Educators are invested in furthering the profession of radiology by delivering high-quality educational content in their field of study. Learn how you can become an honored educator by visiting the website at: https://www.rsna.org/Honored-Educator-Award/ Katherine E. Maturen, MD - 2014 Honored Educator



# Emergency Neuroradiology: Imaging of Infection (Interactive Session)

Monday, Nov. 26 8:30AM - 10:00AM Room: E451A



AMA PRA Category 1 Credits ™: 1.50 ARRT Category A+ Credit: 1.75

### Participants

A. Orlando Ortiz, MD, MBA, Mineola, NY (Moderator) Nothing to Disclose

# LEARNING OBJECTIVES

1) To diagnose head and neck infection on CT. 2) To characterize the nature of the infection. 3) To localize the infection and its spread. 4) To appreciate the potential complications that may result from the infection. 5) To recognize underlying abnormalities that may predispose to head and neck infection. 6) Examine the imaging features of infective conditions of the brain and meninges. 7) Identify the varied CT findings in brain infections as they present in the Emergency Department, and assess the role of MRI in further diagnostic characterization and management. 8) Review the epidemiology of spine infection. 9) Focus on making the diagnosis of infectious spondylitis utilizing: clinical findings, imaging findings, biopsy. 10) Distinguish infectious spondylitis from other radiographic mimics.

### Sub-Events

# RC208A Head and Neck Infection

Participants

Wayne S. Kubal, MD, Tucson, AZ (Presenter) Author, Reed Elsevier; Editor, Reed Elsevier

# LEARNING OBJECTIVES

1) To diagnose head and neck infection on CT. 2) To characterize the nature of the infection. 3) To localize the infection and its spread. 4) To appreciate the potential complications that may result from the infection. 5) To recognize underlying abnormalities that may predispose to head and neck infection.

# RC208B Brain Infection

Participants Diego B. Nunez Jr, MD, MPH, Boston, MA (*Presenter*) Nothing to Disclose

# For information about this presentation, contact:

dnunez@bwh.harvard.edu

# LEARNING OBJECTIVES

1) Examine the imaging features of infective conditions of the brain and meninges. 2) Identify the varied CT findings in brain infections as they present in the Emergency Department, and assess the role of MRI in further diagnostic characterization and management.

# RC208C Spine Infection

Participants

A. Orlando Ortiz, MD, MBA, Mineola, NY (Presenter) Nothing to Disclose

### LEARNING OBJECTIVES

1) Review the epidemiology of spine infection. 2) Focus on making the diagnosis of infectious spondylitis utilizing: clinical findings, imaging findings, biopsy. 3) Distinguish infectious spondylitis from other radiographic mimics.



### **Gastrointestinal Series: Pancreas Imaging**

Monday, Nov. 26 8:30AM - 12:00PM Room: E353C



AMA PRA Category 1 Credits ™: 3.00 ARRT Category A+ Credits: 3.75

**FDA** Discussions may include off-label uses.

### Participants

Eric P. Tamm, MD, Houston, TX (*Moderator*) Institutional Research Grant, General Electric Company Desiree E. Morgan, MD, Birmingham, AL (*Moderator*) Institutional Research Grant, General Electric Company Bhavik N. Patel, MD, MBA, Stanford, CA (*Moderator*) Nothing to Disclose Koenraad J. Mortele, MD, Boston, MA (*Moderator*) Nothing to Disclose So Yeon Kim, MD, Seoul, Korea, Republic Of (*Moderator*) Nothing to Disclose

### For information about this presentation, contact:

dmorgan@uabmc.edu

Sub-Events

## RC209-01 Pancreatic Cancer Staging Update

Monday, Nov. 26 8:30AM - 8:50AM Room: E353C

Participants

Eric P. Tamm, MD, Houston, TX (Presenter) Institutional Research Grant, General Electric Company

### LEARNING OBJECTIVES

1. To understand changes that have occurred recently in the AJCC staging system. 2. To understand the purpose of AJCC staging currently for pancreatic cancer (prognosis versus management). 3. To understand the categorization of cancer as resectable/borderline resectable/clearly unresectable. 4. To understand how to use the above information to guide effective radiology reporting.

## LEARNING OBJECTIVES

1) Understand recent changes in the staging of pancreatic cancer. 2) Understand the differences between societies in the categorization of borderline resectable pancreatic cancer. 3) Apply the above understanding of staging and categorizing pancreatic cancer to improve the clarity and utility of radiology reports for the staging of pancreatic cancer and to aid clinical management.

# RC209-02 Implementation of NCCN Guideline for Assessment of Resectability of Pancreatic Adenocarcinoma: Software Development and Validation

Monday, Nov. 26 8:50AM - 9:00AM Room: E353C

Participants Ying Li, MD, Boston, MA (*Presenter*) Nothing to Disclose Wenli Cai, PhD, Boston, MA (*Abstract Co-Author*) Stockholder, IQ Medical Imaging LLC Sun Ying-Shi, MD, PhD, Beijing, China (*Abstract Co-Author*) Nothing to Disclose

For information about this presentation, contact:

xiaoli2400@126.com

### PURPOSE

The purpose of this study is to develop and evaluate a CAA software to assess the resectability of pancreatic adenocarcinoma by using NCCN guideline and to generate a structured report by using SAR and APA structured reporting template in imaging evaluation of pancreatic adenocarcinoma.

## **METHOD AND MATERIALS**

The CAA software of resectability of pancreatic adenocarcinoma was designed in terms of NCCN guidelines, which consists of three procedures: tumor characterization evaluations, resectability assessment and structured reporting. Forty-five patients with pathologically proven pancreatic adenocarcinoma who underwent CT examination between January 2015 and June 2016 were retrospectively collected to validate the software. Four independent readers (radiologists) assessed the resectability status of pancreatic adenocarcinoma without using (subjective evaluation) and with using the software (CAA evaluation), respectively. The agreements between subjective evaluation and CAA evaluation of four readers were tested by using Cohen's kappa coefficient. The agreement for four subjective evaluations and that for four CAA evaluations were tested with McNemar test and intra-class correlation coefficients (ICCs) were calculated.

The ICC among four subjective evaluations was 0.569 (95% confidence interval (CI):  $0.426 \sim 0.704$ , P < 0.01), moderate agreement, whereas the ICC among four CAA evaluations was 0.687 (95% CI:  $0.565 \sim 0.794$ , P < 0.01), substantial agreement. For the subgroup of 26 patients after excluding 19 unanimous unresectable cases, the ICC among four subjective evaluations was -0.074 (95% CI,  $-0.181 \sim 0.109$ , P = 0.811), indicating no agreement, whereas the ICC among four CAA evaluations was 0.355 (95% CI,  $0.159 \sim 0.579$ , P<0.001), indicating fair to moderate agreement. The inter-observer agreement was statistically significantly improved with the CAA software.

# CONCLUSION

The use of CAA software resulted in a significant improvement in inter-observer agreements of resectability assessment of pancreatic adenocarcinoma among clinicians, and has the potentials to improve the standardization for managing pancreatic adenocarcinoma patients in clinical practice.

# **CLINICAL RELEVANCE/APPLICATION**

The use of CAA software has the potentials to improve the standardization for managing pancreatic adenocarcinoma patients in clinical practice.

# RC209-03 Quantitative Assessment of Tumor Blood Flow with Volume Perfusion CT: A New Imaging Biomarker for Predicting Prognosis in Patients with Pancreatic Cancer after Chemoradiotherapy

Monday, Nov. 26 9:00AM - 9:10AM Room: E353C

Participants

Yutaka Toyomasu, MD, Mie, Japan (*Presenter*) Nothing to Disclose Yasutaka Ichikawa, MD, Tsu, Japan (*Abstract Co-Author*) Nothing to Disclose Motonori Nagata, MD, PhD, Tsu, Japan (*Abstract Co-Author*) Nothing to Disclose Ahmed H. Heussein, MD,MSc, Tsu, Japan (*Abstract Co-Author*) Nothing to Disclose Yoshihito Nomoto, Tsu, Japan (*Abstract Co-Author*) Nothing to Disclose Hajime Sakuma, MD, Tsu, Japan (*Abstract Co-Author*) Nothing to Disclose Hajime Sakuma, MD, Tsu, Japan (*Abstract Co-Author*) Research Grant, Fuji Pharma Co, Ltd; Research Grant, DAIICHI SANKYO Group; Research Grant, FUJIFILM Holdings Corporation; Research Grant, Siemens AG; Research Grant, Nihon Medi-Physics Co, Ltd; Speakers Bureau, Bayer AG Naoki Nagasawa, RT, PhD, Tsu, Japan (*Abstract Co-Author*) Nothing to Disclose Kakuya Kitagawa, MD, PhD, Tsu, Japan (*Abstract Co-Author*) Nothing to Disclose Akinori Takada, MD, Tsu, Japan (*Abstract Co-Author*) Nothing to Disclose Akio Yamazaki, RT, Tsu, Japan (*Abstract Co-Author*) Nothing to Disclose Masayuki Naito, Mie, Japan (*Abstract Co-Author*) Nothing to Disclose Tomoko Kawamura, Mie, Japan (*Abstract Co-Author*) Nothing to Disclose

### PURPOSE

Volume perfusion CT (VPCT) is a new technique that can provide three-dimensional perfusion quantification for the entire pancreas. The aims of this study were to establish a VPCT protocol with a total radiation dose approximately equal to conventional dynamic CT, and to determine the value of quantifying pretreatment perfusion parameters in predicting prognosis of the patients with pancreatic cancer who were scheduled for chemoradiotherapy (CRT).

# METHOD AND MATERIALS

Consecutive 37 patients with biopsy-proven newly diagnosed pancreatic adenocarcinoma who were scheduled for CRT were prospectively recruited. VPCT was performed on a dual-source CT scanner (SOMATOM Force). The CT acquisition parameters included Z-axis coverage of 22.4cm, tube voltage of 80kv, dynamic acquisitions of 40, and acquisition duration of 60s. Blood flow (BF), blood volume (BV), and mean transit time (MTT) in pancreatic cancer were quantified from VPCT images. Univariate and multivariate analyses were performed to evaluate the prognostic value of BF, BV and MTT by VPCT, as well as CA19-9, age, sex, primary tumor site, tumor diameter and surgical indication for the prediction of progression-free survival (PFS) and overall survival (OS).

# RESULTS

The mean dose-length product and estimated effective dose of VPCT was  $619\pm145 \text{ mGy}^{*}\text{cm}$  and  $9.3\pm2.2 \text{ mSv}$ , respectively. Twenty-two (59%) of 37 patients experienced disease recurrence (n=18) or death (n=11) during the median observation period of 14 months. In univariate analysis, BF (<48.4 vs >=48.4 mL/100mL/min) and BV (<4.32 vs >=4.32 mL/100mL) were significant prognostic factors for both PFS (BF, p=0.013; BV, p=0.017) and OS (BF, p=0.007; BV, p=0.045), while MTT was not a significant predictor for PFS (p=0.116) or OS (p=0.236). In multivariate analysis, BF (<48.4 vs >=48.4 mL/100mL/min) was an independent prognostic factor for PFS (Hazard ratio (95% CI), 2.772 (1.154-6.660); p=0.023) and OS (Hazard ratio (95% CI), 6.198 (1.333-28.810); p=0.02).

### CONCLUSION

VPCT allows for perfusion quantification for the entire pancreas with radiation dose approximately equal to conventional dynamic CT. The pretreatment tumor blood flow derived from the VPCT is an independent prognostic factor for patients with pancreatic cancer after CRT.

# **CLINICAL RELEVANCE/APPLICATION**

Tumor blood flow quantified by VPCT is a novel imaging biomarker that permits prediction of the prognosis in patients with newly diagnosed pancreatic cancer who are scheduled for CRT.

# RC209-04 The Prognostic Utility of Differential Enhancement Patterns Measured on Dual Energy CT in Patients with Pancreatic Ductal Adenocarcinoma

Monday, Nov. 26 9:10AM - 9:20AM Room: E353C

Participants Ahmed M. Amer, MD, Birmingham, AL (*Presenter*) Nothing to Disclose Yufeng Li, PhD, Birmingham, AL (*Abstract Co-Author*) Nothing to Disclose David S. Summerlin, MD, Gardendale, AL (*Abstract Co-Author*) Nothing to Disclose Constantine M. Burgan, MD, Pittsburgh, PA (*Abstract Co-Author*) Nothing to Disclose Andrew D. Smith, MD,PhD, Birmingham, AL (*Abstract Co-Author*) President and Owner, Radiostics LLC; President and Owner, eRadioMetrics LLC; President and Owner, Liver Nodularity LLC; President and Owner, Color Enhanced Detection LLC; Patent holder Michelle M. McNamara, MD, Birmingham, AL (*Abstract Co-Author*) Nothing to Disclose Desiree E. Morgan, MD, Birmingham, AL (*Abstract Co-Author*) Institutional Research Grant, General Electric Company

# For information about this presentation, contact:

amamer@uabmc.edu

# PURPOSE

To investigate the prognostic value of baseline DECT imaging biomarkers in patients with pancreatic ductal adenocarcinoma (PDAC).

## **METHOD AND MATERIALS**

Retrospective IRB-approved HIPAA-compliant study of 158 consecutive adult patients (79M/79F, mean age 68) with pathologically proven treatment naïve PDAC who had multiphasic pancreas DECT obtained 12/20/12 through 3/9/17. Regions of interest (ROIs) in tumor core, tumor border, pancreas border, and normal pancreas were recorded on both 52 keV and Iodine images. The Delta across the tumor-normal pancreas interface was calculated. Clinical outcomes included overall survival (OS), distant metastases-free survival (DMFS), and tumor grade/lymphovascular invasion on surgical pathology. Quantitative DECT metrics were associated with clinical outcomes using Cox regression, Pearson correlation, and ROC analysis.

## RESULTS

93 patients with advanced stage (50 locally advanced, 43 metastatic) and 65 with lower stage (48 resectable, 17 borderline). Low peripheral tumor enhancement on Iodine images was associated with shorter OS in lower stage (7.6 vs 19.7 months) (HR=5.89; 95%CI 1.89 to 15.44; P=0.003) and in advanced stage patients (6.8 vs 12.4 months) (HR=2.04; 95%CI 1.09 to 3.58; P=0.027). High Delta tumors on 52 keV were associated with shorter OS in advanced stage compared to Low Delta tumors (10.8 vs 12.9 months) (HR, 1.71; 95%CI 1.07 to 2.74; P=.024). High Delta tumors were associated with shorter DMFS on 52 keV (HR=2.6; 95%CI 1.16 to 5.72; P=0.02) and Iodine images (HR=2.34; 95%CI 1.02 to 5.12; P=0.04). In multivariate analysis adjusting for age, sex, tumor size, and surgery status, High Delta on 52 keV images was associated with shorter DMFS (HR=2.39; 95%CI 1.006 to 5.58; P=0.04). Tumor core enhancement was lower in metastatic population on both 52 keV (P=0.01) and Iodine images (P=0.008) compared to nonmetastatic patients. The Delta across the tumor-normal pancreas interface on 52 keV was associated with lymphovascular invasion (P= 0.04) and associated with tumor grade on Iodine images (P=0.04).

# CONCLUSION

Quantitative DECT metrics in treatment naïve PDAC patients are prognostic of OS and other important clinical outcomes.

### **CLINICAL RELEVANCE/APPLICATION**

DECT-based stratification of patients with PDAC can be accomplished using 52 keV and Iodine images, and can provide prognostic information on survival.

# RC209-05 Factors Affecting Reproducibility of Radiomic Features in Pancreatic Parenchyma and Pancreatic Ductal Adenocarcinoma on Contrast-enhanced CT Imaging

Monday, Nov. 26 9:20AM - 9:30AM Room: E353C

### Participants

Rikiya Yamashita, MD,PhD, New York, NY (*Presenter*) Nothing to Disclose Thomas Perrin, New York, NY (*Abstract Co-Author*) Nothing to Disclose Jayasree Chakraborty, New York, NY (*Abstract Co-Author*) Nothing to Disclose Joanne F. Chou, New York, NY (*Abstract Co-Author*) Nothing to Disclose Natally Horvat, MD, Sao Paulo, Brazil (*Abstract Co-Author*) Nothing to Disclose Maura A. Koszalka, New York, NY (*Abstract Co-Author*) Nothing to Disclose Abhishek Midya, New York, NY (*Abstract Co-Author*) Nothing to Disclose Mithat Gonen, PhD, New York, NY (*Abstract Co-Author*) Nothing to Disclose Peter J. Allen, MD, New York, NY (*Abstract Co-Author*) Nothing to Disclose William Jarnagin, New York, NY (*Abstract Co-Author*) Nothing to Disclose Amber Simpson, New York, NY (*Abstract Co-Author*) Nothing to Disclose Richard Kinh Gian Do, MD, PhD, New York, NY (*Abstract Co-Author*) Consultant, Bayer AG

### For information about this presentation, contact:

rickdom2610@gmail.com

### PURPOSE

To explore the reproducibility of radiomic features in pancreatic parenchyma and pancreatic ductal adenocarcinomas (PDAC) in patients who underwent consecutive contrast-enhanced CT (CECT) scans.

# METHOD AND MATERIALS

In this IRB-approved and HIPAA-compliant retrospective study, consecutive patients with pancreatic tumors who underwent two CECT with variable imaging protocols within two weeks were included. In each patient, pancreas parenchyma and/or PDAC were manually segmented by two radiologists independently using a commercial software. 266 radiomic features, which consist of 12 shape and 254 texture features, were extracted using Matlab. The concordance correlation coefficient (CCC) of each feature was calculated to assess the feature reproducibility for 3 different scenarios, 1) two radiologists performing segmentations on the same CECT, 2) each radiologist performing segmentations on paired CECTs, and 3) one radiologist' segmentation on one CECT, with the other radiologist's segmentation on the paired CECT.

### RESULTS

The study cohort included 37 unique patients for the analyses of pancreas parenchyma and 18 patients with PDAC. Paired CECT scans had different protocols with ranges of slice thickness from 2.5 to 5 mm and contrast injection rates from 1-4 cc/s. For pancreas parenchyma, 47/266 (17.7%) and 48/266 (18.1%) features showed CCC>0.90 for scenario 1, 14/266 (5.3%) and 15/266 (5.6%) features showed CCC>0.90 for scenario 2, and 13/266 (4.9%) and 10/266 (3.8%) features showed CCC>0.90 for scenario 3. For PDAC, 11/266 (4.1%) and 17/266 (6.3%), 1/266 (0.4%) and 5/266 (1.9%), and no features showed CCC>0.90 for scenarios 1, 2, and 3, respectively.

# CONCLUSION

A greater number of radiomic features with high CCC were found for pancreas parenchyma than for PDAC. Reproducibility of radiomic feature may be affected by differences in CECT scanning parameters to a greater degree than radiologist segmentation.

# **CLINICAL RELEVANCE/APPLICATION**

Reproducibility of radiomic features for pancreas parenchyma and PDAC is affected by radiologist segmentation and variability of CECT scanning parameters and requires further prospective investigation.

# RC209-06 Autoimmune Pancreatitis Update

Monday, Nov. 26 9:30AM - 9:50AM Room: E353C

### Participants

So Yeon Kim, MD, Seoul, Korea, Republic Of (Presenter) Nothing to Disclose

### For information about this presentation, contact:

sykimrad@amc.seoul.kr

### LEARNING OBJECTIVES

1) Understand the recent evolution of the concepts and diagnostic criteria for autoimmune pancreatitis. 2) Recognize typical and atypical manifestation of autoimmune pancreatitis. 3) Provide an imaging approach for differentiating autoimmune pancreatitis from its mimickers.

# ABSTRACT

Autoimmune pancreatitis (AIP) is a distinct form of chronic pancreatitis that shows evidence of possible involvement of autoimmune mechanisms such as increased serum levels of IgG or IgG4, or presence of autoantibodies, and effective response to steroid therapy. For the past decade, many different criteria for AIP have been proposed, including the Japanese Pancreas Society (2002, 2006, 2010), the Korean criteria (2007), the HISORt criteria by the Mayo clinic (2006, 2009), the Asian Consensus criteria (2008), and the most recent International Consensus Diagnostic Criteria (2010). As AIP is becoming increasingly recognized as a worldwide entity, it was found that AIP should be divided into two subtypes according to histologic patterns: 1) lymphoplasmacytic sclerosing pancreatitis (LPSP) or AIP without granulocyte epithelial lesions (GELs); 2) idiopathoic duct-centric pancreatitis (IDCP) or AIP with GELs. Furthermore, the two groups of AIP differ in their clinical presentation and outcome. Pancreatic imaging is one of the most important diagnostic criteria in the guidelines. As AIP and its extrapancreatic manifestation have diverse imaging findings, they can mimic other diseases such as pancreatic cancer or lymphoma. Parenchymal involvement of AIP can be diffuse or focal. The diffuse type is more commonly seen than the focal lesion. The diffuse type is seen as diffuse enlargement of the pancreatic parenchyma (i.e., a sausage-like appearance); the absence of normal pancreatic clefts (i.e., featherless); and minimal peripancreatic infiltration. A capsule-like peripancreatic rim appears to be a highly specific finding of AIP. The focal type manifests as an focal enlargement of the pancreas or formation of a mass. The presence of long or multifocal stricture of the pancreatic duct without marked upstream dilatation is frequently noted. Narrowing of the intrapancreatic bile ducts has been observed in up to 90% of AIP patients, corresponding to the finding that the majority of these patients presented with obstructive jaundice. The presence of extrapancreatic organ involvement can be a supportive feature in the diagnosis of type 1 AIP.

# RC209-07 CT Texture Analysis in Differentiating Pancreatic Ductal Adenocarcinoma from Autoimmune Pancreatitis

Monday, Nov. 26 9:50AM - 10:00AM Room: E353C

### Participants

Satomi Kawamoto, MD, Laurel, MD (*Presenter*) Nothing to Disclose Seyoun Park, Baltimore, MD (*Abstract Co-Author*) Nothing to Disclose Linda C. Chu, MD, Baltimore, MD (*Abstract Co-Author*) Nothing to Disclose Shahab Shayesteh, MD, Baltimore, MD (*Abstract Co-Author*) Nothing to Disclose Daniel Fadaei Fouladi, MD, Baltimore, MD (*Abstract Co-Author*) Nothing to Disclose Karen M. Horton, MD, Baltimore, MD (*Abstract Co-Author*) Nothing to Disclose Alan Yuille, Baltimore, MD (*Abstract Co-Author*) Nothing to Disclose Ralph H. Hruban, Baltimore, MD (*Abstract Co-Author*) Board Member, miDiagnostics; Elliot K. Fishman, MD, Baltimore, MD (*Abstract Co-Author*) Institutional Grant support, Siemens AG; Institutional Grant support, General Electric Company; Co-founder, HipGraphics, Inc

### For information about this presentation, contact:

### skawamo1@jhmi.edu

### PURPOSE

Autoimmune pancreatitis (AIP) shares overlapping clinical and imaging features with pancreatic ductal adenocarcinoma (PDAC). Importantly, treatment of the two conditions is different. The purpose of this study is to determine if CT texture feature of AIP and PDAC provide possibility of distinguishing these two conditions.

### **METHOD AND MATERIALS**

As an IRB-approved matched case-control study, 32 patients with AIP (male=25, female=7, average age: 63.0±9.7 years) and 40

patients with PDAC (male=17, female=23, average age: 66.0±8.9 years) who had dedicated pancreas protocol CT between 2004 and 2017 were retrospectively evaluated. All CT imaging was performed in dual-phase imaging with intravenous contrast administration. All images were reconstructed at 0.75 mm thickness and 0.5 mm increment. Segments of pancreas involved by PDAC and autoimmune pancreatitis (areas of enlargement, altered enhancement, effacement of pancreatic duct) as well as uninvolved segments of the pancreas were segmented in 3D using commercially available software, VelocityAI (Varian Medical Systems, USA). 478 radiomics features from the segmented volume using venous phase images were extracted to express pancreas phenotype, and random forest was used for the classification PDAC and AIP. CT reports were reviewed to determine the radiological diagnosis based on CT imaging.

### RESULTS

In AIP, pancreas was diffuse involved in 15 cases, and focally involved in 17 cases. Among 32 cases of AIP, diagnosis of AIP was suspected or included in the differential diagnosis based on the CT reports in 14 cases (44%). Overall accuracy of texture analysis for differentiation of AIP and PDAC with 10 fold cross-validation was 94.4% (68 among 72 cases were correctly classified). Two among 40 PDAC cases were incorrectly classified as AIP, and 2 among 32 AIP cases were incorrectly classified as PDAC, giving sensitivity of 95.0% and specificity of 93.8%.

### CONCLUSION

CT texture analysis is accurate in differentiating autoimmune pancreatitis and pancreatic ductal adenocarcinoma.

### **CLINICAL RELEVANCE/APPLICATION**

Using texture data as a supplemental information in diagnosing pancreatic mass will be helpful for differentiating pancreatic adenocarcinoma and autoimmune pancreatitis.

### **Honored Educators**

Presenters or authors on this event have been recognized as RSNA Honored Educators for participating in multiple qualifying educational activities. Honored Educators are invested in furthering the profession of radiology by delivering high-quality educational content in their field of study. Learn how you can become an honored educator by visiting the website at: https://www.rsna.org/Honored-Educator-Award/ Elliot K. Fishman, MD - 2012 Honored EducatorElliot K. Fishman, MD - 2014 Honored EducatorElliot K. Fishman, MD - 2016 Honored EducatorElliot K. Fishman, MD - 2018 Honored Educator

# RC209-08 Differentiation of Pancreatic Cancer from Focal Mass-forming Pancreatitis: Added Value of Magnetic Resonance Elastography to Dynamic Contrast-enhanced Magnetic Resonance Imaging

Monday, Nov. 26 10:00AM - 10:10AM Room: E353C

Participants Shi Yu, MS, Shenyang, China (*Presenter*) Nothing to Disclose Yanqing Liu, Shenyang, China (*Abstract Co-Author*) Nothing to Disclose Min Wang, Shenyang, China (*Abstract Co-Author*) Nothing to Disclose Qiyong Guo, MD, Shenyang, China (*Abstract Co-Author*) Nothing to Disclose

# For information about this presentation, contact:

18940259980@163.com

# PURPOSE

Thin study is to investigate if incorporating MR elastography (MRE) with conventional dynamic contrast-enhanced MR imaging (DCE-MRI) can provide a benefit in differentiating pancreatic cancer (PC) and focal mass-forming pancreatitis (FMFP).

### **METHOD AND MATERIALS**

We retrospectively identified 21 FMFP patients and 42 PC patients confirmed by histopathological examinations through a prospectively maintained database. The patients did DCE-MRI together with a dual-frequency MRE at 40Hz and 60Hz with a 32-slice, flow-compensated, spin-echo(SE), EPI pulse sequence. A five-point scale for likelihood of PC was used by two experienced radiologist in consensus. To evaluate the added value of MRE, the ROC analysis of a combined technique using both MRE and MR imaging was determined by logistic regression models to calculate probabilities. To estimate how accurately the above classifiers would perform in practice, a leave-one-out cross-validation was applied for all the above ROC analysis.Results from ROC analysis with cross-validation were carried out with 'R' statistical computing software (R version 3.4.0).

### RESULTS

The mean stiffness with FMFP was 2.03kPa (IQR:1.75~2.32kPa) at 40Hz and 3.05kPa (2.71~3.52kPa) at 60Hz, both significantly lower than those of PC, showing 3.21kPa (IQR:2.38~4.41kPa) and 4.95kPa (IQR:3.64~7.23kPa), respectively (Mann-Whitney U test, both P< 0.001). Accuracies for determination of PC using 60Hz-MRE, 40Hz-MRE, DCE-MRI and the combination of DCE/MRI and 60Hz-, 40Hz-MRE, were, 70.2%, 77.4%, 83.3%, 75.0% and 92.9%, respectively. The combined DCE-MRI with 40Hz-MRE significantly improved diagnostic performance to DCE-MRI alone (Area under the ROC curve [AUC]: 0.937 vs 0.783), by increasing specificity (96.9% vs 62.1%), without a significant loss of sensitivity (90.9% vs 94.6%). The combined DCE-MRI with 60Hz-MRE didn't significantly change diagnostic performance of DCE-MRI alone (AUC: 0.761 vs 0.783, P>0.05).

### CONCLUSION

Combined assessment of 40Hz-MRE to DCE-MRI may help to differentiate PC from FMFP in a noninvasive fashion.

### **CLINICAL RELEVANCE/APPLICATION**

The incorporation of 40Hz-MRE into a standard MRI protocol may enhance the value of routine pancreatic MR imaging for better non-invasive differentiation between PC and FMFP.

# RC209-09 Acute Pancreatitis Reporting

Monday, Nov. 26 10:30AM - 10:50AM Room: E353C

Participants Bhavik N. Patel, MD, MBA, Stanford, CA (*Presenter*) Nothing to Disclose

# LEARNING OBJECTIVES

1) Understand the new reporting terminology based on the Revised Atlanta Classification. 2) Be familiar with the morphologic classification of acute pancreatitis and associated fluid collections. 3) Know the reporting template for acute pancreatitis.

# RC209-10 Pancreatic Neuroendocrine Tumors

Monday, Nov. 26 10:50AM - 11:10AM Room: E353C

Participants

Desiree E. Morgan, MD, Birmingham, AL (Presenter) Institutional Research Grant, General Electric Company

## For information about this presentation, contact:

dmorgan@uabmc.edu

# LEARNING OBJECTIVES

1) Identify the imaging features of pancreatic endocrine tumors that differentiate them from pancreatic ductal adenocarcinoma. 2) Understand the World Health Organization grading of pancreatic endocrine tumors and implications for staging and treatment of patients. 3) Apply knowledge of specific strengths and unique clinical utilities of different imaging modalities during evaluation of patients with pancreatic endocrine tumors.

# RC209-11 A Preliminary Study about the Robustness of CT Derived Radiomic Features (RF) In Pancreatic NEN and Their Ability in Predicting Tumors' Histologic Characteristics

Monday, Nov. 26 11:10AM - 11:20AM Room: E353C

Participants Giulia Benedetti, MD, Milan, Italy (*Presenter*) Nothing to Disclose Marta Maria Panzeri, MD, Milan, Italy (*Abstract Co-Author*) Nothing to Disclose Martina Mori, Milan, Italy (*Abstract Co-Author*) Nothing to Disclose Carla Sini, Milan, Italy (*Abstract Co-Author*) Nothing to Disclose Maurizio Barbera, Milan, Italy (*Abstract Co-Author*) Nothing to Disclose Francesca Muffatti, Milan, Italy (*Abstract Co-Author*) Nothing to Disclose Stefano Partelli, Milan, Italy (*Abstract Co-Author*) Nothing to Disclose Massimo Falconi, Milan, Italy (*Abstract Co-Author*) Nothing to Disclose Claudio Fiorino, Milan, Italy (*Abstract Co-Author*) Nothing to Disclose Francesco A. De Cobelli, MD, Milan, Italy (*Abstract Co-Author*) Nothing to Disclose

### For information about this presentation, contact:

benedetti.giulia@hsr.it

### PURPOSE

To assess inter-observer variability in delineating pancreatic neuroendocrine neoplasia (NEN) on CT images, and to evaluate ability of RF in predicting histopathologic characteristics of pancreatic NEN.

## METHOD AND MATERIALS

30 histologically confirmed pancreatic NEN were contoured on CT images by 3 blinded observers. Contours were delineated on arterial or venous phase, and then projected onto the pre-contrast acquisition and adjusted to correct small anatomical discrepancies. Interobserver contouring variability was assessed by DICE-index. 71 RF were extracted from each observer's contours, their robustness was investigated against contour variability with Spearman-R and Intra-Class Correlation (ICC). Histologic data (HD) were collected from the surgical specimen: Ki67 (%), Histologic grade, N, M and vascular invasion (VI). Significant differences of RF according to histologic data were tested.

## RESULTS

Volume mean and median were 14.2 cc and 1.3 cc, respectively. A satisfactory agreement was found, with mean DICE=0.78 and no significant differences between observers. 66/72 RF were very robust (ICC>0.9); 4/72 showed ICC<0.8, mostly in the 'Neighbourhood intensity-difference' RF family. Average R-values were 0.90 for RF with ICC>0.9 and 0.85 for the others. Only 'sphericity' had R-value<0.6. 19 non-redundant features were selected. Patients with VI had higher Mean HU (p=0.039), Entropy (p=0.035), Volume (p=0.002, AUC=0.87) and Low-Intensity Run Emphasis (p=0.021). Second Angular Moment was significantly related to Ki67% (p=0.018) and Volume with M (p=0.41, AUC=0.80).

### CONCLUSION

Despite a small number of patients, results show a good robustness of CT derived RF in NEN and a good ability to predict their histologic characteristics. Therefore, RF have a possible future role in predicting NEN's outcome.

# CLINICAL RELEVANCE/APPLICATION

NEN can present with different macroscopic and histologic features. Unfortunately, only histology has a validated role in predicting NEN's outcome. Therefore, there is a need for implementing clinicians' tools to stratify and predict the prognosis of NEN. Radiomic is a promising field to build predictive models relating imaging features to clinical outcomes, especially for neoplasms. Nevertheless, its robustness is still under investigation. Our study is one of the first to assess RF reliability and its ability to predict hystologic feature in this group of Patients.

# RC209-12 Differentiation Atypical Pancreatic Neuroendocrine Tumors from Pancreatic Ductal Adenocarcinomas: Using Volumetric CT Texture Analysis

Monday, Nov. 26 11:20AM - 11:30AM Room: E353C

Participants Jiali Li, Wuhan, China (*Abstract Co-Author*) Nothing to Disclose Yaqi Shen, PhD, MD, Wuhan, China (*Abstract Co-Author*) Nothing to Disclose Daoyu Hu, Wuhan, China (*Abstract Co-Author*) Nothing to Disclose Zhen Li, MD, PhD, Wuhan, China (*Presenter*) Nothing to Disclose

### For information about this presentation, contact:

m201675924@hust.edu.cn

## PURPOSE

To investigate whether CT texture analysis (CTTA) can be used to differentiate atypical pancreatic neuroendocrine tumors (pNET) from pancreatic ductal adenocarcinomas(PDAC).

### **METHOD AND MATERIALS**

This single-center retrospective study was approved by local institutional review board and the requirement for informed consent was waived. We retrospectively analyzed 210 patients in pathology database between January 2012 and May 2017, according to inclusion and exclusion criterion, 127 patients with 50 PDACs and 77 pNETs were included finally. Traditional imaging manifestations and texture parameters (mean, median, 5th ,10th, 25th, 75th,90th percentiles, skewness, kurtosis and entropy) were extracted from portal images and compared between these two tumors by using proper statistical method. The optimal parameters for differentiating PDACs and atypical pNETs was gained through receiver operating characteristic (ROC) curves and area under curve(AUC) analysis.

## RESULTS

On the basis of arterial enhancement, 52 pNETs (67%,52/77) were typical and 25 pNETs (32%,25/77) were atypical(nonhypervascular). Well-defined margin, homogeneity and no duct dilatation on portal phase were easier to appear in atypical pNET compared to PDAC, although there weas no statistical difference. Atypical pNETs had statistically higher mean, median, 5th ,10th and 25th percentiles (P=0.006,0.024,0.000,0.001,0.021, respectively) and statistically lower skewness(P=0.017) versus PDACs. However, there were no difference for 75th,90th percentiles, kurtosis and entropy between these two tumors (P=0.232,0.415,0.143,0.291, respectively). For differentiating PDACs and atypical pNETs, 5th percentile (AUC=0.811) and5th+skewness (AUC=0.887) were optimal parameters for alone and combined diagnosis respectively.

### CONCLUSION

CT texture features, especially combined diagnosis of 5th+skewness, can be applied as a quantitative tool to distinguish atypical pNETs from PDACs.

### **CLINICAL RELEVANCE/APPLICATION**

CTTA could be used as a non-invasive alternative tool to reduce the number of false diagnoses of atypical pNETs as PDACs. It would be useful for surgery planning and the selection of combined treatments.

# RC209-13 Characterization of Small Insulinomas with Typical and Atypical Appearance on Pancreatic 3T MRI in Comparison to GLP-1-R PET/CT and Histopathology

Monday, Nov. 26 11:30AM - 11:40AM Room: E353C

Participants

Patricia Wiesner, Basel, Switzerland (*Presenter*) Nothing to Disclose Kwadwo Antwi, Basel, Switzerland (*Abstract Co-Author*) Nothing to Disclose Elmar M. Merkle, MD, Basel, Switzerland (*Abstract Co-Author*) Speakers Bureau, Siemens AG Research Grant, Bayer AG Research Grant, Guerbet SA Research Grant, Bracco Group Research Grant, Siemens AG Daniel Boll, Basel, Switzerland (*Abstract Co-Author*) Nothing to Disclose Christoph J. Zech, MD, Basel, Switzerland (*Abstract Co-Author*) Nothing to Disclose Damian Wild, Basel, Switzerland (*Abstract Co-Author*) Nothing to Disclose Tobias Heye, MD, Basel , Switzerland (*Abstract Co-Author*) Nothing to Disclose

### For information about this presentation, contact:

patricia.wiesner@usb.ch

## PURPOSE

To evaluate imaging characteristics of small insulinomas with typical and atypical appearance on 3T MRI in comparison to surgery or GLP-1-R PET/CT.

### **METHOD AND MATERIALS**

31 patients with endogenous hyperinsulinemic hypoglycemia suspicious for insulinoma (24f, 7m, mean 53 y, 19-81 y) were included, patients with multiple lesions were excluded. Patients underwent pancreatic 3T MRI including T1w, T2w, diffusion weighted imaging (DWI) and dynamic contrast enhanced (DCE) imaging using compressed sensing techniques (GRASP; Golden-Angle Radial Sparse Parallel). GLP-1-R (Glucagon like peptide-1 receptor)-PET/CT 2.5h after i.v. administration of 68Ga-DOTA Exendin-4 (all patients) and surgery (29 patients) served as reference standard. One non-blinded reader measured tumor-to-background ratios (T2BR) on MRI data. T2BR were defined as <0.8=hypointense; 0.8-1.2 isointense/less conspicious; >1.2=hyperintense. Three blinded expert readers (>10 years of experience in abdominal radiology) analyzed MRI data for presence of lesions, when at least 2 readers detected the same lesion per case, the lesion was considered detected.

In 31 patients, 30 lesions in total were identified by GLP-1-R PET/CT, one surgically proven insulinoma was not identified. Mean lesion size was 11.9 mm (6-24 mm) on MRI. Three expert readers detected 22 lesions on MRI, resulting in a 71% accuracy. 9 lesions were considered undetected, out of these, the non-blinded reader was able to measure T2BR in 5 lesions. 4 lesions were not visible on MRI. The undetected 5 lesions with a mean size of 8.8 mm (6-12 mm) were less conspicuous with mean T2BR for T1w=0.71; T2w=1.02; high b-value DWI=0.92 compared to detected lesions, mean size 12.6 mm (6-24 mm), mean T2BR for T1w=0.65; T2w=1.63, high b-value DWI=1.3. Arterial hyperenhancement was present in 17/22 (77%) detected lesions and in 3/5 (60%) undetected lesions.

## CONCLUSION

Pancreatic MRI can visualize small lesions in patients with suspected insulinoma. Typical insulinomas show hypointense signal on T1w, hyperintense on T2w and DWI and arterial hyperenhancement on DCE-MRI. Atypical insulinomas may be small, are less conspicuous, show hypo-/isointense signal on T1w and isointense on T2w and DWI.

# **CLINICAL RELEVANCE/APPLICATION**

A proportion (18.5%) of small insulinomas are less conspiciuous on MRI due to atypical presentation. Combination of GLP-1-R PET/CT and MRI facilitates locating a lesion and performing minimal invasive surgery.

# RC209-14 Approach to Cystic Pancreatic Lesions

Monday, Nov. 26 11:40AM - 12:00PM Room: E353C

Participants

Koenraad J. Mortele, MD, Boston, MA (Presenter) Nothing to Disclose

# LEARNING OBJECTIVES

1) Be familiar with the specific imaging features of a vast array of cystic pancreatic lesions. 2) Be able to name the most common cystic pancreatic lesions seen in clinical practice. 3) Have an understanding of how to manage the cystic pancreatic lesions from an imaging follow up standpoint.

### ABSTRACT

Cystic pancreatic neoplasms are a diverse group of tumors which vary in aggressiveness from benign to dysplastic or pre-malignant to frankly invasive cancers. The true prevalence of pancreatic cystic lesions is unknown but has been previously reported to be between 2.4% and 25 % (1-3). At the author's institution, Lee reported the prevalence of incidental pancreatic cystic lesions detected on MRI to be 13.5% and showed that both prevalence and cyst size increased with age (4). Since most cystic pancreatic lesions are neoplastic, accurate diagnosis via a combination of clinical information, imaging, and endoscopic ultrasound (EUS) with cyst fluid analysis is of utmost importance (5-8). The primary purpose of this review is to highlight the key imaging findings for a vast array of cystic pancreatic neoplasms. These include the relatively common ones: intraductal papillary mucinous neoplasm (IPMN), serous microcystic adenoma, and mucinous cystic neoplasm (MCN). Secondly, the radiological features of more rare ones, including cystic endocrine tumors, solid pseudopapillary tumor (SPT), cystic metastases, and lymphangiomas, will also be discussed. Finally, this article also provides a comprehensive management algorithm based on lesion size and patient's symptoms, with recommendations when to reimage patients with those lesions.



## Advances in Gynecologic Ultrasound

Monday, Nov. 26 8:30AM - 10:00AM Room: S504AB

# GU US

AMA PRA Category 1 Credits ™: 1.50 ARRT Category A+ Credit: 1.75

### Sub-Events

### RC210A Uterus and Endometrium: A Primer with Pearls to Perfect Your US Performance

Participants

Loretta M. Strachowski, MD, San Francisco, CA (Presenter) Nothing to Disclose

## LEARNING OBJECTIVES

1) Recognize the varied appearance of the uterus and endometrium throughout a woman's life. 2) Improve sonographic visualization of the endometrium utilizing technical tips and tricks. 3) Recite a basic differential diagnosis for uterine/cervical masses and endometrial thickening. 4) Apply appropriate terminology when describing abnormal bleeding, location of myomas and mullerian duct anomalies. 5) Understand the controversies, cutoffs and considerations in the context of the role of US in postmenopausal bleeding.

# RC210B 3D Ultrasound in Gynecology

Participants

Beryl R. Benacerraf, MD, Boston, MA (Presenter) Nothing to Disclose

### LEARNING OBJECTIVES

1) To discuss the multiplanar reconstruction technique in scanning the pelvis, including the usefulness of looking at the coronal view of the uterus to evaluate the endometrium and uterine shape. 2) To discuss the use of 3D ultrasound to look for causes of pelvic pain. 3) To discuss the use of 3D ultrasound when evaluating a potential hydrosalpinx.

# RC210C Ovarian Cysts and Masses

Participants

Deborah Levine, MD, Boston, MA (Presenter) Editor with royalties, Taylor & Francis Group; Editor with royalties, Reed Elsevier;

## For information about this presentation, contact:

dlevine@bidmc.harvard.edu

### LEARNING OBJECTIVES

1) Review findings of the 'First International Consensus Report on Adnexal Masses: Management Recommendations' . 2) Assess the potential of risk prediction models to improve practice patterns. 3) Improve knowledge of the malignant potential of various sonographic findings. 4) Integrate these findings into daily practice with goal of reducing excess surgery for benign masses while improving triage to gynecology-oncology in women with suspicious adnexal masses.

# RC210D Ultrasound for Deeply Infiltrative Endometriosis

Participants

Luciana P. Chamie, MD, PhD, Sao Paulo, Brazil (Presenter) Nothing to Disclose

For information about this presentation, contact:

# luciana@chamie.com.br

# LEARNING OBJECTIVES

1) Define clinical and epidemiological aspects of endometriosis. 2) Define the importance of imaging mapping for deeply infiltrative endometriosis before clinical counseling. 3) Apply the most appropriate technique to investigate endometriosis. 4) Describe the bowel preparation required for the transvaginal ultrasound to investigate endometriosis. 5) Apply the imaging algorithm to map deeply infiltrative endometriosis. 6) Assess the ultrasonographic findings of deeply infiltrative endometriosis in the most common sites such as bladder, vesicouterine pouch, retrocervical space, vagina, ureters, appendix and rectosigmoid colon.

## ABSTRACT

Endometriosis is a very common gynecological disease affecting millions of women in their reproductive life, often causing pelvic pain and infertility. Clinical history and physical examination may suggest endometriosis, but imaging mapping is necessary to identify the disease and mandatory for clinical couseling and surgical planning. Transvaginal ultrasound after bowel preparation is the best imaging modality as the first-line technique to evaluate patients suspected of endometriosis. The bowel preparation is relatively simple and includes the day before and the day of the examination. This method is highly accurate to identify intestinal endometriosis and to determine which layers of the bowel wall are affected. In addition, it provides better assessment of small peritoneal lesions of the retrocervical space, vagina and bladder. Pelvic adhesions can also be evaluated during the exam.



Nuclear Medicine Series: New PET Tracers for Prostate Cancer (Interactive Session)

Monday, Nov. 26 8:30AM - 12:00PM Room: S505AB



AMA PRA Category 1 Credits ™: 3.50 ARRT Category A+ Credits: 4.00

FDA Discussions may include off-label uses.

## Participants

Terence Z. Wong, MD, PhD, Chapel Hill, NC (Moderator) Consultant, Lucerno Dynamics, LLC;

### Sub-Events

## RC211-01 Logistics: Incorporating New PET Tracers into Practice

Monday, Nov. 26 8:30AM - 8:45AM Room: S505AB

Participants

Nancy M. Swanston, RT, Houston, TX (Presenter) Nothing to Disclose

RC211-02 Validation of the Use of Image-Derived Input Function for the Quantification of Ga-68 PSMA-11 Uptake in Prostate Cancer Patients Using Dynamic PET/MR

Monday, Nov. 26 8:45AM - 8:55AM Room: S505AB

Participants

Anna Maria Ringheim, MSc, BEng, Sao Paulo, Brazil (*Presenter*) Nothing to Disclose Guilherme Campos, Sao Paulo, Brazil (*Abstract Co-Author*) Nothing to Disclose Marcelo L. Cunha, MD, Sao Paulo, Brazil (*Abstract Co-Author*) Nothing to Disclose Taise Vitor, Sao Paulo, Brazil (*Abstract Co-Author*) Nothing to Disclose Karine M. Martins, MS, Sao Paulo, Brazil (*Abstract Co-Author*) Nothing to Disclose Marycel F. de Barboza, MSc, Sao Paulo, Brazil (*Abstract Co-Author*) Nothing to Disclose Jairo Wagner, MD, Sao Paulo, Brazil (*Abstract Co-Author*) Nothing to Disclose Ana Claudia Miranda, Sao Paulo, Brazil (*Abstract Co-Author*) Nothing to Disclose Leonardo L. Fuscaldi, PhD, Sao Paulo, Brazil (*Abstract Co-Author*) Nothing to Disclose Ana Claudia R. Durante, Sao Paulo, Brazil (*Abstract Co-Author*) Nothing to Disclose Gustavo C. Lemos, Sao Paulo, Brazil (*Abstract Co-Author*) Nothing to Disclose Jose Roberto Colombo Jr, Sao Paulo, Brazil (*Abstract Co-Author*) Nothing to Disclose Ronaldo H. Baroni, MD, Sao Paulo, Brazil (*Abstract Co-Author*) Nothing to Disclose

## For information about this presentation, contact:

anna.m.ringheim@gmail.com

# PURPOSE

To validate the use of image-derived input function of the common iliac artery as an alternative to arterial blood sampling in pharmacokinetic modeling of Ga-68 PSMA-11 uptake using hybrid positron emission tomography and magnetic resonance (PET/MR) imaging in primary prostate cancer.

### **METHOD AND MATERIALS**

This observational prospective study was approved by our Institution's Ethics Committee. Eleven patients with clinically significant prostate cancer underwent a 60-minute dynamic PET/MR scan of the pelvis with an injected dose of Ga-68 HBED-CC-PSMA (Ga-68 PSMA-11). Arterial blood activity was measured by an automatic arterial blood sampling device during the first 10 min and manual blood samples were collected for metabolite analysis and for blood to plasma transformation to derive an arterial input function (AIF). One lesion per patient (with the highest uptake) and the common iliac artery were outlined using isocontour volumes on the PET images. Two image-derived input functions (IDIF) were calculated: whole blood curve (IDIF\_bl) and plasma curve (IDIF\_pl) corrected by the average plasma-to-blood ratio. An irreversible two-tissue compartment model, with rate constants K1, k2 and k3, were fitted to the data using AIF, IDIF\_pl and IDID\_bl and the net influx rate Ki=K1k3/(k2+k3) was calculated. The agreement between K1 and Ki from AIF and IDIF\_bl and IDIF\_pl were reported by intraclass correlation coefficients (ICC) with 95% confidence intervals.

# RESULTS

Ga-68 PSMA-11 was stable in-vivo, not necessitating metabolite correction. The mean plasma-to-blood ratio was 1.63. IDIF underestimated the arterial input function by 50% at the bolus peak and by 20% at late times. For K1, ICC between AIF and IDIF\_bl was 0.40 (-0.22, 0.80) and between AIF and IDIF\_pl 0.60 (0.04, 0.87). For Ki, ICC between AIF and IDIF\_bl was 0.77 (0.34, 0.93) and between AIF and IDIF\_pl 0.94 (0.78, 0.98).

### CONCLUSION

IDIF plasma curve can be used in clinical practice as an alternative to arterial blood sampling to calculate the uptake of Ga-68

PSMA-11, but the method requires a known mean plasma-to-blood ratio. Agreement between IDIF whole blood curve and arterial input function was poor to moderate. Underestimation of the IDIF should be explained by partial volume effects.

# **CLINICAL RELEVANCE/APPLICATION**

Image-derived plasma curves can be used in clinical practice as an alternative to arterial blood sampling to quantify uptake of Ga-68 PSMA-11 in prostate cancer.

# RC211-03 Dual-Time 68Ga-PSMA-11 Imaging for Biochemically Recurrent Prostate Cancer Using LYSO and SiPM-Based Detectors PET/CT

Monday, Nov. 26 8:55AM - 9:05AM Room: S505AB

Participants

Heying Duan, Stanford, CA (*Presenter*) Nothing to Disclose Sonya Y. Park, MD, Seoul, Korea, Republic Of (*Abstract Co-Author*) Nothing to Disclose Lucia Baratto, Stanford, CA (*Abstract Co-Author*) Nothing to Disclose Negin Hatami, Stanford, CA (*Abstract Co-Author*) Nothing to Disclose Mohamed H. Khalaf, Stanford, CA (*Abstract Co-Author*) Nothing to Disclose Thomas Yohannan, MD, Chicago, IL (*Abstract Co-Author*) Nothing to Disclose Guido A. Davidzon, MD, Stanford, CA (*Abstract Co-Author*) Nothing to Disclose Andrei Iagaru, MD, Emerald Hills, CA (*Abstract Co-Author*) Research Grant, General Electric Company

## For information about this presentation, contact:

heying@stanford.edu

# PURPOSE

68Ga-labeled prostate-specific membrane antigen (PSMA-11) is a highly specific tracer for biochemically recurrent prostate cancer at low PSA levels. In this study we aim to compare the diagnostic performance of a new PET/CT scanner (Discovery Molecular Insights - DMI) using silicon photomultipliers (SiPM) detectors vs standard LYSO detectors PET/CT (Discovery 690 - D690) in patients with biochemical relapse following a single injection of radiopharmaceutical.

### **METHOD AND MATERIALS**

Forty-four patients were prospectively recruited to undergo imaging on the D690 and DMI scanners, in randomized order. Images from the DMI PET/CT were reconstructed using ToF and a Bayesian penalized likelihood algorithm (Q.Clear®) whereas images from the D690 PET/CT were reconstructed using time-of-flight (ToF) and an ordered subset expectation maximization (OSEM) protocol. Two experienced nuclear medicine physicians reviewed both scans for each patient in random order, recorded the number and location of each lesion, and acquired standardized uptake value (SUV) measurements.

## RESULTS

Twenty-three patients underwent imaging on the D690 PET/CT first followed by the DMI scanner, and twenty-one underwent scanning in the reverse order. The median PSA was 4.33 ng/mL with one outlier of 1170 ng/mL. PSMA PET detected sites of recurrence in 32/44 (73 %) patients, including 6/12 (50 %) patients with PSA below 1 ng/mL with the lowest PSA and a positive scan at 0.05 ng/mL. The mean lesion SUVmax measurements were higher on DMI than D690 regardless of the timely order of the scan (6.5 vs. 5.7 in D690 scan first and 4.6 vs. 4.2 for DMI performed first). However, the difference in mean lesion SUVmax was only significant for patients scanned on the D690 first (p<0.018).

### CONCLUSION

These preliminary results suggest that the SiPM-based DMI PET/CT system offers better performance and superior detector technology and image quality compared to conventional LYSO-based D690 PET/CT. These results need to be confirmed in larger studies.

# CLINICAL RELEVANCE/APPLICATION

SiPM-based DMI PET/CT system seems to offer better performance and superior detector technology and image quality compared to conventional LYSO-based D690 PET/CT.

# RC211-04 Same Day PET/CT and PET/MRI with 68Ga-PSMA in the Evaluation of Biochemical Recurrence of Prostate Cancer

Monday, Nov. 26 9:05AM - 9:15AM Room: S505AB

Participants

Marcelo L. Cunha, MD, Sao Paulo, Brazil (*Abstract Co-Author*) Nothing to Disclose Akemi Osawa, MD, Sao Paulo, Brazil (*Abstract Co-Author*) Nothing to Disclose Guilherme Campos, Sao Paulo, Brazil (*Abstract Co-Author*) Nothing to Disclose Lilian Y. Yamaga, Sao Paulo, Brazil (*Abstract Co-Author*) Nothing to Disclose Julio Cesar Oliveira, MD, Sao Paulo, Brazil (*Abstract Co-Author*) Nothing to Disclose Ricardo C. Fonseca, Sao Paulo, Brazil (*Abstract Co-Author*) Nothing to Disclose Jairo Wagner, MD, Sao Paulo, Brazil (*Abstract Co-Author*) Nothing to Disclose Taise Vitor, Sao Paulo, Brazil (*Abstract Co-Author*) Nothing to Disclose Fernando I. Yamauchi, MD, Sao Paulo, Brazil (*Abstract Co-Author*) Nothing to Disclose Thais Mussi, MD,PhD, Sao Paulo, Brazil (*Presenter*) Nothing to Disclose Ronaldo H. Baroni, MD, Sao Paulo, Brazil (*Abstract Co-Author*) Nothing to Disclose

# PURPOSE

To compare PET/CT and PET/MRI with 68Ga-PSMA in patients with radical prostatectomy and biochemical recurrence (BCR).

# METHOD AND MATERIALS

This is a prospective. IRB approved study. 29 patients with prostate cancer were referred to our department to investigate BCR

and submitted to PET/CT and PET/MR with 68Ga-PSMA in the same day. The first exam started 50 minutes after 68Ga-PSMA injection (15 started with PET/CT while 14 started with PET/MRI). The second study began right after the first one. Readers of each study were aware of clinical data but blinded of eventual findings of the other scan. Patients had age ranging from 52 to 78 years old, had submitted to radical prostatectomy up to 12 years before the exams, and Gleason score ranged from 6 to 9. Serum PSA levels ranged from 0.22 to 12.8 ng/mL at time of the scans.

## RESULTS

There were 16 positive PET/CT and 15 positive PET/MRI. Negative studies (no abnormal area suspicious for prostatic cancer recurrence) counted 11 PET/CT and 13 PET/MR scans. PET/CT found 34 suspicious lesions and PET/MR, 27 lesions. Few equivocal studies were found by both methods: 2 in PET/CT and 1 in PET/MRI, all of them with one uncertain lesion. There were 24/39 studies match studies (positive or negative on both methods).

### CONCLUSION

PET/CT and PET/MRI with 68Ga-PSMA can both be used in BCR scenario, in spite of PET/CT seems to have a slightly higher sensitivity in our population.

### **CLINICAL RELEVANCE/APPLICATION**

PET/CT and PET/MRI are the most important imaging methods in BCR scenario. The comparison among them is essential to perform the right choice in clinical practice.

# RC211-05 Evaluation of Whole-body MRI versus 68Ga-PSMA PET/CT for Detection of Biochemical Recurrence in Prostate Cancer Patients

Monday, Nov. 26 9:15AM - 9:25AM Room: S505AB

### Participants

Lino Sawicki, MD, Dusseldorf, Germany (*Abstract Co-Author*) Nothing to Disclose Carolin Buddensieck, Dusseldorf, Germany (*Abstract Co-Author*) Nothing to Disclose Johannes Boos, MD, Dusseldorf, Germany (*Abstract Co-Author*) Nothing to Disclose Robert Rabenalt, Duesseldorf, Germany (*Abstract Co-Author*) Nothing to Disclose Gerald Antoch, MD, Duesseldorf, Germany (*Abstract Co-Author*) Nothing to Disclose Hubertus Hautzel, MD, Juelich, Germany (*Abstract Co-Author*) Nothing to Disclose Julian Kirchner, Dusseldorf, Germany (*Presenter*) Nothing to Disclose

### PURPOSE

The purpose of our study was to assess whole-body MRI (wb-MRI) for lesion detection of biochemical relapse in prostate cancer (PCa) patients after curative treatment in comparison to 68Ga-PSMA PET/CT.

### METHOD AND MATERIALS

This is a prospective IRB-approved trial of 30 patients (age:  $65.5 \pm 9.6$  years) with newly documented biochemical relapse of PCa (mean prostate-specific antigen (PSA)  $2.11 \pm 1.97$  ng/ml) after curative therapy. All patients underwent both wb-MRI including a dedicated pelvic imaging protocol and PET/CT with  $167 \pm 35$  MBq 68Ga-PSMA within a time window of  $10.5 \pm 9.5$  days. PET/CT and MRI datasets were separately evaluated regarding PCa lesion count, lesion type, localization, and diagnostic confidence (3-point scale; 1-3) by two physicians. The reference standard was based on histopathology results, changes of PSA after targeted irradiation, follow-up imaging, and clinical data. Lesion-based and patient-based detection rates were compared using chi2 test. Differences in diagnostic confidence were assessed by Welch test.

### RESULTS

A total of 58 PCa lesions were found in 22/30 patients in the study cohort. 68Ga-PSMA PET/CT detected 57/58 (98.3 %) lesions in 21/30 (70 %) patients, and 15/58 (25.9 %) lesions were detected in 13/30 (43.3 %) patients using wb-MRI. The higher detection rate of 68Ga-PSMA PET/CT was statistically significant both on a per-lesion (p = 0.001) and per-patient (p = 0.039) basis. In 8/30 patients none of the two modalities actually localized the PCa relapse. Except for one local recurrence in the former prostate fossa that was exclusively detected by wb-MRI, all lesions detected by wb-MRI were also detectable on 68Ga-PSMA PET/CT. 68Ga-PSMA PET/CT offered a superior diagnostic confidence in categorization of PCa lesions compared to wb-MRI (2.7 ± 0.6 vs. 2.3 ± 0.6, p = 0.011).

## CONCLUSION

68Ga-PSMA PET/CT significantly outperforms wb-MRI for detection of biochemical relapse in PCa patients after curative treatment.

# **CLINICAL RELEVANCE/APPLICATION**

Wb-MRI is inferior to 68Ga-PSMA PET/CT for the detection of recurrent PCa. Nevertheless, as one local recurrence in one patient was only detectable with MRI, it might be useful in selected cases.

# RC211-06 The Effect of Various Beta Values on Image Quality and Semi-Quantitative Measurements in 68Ga-Labeled GRPR and PSMA PET/MRI Images Reconstructed With a Block Sequential Regularized Expectation Maximization Algorithm

Monday, Nov. 26 9:25AM - 9:35AM Room: S505AB

Participants

Lucia Baratto, Stanford, CA (*Presenter*) Nothing to Disclose Heying Duan, Stanford, CA (*Abstract Co-Author*) Nothing to Disclose Harsh C. Gandhi, BS,MSc, Saint Louis, MO (*Abstract Co-Author*) Nothing to Disclose Mehdi Khalighi, Palo Alto, CA (*Abstract Co-Author*) Employee, General Electric Company Praveen Gulaka, PhD, Stanford, CA (*Abstract Co-Author*) Nothing to Disclose Andrei Iagaru, MD, Emerald Hills, CA (*Abstract Co-Author*) Research Grant, General Electric Company The block sequential regularized expectation maximization (BSREM) algorithm is a new image reconstruction method that controls noise at higher iterations by applying a relative difference penalty built into the objective function. This enables one to employ more iterations for convergence and better contrast recovery, while mitigating noise amplification. BSREM was recently introduced on the GE SIGNA PET/MRI platform. Here we evaluated how different values influence image quality and SUVmax in a cohort of prostate cancer patients who underwent 68Ga-RM2 or 68Ga-PSMA-11 scans.

## **METHOD AND MATERIALS**

We analyzed 36 prostate cancer patients who underwent either 68Ga-RM2 (15) or 68Ga-PSMA-11 (21) PET/MRI. The raw PET data were retrospectively reconstructed using values of 250, 350, 500, 750 and 1000. Each reconstruction was reviewed independently by 3 nuclear medicine physicians and scored using a Likert scale (1 - poor, 5 - excellent quality). SUVmax values were measured from 68Ga-RM2/PSMA PET/MRI for all the lesions identified as compatible with prostate cancer.

### RESULTS

The mean±SD scores for 68Ga-RM2 PET images were  $2.5\pm0.5$  for =250 reconstructions,  $3.2\pm0.6$  for =350,  $4.1\pm0.6$  for =500,  $4.7\pm0.5$  for =750 and  $4.8\pm0.5$  for =1000. The mean±SD scores for 68Ga-PSMA-11 PET images were  $3.3\pm0.9$  for =250 reconstructions,  $4.2\pm0.9$  for =350,  $4.7\pm0.6$  for =500,  $4.9\pm0.3$  for =750 and  $4.9\pm0.4$  for =1000. The relative observed agreement among readers for the values of 250, 350, 500, 750, 1000 were 49%, 50%, 60%, 70% and 74%, respectively. A total of 24 lesions (6 on RM2 and 18 on PSMA-11) were detected and the mean SUVmax measurements were: 13.1, 12.5, 10.4, 9.3 and 8 for the 68Ga-RM2 values of 250, 350, 500, 750 and 1000, respectively; 22.6, 21.2, 19.7, 18.9 and 16.8 for the 68Ga-PSMA-11 values of 250, 350, 500, 750 and 1000, respectively.

### CONCLUSION

Different values should be used for different 68Ga-labeled radiopharmaceuticals such as those targeting GRPR and PSMA receptors in prostate cancer. Once selected, the same value should be consistently used since SUVmax measurements differ with different values.

### **CLINICAL RELEVANCE/APPLICATION**

BSREM algorithm improves image quality. Different beta values make different image quality and different SUVmax measurements on different 68Ga-labeled radiopharmaceuticals.

# RC211-07 Fluciclovine PET/CT: Practical Approach to Interpretation

Monday, Nov. 26 9:35AM - 9:50AM Room: S505AB

### Participants

Ephraim E. Parent, MD, PhD, Ponta Vedra Beach, FL (*Presenter*) Research support, Blue Earth Diagnostics Ltd; Research support, Advanced Accelerator Applications SA

### For information about this presentation, contact:

ephraim.edward.parent@emory.edu

### LEARNING OBJECTIVES

1) Assess the appropriate clinical indications for 18F-fluciclovine PET and understand the diagnostic accuracy of 18F-fluciclovine PET for local and metastatic prostate cancer. 2) Develop 18F-fluciclovine PET protocols for image optimization. 3) Apply the correct 18F-fluciclovine PET interpretation for local and metastatic prostate cancer and benign physiologic variants.

# ABSTRACT

Anti-1-amino-3-[18F]-flurocyclobutane-1-carboxylic acid (18F-fluciclovine) is a non-naturally occurring amino acid PET radiotracer that is recently United States Food and Drug Administration approved for detection of suspected recurrent prostate cancer. The tumor imaging features of this radiotracer mirror the upregulation of transmembrane amino acid transport that occurs in prostate cancer due to increased amino acid metabolism for energy and protein synthesis. This refresher course provides an overview of 18F-fluciclovine PET diagnostic accuracy for identifying primary and metastatic disease, as well as proper 18F-fluciclovine PET imaging protocols. Correct interpretation criteria will be explored in detail to identify physiologic and pathologic 18F-fluciclovine uptake patterns and potential pitfalls.

# RC211-08 Quantitative Comparison of Standardized Uptake Values of Same-Day Randomized Ga-68 PSMA-11 PET/CT and PET/MR Scans in Recurrent Prostate Cancer Patients

Monday, Nov. 26 9:50AM - 10:00AM Room: S505AB

Participants

Anna Maria Ringheim, MSc,BEng, Sao Paulo, Brazil (*Presenter*) Nothing to Disclose Guilherme Campos, Sao Paulo, Brazil (*Abstract Co-Author*) Nothing to Disclose Karine M. Martins, MS, Sao Paulo, Brazil (*Abstract Co-Author*) Nothing to Disclose Taise Vitor, Sao Paulo, Brazil (*Abstract Co-Author*) Nothing to Disclose Marcelo L. Cunha, MD, Sao Paulo, Brazil (*Abstract Co-Author*) Nothing to Disclose Ronaldo H. Baroni, MD, Sao Paulo, Brazil (*Abstract Co-Author*) Nothing to Disclose

### For information about this presentation, contact:

anna.m.ringheim@gmail.com

## PURPOSE

To determine the reproducibility and agreement of standardized uptake values from same-day Ga-68 PSMA-11 PET/CT and PET/MR scans, randomized in order to eliminate the influence of Ga-68 PSMA-11 accumulation as a function of time, in patients with recurrent prostate cancer.

### METHOD AND MATERIALS

Eighteen patients with recurrent prostate cancer after radical prostatectomy, all with visible lesions on the PET scan, were included in this retrospective study, approved by the Institution's Ethics Committee. All patients underwent PET/CT and PET/MR scans in randomized order after intravenous injection of a single dose of Ga-68 HBED-CC-PSMA (Ga-68 PSMA-11). Volumes of interest on tumor lesions were outlined and maximum standardized uptake value (SUVmax) corrected for lean body mass was calculated. Correlation and agreement between scans were assessed by generalized linear mixed-effects models and Bland Altman analysis. A predictive model of PET/CT SUVmax was developed based on PET/MR SUVmax, patient characteristics and imaging parameters.

## RESULTS

In total, there were 34 visible lesions on the PET scans: 5 local recurrences, 22 lymph node and 7 bone metastases. SUVmax from PET/CT and PET/MR were significantly correlated, described by the following regression model equation:  $(PET/CT SUVmax) = 0.75 + 1.00^{*}$  (PET/MR SUVmax), with a coefficient of determination R2 of 0.77. Bland-Altman analysis showed that SUVmax were on average 20% higher on PET/CT than on PET/MR, with the largest percentage differences for small SUV's. The full predictive model of PET/CT SUVmax showed significant association with PET/MR SUVmax (effect 1.15 (p<0.001)), serum prostate specific antigen (effect 0.99 (p=0.053)), scan time post-injection (effect 0.98 (p=0.003)) and acquisition time per bed position (effect 1.49 (p=0.021)) with a coefficient of determination R2 of 0.85.

# CONCLUSION

SUVmax from PET/CT and PET/MR are comparable and well correlated, but should not be used interchangeably without applying a correction factor.

# **CLINICAL RELEVANCE/APPLICATION**

Since both Ga-68 PSMA-11 PET/CT and PET/MR are increasingly used in clinical practice, the reproducibility of SUVmax measurements is essential in monitoring of disease progression and response to treatment.

# RC211-09 Detection Rate of 18F-FACBC (Fluciclovine) PET/CT Scan as a Function of Prostatic Specific Antigen (PSA) Level: Initial Experience of 76 Patients with Biochemically Recurrent Prostate Cancer

Monday, Nov. 26 10:00AM - 10:10AM Room: S505AB

### Awards

**Trainee Research Prize - Resident** 

Participants

Ali Salavati, MD, MPH, Minneapolis , MN (*Presenter*) Nothing to Disclose Mehmet Gencturk, MD, Istanbul, Turkey (*Abstract Co-Author*) Nothing to Disclose Jerry W. Froelich, MD, Minneapolis, MN (*Abstract Co-Author*) Researcher, Siemens AG

### PURPOSE

In 2016, synthetic amino acid anti-1-amino-3-[18F]-flurocyclobutane-1-carboxylic acid (FACBC, Fluciclovine, Axumin) was approved by U.S. Food and Drug Administration (FDA) as a new PET tracer for the detection and localization of biochemically recurrent prostate cancer. The goal of this study was to determine the impact of PSA level on the detection rate of 18F-FACBC PET/CT.

# METHOD AND MATERIALS

After obtaining IRB approval, we retrospectively enrolled 76 patients with biochemical recurrence of prostate cancer referred for an 18F-FACBC PET/CT scan at our institution. Relevant clinical information including demographic data,PSA level, and Gleason score were collected. Images were interpreted by two experienced nuclear radiologists. Receiver operating characteristic (ROC) curve and bootstrap technique with 2000 iterations were performed to determine the optimal cutoff points of PSA as a predictor of positive and negative 18F-FACBC PET/CT scan.

### RESULTS

The detection rate of 18F-FACBC PET/CT was 67.1% (51 of 76 scans). Positive findings were detected in the prostate/bed and pelvic lymph node regions in 88% of positive scans(45 of 51); metastatic lesion outside the pelvis in 21.5% of positive scans(11 of 51), and bone metastasis in 11.7% of positive scans (6 of 51).18F-FACBC PET/CT scan detected potential sites of recurrence in 23.5% of patients when PSA is <1.0 ng/ml, 66.7 % of patients when PSA is 1.0-2.0 ng/ml, and 86.2% of patients when PSA is >2.0 ng/ml. The ROC curve analysis with bootstrapping demonstrates a PSA >3.38 ng/ml has a likelihood ratio > 10 and positive predictive value > 95% for a positive 18F-FACBC PET/CT scan. The PSA < 0.36 ng/mL has a likelihood ratio > 14 of having a negative 18F-FACBC PET/CT scan and results in positive imaging findings in <2.5% of patients.

## CONCLUSION

Given the high pretest probability of positive imaging findings in patients with PSA > 3.4 ng/ml, they benefit most from 18F-FACBC PET/CT scans. In addition, negative scans of these patients should be interpreted more cautiously. Conversely, considering the low pretest probability of positive PET/CT findings in patients with PSA < 0.36 ng/ml, these patients may benefit from a short follow-up before a diagnostic 18F-FACBC PET/CT scan.

### **CLINICAL RELEVANCE/APPLICATION**

18F-Fluciclovine is a valuable novel clinically-available PET/CT tracer for the detection and localization of biochemically recurrent prostate cancer, particularly when the PSA level is > 2 ng/ml.

# RC211-10 Role of Early Dynamic PET/CT Imaging with 68Ga-PSMA in Staging and Restaging of Prostate Cancer

Monday, Nov. 26 10:10AM - 10:20AM Room: S505AB

# Awards

**Trainee Research Prize - Resident** 

Participants Maria El Homsi, MD, Beirut, Lebanon (*Presenter*) Nothing to Disclose Andrew Barakat, MD, Beirut, Lebanon (*Abstract Co-Author*) Nothing to Disclose Mohamad B. Haidar, MD, Beirut, Lebanon (*Abstract Co-Author*) Nothing to Disclose Basel Yacoub, Beirut, Lebanon (*Abstract Co-Author*) Nothing to Disclose

## PURPOSE

Ga-68 Prostate-Specific Membrane Antigen (PSMA)PET/CT is a new tool for the detection of new and recurrent prostate cancer.Standard imaging time is 60 minutes post injection of radiotracer but some lesions may be obscured by physiologic accumulation of radiotracer in bladder. The aim of the study is to determine if the addition of early imaging at 3 and 6 minutes to standard imaging at 60 minutes can improve the detection of new and recurrent prostate cancer at Ga-68 PSMA PET/CT.

### **METHOD AND MATERIALS**

After obtaining IRB approval, retrospective review of 257 consecutive patients who underwentGa-68 PSMA PET/CT between December 2016 and July 2017 was conducted. 167 patients underwent early (3 and 6 minute) and late (60 minute) imaging. Two readers blinded to the patient's clinical information, independently reviewed the early and late images and qualitatively and quantitatively scored the visibility of prostate lesions on a scale of 1-2 (1: lesion seen, 2: lesion not seen). Qualitatively, focal uptake higher than background that did not correspond to physiologic tracer accumulation was considered cancer. Quantitatively, a cut off maximum standardized uptake value (SUVmax) of 2 was indicative of prostate cancer. Detection of prostate cancer was compared between early and late imaging using McNemar test.

# RESULTS

A total 115 patients (68.9%) had prostate cancer on imaging as seen on early (median SUVmax= 6.4) and late (median SUVmax= 8) PET/CT images. In 106/115 (64%), the cancers were seen on early and delayed imaging, in 8/115 (6.9%) the cancer was only seen on early imaging and masked by bladder activity on delayed imaging, and in 1/115(0.6%) only seen on delayed imaging. The addition of early imaging significantly improved the detection rate of prostate cancer (p=0.039).

### CONCLUSION

The addition of early imaging at 3 and 6 minutes to the standard 60 minute imaging at Ga-68 PSMA PET/CT improves the detection of prostate cancer .

### **CLINICAL RELEVANCE/APPLICATION**

Early imaging at Ga-68 PSMAPET/CT can help in the detection of prostate cancer that is obscured by the bladder activity at 60 minutes.

# RC211-11 Change in Salvage Radiotherapy Management Based On Fluciclovine (18F) PET/CT Guidance in Post-Prostatectomy Recurrent Prostate Cancer

Monday, Nov. 26 10:20AM - 10:30AM Room: S505AB

### Awards

# Student Travel Stipend Award

Participants

Olayinka A. Abiodun-Ojo, MD, MPH, Atlanta, GA (Presenter) Nothing to Disclose Ashesh B. Jani, MD, Atlanta, GA (Abstract Co-Author) Nothing to Disclose Akinyemi A. Akintayo, MD, Atlanta, GA (Abstract Co-Author) Nothing to Disclose Mehrdad Alemozaffar, Atlanta, GA (Abstract Co-Author) Nothing to Disclose Oladunni O. Akin-Akintayo, MD, MPH, Atlanta, GA (*Abstract Co-Author*) Nothing to Disclose Oluwaseun Odewole, MD, MPH, Atlanta, GA (*Abstract Co-Author*) Nothing to Disclose Funmilayo I. Tade, MD, Atlanta, GA (Abstract Co-Author) Nothing to Disclose Peter Nieh, MD, Atlanta, GA (Abstract Co-Author) Nothing to Disclose Viraj Master, MD, Atlanta, GA (Abstract Co-Author) Nothing to Disclose Pretesh Patel, Atlanta, GA (Abstract Co-Author) Nothing to Disclose Joseph W. Shelton, MD, Atlanta, GA (Abstract Co-Author) Nothing to Disclose Omer Kucuk, Atlanta, GA (Abstract Co-Author) Nothing to Disclose Zhengjia Chen, PhD, Atlanta, GA (Abstract Co-Author) Nothing to Disclose Bruce Hershatter, Atlanta, GA (Abstract Co-Author) Nothing to Disclose Bridget Fielder, Atlanta, GA (Abstract Co-Author) Nothing to Disclose Raghuveer K. Halkar, MD, Atlanta, GA (Abstract Co-Author) Research Grant, General Electric Company Research Grant, Gilead Sciences, Inc Royalties, General Electric Company Mark M. Goodman, PhD, Atlanta, GA (Abstract Co-Author) Royalties, Nihon Medi-Physics Co, Ltd David M. Schuster, MD, Decatur, GA (Abstract Co-Author) Institutional Research Grant, Nihon Medi-Physics Co, Ltd; Institutional Research Grant, Blue Earth Diagnostics Ltd; Institutional Research Grant, Advanced Accelerator Applications SA; Consultant, Syncona Ltd; ; ;

# For information about this presentation, contact:

### dschust@emory.edu

### PURPOSE

We previously reported a 40.5% post-prostatectomy salvage radiotherapy management decision change based on guidance with fluciclovine PET/CT in a trial with 87/162 accrual (Clin Nucl Med. 2017 Jan;42(1):e22-e28). We set out to determine if this finding continued at the current accrual of 145/162 patients.

### **METHOD AND MATERIALS**

145 patients with post-prostatectomy biochemical recurrence of prostate cancer and negative bone scan were randomized to undergo treatment planning based on conventional imaging (CT, MRI) or fluciclovine PET/CT in a provider-determined intention-to-treat protocol. Radiotherapy decisions before and after fluciclovine PET/CT were compared and changes in treatment decision and field were noted. Statistical significance of decision changes was determined using Clopper-Pearson (exact) binomial method with significance set at p <0.05.

### RESULTS

70/145 patients underwent fluciclovine PET. Mean PSA ( $\pm$ SD) at scan was 1.89 ( $\pm$ 4.32) ng/ml. 54/70 (77.1%) patients had a positive fluciclovine PET. Radiotherapy decision was changed in 27/70 (38.6%). Four (5.7%) had the decision for radiotherapy withdrawn after the fluciclovine PET findings of extrapelvic uptake. Radiotherapy field decision was changed in 23/66 (34.9%) remaining patients: 13/23 prostate bed only to prostate bed and pelvis; 10/23 prostate bed and pelvis to prostate bed only. There was no significant difference in mean age (62.0 vs. 61.6 years) and treatment-recurrence time interval (991.4 vs. 1403.6 days) between those with change in radiotherapy decision and those without. However, the pre-treatment PSA mean was significantly higher in those with treatment change (2.76ng/ml vs. 1.35ng/ml, p < 0.05). Changes in overall radiotherapy decision (p = 0.01) and field (p < 0.05) were statistically significant.

### CONCLUSION

Fluciclovine PET/CT had a significant effect on radiotherapy planning in post-prostatectomy patients with biochemical recurrent prostate cancer. Radiotherapy planning decision and field changes in the updated analysis is similar to the prior report. Further studies are required to determine if this change in treatment plan has an effect on clinical outcomes. Research support: NIH (R01CA169188), NCT 01666808.

### **CLINICAL RELEVANCE/APPLICATION**

Use of fluciclovine PET/CT resulted in significant change in management (38.6%) in salvage radiotherapy planning in postprostatectomy patients with recurrent prostate cancer.

# RC211-12 Impact of 68Ga-PSMA PET on the Management of Patients with Prostate Cancer: A Systematic Review and Meta-Analysis

Monday, Nov. 26 10:30AM - 10:40AM Room: S505AB

### Participants

Sungmin Woo, MD, Seoul, Korea, Republic Of (*Presenter*) Nothing to Disclose Sangwon Han, Seoul, Korea, Republic Of (*Abstract Co-Author*) Nothing to Disclose Yeon Joo Kim, Seoul, Korea, Republic Of (*Abstract Co-Author*) Nothing to Disclose Chong Hyun Suh, MD, Seoul, Korea, Republic Of (*Abstract Co-Author*) Nothing to Disclose

### PURPOSE

68Gallium prostate-specific membrane antigen positron emission tomography (68Ga-PSMA PET) is a relatively novel imaging modality for assessment of patients with prostate cancer. Recent studies have shown promising results, with their ability to detect recurrent/metastatic prostate cancer foci with superior performance than that of conventional imaging modalities (computed tomography, bone scintigraphy, and choline PET). However, the actual impact that 68Ga-PSMA PET has on management of prostate cancer patients has not been well-established. Therefore, we aimed to systematically review the literature and to perform a meta-analysis on the impact of 68Ga-PSMA PET on management of patients with prostate cancer.

# METHOD AND MATERIALS

Pubmed and EMBASE databases were systematically searched up to January 20, 2018. Studies reporting the proportion of patients with prostate cancer that experienced change in management after 68Ga-PSMA PET were included. Quality of the included studies was evaluated using the GRADE system. The proportion of management changes were pooled using a random-effects model. Subgroup analyses and meta-regression analyses was done to explore potential causes of heterogeneity.

# RESULTS

15 studies (1163 patients) were included. The pooled proportion of management changes was 54% (95% CI 47%-60%). Metaregression analyses revealed that PET-positivity was a significant factor of heterogeneity (p=0.0486). Other variables, including clinical setting, change type (intended vs implemented), responding entity (referring doctor or multidisciplinary committee), D'Amico risk, Gleason score, use of androgen deprivation therapy, PSA at initial diagnosis, pre-PET PSA, and PSA-doubling time, were not significant (p=0.2802-0.9574). In patients with biochemical failure, proportions of radiotherapy, surgery, focal therapy, and multimodal treatment increased, while those of systemic treatment and no treatment decreased after performing 68Ga-PSMA PET.

### CONCLUSION

This meta-analysis showed that 68Ga-PSMA PET had a large impact on the management of prostate cancer patients. PET-positivity affected the proportion of management changes.

# **CLINICAL RELEVANCE/APPLICATION**

We found that 68Ga-PSMA PET alters management in approximately half of the patients with prostate cancer. Studies with higher proportion of patients with 68Ga-PSMA PET-positive lesions tend to have their management altered more frequently.

# RC211-13 Clinician's Perspective: Impact and Applications

Monday, Nov. 26 10:40AM - 10:55AM Room: S505AB

Participants

Steve Cho, MD, Madison, WI (Presenter) Imaging Endpoints; General Electric Company

# For information about this presentation, contact:

scho@uwhealth.org

# LEARNING OBJECTIVES

1) Review current and emerging PET radiotracers for prostate cancer. 2) Assess how PET imaging can address unmet clinical needs in prostate cancer. 3) Address remaining and new clinical and research questions arising from these new PET radiotracers.

# RC211-14 Fluciclovine (18F) Parameters on Targeted Prostate Biopsy Associated With True Positivity in Recurrent Prostate Cancer

Participants

Olayinka A. Abiodun-Ojo, MD,MPH, Atlanta, GA (*Presenter*) Nothing to Disclose Baowei Fei, PhD, Cleveland, OH (*Abstract Co-Author*) Nothing to Disclose Akinyemi A. Akintayo, MD, Atlanta, GA (*Abstract Co-Author*) Nothing to Disclose Peter Nieh, MD, Atlanta, GA (*Abstract Co-Author*) Nothing to Disclose Viraj Master, MD, Atlanta, GA (*Abstract Co-Author*) Nothing to Disclose Funmilayo I. Tade, MD, Atlanta, GA (*Abstract Co-Author*) Nothing to Disclose Oladunni O. Akin-Akintayo, MD,MPH, Atlanta, GA (*Abstract Co-Author*) Nothing to Disclose Mehrdad Alemozaffar, Atlanta, GA (*Abstract Co-Author*) Nothing to Disclose Adeboye Osunkoya, MD, Atlanta, GA (*Abstract Co-Author*) Nothing to Disclose Mark M. Goodman, PhD, Atlanta, GA (*Abstract Co-Author*) Nothing to Disclose Mark M. Schuster, MD, Decatur, GA (*Abstract Co-Author*) Institutional Research Grant, Nihon Medi-Physics Co, Ltd; Institutional Research Grant, Blue Earth Diagnostics Ltd; Institutional Research Grant, Advanced Accelerator Applications SA; Consultant, Syncona Ltd; ; ;

# For information about this presentation, contact:

dschust@emory.edu

# PURPOSE

Fluciclovine is FDA approved for detection of recurrent prostate cancer. We set out to evaluate fluciclovine uptake parameters that correlate with true positivity for local recurrence in non-prostatectomy treated patients.

## **METHOD AND MATERIALS**

21 patients (PSA 7.4±6.8 ng/ml) with nadir PSA+2 after non-prostatectomy local therapy underwent dual time-point fluciclovine (364.1±37.7 MBq) PET/CT (4-15 minutes; 16-25 minutes) from pelvis to diaphragm. Uptake in the prostate over background was delineated and co-registered to a previously obtained planning 3-D ultrasound. Fluciclovine uptake (SUVmax) and target-to-background ratios (TBR) (SUVmax/SUVmean) of blood pool (aorta), prostate, and marrow (L3) were recorded. Uptake pattern (focal vs non-focal), subjective suspicion level [3 (equivocal), 4 (moderate), 5 (high)], and lesion location were noted. Targeted biopsies of the identified lesions with histologic analysis were completed. Statistical significance was determined using univariate regression analysis.

# RESULTS

17/50 (34.0%) targeted lesions were positive for recurrent cancer. Compared to negative lesions, targeted positive lesions had significantly (p<0.01) higher mean SUVmax of lesion ( $6.62\pm1.70 \text{ vs } 4.92\pm1.27$ ), TBR (marrow) ( $2.57\pm0.81 \text{ vs } 1.69\pm0.51$ ), and TBR (blood pool) ( $4.10\pm1.17 \text{ vs } 3.00\pm1.01$ ) at the first time-point, and remained significant at the later time-point except TBR (blood pool). Focal uptake (OR 12.07, [95% CI 2.98-48.80], p<0.01) and subjective high (5) suspicion level (OR 10.91, [95% CI 1.19-99.69], p=0.03) correlated with true positivity. All other parameters did not significantly correlate with true positivity. Of the 17 targeted lesions with focal uptake and subjective high suspicion, 11/17 (64.7%) were true positive. 16/33 (48.5%) false positive targeted lesions had evidence of prostatitis or radiation changes.

# CONCLUSION

True positivity of fluciclovine targeted prostate biopsy in non-prostatectomy treated patients correlates with focal uptake, higher SUV, target-to-background (blood pool and marrow) ratios and subjective high suspicion level. These parameters may be utilized for future modification of interpretative criteria. Research Support: NIH (CA156775, CA204254 and CA176684)

### **CLINICAL RELEVANCE/APPLICATION**

Targeted biopsy of lesions with focal uptake and subjective high suspicion on fluciclovine PET-CT increases the true positivity rate from 34.0% to 64.7% in non-prostatectomy treated patients.

### RC211-15 Evaluation of 18F-DCFPyL PSMA-Based PET/CT and mpMRI in Patients with Localized Prostate Cancer

Monday, Nov. 26 11:05AM - 11:15AM Room: S505AB

Participants

Marcin Czarniecki, MD, Bethesda, MD (Presenter) Nothing to Disclose

Stephanie A. Harmon, PhD , Bethesda, MD (Abstract Co-Author) Research funded, NCI

Esther Mena, MD, Bethesda, MD (Abstract Co-Author) Nothing to Disclose

Maria Lindenberg, MD, Bethesda, MD (Abstract Co-Author) Nothing to Disclose

Yolanda Mckinney, Bethesda, MD (Abstract Co-Author) Nothing to Disclose

Deborah Citrin, MD, Bethesda, MD (Abstract Co-Author) Nothing to Disclose

Bradford J. Wood, MD, Bethesda, MD (*Abstract Co-Author*) Researcher, Koninklijke Philips NV; Researcher, Celsion Corporation; Researcher, BTG International Ltd; Researcher, Siemens AG; Researcher, XAct Robotics; Researcher, NVIDIA Corporation; Intellectual property, Koninklijke Philips NV; Intellectual property, BTG International Ltd; Royalties, Invivo Corporation; Royalties, Koninklijke Philips NV; ; ;

Peter Pinto, Bethesda, MD (Abstract Co-Author) Nothing to Disclose

Ronnie Mease, PhD, Baltimore, MD (Abstract Co-Author) Inventor, Progenics Pharmaceuticals, Inc; Inventor, Advanced Accelerator Applications SA

Martin G. Pomper, MD, PhD, Baltimore, MD (*Abstract Co-Author*) Researcher, Progenics Pharmaceuticals, Inc; License agreement, Progenics Pharmaceuticals, Inc; Researcher, Advanced Accelerator Applications SA; License agreement, Advanced Accelerator Applications SA; Co-founder, Cancer Targeting Systems, Inc; Board Member, Cancer Targeting Systems, Inc; Researcher, Celgene Corporation, Inc; License agreement, Celgene Corporation, Inc; Co-founder, Neurly; Board Member, Neurly; Co-founder, Theraly Pharmaceuticals, Inc; Board Member, Theraly Pharmaceuticals, Inc

Peter L. Choyke, MD, Rockville, MD (*Abstract Co-Author*) Nothing to Disclose Baris Turkbey, MD, Bethesda, MD (*Abstract Co-Author*) Nothing to Disclose

### For information about this presentation, contact:

marcin.czarniecki@nih.gov

### PURPOSE

To assess the ability of 18F-DCFPyL PET/CT to predict prostate cancer Gleason grade and its role as a potential adjunct to multiparametric prostate MRI.

# METHOD AND MATERIALS

Patients with prostate cancer (PCa) underwent multi-parametric MRI (mpMRI) and 18F-DCFPyL PET/CT imaging. MpMRI lesion characteristics (PIRADS, ADCmean, ADCmin, ADC10, MRIvol) were derived manually and 18F-DCFPyL PET/CT metrics SUVmax, SUVmean, MTV and TLG (SUVmean\*MTV) were extracted from tracer-specific regions of interest (ROI). Lesion metrics were correlated with each other using the Spearman rank test, and their ability to differentiate tumor pathology Gleason grade (GG) <3 vs. GG 3-5 was performed using the Wilcoxon rank sum test.

## RESULTS

Thirteen patients with high-risk PCa were included in the study, with 25 (12 GG<3, 12 GG 3-5) lesions found across the two modalities (median age 70.6, MRI volume 62mL, and PSA 18.87ng/mL). Seven patients did not have findings suspicious for metastatic disease on 18F-DCFPyL-PET/CT. MpMRI and 18F-DCFPyL PET/CT both detected 22/25 lesions, while 3 were not detected by any of the two modalities. 18F-DCFPyL PET/CT (SUVmax, SUVmean and TLG) as well as mpMRI metrics (ADCmin and MRI size) were significantly associated with GG 3-5 pathology (p=0.017, 0.020, 0.004, 0.028, 0.008, respectively). Additionally, MRI size correlated significantly with SUVmax, MTV and TLG (p=0.01, 0.02, 0.02, respectively) and SUVmax, SUVmean correlated significantly to ADCmin. All SUV metrics correlated positively with PIRADS 5 lesions vs. the remaining categories. In some cases, MRI findings did not entirely colocalize with PET avidity indicating MRI underestimation of functional burden.

### CONCLUSION

18F-DCFPyL PET-identified prostatic lesions and mpMRI findings correlate with each other, Gleason grades and PIRADS. MpMRI may underestimate the tumor burden seen on 18F-DCFPyL PET/CT imaging, which may aid focal therapy decisions.

## **CLINICAL RELEVANCE/APPLICATION**

Quantitative metrics of 18F-DCFPyL PET/CT and mpMRI correlate well with each other and with PCa Gleason grade and PIRADS. 18F-DCFPyL PET/CT adds additional functional metrics which may be meaningful in determining tumour heterogeneity and burden.

# RC211-16 Quantification of the Pharmacokinetics of Ga-68 PSMA-11 in Prostate Cancer Patients using Hybrid Positron Emission Tomography and Magnetic Resonance Imaging

### Monday, Nov. 26 11:15AM - 11:25AM Room: S505AB

### Participants

Anna Maria Ringheim, MSc, BEng, Sao Paulo, Brazil (*Presenter*) Nothing to Disclose Guilherme Campos, Sao Paulo, Brazil (*Abstract Co-Author*) Nothing to Disclose Marcelo L. Cunha, MD, Sao Paulo, Brazil (*Abstract Co-Author*) Nothing to Disclose Karine M. Martins, MS, Sao Paulo, Brazil (*Abstract Co-Author*) Nothing to Disclose Taise Vitor, Sao Paulo, Brazil (*Abstract Co-Author*) Nothing to Disclose Marycel F. de Barboza, MSc, Sao Paulo, Brazil (*Abstract Co-Author*) Nothing to Disclose Jairo Wagner, MD, Sao Paulo, Brazil (*Abstract Co-Author*) Nothing to Disclose Ana Claudia Miranda, Sao Paulo, Brazil (*Abstract Co-Author*) Nothing to Disclose Leonardo L. Fuscaldi, PhD, Sao Paulo, Brazil (*Abstract Co-Author*) Nothing to Disclose Gustavo C. Lemos, Sao Paulo, Brazil (*Abstract Co-Author*) Nothing to Disclose Jose Roberto Colombo Jr, Sao Paulo, Brazil (*Abstract Co-Author*) Nothing to Disclose Ronaldo H. Baroni, MD, Sao Paulo, Brazil (*Abstract Co-Author*) Nothing to Disclose

## For information about this presentation, contact:

anna.m.ringheim@gmail.com

### PURPOSE

To quantify Ga-68 PSMA-11 uptake by pharmacokinetic modeling using arterial blood sampling and hybrid positron emission tomography and magnetic resonance (PET/MR) imaging in primary prostate cancer.

## **METHOD AND MATERIALS**

This observational prospective study was approved by our Institution's Ethics Committee. Eleven patients with clinically significant prostate cancer underwent a 60-minute dynamic PET/MR scan of the pelvis with an injected dose of Ga-68 HBED-CC-PSMA (Ga-68 PSMA-11). Simultaneously, axial T1 Dixon, T2 and diffusion-weighted MR images were acquired. Arterial blood activity was measured by an automatic arterial blood sampling device during the first 10 min. Manual blood samples at time points 3, 7, 15, 25, 40 and 60 min were collected for metabolite analysis and for blood to plasma transformation to derive an arterial input function. Time-activity curves of lesion, prostate and muscle were generated and mean standardized uptake values (SUVmean) calculated. An irreversible two-tissue compartment model, with rate constants K1, k2 and k3, were fitted to the data and the net influx rate Ki=K1k3/(k2+k3) was calculated. Ki was correlated to SUVmean, patient data and MR parameters.

### RESULTS

In total 13 lesions located in the prostate were identified. Ga-68 PSMA-11 was stable in-vivo, not necessitating metabolite correction. The mean plasma-to-blood ratio was 1.63, stable over time. The kinetics could be described by an irreversible two-tissue compartment model. K1, k3 and Ki were all significantly higher in lesion compared to normal tissue (p<0.05): mean K1 in lesion, prostate and muscle 0.086, 0.063 and 0.018 mL/min/mL, mean k3 in lesion, prostate and muscle 0.075, 0.033 and 0.034 min-1 and mean Ki in lesion, prostate and muscle 0.031, 0.011 and 0.003 min-1. Ki showed strong correlation with SUVmean (Spearman rho 0.92, p<0.001). There was no significant correlation between Ki and patient data and MR parameters (p<0.060).

### CONCLUSION

The kinetics of Ga-68 PSMA-11 can be described by an irreversible two-tissue compartment model. SUVmean showed strong correlation with Ki and can be used in clinical practice to quantify Ga-68 PSMA-11 uptake.

### **CLINICAL RELEVANCE/APPLICATION**

Pharmacokinetic modeling is the gold standard for PET quantification. SUV strongly correlates with net influx rate Ki and can therefore be used in clinical practice to quantify Ga-68 PSMA-11 uptake.

# RC211-17 Localization and Restaging of Carcinoma Prostate by 68Ga PSMA PET/CT in Patients with Biochemical Recurrence: A Descriptive Study

Monday, Nov. 26 11:25AM - 11:35AM Room: S505AB

Participants

Nikhil Seniaray, New Delhi, India (*Abstract Co-Author*) Nothing to Disclose Ritu Verma, New Delhi, India (*Presenter*) Nothing to Disclose Harsh Mahajan, MD, MBBS, New Delhi, India (*Abstract Co-Author*) Nothing to Disclose Vidur Mahajan, MBBS, New Delhi, India (*Abstract Co-Author*) Nothing to Disclose Sudhir Khanna, New Delhi, India (*Abstract Co-Author*) Nothing to Disclose Ethel S. Belho, New Delhi, India (*Abstract Co-Author*) Nothing to Disclose Vanshika Gupta, New Delhi, India (*Abstract Co-Author*) Nothing to Disclose Ankur Pruthi, New Delhi, India (*Abstract Co-Author*) Nothing to Disclose

# For information about this presentation, contact:

vidur@mahajanimaging.com

### PURPOSE

Prostate cancer is the most common solid cancer in men. Following definitive treatment of prostate cancer by radical prostatectomy (RP) or radiotherapy, cancer recurrence is heralded by an increase in serum prostate-specific antigen (PSA) which is called biochemical recurrence. We investigate the relationship between prostate specific antigen (PSA) level and detection of suspected cancer recurrence using 68 Ga-PSMA PET/CT in patients with biochemical recurrence after radical prostatectomy (RP) or radiotherapy.

### **METHOD AND MATERIALS**

We analyzed retrospective data of 150 men with carcinoma prostate post RP and post radiotherapy with biochemical recurrence from May 2014 to Jan 2018 by 68 Ga-PSMA PET/CT We included men with suspected recurrent prostate cancer based on an elevated post treatment PSA level. The data collected analyzed the relationship of the pre-scan PSA level to the probability of a positive scan finding for recurrent prostate cancer.

### RESULTS

Our cohort included 150 men, all had adenocarcinoma of prostate, 126/150 had a previous RP and 24/150 had prior radiotherapy. The mean PSA of the RP group was 4.8 ng/mL and 22.8 ng/mL in the radiotherapy group. In the post RP cohort, the detection rate of 68 Ga-PSMA PET/ CT was 39.3% for PSA 0.2 to <0.5 ng/mL, 45.3% for PSA 0.5 to <1 ng/mL, 88.2% for PSA 1 to <2 ng/mL and 95.5% for PSA >=2. Lymph node metastasis post RP was identified in 52% of men with suspected disease recurrence. In the post radiotherapy cohort the detection rate was 96.1% for PSA 2 to 4 ng/mL, 99.2% for PSA 4 to 6 ng/ mL and 100% for PSA >=6. Local recurrence after radiotherapy was present in 62% of the cohort and 58% had lymph node metastasis.

# CONCLUSION

68Ga-PSMA PET/CT provides a novel imaging modality for the detection of prostate cancer recurrence and metastasis. Suspected PSMA avid metastatic lesions are common and are identified at low post treatment PSA levels, which if detected will help direct appropriate salvage treatments.

# **CLINICAL RELEVANCE/APPLICATION**

PSMA PET/CT should be considered a routine part of follow-up of treated prostate cancer patients since metastasis may present with low PSA levels leading to delay in addressing relapses.

## RC211-18 68Ga-PSMA PET/PSMA for Prostate Cancer Staging Correlated to Prostatectomy Specimen

Monday, Nov. 26 11:35AM - 11:45AM Room: S505AB

Participants Thais Mussi, MD,PhD, Sao Paulo, Brazil (*Presenter*) Nothing to Disclose Marcelo L. Cunha, MD, Sao Paulo, Brazil (*Abstract Co-Author*) Nothing to Disclose Ronaldo H. Baroni, MD, Sao Paulo, Brazil (*Abstract Co-Author*) Nothing to Disclose

For information about this presentation, contact:

thaiscaldara@gmail.com

# PURPOSE

To evaluate the accuracy of 68Ga-PSMA PET/PSMA for prostate cancer staging using prostatectomy specimen as gold standard for local staging.

### **METHOD AND MATERIALS**

IRB approved retrospective study. We reviewed our database from February 2016 to February 2018 and found 214 patients who had submitted to a 68Ga-PSMA PET/PSMA and had no prior prostatectomy. 162 patients were excluded because had no prostatectomy in our hospital and eight had not performed lymphadenectomy. A total of 44 patients were included in the study.

### RESULTS

Histology in 16, 17, 5 and 6 patients were ISUP 2, 3, 4 and 5, respectively. From the 44 patients, six had lymph node uptake and ten had uptake in bone lesions suggestive of benignity/fibrous dysplasia. On pathology, tree patient had lymph nodes metastasis, not seen on PET/PSMA. Sensitivity for lymph node was 62% and specificity was 95%.

### CONCLUSION

68Ga-PSMA PET/PSMA showed high specificity for lymph node metastasis and low specificity for bone lesions.

### **CLINICAL RELEVANCE/APPLICATION**

68Ga-PSMA PET/PSMA is an advance in a new imaging method for prostate cancer staging, with high level of specificity for lymph node metastasis.

# RC211-19 Panel Discussion

Monday, Nov. 26 11:45AM - 12:00PM Room: S505AB

Participants

Nancy M. Swanston, RT, Houston, TX (*Presenter*) Nothing to Disclose Ephraim E. Parent, MD,PhD, Ponta Vedra Beach, FL (*Presenter*) Research support, Blue Earth Diagnostics Ltd; Research support, Advanced Accelerator Applications SA Steve Cho, MD, Madison, WI (*Presenter*) Imaging Endpoints; General Electric Company

# For information about this presentation, contact:

ephraim.edward.parent@emory.edu

# LEARNING OBJECTIVES

1) Assess the appropriate clinical indications for 18F-fluciclovine PET and understand the diagnostic accuracy of 18F-fluciclovine PET for local and metastatic prostate cancer. 2) Develop 18F-fluciclovine PET protocols for image optimization. 3) Apply the correct 18F-fluciclovine PET interpretation for local and metastatic prostate cancer and benign physiologic variants.

### ABSTRACT

Anti-1-amino-3-[18F]-flurocyclobutane-1-carboxylic acid (18F-fluciclovine) is a non-naturally occurring amino acid PET radiotracer that is recently United States Food and Drug Administration approved for detection of suspected recurrent prostate cancer. The tumor imaging features of this radiotracer mirror the upregulation of transmembrane amino acid transport that occurs in prostate cancer due to increased amino acid metabolism for energy and protein synthesis. This refresher course provides an overview of 18F-fluciclovine PET diagnostic accuracy for identifying primary and metastatic disease, as well as proper 18F-fluciclovine PET imaging protocols. Correct interpretation criteria will be explored in detail to identify physiologic and pathologic 18F-fluciclovine uptake patterns and potential pitfalls.



# MR Angiography: 2018 Update

Monday, Nov. 26 8:30AM - 10:00AM Room: E352



AMA PRA Category 1 Credits ™: 1.50 ARRT Category A+ Credit: 1.75

FDA Discussions may include off-label uses.

### Participants

Martin R. Prince, MD,PhD, New York, NY (*Moderator*) Patent agreement, General Electric Company; Patent agreement, Hitachi, Ltd; Patent agreement, Siemens AG; Patent agreement, Canon Medical Systems Corporation; Patent agreement, Koninklijke Philips NV; Patent agreement, Nemoto Kyorindo Co, Ltd; Patent agreement, Bayer AG; Patent agreement, Lantheus Medical Imaging, Inc; Patent agreement, Bracco Group; Patent agreement, Mallinckrodt plc; Patent agreement, Guerbet SA; Maureen N. Hood, PhD,RN, Bethesda, MD (*Moderator*) Research support, General Electric Company

### Sub-Events

## RC212A MRA Techniques

Participants

Scott B. Reeder, MD, PhD, Madison, WI (*Presenter*) Institutional research support, General Electric Company; Institutional research support, Bracco Group; Founder, Calimetrix, LLC; Shareholder, Elucent Medical; Consultant, ArTara

### **LEARNING OBJECTIVES**

1) Understand the fundamental principles of contrast enhanced MRA2) Understand the fundamental principles of non-contrast enhanced MRA3) Understand the fundamental principles of phase velocity MRA

# RC212B Thoracic MRA: Clinical Applications

Participants

P. Gabriel Peterson, MD, Bethesda, MD (Presenter) Nothing to Disclose

# For information about this presentation, contact:

paul.g.peterson3.mil@mail.mil

## LEARNING OBJECTIVES

1) Identify common clinical applications for thoracic MRA. 2) Describe the role for non-contrast versus contrast-enhanced thoracic MRA.

# RC212C Abdominal/Pelvic MRA: Clinical Applications

Participants Pamela J. Lombardi, MD, Chicago, IL (*Presenter*) Nothing to Disclose

# LEARNING OBJECTIVES

1) Describe current contrast enhanced and non contrast MR angiography techniques. 2) Present clinical applications of MR angiography. 3) Introduce future perspectives for MRA.

# RC212D MR Safety Concerns in Cardiovascular Patients

Participants Maureen N. Hood, PhD,RN, Bethesda, MD (*Presenter*) Research support, General Electric Company

# For information about this presentation, contact:

maureen.hood@usuhs.edu

### LEARNING OBJECTIVES

1) Discuss the importance of an MR Safety Program in your institution. 2) List several safety concerns in MR exams for cardiovascular patients. 3) Explain the evaluation MR safety procedures for electronic devices. 4) Describe safety concerns related passive and active cardiovascular devices.

### Active Handout: Maureen Nanette Hood

http://abstract.rsna.org/uploads/2018/18002591/RC 212D Hood MR Safety Concerns 2018 RC212D.pdf



# Pediatric Series: Pediatric Chest/Cardiovascular Imaging

Monday, Nov. 26 8:30AM - 12:00PM Room: E353B



AMA PRA Category 1 Credits ™: 3.00 ARRT Category A+ Credits: 3.75

**FDA** Discussions may include off-label uses.

### Participants

Edward Y. Lee, MD, Boston, MA (*Moderator*) Nothing to Disclose Ladonna J. Malone, MD, Aurora, CO (*Moderator*) Nothing to Disclose David M. Biko, MD, Philadelphia, PA (*Moderator*) Nothing to Disclose Randolph K. Otto, MD, Seattle, WA (*Moderator*) Nothing to Disclose Demetrios A. Raptis, MD, Saint Louis, MO (*Moderator*) Nothing to Disclose

### Sub-Events

## RC213-01 Cardiac CT in Neonates

Monday, Nov. 26 8:30AM - 8:50AM Room: E353B

Participants Ladonna J. Malone, MD, Aurora, CO (*Presenter*) Nothing to Disclose

### LEARNING OBJECTIVES

1) Describe different cardiac CT techniques used in infants with congenital heart disease. 2) Discuss the common scenarios that cardiac CT can be useful in infants including evaluation of a. systemic arteries, b. pulmonary arteries and veins, c. evaluation of common shunts performed for palliation (BT, Sano, central), d. coronary arteries, and e. Heterotaxy.

# RC213-02 Image Quality and Incidental Findings of Chest MRI in a Large Pediatric Population-Based Study

Monday, Nov. 26 8:50AM - 9:00AM Room: E353B

Participants

Alice Pittaro, Rotterdam, Netherlands (*Presenter*) Nothing to Disclose Liesbeth Duijts, Rotterdam, Netherlands (*Abstract Co-Author*) Nothing to Disclose Piotr A. Wielopolski, PhD, Rotterdam, Netherlands (*Abstract Co-Author*) Nothing to Disclose Harm A. Tiddens, MD, Rotterdam, Netherlands (*Abstract Co-Author*) Nothing to Disclose Meike W. Vernooij, MD, Rotterdam, Netherlands (*Abstract Co-Author*) Nothing to Disclose Mariette Kemner - Corput van de M.P.C., Rotterdam, Netherlands (*Abstract Co-Author*) Nothing to Disclose Vincent Jaddoe, Rotterdam, Netherlands (*Abstract Co-Author*) Nothing to Disclose Pierluigi Ciet, MD, Rotterdam, Netherlands (*Abstract Co-Author*) Nothing to Disclose

### For information about this presentation, contact:

p.ciet@erasmusmc.nl

### PURPOSE

To describe image quality (IQ) and incidental findings (IF) of chest MRI in a large pediatric cohort from a population-based prospective multi ethnic study.

# METHOD AND MATERIALS

Two end-inspiratory (INSP) and end-expiratory (EXP) breath-old chest MRI scans were performed in 2498 healthy children using a spirometry-gated 3D spoiled gradient echo sequence (TR/TE/FA/voxel-resolution=1.6ms/0.7ms/2°/2mm isotropic) in a 3 Tesla scanner. IQ was assessed using 5-point scale from poor (score 1) to excellent (score 5). IFs were classified in clinically relevant or non clinically relevant. Imaging artifacts included four main categories (motion, wrap, ghosting, low signal-to-noise ratio). Analysis was conducted by two indipendent observers. Descriptive statistic was used to assess IQ, IFs and artifacts. Inter-observer agreement of IQ was assessed with Intra-class Correlation Coefficient (ICC) and Bland-Altman plots. Significant differences between IQ-INSP and IQ-EXP were assessed with Wilcoxon test.

### RESULTS

47 children were excluded for missing data (i.e. no inspiratory or expiratory scans). Final analysis included 2451 children (median age 9.9 years, range 9.5-11.9). Median IQ was good to excellent 4.5 (Interquartile Range, IQR=4-5). Median IQ-INSP and IQ-EXP was 4.5 (IQR=4-5) for both. Despite deemed excellent, IQ-EXP was significantly lower than IQ-INSP (Z=-8.487, p<0.0001). 1,7% of the cohort subjects had clinically relevant IFs, 45% had non-clinically relevant IFs. Clinically relevant IFs included pulmonary nodules (diameter >10 mm), severe tracheomalacia (collapse>70%), severe trapped-air (>25% lung lobe volume) and congenital abnormalities (i.e. sequester). Non-clinically relevant IFs were: mild trapped-air (23,8%), atelectasis (15,4%) and mild tracheomalacia (4,5%). IQ was mostly affected by motion artifact (31,9%), fat ghosting (7,9%) or both (6,3%). Inter-observer agreement for IQ was good (ICC=0.7, 95% C.I 0.48-0.83).

### CONCLUSION

Chest MRI is a robust technique for large cohort studies in children. Clinically relevant IFs are rare in children, but a large percentage of the cohort had non-clinically relevant IFs.

## **CLINICAL RELEVANCE/APPLICATION**

Trapped-air, atelectasis and mild tracheomalacia are common non-clinically relevant incidental findings on chest MRI in healthy children.

# RC213-03 Pediatric Heart Transplant Patients Demonstrate Altered Regional Left and Right Ventricular Velocities

Monday, Nov. 26 9:00AM - 9:10AM Room: E353B

Participants

Haben Berhane, Chicago, IL (*Presenter*) Nothing to Disclose Alexander Ruh, PhD, Chicago, IL (*Abstract Co-Author*) Nothing to Disclose Joshua D. Robinson, MD, Chicago, IL (*Abstract Co-Author*) Nothing to Disclose Cynthia K. Rigsby, MD, Chicago, IL (*Abstract Co-Author*) Nothing to Disclose Michael Markl, PhD, Chicago, IL (*Abstract Co-Author*) Institutional research support, Siemens AG; Consultant, Circle Cardiovascular Imaging Inc; Nazia Husain, MBBS,MPH, Chicago, IL (*Abstract Co-Author*) Nothing to Disclose

### For information about this presentation, contact:

hberhane@luriechildrens.org

### PURPOSE

Endomyocardial biopsy is the gold standard for rejection monitoring after heart transplantation (Tx) at the expenses of invasiveness, cost and possible sampling errors. Alternatively, MRI has emerged as a potential noninvasive tool for assessing changes in left ventricular (LV) adult Tx graft structure (e.g. T2-mapping) and function (e.g. strain). However, few have studied these findings in children or explored post-Tx right ventricular (RV) function. Our goal was to apply MRI tissue phase mapping (TPM), which quantifies 3-directional biventricular myocardial velocities, to investigate LV and RV mechanics and interventricular dyssynchrony in pediatric Tx patients compared to healthy controls.

## **METHOD AND MATERIALS**

Cardiac MRI, including TPM, was performed on 1.5T system Siemens Aera for 17 pediatric Tx patients (age:  $16.1 \pm 2.9$  yrs, 9 males, time after Tx:  $5\pm5$  yrs) and 10 healthy controls (age:  $15.3 \pm 2.5$  yrs, 4 males). TPM was acquired during breath-holding in short axis orientation at base, mid, and apex (TR=20.8-24.8 ms, in-plane voxel size=1.5-2.5 mm2, slice thickness=5-8 mm, venc = 25 cm/s). TPM data analysis involved endo- and epicardium contouring and the transformation of the acquired velocities into radial, circumferential, and long-axis motion components (vr, v $\phi$ , vz). Peak systolic and diastolic vr and vz were calculated from time-velocity curves and mapped onto an extended 16+10 AHA segment LV-RV model. Peak velocity twist was quantified from the difference in v $\phi$  between base and apex. Cross-correlations between slice-averaged LV and RV velocity time courses were used to assess interventricular dyssynchrony.

### RESULTS

Global (averaged over segments) peak systolic and diastolic vz in the LV and RV were significantly lower in Tx patients compared to controls (p<0.01). RV peak twist showed significant reduction in systole (p<0.01) and diastole (p<0.05). Tx patients also showed increased interventricular circumferential (p<0.01) and long-axis (p<0.05) dyssynchrony compared to controls. Moreover, diastolic LV peak vr was inversely correlated to time after Tx (r=0.52, p=0.03).

### CONCLUSION

The findings of this feasibility study indicate the potential of TPM for noninvasive monitoring of graft function.

# **CLINICAL RELEVANCE/APPLICATION**

Tissue phase mapping can detect alterations in LV and RV myocardial velocities in pediatric Tx patients and may add to noninvasive monitoring of graft function.

# RC213-04 First Experience of Application in Pediatric Cardiac CT: 640-Slice Volume Computed Tomography Angiography in Children with Congenital Heart Disease

### Monday, Nov. 26 9:10AM - 9:20AM Room: E353B

#### Participants

Djuraeva Nigora, PhD,DSc, Tashkent, Uzbekistan (*Presenter*) Nothing to Disclose Vaxidova Nargiza, Tashkent, Uzbekistan (*Abstract Co-Author*) Nothing to Disclose Amirxamzaev Aybek, MD, Tashkent, Uzbekistan (*Abstract Co-Author*) Nothing to Disclose Sultanov Alisher, Tashkent, Uzbekistan (*Abstract Co-Author*) Nothing to Disclose Ikramov Adham, Tashkent, Uzbekistan (*Abstract Co-Author*) Nothing to Disclose Abralov Xakimjon, Tashkent, Uzbekistan (*Abstract Co-Author*) Nothing to Disclose Xakim Shamirzaev, Tashkent, Uzbekistan (*Abstract Co-Author*) Nothing to Disclose

# For information about this presentation, contact:

nika.kt@rambler.ru

### PURPOSE

to evaluate the quality of the images and radiation dose (RD) in children with congenital heart disease (CHD) with a heart rate of up to 180 beats/min.

48 patients from 1 month to 18 years, weighting 4,5 to 52 kg, heart rate 81-172 (117.3±27.26) were examined. The amount of contrast agent (CA) was 1-1.5 ml/kg, kV80/100, mA200/350, the effective radiation dose (ERD) was 0.9-3.2mSv. ERD was calculated using DLP (mGy\*cm) multiplied to e (e is the dose coefficient for the corresponding anatomical region (0.017mSv/mGy\*cm)) and multiplied by the age coefficient. Patients were divided: A - HR of up to 120beats/min(one volume scanning) (27patients 56,25%), B-HR over 120 beats/minute (two volumes) (21patients 43,75%). 5 patients underwent postoperative control CTA of the heart.

## RESULTS

RD in group A-1,57 $\pm$ 0,62mSv; B-1,84 $\pm$ 0,58, mean dispersion within the group was 0,36, intergroup dispersion 0.018, total dispersion 0.387, and the empirical correlation ratio was 0.22, which clearly demonstrates the weak effect of heart rate on the choice of the scan mode. The CTA results coincided with the intraoperative in 100% of cases.

### CONCLUSION

Volume CTA of the heart in children can adapt heart rate even 180 beats/min and provides high image quality with low RD up to 0.92mSv.

# **CLINICAL RELEVANCE/APPLICATION**

Cardiac CT in pediatric: Row-640 MSCT recomending in diagnosting and planning of surgical treatment.

RC213-05 Automatic Computation of Iso-Perimetric Ratio as Quantitative Index for Degree of Left Ventricular Trabeculation in Adolescents and Young Adults: Potential Indicator for Left Ventricular Non-Compaction

Monday, Nov. 26 9:20AM - 9:30AM Room: E353B

Participants

Amol Pednekar, PhD, Houston, TX (*Presenter*) Nothing to Disclose Siddharth P. Jadhav, MD, Houston, TX (*Abstract Co-Author*) Nothing to Disclose Cory Noel, Houston, TX (*Abstract Co-Author*) Nothing to Disclose Prakash M. Masand, MD, Houston, TX (*Abstract Co-Author*) Nothing to Disclose

## For information about this presentation, contact:

vedamol@gmail.com

### PURPOSE

The purpose of this study is to assess the discriminating power of fractal analysis and perimetric ratio to distinguish between pathologic left ventricular noncompaction (LVNC) and physiologic variant of hyper-trabeculation in bright blood cine balanced steady-state free precession (bSSFP) MR images at end-diastole using an automated analysis tool in a pediatric population.

# **METHOD AND MATERIALS**

Short-axis stack of end-diastolic balanced SSFP images from 26 (age 15±4.9, range 8-31yrs, 21m) LVNC positive (noncompacted(NC)/compacted(C) length ratio (LR)>2.3 and mass ratio(MR)>35%), 20 (age 16±6.6, range 6-35yrs, 12m) hyper trabeculated (NC/C LR<2.3 and MR>35%), and 18 (age 16±5.5, range 6-28yrs, 12m) LVNC negative (NC/C LR<2.3 and MR<35%, anomalous coronary origins or Kawasaki) patients with normal anatomy, preload and afterload, were analyzed with an automated tool. Manually drawn epicardial contours were used to automatically segment the blood pool and extract endocardial boundaries. Using blood pool edges and endocardial contour fractal dimension (FD) and iso-perimetric ratio (PR) i.e. ratio of blood pool to endocardial contour perimeter, are computed for each slice. Mean of top half - 50 percentile FD (mthFD) and cumulative PR (cPR) were used as geometric markers to quantify degree of hyper-trabeculation. Rays normal to and from epicardial contour are generated to compute Endo-blood/Epi-Endo length ratios. The 95 percentile of length ratios in apical third is used as LR.

# RESULTS

Both NC/C LR and MR increase with degree of trabeculation as a continuous spectrum. Values for both mthFD and cPR were statistically significantly higher (p<0.0001) for LVNC +ve compared to LVNC -ve subjects. However, mthFD values have overlap between LVNC +ve and -ve subjects.Values for mthFD and cPR for patients with MR>35 and LR<2.3 overlap with both LVNC +ve and LVNC -ve subjects.

### CONCLUSION

This study indicates that automatic computation of cPR can be used for quick assessment of degree of trabeculation. This quantification can serve as potential indication for LVNC which can be assessed further by manual drawings of epi- and endocardial contours to check against established diagnostic criteria

### **CLINICAL RELEVANCE/APPLICATION**

Automatic computation of cumulative iso-perimetric ratio as quantitative index for degree of trabeculation is feasible and can serve as a potential indicator for further evaluation of LVNC.

# RC213-06 Splenic Switch-Off and Hemodynamic Changes in Pediatric Adenosine Stress Perfusion Cardiac Magnetic Resonance Imaging

Monday, Nov. 26 9:30AM - 9:40AM Room: E353B

Participants

Kenneth K. Cheung, MBBS,FRCR, Toronto, ON (*Presenter*) Nothing to Disclose Lars Grosse-Wortmann, MD, Toronto, ON (*Abstract Co-Author*) Nothing to Disclose Mike Seed, MBBS, FRCR, Toronto, ON (*Abstract Co-Author*) Nothing to Disclose Shi-Joon Yoo, MD, Toronto, ON (*Abstract Co-Author*) Owner, 3D HOPE Medical; CEO, IMIB-CHD; Spouse, CEO, 3D PrintHeart;

## PURPOSE

Adenosine stress perfusion cardiac magnetic resonance imaging (CMR) is well established to be useful in detecting adult coronary artery disease. A positive drug response to adenosine is signified by an increase in heart rate and change in blood pressure (haemodynamic response). 'Splenic switch-off' (SSO) has recently been proposed as a new marker for drug response in adults. Due to the different disease spectrum and physiology, the use of adenosine as a stressor agent in children is not well established. By observing the prevalence of haemodynamic response and SSO, we aim to investigate the utility of adenosine as a stressor agent in the paediatric population.

# METHOD AND MATERIALS

Retrospective analysis of 52 studies in 48 patients of stress perfusion CMR from July 2014 to March 2018 using adenosine was performed. Visual and semi-quantitative analysis of SSO was performed. Haemodynamic changes (blood pressure and heart rate changes of more than 20% of baseline rates) and imaging findings in the stress perfusion CMR examination were correlated with presence of SSO.

### RESULTS

Splenic switch-off was visualised in 46.2% (24/52) cases, and was present in 66.7% (16/24) of patients with positive haemodynamic response. Both rates were lower than the reported rates in adults. Splenic switch-off was not associated with haemodynamic response (p=0.22). Presence of inducible stress perfusion defects was associated with positive SSO (p=0.01), but not with positive haemodynamic response (p=0.47). The optimal threshold for SIR as an indicator of SSO was 0.44 (sensitivity = 91.7%, specificity=89.3%, AUC=0.94). Use of general anaesthesia (GA) was associated with less overall haemodynamic response (p=0.01) and reduced increase in heart rate (p<0.001) on adenosine infusion, but was not associated with absence of splenic switch-off (p=0.25).

## CONCLUSION

Presence of inducible stress perfusion defects was associated with positive splenic switch-off, which may signify adequate stress response. There was a lower rate of splenic switch-off and absent association with haemodynamic response in children. Children under GA displayed less overall haemodynamic response to adenosine.

### **CLINICAL RELEVANCE/APPLICATION**

Adenosine may not be a reliable stressor agent in children. A lower incidence of splenic-switch off may infer a higher incidence of understress even with a standard pharmacological protocol.

# RC213-07 Imaging of Tetralogy of Fallot

Monday, Nov. 26 9:40AM - 10:00AM Room: E353B

Participants

Randolph K. Otto, MD, Seattle, WA (Presenter) Nothing to Disclose

# LEARNING OBJECTIVES

1) Describe the classic imaging findings in tetralogy of Fallot. 2) Recognize, differentiate, and describe common variants and anomalies with this syndrome. 3) Understand requisite imaging data used for pre-surgical or pre-interventional planning both initially and in the post-operative patient undergoing surveillance imaging. 4) List the appropriate modality and salient imaging features for reporting. 5) Review current management recommendations.

# RC213-08 Lymphatic System in Congenital Heart Disease

Monday, Nov. 26 10:20AM - 10:40AM Room: E353B

Participants

David M. Biko, MD, Philadelphia, PA (Presenter) Nothing to Disclose

## For information about this presentation, contact:

bikod@email.chop.edu

### LEARNING OBJECTIVES

1) Improve knowledge of MR techniques to image the lymphatic system in pediatric congenital heart disease. 2) Understand the relationship between the complications of surgical palliation of congenital heart disease and the lymphatic system. 3) Expand knowledge of lymphatic disorders and how they relate to congenital heart disease.

# RC213-09 PedsCheXNet: Deep Learning-Based Automated Detection of Pediatric Thoracic Diseases

Monday, Nov. 26 10:40AM - 10:50AM Room: E353B

Participants

Tae Kyung Kim, Baltimore, MD (*Abstract Co-Author*) Nothing to Disclose Paul H. Yi, MD, Baltimore, MD (*Presenter*) Nothing to Disclose Ji Won Shin, Baltimore, MD (*Abstract Co-Author*) Nothing to Disclose Jinchi Wei, Baltimore, MD (*Abstract Co-Author*) Nothing to Disclose Tae Soo Kim, Baltimore, MD (*Abstract Co-Author*) Nothing to Disclose Gregory D. Hager, PhD, MSc, Baltimore, MD (*Abstract Co-Author*) Co-founder, Clear Guide Medical LLC CEO, Clear Guide Medical LLC Haris I. Sair, MD, Baltimore, MD (*Abstract Co-Author*) Nothing to Disclose Ferdinand K. Hui, MD, Richmond, VA (*Abstract Co-Author*) Speakers Bureau, Terumo Corporation Speakers Bureau, Penumbra, Inc Stockholder, Blockade Medical Inc Cheng Ting Lin, MD, Baltimore, MD (*Abstract Co-Author*) Nothing to Disclose

### For information about this presentation, contact:

## pyi10@jhmi.edu

### PURPOSE

The purpose of this study was to develop and test the performance of a deep convolutional neural network (DCNN) called PedsCheXNet for the automated detection of pediatric thoracic diseases.

### METHOD AND MATERIALS

We obtained a subset of 5941 (5.2%) pediatric chest radiographs (CXRs) from the NIH ChestX-ray14 database, the largest publiclyavailable CXR database containing 112,120 CXRs labeled with 14 thoracic diseases. For each thoracic disease of interest, the 5941 pediatric CXRs were randomly split into training (70%), validation (10%), and test (20%) datasets. In total, we evaluated 11 diseases (Table 1), while excluding fibrosis, hernia, and pneumonia due to low number of positive cases (<30). The CXRs were used to train, validate, and test the ResNet-18 DCNN pretrained on ImageNet for each disease of interest. During each training epoch, each image was augmented by random rotations, cropping, and horizontal flipping. Receiver operating characteristic (ROC) curves with area under the curve (AUC) and standard diagnostic measures were used to evaluate the DCNNs' performance on the test datasets.

### RESULTS

Our DCNNs trained on only pediatric patients from the NIH ChestX-ray14 database for detection of thoracic pathology achieved AUCs ranging from 0.66 for atelectasis to 0.94 for pneumothorax, which are comparable to prior state-of-the-art work using the entire NIH ChestX-ray14 database (Figure 1). In some cases, such as pneumothorax, our AUC outperformed that achieved by prior work utilizing the entire database. Accuracy of each DCNN ranged from a low of 81% for infiltrate to a high of 98% for edema; in fact, infiltrate was the only DCNN to have accuracy <90%.

### CONCLUSION

PedsCheXNet is our in-house DCNN specifically trained to detect thoracic pathology utilizing a pediatric subset of the NIH ChestXray14 database. PedsCheXNet achieved similar overall performance and improved accuracy for certain diagnoses compared to prior DCNNs utilizing the entire database, demonstrating that DCNNs can optimize diagnostic accuracy when stratifying by age.

### **CLINICAL RELEVANCE/APPLICATION**

We have developed a deep convolutional neural network specifically trained to detect pediatric thoracic pathology utilizing a subset of the NIH ChestX-ray14 database with AUC as high as 0.94 for pneumothorax.

# RC213-10 Quantifying Dynamic Tracheal Collapse in Neonates with Bronchopulmonary Dysplasia Using Respiratory-gated MRI

Monday, Nov. 26 10:50AM - 11:00AM Room: E353B

Participants

Nara Ś. Higano, PhD, Cincinnati, OH (*Presenter*) Nothing to Disclose Alister Bates, PhD, Cincinnati, OH (*Abstract Co-Author*) Nothing to Disclose Robert J. Fleck JR, MD, Cincinnati, OH (*Abstract Co-Author*) Nothing to Disclose Andrew Hahn, PhD, Madison, WI (*Abstract Co-Author*) Nothing to Disclose Sean B. Fain, PhD, Madison, WI (*Abstract Co-Author*) Research Grant, General Electric Company Research Consultant, Marvel Medtech, LLC Paul Kingma, Cincinnati, OH (*Abstract Co-Author*) Nothing to Disclose Erik Hysinger, MD, Cincinnati, OH (*Abstract Co-Author*) Nothing to Disclose Jason C. Woods, PhD, Saint Louis, MO (*Abstract Co-Author*) Nothing to Disclose

### For information about this presentation, contact:

nara.higano@cchmc.org

# PURPOSE

Extremely preterm infants face serious chronic lung disease (bronchopulmonary dysplasia, BPD), often complicated by comorbid dynamic tracheal collapse (tracheomalacia, TM). Tracheostomy can be used to bypass segments of the collapsing airway or to provide long-term positive pressure to improve respiratory mechanics in patients with TM or who otherwise struggle to wean from intubated support. Bronchoscopy is the gold standard for diagnosis of airway collapse but requires sedation and increased risk to patients. We present an innovative MRI technique for quantitative evaluation of dynamic tracheal collapse in non-sedated neonates.

### **METHOD AND MATERIALS**

High-resolution (0.7mm isotropic) 3D radial ultrashort echo-time (UTE) MRI was obtained in 23 neonates (11 severe BPD, 1 moderate, 5 mild, 6 non-BPD control [4 preterm control]; gestational age 28±5 wks) on a NICU-sited 1.5T neonatal-sized scanner. Images were retrospectively gated to end-inspiration (EI) and end-expiration (EE) using the respiratory-modulated time-course of the MRI k-space center. Tracheas were segmented from gated images, and airway surfaces were geometrically analyzed to calculate minimum minor:major ratios of tracheal diameter (Rmin) at EI and EE along the trachea. MRI values of Rmin were compared to preterm subjects' clinical need for tracheostomy (required by 7 severe patients 15±13 days after MRI).

# RESULTS

EI and EE images demonstrated clear changes in tracheal lumen size during respiration. Severe BPD subjects had significantly smaller values of Rmin at EE ( $0.69\pm0.18$ ) than combined control, mild, and moderate subjects ( $0.80\pm0.04$ ; P=0.042) and also exhibited a larger Rmin range. Values of Rmin at EE significantly correlated with preterm subjects' need for tracheostomy ( $0.62\pm0.20$  and  $0.80\pm0.04$  for patients who did and did not receive tracheostomy, respectively; P=0.002).

### CONCLUSION

This work demonstrates an innovative, quantitative MRI assessment of dynamic tracheal collapse in neonates with BPD, without

requiring invasive procedures, sedation, or ionizing radiation. Excessive tracheal collapse on MRI was predictive of later tracheostomy requirement and thus has potential to be used in a comprehensive clinical evaluation of neonatal BPD.

# **CLINICAL RELEVANCE/APPLICATION**

MRI of neonates with BPD can quantify dynamic tracheal collapse, is predictive of eventual tracheostomy, and advantageously is non-invasive, non-ionizing, and does not require sedation.

# RC213-11 Kids Don't Follow the Rules: Underperformance of E-FAST in the Pediatric Population for Detection of Pneumothorax

Monday, Nov. 26 11:00AM - 11:10AM Room: E353B

Participants

Serge G. Srour, DO , Wichita, KS (*Presenter*) Nothing to Disclose Donald Vasquez, MD, Wichita, KS (*Abstract Co-Author*) Nothing to Disclose Gina Berg, PhD, Wichita, KS (*Abstract Co-Author*) Nothing to Disclose Kamran Ali, MD, Wichita, KS (*Abstract Co-Author*) Nothing to Disclose

## PURPOSE

Chest trauma is a common cause of pneumothorax in the pediatric population and is often seen associated with rib fractures and pulmonary contusions. Multiple modalities are currently used to evaluate the chest offering variable sensitivities for pneumothorax detection including CT, ultrasound, and chest x-ray. CT is currently the gold-standard for pneumothorax detection, however this modality delivers a higher radiation dose. Therefore radiation-related increased risk of cancer must be outweighed with the potential benefits. Chest ultrasound has been gaining popularity due to reports of superior sensitivity compared to the chest radiograph and it offers a desirable safety profile. The current literature describes sensitivities ranging from 58.9%-98.2%. Despite the growing body of evidence supporting its use in the adult patient, there is a paucity of supporting data in the pediatric population. Therefore we performed a single institution retrospective analysis of chest ultrasound in the trauma patient.

## METHOD AND MATERIALS

This was an Institutional Review Board approved retrospective medical record review of pediatric trauma patients that received extended focused assessment with sonography (EFAST) between May 1, 2016 and September 21, 2017. Mean comparison was evaluated using an independent samples t-test with .05 defined as statistically significant. Statistical analysis was performed including the sensitivity, specificity, and accuracy.

### RESULTS

403 of the 750 pediatric trauma patients identified underwent EFAST exam as part of the initial work up in the trauma bay. There were 226 patients (56%) whose EFAST findings were confirmed with either a chest x-ray or a CT scan. The remaining 177 (44%) were confirmed by observation and clinical outcome. A total of 11 pneumothoraces were observed of which 6 were were falsely negative on the chest ultrasound compatible with 45.5 % sensitivity and 99.2 % sensitivity.

# CONCLUSION

Although there were only a total of 11 confirmed pneumothorax cases (2.7%), chest ultrasound demonstrated a low sensitivity in the pediatric population (45.5%). Further research in the pediatric population is needed to reproduce the findings described in the adult population. Additionally there is a need for a standardized protocol which optimizes the sensitivity while maintaining a time sensitive exam in the trauma setting.

### **CLINICAL RELEVANCE/APPLICATION**

Pediatric E-fast underperforms in excluding pneumothorax.

# RC213-12 Evaluation of Respiratory Gated Stationary Digital Chest Tomosynthesis in Pediatric Cystic Fibrosis Patients

Monday, Nov. 26 11:10AM - 11:20AM Room: E353B

# Participants

Elias T. Gunnell, MD, Chapel Hill, NC (*Presenter*) Nothing to Disclose Christy Inscoe, MS, BS, Chapel Hill, NC (*Abstract Co-Author*) Nothing to Disclose Connor Puett, Chapel Hill, NC (*Abstract Co-Author*) Nothing to Disclose Benjamin D. Smith, MD, Chapel Hill, NC (*Abstract Co-Author*) Nothing to Disclose Brian Handly, MD, Chapel Hill, NC (*Abstract Co-Author*) Nothing to Disclose Lynn A. Fordham, MD, Chapel Hill, NC (*Abstract Co-Author*) Nothing to Disclose Jianping Lu, Chapel Hill, NC (*Abstract Co-Author*) Nothing to Disclose Jianping Lu, Chapel Hill, NC (*Abstract Co-Author*) Nothing to Disclose Jianping Lu, Chapel Hill, NC (*Abstract Co-Author*) Consultant, Xintek Inc; Consultant, XinVivo Inc; Consultant, XinRay Systems Inc Otto Zhou, PhD, Chapel Hill, NC (*Abstract Co-Author*) Board of Directors, XinRay Systems Inc Yueh Z. Lee, MD,PhD, Chapel Hill, NC (*Abstract Co-Author*) License agreement, XinRay Systems Inc

### For information about this presentation, contact:

elias.gunnell@gmail.com

## PURPOSE

Cystic fibrosis is a common disease in the pediatric population reliant on imaging for accurate disease assessment. During imaging extended breath holds can be challenging for younger patients. The primary goal of this study was to perform the first clinical evaluation of our prospective respiratory gated stationary digital chest tomosynthesis (RG s-DCT) system using a carbon nanotube (CNT) x-ray source array.

### **METHOD AND MATERIALS**

Pediatric CF patients undergoing indicated CXR were recruited for this study. Following CXR, patients underwent RG s-DCT using our CNT x-ray source array. Prior to imaging, the respiratory signal was obtained (DTU300 BIOPAC system) and a gating window was

selected at the inspiratory peak. Accuracy of gating was determined by comparing the relative respiratory trace height with the breath with the maximum peak height of the 29 projections. Retrospective analysis was used to remove projections with significant motion. Custom Matlab code measured diaphragm sharpness to evaluate between original s-DCT sets and motion corrected sets. A reader study was performed with three pediatric radiologists to compare CXR and s-DCT. Image quality, motion blur, and CF pathology was assessed. A Wilcoxon sign-rank test was used for statistical analysis.

## RESULTS

A total of thirteen pediatric patients were successfully imaged using our system. The average age of the patients was 9.6 +/- 3.4 years. The mean peak breath ratio was 0.89 +/- 0.06. Pixel widths of the diaphragm border were 27.08 +/- 6.20 for the original s-DCT set and 21.31 +/- 6.94 for the corrected set. Comparison yielded a t-value of -3.18, p-value of 0.0079. Summed quality and pathology assessment scores were significantly improved on motion corrected images, z-value-2.76 and p-value 0.006. Blur was also significantly decreased in corrected images, z-value -3.12 and p-value 0.002. CXR scores were significantly higher than s-DCT.

# CONCLUSION

Prospective respiratory gated tomosynthesis imaging is possible using our CNT RG s-DCT system. Precision gating and analysis of gating allows for significantly reduced respiratory motion blur. Quality and CF pathology scores determined by reader study are improved in motion corrected sets, however more work is required to reach the quality found on conventional imaging.

### **CLINICAL RELEVANCE/APPLICATION**

Respiratory gated s-DCT has the potential to be an effective method of performing CF imaging without the need for a breath hold.

# RC213-13 Magnetic Resonance T1 Mapping And Ultrashort Echo Time (UTE) Magnetic Resonance Imaging (MRI) of the Lung in the Evaluation of Early Regional Pulmonary Disease in Pediatric Cystic Fibrosis (CF) Patients: A Cross-Sectional Pilot Study

Monday, Nov. 26 11:20AM - 11:30AM Room: E353B

### Participants

Maryam Ghadimi Mahani, MD, Ann Arbor, MI (*Presenter*) Nothing to Disclose Fatima Neemuchwala, Ann Arbor, MI (*Abstract Co-Author*) Nothing to Disclose Ramon Sanchez, MD, Ann Arbor, MI (*Abstract Co-Author*) Nothing to Disclose Eunjee Lee, Ann Arbor, MI (*Abstract Co-Author*) Nothing to Disclose Yuxi Pang, PhD, Ann Arbor, MI (*Abstract Co-Author*) Nothing to Disclose Samya Z. Nasr, Ann Arbor, MI (*Abstract Co-Author*) Nothing to Disclose Craig J. Galban, PhD, Ann Arbor, MI (*Abstract Co-Author*) Nothing to Disclose Fortuna B. Aleksa, Ann Arbor, MI (*Abstract Co-Author*) Nothing to Disclose Chris A. Flask, PhD, Cleveland, OH (*Abstract Co-Author*) Nothing to Disclose

### For information about this presentation, contact:

maryamg@med.umich.edu

### PURPOSE

To compare the normalized T1 (nT1) relaxation metric and UTE MRI of the lungs in early pediatric pulmonary CF disease with healthy subjects

# METHOD AND MATERIALS

In this institutional review board- approved prospective study 5 CF patients (mean  $11 \pm 3$  years) with normal spirometry tests and 5 age and sex -matched healthy subjects (mean  $11 \pm 4$  years) were recruited. Signed informed assents/consents were obtained. Subjects completed a non-contrast chest MRI, using UTE and T1 mapping (modified look-locker inversion recovery) of the lung. Spirometry and CF Respiratory Symptom Diary (CFRSD) questionnaire were obtained on a same day. CF MRI scoring (Eichinger) was performed by two experienced pediatric radiologists blinded to the patients' clinical information. T1 mapping was used as a surrogate for perfusion images for functional scoring. A region of interest analysis on T1 mapping images was used to calculate the mean nT1 values for all lobes. The primary outcome was to assess the differences in mean nT1 and MRI scores between two groups. Correlation between the mean nT1 and MRI scoring with spirometry and CFRSD were evaluated. Reproducibility of T1 mapping images was evaluated by repeating right lung MRI. Statistical analysis was performed by t-test to compare means. A normality assumption was validated by a Shapiro-Wilk normality test. Pearson, Spearman's, and Kendall's correlation tests were conducted to evaluate relationship between two variables. P< 0.05 were considered significant.

### RESULTS

Mean nT1 values were lower in CF patients compared to healthy subjects (p<0.05). Repeat T1 mapping results of the lung were similar to the first results (p> 0.1). Negative correlation between mean nT1 and CFRSD was found (r-0.94, p 0.05). No correlation between mean nT1 and spirometry results was found. Morphologic MRI scoring in CF and healthy group was similar (p 0.11), yet the T1 scoring was different (p 0.03)

# CONCLUSION

MR T1 mapping of lung was different between our CF patients with normal spirometry and healthy subjects. Combining T1 mapping with a morphologic MRI assessment of the lung can detect early pulmonary disease in pediatric CF patients without risk of radiation or contrast agent.

# **CLINICAL RELEVANCE/APPLICATION**

MR T1 mapping of the lung detects early regional pulmonary CF disease on MRI, before morphologic changes. This can be used to individualize treatment and introduce therapies before irreversible lung damage occurs.

# RC213-15 Pediatric Cardiac Masses

Monday, Nov. 26 11:40AM - 12:00PM Room: E353B

Participants Demetrios A. Raptis, MD, Saint Louis, MO (*Presenter*) Nothing to Disclose

# LEARNING OBJECTIVES

1. Review the more commonly encountered pediatric cardiac masses2. Distinguish rare tumors and mimickers from the common pediatric cardiac tumors3. Develop an age and location based approach for evaluation of cardiac tumors

# LEARNING OBJECTIVES

1) Review the commonly encountered cardiac masses in the pediatric patient and their CT and MRI imaging findings. 2) Develop a differential diagnosis for pediatric cardiac masses based on age, location, and imaging findings. 3) Discuss tips for applying CT and MRI to evaluate pediatric cardiac masses.



# **Interventional Series: Embolotherapy**

Monday, Nov. 26 8:30AM - 12:00PM Room: E350

IR AMA PRA Category 1 Credits ™: 3.25 ARRT Category A+ Credits: 3.75

FDA Discussions may include off-label uses.

### Participants

Wael E. Saad, MBBCh, Ann Arbor, MI (*Moderator*) Speaker, W. L. Gore & Associates, Inc; Consultant, Siemens AG Laura K. Findeiss, MD, Atlanta, GA (*Moderator*) Nothing to Disclose

### For information about this presentation, contact:

wspikes@yahoo.com

### LEARNING OBJECTIVES

1) Describe rationale of bariatric embolization. 2) Explain the rationale and treatment of high flow malformations. 3) Describe the preparation of cyanoacrylates for embolization. 4) List two complications related to embolization. 5) Recognize the significance of Type III endoleaks. 6) Describe approach to treatment of visceral aneurysms.

### Sub-Events

### RC214-01 Embolization of Hemorrhoids

Monday, Nov. 26 8:30AM - 8:45AM Room: E350

Participants

Farouk Tradi, MBBS, Marseille, France (Presenter) Nothing to Disclose

### LEARNING OBJECTIVES

1) Describe the anatomy of superior rectal arteries. 2) List the indications of embolization of hemorrhoids. 3) Explain the results of embolization of hemorrhoids.

## RC214-02 Advanced Endoleak Treatment

Monday, Nov. 26 8:45AM - 9:00AM Room: E350

Participants Laura K. Findeiss, MD, Atlanta, GA (*Presenter*) Nothing to Disclose

For information about this presentation, contact:

lfindei@emory.edu

## LEARNING OBJECTIVES

1) To be able to asses the options for access to the source of an endoleak for treatment. 2) To be able to apply knowledge of the behavior of flow channels to select locations for embolization.

# RC214-03 TIPS Reduction: A Revising Concept

Monday, Nov. 26 9:00AM - 9:10AM Room: E350

Participants Rakesh K. Varma, MD, Birmingham, AL (*Presenter*) Nothing to Disclose Alex El-Ali, MD, Pittsburgh, PA (*Abstract Co-Author*) Nothing to Disclose Ahmed K. Abdel Aal, MD, PhD, Birmingham, AL (*Abstract Co-Author*) Consultant, Abbott Laboratories; Consultant, Baxter International Inc; Consultant, C. R. Bard, Inc; Consultant, Boston Scientific Corporation; Consultant, W. L. Gore & Associates, Inc; Consultant, Sirtex Medical Ltd Avinash N. Medsinge, MBBS, MD, Cleveland, OH (*Abstract Co-Author*) Nothing to Disclose

### For information about this presentation, contact:

rvarma@uabmc.edu

### PURPOSE

TIPS reduction/occlusion remains a favored option for patients with adverse outcomes from TIPS placement (i.e hepatic encephalopathy and acute hepatic failure)refractory to medical therapy. Herein we review the available data substantiating this practice and present our single-center experience, specifically assessing the role of pre-operative evaluation on patient selection.

### METHOD AND MATERIALS

Single center retrospective review was performed for cases of TIPS reduction/occlusion over the past 10 years. Only cases utilizing covered stents grafts were included for review. Clinical data related to their TIPS reduction were gathered from the medical record (including MELD, NH3, hepatic encephalopathy grade and survival). Two-tailed paired students T test when applicable.

## RESULTS

Out of a total of 157 TIPS revisions, 7 patient underwent TIPS reduction/occlusion.1 patient was female. Average age was 64. Methods for treatment included placement of a parallel stent graft or an amplatzer plug (TIPS occlusion).Technical success was 100%. Average MELD at reduction was 28 (range: 15-49). Average survival after intervention was 154 days. In fact, if the single surviving patient is removed from the series (MELD=15, currently at over 2 years survival), the average survival plummets to 38 days. 4 patients had significant decreases in serum NH3 after TIPS reduction (p0.05). None of the patients with MELD > 20 and refractory encephalopathy had complete improvement in mental status. No patients had significant decreases in their MELD score post TIPS reduction. Only a weak correlation existed between MELD and average survival (r2=0.23), all 4 patients with MELD score > 20 survived less than 20 days after their TIPS intervention.

### CONCLUSION

Our cohort had signifcantly worse clinical outcomes than reported in the literature. This is attributable to the inherently sicker patients included in this review with higher MELD score>20. None of these patients with MELD >20 and refractory encephalopathy had clinical improvement in mental status with overall survival less than 20 days, post reduction. TIPS reduction/occlusion in patients with high MELD score and refractory encephalopathy have guarded outcomes. Larger cohorts need to be evaluated to validate the conclusion.

# **CLINICAL RELEVANCE/APPLICATION**

TIPS reduction/occlusion for patient with high MELD scores for refractory encephalopathy or acute hepatic failure have guarded outcomes.

## RC214-04 Bioengineered Liquid Embolic For Vascular Embolization

Monday, Nov. 26 9:10AM - 9:20AM Room: E350

Participants

Hassan Albadawi, MD, Phoenix, AZ (*Abstract Co-Author*) Nothing to Disclose Avery A. Witting, Phoenix, AZ (*Abstract Co-Author*) Nothing to Disclose Patrick T. Hangge, MD, Phoenix, AZ (*Abstract Co-Author*) Nothing to Disclose Ali Khademhosseini, PhD, Boston, MA (*Abstract Co-Author*) Nothing to Disclose Rahmi Oklu, MD,PhD, Phoenix, AZ (*Presenter*) Nothing to Disclose

### For information about this presentation, contact:

Oklu.rahmi@mayo.edu

## PURPOSE

We developed a novel class of hemostatic shear-thinning biomaterials (STB) with unique properties. The goal of this study was to examine the embolic property in a model of arterial embolization in rats to rule out STB breakdown/fragmentation that can potentially cause non-target emoblization.

## **METHOD AND MATERIALS**

Rats underwent unilaterial femoral artery (FA) injection with STB containing Iohexol. Hind limb microperfusion was measured using laser speckle imaging. FA tissue was harvested at 0, 3, 7, 21, days after STB injection; extensive histologic, immunohistochemichal and micro-computed tomography (micro-CT) sudies were performed. High resolution micro-CT images of fixed FA tissues were aquired and reconstructed using SkyScan-1275 scanner at 10µm. Structural analyses was performed on binarized volume of interest of each scan with standardized global theshold for all frames. In addition, cytokine arrays were analyzed.

### RESULTS

STB injection caused 50% decrease in hind limb perfusion that persisted for 21 days after surgery (p=0.0001); however, digital perfusion was preserved without necrosis. Micro-CT imaging showed intact STB casting FA lumen which remodels by 21 days after injection. Micro-CT structural analysis revealed an increase in surface to volume ratio (p=0.006), surface convexity index (p=0.002), and structure model index (p=0.037) at 21 days compared to baseline at 0 days after injection. Hisology revealed ongoing STB degradation and intraluminal remodling with transient increase in inflammatory cells infiltrated at 3 days and granulation tissue formation at 21 days after injection.

### CONCLUSION

STB arterial injection led to persistent focal embolization of FA without migration or fragmentation; there were no distal limb perfusion deficits and motor function was unchanged. Extensive Micro-CT and histologic and cytokine sudies revealed STB biocompatability and biodegradation consistent with expected safety profile. This study suggests STB can be used as a permanent or potentially reversible biocompatable liquid embolic agent.

# **CLINICAL RELEVANCE/APPLICATION**

This novel embolic biomaterial may be an effective embolization agent, which can be delivered through clinical catheters using image guided minimally invasive techniques.

# RC214-05 AVM Embolization

Monday, Nov. 26 9:20AM - 9:35AM Room: E350

#### Participants

William S. Rilling, MD, Milwaukee, WI (*Presenter*) Research support, B. Braun Melsungen AG; Research support, Sirtex Medical Ltd; Research support, Siemens AG; Consultant, B. Braun Melsungen AG; Consultant, Cook Group Incorporated ; Consultant, Terumo

Corporation; Advisory Board, Terumo Corporation

### LEARNING OBJECTIVES

View learning objectives under main course title.

### RC214-06 Bariatric Embolization

Monday, Nov. 26 9:35AM - 9:50AM Room: E350

Participants

Jafar Golzarian, MD, Minneapolis, MN (*Presenter*) Officer, EmboMedics Inc; Consultant, Boston Scientific Corporation; Consultant, Medtronic plc; Consultant, Penumbra, Inc

# LEARNING OBJECTIVES

1) Understand the rationale for GAE. 2) Review the state of the results. 3) Discuss future directions.

# RC214-07 Clinical Value of C-Arm Cone-Beam CT in Patients with Hemoptysis for Intra-Procedural Bronchial Artery Embolization Planning

Monday, Nov. 26 9:50AM - 10:00AM Room: E350

Participants

Tanja Zitzelsberger, MD, Tuebingen, Germany (*Presenter*) Nothing to Disclose Ulrich Grosse, MD, Tuebingen, Germany (*Abstract Co-Author*) Nothing to Disclose Gerd Grozinger, MD, Tuebingen, Germany (*Abstract Co-Author*) Nothing to Disclose Roland Syha, MD, Tuebingen, Germany (*Abstract Co-Author*) Nothing to Disclose Dominik Ketelsen, MD, Tuebingen, Germany (*Abstract Co-Author*) Nothing to Disclose Sasan Partovi, MD, Cleveland, OH (*Abstract Co-Author*) Nothing to Disclose Konstantin Nikolaou, MD, Tuebingen, Germany (*Abstract Co-Author*) Nothing to Disclose Speaker Bureau, Bayer AG Rudiger Hoffmann, Tubingen, Germany (*Abstract Co-Author*) Nothing to Disclose

### PURPOSE

Pulmonary hemoptysis is a potentially life-threatening symptom and frequently a sign for underlying severe pulmonary disease. Bronchial artery embolization has been established as a first line approach in pulmonary hemoptysis. Purpose of this study was to evaluate the clinical value of CBCT for embolization procedures in unclear detection of the bronchial arteries (BA) on pre-operative imaging.

### METHOD AND MATERIALS

From 11/2016 to 07/2017, 17 patients (64.3±14.7years) with haemoptysis underwent BAE including pre-interventional CT, angiography and CBCT during the procedure. CBCT, angiography and CT were independently evaluated by two interventional radiologists with limited experience (1 and 3 years) with regard to image quality, number and origin of BA and diagnostic confidence. Consensus reading by two experienced interventional radiologists of all available data served as a gold standard (GS). 17 patients who underwent BAE without CBCT guidance served as controls regarding procedural time and number of acquired angiographic series. Spearman rank correlation and Wilcoxon signed-rank test was performed.

# RESULTS

Both readers showed a statistically significant increase in diagnostic confidence for CBCT compared to pre-procedural CT (A: p=0.003; B: p=0.03) and compared to angiography (A&B: p<0.001). Regarding the number of detected BA, correlation coefficient between GS and CBCT was: r=0.8553 (A), r=0.8773 (B); GS and pre-procedural CT: r=0.2504 (A), r=0.3174 (B); GS and angiography: r=0.2901 (A); r=0.4292 (B). Time to BA embolization was  $32.6\pm12.5$ min in the group with CBCT (control group  $38.5\pm24.6$ min; p=0.7204). Significantly less angiographic series were acquired when utilizing CBCT ( $1.3\pm0.7$  vs.  $3.6\pm2.9$ ; p=0.0029). Mean cumulative dose area product didn't show any significant difference between angiography with CBCT ( $2495.4 \pm 1428.5 \mu$ Gym<sup>2</sup>) and without CBCT ( $2347.2 \pm 1984.9 \mu$ Gym<sup>2</sup>, p=0.6745).

### CONCLUSION

In patients with hemoptysis and pre-procedural CT revealing unclear visualization of bronchial arteries, CBCT is a helpful and reliable technique for improving detection of bronchial arteries and is particularly beneficial for unexperienced interventional radiologists.

# **CLINICAL RELEVANCE/APPLICATION**

This study showed that utilizing CBCT decreased the number of DSA until successful selection of the target bronchial artery. Therefore, especially less experienced interventional radiologists are likely to benefit from CBCT.

# **RC214-08** Embolization in the Trauma Patient

Monday, Nov. 26 10:00AM - 10:15AM Room: E350

Participants

Ahmed K. Abdel Aal, MD, PhD, Birmingham, AL (*Presenter*) Consultant, Abbott Laboratories; Consultant, Baxter International Inc; Consultant, C. R. Bard, Inc; Consultant, Boston Scientific Corporation; Consultant, W. L. Gore & Associates, Inc; Consultant, Sirtex Medical Ltd

### For information about this presentation, contact:

akamel@uabmc.edu

### **LEARNING OBJECTIVES**

1) The angiographic findings in trauma patients. 2) The different modalities & materials used in treatment of trauma patients. 3) The outcomes of interventional treatment in trauma patients.

# RC214-09 Prophylactic Embolization Pre-Y90

Monday, Nov. 26 10:30AM - 10:45AM Room: E350

Participants Naganathan B. Mani, MD, Chesterfield, MO (*Presenter*) Nothing to Disclose

# LEARNING OBJECTIVES

1) Understand the rationale of prophylactic embolization prior to Y90 treatment. 2) Have a basic understanding of the arterial anatomy relevant to Y90 and specific arteries of interest. 3) Tips and techniques to achieve a safe embolization of hepatoenteric branches. 4) Complications associated with prophylactic embolization. 5) Consensus/update of literature on prophylactic embolization prior to Y90. 6) Devices used to avoid doing prophylactic embolization.

# RC214-10 Cost-Effectiveness of Steerable Microcatheter Use in Super-selective Angiography and/or Embolization

Monday, Nov. 26 10:45AM - 10:55AM Room: E350

Participants Jung H. Yun, Closter, NJ (*Presenter*) Nothing to Disclose Abieyuwa Eweka, MD, Mineola, NY (*Abstract Co-Author*) Nothing to Disclose Jonathan Minkin, Mineola, NY (*Abstract Co-Author*) Nothing to Disclose Jason C. Hoffmann, MD, Mineola, NY (*Abstract Co-Author*) Speakers Bureau, Merit Medical Systems, Inc; ;

### For information about this presentation, contact:

Jason.Hoffmann@nyulangone.org

### PURPOSE

To perform a cost analysis comparing steerable microcatheter (SM) and conventional microcatheter (CM) use in moderate and highly difficult vessel selection.

### **METHOD AND MATERIALS**

IRB-approved single institution prospective cohort analysis of 40 complex angiographic procedures with superselective microcatheter use during a 3-month period in 2017 was performed. Data collected included number and types of microcatheters and microwires used, procedure time, radiation exposure index (dose area product/DAP), time to target vessel selection (TTVS), cost associated with microcatheter/wire use, and time-specific room-related cost (cost per minute to run room). Multivariate statistical analyses were conducted with Microsoft Excel (Microsoft, Redmond, WA). Discrete variables between SM and CM use were evaluated by Wilcoxon and two-tailed t-test. Statistical significance was expressed as a P value of <.05.

# RESULTS

A SM (SwiftNINJA, Merit Medical, South Jordan, UT, USA) was used to select 46 vessels in 20 patients. One or more CMs were used in 20 patients to select 34 vessels. Mean vessel selection cost specific to microcatheter and microwire use was \$1914.81 (SD \$242.03) in the SM group and \$878.69 (SD \$371.02) in the CM group (P<.05). Mean cost associated with procedure time was \$14,319.5 (SD \$3,715.31) in the SM group and \$19,871.06 (SD \$7652.67) in the CM group (P<.05). When combining these variables, the mean total adjusted cost was \$16,234.31 (SD \$3,789.58) in the SM group and \$20,749.75 (SD \$7,886.57) in the CM group (P<.05). Median TTVS was 12 seconds (range 4-155 seconds) in the SM group and 47.5 seconds (range 12-480 seconds) in the CM group (P<.001). No guidewire was used when selecting 33 SM vessels, with median guidewire use of 0 in the SM group and 2 in the CM group (P<.001). Median total procedure time in the SM group was 75 minutes and 112 minutes in the CM group (P=0.03). Median DAP (microGray.m2) was 26,948 in the SM group and 30,904 in the CM group (P=0.29).

### CONCLUSION

When taking into consideration the dollar value associated with procedural efficiency and resulting procedure room cost, utilization of a steerable microcatheter leads to cost savings in appropriately selected superselective angiography cases.

# **CLINICAL RELEVANCE/APPLICATION**

Steerable microcatheter benefits include improved procedural efficiency, shorter TTVS, and an overall cost benefit that is driven by resultant shorter procedure times and improved efficiency.

# RC214-11 Single-Center Experience of Endovascular Repair of 40 Visceral Artery Aneurysms (VAAs) and Pseudoaneurysms (VAPAs) with the Viabahn Stent-Graft: Technical Aspects, Clinical Outcome, and Mid-Term Patency

Monday, Nov. 26 10:55AM - 11:05AM Room: E350

Participants

Luigi Augello, MD, Milan, Italy (*Presenter*) Nothing to Disclose Massimo Venturini, MD, Milano, Italy (*Abstract Co-Author*) Nothing to Disclose Paolo Marra, Milan, Italy (*Abstract Co-Author*) Nothing to Disclose Simone Gusmini, MD, Milan, Italy (*Abstract Co-Author*) Nothing to Disclose Francesco A. De Cobelli, MD, Milan, Italy (*Abstract Co-Author*) Nothing to Disclose Alessandro Del Maschio, MD, Milan, Italy (*Abstract Co-Author*) Nothing to Disclose

#### PURPOSE

Endovascular repair of VAAs and VAPAs with stent-grafting (SG) can simultaneously allow aneurysm exclusion and vessel preservation, minimizing the risk of ischemic complications. Our aim was to report endovascular repair of 40 VAAs and VAPAs with the Viabahn stent-graft, focusing on technical aspects, clinical outcome and mid-term patency.

Consecutive patients affected by VAAs-VAPAs and submitted to SG with the self-expandable Viabahn stent-graft (Gore) were retrospectively analyzed. Aneurysm type, patient number, SG clinical setting, procedural data, peri-procedural complications, technical success, 30-day clinical success, 30-day mortality and follow-up period (aneurysm exclusion, stent-graft patency, ischemic complications) were assessed.

### RESULTS

SG was performed in 40 patients (24 VAPAs/16 VAAs) and in 44 procedures (25 in emergency, 19 in elective treatments), via transfemoral in 37 cases (transaxillary in 7 cases). One peri-procedural complication was recorded (a splenic artery dissection successfully converted to transcatheter embolization). The overall technical and clinical success rates were, respectively, 96 and 84%, with excellent trend in elective treatments (both 100%). Overall 30-day mortality was 12.5% (septic shock after pancreatic surgery). Stent-graft thrombosis occurred in 2 patients within 3 months, with aneurysm exclusion and without ischemic complications. Stent-graft patency and aneurysm exclusion were confirmed at 6, 12 and 36 months in 18, 12 and 7 patients, respectively.

#### CONCLUSION

SG of VAAs and VAPAs was safe and effective, particularly in elective treatments. The Viabahn stent-graft, flexible and without shape memory, is suitable for endovascular repair of tortuous visceral arteries.

### **CLINICAL RELEVANCE/APPLICATION**

The self-expandable peripheral Viabahn SG is suitable for the endovascular repair of VAAs and VAPAs.

#### RC214-12 Prostate Embolization: Lessons Learned

Monday, Nov. 26 11:05AM - 11:20AM Room: E350

#### Participants

Alex Kim, MD, Bethesda, MD (*Presenter*) Research Grant, Surefire Medical, Inc; Speakers Bureau, Surefire Medical, Inc; Advisory Board, Surefire Medical, Inc; Stockholder, Surefire Medical, Inc; Speakers Bureau, Sirtex Medical Ltd; Proctor, Sirtex Medical Ltd; Stockholder, Pfizer Inc; ;

### **LEARNING OBJECTIVES**

To review the latest literature, technical details and potential complications related to PAE.

### RC214-13 Embolization: New Tools and Techniques

Monday, Nov. 26 11:20AM - 11:35AM Room: E350

Participants

D. T. Johnson, MD, PhD, South San Francisco, CA (*Presenter*) Speaker, Surefire Medical, Inc; Consultant, Surefire Medical, Inc; Advisory Board, Bristol-Myers Squibb Company; Speaker, BTG International Ltd; Advisory Board, Boston Scientific Corporation; Advisory Board, Merck & Co, Inc; Advisory Board, Dova Pharmaceuticals

### For information about this presentation, contact:

thor.johnson@ucdenver.edu

### LEARNING OBJECTIVES

Learners during this session should be able to describe the currently available embolic materials for chemoembolization and be able to describe the proper uses, advantages, and drawbacks for these treatments.

#### ABSTRACT

There are several choices for treatment of tumors in the liver presently. This presentation seeks to describe the differences of the devices available based on characteristics and performance as well as new devices available for delivery.

# RC214-14 Body Composition Changes at Computed Tomography after Left Gastric Artery Embolization in Overweight and Obese Individuals

Monday, Nov. 26 11:35AM - 11:45AM Room: E350

# Awards

### **Student Travel Stipend Award**

Participants Edwin A. Takahashi, MD, Rochester, MN (*Presenter*) Nothing to Disclose Naoki Takahashi, MD, Rochester, MN (*Abstract Co-Author*) Nothing to Disclose Chris Reisenauer, MD, Rochester, MN (*Abstract Co-Author*) Nothing to Disclose Michael R. Moynagh, MD, FFR(RCSI), Dublin 7, Ireland (*Abstract Co-Author*) Nothing to Disclose Sanjay Misra, MD, Rochester, MN (*Abstract Co-Author*) Cardinal Health, Inc

# For information about this presentation, contact:

takahashi.edwin@mayo.edu

# PURPOSE

Left gastric artery embolization (LGAE) is currently under investigation as a potential bariatric therapy. This study aimed to characterize body composition changes in overweight and obese individuals who underwent LGAE.

# METHOD AND MATERIALS

Institutional review board approval was obtained for this study. Eighty-nine patients who underwent LGAE for gastric bleeding

between 1/2006 and 3/2018 were retrospectively reviewed. Of these, 61 patients were excluded for unavailable imaging or followup and 12 more patients were excluded for body mass index (BMI) below 25 kg/m2. Computed tomography body composition parameters were analyzed at the L1, L3 and L5 lumbar levels in the remaining 16 overweight or obese patients with semiautomated imaging processing algorithms (MATLAB 13.0, Math Works, MA). Adipose tissue and skeletal muscle area were measured using threshold attenuation values between -190 to -30 Hounsfield Units (HU) and -29 to +150 HU, respectively. Total body fat index (BFI), subcutaneous fat index (SFI), visceral fat index (VFI) and skeletal muscle index (SMI) were determined ([tissue area (cm)]2/[height (m)]2) at each lumbar level and summed. Excess body weight (EBW) was determined based on the Lorentz formula for ideal body weight. Changes in weight and body composition were analyzed with either Wilcoxon signed-rank test or paired Student's t tests based on the normality of the distributions.

### RESULTS

Mean follow-up was  $1.5 \pm 0.8$  months. Mean weight and body composition parameters pre-LGAE vs. post-LGAE as well as per cent change were calculated for body weight (87.9±12.5 vs. 82.3±13.9 kg, -6.4%, p=0.03), BMI (30.0±4.3 vs. 28.3±4.9 kg/m2, -6.3%, p=0.005), EBW (23.3±10.6 vs. 17.7±12.6 kg, -24.1%, p=0.003), BFI (128.6±54.7 vs 123.9±59.5 cm2/m2, -3.7%, p=0.03), SFI (81.7±44.5 vs. 78.4±43.7 cm2/m2, -4.1%, p=0.03), VFI (35.8±17.8 vs. 34.3±21.6 cm2/m2, -4.1%, P=0.13) and SMI (44.5±7.2 vs. 41.5±6.9 cm2/m2, -6.8%, p<0.001).

### CONCLUSION

Overweight and obese individuals who underwent LGAE had significant weight loss as a result of decreased body fat and skeletal muscle. However, visceral fat did not significantly decrease over the course of follow-up.

# **CLINICAL RELEVANCE/APPLICATION**

This study quantitatively characterized changes in body composition as they pertain to weight loss after LGAE and highlights how this procedure may affect body fat and muscle mass.

### **Honored Educators**

Presenters or authors on this event have been recognized as RSNA Honored Educators for participating in multiple qualifying educational activities. Honored Educators are invested in furthering the profession of radiology by delivering high-quality educational content in their field of study. Learn how you can become an honored educator by visiting the website at: https://www.rsna.org/Honored-Educator-Award/ Naoki Takahashi, MD - 2012 Honored Educator

# RC214-15 Anatomy and Basic Technique for BRTO/BATO

Monday, Nov. 26 11:45AM - 12:00PM Room: E350

#### Participants

Wael E. Saad, MBBCh, Ann Arbor, MI (Presenter) Speaker, W. L. Gore & Associates, Inc; Consultant, Siemens AG

# LEARNING OBJECTIVES

1) To recognize standard variceal inflow and outflow anatomy. 2) To understand to basic principles that underlie variceal obliteration. 3) To be familiar with standard technical approaches to variceal obliteration.



Breast Series: Hot Topics (The In-Person Presentation is Supported by an Unrestricted Educational Grant from Hologic)

Monday, Nov. 26 8:30AM - 12:00PM Room: Arie Crown Theater



AMA PRA Category 1 Credits ™: 3.50 ARRT Category A+ Credits: 4.00

**FDA** Discussions may include off-label uses.

### Participants

Linda Moy, MD, New York, NY (Moderator) Nothing to Disclose

Fiona J. Gilbert, MD, Cambridge, United Kingdom (*Moderator*) Research Grant, Hologic, Inc; Research Grant, General Electric Company; Research Grant, GlaxoSmithKline plc; Research Consultant, Alphabet Inc

### Sub-Events

RC215-01 Radiomics

Monday, Nov. 26 8:30AM - 8:50AM Room: Arie Crown Theater

Participants Karen Drukker, PhD, Chicago, IL (*Presenter*) Royalties, Hologic, Inc

For information about this presentation, contact:

kdrukker@uchicago.edu

### **Active Handout:Karen Drukker**

http://abstract.rsna.org/uploads/2018/18000478/RSNA2018\_Drukker\_Handout RC215-01.pdf

### LEARNING OBJECTIVES

1) Identify the scientific premise, motivation, and increasing role of radiomics in medical imaging. 2) Compare 'conventional' radiomics methods and deep learning-based radiomics methods. 3) Assess some of the challenges for radiomics-based decision support systems in becoming powerful players in modern precision medicine.

### RC215-02 Quantitative Diffusion-Weighted MRI of Estrogen Receptor-Positive, Lymph Node-Negative Invasive Breast Cancer: Association between Whole-Lesion Apparent Diffusion Coefficient Metrics and Recurrence Risk

Monday, Nov. 26 8:50AM - 9:00AM Room: Arie Crown Theater

Participants

Jin You Kim, MD, Busan, Korea, Republic Of (*Presenter*) Nothing to Disclose Lee Hwangbo, MD, Pusan, Korea, Republic Of (*Abstract Co-Author*) Nothing to Disclose Jin Joo Kim, MD, Busan, Korea, Republic Of (*Abstract Co-Author*) Nothing to Disclose Suk Kim, MD, Pusan, Korea, Republic Of (*Abstract Co-Author*) Nothing to Disclose

For information about this presentation, contact:

youdosa@naver.com

### PURPOSE

To investigate possible associations between quantitative apparent diffusion coefficient (ADC) metrics derived from whole-lesion histogram analysis and breast cancer recurrence risk in patients with estrogen receptor (ER)-positive, lymph node-negative invasive breast cancer who underwent the Oncotype DX assay.

### **METHOD AND MATERIALS**

Institutional review board approval was obtained for this retrospective study, which was conducted on 74 women (mean age, 49.3 years) with ER-positive, lymph node-negative invasive breast cancer who underwent the Oncotype DX assay and preoperative diffusion-weighted MRI from July 2015 to January 2018. Histogram analysis of pixel-based ADC data of whole tumors was performed by two radiologists using a software tool and various ADC histogram parameters (mean, minimum, maximum, and 5th, 25th, 50th, 75th, and 95th percentile ADCs) were extracted. The ADC difference value (defined as the difference between minimum and maximum ADC) was calculated to assess intratumoral heterogeneity. Associations between quantitative ADC metrics and Oncotype DX risk groups (low [recurrence score (RS) <18], intermediate (RS 18-30), and high [RS >30]) were evaluated by receiver operating characteristic (ROC) curve and logistic regression analyses.

### RESULTS

Whole-lesion histogram analysis showed minimum ADCs, maximum ADCs, and ADC difference values were significantly different between low and non-low (ie, intermediate and high) risk groups (0.604, 1.478, and  $0.874 \times 10$ -3mm2/s versus 0.374, 1.687, and

 $1.321 \times 10$ -3mm2/s, respectively; P<0.001, P=0.010, and P<0.001, respectively). The ADC difference value yielded the largest area under the ROC curve (0.771; 95% confidence interval [CI]: 0.650, 0.891; P<0.001) for differentiating the two groups. Multivariate regression analysis showed that the ADC difference value was the only significant factor associated with low Oncotype DX risk group (adjusted odds ratio = 0.998; 95% CI: 0.996, 0.999; P<0.001).

# CONCLUSION

The ADC difference value derived from whole-lesion histogram analysis could be helpful for identifying ER-positive, lymph nodenegative invasive breast cancer patients with low risk of recurrence.

# **CLINICAL RELEVANCE/APPLICATION**

In estrogen receptor-positive, lymph node-negative breast cancer, the ADC difference value derived from whole-lesion histogram assessments might serve as quantitative biomarkers of recurrence risk.

# RC215-03 Radiomic Phenotypes of Tumor Heterogeneity from Pre-Operative DCE-MRI Predict Breast Cancer Recurrence after 10-Year Follow-Up: Phenotype Discovery and Independent Validation

Monday, Nov. 26 9:00AM - 9:10AM Room: Arie Crown Theater

Participants

Rhea Chitalia, Philadelphia, PA (*Presenter*) Nothing to Disclose Jennifer Rowland, MD, Philadelphia, PA (*Abstract Co-Author*) Nothing to Disclose Elizabeth S. McDonald, MD, Philadelphia, PA (*Abstract Co-Author*) Nothing to Disclose Lauren Pantalone, BS, Philadelphia, PA (*Abstract Co-Author*) Nothing to Disclose Eric A. Cohen, Philadelphia, PA (*Abstract Co-Author*) Nothing to Disclose Aimilia Gastounioti, Philadelphia, PA (*Abstract Co-Author*) Nothing to Disclose Kathleen M. Thomas, BS, Philadelphia, PA (*Abstract Co-Author*) Nothing to Disclose Rebecca Batiste, Philadelphia, PA (*Abstract Co-Author*) Nothing to Disclose Michael D. Feldman, MD, PhD, Philadelphia, PA (*Abstract Co-Author*) Nothing to Disclose NV Advisory Board, XIFIN, Inc Mitchell D. Schnall, MD, PhD, Philadelphia, PA (*Abstract Co-Author*) Nothing to Disclose Emily F. Conant, MD, Philadelphia, PA (*Abstract Co-Author*) Nothing to Disclose Emily F. Conant, MD, Philadelphia, PA (*Abstract Co-Author*) Nothing to Disclose Emily F. Conant, MD, Philadelphia, PA (*Abstract Co-Author*) Nothing to Disclose Emily F. Conant, MD, Philadelphia, PA (*Abstract Co-Author*) Nothing to Disclose Emily F. Conant, MD, Philadelphia, PA (*Abstract Co-Author*) Nothing to Disclose Emily F. Conant, MD, Philadelphia, PA (*Abstract Co-Author*) Nothing to Disclose Emily F. Conant, MD, Philadelphia, PA (*Abstract Co-Author*) Nothing to Disclose Emily F. Conant, MD, Philadelphia, PA (*Abstract Co-Author*) Nothing to Disclose

# For information about this presentation, contact:

rhea.chitalia@uphs.upenn.edu

# PURPOSE

To validate intrinsic imaging phenotypes of tumor heterogeneity and evaluate their prognostic performance in predicting 10-year recurrence.

# METHOD AND MATERIALS

Pre-treatment DCE-MRI scans of 94 women with primary invasive breast cancer and 10-year follow up data available were retrospectively analyzed from a clinical trial cohort at our institution (2002-2006). For each woman, a signal enhancement ratio map was generated for the most representative slice of the primary lesion from which morphologic features were calculated. Radiomic features (histogram, run-length, structural, and co-occurrence matrix features) were extracted and summarized over tumor quadrants. Intrinsic phenotypes of tumor heterogeneity were identified via unsupervised hierarchical clustering applied to the extracted feature vectors, with significant clusters found using Consensus Clustering and the SigClust method. Differences across phenotypes by hormone receptor status, tumor size, post-surgery therapy, TNM staging, and recurrence outcomes were assessed using Chi-square and Kruskal-Wallis tests. An independent dataset of 116 women diagnosed with primary invasive breast cancer (2002-2006), available via The Cancer Imaging Archive, was used to validate phenotype reproducibility. Survival probabilities across phenotypes were evaluated using Kaplan-Meier curves and phenotype cluster assignments were added to a baseline Cox proportional hazards model with established histopathologic prognostic factors to predict RFS.

### RESULTS

Three significant phenotypes of low, medium, and high heterogeneity were identified in the discovery cohort and reproduced in the validation cohort (p<0.001). No recurrent cases were found in the low heterogeneity phenotype (p<0.001). Clinical stage, mitotic grade, lymph invasion, and nuclear grade were different across phenotypes (p<=0.02). Kaplan-Meier curves showed significant differences (p<0.001) in RFS probabilities across phenotypes. The augmented model including phenotype assignment had a higher discriminatory capacity (c-statistic= 0.80) compared to a baseline model with only established prognostic factors (c-statistic= 0.65, p<0.01).

# CONCLUSION

Intrinsic imaging phenotypes of tumor heterogeneity can predict 10-year recurrence as validated in an independent dataset.

# **CLINICAL RELEVANCE/APPLICATION**

Radiomic phenotypes could provide a non-invasive characterization of tumor heterogeneity to augment personalized prognosis and treatment.

# **Honored Educators**

Presenters or authors on this event have been recognized as RSNA Honored Educators for participating in multiple qualifying educational activities. Honored Educators are invested in furthering the profession of radiology by delivering high-quality educational content in their field of study. Learn how you can become an honored educator by visiting the website at: https://www.rsna.org/Honored-Educator-Award/ Mitchell D. Schnall, MD, PhD - 2013 Honored Educator

# RC215-04 Robustness of Computer-aided Diagnosis of Breast Cancer Using Radiomics and Machine Learning Classification of 1,461 Lesions across Populations in China and the United States

### Participants

Heather Whitney, PhD, Wheaton, IL (Presenter) Nothing to Disclose

Hui Li, PHD, Chicago, IL (Abstract Co-Author) Nothing to Disclose

Yu Ji, MD, Chicago, IL (Abstract Co-Author) Nothing to Disclose

Alexandra V. Edwards, Chicago, IL (*Abstract Co-Author*) Research Consultant, QView Medical, Inc; Research Consultant, Quantitative Insights, Inc

John Papaioannou, MSc, Chicago, IL (Abstract Co-Author) Research Consultant, QView Medical, Inc.

Peifang Liu, MD, PhD, Tianjin, China (*Abstract Co-Author*) Nothing to Disclose

Maryellen L. Giger, PhD, Chicago, IL (*Abstract Co-Author*) Stockholder, Hologic, Inc; Shareholder, Quantitative Insights, Inc; Shareholder, QView Medical, Inc; Co-founder, Quantitative Insights, Inc; Royalties, Hologic, Inc; Royalties, General Electric Company; Royalties, MEDIAN Technologies; Royalties, Riverain Technologies, LLC; Royalties, Mitsubishi Corporation; Royalties, Canon Medical Systems Corporation

# For information about this presentation, contact:

hwhitney@uchicago.edu

### PURPOSE

To assess the performance of computer aided diagnosis (CADx) in breast lesions imaged with DCE-MR in two patient cohorts, one in China and one in the United States (US), using extracted radiomic features and machine learning classification.

### **METHOD AND MATERIALS**

Dynamic contrast-enhanced magnetic resonance (DCE-MR) images of 1,461 breast lesions (from China, GE scanners: 300 benign lesions, 302 malignant cancers; from the US, Philips scanners: 268 benign lesions, 591 malignant cancers) were collected under HIPAA and IRB compliance. The lesions were segmented automatically using a fuzzy c-means method. Thirty-eight radiomic features describing size, shape, morphology, kinetics, and texture were extracted using previously reported methods. The performance of CADx for classification between benign lesions and malignant cancers was evaluated with two methodologies: (a) independent training and testing of the datasets, with each set serving as a training set while the other served as a testing set; and (b) tenfold cross validation within each set. Classification was performed using support vector machines with optimization of the hyperparameters. The area under the ROC curve (AUC) served as figure of merit, with its value and standard error determined using the conventional binormal model. The AUCs resulting from (a) and (b) were compared within and between each methodology. Difference in AUC was significantly different when p < 0.05.

#### RESULTS

When radiomic features extracted from MRIs acquired in China were used to train the machine classifiers and independent testing was conducted on MRIs acquired in the US, AUC = 0.77 (0.02), while the reverse resulted in AUC = 0.79 (0.02). For cross-validation within each set, AUC = 0.82 (0.02) for the US database and AUC = 0.80 (0.02) for the China database. AUCs compared across methodologies failed to show significant difference.

### CONCLUSION

Computer aided diagnosis of breast lesions demonstrated potential robustness across independent populations in both independent training/testing and in cross validation.

# CLINICAL RELEVANCE/APPLICATION

Radiomic features extracted from DCE-MRI may be robust for classifying breast lesions as benign or malignant across two cohorts (one in China, one in US), enhancing translation to clinical use.

# RC215-05 Radiogenomics

Monday, Nov. 26 9:20AM - 9:40AM Room: Arie Crown Theater

# Participants

Lars J. Grimm, MD, Durham, NC (Presenter) Editorial Advisory Board, Medscape, LLC; Educational program support, Hologic, Inc

For information about this presentation, contact:

lars.grimm@duke.edu

### LEARNING OBJECTIVES

1) Define radiogenomics and describe how it differs from radiomics. 2) Examine the limitations of current radiogenomics research. 3) Assess the utility of radiogenomics in clinical practice. 4) Develop a framework to evaluate future radiogenomics research.

# RC215-06 Proteomic Expression Underlying Quantitative MRI Features in Breast Cancer: A Radioproteomics Study

Monday, Nov. 26 9:40AM - 9:50AM Room: Arie Crown Theater

Participants

Ryan M. Hausler, BS, Pittsburgh, PA (*Presenter*) Nothing to Disclose Ruimei Chai, Shenyang, China (*Abstract Co-Author*) Nothing to Disclose Dooman Arefan, PhD, Pittsburgh, PA (*Abstract Co-Author*) Nothing to Disclose Jules H. Sumkin, DO, Pittsburgh, PA (*Abstract Co-Author*) Research Grant, Hologic, Inc; Research Grant, General Electric Company Min Sun, MD,PhD, Pittsburgh, PA (*Abstract Co-Author*) Nothing to Disclose Shandong Wu, PhD, MSc, Philadelphia, PA (*Abstract Co-Author*) Nothing to Disclose

For information about this presentation, contact:

### PURPOSE

The complementary analysis of breast cancer via radiology imaging and molecular pathology approaches has spurred radiogenomics and radioproteomics studies. We performed an investigation of the relationships between quantitative radiomic imaging phenotype data and underlying proteomic expression, with the goal of improving precise breast cancer diagnosis and cancer behavior characterization.

# METHOD AND MATERIALS

We identified a retrospective cohort of 40 invasive breast cancer patients from a single medical center. Their integrated protein expression data were obtained from The Cancer Genome Atlas study. The proteomic data was acquired via Reverse Phase Protein Array (RPPA) to measure the expression of 217 breast cancer related proteins and phospho-proteins. Dynamic Contrast Enhanced Magnetic Resonance Imaging (DCE-MRI) data of the 40 patients were collected from clinical archive, all acquired with a 1.5T same-vendor scanner. A set of 30 radiomic imaging features were extracted from automatically-segmented tumor volume in all 40 DCE-MRIs to capture tumor morphological and contrast enhancement characteristics. Multivariate linear regression was used to map the associations between each imaging feature with each of the 217 protein expressions, controlling for patient age and cancer stage. A p value was obtained evaluating the significance of the association and was adjusted for multiple comparisons of the selected radiomic feature against every protein. Adjusted p values less than 0.05 were recorded.

# RESULTS

The average patient age at scan was 38.7±12 years, 10 (25%) of which were pre- with the rest post-menopausal. We found a variety of expression of cancer related proteins were significantly associated (positively or negatively) with a subset of morphological and contrast enhancement kinetics related imaging features. For example, ERCC5 (a protein responsible for DNA repair following UV-induced damage) is negatively associated with the tumor brightness and contrast agent uptake rates. The full association map is shown in the attached figure.

### CONCLUSION

Our study showed that the expression of several cancer related proteins were found to be linearly associated with quantitative DCE-MRI-derived phenotype features in invasive breast tumors.

# **CLINICAL RELEVANCE/APPLICATION**

Radioproteomic studies of cancer can help to decipher how molecular mechanisms may regulate the development of specific tumor phenotypes.

# RC215-07 Prediction of 21-gene Recurrence Score in Patients with Estrogen Receptor-positive Early-Stage Breast Cancer Using MRI-based Radiomics Nomogram

Monday, Nov. 26 9:50AM - 10:00AM Room: Arie Crown Theater

# Participants

Nam Joo Lee, Seoul, Korea, Republic Of (*Presenter*) Nothing to Disclose Hee Jung Shin, MD, Seoul, Korea, Republic Of (*Abstract Co-Author*) Nothing to Disclose Hwa Jung Kim, Seoul, Korea, Republic Of (*Abstract Co-Author*) Nothing to Disclose Ki Chang Shin, Seoul, Korea, Republic Of (*Abstract Co-Author*) Nothing to Disclose Jong Won Lee, Seoul, Korea, Republic Of (*Abstract Co-Author*) Nothing to Disclose Sae Byul Lee, Seoul, Korea, Republic Of (*Abstract Co-Author*) Nothing to Disclose Eun Young Chae, Seoul, Korea, Republic Of (*Abstract Co-Author*) Nothing to Disclose Woo Jung Choi, MD, Seoul, Korea, Republic Of (*Abstract Co-Author*) Nothing to Disclose Joo Hee Cha, MD, Seoul, Korea, Republic Of (*Abstract Co-Author*) Nothing to Disclose Hak Hee Kim, MD, Seoul, Korea, Republic Of (*Abstract Co-Author*) Nothing to Disclose Ga Young Yoon, MD, Seoul, Korea, Republic Of (*Abstract Co-Author*) Nothing to Disclose

# For information about this presentation, contact:

docshin@amc.seoul.kr

# PURPOSE

To develop a breast MRI-based radiomics nomogram including pathologic factors which can predict low-risk recurrence score (RS) on 21-gene RS assay in patients with estrogen receptor-positive early-stage breast cancer (EBC).

# **METHOD AND MATERIALS**

From 2011 to 2017, a total of 547 tumors in 539 patients with EBC who underwent preoperative breast MRI were retrospectively included in this study. Among them, low-risk was 320 (58.5%), intermediate-risk was 180 (32.9%), and high-risk was 47 (8.6%). We extracted 744 quantitative MR radiomic features from computerized three-dimensional segmentations of each tumor generated computer-extracted image phenotypes (CEIP) within the intratumoral regions of early post-contrast T1-weighted images, percent enhancement (PE) map, signal enhancement ratio (SER) map, and T2-weighted images. We divided 547 cases into a training set (n=365) and a validation set (n=182). Elastic net was used for feature selection and radiomics score building. Multivariate logistic regression analysis was used to develop a prediction model, we incorporated the radiomics score and independent pathologic risk factors and build a radiomics nomogram. Internal validation for an independent validation set (n=182) was performed.

#### RESULTS

The radiomics score, which consisted of 24 selected CEIPs, was significantly associated with the prediction of recurrence (C-index, 0.769 for training set and 0.745 for validation set). Independent pathologic predictors contained in the nomogram were progesterone receptor status, nuclear grade, histologic grade, extensive intraductal component, lymphovascular invasion, P53, and Ki67 status, and their C-index was 0.858 for training set and 0.774 for validation set. Addition of radiomics score to the pathologic nomogram showed an incremental value of 0.054 and 0.092, respectively. Radiomics nomogram showed good prediction of low-risk RS, with a C-index of 0.912 for training set and 0.866 for validation set.

### CONCLUSION

This study shows that a radiomics nomogram which incorporates the MRI-based radiomics score and pathologic features, can be used to help the preoperative individualized prediction of low-risk RS in patients with EBC.

### **CLINICAL RELEVANCE/APPLICATION**

Prediction nomogram using breast MRI-based radiomics score and pathologic predictors can be used to facilitate the preoperative individualized prediction of low-risk RS on 21-gene RS assay in patients with EBC.

# RC215-08 Can Histogram Analysis of Dynamic Contrast-Enhanced MRI and Apparent Diffusion Coefficient Map Predict Molecular Subtypes of Invasive Breast Cancers?

Monday, Nov. 26 10:00AM - 10:10AM Room: Arie Crown Theater

Participants

Joao V. Horvat, MD, Sao Paulo, Brazil (*Presenter*) Nothing to Disclose Doris Leithner, MD, New York, NY (*Abstract Co-Author*) Nothing to Disclose Blanca Bernard-Davila, MPH,MS, New York, NY (*Abstract Co-Author*) Nothing to Disclose Rosa E. Ochoa Albiztegui II, MD, Mexico CIty, Mexico (*Abstract Co-Author*) Nothing to Disclose Danny F. Martinez, BSC,MSc, New York, NY (*Abstract Co-Author*) Nothing to Disclose Olivia Sutton, New York, NY (*Abstract Co-Author*) Nothing to Disclose Elizabeth A. Morris, MD, New York, NY (*Abstract Co-Author*) Nothing to Disclose Sunitha Thakur, PhD, MS, New York, NY (*Abstract Co-Author*) Nothing to Disclose Katja Pinker-Domenig, MD, Vienna, Austria (*Abstract Co-Author*) Nothing to Disclose

### For information about this presentation, contact:

joaohorvat@gmail.com

# PURPOSE

To evaluate if histogram analysis of dynamic contrast-enhanced (DCE) MRI and apparent diffusion coefficient (ADC) maps with diffusion-weighted imaging (DWI) can predict molecular subtypes of invasive breast cancers.

### **METHOD AND MATERIALS**

In this HIPAA-compliant and IRB-approved study we retrospectively evaluated 91 consecutive patients from January 2011 to January 2013 with invasive ductal carcinoma of the breast who underwent multiparametric MRI with DCE and DWI at our institution. The exclusion criteria were 1) lesion smaller than 1 cm, 2) previous treatment for breast cancer, 3) pathology report unavailable, and 4) poor image quality. One experienced breast radiologist drew a region of interest on DCE MRI and ADC maps on the slice with the largest diameter of the solid portion of the lesion avoiding cystic areas and biopsy markers. The histogram analysis was performed and the mean, variance, kurtosis and skewness were calculated. Molecular breast cancer subtypes were derived by IHC surrogates. Tumors were classified as luminal A if either ER or PR was positive and HER2 was negative, Luminal B if either ER or PR was positive and HER2 positive and triple-negative if ER, PR and HER2 were negative. Nonparametric Mann-Whitney U test and Kruskal-Wallis were used to compare groups of molecular subtypes. P-values <0.05 were accepted to be statistically significant.

#### RESULTS

The histogram analysis of DCE images and ADC maps of 91 breast cancers demonstrated no significant difference among breast tumor molecular subtypes. Measurements of the mean, variance, kurtosis and skewness were used to compare luminal A/B with HER-2 enriched/triple-negative cancers, without significant results for both DCE (p-value = 0.405, 0.252, 0.667, 0.809) and ADC (0.204, 0.081, 0.941, 0.574), respectively. Histogram measurements were also used to compare luminal A with other subtypes and also demonstrated no significant difference for DCE (0.659, 0.162, 0.516, 0.833) and ADC (0.204, 0.222, 0.495, 0.896).

### CONCLUSION

Histogram analysis of DCE MRI and ADC map cannot predict molecular subtypes of invasive breast cancers.

### **CLINICAL RELEVANCE/APPLICATION**

Despite many valuable applications of histogram analysis in diagnostic imaging, it cannot predict molecular subtypes of invasive breast cancers.

# RC215-09 CESM Enhancement Pattern and Intensity and Its Correlation to Breast Cancer Immunophenotype: Preliminary Results

Monday, Nov. 26 10:10AM - 10:20AM Room: Arie Crown Theater

Participants

Elzbieta Luczynska, MD, Cracow, Poland (*Presenter*) Nothing to Disclose Sylwia Heinze, PhD, Cracow, Poland (*Abstract Co-Author*) Nothing to Disclose Joanna Niemiec, Cracow, Poland (*Abstract Co-Author*) Nothing to Disclose Agnieszka Adamczyk, Cracow, Poland (*Abstract Co-Author*) Wojciech Rudnicki, MD, Krakow, Poland (*Abstract Co-Author*) Nothing to Disclose

### For information about this presentation, contact:

#### z5luczyn@cyfronet.pl

### PURPOSE

The differences in the intensity and pattern of enhancement in CESM between breast carcinomas might result from the differences in the amount of contrast that leaked out from the blood vessels and timely arrested in the interstitium. The aim of this paper is to study the expression of podoplanin in cancer stroma and its relation to breast cancer immunophenotype. Patients with lesions enhancing on CESM were subjected to biopsy - material obtained during biopsies was histopathologically verified. In the present study we retrospectively investigated 97 invasive breast carcinomas diagnosed in 94 patients. This study was performed in compliance with the Declaration of Helsinki and it received the approval of Ethical Committee at the Regional Medical Chamber. For each tumor enhancing on CESM, the intensity and the pattern of enhancement were evaluated. The enhancement of contrast agent uptake was qualitatively assessed as weak/medium or strong ,while the pattern as heterogenous or homogenous. Lymphatic vessels were defined as strongly podoplanin-stained structures with lymphatic vessel characteristics , clearly distinguishable from other tissue structures and cells. We classified tumor stroma as: podoplanin-sparse and podoplanin-rich.

### RESULTS

Strong enhancement on CESM was found more frequently in: large tumors (pT>1), node-positive carcinomas, in tumors with podoplanin-sparse stroma vs. tumors with podoplanin-rich stroma . We found no relationship between enhancement on CESM and: tumor grade, histological type of cancer, breast cancer immunophenotype and Ki-67LI. However, in luminal A tumors strong enhancement on CESM was insignificantly more frequent as compared to neoplasms with non-luminal A subtype .

# CONCLUSION

In our study prognostic significance of selected CESM features was found for the first time: strong and heterogenous enhancement on CESM was related to poor patients' outcome. In this study, the aforementioned correlation was additionally confirmed by the relationship between strong enhancement on CESM and nodal involvement or large tumor size.

# **CLINICAL RELEVANCE/APPLICATION**

Our results may suggest that intensity and pattern of enhancement on CESM might bring (together with the results of diagnostic imaging methods) not only the confirmation of presence or absence of tumor, but also prognostic information.

# RC215-10 Development of MRI-based Radiomics Nomogram for the Prediction of Recurrence in Patients with Luminal-type Breast Cancer: A Nested Case-Control Study

Monday, Nov. 26 10:20AM - 10:30AM Room: Arie Crown Theater

Participants

Bo Yong Chung, Seoul, Korea, Republic Of (*Presenter*) Nothing to Disclose Hee Jung Shin, MD, Seoul, Korea, Republic Of (*Abstract Co-Author*) Nothing to Disclose Hwa Jung Kim, Seoul, Korea, Republic Of (*Abstract Co-Author*) Nothing to Disclose Ki Chang Shin, Seoul, Korea, Republic Of (*Abstract Co-Author*) Nothing to Disclose Eun Young Chae, Seoul, Korea, Republic Of (*Abstract Co-Author*) Nothing to Disclose Woo Jung Choi, MD, Seoul, Korea, Republic Of (*Abstract Co-Author*) Nothing to Disclose Joo Hee Cha, MD, Seoul, Korea, Republic Of (*Abstract Co-Author*) Nothing to Disclose Hak Hee Kim, MD, Seoul, Korea, Republic Of (*Abstract Co-Author*) Nothing to Disclose Ga Young Yoon, MD, Seoul, Korea, Republic Of (*Abstract Co-Author*) Nothing to Disclose

For information about this presentation, contact:

docshin@amnc.seoul.kr

### PURPOSE

To determine whether breast MRI-based radiomics nomogram including pathologic factors can predict recurrences or distant metastasis in patients with luminal-type breast cancer (LTBC).

# METHOD AND MATERIALS

From 2006 to 2012, a total of 348 patients with LTBC who underwent preoperative breast MRI were retrospectively included in this study. Patients with recurrence were 174. Patients without recurrence were matched in terms of age, stage, and type of chemotherapy, and developed 174 nested case-control pairs. We extracted 804 quantitative MR radiomic features of computerized three-dimensional segmentations of each cancer generated computer-extracted image phenotypes (CEIP) within the intratumoral regions of early post-contrast T1-weighted images, percent enhancement (PE) map, signal enhancement ratio (SER) map, and T2-weighted images. We divided 174 case-control matches into a training set (n=232) and a validation set (n=116). Elastic net was used for feature selection and radiomics score building. Multivariate logistic regression analysis was used to develop the prediction model, we incorporated the radiomics score and independent pathologic risk factors and build a radiomics nomogram. Internal validation for an independent validation set (n=76) was performed.

# RESULTS

The radiomics score, which consisted of 14 selected CEIPs, was significantly associated with the prediction of recurrence (C-index, 0.864 for training set and 0.815 for validation set). Independent pathologic predictors contained in the nomogram were progesterone receptor status, P53, lymphovascular invasion, Ki67 status, and lymph node ratio, and their C-index was 0.695 for training set and 0.701 for validation set. Addition of radiomics score to the pathologic nomogram showed an incremental value of 0.211 and 0.177, respectively. Radiomics nomogram showed good prediction of recurrence, with a C-index of 0.906 for training set and 0.878 for validation set.

### CONCLUSION

This study shows that a radiomics nomogram which incorporates the MRI-based radiomics score and pathologic features, can be used to help the individualized prediction of local or distant recurrence in patients with LTBC.

# **CLINICAL RELEVANCE/APPLICATION**

Nomogram using breast MRI-based radiomics score and pathologic predictors can be used to facilitate the individualized prediction of recurrence in patients with LTBC.

# RC215-11 Horizons with Deep Learning

Monday, Nov. 26 10:40AM - 11:00AM Room: Arie Crown Theater

Participants

Robert M. Nishikawa, PhD, Pittsburgh, PA (*Presenter*) Royalties, Hologic, Inc; Research Grant, Hologic, Inc; Research Consultant, iCAD, Inc; Research Grant, Koios Medical

For information about this presentation, contact:

nishikawarm@upmc.edu

### LEARNING OBJECTIVES

1) To understand the importance implementing deep learning tools into a breast imager's workflow. 2) To understand applications of deep learning outside of detection and characterization of breast lesions.

# RC215-12 Incorporating Patient Characteristics in Breast Cancer Screening with Deep Convolutional Neural (DCN) Network

Monday, Nov. 26 11:00AM - 11:10AM Room: Arie Crown Theater

Participants

Eric Kim, MD, New York, NY (*Presenter*) Nothing to Disclose Krzysztof J. Geras, New York City, NY (*Abstract Co-Author*) Nothing to Disclose Nan Wu, New York City, NY (*Abstract Co-Author*) Nothing to Disclose Yiqiu Shen, New York City, NY (*Abstract Co-Author*) Nothing to Disclose Jingyi Su, New York City, NY (*Abstract Co-Author*) Nothing to Disclose Sungheon Kim, PhD, New York, NY (*Abstract Co-Author*) Nothing to Disclose Stacey Wolfson, New York, NY (*Abstract Co-Author*) Nothing to Disclose Linda Moy, MD, New York, NY (*Abstract Co-Author*) Nothing to Disclose Kyunghyun Cho, New York City, NY (*Abstract Co-Author*) Nothing to Disclose

For information about this presentation, contact:

kime18@nyumc.org

# PURPOSE

To determine if the addition of patient characteristics obtained from the electronic health records may improve the ability of a DCN network to detect and classify lesions on screening mammography.

# METHOD AND MATERIALS

This is a retrospective study of a DCN network trained on over 250,000 screening mammograms performed at our institution from 2010-2016. The patients were sorted according to the date of their latest exam and divided into training (first 80%), validation (next 10%), and test (last 10%) sets. In the test phase, only the most recent exam was used for each patient. Patient characteristics including age, family history of breast cancer, and history of prior examinations were extracted from the radiologist reports. The original high-resolution images and extracted side information were utilized as inputs by a multi-column DCN network to classify BI-RADS category. The model was evaluated using area under the receiver operating characteristic curve (AUC) analysis. Analysis was also performed after stratifying patients by age-group and breast density (dense vs non-dense).

# RESULTS

The overall performance of the DCN network improved with the addition of patient characteristics in comparison to using images alone (AUC 0.750 vs 0.733). This improvement was especially notable for BI-RADS 0 cases, with an AUC of 0.664 vs 0.618. Performance also generally improved with increasing age, with an average AUC of 0.759 in patients over 70 years of age. Finally, performance of the model is superior in dense breasts vs non-dense breasts (AUC 0.740 vs AUC 0.707).

# CONCLUSION

The performance of DCN networks in evaluating screening mammograms increases with the addition of patient characteristics information, especially in the abnormal BI-RADS 0 cases which are the most difficult to evaluate.

# **CLINICAL RELEVANCE/APPLICATION**

End-to-end architectures of DCN networks, like ours, support the incorporation of patient characteristics to increase the accuracy of deep learning algorithms in breast cancer screening.

# RC215-13 Detecting Breast Cancer in Mammography: A Deep Learning-Based Computer System versus 101 Radiologists

Monday, Nov. 26 11:10AM - 11:20AM Room: Arie Crown Theater

Participants

Alejandro Rodriguez-Ruiz, Nijmegen, Netherlands (*Abstract Co-Author*) Nothing to Disclose Albert Gubern-Merida, PhD, Nijmegen, Netherlands (*Abstract Co-Author*) Employee, ScreenPoint Medical Kristina Lang, MD,PhD, Malmo, Sweden (*Abstract Co-Author*) Travel support, Siemens AG Speaker, Siemens AG Mireille Broeders, PhD, Nijmegen, Netherlands (*Abstract Co-Author*) Nothing to Disclose Gisella Gennaro, PhD, Padua, Italy (*Abstract Co-Author*) Nothing to Disclose Paola Clauser, MD, Vienna, Austria (*Abstract Co-Author*) Nothing to Disclose Margarita Chevalier, PhD, Madrid, Spain (*Abstract Co-Author*) Nothing to Disclose Thomas H. Helbich, MD, Vienna, Austria (*Abstract Co-Author*) Nothing to Disclose Thomas H. Helbich, MD, Vienna, Austria (*Abstract Co-Author*) Research Grant, Medicor, Inc Research Grant, Siemens AG Research Grant, C. R. Bard, Inc Tao Tan, Nijmegen, Netherlands (*Abstract Co-Author*) Research Grant, QView Medical, Inc Thomas Mertelmeier, PHD, Forchheim, Germany (*Abstract Co-Author*) Employee, Siemens AG; Stockholder, Siemens AG Matthew G. Wallis, MD, Cambridge, United Kingdom (Abstract Co-Author) Nothing to Disclose

Ingvar T. Andersson, MD, PhD, Malmo, Sweden (*Abstract Co-Author*) Nothing to Disclose

Sophia Zackrisson, Malmo, Sweden (*Abstract Co-Author*) Speaker, AstraZeneca PLC ; Speaker, Siemens AG; Travel support, AstraZeneca PLC; Travel support, Siemens AG

Ritse M. Mann, MD, PhD, Nijmegen, Netherlands (*Abstract Co-Author*) Researcher, Siemens AG ; Researcher, Seno Medical Instruments, Inc; Researcher, Identification Solutions, Inc; Researcher, Micrima Limited; Researcher, Medtronic plc; Scientific Advisor, ScreenPoint Medical BV; Scientific Advisor, Transonic Imaging, Inc; Stockholder, Transonic Imaging, Inc Ioannis Sechopoulos, PhD, Atlanta, GA (*Presenter*) Research Grant, Siemens AG; Research Grant, Canon Medical Systems Corporation; Speakers Bureau, Siemens AG; Scientific Advisory Board, Fischer Medical

# PURPOSE

To compare the stand-alone performance of a computer-based detection system to that of radiologists in detecting breast cancer on digital mammography (DM).

### METHOD AND MATERIALS

Nine multi-reader multi-case (MRMC) study datasets previously used for different performance evaluation purposes in seven countries were collected. Each dataset consisted of DM exams acquired with systems from four different vendors, multiple radiologists' assessments per exam (BI-RADS or probability-of-malignancy scores), and ground truth: yielding a total of 2,458 exams (608 malignant) and interpretations by 101 radiologists (28,373 independent exam interpretations). A deep learning-based computer system (Transpara, ScreenPoint Medical, Nijmegen, The Netherlands) was used to automatically analyze each exam, resulting in a score for suspiciousness of cancer (1-100). Independently for each dataset, the area under the receiver operating characteristic curve (AUC) and the sensitivity at the radiologists' specificity level (case recall) were compared between the computer and radiologists using MRMC analysis of variance.

### RESULTS

The performance of the computer system was not significantly different to that of the average of radiologists in eight of nine datasets (AUC differences ranged between -2.6% and +2.5%, P>0.329) and was significantly better in the ninth (+4.6%, P=0.036). At the average specificity of the radiologists, the computer had an equal or higher sensitivity (+0-9%, P>0.083) in all datasets but one (-13%, P=0.066). Comparing individually, the computer had an AUC and sensitivity higher than 53% and 65% of all radiologists, respectively.

### CONCLUSION

A computer system based on deep learning has an equivalent performance to radiologists for detecting breast cancer in mammography.

### **CLINICAL RELEVANCE/APPLICATION**

Whether used for decision support (preventing overlook and interpretation errors that are relatively common in the reading of mammography) or as stand-alone readers, computer systems performing at radiologist-like level might herald a breakthrough in the breast cancer detection workflow with mammography. In some situations, where there is a lack of experienced breast radiologists, it might even allow the development or continuation of screening programs.

# RC215-14 Improving Accuracy and Efficiency with Concurrent Use of Artificial Intelligence for Digital Breast Tomosynthesis Screening

Monday, Nov. 26 11:20AM - 11:30AM Room: Arie Crown Theater

Participants

Emily F. Conant, MD, Philadelphia, PA (*Presenter*) Grant, Hologic, Inc; Consultant, Hologic, Inc; Grant, iCAD, Inc; Consultant, iCAD, Inc; Speaker, iiCME

Alicia Y. Toledano, DSc, Kensington, MD (Abstract Co-Author) Consultant, iCAD, Inc

Senthil Periaswamy, PhD, Nashua, NH (Abstract Co-Author) Vice President, iCAD, Inc

Sergei V. Fotin, PhD, Nashua, NH (Abstract Co-Author) Principal Scientist, iCAD, Inc; Stockholder, iCAD, Inc

Jonathan Go, Nashua, NH (Abstract Co-Author) Sr. Vice President, iCAD, Inc; ;

Jeffrey W. Hoffmeister, MD, Nashua, NH (Abstract Co-Author) Employee, iCAD, Inc; Stockholder, iCAD, Inc

Justin E. Boatsman, MD, San Antonio, TX (Abstract Co-Author) Consultant, iCad, Inc

# For information about this presentation, contact:

Emily.Conant@uphs.upenn.edu

# PURPOSE

Screening with Digital Breast Tomosynthesis (DBT) improves accuracy but prolongs reading time when compared to Full-Field Digital Mammography (FFDM) alone. A reader study evaluated concurrent use of Artificial Intelligence (AI) to shorten reading time, while maintaining or improving sensitivity and specificity.

# **METHOD AND MATERIALS**

An AI system based on deep convolutional neural networks was developed to identify suspicious soft tissue and calcific lesions in DBT slices. Findings are outlined in slices, indicating AI's confidence of malignancy with 0-100 scores. A retrospective, fullycrossed, multi-reader, multi-case designed study compared performance of 24 radiologists reading 260 DBT cases both with and without AI. The case set included 65 cancer cases with 66 malignant lesions and 65 cases with biopsy-proven benign lesions. Readings with and without AI occurred in 2 visits separated by a memory washout period of at least 4 weeks. Performance was assessed by measuring Area Under the ROC Curve (AUC) for malignant lesions with AI versus without AI. Reading time, sensitivity, specificity and recall rate were also assessed.

# RESULTS

Radiologist performance for detection of malignant lesions, measured by mean AUC, increased 0.057 with use of AI (95% CI: 0.028, 0.087; p < 0.01), from 0.795 without AI to 0.852 with AI. Reading time decreased 52.7% with use of AI (95% CI: 41.8%, 61.5%; p < 0.01), from 64.1 sec without AI to 30.4 sec with AI, using a normalizing transformation to appropriately assess reading times that

were not normally distributed. Sensitivity increased from 77.0% without AI to 85.0% with AI (8.0%; 95% CI: 2.6%, 13.4%; p < 0.01), specificity increased from 62.7% without AI to 69.6% with AI (6.9%; 95% CI: 3.0%, 10.8%; p < 0.01), and recall rate for non-cancers decreased from 38.0% without AI to 30.9% with AI (7.2%; 95% CI: 3.1%, 11.2%; p < 0.01).

### CONCLUSION

Concurrent use of AI improves cancer detection with increases of 0.057 in AUC, 8.0% in sensitivity, and 6.9% in specificity; and decreases of 7.2% in recall rate and 52.7% in reading time.

### CLINICAL RELEVANCE/APPLICATION

Radiologist's concurrent use of AI for DBT with certainty of finding scores increases detection of breast cancer with significant reduction in reading time while improving sensitivity and specificity.

# RC215-15 Breast Cancer Temporal Risk Prediction by Deep Learning and Longitudinal Digital Mammogram Images

Monday, Nov. 26 11:30AM - 11:40AM Room: Arie Crown Theater

Participants

Aly A. Mohamed, PhD, Pittsburgh, PA (*Presenter*) Nothing to Disclose
Wendie A. Berg, MD, PhD, Pittsburgh, PA (*Abstract Co-Author*) Nothing to Disclose
Dooman Arefan, PhD, Pittsburgh, PA (*Abstract Co-Author*) Nothing to Disclose
Jules H. Sumkin, DO, Pittsburgh, PA (*Abstract Co-Author*) Research Grant, Hologic, Inc; Research Grant, General Electric Company
Margarita L. Zuley, MD, Pittsburgh, PA (*Abstract Co-Author*) Investigator, Hologic, Inc
Shandong Wu, PhD, MSc, Philadelphia, PA (*Abstract Co-Author*) Nothing to Disclose

# For information about this presentation, contact:

wus3@upmc.edu

### PURPOSE

Mammographic breast density is a risk factor and recent studies showed deep learning may identify more predictive imaging risk features than breast density. We performed a study to investigate temporal breast cancer risk prediction by using deep learning models on longitudinal 'normal' screening mammograms acquired prior to diagnosis of breast cancer.

#### **METHOD AND MATERIALS**

We conducted a retrospective case-control study on a cohort of 226 patients (1:1 case-control ratio) who underwent standard mammographic screening at our institution during 2006-2013. The unilateral cancer cases (61.3±10.3YO) were all newly diagnosed at 2013 and confirmed by pathology. Asymptomatic cancer-free controls (60.1±10.0 YO) are matched to the cancer cases by age and year of the cancer-diagnosis imaging. All studied women did not have any prior biopsy or recall on mammography. For all cohort, a set of sequential prior 'normal' (negative or benign findings) screening mammogram exams acquired during 2006-2012 were collected (2-8 exams per patient), generating a total of 3263 'normal' images (913 for cancer cases, and 2350 for controls). Those prior images of the cancer-affected breast (for cancer cases) and side-matched breast (for controls) were used to predict the outcome (i.e., case/control status). We compared the prediction in terms of three time periods: (A) all priors from 2006 to 2012, (B) recent priors (1548 images) from 2010 to 2012, and (C) distant priors (1715 images) from 2006 to 2009. The outcome prediction was based on a pre-trained convolutional neural network model (ResNet-50) that was further fine-tuned on our mammograms. 10-fold cross-validation and AUC were used to measure model performance.

### RESULTS

81% of cancers and 82% of controls were post- with the rest pre-menopausal, and neither menopausal status nor family history of breast cancer was associated with the outcome. AUC was 0.84 when using all priors, while it was 0.77 or 0.75 when using only the recent or only the distant priors, respectively.

### CONCLUSION

Sequential recent or distant prior 'normal' screening mammograms can predict, and their combination is more predictive of, breast cancer development using deep learning models.

# **CLINICAL RELEVANCE/APPLICATION**

Deep learning modeling on longitudinally acquired prior 'normal' screening mammogram images through up to 7 years earlier can enhance temporal prediction of breast cancer development.

### RC215-16 Novel Radiomic Descriptor of Tumor Vascular Morphology Identifies Responders to Neo-Adjuvant Chemotherapy on Pre-Treatment Breast MRI

Monday, Nov. 26 11:40AM - 11:50AM Room: Arie Crown Theater

#### Awards

### **Trainee Research Prize - Medical Student**

Participants Nathaniel Braman, Cleveland, OH (*Presenter*) Nothing to Disclose Prateek Prasanna, Cleveland, OH (*Abstract Co-Author*) Nothing to Disclose Maryam Etesami, MD, New Haven, CT (*Abstract Co-Author*) Nothing to Disclose Donna M. Plecha, MD, Strongsville, OH (*Abstract Co-Author*) Research Grant, Hologic, Inc Anant Madabhushi, PhD, Cleveland, OH (*Abstract Co-Author*) Research funded, Koninklijke Philips NV

### For information about this presentation, contact:

nathaniel.braman@case.edu

PURPOSE

Despite significant interest in predicting treatment response prior to breast cancer neo-adjuvant chemotherapy (NAC) from DCE-MRI, prior work has focused on textural patterns of the tumor or parenchyma or deep learning-based approaches that lack direct biological interpretability. In this work, we introduce functional radiomic descriptors of vascular network disorder (VND) and evaluate whether differences in the complexity of tumor-associated vasculature on pre-treatment DCE-MRI can discriminate between patients who do and do not respond to NAC.

# METHOD AND MATERIALS

1.5 or 3T DCE-MRI scans of 76 NAC recipients, 24 of whom had surgically confirmed pathological complete response (pCR), were retrospectively analyzed. Average pixel width and slice thickness were .77 mm and 1.22 mm, respectively. Patients were randomly divided into training (n=53, 14 pCR) and testing (n=23, 10 pCR) sets. A semi-interactive scheme was employed to segment the tumor and vascular network. Within a sliding window, vessel orientation was computed for a series of 2-dimensional representations of the vasculature relative to the tumor centroid. Statistics (mean, median, st. dev, skewness, and kurtosis) of the distribution of vessel orientations for each representation were computed, yielding 20 VND features total. Top VND features were selected in the training set using the Wilcoxon rank sum test via three-fold cross validation, then used to train a linear discriminant analysis classifier to predict response in the test set. Performance was compared against (1) intra- and peri-tumoral texture features and (2) a 3 layer LeNet convolutional neural network (CNN).

# RESULTS

The top 4 VND features distinguished pCR with an AUC=0.75. pCR was characterized by reduced vascular disorder relative to nonpCR. VND performed comparably or better than other state of the art radiomic approaches, including intra- and peri-tumoral texture (AUC=.75) and deep learning (AUC=.67). Combining predictions from VND, texture features, and CNN yielded the best response prediction accuracy (AUC=0.80).

### CONCLUSION

VND features, which capture chaotic vessel network architecture, appear to be associated with NAC response and added predictive value to established radiomic and deep learning approaches.

# **CLINICAL RELEVANCE/APPLICATION**

Quantitative assessment of vessel network architecture as a functional radiomic biomarker could provide interpretable NAC response prediction in breast cancer.

# RC215-17 Using Machine Learning to Assess Tumor Metastatic Lymph Nodes and Ki-67 Expression Aggressiveness from Breast MRI Using a Large Clinical Dataset of 300 Cancers from China

Monday, Nov. 26 11:50AM - 12:00PM Room: Arie Crown Theater

### Participants

Yu Ji, MD, Chicago, IL (Presenter) Nothing to Disclose

Hui Li, PHD, Chicago, IL (Abstract Co-Author) Nothing to Disclose

Alexandra V. Edwards, Chicago, IL (*Abstract Co-Author*) Research Consultant, QView Medical, Inc; Research Consultant, Quantitative Insights, Inc

John Papaioannou, MSc, Chicago, IL (Abstract Co-Author) Research Consultant, QView Medical, Inc

Peifang Liu, MD, PhD, Tianjin, China (Abstract Co-Author) Nothing to Disclose

Maryellen L. Giger, PhD, Chicago, IL (*Abstract Co-Author*) Stockholder, Hologic, Inc; Shareholder, Quantitative Insights, Inc; Shareholder, QView Medical, Inc; Co-founder, Quantitative Insights, Inc; Royalties, Hologic, Inc; Royalties, General Electric Company; Royalties, MEDIAN Technologies; Royalties, Riverain Technologies, LLC; Royalties, Mitsubishi Corporation; Royalties, Canon Medical Systems Corporation

# For information about this presentation, contact:

yuji710@uchicago.edu

# PURPOSE

To evaluate quantitative MRI radiomics in the task of identifying metastatic versus nonmetastatic axillary lymph nodes and Ki-67 expression aggressiveness.

### **METHOD AND MATERIALS**

Our research involved a HIPAA-compliant, DCE-MRI database of 300 breast cancer cases. The average age was 47.2 years with a standard deviation of 9.6 years and a range from 25 to 77 years with a median of 47 years. The clinical cohort included 48 low Ki-67 expression (Ki-67 proliferation index < 14%) and 252 cases with high Ki-67 expression (Ki-67 proliferation index >= 14%), indicating a range of tumor aggressiveness. The cohort also included 93 cases with axillary lymph node metastasis and 201 cases without metastasis. The images had been obtained with a gadodiamide-enhanced T1-weighted spoiled gradient-recalled acquisition in the steady state sequence. Primary lesions underwent computerized radiomic analysis in which tumor segmentation and extraction were automatically conducted on an existing CADx workstation. These computer-extracted features included MRI-based phenotypes from six categories: size, shape, morphology, enhancement texture, kinetics, and enhancement-variance kinetics. Radiomic features were input to a Bayesian artificial neural network classifier (BANN) and underwent leave-one-case-out cross validation. Area under the ROC curve (AUC) served as the figure of merit in the classification tasks.

### RESULTS

In the task of identifying Ki-67 expression and lymph node status, the analyses of the various radiomic phenotypes yielded AUCs ranging from 0.50 (se = 0.05) to 0.69 (se = 0.04). The Ki-67 MRI-based tumor signature produced an AUC value of 0.71 (se = 0.04). In the task of assessing the status of axillary lymph nodes, the radiomics tumor signature yielded an AUC value of 0.67 (se = 0.03). Both signatures were found to be statistically different from random guessing.

# CONCLUSION

Quantitative MRI radiomics conducted on depicted primary breast tumors can contribute to identifying aggressive tumors, including identifying Ki-67 expression and discriminating between metastatic and nonmetastatic lymph nodes, yielding automatic MRI-based prognostic markers for ultimate use in radiogenomics and patient care.

# **CLINICAL RELEVANCE/APPLICATION**

The ability to assess automatically the potential aggressiveness of tumors may elucidate the characteristics of breast cancers for radiogenomics and for use in helping clinician estimate prognosis.



Medicolegal Issues for Radiologists-To Divulge or Not to Divulge: Diagnostic Misses and Errors (Sponsored by the RSNA Professionalism Committee)

Monday, Nov. 26 8:30AM - 10:00AM Room: N230B

PR

AMA PRA Category 1 Credits ™: 1.50 ARRT Category A+ Credit: 0

### **Participants**

Ronald L. Eisenberg, MD, JD, Boston, MA (*Moderator*) Nothing to Disclose Priscilla J. Slanetz, MD, MPH, Belmont, MA (*Presenter*) Nothing to Disclose Stephen D. Brown, MD, Boston, MA (*Presenter*) Nothing to Disclose Brent J. Wagner, MD, West Reading, PA (*Presenter*) Nothing to Disclose Darlene King, Lancaster, PA (*Presenter*) Nothing to Disclose

For information about this presentation, contact:

stephen.brown@childrens.harvard.edu

rleisenb@bidmc.harvard.edu

pslanetz@bidmc.harvard.edu

### LEARNING OBJECTIVES

Describe the responsibilities of the radiologist in terms of the peer review role inherent in the assessment of a comparison study.
 Develop an approach to a robust peer review program that encourages reporting and review of diagnostic errors.
 Define the parameters that impact the balance of error disclosure in the context of the potential missed finding.

### ABSTRACT

The radiologic interpretation involves multiple facets. Most importantly, it is intended to convey a meaningful assessment that will result in either the exclusion of a diagnosis - in which case the clinical evaluation can proceed along a different path - or the establishment of a diagnosis (or set of diagnostic possibilities) to guide further management. For a wide variety of reasons, imaging findings often identified in retrospect were not detected during the initial interpretation. This is especially problematic when balancing two distinct functions of a diagnostic interpretation - the review of the current examination and the comparison to (and, therefore, independent review of) a prior study dictated by a colleague. When there is a difference in the assessment of the prior study, the radiologist is potentially faced with two competing obligations. The first is the overriding interests of the individual patient. The second is the critical role of a structured peer review process that is now an inherent part of modern-day safety culture and professional quality improvement. This exercise in peer review requires us to examine the nuances involved in distinguishing 'missed diagnoses,' 'interpretative errors,' and 'findings identified in retrospect.' While radiologists recognize the ethical argument concerning respect for patient autonomy and the patient's right to know everything about one's own body and health, it is also important for radiologists to know how to communicate such imaging findings with care, sensitivity, and a lack of defensiveness.



# Emerging Technology: Elastography - Update 2018

Monday, Nov. 26 8:30AM - 10:00AM Room: S504CD



AMA PRA Category 1 Credits ™: 1.50 ARRT Category A+ Credit: 1.75

### Participants

Richard L. Ehman, MD, Rochester, MN (Moderator) CEO, Resoundant, Inc Stockholder, Resoundant, Inc

# LEARNING OBJECTIVES

1) To understand how elastography measurements are integrated into the management of patients with chronic liver disease. 2) To learn imaging techniques and protocols of ultrasound and MR elastography. 3) To compare US and MR elastography in assessing liver fibrosis. 4) To review emerging clinical indications of US and MR elastography. 5) To understand limitations of current elastography techniques.

### Sub-Events

# RC217A Elastography of the Liver: What the Clinician Wants to Know

Participants

Mindie Nguyen, MD, Stanford, CA (*Presenter*) Consultant, Intercept Pharmaceuticals, Inc; Consultant, Johnson & Johnson; Consultant, Gilead Sciences, Inc; Consultant, Alynam Pharmaceuticals, Inc; Consultant, Dynavax Technologies Corporation; Consultant, Spring Bank Pharmaceuticals, Inc; Consultant, Novartis AG; Consultant, Eisas; Research Grant, Johnson & Johnson; Research Grant, Gilead Sciences, Inc; Research Grant, Bristol-Myers Squibb Company; Research Grant, Pfizer Inc

# LEARNING OBJECTIVES

View learning objectives under the main course title.

# RC217B Ultrasound Elastography: How and When?

Participants

Richard G. Barr, MD, PhD, Campbell, OH (*Presenter*) Consultant, Siemens AG; Consultant, Koninklijke Philips NV; Research Grant, Siemens AG; Research Grant, SuperSonic Imagine; Speakers Bureau, Koninklijke Philips NV; Research Grant, Bracco Group; Speakers Bureau, Siemens AG; Consultant, Canon Medical Systems Corporation; Research Grant, Esaote SpA; Research Grant, BK Ultrasound; Research Grant, Hitachi, Ltd

# LEARNING OBJECTIVES

1) Understand the clinical indications of ultrasound elastography (USE). 2) Learn about the various techniques and imaging protocols of USE. 3) Review the diagnostic accuracy of USE in the assessment of elasticity in liver fibrosis and other clinical applications in the body. 4) Compare USE with MR elastography. 5) Understand current limitations of USE.

### ABSTRACT

Ultrasound elastography (USE) is a general term for various techniques available for objectively and quantitatively assessing tissue stiffness using ultrasonic techniques, creating noninvasive images of mechanical characteristics of tissues. Elastography is based on the fact that the elasticity of a tissue is changed by pathological or physiological processes. For example, cancer or fibrosis associated with various disease processes including chronic liver disease or chronic pancreatitis result in increased tissue stiffness. Recently, various USE techniques have been cleared by the FDA and all major ultrasound companies offer different approaches of measuring tissue stiffness on their ultrasound machines. The objective of this talk is to familiarize the audience with the clinical indications, imaging techniques and protocols, interpretation, diagnostic accuracy, and limitations of the various USE technique for assessment of tissue stiffness, with special focus on assessment of fibrosis in chronic liver disease.

### **Honored Educators**

Presenters or authors on this event have been recognized as RSNA Honored Educators for participating in multiple qualifying educational activities. Honored Educators are invested in furthering the profession of radiology by delivering high-quality educational content in their field of study. Learn how you can become an honored educator by visiting the website at: https://www.rsna.org/Honored-Educator-Award/ Richard G. Barr, MD, PhD - 2017 Honored Educator

# RC217C MR Elastography: How and When?

Participants

Richard L. Ehman, MD, Rochester, MN (Presenter) CEO, Resoundant, Inc Stockholder, Resoundant, Inc

# LEARNING OBJECTIVES

1) To be able to understand the basic physical principles of MR Elastography (MRE). 2) To be able to describe the clinical indications for MRE in liver disease. 3) To be able to describe published evidence on the diagnostic performance of MRE in assessing liver fibrosis. 4) To be able to compare ultrasound based elastography to MRE. 5) To be able to describe the current limitations of MRE.

### **Honored Educators**

Presenters or authors on this event have been recognized as RSNA Honored Educators for participating in multiple qualifying educational activities. Honored Educators are invested in furthering the profession of radiology by delivering high-quality educational content in their field of study. Learn how you can become an honored educator by visiting the website at: https://www.rsna.org/Honored-Educator-Award/ Richard L. Ehman, MD - 2016 Honored Educator



Whole-body MRI for Oncologic Decision Making in Bone Disease

Monday, Nov. 26 8:30AM - 10:00AM Room: S103AB



AMA PRA Category 1 Credits ™: 1.50 ARRT Category A+ Credit: 1.75

FDA Discussions may include off-label uses.

#### Participants

Evis Sala, MD, PhD, Cambridge, United Kingdom (Moderator) Nothing to Disclose

#### LEARNING OBJECTIVES

1) Describe the limitations of current imaging modalities in evaluation of metastatic bone disease. 2) Learn the added value of whole body MRI in evaluation of metastatic bone disease in various malignancies including prostate cancer and multiple myeloma. 3) Understand the role of quantitative whole body MRI in delivering precision medicine in oncology.

#### Sub-Events

# RC218A Imaging of Metastatic Bone Disease: Current Limitations

Participants

Hebert Alberto Vargas, MD, Cambridge, United Kingdom (Presenter) Nothing to Disclose

# LEARNING OBJECTIVES

1) Discuss the challenges associated with the diagnosis and interpretation of bone findings in patients with metastatic disease.

### ABSTRACT

Conventional imaging of metastatic disease to the bone is notoriously difficult. Unlike soft tissue metastases, significant cortical disruption is required before a bone metastases is visible on CT, and bone scan demonstrates the effect of the metastases on bone, rather than the metastases themselves. MR partially overcomes these limitations, as early bone metastases can be detected. However, even after bone metastases are apparent on imaging, it is difficult to assess their evolution with regards to therapy response.

# RC218B WB-MRI of Metastatic Bone: MET- RADS

#### Participants

Anwar R. Padhani, MD, FRCR, Northwood, United Kingdom (*Presenter*) Advisory Board, Siemens AG ; Speakers Bureau, Siemens AG ; Speakers Bureau, Sanofi-aventis Group; Speakers Bureau, Johnson & Johnson

### For information about this presentation, contact:

anwar.padhani@sticklandscanner.org.uk

### LEARNING OBJECTIVES

1) To show how measurements are acquired distinguishing between tumor detection (core) and response assessment (comprehensive) protocols that are MET-RADS compliant. 2) To highlight and review the MET-RADS response assessment criteria and their application. 3) To illustrate MET-RADS usage with case examples and to provide data on MET-RADS use in clinical practice. 4) Outline the next steps for MET-RADS development.

### ABSTRACT

MET-RADS provides the minimum standards for whole body MRI with DWI regarding image acquisitions, interpretation, and reporting of both baseline and follow-up monitoring examinations of patients with advanced, metastatic cancers. MET-RADS is suitable for guiding patient care in practice (using the regional and overall assessment criteria), but can also be incorporated into clinical trials when accurate lesion size and ADC measurements become more important (the recording of measurements is not mandated for clinical practice). MET-RADS enables the evaluation of the benefits of continuing therapy to be assessed, when there are signs that the disease is progressing (discordant responses). MET-RAD requires validation within clinical trials initially in studies that assess the effects of known efficacious treatments. METRADS measures should be correlated to other tumor response biomarkers, quality of life measures, rates of skeletal events, radiographic progression free survival and overall survival. The latter will be needed for the introduction of WB-MRI into longer term follow-up studies, that will allow objective assessments of whether WB-MRI is effective in supporting patient care.

#### **Honored Educators**

Presenters or authors on this event have been recognized as RSNA Honored Educators for participating in multiple qualifying educational activities. Honored Educators are invested in furthering the profession of radiology by delivering high-quality educational content in their field of study. Learn how you can become an honored educator by visiting the website at: https://www.rsna.org/Honored-Educator-Award/ Anwar R. Padhani, MD, FRCR - 2012 Honored Educator

For information about this presentation, contact:

Christina.Messiou@rmh.nhs.uk

# LEARNING OBJECTIVES

1) List indications for WB-MRI in multiple myeloma. 2) Describe the core and comprehensive protocols for WB-MRI in multiple myeloma. 3) Apply a systematic approach to reporting WB-MRI in multiple myeloma as outlined in MY-RADS. 4) Review the MY-RADS criteria for assessing disease phenotype, burden and response assessment with case examples.

# ABSTRACT

Acknowledging the increasingly important role of WB-MRI for directing myeloma patient care, a multidisciplinary international expert panel of radiologists, medical physicists and haematologists convened to discuss the performance standards, merits and limitations of WB-MRI in myeloma. The MY-RADS imaging recommendations are designed to promote standardization and diminish variations in the acquisition, interpretation, and reporting of WB-MRI in myeloma both in the clinical setting and within clinical trials. MY-RADS comprehensive disease classification requires validation within clinical trials including assessments of reproducibility.

# **Active Handout:Christina Messiou**

http://abstract.rsna.org/uploads/2018/18001097/Handout. Messiou Final RSNA 2018 RC218C.pdf

# RC218D Quantitative WB-MRI for Promoting Precision Oncology

Participants

Dow-Mu Koh, MD, FRCR, Sutton, United Kingdom (Presenter) Nothing to Disclose

# LEARNING OBJECTIVES

1) To review the quantitative parameters that can be derived from WB-MRI studies. 2) To understand the evolving role of quantitative WB-MRI for the evaluation of metastatic bone disease. 3) To appreciate the application of quantitative WB-MRI for precision oncology in assessing tumour treatment response and disease heterogeneity.



# What Radiologists Need to Know about the Evolving Treatment of Brain Metastases?

Monday, Nov. 26 8:30AM - 10:00AM Room: S404CD



AMA PRA Category 1 Credits ™: 1.50 ARRT Category A+ Credit: 1.75

#### **Participants**

Timothy J. Kruser, MD, Chicago, IL (Moderator) Nothing to Disclose

### For information about this presentation, contact:

tkruser@nm.org

# LEARNING OBJECTIVES

1) Identify clinical factors that may favor radiosurgery versus whole brain RT. 2) Describe the imaging changes seen when immunotherapy is combined with radiosurgery. 3) Define current Response Assessment in Neuro-Oncology Brain Metastases guidelines. 4) Differentiate the role of steroids and bevacizumab in management of post-radiosurgery inflammation.

### Active Handout: Timothy J. Kruser

http://abstract.rsna.org/uploads/2018/18001718/Brain met RSNA kruser handout RC220.pdf

### Sub-Events

RC220A The Evolving Role of Radiosurgery and Whole Brain RT in Brain Metastases

### Participants

Timothy J. Kruser, MD, Chicago, IL (Presenter) Nothing to Disclose

### LEARNING OBJECTIVES

View learning objectives under main course title.

### Active Handout: Timothy J. Kruser

http://abstract.rsna.org/uploads/2018/18001719/Brain met RSNA kruser handout RC220A.pdf

RC220B Combining Stereotactic Radiosurgery with Immunotherapy/Targeted Therapy for Brain Metastases

Participants Veronica Chiang, MD, New Haven, CT (*Presenter*) Nothing to Disclose

### LEARNING OBJECTIVES

View learning objectives under main course title.

### **Active Handout:Veronica Chiang**

http://abstract.rsna.org/uploads/2018/18001720/RC220B 11.24.pdf

# RC220C Imaging Response Assessment for Brain Metastases

Participants Timothy J. Kaufmann, MD, Rochester, MN (*Presenter*) Consultant, SpineThera

# LEARNING OBJECTIVES

View learning objectives under main course title.

# RC220D Reirradiation of Brain Metastases; Management of Local Failures

Participants

Caroline Chung, MD, FRCPC, Houston, TX (*Presenter*) Research Grant, Elekta AB; Research Grant, RaySearch Laboratories AB; Advisory Board, RaySearch Laboratories AB; Advisory Board, Novocure Ltd

# LEARNING OBJECTIVES

View learning objectives under main course title.



Advances in CT: Technologies, Applications, Operations-Special Purpose CT

Monday, Nov. 26 8:30AM - 10:00AM Room: S102CD



AMA PRA Category 1 Credits ™: 1.50 ARRT Category A+ Credit: 1.75

# Participants

Ehsan Samei, PhD, Durham, NC (*Coordinator*) Research Grant, General Electric Company; Research Grant, Siemens AG; Advisory Board, medInt Holdings, LLC; License agreement, 12 Sigma Technologies; License agreement, Gammex, Inc Lifeng Yu, PhD, Chicago, IL (*Coordinator*) Nothing to Disclose

# ABSTRACT

CT has become a leading medical imaging modality, thanks to its superb spatial and temporal resolution to depict anatomical details. New advances have enabled extending the technology to depict physiological information. This has enabled a wide and expanding range of clinical applications. These advances are highlighted in this multi-session course. The course offers a comprehensive and topical depiction of these advances with material covering CT system innovations, CT operation, CT performance characterization, functional and quantitative applications, and CT systems devised for specific anatomical applications. The sessions include advances in CT system hardware and software, CT performance optimization, CT practice management and monitoring, spectral CT techniques, quantitative CT techniques, functional CT methods, and special CT use in breast, musculoskeletal, and interventional applications.

# Sub-Events

# RC221A Breast CT Applications

Participants

John M. Boone, PhD, Sacramento, CA (Presenter) Patent agreement, Isotropic Imaging Corporation Consultant, RadSite

# LEARNING OBJECTIVES

1) Introduce the technology of cone beam breast CT to audience. 2) Show both qualitative parameters describing image quality and qualitative images. 3) Demonstrate breast CT performance using metrics such as anatomical noise metrics, computer and human observer studies. 4) Illustrate the future potential of breast CT in diagnostic and screening breast imaging.

# RC221B MSK CT Applications

Participants

Wojciech Zbijewski, PhD, Baltimore, MD (Presenter) Research Grant, Carestream Health, Inc; Research Grant, Siemens AG

### For information about this presentation, contact:

wzbijewski@jhu.edu

# LEARNING OBJECTIVES

1) Explain the technology of musculoskeletal (MSK) cone-beam CT (CBCT). 2) Identify key differences between MSK CBCT and other orthopedic imaging modalities. 3) Discuss emerging clinical applications of MSK CBCT.

# RC221C Interventional CT Applications

Participants Christopher P. Favazza, PhD, Rochester, MN (*Presenter*) Nothing to Disclose



Functional MR Imaging for Tumor Targeting in Radiotherapy

Monday, Nov. 26 8:30AM - 10:00AM Room: S502AB



AMA PRA Category 1 Credits ™: 1.50 ARRT Category A+ Credit: 1.75

**FDA** Discussions may include off-label uses.

### Participants

Kristy K. Brock, PhD, Houston, TX (Moderator) License agreement, RaySearch Laboratories AB

### Sub-Events

# RC222A State of the Art in Functional MR Imaging for Tumor Targeting

Participants

R. Jason Stafford, PhD, Houston, TX (Presenter) Nothing to Disclose

For information about this presentation, contact:

jstafford@mdanderson.org

# LEARNING OBJECTIVES

1) Identify some advanced and emerging MRI techniques which inform on tumor physiology and metabolism. 2) Explain the relevance of functional MR observations to basic underlying tumor physiology and biology. 3) Understand key limitations and tradeoffs of functional MR techniques for tumor assessment.

# RC222B Clinical Need for Functional MR Imaging for Tumor Targeting in Radiation Therapy

Participants

Michelle M. Kim, MD, Ann Arbor, MI (Presenter) Nothing to Disclose

### For information about this presentation, contact:

michekim@med.umich.edu

# LEARNING OBJECTIVES

1) Describe the major limitations of anatomic imaging for tumor target delineation in radiation therapy2) Identify key physiologic and functional MRI techniques of value in radiation treatment planning3) Explain emerging concepts of radiation treatment-individualization using advanced MRI techniques

# RC222C Technical Challenges in the Integration of Functional MR Imaging for Tumor Targeting into Radiotherapy

Participants Ning Wen, PHD, Detroit, MI (*Presenter*) Nothing to Disclose

# For information about this presentation, contact:

nwen1@hfhs.org

# **LEARNING OBJECTIVES**

This presentation is going to review the technical challenges to integrate the functional MR Imaging into radiotherapy including the following aspects: 1) Patient positioning variation; 2) geometrical accuracy consideration; 3) reproducibility of functional imaging across different institutions/scanners/protocols; 4) precision to identify the boundary of the targets; 5) quantitative relationships among different imaging modalities.



# **ACR Accreditation Updates II**

Monday, Nov. 26 8:30AM - 10:00AM Room: E260

PH

AMA PRA Category 1 Credits ™: 1.50 ARRT Category A+ Credit: 1.75

### **Participants**

James M. Kofler JR, PhD, Jacksonville, FL (Coordinator) Nothing to Disclose

### LEARNING OBJECTIVES

1) Learn new and updated information for the ACR breast x-ray imaging accreditation program. 2) Become familiar with the requirements for the ACR ultrasound accreditation program, including data acquisition methods and common deficiencies. 3) Understand how to prepare for an ACR site visit.

### Sub-Events

# RC223A ACR Breast X-Ray Imaging Accreditation Update

Participants

Eric A. Berns, PhD, Denver, CO (Presenter) Nothing to Disclose

# LEARNING OBJECTIVES

1) Understand the ACR Mammography accreditation program requirements. 2) Understand the 2D and DBT recent changes. 3) Review frequently asked questions on the program. 5) Present resources for personnel and facilities undergoing accreditation.

# RC223B ACR US Accreditation Update

Participants

Zheng Feng Lu, PhD, Chicago, IL (Presenter) Nothing to Disclose

# LEARNING OBJECTIVES

1) Understand ACR ultrasound accreditation requirements. 2) Describe the methods and tools for ultrasound QA/QC with an explanation of common deficiencies. 3) List key resources for ACR ultrasound accreditation.

### Active Handout: Zheng Feng Lu

http://abstract.rsna.org/uploads/2018/18001931/Presentation Title Here Presentation Subtitle RC223B.pdf

# RC223C ACR Accreditation: Preparing for a Site Visit

Participants

Heidi A. Edmonson, PhD, Rochester, MN (Presenter) Nothing to Disclose

# LEARNING OBJECTIVES

1) Identify key elements of an ACR Accreditation Program. 2) Understand what data to prepare for an ACR Site Visit. 3) Improve departmental organization for continual accreditation readiness.

# Active Handout:Heidi A. Edmonson

http://abstract.rsna.org/uploads/2018/18001932/Edmonson\_PrepForACRSiteVisit RC223C.pdf



# CT Dose Monitoring: Nuts, Bolts, and Tools... and What We Need to Build

Monday, Nov. 26 8:30AM - 10:00AM Room: N229



AMA PRA Category 1 Credits ™: 1.50 ARRT Category A+ Credit: 1.75

#### Participants

Donald P. Frush, MD, Durham, NC (Moderator) Nothing to Disclose

### For information about this presentation, contact:

donald.frush@duke.edu

# LEARNING OBJECTIVES

1) To learn fundamental elements of a CT dose monitoring program. 2) To review current programs (products) and resources available. 3) To understand current status, including challenges of dose monitoring in adults. 4) To be able to describe current status, including challenges of dose monitoring. 5) To be able to discuss potential advances in dose monitoring.

#### Sub-Events

### RC224A Fundamentals (Nuts and Bolts) and Current Products (Tools)

Participants

Sarah E. McKenney, PhD, Sacramento , CA (Presenter) Nothing to Disclose

### For information about this presentation, contact:

semckenney@ucdavis.edu

### LEARNING OBJECTIVES

1) Evaluate clinical needs for radiation dose monitoring within their institution. 2) Identify resources necessary to ensure a successful monitoring program. 3) Classify the different features of dose monitoring software.

#### **Active Handout:Sarah Eva McKenney**

http://abstract.rsna.org/uploads/2018/18003143/Fundamentals Ideal and Current Dose MonitoringRC224A.pdf

# RC224B CT Dose Monitoring Status in Adults (Including Diagnostic Reference Levels)

Participants Kalpana M. Kanal, PhD, Seattle, WA (*Presenter*) Nothing to Disclose

# For information about this presentation, contact:

kkanal@uw.edu

# LEARNING OBJECTIVES

1) To discuss CT dose monitoring for adults. 2) To learn about diagnostic reference levels in CT. 3) To understand how to implement dose monitoring and diagnostic reference levels in practice.

# RC224C CT Dose Monitoring Status in Children (Including Diagnostic Reference Levels)

Participants Donald P. Frush, MD, Durham, NC (*Presenter*) Nothing to Disclose

# For information about this presentation, contact:

donald.frush@duke.edu

# LEARNING OBJECTIVES

1) To understand the unique considerations in CT dose monitoring program for children. 2) To learn challenges and obstacles in CT dose monitoring programs in children. 3) To be able to discuss future opportunities for CT dose monitoring program in children.

# RC224D Designing the Program of the Future

Participants

Ehsan Samei, PhD, Durham, NC (*Presenter*) Research Grant, General Electric Company; Research Grant, Siemens AG; Advisory Board, medInt Holdings, LLC; License agreement, 12 Sigma Technologies; License agreement, Gammex, Inc

### LEARNING OBJECTIVES

1) To understand the importance of analytics in extracting meaninoful and actionable knowledge from performance data 2) To

understand the role and components of image quality characterization based on patient images. 3) To understand performance monitoring as the overarching objective of dose monitoring.



Mini-course: Image Interpretation Science - Clinical Foundations of Medical Image Perception: Why Study Radiologists

Monday, Nov. 26 8:30AM - 10:00AM Room: S104A

# PH

AMA PRA Category 1 Credits ™: 1.50 ARRT Category A+ Credit: 0

### Participants

Elizabeth A. Krupinski, PhD, Atlanta, GA (*Coordinator*) Nothing to Disclose Ehsan Samei, PhD, Durham, NC (*Coordinator*) Research Grant, General Electric Company; Research Grant, Siemens AG; Advisory Board, medInt Holdings, LLC; License agreement, 12 Sigma Technologies; License agreement, Gammex, Inc

### For information about this presentation, contact:

ekrupin@emory.edu

# LEARNING OBJECTIVES

1) Define the perception factors and considerations in interpreting a medical image. 2) Delineate how perception considerations impact the radiologist's practice in terms of increasing sensitivity and reducing errors. 3) Describe perceptual factors while interpreting medical images including cognitive overload, satisfaction of search, CAD influence, color presentation, image processing, and graphical user interface. 4) Describe the origins of the inter and intra-observer variability issue. 5) Trace the roots of visual search studies in radiology. 6) Show when Receiver Operating Characteristic (ROC) analysis comes into the picture. 7) Delineate why vision models are important for image perception research. 8) Describe the role of medical image perception in modern medicine. 9) Outline the cost, frequency, and patient care impact of image interpretation. 10) Provide an overview of common issues explored in studies of interpretation processes. 11) Delineate what difference perception considerations can make in day-to-day practice of radiology.

### ABSTRACT

Medical images constitute a core portion of the information physicians utilize to render diagnostic and treatment decisions. At a fundamental level, the diagnostic process involves two aspects - visually inspecting the image (perception) and rendering an interpretation (cognition). Key indications of expert interpretation of medical images are consistent, accurate and efficient diagnostic performance, but how do we know when someone has attained the level of training required to be considered an expert? How do we know the best way to present images to the clinician in order to optimize accuracy and efficiency? The advent of digital imaging in many clinical specialties, including radiology, pathology and dermatology, has dramatically changed the way that clinicians view images, how residents are trained, and thus potentially the way they interpret image information, emphasizing our need to understand how clinicians interact with the information in an image during the interpretation process. With improved understanding we can develop ways to further improve decision-making and thus improve patient care.

# Sub-Events

# RC225A Clinical Relevance of Perceptual Issues in Radiology

Participants

Francine L. Jacobson, MD, MPH, Boston, MA (Presenter) Research Grant, Hummingbird Diagnostics GmbH

# For information about this presentation, contact:

### fjacobson@bwh.harvard.edu

# LEARNING OBJECTIVES

1) Define the perception factors and considerations in interpreting a medical image. 2) Delineate how perception considerations impact the radiologist's practice in terms of increasing sensitivity and reducing errors. 3) Describe perceptual factors while interpreting medical images including cognitive overload, satisfaction of search, CAD influence, color presentation, image processing, and graphical user interface.

### ABSTRACT

In the 21st Century, technology has led to increased workloads for radiologists with advanced modalities and image processing dramatically increasing the volume of images to be studied by the Radiologist. Information overload is not limited to visual data in the era of the electronic medical record. Increasingly, radiologists are being asked to perform the physical examination of the patient without the opportunity to interact with the patient directly to localize pain and acquire additional history about prior ilnesses and surgical treatments. Set against a background of changing diagnostic criteria and individualization of treatment, critical decisions are increasingly made by radiologists using a variety of diagnostic and non-diagnostic quality image displays. Perception science provides keys to evolving the human visual processes in evaluating medical images. It is through perception science that we can move with technology to newer image presentation paradigms and maintain the efficacy of radiology.

# RC225B A Short History of Image Perception in Radiology

Participants Elizabeth A. Krupinski, PhD, Atlanta, GA (*Presenter*) Nothing to Disclose

### For information about this presentation, contact:

#### ekrupin@emory.edu

#### **LEARNING OBJECTIVES**

1) Describe the origins of the inter and intra-observer variability issue. 2) Trace the roots of visual search studies in radiology. 3) Show when Receiver Operating Characteristic (ROC) analysis comes into the picture. 4) Delineate why vision models are important for image perception research.

### ABSTRACT

Medical images constitute a core portion of the information physicians utilize to render diagnostic and treatment decisions. At a fundamental level, the diagnostic process involves two aspects - visually inspecting the image (perception) and rendering an interpretation (cognition). Key indications of expert interpretation of medical images are consistent, accurate and efficient diagnostic performance, but how do we know when someone has attained the level of training required to be considered an expert? How do we know the best way to present images to the clinician in order to optimize accuracy and efficiency? The advent of digital imaging in many clinical specialties, including radiology, pathology and dermatology, has dramatically changed the way that clinicians view images, how residents are trained, and thus potentially the way they interpret image information, emphasizing our need to understand how clinicians interact with the information in an image during the interpretation process. With improved understanding we can develop ways to further improve decision-making and thus improve patient care.

### **Honored Educators**

Presenters or authors on this event have been recognized as RSNA Honored Educators for participating in multiple qualifying educational activities. Honored Educators are invested in furthering the profession of radiology by delivering high-quality educational content in their field of study. Learn how you can become an honored educator by visiting the website at: https://www.rsna.org/Honored-Educator-Award/ Elizabeth A. Krupinski, PhD - 2017 Honored Educator



# Patient Centered Imaging: Research, Dissemination and Practice

Monday, Nov. 26 8:30AM - 10:00AM Room: E353A



AMA PRA Category 1 Credits ™: 1.50 ARRT Category A+ Credit: 1.75

### **Participants**

Ruth C. Carlos, MD, MS, Ann Arbor, MI (Moderator) Nothing to Disclose

### Sub-Events

# RC227A Patient Engagement and Comparative Effectiveness Research in Imaging

Participants

Ruth C. Carlos, MD, MS, Ann Arbor, MI (Presenter) Nothing to Disclose

# LEARNING OBJECTIVES

1) Summarize the state of comparative effectiveness research (CER) in imaging. 2) Discuss concepts of patient engagement in imaging CER.

### **Honored Educators**

Presenters or authors on this event have been recognized as RSNA Honored Educators for participating in multiple qualifying educational activities. Honored Educators are invested in furthering the profession of radiology by delivering high-quality educational content in their field of study. Learn how you can become an honored educator by visiting the website at: https://www.rsna.org/Honored-Educator-Award/ Ruth C. Carlos, MD, MS - 2015 Honored EducatorRuth C. Carlos, MD, MS - 2018 Honored Educator

# RC227B Patient Centered Research in Imaging Care Delivery

Participants Hanna M. Zafar, MD, Philadelphia, PA (*Presenter*) Nothing to Disclose Ilana F. Gareen, PhD, Providence, RI (*Presenter*) Nothing to Disclose Ruth C. Carlos, MD, MS, Ann Arbor, MI (*Presenter*) Nothing to Disclose

### LEARNING OBJECTIVES

1) Illustrate patient-centered research in care delivery using contemporary examples.

# RC227C Emerging Topics in Patient Centered Research and Dissemination

Participants Sheetal M. Kircher, MD, Chicago, IL (*Presenter*) Nothing to Disclose Bruce J. Hillman, MD, Wake Forest, NC (*Presenter*) Nothing to Disclose

For information about this presentation, contact:

bjh8a@virginia.edu

skirche1@nm.org

### LEARNING OBJECTIVES

1) Introduce concepts of financial burden of care. 2) Understand the arguments posed for researchers supplying their raw data as a pre-requisite of publication. 3) Familiarize themselves with how medical journals are dealing with patient demands for greater access to and clarity of research findings.



MRI Safety Issue for Implants, Devices, and Contrast: Update 2018 (Interactive Session)

Monday, Nov. 26 8:30AM - 10:00AM Room: N228



AMA PRA Category 1 Credits ™: 1.50 ARRT Category A+ Credit: 1.75

FDA Discussions may include off-label uses.

# Participants

Jeffrey C. Weinreb, MD, New Haven, CT (Moderator) Consultant, Bracco Group; Author, Siemens AG

For information about this presentation, contact:

jeffrey.weinreb@yale.edu

### LEARNING OBJECTIVES

1) Understand the various MRI issues that impact passive and active, implants and devices. 2) Define the terms applied to MRI labeling of implants and devices. 3) Appreciate the controversies that exist for certain implants and understand the latest labeling information for implanted medical products. 4) Describe current data about safety of gadolinium-based contact agents. 5) Compare the association of various GBCAs with NSF and gadolinium retention. 6) Review updated recommendations about use of gadolinium-based contrast agents. 7) Through case presentation format multiple common clinical scenarios will be presented that reflect potential MRI safety events. 8) Best practices and literature will be reviewed to inform participants on how to best address these scenarios with an emphasis on MR and patient safety principles.

### Sub-Events

# RC229A MRI Issues for Implants and Devices

Participants

Frank G. Shellock, PhD, Playa Del Rey, CA (Presenter) Nothing to Disclose

### For information about this presentation, contact:

frank.shellock@gte.net

# LEARNING OBJECTIVES

1) Understand the various MRI issues that impact passive and active, implants and devices. 2) Define the terms applied to MRI labeling of implants and devices. 3) Know the differences in the labeling information that is applied to passive and active medical products. 4) Appreciate the controversies that exist for certain implants and comprehend the latest labeling information for implanted medical products.

# RC229B Update on the Risks of Gadolinium-Based Contrast Agents

Participants

Jeffrey C. Weinreb, MD, New Haven, CT (Presenter) Consultant, Bracco Group; Author, Siemens AG

# **LEARNING OBJECTIVES**

1) Describe current data about safety of gadolinium-based contact agents. 2) Compare the association of various GBCAs with NSF and gadolinium retention. 3) Review updated recommendations about use of gadolinium-based contrast agents.

#### **Honored Educators**

Presenters or authors on this event have been recognized as RSNA Honored Educators for participating in multiple qualifying educational activities. Honored Educators are invested in furthering the profession of radiology by delivering high-quality educational content in their field of study. Learn how you can become an honored educator by visiting the website at: https://www.rsna.org/Honored-Educator-Award/ Jeffrey C. Weinreb, MD - 2018 Honored Educator

# RC229C Common Clinical MRI Safety Scenarios

Participants

Jay K. Pahade, MD, New Haven, CT (Presenter) Consultant, General Electric Company

# LEARNING OBJECTIVES

Through case presentation format multiple common clinical scenarios will be presented that reflect potential MRI safety events.
 Best practices and literature will be reviewed to inform participants on how to best address these scenarios with an emphasis on MR and patient safety principles.

# RC229D Questions and Answers

Participants

Frank G. Shellock, PhD, Playa Del Rey, CA (*Presenter*) Nothing to Disclose Jay K. Pahade, MD, New Haven, CT (*Presenter*) Consultant, General Electric Company Jeffrey C. Weinreb, MD, New Haven, CT (*Presenter*) Consultant, Bracco Group; Author, Siemens AG

# **Honored Educators**

Presenters or authors on this event have been recognized as RSNA Honored Educators for participating in multiple qualifying educational activities. Honored Educators are invested in furthering the profession of radiology by delivering high-quality educational content in their field of study. Learn how you can become an honored educator by visiting the website at: https://www.rsna.org/Honored-Educator-Award/ Jeffrey C. Weinreb, MD - 2018 Honored Educator



# Hands-on Musculoskeletal Ultrasound: A Forum for Question and Answer (Hands-on)

Monday, Nov. 26 8:30AM - 10:00AM Room: E258



AMA PRA Category 1 Credits ™: 1.50 ARRT Category A+ Credit: 1.75

### Participants

Marnix T. van Holsbeeck, MD, Detroit, MI (*Presenter*) Minor stockholder, Koninklijke Philips NV; Minor stockholder, General Electric Company; Stockholder, MedEd3D; Grant, Siemens AG; Grant, General Electric Company; Lodewijk J. van Holsbeeck, MD, Lansing, MI (*Presenter*) Nothing to Disclose Joseph H. Introcaso, MD, Neenah, WI (*Presenter*) Nothing to Disclose Humberto G. Rosas, MD, Madison, WI (*Presenter*) Nothing to Disclose

### **LEARNING OBJECTIVES**

1) Recognize and identify pitfalls of scanning that lead to false positive or false negative musculoskeletal ultrasound results. 2) Perform skills for scanning difficult patients. 3) Follow rigorous protocols for the examination of different anatomic regions. 4) Position patients for more complicated musculoskeletal ultrasound examinations. 5) Recognize and integrate the importance of tissue movement in judging the functionality of the extremities.

### ABSTRACT

In this Musculoskeletal Ultrasound Master class, an opportunity will be given to participants to start a written dialogue in advance to RSNA 2018. The electronically submitted questions will be sorted by instructors and organized per topic. A select number of recurrent themes in these questions will be prepared for dialogue on stage. When the questions focus on a particular scanning skill, the authors of the questions will be invited on the examination platform to show problems they encounter in their practice. By using a step-by step approach in solving the scanning issues, all who are present should benefit from the technical interactions on stage. Cameras will project scanning details on large screens. The seating in the class will guarantee close proximity for an enriching interaction between audience and stage.



# **Burnout of a Radiology Physician Workforce**

Monday, Nov. 26 8:30AM - 10:00AM Room: N226

# LM

AMA PRA Category 1 Credits ™: 1.50 ARRT Category A+ Credit: 0

### **Participants**

Cheri L. Canon, MD, Birmingham, AL (Moderator) Royalties, The McGraw-Hill Companies

### For information about this presentation, contact:

ccanon@uabmc.edu

#### Sub-Events

RC232A Burnout in Radiology

Participants Felix S. Chew, MD, Seattle, WA (*Presenter*) Nothing to Disclose

For information about this presentation, contact:

fchew@uw.edu

### LEARNING OBJECTIVES

1) Define burnout and discuss its prevalence and potential causes in radiologists. 2) Discuss burnout among radiologist trainees and its potential effects on their education. 3) Describe approaches to mitigating burnout in the radiologist's workplace.

### **Honored Educators**

Presenters or authors on this event have been recognized as RSNA Honored Educators for participating in multiple qualifying educational activities. Honored Educators are invested in furthering the profession of radiology by delivering high-quality educational content in their field of study. Learn how you can become an honored educator by visiting the website at: https://www.rsna.org/Honored-Educator-Award/ Felix S. Chew, MD - 2012 Honored EducatorFelix S. Chew, MD - 2016 Honored Educator

# RC232B How to Address Radiology Trainees' Burnout

Participants

Stacy E. Smith, MD, Boston, MA (Presenter) Nothing to Disclose

# RC232C Remedies to Mitigate Burnout in the Workplace

Participants

Cheri L. Canon, MD, Birmingham, AL (Presenter) Royalties, The McGraw-Hill Companies

For information about this presentation, contact:

ccanon@uabmc.edu

# LEARNING OBJECTIVES

1) List activities that can mitigate burnout.



Targeted Treatment and Imaging of Liver Cancers: Basic to Advanced Techniques in Minimally-Invasive Therapies and Imaging

Monday, Nov. 26 8:30AM - 10:00AM Room: E261



AMA PRA Category 1 Credits ™: 1.50 ARRT Category A+ Credit: 1.75

**FDA** Discussions may include off-label uses.

# Participants

John J. Park, MD, PhD, Duarte, CA (*Moderator*) Proctor, Sirtex Medical Ltd; Speaker, Medtronic plc; Speaker, Galil Medical Ltd; Speaker, BTG International Ltd; Speaker, Biocompatibles International plc; Consultant, Biocompatibles International plc; Consultant, BTG International Ltd; Advisory Board, Eisai Co, Ltd

Jinha Park, MD, PhD, Iowa City, IA (Moderator) Nothing to Disclose

John J. Park, MD, PhD, Duarte, CA (*Presenter*) Proctor, Sirtex Medical Ltd; Speaker, Medtronic plc; Speaker, Galil Medical Ltd; Speaker, BTG International Ltd; Speaker, Biocompatibles International plc; Consultant, Biocompatibles International plc; Consultant, BTG International Ltd; Advisory Board, Eisai Co, Ltd

Jinha Park, MD, PhD, Iowa City, IA (Presenter) Nothing to Disclose

Marcelo S. Guimaraes, MD, Charleston, SC (*Presenter*) Consultant, Baylis Medical Company; Consultant, Terumo Corporation; Consultant, General Electric Company; Consultant, Medtronic plc

Andrew C. Price, MD, Gilbert, AZ (Presenter) Nothing to Disclose

Sandeep T. Laroia, MD, Iowa City, IA (Presenter) Nothing to Disclose

# For information about this presentation, contact:

Andrew.Price@bannerhealth.com

# jinha-park@uiowa.edu

# LEARNING OBJECTIVES

1) Discuss the role of the interventional radiologist in the treatment and management of patients with primary and metastatic liver cancer as part of the multidisciplinary team. 2) Learn best practice techniques in the treatment of liver cancers, with emphasis on both locoregional and focal therapeutic approaches, and indications for treatment. 3) Explore various tips and tricks for each treatment modality and learn how to avoid complications through good patient selection, choosing the appropriate techniques, and knowing what common mistakes to avoid. 4) Learn about newer and developing techniques and devices, their potential roles and indications, and potential pitfalls. 5) Explore advanced imaging modalities in the detection of tumors and for monitoring treatment response.

# ABSTRACT

Primary and metastatic liver disease may benefit from combined techniques such as bland/chemoembolization and liver ablation. The presentation will provide the rationale for the association of techniques, patient selection, tips and tricks, equipment and supplies necessary, protective techniques and how to avoid complications. Also, it will be discussed the results and current literature to support the association of techniques.



# Carotid and Renal Doppler (Hands-on)

Monday, Nov. 26 8:30AM - 10:00AM Room: E264



AMA PRA Category 1 Credits ™: 1.50 ARRT Category A+ Credit: 1.75

# Participants

Gowthaman Gunabushanam, MD, New Haven, CT (*Presenter*) Nothing to Disclose Shweta Bhatt, MD,MBBS, Rochester, NY (*Presenter*) Nothing to Disclose Wui K. Chong, MD, Houston, TX (*Presenter*) Nothing to Disclose Corinne Deurdulian, MD, Los Angeles, CA (*Presenter*) Nothing to Disclose Vikram S. Dogra, MD, Rochester, NY (*Presenter*) Editor, Wolters Kluwer nv; Ulrike M. Hamper, MD, MBA, Baltimore, MD (*Presenter*) Nothing to Disclose Davida Jones-Manns, Hampstead, MD (*Presenter*) Nothing to Disclose Mark E. Lockhart, MD, Birmingham, AL (*Presenter*) Nothing to Disclose Mark E. Lockhart, MD, Birmingham, AL (*Presenter*) Nothing to Disclose Margarita V. Revzin, MD, Wilton, CT (*Presenter*) Nothing to Disclose Michelle L. Robbin, MD, Birmingham, AL (*Presenter*) Consultant, Koninklijke Philips NV; Speaker, Koninklijke Philips NV; Leslie M. Scoutt, MD, New Haven, CT (*Presenter*) Speaker, Koninklijke Philips NV Ravinder Sidhu, MD, Rochester, NY (*Presenter*) Nothing to Disclose Sadhna Verma, MD, Cincinnati, OH (*Presenter*) Nothing to Disclose Sadhna Verma, MD, Cincinnati, OH (*Presenter*) Nothing to Disclose William D. Middleton, MD, Saint Louis, MO (*Presenter*) Nothing to Disclose

### For information about this presentation, contact:

corinne.deurdulian@med.usc.edu

Drsadhnaverma@gmail.com

mrobbin@uabmc.edu

### LEARNING OBJECTIVES

1) Describe the technique and optimally perform carotid Doppler ultrasound. 2) Describe the technique and optimally perform renal Doppler ultrasound. 3) Review qualitative and quantitative criteria for diagnosing abnormalities in carotid and renal ultrasound Doppler examinations.

# ABSTRACT

This hands-on course will provide participants with a combination of didactic lectures and an extended 'live' scanning opportunity on normal human volunteers, as follows: Didactic lectures (30 minutes): Carotid Doppler ultrasound: scanning technique, diagnostic criteria and interesting teaching cases. Renal Doppler ultrasound: scanning technique, diagnostic criteria and interesting teaching cases. Mentored scanning (60 minutes): Following the didactic lectures, the participants will proceed to a scanning area with normal human volunteers and ultrasound machines from different manufacturers. Participants will be able to perform live scanning with direct assistance, as needed, by faculty. Faculty will be able to offer feedback, help participants improve their scanning technique as well as answer any questions. Time permitting, faculty will also be available to answer general questions relating to all aspects of vascular ultrasound, not just limited to carotid and renal Doppler studies.

### Active Handout:Wui Kheong Chong

http://abstract.rsna.org/uploads/2018/15000037/RSNA doppler 2018 RC252.pdf

# **Honored Educators**

Presenters or authors on this event have been recognized as RSNA Honored Educators for participating in multiple qualifying educational activities. Honored Educators are invested in furthering the profession of radiology by delivering high-quality educational content in their field of study. Learn how you can become an honored educator by visiting the website at: https://www.rsna.org/Honored-Educator-Award/ Margarita V. Revzin, MD - 2017 Honored EducatorLeslie M. Scoutt, MD - 2014 Honored EducatorSadhna Verma, MD - 2013 Honored Educator



# Preparing your Radiology Practice and IT Department for Big Data

Monday, Nov. 26 8:30AM - 10:00AM Room: S503AB



AMA PRA Category 1 Credits ™: 1.50 ARRT Category A+ Credit: 1.75

### Participants

Paul J. Chang, MD, Chicago, IL (*Moderator*) Co-founder, Koninklijke Philips NV; Researcher, Koninklijke Philips NV; Researcher, Bayer AG; Advisory Board, Aidoc Ltd; Advisory Board, EnvoyAI; Advisory Board, Inference Analytics

# **LEARNING OBJECTIVES**

1) The potential of applying "Big Data" approaches to radiology will be discussed. 2) The participant will be introduced to the importance of developing a comprehensive IT architecture and capability beyond the EMR in order to effectively use "Big Data" tools. 3) Strategies for preparing IT for "Big Data" will be discussed.

### ABSTRACT

Current and near future requirements and constraints will require radiology practices to continuously improve and demonstrate the value they add to the enterprise. Merely 'managing the practice' will not be sufficient; groups will be required to compete in an environment where the goal will be measurable improvements in efficiency, productivity, quality, and safety. This will require optimally leveraging IT enabled business intelligence, analytics, and data driven workflow. In many ways, this challenge can be described as a "Big Data" problem, requiring the application of newer "Big Data" approaches and tools. Unfortunately, many have discovered that an "EMR centric" IT perspective may severely limit the ability for the enterprise to maximally leverage these newer tools to create differentiable value. This session will provide an introduction to the importance of developing a comprehensive architectural strategy to augment the existing EMR to more effectively consume "Big Data" tools.

### Sub-Events

# RC253A Getting Your IT Infrastructure Ready for Big Data

Participants

Paul J. Chang, MD, Chicago, IL (*Presenter*) Co-founder, Koninklijke Philips NV; Researcher, Koninklijke Philips NV; Researcher, Bayer AG; Advisory Board, Aidoc Ltd; Advisory Board, EnvoyAI; Advisory Board, Inference Analytics

### LEARNING OBJECTIVES

1) The potential of applying "Big Data" and noSQL approaches to radiology will be discussed. 2) The participant will be introduced to the importance of developing a comprehensive IT architecture and capability beyond the EMR in order to effectively use "Big Data" tools. 3) Strategies for preparing IT for business intelligence and analytics will be discussed.

# ABSTRACT

Current and near future requirements and constraints will require radiology practices to continuously improve and demonstrate the value they add to the enterprise. Merely 'managing the practice' will not be sufficient; groups will be required to compete in an environment where the goal will be measurable improvements in efficiency, productivity, quality, and safety. This will require optimally leveraging IT enabled business intelligence, analytics, and data driven workflow. In many ways, this challenge can be described as a "Big Data" problem, requiring the application of newer "Big Data" approaches and tools. Unfortunately, many have discovered that an "EMR centric" IT perspective may severely limit the ability for the enterprise to maximally leverage these newer tools to create differentiable value. This session will provide an introduction to the importance of developing a comprehensive architectural strategy to augment the existing EMR to more effectively consume "Big Data" approaches and fully leverage business intelligence and analytics.

# RC253B NoSQL Approaches: Beyond the Traditional Relational Database

#### Participants

Paul J. Chang, MD, Chicago, IL (*Presenter*) Co-founder, Koninklijke Philips NV; Researcher, Koninklijke Philips NV; Researcher, Bayer AG; Advisory Board, Aidoc Ltd; Advisory Board, EnvoyAI; Advisory Board, Inference Analytics

# LEARNING OBJECTIVES

1) The distinction between the traditional relational (SQL) database and "NoSQL" approaches will be discussed. 2) The attendees will be given a basic introduction to how "NoSQL" tools, such as Hadoop, MapReduce, MongoDB can be complementary to existing approaches. 3) NoSQL applications and their relevance to radiology will be discussed.

# ABSTRACT

Current and near future requirements and constraints will require radiology practices to continuously improve and demonstrate the value they add to the enterprise. Merely 'managing the practice' will not be sufficient; groups will be required to compete in an environment where the goal will be measurable improvements in efficiency, productivity, quality, and safety. This will require optimally leveraging IT enabled business intelligence, analytics, and data driven workflow. These approaches will require the ability to consume and utilize all available enterprise data, including unstructured reports, multimedia objects, etc. Other industries have realized that traditional IT approaches, such as the relational (SQL) database, cannot optimally address these "difficult" data

objects. Many outside of the medical domain have successfully augmented traditional approaches by newer "Big Data" and "NoSQL" methodologies, such as Hadoop, MapReduce, MongoDB, etc. In this session, an introduction to these newer tools will be presented.

# RC253C Radiologist Workflow and AI: Challenges and Opportunities

Participants

William W. Boonn, MD, Philadelphia, PA (Presenter) Officer, Nuance Communications, Inc; Shareholder, Nuance Communications, Inc

# LEARNING OBJECTIVES

1) A technical overview of machine learning and deep learning will be presented. 2) Applications of machine learning and deep learning in radiology will be illustrated. 3) Challenges in deploying machine learning and deep learning in radiologist workflow and productivity demands will be discussed.

#### ABSTRACT

Computers in radiology have often promised to deliver faster clinical decisions, more accurate diagnoses, and transformative visualizations. Computer aided diagnostics (CAD) has been deployed to guide radiologists in their detection of abnormalities and identification of disease. Historically, CAD has been based on domain-driven heuristics, and more recently used simple machine learning on structured data. Both of these require extensive manual engineering making them very slow to build, limited in their flexibility, and less accurate than we would like. Deep learning is a new paradigm that offers a transformative solution. Instead of demanding countless human hours of painstaking feature generation and selection, deep learning automatically discovers clinically-relevant features by first architecting a hierarchy of patterns (loosely modelled on the brain's own neural neural networks) and then updating those patterns upon observing examples. As radiology requires complex associative pattern recognition, deep learning is the ideal companion tool. Enlitic is developing a deep neural network of the entire human body that will offer a new way forward in which the radiologist has immediate access to the most relevant clinical information. In this talk, we will present a technical overview of machine learning and deep learning, illustrate its applications in radiology, and detail some of the challenges improving radiological workflow using deep learning poses.

#### **Honored Educators**

Presenters or authors on this event have been recognized as RSNA Honored Educators for participating in multiple qualifying educational activities. Honored Educators are invested in furthering the profession of radiology by delivering high-quality educational content in their field of study. Learn how you can become an honored educator by visiting the website at: https://www.rsna.org/Honored-Educator-Award/ William W. Boonn, MD - 2012 Honored Educator



#### RC254

# Next Frontier in Imaging: Disease-specific Radiology Reports

Monday, Nov. 26 8:30AM - 10:00AM Room: S402AB

IN

AMA PRA Category 1 Credits ™: 1.50 ARRT Category A+ Credit: 0

#### **Participants**

Olga R. Brook, MD, Boston, MA (Moderator) Nothing to Disclose

#### For information about this presentation, contact:

obrook@bidmc.harvard.edu

# LEARNING OBJECTIVES

1) Demonstrate the advantages of disease-specific reporting over organ-system-based reporting. 2) Provide specific examples of the disease-specific templates that have been shown to improve value of imaging in diagnostic and interventional radiology

#### Sub-Events

# RC254A Contextual Radiology Reporting: The Next Generation of Structured Reports

Participants Mark D. Mamlouk, MD, Santa Clara, CA (*Presenter*) Nothing to Disclose

#### For information about this presentation, contact:

mark.d.mamlouk@kp.org

#### LEARNING OBJECTIVES

1) Define what contextual reporting is and demonstrate how to create disease-specific templates. 2) Explain the advantages of contextual reporting over conventional structured reporting through the use of imaging examples and contextual templates.

# RC254B Reporting Prostate MRI: Optimizing Content for Referring Providers

Participants Benjamin D. Spilseth, MD, Minneapolis, MN (*Presenter*) Consultant, NxThera, Inc

For information about this presentation, contact:

spil0042@umn.edu

#### **LEARNING OBJECTIVES**

1) Learn urologists' and radiologists' opinions on prostate MRI reporting. 2) Learn how reports and reporting templates can be improved to include the most relevant clinical data. 3) Understand patterns in how referring provider's opinions may be different from radiologists on optimal imaging report content.

# RC254C Interventional Radiology Standardized Reporting: Latest Developments and Opportunities

Participants

Stephanie Dybul, MBA, RT, Milwaukee, WI (Presenter) Nothing to Disclose

# LEARNING OBJECTIVES

1) Understand how to integrate IR standardized reports in your practice. 2) Understand the intent behind IR standardized report design and data element selection, as well as how data is collected in the IR Registry.

# RC254D Why RADS? Standardized Terminologies and Templates Allow Unambiguous Communication of Risk

Participants

Thomas W. Loehfelm, MD, PhD, Atlanta, GA (Presenter) Nothing to Disclose

# For information about this presentation, contact:

twloehfelm@ucdavis.edu

# LEARNING OBJECTIVES

1) Understand basic principles of clear communication, recognize quirky dictation habits that confound communication. 2) Learn the advantages of structured declarations to unambiguously convey meaning.

# RC254E Disease-specific Structured Reporting in Thoracic Imaging: Added Value from a Quality Perspective

#### Participants

Jonathan H. Chung, MD, Chicago, IL (*Presenter*) Royalties, Reed Elsevier; Consultant, Boehringer Ingelheim GmbH; Consultant, F. Hoffmann-La Roche Ltd; Consultant, Applied Clinical Intelligence LLC; Consultant, Veracyte, Inc; Speakers Bureau, Boehringer Ingelheim GmbH; Speakers Bureau, F. Hoffmann-La Roche Ltd

# LEARNING OBJECTIVES

1) Understand that structured reports encourage positive radiologist behavior. 2) Recognize how structured, disease specific templates can aid in quality improvement. 3) Understand how structured, disease specific templates can help our clinical colleagues.

# **Honored Educators**

Presenters or authors on this event have been recognized as RSNA Honored Educators for participating in multiple qualifying educational activities. Honored Educators are invested in furthering the profession of radiology by delivering high-quality educational content in their field of study. Learn how you can become an honored educator by visiting the website at: https://www.rsna.org/Honored-Educator-Award/ Jonathan H. Chung, MD - 2013 Honored Educator



#### RCB21

# Deploying an Open-Source DICOM Archive and Web Viewer with OHIF and Orthanc (Hands-on)

Monday, Nov. 26 8:30AM - 10:00AM Room: S401CD

# IN

AMA PRA Category 1 Credits ™: 1.50 ARRT Category A+ Credit: 1.75

# Participants

Simon Rascovsky, MD, MSc, Bogota, Colombia (*Moderator*) Director, Nucleus Health, LLC Marc D. Kohli, MD, San Francisco, CA (*Presenter*) Nothing to Disclose Ross W. Filice, MD, Chevy Chase, MD (*Presenter*) Co-founder, DexNote, LLC; Research Grant, NVIDIA Corporation; Advisor, BunkerHill Health, Inc Simon Rascovsky, MD, MSc, Bogota, Colombia (*Presenter*) Director, Nucleus Health, LLC

#### For information about this presentation, contact:

ross.w.filice@gunet.georgetown.edu

# LEARNING OBJECTIVES

1) Learn how to deploy an instance of Orthanc and OHIF on your personal machine in a way that's translatable to your server architecture back home. 2) Learn how to query, retrieve, and store images to the DICOM archive as well as view these images in the OHIF viewer.



#### RCC21

# Getting Stuff Done: A Mindful Approach to Personal Productivity

Monday, Nov. 26 8:30AM - 10:00AM Room: S501ABC

# IN

AMA PRA Category 1 Credits ™: 1.50 ARRT Category A+ Credit: 1.75

## Participants

Puneet Bhargava, MD, Seattle, WA (*Moderator*) Nothing to Disclose Matthew B. Morgan, MD, Sandy, UT (*Presenter*) Consultant, Reed Elsevier Puneet Bhargava, MD, Seattle, WA (*Presenter*) Nothing to Disclose

#### For information about this presentation, contact:

Bhargp@uw.edu

#### LEARNING OBJECTIVES

1) Introduce the concept of "Getting Things Done.' Learn the concepts of Inbox Zero and other email management techniques. 2) Using tools such as note-taking applications, citation and password managers.3) Using self-inquiry techniques, review how to make meaningful and powerful changes in how we engage with technology.

#### **Active Handout: Puneet Bhargava**

http://abstract.rsna.org/uploads/2018/18001626/Productivity Primer RCC21.pdf

#### **Honored Educators**

Presenters or authors on this event have been recognized as RSNA Honored Educators for participating in multiple qualifying educational activities. Honored Educators are invested in furthering the profession of radiology by delivering high-quality educational content in their field of study. Learn how you can become an honored educator by visiting the website at: https://www.rsna.org/Honored-Educator-Award/ Puneet Bhargava, MD - 2015 Honored Educator



#### MSAS22

Evolving Imaging Methods for the Cancer Patient - Part 2 (Sponsored by the Associated Sciences Consortium) (Interactive Session)

Monday, Nov. 26 10:30AM - 12:00PM Room: S105AB



AMA PRA Category 1 Credits ™: 1.50 ARRT Category A+ Credit: 1.75

#### **Participants**

Nancy McDonald, MS, Chicago, IL (*Moderator*) Nothing to Disclose William A. Undie, PhD, RT, Houston, TX (*Moderator*) Nothing to Disclose Bernie McKay, BS, Chicago, IL (*Presenter*) Employee, Triad Isotopes Katie Tucker, BS, Chicago, IL (*Presenter*) Nothing to Disclose

# LEARNING OBJECTIVES

1) Improve basic knowledge and skills relevant to new imaging procedures and treatments for the cancer patient. 2) Assess the potential applications to clinical practice and the treatments to these patients. 3) Assess the potential of new radiopharmaceuticals to imaging and the treatment of the cancer patient. 4) How Nuclear Medicine is integrated with other modalities in the treatment of the cancer patient.



#### MSCM22

Case-based Review of Magnetic Resonance (Interactive Session)

Monday, Nov. 26 10:30AM - 12:00PM Room: S100AB



AMA PRA Category 1 Credits ™: 1.50 ARRT Category A+ Credit: 1.75

FDA Discussions may include off-label uses.

#### Participants

Jorge A. Soto, MD, Boston, MA (Director) Royalties, Reed Elsevier

#### Sub-Events

# MSCM22A MRI of the Kidneys, Adrenals, and Retroperitoneum

Participants Christine O. Menias, MD, Chicago, IL (*Presenter*) Nothing to Disclose

For information about this presentation, contact:

menias.christine@mayo.edu

#### LEARNING OBJECTIVES

1) Discuss MR imaging features of several GU cases in a case-based format. 2) Review imaging pitfalls and differential diagnoses of GU cases at MR imaging. 3) Pathology of the kidneys, bladder, seminal vesicles, testes, retroperitoneum, and adrenals will be discussed in a case based format.

#### **Honored Educators**

Presenters or authors on this event have been recognized as RSNA Honored Educators for participating in multiple qualifying educational activities. Honored Educators are invested in furthering the profession of radiology by delivering high-quality educational content in their field of study. Learn how you can become an honored educator by visiting the website at: https://www.rsna.org/Honored-Educator-Award/ Christine O. Menias, MD - 2013 Honored EducatorChristine O. Menias, MD - 2014 Honored EducatorChristine O. Menias, MD - 2015 Honored EducatorChristine O. Menias, MD - 2016 Honored EducatorChristine O. Menias, MD - 2018 Honored Educator

#### MSCM22B MRI of the Female Pelvis

Participants Marcia C. Javitt, MD, Haifa, Israel (*Presenter*) Nothing to Disclose

#### LEARNING OBJECTIVES

1) Learn appropriate use of and technique for female pelvic MRI. 2) Recognize imaging patterns of benign and malignant disease, triage emergencies, and analyze key findings that enable an informed interpretation. 3) Be mindful of the need for accurate, safe, and efficient patient management.

#### ABSTRACT

This presentation will review basics for performance and interpretation of pelvic MRI with emphasis on differential diagnosis of common findings. Important and unusual complications of common problems will be reviewed.

#### MSCM22C MRI of the Ankle and Foot

Participants Hilary R. Umans, MD, Ardsley, NY (*Presenter*) Nothing to Disclose

# LEARNING OBJECTIVES

1) To better understand the MR imaging findings in a series of cases that emphasize common and clinically important disorders of the ankle and foot. 2) To present MR imaging features that allow accurate differential diagnosis among other diagnostic possibilities for each of these cases.

# MSCM22D MRI of the Shoulder

Participants Bruce B. Forster, MD, Vancouver, BC (*Presenter*) Stockholder, Canada Diagnostic Centres

# For information about this presentation, contact:

bruce.forster@vch.ca

LEARNING OBJECTIVES

1) Recognize common pathology of the rotator cuff on MRI, including differentiating tendinopathy from partial and full thickness tears, and to understand how imaging findings potentially change management. 2) Differentiate normal labral variants from labral tears on MR arthrography, and appreciate the appearance of Bankart tear variants. 3) Understand the role of 1.5T and 3T MRI vs arthrography in the workup of rotator cuff disease and shoulder instability.



#### MSMC22

Cardiac CT Mentored Case Review: Part II (In Conjunction with the North American Society for Cardiovascular Imaging) (Interactive Session)

Monday, Nov. 26 10:30AM - 12:15PM Room: S406A



AMA PRA Category 1 Credits ™: 1.75 ARRT Category A+ Credits: 2.00

#### **Participants**

Jill E. Jacobs, MD, New York, NY (*Director*) Nothing to Disclose Charles S. White, MD, Baltimore, MD (*Moderator*) Consultant, Koninklijke Philips NV

#### For information about this presentation, contact:

jill.jacobs@nyumc.org

#### LEARNING OBJECTIVES

1) Identify cardiac and coronary artery anatomy. 2) Recognize cardiac disease processes, including coronary atherosclerosis, as diagnosed on CT. 3) Understand methods of cardiac CT and coronary CT angiography post-processing.

#### Sub-Events

# MSMC22A Coronary Atherosclerosis I

Participants

Geoffrey D. Rubin, MD, Durham, NC (*Presenter*) Consultant, Fovia, Inc; Consultant, HeartFlow, Inc; Consultant, General Electric Company;

#### LEARNING OBJECTIVES

View learning objectives under main course title.

#### MSMC22B Coronary Atherosclerosis II

Participants Karin E. Dill, MD, Worcester, MA (*Presenter*) Nothing to Disclose

# LEARNING OBJECTIVES

View learning objectives under main course title.

# MSMC22C Valves and Cardiac Function

Participants

Suhny Abbara, MD, Dallas, TX (*Presenter*) Royalties, Reed Elsevier; Institutional research agreement, Koninklijke Philips NV; Institutional research agreement, Siemens AG

#### LEARNING OBJECTIVES

View learning objectives under main course title.

#### **Honored Educators**

Presenters or authors on this event have been recognized as RSNA Honored Educators for participating in multiple qualifying educational activities. Honored Educators are invested in furthering the profession of radiology by delivering high-quality educational content in their field of study. Learn how you can become an honored educator by visiting the website at: https://www.rsna.org/Honored-Educator-Award/ Suhny Abbara, MD - 2014 Honored EducatorSuhny Abbara, MD - 2017 Honored Educator



# MSMI22

Molecular Imaging Symposium: Oncologic MI Applications

Monday, Nov. 26 10:30AM - 12:00PM Room: S405AB



AMA PRA Category 1 Credits ™: 1.50 ARRT Category A+ Credit: 1.75

**FDA** Discussions may include off-label uses.

#### Participants

Peter L. Choyke, MD, Rockville, MD (*Moderator*) Nothing to Disclose Vikas Kundra, MD, PhD, Houston, TX (*Moderator*) Institutional license agreement, Introgen Therapeutics, Inc; Research Grant, General Electric Company

#### For information about this presentation, contact:

pchoyke@nih.gov

### LEARNING OBJECTIVES

1) To understand current advances in PET molecular imaging and clinical applications. 2) To understand new applications of advanced MRI techniques. 3) To improve understanding of theranostic agents based on targeted imaging agents.

#### Sub-Events

## MSMI22A Hyperpolarized MRI of Prostate Cancer

Participants Daniel B. Vigneron, PhD, San Francisco, CA (*Presenter*) Research Grant, General Electric Company;

# LEARNING OBJECTIVES

1) To understand the biochemical information that Hyperpolarized pyruvate MRI can provide. 2) Learn the value of detecting increased conversion of pyruvate to lactate in cancer reflecting upregulated lactate dehydrogenase expression. 3). To describe initial results in prostate cancer, brain tumors and metastatic lung cancers.

# MSMI22B Somatostatin Receptor Imaging

Participants

Corina Millo, MD, Bethesda, MD (Presenter) Nothing to Disclose

#### For information about this presentation, contact:

millocm@nih.gov

# LEARNING OBJECTIVES

1) Identify clinical scenarios in which performing 68Ga-somatostatin PET/CT imaging can benefit patient's care based on published appropriate use criteria. 2) Examine a range of 68Ga-somatostatin PET/CT cases from basic to complex and/or unusual. 3) Discuss peptide receptor radiotherapy (PRRT).

# ABSTRACT

68Ga-labeled somatostatin analogs (DOTATATE, DOTATOC and DOTANOC) PET/CT imaging provides both higher resolution and enhanced receptor affinity compared with In-111-DTPA-octreotide, with less radiation, comparable cost, and imaging completion within 2 hours vs. 2-3 days. 68Ga-somatostatin analogs have a higher impact on patient management than In-111-DTPAoctreotide, including the ability to identify patients likely to benefit from PRRT. This activity will provide results from the literature and the author's experience to illustrate the potential of 68Ga-somatostatin analogues PET/CT in imaging of neuroendocrine tumors.

# MSMI22C Multimodal MI in Oncology

Participants

Mukesh G. Harisinghani, MD, Boston, MA (Presenter) Nothing to Disclose

# LEARNING OBJECTIVES

1) To understand imaging applications for commercially available iron oxide nanoparticles. 2) To understand mechanism of action for magnetic iron oxide nanoparticles. 3) To describe MR technique for imaging with magnetic nanoparticles.

# MSMI22D Imaging of Delivered Gene Expression

Participants

Vikas Kundra, MD, PhD, Houston, TX (*Presenter*) Institutional license agreement, Introgen Therapeutics, Inc; Research Grant, General Electric Company

# MSMI22E PSMA Imaging in Prostate Cancer

Participants Peter L. Choyke, MD, Rockville, MD (*Presenter*) Nothing to Disclose

For information about this presentation, contact:

pchoyke@nih.gov

# LEARNING OBJECTIVES

1) Describe the various forms of PSMA PET ligands. 2) Illustrate the most common uses of PSMA PET. 3) Demonstrate pitfalls of interpreting PSMA PET.



#### MSRO22

# BOOST: CNS-Case-based Multidisciplinary Review (Interactive Session)

Monday, Nov. 26 10:30AM - 12:00PM Room: S103AB



AMA PRA Category 1 Credits ™: 1.50 ARRT Category A+ Credit: 1.75

# Participants

Christina I. Tsien, MD, Saint Louis, MO (*Presenter*) Advisory Board, AbbVie Inc; Advisory Board, NovoCure Ltd; Speakers Bureau, Varian, Inc; Speakers Bureau, Merck & Co, Inc

Soonmee Cha, MD, San Francisco, CA (Presenter) Nothing to Disclose

Roger Stupp, MD, Chicago, IL (*Presenter*) Spouse, Employee, Novartis AG; Research Consultant, Celgene Corporation; Research Consultant, AbbVie Inc; Research Consultant, Boehringer Ingelheim

Gavin P. Dunn, MD, PhD, Saint Louis, MO (Presenter) Nothing to Disclose

# LEARNING OBJECTIVES

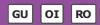
1) Review latest advances in imaging for assessment of gliomas before, during, and after therapy in the context of WHO 2016 molecular/genetic classification gliomas 2) Discuss challenges and strategies for accurate imaging characterization of gliomas following therapy in a case based format. 3) Recognize the need to incorporate molecular/genetic features and types of therapy in imaging assessment of gliomas



#### MSRO26

# BOOST: Gynecologic-Case-based Multidisciplinary Review (Interactive Session)

Monday, Nov. 26 10:30AM - 12:00PM Room: S103CD



AMA PRA Category 1 Credits ™: 1.50 ARRT Category A+ Credit: 1.75

## Participants

Susanna I. Lee, MD,PhD, Boston, MA (*Moderator*) Editor, Wolters Kluwer nv Lilie Lin, MD, Houston, TX (*Presenter*) Investigator, AstraZeneca PLC Aoife Kilcoyne, MBBCh, Boston, MA (*Presenter*) Nothing to Disclose Marcela G. Del Carmen, MD, Boston, MA (*Presenter*) Nothing to Disclose

# For information about this presentation, contact:

slee0@mgh.harvard.edu

#### LEARNING OBJECTIVES

Understand the surgical treatment of gynecologic cancers based on standard of care current treatment strategies. 2)
 Understand systemic therapies available for the management of gynecologic cancers based on current standard of care regimens.
 Understand the use of radiotherapy techniques used for the adjuvant and definitive management of gynecologic cancers. 4)
 Identify key imaging findings on MR and PET CT pertinent to pre-operative treatment planning as well as post treatment follow up.
 Detect common pitfalls on MR and PET CT imaging in the pre and post treatment evaluation of patients with gynecologic cancer.

#### ABSTRACT

This is a case based, multidisciplinary review of gynecologic malignancies.



#### RCA22

# Case Review: Rectal MRI - Bring Your Own Device (Hands-on)

Monday, Nov. 26 10:30AM - 12:00PM Room: S404CD



AMA PRA Category 1 Credits ™: 1.50 ARRT Category A+ Credit: 1.75

# Participants

David H. Kim, MD, Middleton, WI (*Moderator*) Shareholder, Cellectar Biosciences, Inc; Shareholder, Elucent Medical; Mukesh G. Harisinghani, MD, Boston, MA (*Presenter*) Nothing to Disclose Courtney C. Moreno, MD, Suwanee, GA (*Presenter*) Researcher, General Electric Company; Zahra Kassam, MD, London, ON (*Presenter*) Nothing to Disclose Thomas A. Hope, MD, San Francisco, CA (*Presenter*) Research support, General Electric Company Gaiane M. Rauch, MD, PhD, Houston, TX (*Presenter*) Nothing to Disclose Raj M. Paspulati, MD, Cleveland, OH (*Presenter*) Nothing to Disclose

# LEARNING OBJECTIVES

1) Critically evaluate the primary tumor, particularly in the differentiation between T2/early T3 -and- advanced T3 status. 2) Apply criteria to determine regional lymph node status. 3) Recognize relevant anatomic landmarks used in Rectal MR cancer staging.

#### ABSTRACT

Participants will review cases on their own devices and answer questions. The cases will then be reviewed by the presenters. Note: this activity is best done on a laptop or tablet. Although phones will work, their small size limits optimal image view. This workshop will be led by members of the Society of Abdominal Radiology Rectal Cancer Disease Focused Panel. This group helps set the interpretation standards for rectal cancer MRI in the United States. In this 1.5 hour Hands-on Workshop, the participants will have the opportunity to review a number of rectal staging MRI cases on stand-alone computers or on a personal mobile device. The selected cases are intended to give a broad overview of the common issues encountered in rectal cancer staging, including appropriately categorizing the correct T category of the tumor as well as determining regional lymph node status. The relevant anatomic relationships of the tumor with adjacent structures for surgical and potential neoadjuvant options will be emphasized. An interactive platform will allow participants to see overall class performance for questions posed by the expert reviewer. Each case will be reviewed after a short interval to allow a participant to form an opinion prior to the expert review. This workshop is intended to give a practical, hands-on approach to rectal cancer staging by MRI.



#### RCB22

# Getting Stuff Done: A Hands-on Technology Workshop to Enhance Personal Productivity (Hands-on)

Monday, Nov. 26 10:30AM - 12:00PM Room: S401CD

# IN

AMA PRA Category 1 Credits ™: 1.50 ARRT Category A+ Credit: 1.75

# Participants

Puneet Bhargava, MD, Seattle, WA (*Moderator*) Nothing to Disclose Matthew B. Morgan, MD, Sandy, UT (*Presenter*) Consultant, Reed Elsevier Puneet Bhargava, MD, Seattle, WA (*Presenter*) Nothing to Disclose Amanda Lackey, MD, Springfield, MO (*Presenter*) Nothing to Disclose Tarun Pandey, MD, FRCR, Little Rock, AR (*Presenter*) Nothing to Disclose

#### For information about this presentation, contact:

Bhargp@uw.edu

# LEARNING OBJECTIVES

1) Introduce the concept of "Getting Things Done.' Learn the concepts of Inbox Zero and other email management techniques. 2) Using tools such as note-taking applications, citation and password managers.3) Using self-inquiry techniques, review how to make meaningful and powerful changes in how we engage with technology.

#### Active Handout:Puneet Bhargava

http://abstract.rsna.org/uploads/2018/18003025/Productivity Primer RCB22.pdf

#### **Active Handout:Tarun Pandey**

http://abstract.rsna.org/uploads/2018/18003025/Pandey\_RSNA 2018 Productivity Exercises FINAL RCB22.pdf

#### **Honored Educators**

Presenters or authors on this event have been recognized as RSNA Honored Educators for participating in multiple qualifying educational activities. Honored Educators are invested in furthering the profession of radiology by delivering high-quality educational content in their field of study. Learn how you can become an honored educator by visiting the website at: https://www.rsna.org/Honored-Educator-Award/ Puneet Bhargava, MD - 2015 Honored Educator



#### RCC22

# Using Imaging Informatics to Enable Patient Experience Improvements in Radiology

Monday, Nov. 26 10:30AM - 12:00PM Room: S501ABC

#### LM IN

AMA PRA Category 1 Credits ™: 1.50 ARRT Category A+ Credit: 1.75

## Participants

Ramin Khorasani, MD, Boston, MA (Moderator) Nothing to Disclose

# Sub-Events

#### RCC22A Patient Experience in Radiology: The Case for Urgent Action

Participants

Ramin Khorasani, MD, Boston, MA (Presenter) Nothing to Disclose

#### RCC22B **Patient-centered Imaging Informatics Innovations**

Participants Tessa S. Cook, MD, PhD, Philadelphia, PA (Presenter) Royalties, Osler Institute

# For information about this presentation, contact:

tessa.cook@uphs.upenn.edu

# LEARNING OBJECTIVES

1) Discuss how imaging informatics can be used to design innovations that help patients to better understand their radiology reports as well as to more effectively connect directly with the radiologists caring for them or their family members.

#### RCC22C **Using Patient Experience Survey Results to Motivate Change**

Participants

Neena Kapoor, MD, Boston, MA (Presenter) Nothing to Disclose

# LEARNING OBJECTIVES

1) Learn how IT tools can help analyze patient experience comments to identify targets for improvement initiatives.

#### RCC22D Patient Experience: Numbers, Culture, or ?

Participants

Keith D. Hentel, MD, MS, New York, NY (Presenter) Nothing to Disclose

#### RCC22E **Patient Challenges and Wish List for Imaging Informatics**

Participants

Andrea K. Borondy Kitts, MS, MPH, South Glastonbury, CT (Presenter) Stockholder, Abbott Laboratories; Stockholder, AbbVie Inc; Stockholder, F. Hoffmann-La Roche Ltd; Stockholder, Johnson & Johnson; Officer, Prosumer Health; Investor, Prosumer Health

For information about this presentation, contact:

Borondy@msn.com

#### **LEARNING OBJECTIVES**

Help radiologists assess the challenges and barriers faced by patients in finding information about imaging tests and procedures online, in accessing and understanding radiologist reports on patient portals, and in understanding, arranging for, and committing to, appropriate follow-up. Provide suggestions for interventions for radiologists and radiology practices to use to help patients find and understand information on appropriate imaging tests for their health/medical situation, find and understand their radiologist report, and understand and arrange for appropriate follow-up.

### **Active Handout: Andrea K Borondy Kitts**

http://abstract.rsna.org/uploads/2018/18024154/Patient Challenges and Wish List for Imaging RCC22E.pdf



# SPCP21

# Australia and New Zealand Present: Clinical Radiology and Radiation Oncology

Monday, Nov. 26 10:30AM - 12:00PM Room: E351



AMA PRA Category 1 Credits ™: 1.50 ARRT Category A+ Credit: 0

#### LEARNING OBJECTIVES

1) Overview of the RANZCR Clinical Radiology Curriculum and its adoption of the CanMEDS framework. 2) Insight into the aims of RANZCR's 2016-2020 Training and Assessment Reform project and the progress to date. 3) Describe RANZCR assessment processes for radiology training - existing methods and reform initiatives. 4) Understand how RANZCR's approach fits into the broader context of specialty training programs in Australia and New Zealand. 5) Understand how RANZCR's educational model compares with correspondent radiology training programs in North America and Europe.

#### ABSTRACT

In 2014 the RANZCR commissioned a full review of its assessment and examination processes for Fellowship training, across both its Faculties. Expert educationalists were engaged to evaluate the quality and sustainability of RANZCR's assessment and examination program at both the operational and strategic levels, and to recommend and facilitate suitable strategies for improvement. In 2016 the College commenced a comprehensive set of work packages to implement the recommendations and develop a best-practice medical education program.

# Sub-Events

# SPCP21A Introduction

Participants John P. Slavotinek, MBBS, Adelaide, Australia (*Presenter*) Nothing to Disclose

#### For information about this presentation, contact:

john.slavotinek@sa.gov.au

#### LEARNING OBJECTIVES

1. To provide a basic overview of Australian and New Zealand demographics in comparison to other entities such as the USA, the European Union and the UK. 2. To convey brief insight into similarities and differences between the Australian and New Zealand health care environments and other countries. 3. To give perspective regarding radiology and radiation oncology services in Australia and New Zealand compared to other entities such as the USA, Europe and the UK.

# SPCP21B Education, Training and Reform Initiatives in Australia and New Zealand in Radiology

#### Participants

Dinesh K. Varma, FRANZCR, Brighton, Australia (Presenter) Nothing to Disclose

#### LEARNING OBJECTIVES

1) Overview of the RANZCR Clinical Radiology Curriculum and its adoption of the CanMEDS framework. 2) Insight into the aims of RANZCR's 2016-2020 Training and Assessment Reform project and the progress to date. 3) Describe RANZCR assessment processes for radiology training - existing methods and reform initiatives. 4) Understand how RANZCR's approach fits into the broader context of specialty training programs in Australia and New Zealand. 5) Understand how RANZCR's educational model compares with correspondent radiology training programs in North America and Europe.

#### ABSTRACT

In 2014 the RANZCR commissioned a full review of its assessment and examination processes for Fellowship training, across both its Faculties. Expert educationalists were engaged to evaluate the quality and sustainability of RANZCR's assessment and examination program at both the operational and strategic levels, and to recommend and facilitate suitable strategies for improvement. In 2016 the College commenced a comprehensive recommend and facilitate suitable strategies for improvement. In 2016 the College commenced a comprehensive set of work packages to implement the recommendations and develop a best-practice medical education program.

# SPCP21C Radiation Oncology and Interventional Oncology: A Marriage Made in Heaven

Participants Lizbeth Kenny, MD, FRANZCR, Herston, Australia (*Presenter*) Nothing to Disclose

For information about this presentation, contact:

lizkenny@bigpond.net.au

# LEARNING OBJECTIVES

View learning objectives under main course title.

#### ABSTRACT

Radiation Oncology and Radiology started as the one discipline with all knowledge housed within one person and one specialty, they diverged and are now coming closer together once more. Both, by their very nature are imaging guided specialties. Interventional Radiology and in particular Interventional Oncology and Radiation Oncology are two sides of a coin, same aim, different modalities. Radiation Oncology has a century of science and collaboration behind its practice, with a massive evidence base, hard core clinical practice and a robust research capability. Interventional Oncology internationally, is still at its infancy, but in partnership with radiation oncology, we can refocus the importance of local cancer control which the world has largely forgone in pursuit of systemic therapy. The partnership can provide a robust framework within which to practice and research. The partnership between radiation oncology and interventional oncology will rapidly propell the importance of local cancer treatment and the amazing benefit that this brings to patients and to the system. This partnership can not only help the world at large to refocus on the importance of local cancer control, but can help us reshape the evidence paradigm, which using current accepted international criteria, makes it almost impossible to obtain high level evidence in our fields of rapidly evolving technology. With a major re-focus on patient reported outcome measures, quality of life and overall economic burden, local image guided therapy, by any modality, can bring great benefit to patients and to the system alike. This is a time for overt collaboration, given the burden of cancer in the community and the lack of resources world wide. With a clear appreciation of the overall benefit of such a relationship, within Australia and New Zealand, Interventional Oncology has now formed a special interest group within our highly successful bi-national radiation oncology research group - the Trans Tasman Radiation Oncology Group (TROG) and a number of major hospital facilities in Australia are considering partnership arrangments within their services.

# SPCP21D A Journey in Vascular Interventional Research: Lessons Learnt and Future Prospects

Participants

Andrew H. Holden, FRANZCR, Auckland, New Zealand (Presenter) Nothing to Disclose

# LEARNING OBJECTIVES

View learning objectives under main course title.

# SPCP21E The Role of Iron in Neurodegeneration

Participants

Patricia Desmond, MD, Melbourne, Australia (Presenter) Nothing to Disclose

# LEARNING OBJECTIVES

Learning objectives 1. Understand the importance of iron in normal brain function 2. Understand how iron can led to neurodegeneration 3. Appreciate that Iron can be measured and imaged with MRI 4. Give insight into the role that iron may play in predicting cognitive decline.

# ABSTRACT

Iron plays an essential role in normal brain function. It is important in synaptic transmission, mitochondrial respiration and myelin synthesis. Iron in the brain increase with age. However, too much iron is toxic and leads to oxidative stress and neurodegeneration. Iron is associated with neurodegeneration in Parkinson's disease and Parkinson's dementia and has also been linked to other neurodegenerative diseases including Alzheimer's disease. Increase iron levels and found in the brain of AD patients at post mortem. Increase iron in the CSF is a predictor of cognitive decline in amyloid positive patients Amyloid imaging has revolutionised our understanding of AD disease. It points to a long preclinical phase, 20 to 30 years of gradual build up before the onset of clinical disease. However, amyloid does not tell us about when a patient will dement. Approximately 30% of normal healthy elderly will have a positive amyloid scan. Iron can now be imaged quantitatively with MRI by a technique known as Quantitative Susceptibility Mapping (QSM). Increase iron in the hippocampus, measured with QSM in amyloid positive patients predicts decline 5 years before onset. Iron chelation in amyloid positive patients is currently being trialed as a way of delaying onset of cognitive impairment

# SPCP21F Closing Remarks

Participants Vijay M. Rao, MD, Philadelphia, PA (*Presenter*) Nothing to Disclose



#### SSC01

# Science Session with Keynote: Cardiac (Coronary Artery Disease: Practice and Prognosis)

Monday, Nov. 26 10:30AM - 12:00PM Room: S504CD

# САСТ

AMA PRA Category 1 Credits ™: 1.50 ARRT Category A+ Credit: 1.75

#### **Participants**

Yeon Hyeon Choe, MD, PhD, Seoul, Korea, Republic Of (*Moderator*) Nothing to Disclose Gregory Kicska, MD, PhD, Seattle, WA (*Moderator*) Nothing to Disclose

# Sub-Events

# SSC01-01 Cardiac Keynote Speaker: Prognostic Role of Coronary CT Angiography

Monday, Nov. 26 10:30AM - 10:50AM Room: S504CD

Participants

Gregory Kicska, MD, PhD, Seattle, WA (Presenter) Nothing to Disclose

# SSC01-03 The Intermediate-Term Impact of Coronary CT Compared to Stress Echocardiography During Risk Assessment in Patients Undergoing Liver Transplantation: A Prospective Follow-Up Study in a Consecutive Patient Population

Monday, Nov. 26 10:50AM - 11:00AM Room: S504CD

#### Participants

Patricia Tischendorf, Frankfurt, Germany (*Presenter*) Nothing to Disclose Claudia Frellesen, Frankfurt, Germany (*Abstract Co-Author*) Nothing to Disclose Christophe Arendt, MD, Frankfurt am Main, Germany (*Abstract Co-Author*) Nothing to Disclose Thomas J. Vogl, MD, PhD, Frankfurt, Germany (*Abstract Co-Author*) Nothing to Disclose Ralf W. Bauer, MD, Frankfurt, Germany (*Abstract Co-Author*) Speakers Bureau, Siemens AG; Speakers Bureau, Bayer AG; Speakers Bureau, General Electric Company

#### PURPOSE

Aim of this study was to evaluate the intermediate-term impact of coronary Computed Tomography (cCT) versus Stress Echocardiography (STE) as a cardiac risk stratification prior to liver transplantation in a consecutive patient population with unknown coronary artery disease (CAD).

# METHOD AND MATERIALS

From 2014 to 2017, 139 consecutive patients, who underwent cCT or STE as a part of the institutional liver transplantation evaluation procedure, were enrolled unless they met the predefined exclusion criteria. 67 patients underwent non-enhanced CaSc followed by prospectively ECG-triggered sequential coronary CTA, in addition to the Agatston-Score, we used the CAD-RADS classification for risk assessment. 72 patients were examined by STE. Follow-up information concerning the primary endpoint, consist of cardiac or non-cardiac death and the combined endpoint of cardiac death, myocardial infarction, revascularisation and stroke was obtained from general practitioners, or treating hospitals, respectively.

#### RESULTS

The mean follow-up period was 569±442 days. During this time, 40 primary endpoints and 7 combined endpoints occurred. There was no significant difference in the incidence of primary endpoints in patients with pos. cCT or STE compared to patients without a pathological finding. In patients with pos. cCT, significantly more combined endpoint were observed than in the control group (p=0.0004). Moreover, the absence of a pathological finding in cCT or STE was shown to exhibit high negative predictive value. On multivariate analysis, Child-Pugh C liver status was the strongest independent predictor for an primary endpoint, with a 5-fold increased risk. While pos. cCT was the strongest independent predictor for an combined entpoint.

# CONCLUSION

cCT and STE both provide excellent risk stratification and intermediate-term prognostic value in patients with unknown CAD. cCTA shows promising results in the initial work-up of unselected liver transplantation candicates with perviously unknown CAD. Patients with positive findings in cCT were successfully routed towards revascularization leading to a non-significant difference concerning the primary endpoint combared to patients with neg. cCT (p=0.47).

#### **CLINICAL RELEVANCE/APPLICATION**

Different cardiac imaging methods need to be investigated to avoid cardiac complications in patients undergoing liver transplantation, because the prevalence of asymptomatic CAD is relatively high in this population.

# SSC01-04 Utilization of Coronary CT Angiography in Private Offices and Hospitals: Reversal of Earlier Trends and Implications for Radiologists

Participants David C. Levin, MD, Philadelphia, PA (*Presenter*) Consultant, HealthHelp, LLC; Board Member, Outpatient Imaging Affiliates, LLC Laurence Parker, PhD, Philadelphia, PA (*Abstract Co-Author*) Nothing to Disclose Ethan J. Halpern, MD, Philadelphia, PA (*Abstract Co-Author*) Nothing to Disclose Vijay M. Rao, MD, Philadelphia, PA (*Abstract Co-Author*) Nothing to Disclose

#### For information about this presentation, contact:

david.levin@jefferson.edu

## PURPOSE

To assess recent trends in utilization of coronary CT angiography (CCTA), based upon place-of-service and provider specialty.

# **METHOD AND MATERIALS**

The nationwide Medicare Part B Physician/Supplier Procedure Procedure Summary Master Files for 2006-2016 were the data source. CPT-4 codes for CCTA were selected. The files provided procedure volume for each code. Utilization rates per 100,000 Medicare fee-for-service enrollees were then calculated. Medicare's place-of-service codes were used to identify CCTAs performed in private offices, hospital outpatient departments (HOPDs), emergency departments (EDs), and inpatient settings. Physician specialty codes were used to identify CCTAs interpreted by radiologists, cardiologists, and all other physicians as a group. Because these files represent an entire population count, sample statistics are not required.

# RESULTS

The overall CCTA utilization rate per 100,000 Medicare enrollees rose abruptly from 99.1 in 2006 to 210.3 in 2007, but then progressively dropped to 107.1 by 2013. However, thereafter it rose each year, reaching 131.0 in 2016. The private office CCTA utilization rate increased abruptly from 70.3 in 2006 to a peak of 150.1 in 2007, but thereafter dropped rapidly to 39.5 in 2016. The HOPD rate rose from 22.9 in 2006 to 46.1 in 2007, then declined to 36.1 by 2010. However, it thereafter increased progressively to 69.8 in 2016. The ED rate increased continually from 0.4 in 2006 to 5.3 in 2016. Among inpatients, the rate was 11.0 in 2007 and remained relatively unchanged through 2013. But in the 3 subsequent years, it increased to 16.4 by 2016. Radiologists' CCTA market share in the 4 venues in 2016 were: offices 44%, HOPDs 62%, EDs 85%, inpatients 66%. Radiologists' overall share had been 32% in 2007 (the peak year), compared with 60% for cardiologists. However, by 2016, radiologists' overall share was 58%, compared with 38% for cardiologists.

#### CONCLUSION

After years of declining CCTA utilization, the rate is now increasing, primarily in hospital settings. The private office rate has declined sharply. In a noteworthy reversal of another earlier trend, radiologists currently predominate in this procedure.

# **CLINICAL RELEVANCE/APPLICATION**

After years of decline, the frequency of use of CCTA appears to be increasing, especially in hospital settings and among radiologists.

# SSC01-05 Radiomics-Based Machine Learning Differentiates Early from Advanced Coronary Lesions: A Proof of Concept

Monday, Nov. 26 11:10AM - 11:20AM Room: S504CD

#### Awards

# **Trainee Research Prize - Fellow**

# Participants

Marton Kolossvary, MD, Budapest, Hungary (*Presenter*) Creator and Developer - Radiomics Image Analysis Julia Karady, MD, Budapest, Hungary (*Abstract Co-Author*) Nothing to Disclose Yasuka Kikuchi, MD, Sapporo, Japan (*Abstract Co-Author*) Nothing to Disclose Alexander Ivanov, Moscow, Russia (*Abstract Co-Author*) Nothing to Disclose Christopher L. Schlett, MD, MPH, Heidelberg, Germany (*Abstract Co-Author*) Nothing to Disclose Michael T. Lu, MD, Boston, MA (*Abstract Co-Author*) Nothing to Disclose Borek Foldyna, MD, Boston, MA (*Abstract Co-Author*) Nothing to Disclose Hugo Aerts, PhD, Boston, MA (*Abstract Co-Author*) Stockholder, Sphera Inc Pal Maurovich-Horvat, MD, PhD, Pecs, Hungary (*Abstract Co-Author*) Nothing to Disclose Udo Hoffmann, MD, Boston, MA (*Abstract Co-Author*) Institutional Research Grant, Kowa Company, Ltd; Institutional Research Grant, Abbott Laboratories; Institutional Research Grant, HeartFlow, Inc; Institutional Research Grant, AstraZeneca PLC

# For information about this presentation, contact:

marton.kolossvary@gmail.com

# PURPOSE

Coronary plaques can be classified into the following histological categories: adaptive and pathological intimal thickening (AIT, PIT), fibrous plaque (Fib), early and late fibroatheroma (EFA, LFA) and thin-cap fibroatheroma (TCFA). Advanced atherosclerotic lesions (EFA, LFA, TCFA) carry higher risk versus early plaques (AIT, PIT, Fib). We sought to assess if radiomic analysis of coronary CTA is superior to conventional CTA plaque assessment performed by experts to identify early vs. advanced lesions and to classify plaques into the six histological categories.

#### **METHOD AND MATERIALS**

Coronary cross-sections of 95 plaques in 7 ex-vivo hearts were analyzed. Overall, 607 histology slides and coronary CTA crosssections were co-registered and analyzed in random order. We derived 1015 radiomic features from each CTA plaque cross-section. Principal components accounting for 90% of the variation were derived. A multivariate k-nearest neighbors machine learning (ML) model was built based-on these parameters. We calculated the diagnostic accuracy of the radiomics-ML model and plaque attenuation pattern classification by experts to differentiate early from advanced atherosclerotic plaques and to classify CTA cross-sections into the six histological categories. We compared the diagnostic accuracies between the models using the McNemartest.

# RESULTS

After excluding sections with heavy calcium (n=32) and no visible atherosclerotic plaque on CTA (n=134), we analyzed 411 crosssections of which 30.4% (134/441) were advanced atherosclerotic lesions. The radiomics-ML model which included 13 parameters correctly differentiated early from advanced plaques with a diagnostic accuracy of 82.3%, whereas the expert classification had a diagnostic accuracy of 76.0% (p=0.001). Our ML model was able to classify 63.0% of the CTA cross-sections into the six histological categories correctly.

#### CONCLUSION

Radiomics-based ML outperforms experts to identify advanced atherosclerotic lesions on coronary CTA. However, ML-based classification of coronary plaques into the corresponding six histological categories has moderate accuracy. Further analysis with larger samples size and validation is needed.

## CLINICAL RELEVANCE/APPLICATION

Radiomics-based machine learning could increase the diagnostic accuracy of coronary CT angiography to identify gold-standard histological entities.

# **Honored Educators**

Presenters or authors on this event have been recognized as RSNA Honored Educators for participating in multiple qualifying educational activities. Honored Educators are invested in furthering the profession of radiology by delivering high-quality educational content in their field of study. Learn how you can become an honored educator by visiting the website at: https://www.rsna.org/Honored-Educator-Award/ Udo Hoffmann, MD - 2015 Honored Educator

# SSC01-06 Diagnostic Accuracy of Low Dose Dynamic Stress Computed Tomography Myocardial Perfusion (CTP) in Intermediate-to-High-Risk Patients for Suspected Coronary Artery Disease (CAD)

Monday, Nov. 26 11:20AM - 11:30AM Room: S504CD

Participants

Andrea Baggiano, Milan, Italy (*Abstract Co-Author*) Nothing to Disclose Margherita Soldi, Milan, Italy (*Abstract Co-Author*) Nothing to Disclose Giuseppe Muscogiuri, MD, Charleston, SC (*Presenter*) Nothing to Disclose Marco Guglielmo, Milan, Italy (*Abstract Co-Author*) Nothing to Disclose Andrea Guaricci, MD, Foggia, Italy (*Abstract Co-Author*) Nothing to Disclose Daniele Andreini, MD, Milan, Italy (*Abstract Co-Author*) Consultant, General Electric Company Saima Mushtaq, Milan, Italy (*Abstract Co-Author*) Nothing to Disclose Edoardo Conte, Milan, Italy (*Abstract Co-Author*) Nothing to Disclose Andrea D. Annoni, MD, Milan, Italy (*Abstract Co-Author*) Nothing to Disclose Maria E. Mancini, Milan, Italy (*Abstract Co-Author*) Nothing to Disclose Maria E. Mancini, Milan, Italy (*Abstract Co-Author*) Nothing to Disclose Maria E. Mancini, Milan, Italy (*Abstract Co-Author*) Nothing to Disclose Maria E. Mancini, Milan, Italy (*Abstract Co-Author*) Nothing to Disclose Maria E. Mancini, Milan, Italy (*Abstract Co-Author*) Nothing to Disclose Mauro Pepi, Milan, Italy (*Abstract Co-Author*) Nothing to Disclose Gianluca Pontone, MD, Milan, Italy (*Abstract Co-Author*) Nothing to Disclose Gianluca Pontone, MD, Milan, Italy (*Abstract Co-Author*) Nothing to Disclose Gianluca Pontone, MD, Milan, Italy (*Abstract Co-Author*) Nothing to Disclose Gianluca Pontone, MD, Milan, Italy (*Abstract Co-Author*) Nothing to Disclose Gianluca Pontone, MD, Milan, Italy (*Abstract Co-Author*) Speakers Bureau, General Electric Company Consultant, General Electric Company Research Consultant, HeartFlow, Inc Speakers Bureau, HeartFlow, Inc Speakers Bureau, Medtronic plc Speakers Bureau, Bayer AG

For information about this presentation, contact:

andrea.baggiano@centrocardiologicomonzino.it

#### PURPOSE

The aim of this study is to evaluate the incremental diagnostic value of stress CTPdyn over CCTA in intermediate to high risk patients scheduled for invasive coronary angiography (ICA) plus clinically indicated invasive fractional flow reserve (FFR) for suspected CAD by using a low dose acquisition protocol with last generation of whole-heart single beat CT scanner.

# **METHOD AND MATERIALS**

Consecutive symptomatic patients with intermediate-to-high pre-test probability of CAD and scheduled for clinically indicated ICA+FFR, were prospectively enrolled. All patients underwent rest-CCTA followed by stress-CTP protocol with adenosine and with injection of 0.7 ml/kg of iodixanol 320 as additional test. CCTA and CTP were defined positive for the presence of >= 50% stenosis and for the presence of subendocardial hypoenhancement encompassing >= 25% of transmural myocardial thickness within a specific coronary territory, respectively. At ICA, obstructive CAD was defined by the presence of >= 50% stenosis and hemodynamically significant CAD was defined by the presence of > 50% stenosis on left main coronary artery, severe (> 80%) or occlusive stenosis or FFR < 0.80. The additive value of CTP versus CCTA alone to rule out the presence of hemodynamically relevant stenosis was assessed on a per-vessel basis.

# RESULTS

Forty-eight patients [mean age:  $65 \pm 8$  years, male: 35 (73%)] were included in our study. Obstructive CAD was found in 38% (54/144) of vessels and in 73% (35/48) of patients. Hemodynamically significant CAD was present in 23% (36/144) of vessel and in 54% (26/48) of patients. In a vessel-based model, CCTA alone and CCTA+CTPdyn showed a sensitivity, specificity, negative predictive value, positive predictive value and diagnostic accuracy of 92%, 64%, 96%, 46%, 71% and 89%, 89%, 96%, 76%, 89%, respectively. CCTA+CTPdyn showed a significant improvement in specificity (p: <0.001), positive predictive value (p: 0.002) and diagnostic accuracy (p: <0.001) to rule out haemodynamically significant CAD as compared to CCTA alone. The mean radiation exposure due to CTPdyn alone is  $5.13 \pm 1.51$  mSv.

# CONCLUSION

In patients with intermediate-to-high pre-test likelihood of CAD, low dose dynamic CTP had incremental value over CCTA alone to diagnose the presence of hemodynamically significant CAD.

#### **CLINICAL RELEVANCE/APPLICATION**

Combination of CTP an CCTA can improve diagnosis of hemodynamically significant CAD.

# SSC01-07 Triple-Rule-Out CT Angiography in Low-intermediate and High Risk Patients with Acute Chest Pain: Impact on Patient Management

Monday, Nov. 26 11:30AM - 11:40AM Room: S504CD

Participants

Christian Tesche, MD, Munich, Germany (Presenter) Nothing to Disclose Katharina Otani, PhD, Tokyo, Japan (Abstract Co-Author) Employee, Siemens AG Julian L. Wichmann, MD, Frankfurt, Germany (Abstract Co-Author) Speaker, General Electric Company; Speaker, Siemens AG Carlo N. De Cecco, MD, PhD, Atlanta, GA (Abstract Co-Author) Research Grant, Siemens AG Taylor M. Duguay, Charleston, SC (Abstract Co-Author) Nothing to Disclose U. Joseph Schoepf, MD, Charleston, SC (Abstract Co-Author) Research Grant, Astellas Group; Research Grant, Bayer AG; Research Grant, Siemens AG; Research support, Bayer AG; Consultant, Guerbet SA; Consultant, General Electric Company; Consultant, HeartFlow, Inc; Consultant, Bayer AG; Consultant, Siemens AG; ; ; Moritz H. Albrecht, MD, Frankfurt am Main, Germany (Abstract Co-Author) Speaker, Siemens AG Richard A. Takx, MD, Boston, MA (Abstract Co-Author) Nothing to Disclose Sheldon Litwin, Charleston, SC (Abstract Co-Author) Nothing to Disclose Akos Varga-Szemes, MD, PhD, Charleston, SC (Abstract Co-Author) Research Grant, Siemens AG Brian E. Jacobs, BS, Charleston, SC (Abstract Co-Author) Nothing to Disclose Christine M. Carr, MD, Charleston, SC (Abstract Co-Author) Nothing to Disclose Richard Bayer, Charleston, SC (Abstract Co-Author) Nothing to Disclose John W. Nance JR, MD, Charleston, SC (Abstract Co-Author) Nothing to Disclose Pal Suranyi, MD, PhD, Charleston, SC (Abstract Co-Author) Nothing to Disclose

# For information about this presentation, contact:

schoepf@musc.edu

#### PURPOSE

To investigate the impact of triple-rule-out cardiac CT angiography (TRO-CTA) on patient management in patients presenting with chest pain to the emergency department (ED) compared to standard of care (SOC) work-up.

#### METHOD AND MATERIALS

In this IRB-approved, HIPAA-compliant study we analyzed data of 2156 patients who presented to the ED with chest pain. Patients were divided into two groups according to their cardiovascular risk: low-intermediate risk (<=1 risk factor regardless of body-mass-index [BMI]) and high risk (>=2 risk factors and BMI >=30kg/m2 or >=4 risk factors regardless of BMI). Patients received either TRO-CTA as an initial test or SOC without initial CTA. ED length of stay, downstream utilization of additional tests, and hospital costs were compared between both groups.

#### RESULTS

515 patients were assigned to the high-risk group (TRO-CTA, n=274; SOC, n=241) and 1610 to the low-intermediate risk group (TRO-CTA, n=837; SOC, n=773). No significant differences between groups and corresponding treatment arms were observed for age, gender, or race. The rate of diagnosis of coronary artery disease (CAD), pulmonary embolism (PE), or aortic dissection (AD) was significantly higher in the TRO-CTA vs. the SOC arm for the low-intermediate risk group (all p<0.05). Median ED wait time (5.0 vs. 7.0hrs, p<0.001), median total length of hospital stay (48.0 vs. 72.0hrs, p<0.001), additional downstream testing, rate of invasive coronary angiography (11.6% vs. 38.7%, p<0.001), and total costs (9.184\$ vs. 17.253\$, p<0.001) were significantly lower in the TRO-CTA vs. the SOC arm. No significant difference in the diagnosis of CAD, PE, or AD was found between TRO-CTA vs. SOC in the high-risk group with significant lower median ED waiting time (4.0 vs. 8.0hrs, p<0.001), median total length of hospital stay (48.0 vs. 72.0hrs, p<0.001), and total costs (9.184\$ vs. 17.253\$, p<0.001) were significantly lower in the TRO-CTA vs. the SOC arm. No significant difference in the diagnosis of CAD, PE, or AD was found between TRO-CTA vs. SOC in the high-risk group with significant lower median ED waiting time (4.0 vs. 8.0hrs, p<0.001), median total length of hospital stay (48.0 vs. 72.0hrs, p<0.001), additional downstream testing, invasive coronary angiography (16.4% vs. 34.0%, p<0.001), and total costs (\$10,532 vs. \$21,518, p<0.001) in the TRO-CTA vs. the SOC arm.

# CONCLUSION

TRO-CTA as an initial imaging test in ED patients presenting with acute chest pain was associated with shorter ED and hospital length of stay, lower utilization of downstream testing, and lower total cost both for the episode of care and overall.

# **CLINICAL RELEVANCE/APPLICATION**

TRO-CTA is a robust imaging modality with lower resource use and lower cost in the work-up of patients presenting to the ED with chest pain regardless of their a-priori risk.

# SSC01-08 Prognostic Role of Adenosine Stress Cardiac Magnetic Resonance Compared to CCTA in the Long-Term Outcome of Heart Disease Patient

Monday, Nov. 26 11:40AM - 11:50AM Room: S504CD

Participants

Pierpaolo Palumbo, MD, L'Aquila, Italy (*Presenter*) Nothing to Disclose Ester Cannizzaro, MD, L'Aquila, Italy (*Abstract Co-Author*) Nothing to Disclose Camilla De Cataldo, L'Aquila, Italy (*Abstract Co-Author*) Nothing to Disclose Silvia Torlone, L'Aquila, Italy (*Abstract Co-Author*) Nothing to Disclose Antonella Corridore, L'Aquila, Italy (*Abstract Co-Author*) Nothing to Disclose Alessandra di Sibio, L'Aquila, Italy (*Abstract Co-Author*) Nothing to Disclose Margherita Di Luzio, L'Aquila, Italy (*Abstract Co-Author*) Nothing to Disclose Ernesto E. Di Cesare, MD, L'Aquila, Italy (*Abstract Co-Author*) Nothing to Disclose Carlo Masciocchi, MD, L'Aquila, Italy (*Abstract Co-Author*) Nothing to Disclose

#### palumbopierpaolo89@gmail.com

#### PURPOSE

Coronary heart disease is still the leading cause of death and the need for a prognostic assessment of CAD patients is continuously increasing. With this regard, the anatomic and morphological approach is not completely satisfying in the CAD definition. The purpose of our study was assessing the prognostic role of Adenosine Stress Cardiac Magnetic Resonance compared to Computed Tomography Angiography (CTA) in the outcome of the heart patient

#### **METHOD AND MATERIALS**

55 patients with previous PTCA-stenting who underwent CTA examination and CMR with adenosine were included in our study. A 5year follow-up was carried out to evaluate the clinical evolution of these patients

#### RESULTS

Nine patients showed negative CTA and CMR under stress, with reported well-being in the 5-year follow-up. 78% of the remaining patients showed stent filling defects in the CTA examination; among these, 86% showed also perfusion defect in the CMR, associated to major cardiovascular symptoms referred in the follow-up, while the remaining 14% were negative for perfusion CMR and for symptoms.22% of patients who showed perfusion alterations in CMR, although in absence of stent apparent filling defects in CTA examination, reported acute myocardial infarction treated with re-stenting. 5 patients out of 18 with positive LGE images developed MACE (arrhythmias, cardiac death).

# CONCLUSION

Our experience shows how, despite a CTA examination positive for the presence of moderate stenosis, a negative Adenosine Stress CMR represents a positive prognostic factor for the patient outcome. On the other hand, also with a negative CTA, the positivity of Adenosine Stress CMR is strongly associated with a high probability of developing a cardiovascular accident and constitutes a negative prognostic factor

#### **CLINICAL RELEVANCE/APPLICATION**

Our study demonstrates the prevalent role of Stress CMR in comparison to Computed Tomography as a predictive prognostic factor in the outcome of heart patient

# SSC01-09 Additional Diagnostic Value of CT Perfusion Over Coronary CT Angiography in Stented Patients with Suspected In-Stent Restenosis or Coronary Artery Disease Progression: ADVANTAGE Study -Preliminary Results

Monday, Nov. 26 11:50AM - 12:00PM Room: S504CD

Alberto Formenti, Milan, Italy (Abstract Co-Author) Nothing to Disclose

Daniele Andreini, MD, Milan, Italy (Abstract Co-Author) Consultant, General Electric Company

Participants

Saima Mushtaq, Milan, Italy (*Presenter*) Nothing to Disclose Edoardo Conte, Milan, Italy (*Abstract Co-Author*) Nothing to Disclose Gianluca Pontone, MD, Milan, Italy (*Abstract Co-Author*) Speakers Bureau, General Electric Company Consultant, General Electric Company Research Consultant, HeartFlow, Inc Speakers Bureau, HeartFlow, Inc Speakers Bureau, Medtronic plc Speakers Bureau, Bayer AG Elisabetta Mancini, Milan, Italy (*Abstract Co-Author*) Nothing to Disclose Andrea Baggiano, Milan, Italy (*Abstract Co-Author*) Nothing to Disclose Marco Guglielmo, Milan, Italy (*Abstract Co-Author*) Nothing to Disclose Giuseppe Muscogiuri, MD, Charleston, SC (*Abstract Co-Author*) Nothing to Disclose Andrea D. Annoni, MD, Milan, Italy (*Abstract Co-Author*) Nothing to Disclose

# For information about this presentation, contact:

saima.mushtaq@ccfm.it

#### PURPOSE

Aim of the study is to assess the diagnostic performance of CCTA alone, CTP alone and CCTA plus CTP performed with the latest scanner generation that combine a whole-heart coverage with high spatial and temporal resolution, by using invasive coronary angiography (ICA) as standard of reference.

#### **METHOD AND MATERIALS**

A cohort of consecutive patients referred for a clinically ICA for suspicion of ISR or progression of native CAD were enrolled. The feasibility of CCTA, CTP and the combined evaluation CCTA plus CTP were calculated in a stent-based, territory-based and patient-based analysis. Sensitivity, specificity, positive predictive value, negative predictive value and diagnostic accuracy of CCTA, CTP, combined evaluation CCTA-CTP vs. ICA in a stent-based, territory-based and patient-based analysis. Radiation exposure of CCTA, CTP, and ICA was recorded.

#### RESULTS

Ninety-eight patients were enrolled (83 male, mean age  $64 \pm 9$  years-old). CTP feasibility was significantly higher than CCTA feasibility in a stent-based, territory-based and patient based analysis (97% vs. 87%, p=0.001; 98% vs. 92%, p=0.001; 97% vs. 70%, p<0.0001, respectively). The feasibility of the combined evaluation CCTA-CTP was significantly higher than CCTA feasibility in a stent-based, territory-based and patient based analysis (96% vs. 87%, p=0.001; 99% vs. 92%, p<0.001; 100% vs. 70%, p<0.0001, respectively). The diagnostic accuracy of CCTA was 81%, 85% and 79%, in a stent-based, territory-based and patient based analysis, respectively; the diagnostic accuracy of CTP was 90%, 93% and 84%, respectively; the diagnostic accuracy of combined CCTA-CTP was 85%, 90% and 83%, respectively; the diagnostic accuracy of CTP was 90%, 00% and 84%, respectively; the diagnostic accuracy of combined CCTA-CTP was 95% and 92% in a territory and patient-based analysis, respectively. The diagnostic accuracy of CTP was higher than that of CCTA in a stent-based (p=0.001) and territory-based (p<0.0001) analysis. The mean effective dose of the entire CT assessment (CCTA-CTP) was 2.76 ± 2.32 mSv.

# CONCLUSION

The CTP assessment appears as more feasible and more accurate than the anatomical evaluation alone by CCTA in patients with coronary stents. When results of CCTA and CTP are concordant, the diagnostic accuracy of the combined evaluation is very high and associated with very low radiation exposure.

# **CLINICAL RELEVANCE/APPLICATION**

Evaluation with cardiac CT of both anatomy and perfusion



#### SSC02

# Cardiac (Myocardial Ischemia and Viability (MRI): I)

Monday, Nov. 26 10:30AM - 12:00PM Room: S502AB



AMA PRA Category 1 Credits ™: 1.50 ARRT Category A+ Credit: 1.75

**FDA** Discussions may include off-label uses.

#### Participants

Hajime Sakuma, MD, Tsu, Japan (*Moderator*) Research Grant, Fuji Pharma Co, Ltd; Research Grant, DAIICHI SANKYO Group; Research Grant, FUJIFILM Holdings Corporation; Research Grant, Siemens AG; Research Grant, Nihon Medi-Physics Co, Ltd; Speakers Bureau, Bayer AG

Friedrich D. Knollmann, MD, PhD, Wynnewood, PA (Moderator) Nothing to Disclose

#### Sub-Events

# SSC02-01 Comparison Between Radio-Water PET and Model-Based Quantitative Analysis of 3.0T Myocardial Perfusion Magnetic Resonance Imaging

Monday, Nov. 26 10:30AM - 10:40AM Room: S502AB

Participants

Masak<sup>i</sup> Ishida, MD, PhD, Tsu, Japan (*Presenter*) Nothing to Disclose Yasutaka Ichikawa, MD, Tsu, Japan (*Abstract Co-Author*) Nothing to Disclose Takashi Ichihara, PhD, Tsu, Japan (*Abstract Co-Author*) Nothing to Disclose Yoshitaka Goto, MD, Tsu, Japan (*Abstract Co-Author*) Nothing to Disclose Masafumi Takafuji, Tsu, Japan (*Abstract Co-Author*) Nothing to Disclose Haruno Ito, Tsu, Japan (*Abstract Co-Author*) Nothing to Disclose Kakuya Kitagawa, MD, PhD, Tsu, Japan (*Abstract Co-Author*) Nothing to Disclose Hajime Sakuma, MD, Tsu, Japan (*Abstract Co-Author*) Research Grant, Fuji Pharma Co, Ltd; Research Grant, DAIICHI SANKYO Group; Research Grant, FUJIFILM Holdings Corporation; Research Grant, Siemens AG; Research Grant, Nihon Medi-Physics Co, Ltd; Speakers Bureau, Bayer AG

For information about this presentation, contact:

mishida@clin.medic.mie-u.ac.jp

#### PURPOSE

Radio-water PET is the most accurate method in quantifying myocardial blood flow (MBF). Model-based analysis of perfusion MRI with corrections of blood saturation and flow-dependent alteration in extraction fraction of gadolinium contrast medium may permit quantification of absolute MBF. The purpose of this study was to determine the accuracy of MR measurements of rest and stress MBF at 3.0T by using radio-water PET as a reference.

# METHOD AND MATERIALS

Twenty-nine patients with suspected coronary artery disease underwent MRI including stress and rest perfusion MRI and LGE MRI at 3.0T and radio-water PET. ATP stress and rest perfusion MRI were performed with injections of 0.03mmol/kg of Gd-DOTA. Dual bolus method was used to correct blood saturation. Patlak plot method was employed in quantifying MBF. Myocardial unidirectional influx constant (K1) was determined from blood input and myocardial output functions in 16 myocardial segments. The extraction fraction of Gd-DOTA (E) was determined using K1 and PET-derived MBF (MBFPET) for the first 15 patients. For validation, MRI-derived absolute MBF (MBFMRI) was calculated using the relation between E and MBF for the remaining 14 patients and compared with MBFPET. The segments including myocardial infarction were excluded from the analysis.

#### RESULTS

In the first 15 patients, K1 by perfusion MRI was  $0.60\pm0.21$  ml/min/g at rest and  $1.07\pm0.37$  ml/min/g during stress, while MBFPET was  $1.15\pm0.35$  ml/min/g at rest and  $3.08\pm0.81$  ml/min/g during stress. The relationship between E and MBF was E=1-exp(-(0.24xMBF+0.63)/MBF). In the remaining 14 patients, MBFMRI at rest and during stress were  $1.24\pm1.16$  ml/min/g and  $2.63\pm1.48$  ml/min/g, while MBFPET at rest and during stress were  $1.17\pm0.61$  ml/min/g and  $2.69\pm0.70$  ml/min/g, respectively. MBFMRI showed a good linear correlation with MBFPET (r=0.71, p<0.001). The measurement bias in measuring MBF between MRI and PET was  $0.01\pm1.06$ ml/min/g.

# CONCLUSION

Model-based analysis of perfusion MRI at 3.0T with corrections of blood saturation and flow-dependent alteration of extraction of gadolinium contrast medium allows for accurate quantification of MBF both at rest and during ATP stress.

# **CLINICAL RELEVANCE/APPLICATION**

Accurate quantification of myocardial blood flow by using perfusion MRI may permit objective assessment of myocardial ischemia and early detection of high risk patients in the routine cardiac MRI.

# SSC02-02 Oxygenation-Sensitive Cardiovascular Magnetic Resonance for Differentiation of Reversible and Irreversible Myocardial Damage by Evaluation of the Balance between Supply/Demand in Myocardial Oxygenation after ST-Segment-Elevation Myocardial Infarct

Monday, Nov. 26 10:40AM - 10:50AM Room: S502AB

Participants Binghua Chen, Shanghai, China (*Presenter*) Nothing to Disclose Lian-Ming Wu, Shanghai, China (*Abstract Co-Author*) Nothing to Disclose Jian-Rong Xu, MD, PhD, Shanghai, China (*Abstract Co-Author*) Nothing to Disclose

#### For information about this presentation, contact:

chenbinghua0311@163.com

# PURPOSE

T2\* BOLD imaging is a quantitative magnetic resonance imaging(MRI) technique allowing for evaluation of the balance between supply/demand in myocardial oxygenation and myocardial hemorrhage. We sought to investigate the ability of T2\* BOLD imaging to differentiate reversible and irreversible myocardial injury as well as the time course of myocardial oxygenation after reperfusion in patients with ST-segment elevation myocardial infarction (STEMI).

#### **METHOD AND MATERIALS**

Twenty two patients(age, 60±11 years;77.27% male)with STEMI underwent cardiac MRI on four occasions: at 1 day, 3 days, 7 days, and 30 days after (percutaneous coronary intervention)PCI. T2\* BOLD MRI was performed on a 3T scanner to assess myocardial oxygenation in myocardial infarcted regions with or without intramyocardial hemorrhage (IMH), salvaged myocardium, remote myocardium and normal myocardium.

#### RESULTS

T2\* BOLD value in myocardial infarction(MI) with IMH was lowest( $9.77\pm3.29ms$ ), while that of the salvaged zone was the highest( $33.97\pm3.42ms$ ). Hyperemia induced by inflammation may increase blood flow in the salvaged area. T2\* BOLD value in salvaged myocardium demonstrated a unimodal temporal pattern from 1 day( $37.91\pm2.23ms$ ) to 30 days( $30.68\pm1.59ms$ ).

# CONCLUSION

T2\* BOLD MRI performed in post-STEMI patients allows for accurate evaluation of myocardial damage severity, and can discriminate between reversible and irreversible myocardial injury. The increased T2\* BOLD values may imply the pathophysiological mechanism of salvaged myocardium. T2\* BOLD could represent a more accurate alternative without contrast to late gadolinium enhancement (LGE) imaging in acute STEMI patients.

# **CLINICAL RELEVANCE/APPLICATION**

BOLD MRI could evaluate the balance between supply/demand in myocardial oxygenation and myocardial damage severity, and discriminate between reversible and irreversible myocardial injury and is recommended in the initial evaluation of STEMI patients.

# SSC02-03 Intra-Myocardial Hemorrhage and Microvascular Obstruction After Acute Re-Perfused Myocardial Infarction: Are They Really Two Different Complications?

Monday, Nov. 26 10:50AM - 11:00AM Room: S502AB

Participants

Veronica Bordonaro, MD, Rome, Italy (*Presenter*) Nothing to Disclose Vincenzo Vingiani, MD, Castellammare di Stabia, Italy (*Abstract Co-Author*) Nothing to Disclose Agostino Meduri, MD, Rome, Italy (*Abstract Co-Author*) Nothing to Disclose Riccardo Marano, MD, Rome, Italy (*Abstract Co-Author*) Nothing to Disclose Luigi Natale, MD, Florence, Italy (*Abstract Co-Author*) Nothing to Disclose Riccardo Manfredi, MD, Rome, Italy (*Abstract Co-Author*) Nothing to Disclose

#### For information about this presentation, contact:

bordonaroveronica@gmail.com

#### PURPOSE

To evaluate the performance of T2\* mapping for intra-myocardial hemorrhage (IMH) detection in acute re-perfused myocardial infarction and to demonstrate in vivo the pathophysiological coincidence of microvascular obstruction (MVO) and intra-myocardial hemorrhage (IMH) at the level of the infarcted zone.

# **METHOD AND MATERIALS**

74 consecutive Patients (Pts) after primary percutaneous intervention for first acute myocardial infarction (AMI) underwent cardiovascular MR (CMR) within 1 week after treatment, using a standard protocol (T2 3IR-FSE, cine-SSFP, rest FGRET and 2D IR-FGRE). Before gadolinium administration, we performed T2\* mapping at the level of the infarct zone. T2\* images were analyzed with a dedicated software (Reportcard 4.0, GE Medical Systems), considering a T2\* value <=20 ms as positive for IHM. First-pass perfusion images were acquired during administration of different Gadolinium chelates at a standard dose of 0.1 mmol/kg; early and late gadolinium enhancement (EGE and LGE) were obtained at 2-3 and 12-15 minutes after contrast injection, respectively.

#### RESULTS

On the basis of post-Gadolinium sequences, MVO in the infarct area was demonstrated in 34 Pts at the first pass perfusion images, in 29 Pts at EGE and in 26 Pts in LGE images. A focal IMH was identified in 13/74 Pts at T2 3IR-FSE images, while on the basis of T2\* mapping IMH was detected in 28/74 Pts. We found that IMH coincided with the area of MVO: all 13 Pts with IMH at T2 3IR-FSE images showed MVO at first pass perfusion and/or at EGE and LGE; all 28 Pts positive for IMH at T2\* mapping showed MVO at EGE, while only 2 Pts did not show MVO at LGE.

#### CONCLUSION

T2\* imaging should be the preferred CMR method for assessment of IMH because its higher sensitivity than conventional T2 images. Reperfusion IMH is closely associated with the presence of MVO and they represent patho-physiologically the same complication of the ischemia-reperfusion injury.

# **CLINICAL RELEVANCE/APPLICATION**

We demonstrated that MVO and IMH represent the same complication in re-perfused AMI. T2\* mapping (better than T2) can be used to assess MVO also in Pts not suitable for gadolinium administration.

# SSC02-04 Intramyocardial Hemorrhage May Not Change from 48 Hours to 7days While Myocardial Ischemia and Myocardial Edema Decrease After Reperfusion: A Rat Study at 7T

Monday, Nov. 26 11:00AM - 11:10AM Room: S502AB

Participants

Rui Xia, Chongqing, China (*Presenter*) Nothing to Disclose Tong Zhu, Chengdu, China (*Abstract Co-Author*) Nothing to Disclose Yu Zhang, Chengdu, China (*Abstract Co-Author*) Nothing to Disclose Yushu Chen, BSc, Chengdu, China (*Abstract Co-Author*) Nothing to Disclose Lei Wang, BA, Chengdu, China (*Abstract Co-Author*) Nothing to Disclose Wei Chen, PhD, Chengdu, China (*Abstract Co-Author*) Nothing to Disclose Yongmei Li, MD, PhD, Chongqing, China (*Abstract Co-Author*) Nothing to Disclose Fajin Lv, MD, Chongqing, China (*Abstract Co-Author*) Nothing to Disclose Tianyou Luo, Chongqing, China (*Abstract Co-Author*) Nothing to Disclose Jie Zheng, PhD, Saint Louis, MO (*Abstract Co-Author*) Nothing to Disclose Fabao Gao, MD, PhD, Chengdu, China (*Abstract Co-Author*) Nothing to Disclose

# For information about this presentation, contact:

gaofabao@yahoo.com

### PURPOSE

To study the change of intramyocardial hemorrhage(IMH), myocardial edema(ME) and myocardial ischemia(MI) in reperfused myocardial ischemic rat from 48h to 7d in a 7.0T MR scanner.

# METHOD AND MATERIALS

Nine rats (SD, 250-300g, male) with 60min myocardial ischemia followed by 48h and 7d were investigated. The myocardial ischemia was induced by occluding the proximal left anterior descending coronary artery, which was then released for reperfusion. The T2\*-mapping and T2-mapping pulse sequences (T2-mapping: TR/TE=1500ms/10,20,30 ms, MTX=192×192, FOV=50×50mm, slice thickness=1.5mm. T2\*-mapping: TR/TE=1000ms/3.5,7,10.5,14,17.5,21,24.5,28,31.5 ms, FA (Flip angle)=30°, MTX=192×192, FOV=50×50mm, slice thickness=1.5mm) were implemented and optimized on a 7.0T MR system (BRUKER BIOSPEC 70/30, Germany). Images were acquired on the short axis slices during mid-diastolic phase in each end-inspiratory period using both ECG and respiratory gating systems. After the acquisition of T2\*-mapping and T2-mapping images, Late gadolinium enhancement (LGE) imaging was performed by FISP(TR/TE=5.2ms/1.8ms, FA=25°, MTX=256×256, FOV=50×50mm, slice thickness=1.5mm) to evaluate the extent of myocardial ischemia after an injection of gadolinium diethylenetriamine pentaacetic acid (Gd-DTPA, Magnevist, Bayer Health Care Pharmaceuticals) at a dose of 0.15 mmol/kg. The T2\*-maps and T2-maps were calculated using a custom-made software. The areas of edema regions were defined by high T2 values (> mean ± 2SD in remote areas) on T2 maps. The areas of hemorrhage were identified as a hypointense core within a hyperintense territory on T2\* maps. All areas were expressed as a percentage of the whole myocardial tissue of left ventricle.

#### RESULTS

The area of ME and MI decreased from 48h ( $31.2\pm7.9\%$ ;  $21.9\pm10.2\%$ ) to 7d ( $23.6\pm3.8\%$ , p<0.01;  $10.8\pm6.6\%$ , p<0.01). However, they were not significant different between the area of IMH at 48h ( $4.8\pm3.3\%$ ) and 7d ( $5.1\pm3.4\%$ , p>0.05).

# CONCLUSION

The area of ME and MI decreased, which may indicate the self-healing of myocardial edema and myocardial ischemia after reperfusion. However, intramyocardial hemorrhage, caused by reperfusion injury, would not recover in this duration.

# **CLINICAL RELEVANCE/APPLICATION**

Reperfusion will decrease myocardial ischemia and myocardial edema, but also cause sustained intramyocardial hemorrhage, which should be recommended as an important risk point for percutaneous coronary intervention of myocardial ischemic patients.

# SSC02-05 Larger Myocardial Ischemia May Cause Larger Intramyocardial Hemorrhage and Smaller Area at Risk in Acute Reperfused Myocardial Ischemic Rats

Monday, Nov. 26 11:10AM - 11:20AM Room: S502AB

Participants

Rui Xia, Chongqing, China (*Presenter*) Nothing to Disclose Yu Zhang, Chengdu, China (*Abstract Co-Author*) Nothing to Disclose Tong Zhu, Chengdu, China (*Abstract Co-Author*) Nothing to Disclose Yushu Chen, BSc, Chengdu, China (*Abstract Co-Author*) Nothing to Disclose Lei Wang, BA, Chengdu, China (*Abstract Co-Author*) Nothing to Disclose Wei Chen, PhD, Chengdu, China (*Abstract Co-Author*) Nothing to Disclose Yongmei Li, MD, PhD, Chongqing, China (*Abstract Co-Author*) Nothing to Disclose Fajin Lv, MD, Chongqing, China (*Abstract Co-Author*) Nothing to Disclose Tianyou Luo, Chongqing, China (*Abstract Co-Author*) Nothing to Disclose Jie Zheng, PhD, Saint Louis, MO (*Abstract Co-Author*) Nothing to Disclose Fabao Gao, MD, PhD, Chengdu, China (*Abstract Co-Author*) Nothing to Disclose

#### For information about this presentation, contact:

#### gaofabao@yahoo.com

#### PURPOSE

To study the correlations between myocardial infarction and intramyocardial hemorrhage, area at risk in reperfused myocardial ischemic rats with a comprehensive method on 7.0T MR.

#### METHOD AND MATERIALS

Eleven rats (SD, 250-300g, male) with 60min myocardial ischemia followed by 48hours reperfusion were investigated. The different degrees of myocardial ischemia were induced by occluding the different section of proximal left anterior descending coronary artery. The T2\*-mapping and T2-mapping pulse sequences (T2-mapping: TR/TE=1500ms/10,20,30 ms. T2\*-mapping: TR/TE=1000ms/3.5,7,10.5,14,17.5,21,24.5,28,31.5 ms, FA (Flip angle)=30°) were implemented and optimized on a 7.0T MR system (BRUKER BIOSPEC 70/30, Germany). Images were acquired on the short axis slices during mid-diastolic phase in each end-inspiratory period using both ECG and respiratory gating systems. After the acquisition of T2\*-mapping and T2-mapping images, Late gadolinium enhancement (LGE) imaging was performed by FISP(TR/TE=5.2ms/1.8ms, FA=25°) to evaluate the extent of myocardial ischemia after an injection of gadolinium diethylenetriamine pentaacetic acid (Gd-DTPA) at a dose of 0.15 mmol/kg. The T2\*-maps and T2-maps were calculated using a custom-made software. Area at risk were defined as the difference between edema areas with high T2 values(> mean ± 2SD in remote normal tissue areas) in T2 maps and positive enhanced area in LGE images. The areas of hemorrhage were identified as a hypointense core within a hyperintense territory on T2\* maps. All areas were expressed as a percentage of the whole myocardial tissue of left ventricle.

#### RESULTS

Myocardial ischemia ranged from 9.5% to 47% (22.7 $\pm$ 10.4%), intramyocardial hemorrhage ranged from 1.25% to 17% (5.3 $\pm$ 4.5%), area at risk ranged from 2.8% to 15.2% (8.4 $\pm$ 3.9%). There was a significant positive correlation between myocardial ischemia and intramyocardial hemorrhage (r=0.85, P<0.01), while a negtive correlation was found between myocardial ischemia and area at risk (r=0.77, P<0.01).

# CONCLUSION

Larger myocardial ischemia may cause larger intramyocardial hemorrhage and smaller area at risk in 48h reperfused myocardial ischemic rats.

# **CLINICAL RELEVANCE/APPLICATION**

The prognosis of intramyocardial hemorrhage and area at risk could be made by the area of reperfused myocardial ischemia, which should be recommended as a critical index before percutaneous coronary intervention of myocardial ischemic patients.

# SSC02-06 Fully Automated Analysis of LGE MRI in Post-Infarct Patients Using Convolutional Neural Networks: Simultaneous Segmentation of Ventricular Myocardium and Myocardial Infarction

Monday, Nov. 26 11:20AM - 11:30AM Room: S502AB

Participants

Qian Tao, Leiden, Netherlands (*Presenter*) Nothing to Disclose Wenjun Yan, MSc, Shanghai, China (*Abstract Co-Author*) Nothing to Disclose Yuanyuan Wang, PhD, Shanghai, China (*Abstract Co-Author*) Nothing to Disclose Rob J. van der Geest, PhD, Leiden, Netherlands (*Abstract Co-Author*) Nothing to Disclose

#### For information about this presentation, contact:

q.tao@lumc.nl

#### PURPOSE

To investigate the feasibility of deep-learning convolutional neural network (CNN) image segmentation for fully automated analysis of late gadolinium enhanced (LGE) MRI in post-infarct patients.

# METHOD AND MATERIALS

In 180 consecutive post-infarct patients LGE MRI was acquired prior to ICD implantation. An inversion-recovery 3D turbo-field echo sequence was used with parallel imaging, in one or two breath-holds and reconstructed into 20-24 levels in the short-axis view with a typical image resolution of  $1.56 \times 1.56 \times 5$  mm. For reference, an experienced observer manually traced the endocardial and epicardial contours and assessed the region of myocardial scar using the Full Width Half Maximum (FWHM) method, followed by visual correction, if needed. The cohort was randomly divided into a training set of 150 (3,606 images) and a testing set of 30 subjects (726 images). The training images were augmented into a total of 144,240 images by applying moderate rotation (-15 to 15 degree) and scaling (0.8 to 1.25). The U-Net CNN architecture was adopted to learn the manual segmentation from the training set, using cross entropy as the metric, with a learning rate of 10-4, in 50 epochs, initialized from a previously trained network for cine MR segmentation. The trained network was evaluated on the 30 independent testing subjects. We evaluated: (1) the accuracy of endocardial and epicardial contour in terms of average perpendicular distance (APD) in pixels, and (2) the accuracy of identified myocardial scar size per subject.

### RESULTS

On the independent training set, the APD was  $1.10\pm0.39$  and  $1.09\pm0.29$  pixels for the endocardial and epicardial contours, respectively. The identified scar size per subject was not significantly different between the CNN and the human observer:  $29.1\pm21.3$  g vs.  $31.7\pm20.8$  g (p=0.2). The processing time for CNN based segmentation was less than 0.2 seconds per subject.

# CONCLUSION

Deep-learning CNN shows great promise in the challenging segmentation problem of automated LGE MRI quantification in postinfarct patients, by simultaneously identifying the left ventricle and myocardial scar in a fully automated manner.

# **CLINICAL RELEVANCE/APPLICATION**

With further validation, the developed deep-learning CNN can be used to rapidly identify and quantify the myocardial scar from LGE MRI, avoiding time-consuming and user-dependent scar assessment and contour tracing.

# SSC02-07 Myocardial Edema and Necrosis after ST-Segment Elevation Myocardial Infarction by T2-Weighted and Late Gadolinium Enhancement MR Imaging: A Meta-Analysis

Monday, Nov. 26 11:30AM - 11:40AM Room: S502AB

Participants

Benjamin Kendziora, Berlin, Germany (Presenter) Nothing to Disclose

Peter Schlattmann, PhD, Berlin, Germany (Abstract Co-Author) Nothing to Disclose

Marc Dewey, MD, Berlin, Germany (*Abstract Co-Author*) Research Grant, General Electric Company; Research Grant, Bracco Group; Research Grant, Guerbet SA; Research Grant, Canon Medical Systems Corporation; Research Grant, European Commission; Research Grant, BIH Digital Health Accelerator; Speakers Bureau, Canon Medical Systems Corporation; Speakers Bureau, Guerbet SA; Speakers Bureau, Bayer AG; Consultant, Guerbet SA; Author, Springer Nature; Editor, Springer Nature; Institutional research agreement, Siemens AG; Institutional research agreement, Koninklijke Philips NV; Institutional research agreement, Canon Medical Systems Corporation; ; ; ; ; ; ; ;

For information about this presentation, contact:

benjamin.kendziora@charite.de

### PURPOSE

To analyze existing data on the extent of myocardial edema and necrosis measured by T2-weighted and late gadolinium enhancement (LGE) magnetic resonance (MR) imaging after ST-segment elevation myocardial infarction (STEMI).

#### **METHOD AND MATERIALS**

We searched MEDLINE, EMBASE, and ISI Web of Science for patient studies reporting the extent of myocardial edema and necrosis measured by T2-weighted and LGE MR imaging after STEMI. All information on patient demographics, treatment features, and imaging techniques reported by included studies were extracted. Multiple imputation was used for missing data and mixed-effects models to identify significant predictors of edema and necrosis. Follow-up data were used to evaluate the further temporal evolution of edema and necrosis.

# RESULTS

Forty-four studies with 5028 patients were included. Overall, edema area measured using T2-weighted MR imaging during the first week after STEMI was 33.8% of left ventricular (LV) myocardium (confidence interval [CI]: 31.9, 36.5), necrosis area measured using LGE MR imaging was 18.1% of LV myocardium (CI: 14.7, 21.4), and the proportion of edematous myocardium without necrosis was 42.0% (CI: 34.6, 49.4). Each hour of delay in revascularization increased necrosis by 3.6% of LV myocardium (95% CI: 1.1, 6.0; P = .013) and decreased the proportion of edematous myocardium without necrosis by 12.5% (95% CI: 6.9, 18.1; P = .002), while edema was not significantly affected. Other significant predictors were the degree of obstruction of the culprit artery before revascularization and the applied method for interpreting MR images. Within 6 months after STEMI, edema disappeared, while necrosis decreased only slightly but significantly.

# CONCLUSION

This meta-analysis indicates that myocardial edema on T2-weighted MR imaging delineates the area at risk after STEMI and can be used to quantify the proportion of reversibly injured myocardium, commonly defined as myocardial salvage index, when combined with LGE MR imaging of necrotic myocardium.

# **CLINICAL RELEVANCE/APPLICATION**

Quantification of the proportion of reversibly injured, salvaged myocardium after STEMI by T2-weighted and LGE MR imaging allows evaluation of therapeutic efficiency.

# SSC02-08 Detection of Occult Myocardial Scars with Cardiovascular Magnetic Resonance Imaging in Patients with Asymptomatic Type 2 Diabetes Mellitus: The ACCREDIT Study

Monday, Nov. 26 11:40AM - 11:50AM Room: S502AB

Participants

Joon-Won Kang, MD, Seoul, Korea, Republic Of (*Presenter*) Nothing to Disclose Sang Il Choi, MD, Seongnam-Si, Korea, Republic Of (*Abstract Co-Author*) Nothing to Disclose Sung Min Ko, Seoul, Korea, Republic Of (*Abstract Co-Author*) Nothing to Disclose Yeon Hyeon Choe, MD, PhD, Seoul, Korea, Republic Of (*Abstract Co-Author*) Nothing to Disclose Byoung Wook Choi, MD, Seoul, Korea, Republic Of (*Abstract Co-Author*) Nothing to Disclose Whal Lee, MD, PhD, Seoul, Korea, Republic Of (*Abstract Co-Author*) Nothing to Disclose Tae-Hwan Lim, MD, PhD, Seoul, Korea, Republic Of (*Abstract Co-Author*) Nothing to Disclose

#### PURPOSE

To determine the prevalence of occult myocardial scars (OMS) on contrast-enhanced cardiovascular magnetic resonance imaging (CMR) in asymptomatic patients with type 2 diabetes mellitus (DM) and to assess the relationship between the occurrence of OMS detected with CMR and coronary atherosclerosis observed with contrast-enhanced coronary computed tomography angiography (CCTA).

#### **METHOD AND MATERIALS**

This multi-center, prospective, open-label study included asymptomatic patients with type 2 DM and at least two identified cardiac risk factors, scheduled to undergo CMR and CCTA procedures. CMR and CCTA were performed with gadoterate meglumine (Dotarem®, Guerbet) and iobitridol (Xenetix®, Guerbet), respectively. The prevalence of OMS was calculated on CMR. For each main coronary artery, stenosis degree and plaque characteristics were assessed on CCTA. For each myocardial segment with OMS, the corresponding infarct-related artery (IRA) was identified according to the American Heart Association recommendations. The

characteristics of the plaques located in IRA were compared to those located in non-IRA.

# RESULTS

Among the 348 patients included (mean (±SD) age: 60.2±6.5 years; male: 60.9%; mean BMI: 25.4±3.1 kg/m2), 322 patients completed both CMR and CCTA procedures. At least one OMS was detected by CMR in 23 patients (7.1%). CCTA showed a significant stenosis (>50% diameter reduction) or occlusion for 13 (56.5%) of the 23 patients with OMS and for 67 (22.4%) of the 299 patients without OMS. Sixty-two IRA plaques and 52 non-IRA plaques were identified with CCTA in patients with OMS. In IRA, 16.1% plaques were non-calcified, 22.6% mixed and 61.3% calcified while in the non-IRA, 30.8% were non-calcified, 17.3% mixed and 51.9% calcified. No differences in calcification status were demonstrated between IRA and non-IRA plaques (p=0.175, Chi<sup>2</sup>).

# CONCLUSION

OMS were identified with CMR in 7.1% of asymptomatic patients with type 2 DM. No significant difference was demonstrated in plaque characteristics between IRA and non-IRA in patients with OMS. Further investigations are still required to determine whether the occurrence of OMS is related to atherosclerosis detected with CCTA.

#### **CLINICAL RELEVANCE/APPLICATION**

CT and MRI screening in diabetes patients without chest pain can provide the information of occult myocardial infarction and its relationship to coronary arterial disease.

# SSC02-09 Multi-Parametric Rest and Dobutamine Stress Cardiovascular Magnetic Resonance in Assessment of Myocardial Viability: Could Feature Tracking Strain Analysis Add Value?

Monday, Nov. 26 11:50AM - 12:00PM Room: S502AB

#### Awards

#### Student Travel Stipend Award

Participants

Mahmoud N. Shaaban, MSc,MBChB, Aswan, Egypt (*Presenter*) Nothing to Disclose Sara W. Tantawy, MBBCh, Aswan, Egypt (*Abstract Co-Author*) Nothing to Disclose Dina F. Haroun, MBBCh, Cairo, Egypt (*Abstract Co-Author*) Nothing to Disclose Fatma R. Elkafrawy, MBBCh,MSc, Aswan, Egypt (*Abstract Co-Author*) Nothing to Disclose Dina Labib, Aswan, Egypt (*Abstract Co-Author*) Nothing to Disclose Noha Behairy, MD, Cairo, Egypt (*Abstract Co-Author*) Nothing to Disclose Ahmed E. Kharabish, MD,MSc, Freiburg, Germany (*Abstract Co-Author*) Nothing to Disclose Soha Romeih, Aswan, Egypt (*Abstract Co-Author*) Nothing to Disclose Wesam El Mozy, Cairo, Egypt (*Abstract Co-Author*) Nothing to Disclose

#### For information about this presentation, contact:

mahmoud.shaban@med.tanta.edu.eg

#### PURPOSE

To evaluate the diagnostic accuracy of multi-parametric CMR in assessment of myocardial viability in chronic ischemic patients using 4 different techniques; delayed gadolinium enhancement(DGE) as gold standard for detection of scar burden, CMR feature tracking(CMR-FT) at rest and with low dose dobutamine(LDD), visual assessment of myocardial contractility with LDD and LV end-diastolic wall thickness(EDWT)

# METHOD AND MATERIALS

15 patients(53±12years) &10 controls(38±11years) were prospectively enrolled. All subjects had CMR exams on 1.5T scanner. A LDD IV infusion was administrated in 2 stages, 3 minutes each, with a dose of 5  $\mu$ g/kg/min that is increased to 10  $\mu$ g/kg/min in 2nd stage. LV was divided into 16 segments and FT parameters were derived from SSFP Cine images using dedicated software. Viable myocardium was defined as a dobutamine induced increase in resting FT values of >20 % & systolic wall thickening of >=2 mm by visual assessment. A segment with no or <=50 % fibrosis on DGE & EDWT of >5 mm was defined as viable

#### RESULTS

240 segments were analyzed for patients at rest & with LDD &160 segments for controls at rest. 44 segments were non-viable based on DGE &196 were viable. Both peak global circumferential(Ecc) & radial(Err) strains were significantly impaired in ischemic patients compared to healthy(-12.84±7.72 vs -19.63±7.08,P<0.0001 & 22.07±15.19 vs 30.90±18.59,P=0.0039)respectively. With segmental Ecc, 50 segments were identified as non-viable & 190 as viable(sensitivity 72%,specificity 91% &diagnostic accuracy 87%). With segmental Err, 49 segments were identified as non-viable & 191 as viable(sensitivity 54%,specificity 87% & diagnostic accuracy 81%). By visual assessment of myocardial contractility with LDD, 43 segments were identified as non-viable & 197 as viable(sensitivity 70%,specificity 86% & diagnostic accuracy 88%). Based on EDWT assessment, 41 segments were identified as non-viable & 199 as viable(sensitivity 50%,specificity 90%& diagnostic accuracy 83%)

# CONCLUSION

Quantitative assessment of Ecc & Err with FT, along with EDWT & qualitative visual assessment of myocardial contractility at rest & with LDD may improve diagnostic accuracy of non-viable segments with moderate sensitivity & high specificity

# **CLINICAL RELEVANCE/APPLICATION**

FT and EDWT are non-contrast parameters that could be of particular importance in determining viability in patients with impaired glomerular filtration rate or patients with known hypersensitivity to contrast agents



#### SSC03

#### Chest (Lung Cancer Screening)

Monday, Nov. 26 10:30AM - 12:00PM Room: E451A



AMA PRA Category 1 Credits ™: 1.50 ARRT Category A+ Credit: 1.75

#### Participants

Jo-Anne O. Shepard, MD, Boston, MA (*Moderator*) Nothing to Disclose Jane P. Ko, MD, New York, NY (*Moderator*) Research collaboration, Siemens AG

# Sub-Events

# SSC03-01 Predicting the Likelihood of Various Major Diseases from Lung Cancer Screening Chest CT Using 3D Convolutional Neural Networks

Monday, Nov. 26 10:30AM - 10:40AM Room: E451A

Participants

Aditya U. Sheth, Berkeley, CA (*Presenter*) Nothing to Disclose Youngho Seo, PhD, San Francisco, CA (*Abstract Co-Author*) Consultant, BioLaurus, Inc Peter Chang, MD, San Francisco, CA (*Abstract Co-Author*) Nothing to Disclose Thienkhai H. Vu, MD, PhD, San Francisco, CA (*Abstract Co-Author*) Nothing to Disclose Dmytro Lituiev, San Francisco, CA (*Abstract Co-Author*) Nothing to Disclose Jae Ho Sohn, MD, San Francisco, CA (*Abstract Co-Author*) Nothing to Disclose

# For information about this presentation, contact:

sohn87@gmail.com

# PURPOSE

A large number of patients undergo annual lung cancer screening with low-dose chest CT. The CT data contains significant information about health of the patient, beyond simple lung cancer status. The National Lung Cancer Screening (NLST) database provides a large dataset with correlated clinical metadata, which can be used to train machine learning algorithms to extract as much useful health information as possible. The aim of the study is to develop and validate a 3D convolutional neural network algorithm on these CT studies to predict the likelihood of various major diseases: diabetes, heart disease, COPD, and stroke.

#### **METHOD AND MATERIALS**

We extracted random samples of 16,780 scans from NLST. Data preprocessing consisted of isotropic resolution resizing and standardization to 350 x 350 x 35 pixel size. Data was augmented with random rotations between -15 and 15 degrees. The processed samples were passed through a 3D convolutional neural network (CNN) with architecture loosely inspired by the VGG-Net. Modifications included generalization to 3D dataset, more gradual pooling across the z-axis, and use of batch normalization. Stochastic gradient descent optimizer and sparse categorical crossentropy loss function were utilized. Final results were gathered using a separate testing set extracted from the NLST dataset. Error analysis was conducted.

#### RESULTS

We performed training and testing for classification of the following diseases: diabetes, heart disease, COPD, and stroke. For each disease respectively, we achieved an ROC AUC of 0.75, 0.70, 0.74, 0.69 on the test sets. ROC curves are displayed in Figure (1). For each of these results, a single radiologist with deep learning expertise manually inspected random samples of correct and incorrect predictions to ensure absence of any systematic errors. None was identified. Testing sets were confirmed to be an accurate representation of the training sets with regards to positive/negative example ratios.

#### CONCLUSION

Our 3D CNN model successfully predicted the likelihood of various diseases from lung cancer screening chest CT studies.

# **CLINICAL RELEVANCE/APPLICATION**

The algorithm can be used to provide patients with useful health information about major diseases, in addition to the formal lung cancer screening interpretations by radiologists.

# SSC03-02 Improving Specificity of Lung Cancer Screening CT Using Deep Learning

Monday, Nov. 26 10:40AM - 10:50AM Room: E451A

Participants

Diego Ardila, Mountain View, CA (*Presenter*) Employee, Alphabet Inc Bokyung Choi, PhD, Mountain View, CA (*Abstract Co-Author*) Employee, Alphabet Inc Atilla P. Kiraly, PhD, Mountain View,, CA (*Abstract Co-Author*) Former Employee, Siemens AG; Employee, Alphabet Inc Sujeeth Bharadwaj, PhD, Mountain View, CA (*Abstract Co-Author*) Employee, Alphabet Inc Joshua J. Reicher, MD, Stanford, CA (*Abstract Co-Author*) Investor, Health Companion, Inc; Consultant, Alphabet Inc Greg Corrado, PhD, Mountain View, CA (*Abstract Co-Author*) Employee, Alphabet Inc Daniel Tse, MD, Mountain View, CA (*Abstract Co-Author*) Employee, Alphabet Inc Lily Peng, MD,PhD, Mountain View, CA (*Abstract Co-Author*) Employee, Alphabet Inc Shravya Shetty, Mountain View, CA (*Abstract Co-Author*) Employee, Alphabet Inc

#### For information about this presentation, contact:

sshetty@google.com

#### PURPOSE

Evaluate the utility of deep learning to improve the specificity and sensitivity of lung cancer screening with low-dose helical computed tomography (LDCT), relative to the Lung-RADS guidelines.

#### **METHOD AND MATERIALS**

We analyzed 42,943 CT studies from 14,863 patients, 620 of which developed biopsy-confirmed cancer. All cases were from the National Lung Screening Trial (NLST) study. We randomly split patients into a training (70%), tuning (15%) and test (15%) sets. A study was marked "true" if the patient was diagnosed with biopsy confirmed lung cancer in the same screening year as the study. A deep learning model was trained over 3D CT volumes (400x512x512) as input. We used the 95% specificity operating point based on the tuning set, and evaluated our approach on the test set. To estimate radiologist performance, we retrospectively applied Lung-RADS criteria to each study in the test set. Lung-RADS categories 1 to 2 constitute negative screening results, and categories 3 to 4 constitute positive results. Neither the model nor the Lung-RADS results took into account prior studies, but all screening years were utilized in evaluation.

# RESULTS

The area under the receiver operator curve of the deep learning model was 94.2% (95% CI 91.0, 96.9). Compared to Lung-RADS on the test set, the trained model achieved a statistically significant absolute 9.2% (95% CI 8.4, 10.1) higher specificity and trended a 3.4% (95% CI -5.2, 12.6) higher sensitivity (not statistically significant).Radiologists qualitatively reviewed disagreements between the model and Lung-RADS. Preliminary analysis suggests that the model may be superior in distinguishing scarring from early malignancy.

#### CONCLUSION

A deep learning based model improved the specificity of lung cancer screening over Lung-RADS on the NLST dataset and could potentially help reduce unnecessary procedures. This research could supplement future versions of Lung-RADS; or support assisted read or second read workflows.

#### CLINICAL RELEVANCE/APPLICATION

While Lung-RADS criteria is recommended for lung cancer screening with LDCT, there is still an opportunity to reduce false-positive rates which lead to unnecessary invasive procedures.

# SSC03-03 New Algorithm Incorporating Machine Learning Improves Lung Cancer Risk Calculation on Screening CT Scans

Monday, Nov. 26 10:50AM - 11:00AM Room: E451A

Participants

Cheng Ting Lin, MD, Baltimore, MD (*Presenter*) Nothing to Disclose Yuliang Li, Baltimore, MD (*Abstract Co-Author*) Nothing to Disclose Matthew Garner, Baltimore, MD (*Abstract Co-Author*) Nothing to Disclose Nadege Fackche, Baltimore, MD (*Abstract Co-Author*) Nothing to Disclose Samata Kakkad, Baltimore, MD (*Abstract Co-Author*) Nothing to Disclose Zaver M. Bhujwalla, PhD, Baltimore, MD (*Abstract Co-Author*) Nothing to Disclose Susumu Mori, PhD, Baltimore, MD (*Abstract Co-Author*) Nothing to Disclose Susumu Mori, PhD, Baltimore, MD (*Abstract Co-Author*) Nothing to Disclose Calum MacAulay, Vancouver, BC (*Abstract Co-Author*) Nothing to Disclose David Ettinger, Baltimore, MD (*Abstract Co-Author*) Nothing to Disclose Malcolm Brock, Baltimore, MD (*Abstract Co-Author*) Nothing to Disclose Stephen Lam, MD, Vancouver, BC (*Abstract Co-Author*) Nothing to Disclose Peng Huang, Baltimore, MD (*Abstract Co-Author*) Nothing to Disclose

#### For information about this presentation, contact:

clin97@jhmi.edu

#### PURPOSE

Lung-RADS is widely used to classify nodules detected on lung cancer screening CT. Using data from the National Lung Cancer Screening Trial (NLST), we examined whether integration of patient demographics, clinical history, and CT texture features could improve our ability to predict long-term lung cancer development. Since most screening CTs detect early stage lung cancers, we further examined if our algorithm could predict cancer progression and overall survival in patients with resected stage I lung cancers.

#### **METHOD AND MATERIALS**

Demographics, clinical history, and baseline CT images from 24,386 NLST participants were analyzed using survival machine learning (SML). Nodule volume was calculated by V=3.14LR2 where L=longest diameter, R=longest perpendicular diameter/2. Subjects were partitioned into 4 risk groups to test hazards ratios (HR). The SML partition was compared to that from Lung-RADS. For the stage I lung cancer subgroup, the time from lung cancer diagnosis to death was used as the SML endpoint.

#### RESULTS

At the time of baseline CTs, the 4 risk groups were classified by: high (largest nodule L>10mm, V>6358mm3; n=85), mid-high (largest nodule L>10mm, V<=6358mm3; n=1219), mid-low (largest nodule L= $5\sim10$ mm, smoking>40 years; n=1736), and low (all

others; n=21346). Compared to our low risk group, HRs for time to lung cancer onset were 91.5, 11.1, 4.0 for high, mid-high, and mid-low risk groups respectively (all p<0.0001). In contrast, the HRs from Lung-RADS categories 4, 3, and 2 were 5.68, 1.27, and 0.75 respectively as compared to category 1 (p values: <0.0001, 0.056, 0.058). For stage 1 lung cancers, demographics, nodule margins, lymph node enlargement, and blood vessel involvement jointly affected the rate of cancer progression and overall patient survival.

# CONCLUSION

Using the NLST data, our new classification outperforms Lung-RADS in stratifying risk and predicting long-term lung cancer development. Furthermore, in pathologically defined stage 1 patients who received surgery, our new classification can identify those with poor survival suggesting that it can do so independently of cancer stage.

# **CLINICAL RELEVANCE/APPLICATION**

Our new classification outperforms Lung-RADS in stratifying risk and predicting long-term lung cancer development and can identify stage 1 patients with poor survival suggesting that it can do so independently of cancer stage.

# SSC03-04 Effect of Semiautomated Segmentation and Computer-Aided Detection of Lung Nodules on Lung Cancer Screening with Low Dose CT: Experience from a Nationwide Lung Cancer Screening Project

Monday, Nov. 26 11:00AM - 11:10AM Room: E451A

Participants

Eui Jin Hwang, Seoul, Korea, Republic Of (*Presenter*) Nothing to Disclose Jin Mo Goo, MD, PhD, Seoul, Korea, Republic Of (*Abstract Co-Author*) Research Grant, Samsung Electronics Co, Ltd; Research Grant, Lunit Inc Hyae Young Kim, MD, PhD, Goyang-si, Korea, Republic Of (*Abstract Co-Author*) Nothing to Disclose Jaeyoun Yi, Seoul, Korea, Republic Of (*Abstract Co-Author*) Officer, Coreline Soft, Co Ltd Yeol Kim I, Goyang-Si, Korea, Republic Of (*Abstract Co-Author*) Nothing to Disclose

#### For information about this presentation, contact:

ken921004@hotmail.com

#### PURPOSE

To evaluate the effect of semiautomated segmentation and computer-aided detection (CAD) system for lung nodule on lung cancer screening based on the Lung-RADS.

# METHOD AND MATERIALS

We utilized the data from an ongoing nationwide multi-center lung cancer screening project with low dose chest CT. This project started with a visual assessment and manual measurement system (a manual system) and changed into a cloud-based software system which equipped with a semiautomated nodule segmentation and CAD system (a software system). In a software system, an average diameter of a nodule for the Lung-RADS was calculated on a plane showing the maximal cross sectional area of a nodule. For this study, an average diameter on axial planes was also calculated. We compared the number of detected lung nodules and distribution of Lung-RADS categories between two systems. When the results of before and after CAD were available (the number of cases, 2374), the effect of CAD was evaluated.

# RESULTS

The number of cases and the number of nodules for both systems are as follows: a manual system, 1821 cases, 1630 nodules; a software system, 4665 cases, 6116 nodules. Significantly greater number of nodules (0.90 vs. 1.31 nodule/case) were detected at a software system. The size of nodule was significantly larger (5.5 vs. 4.6 mm) at a software system, but there was no significant difference in the size of nodules between two systems when axial planes were used in calculating an average diameter in a software system. Both the per-case (9.8% vs. 17.4%) and per-nodule (12.9% vs. 17.9%) proportion of positive test (category 3/4) were significantly higher at a software system. By applying the CAD results, not only the number of the detected nodules (0.77 vs. 1.23 nodule/case) but also the per-case proportion of positive test (11.6% vs. 17.1%) were significantly increased.

# CONCLUSION

By applying a semi-automated segmentation and CAD system, the number of detected nodules and the proportion of positive test were significantly increased.

# **CLINICAL RELEVANCE/APPLICATION**

Semiautomated segmentation and CAD have important effects on the Lung-RADS positive rate. Therefore, detailed guidelines should be provided for the use of software in lung cancer screening.

# SSC03-05 Randomized Clinical Trial of CAD versus No CAD as First Reader of Lung Cancer Screening CT: Preliminary Report

Monday, Nov. 26 11:10AM - 11:20AM Room: E451A

Participants

Ren Yuan, MD,PhD, Vancouver, BC (*Presenter*) Nothing to Disclose John R. Mayo, MD, Vancouver, BC (*Abstract Co-Author*) Speaker, Siemens AG Renelle Myers, MD, Vancouver, BC (*Abstract Co-Author*) Nothing to Disclose Sukhinder Atkar-Khattra, BSC, Vancouver, BC (*Abstract Co-Author*) Nothing to Disclose Isaac Streit, Vancouver, BC (*Abstract Co-Author*) Nothing to Disclose John Yee, MD, Vancouver, BC (*Abstract Co-Author*) Nothing to Disclose Kyle Grant, MD, Vancouver, BC (*Abstract Co-Author*) Nothing to Disclose Alexander Lee, MD, Vancouver, BC (*Abstract Co-Author*) Nothing to Disclose Anna L. Mcguire, MD, Vancouver, BC (*Abstract Co-Author*) Nothing to Disclose Colin Jacobs, PhD, Nijmegen, Netherlands (*Abstract Co-Author*) Research Grant, MeVis Medical Solutions AG Bram Van Ginneken, PhD, Nijmegen, Netherlands (*Abstract Co-Author*) Stockholder, Thirona BV; Co-founder, Thirona BV; Research Grant, Varian Medical Systems, Inc; Research Grant, Canon Medical Systems Corporation Martin Tammemagi, St. Catharines, ON (*Abstract Co-Author*) Nothing to Disclose Stephen Lam, MD, Vancouver, BC (*Abstract Co-Author*) Nothing to Disclose

#### For information about this presentation, contact:

ren.yuan@bccancer.bc.ca

#### PURPOSE

The accuracy of radiologists reading lung cancer screening CT in a previous study shows a false-negative rate (FN) of 3.5% to 8.1%. The purpose of this study was to assesses if CAD can reduce the FN and CT reading time.

# **METHOD AND MATERIALS**

We conducted a randomized trial in 148 smokers participating in our ongoing Lung Cancer Screening Project (75M:73F, 66±7yrs, 59 ex- vs. 89 current-smoker). Chest CTs were randomized into two arms. In the CAD and Technician first arm (CAD+Tech-1st), CAD findings were displayed first, a technician accepted or rejected CAD findings and added probable nodule(s), then a chest radiologist accepted or rejected the CAD +Tech findings additional nodule(s). In the RAD-first arm (RAD-1st) the same radiologist read the CT first with CAD marks hidden, then turned on CAD to accept true nodules including those only found by CAD and delete the non-nodule CAD findings. The number of true nodules and reading time were recorded.

#### RESULTS

The reading times were  $6.2 \pm 3.4$  min (range: 2-18) vs.  $8.3 \pm 5.4$  min (range: 3-30) for CAD+Tech-1st vs. RAD-1st arms (p=0.012) for CTs with >=1 nodule; and  $4.4\pm1.5$  min (range: 2-10) vs.  $8.7\pm9.5$  min (range: 3-30) for those without nodules (p=0.07). By the three detection methods, 212 true nodules were found in 97 CTs in the CAD+Tech-1st arm. CAD detected 82 and technician added 93 true nodules, giving a combined sensitivity of 83%. There were 37/212 nodules found only by the radiologist; 12/37 were the most important nodule, and 1/37 was the only nodule that drove follow-up. In the RAD-1st arm 71 true nodules were found in 51 CTs; 36/71 (51%) were found by both CAD and radiologist. The radiologist missed 2 true nodules in 2 participants (2/51, 4%) which were detected by CAD and altered their follow-up protocol. The radiologist's detection sensitivity slightly increased with CAD (97% to 100%). CAD missed 33/71(46%) true nodules found by the radiologist, 16/33 (48%) were key nodules and 11/16 were the only nodule, changing follow-up.

#### CONCLUSION

CAD+Tech speed up the radiologist's nodule detection on screening chest CT. CAD detected nodules in 4% subjects where no nodule was identified by the radiologist, changing imaging follow-up protocol.

#### **CLINICAL RELEVANCE/APPLICATION**

While CAD+Tech as first reader cannot replace the radiologist, CAD could play an important role in lung cancer screening by saving radiologists' time, and importantly reduce their FN rate by 4%.

# SSC03-06 Understanding Gaps Between Mental Health and Radiology Care: Population-based Cross-Sectional Survey Analysis of Lung Cancer Screening Eligibility and Smoking Prevalence Among Patients with Mental Illness

Monday, Nov. 26 11:20AM - 11:30AM Room: E451A

Participants

Efren J. Flores, MD, Boston, MA (*Presenter*) Nothing to Disclose Diego Lopez, Boston, MA (*Abstract Co-Author*) Nothing to Disclose Gary X. Wang, MD, PhD, Boston, MA (*Abstract Co-Author*) Nothing to Disclose McKinley Glover IV, MD, Boston, MA (*Abstract Co-Author*) Nothing to Disclose Kelly E. Irwin, MD, MPH, Boston, MA (*Abstract Co-Author*) Nothing to Disclose Elyse Park, PhD, MPH, Boston, MA (*Abstract Co-Author*) Nothing to Disclose Constance D. Lehman, MD, PhD, Boston, MA (*Abstract Co-Author*) Nothing to Disclose Soard, General Electric Company Jo-Anne O. Shepard, MD, Boston, MA (*Abstract Co-Author*) Nothing to Disclose Anand K. Narayan, MD, PhD, Boston, MA (*Abstract Co-Author*) Nothing to Disclose

#### For information about this presentation, contact:

ejflores@mgh.harvard.edu

#### PURPOSE

Prior studies have found that patients with mental illness are more likely to smoke compared with patients without mental illness. Lung Cancer Screening (LCS) with LDCT decreases lung cancer mortality in eligible current or former smokers. There is limited population-based information about LCS eligibility in patients with mental illness. Our purpose was to determine if patients with selfreported mental illness are more likely to be eligible for LCS and smoking cessation interventions compared to patients without mental illness using nationally representative federal cross-sectional survey data.

# METHOD AND MATERIALS

Retrospective analysis of 2015 National Health Interview Survey (NHIS), a nationally representative, federal cross sectional survey was conducted. Individuals 55-77 yrs without lung cancer were included. The proportion of survey participants eligible for LCS was calculated and compared in patients with and without self-reported mental illness. Multiple variable logistic regression analyses were conducted comparing LCS eligibility in patients with and without self-reported mental illness, adjusted for potential confounders (age, race, and insurance status). Adjusted odds ratios were calculated with 95% confidence intervals. Analyses were performed accounting for complex survey design elements.

# RESULTS

11,325 individuals between ages 55-77 were included (mean age 64.1, 52.8% female, 74.9% white) of whom 2.8% reported at least

one mental illness. Of individuals with self reported mental illness, 18.7% met eligibility criteria for LCS and 25.8% were current smokers. Of individuals without self reported mental illness, 10.6% met eligibility criteria for LCS and 12.9% were current smokers. Patients self-reporting mental illness were more likely to be eligible for LCS (Adjusted OR 1.89, 95% CI 1.30 to 2.75, p = 0.001) and more likely to be current smokers (Adjusted OR 2.20, 95% CI 1.59 to 3.07, p < 0.001) than patients without mental illness.

# CONCLUSION

Patients with self-reported mental illness have a higher smoking prevalence and are nearly twice as likely to be eligible for LCS compared with patients without mental illness.

#### **CLINICAL RELEVANCE/APPLICATION**

Radiologists have an opportunity to collaborate with psychiatry and primary care in developing targeted LCS outreach efforts for patients with mental illness who are at increased risk of developing lung cancer due to their higher smoking prevalence.

# SSC03-07 Lung Cancer Screening in a Socioeconomically Disadvantaged Population: Baseline and 1st Annual Rescreening Results

Monday, Nov. 26 11:30AM - 11:40AM Room: E451A

# Awards

# **Trainee Research Prize - Resident**

Participants

Charles H. Li, MD, Los Angeles, CA (*Presenter*) Nothing to Disclose Phillip Guichet, MD, New York, NY (*Abstract Co-Author*) Nothing to Disclose Steven Cen, PhD, Los Angeles, CA (*Abstract Co-Author*) Nothing to Disclose Beringia Liu, MPH, Los Angeles, CA (*Abstract Co-Author*) Nothing to Disclose Bhushan Desai, MBBS, MS, Los Angeles, CA (*Abstract Co-Author*) Nothing to Disclose Cameron Hassani, MD, Los Angeles, CA (*Abstract Co-Author*) Nothing to Disclose Leah M. Lin, MD, Los Angeles, CA (*Abstract Co-Author*) Nothing to Disclose Farhood Saremi, MD, Los Angeles, CA (*Abstract Co-Author*) Nothing to Disclose Bonnie Garon, MD, Los Angeles, CA (*Abstract Co-Author*) Nothing to Disclose Ana Maliglig, MD, MPH, Los Angeles, CA (*Abstract Co-Author*) Nothing to Disclose Alison Wilcox, MD, Los Angeles, CA (*Abstract Co-Author*) Nothing to Disclose Alison Wilcox, MD, Los Angeles, CA (*Abstract Co-Author*) Nothing to Disclose

#### For information about this presentation, contact:

chrisleemd@gmail.com

# PURPOSE

To describe the results of the first two rounds of screening of our clinical low-dose CT lung cancer screening program targeting a minority, socioeconomically disadvantaged, high-risk population different from that studied in the National Lung Screening Trial.

# **METHOD AND MATERIALS**

All participants met USPSTF and/or NCCN eligibility criteria for lung cancer screening. A coordinator enrolled eligible individuals, scheduled their screening exams, and organized their transportation.

# RESULTS

1029 individuals were referred from 7/21/2015 through 3/20/2018. 119 individuals declined screening, and 230 were unable to be contacted. Of 717 participants who agreed to participate, 411 met eligibility criteria for lung cancer screening. 370 patients underwent their baseline LDCT during this time period. 203 males (55%) and 167 females received baseline LDCT, with a mean age of 60 years. The median pack-years was 42 (range 20-132), and 81% of participants were current smokers. The ethnic makeup of the population was 77% black, 9% white, 8% Hispanic/Latino, and 5% Asian. 57% of participants had no more than a high school education. 33% of participants reported occupational exposure to one or more lung carcinogens. 84% (312) of patients received a Lung-RADS score of 1 (92) or 2 (220), 8% (29) received a score of 3, 5% (19) a score of 4A, and 3% a score of 4B (8) or 4X (2). 3 patients have been diagnosed with lung cancer to date: 1 stage IIB, 1 stage IIIB, and 1 stage IV. 28% (105) of patients had potentially significant incidental findings including interstitial lung disease (16), severe emphysema (14), aortic aneurysm (7), moderate-severe coronary calcifications (45), extrapulmonary masses (32), and pulmonary hypertension (4). 54% (147/271) of participants who were due for annual rescreening returned for their first annual LDCT. 93% (136) of these patients received a Lung-RADS score of 1 (21) or 2 (115), 3% (4) received a score of 3, 1% (2) a score of 4A, and 3% a score of 4B (5) or 4X (0).

# CONCLUSION

Lung cancer screening with LDCT in a minority, socioeconomically disadvantaged, high-risk population is feasible but may yield a different lung cancer profile than screening in more privileged communities. Adherence to annual rescreening and follow-up recommendations is challenging in this population.

#### **CLINICAL RELEVANCE/APPLICATION**

Minority, socioeconomically disadvantaged populations may experience different benefits from LDCT lung cancer screening.

#### **Honored Educators**

Presenters or authors on this event have been recognized as RSNA Honored Educators for participating in multiple qualifying educational activities. Honored Educators are invested in furthering the profession of radiology by delivering high-quality educational content in their field of study. Learn how you can become an honored educator by visiting the website at: https://www.rsna.org/Honored-Educator-Award/ Cameron Hassani, MD - 2018 Honored EducatorFarhood Saremi, MD - 2015 Honored Educator

# SSC03-08 Performance of the Vancouver Risk Calculator Compared to ACR Lung-RADS in an Urban, Diverse Clinical Lung Cancer Screening Cohort

Participants Abraham Kessler, BA, Bronx, NY (*Abstract Co-Author*) Nothing to Disclose Robert Peng, MD, Bronx, NY (*Presenter*) Nothing to Disclose Edward Mardakhaev, MD, Bronx, NY (*Abstract Co-Author*) Nothing to Disclose Charles S. White, MD, Baltimore, MD (*Abstract Co-Author*) Consultant, Koninklijke Philips NV Linda B. Haramati, MD, MS, Bronx, NY (*Abstract Co-Author*) Spouse, Board Member, Kryon Systems Ltd

# For information about this presentation, contact:

kessler.abraham@gmail.com

#### PURPOSE

To compare the performance of the Vancouver Risk Calculator (VRC) with ACR Lung-RADS for a lung cancer screening cohort in an urban, diverse clinical setting.

# METHOD AND MATERIALS

IRB approval was obtained. All lung cancer screening patients who had their initial screening CT from December 2012-June 2016 demonstrating a nodule comprised the study population. Each exam was assigned a Lung-RADS score, with 4A and 4B considered positive. The VRC calculates the risk of cancer at different thresholds using 9 patient and imaging variables, with a 5% threshold considered positive. Analysis was performed on a per-patient level based on the largest nodule. Follow-up information was obtained via EMR, cancer registry and NDI. Patients with initial studies suspicious for malignancy but without histologic confirmation were adjudicated on a case-by-case basis. Performance characteristics to predict lung cancer were compared for Lung-RADS and VRC.

#### RESULTS

486 patients, 261(53.7%) women, mean age  $63\pm5.2$ , comprised the study population. Mean follow-up time was  $36.9\pm11.1$  months, and 61(12.6%) patients were lost to follow-up. Lung cancer was diagnosed in 35(7.2%). Lung-RADS had 10 FP and 14 FN while VRC 5% had 30 FP and 8 FN. Overall sensitivity, specificity and accuracy for Lung-RADS was 61.1%, 97.8%, and 94.9% and for VRC 5% was 77.8%, 93.3%, and 92.2%, respectively.

# CONCLUSION

In comparison with Lung-RADS, the VRC demonstrated higher sensitivity but lower specificity and accuracy in predicting malignancy among patients in a diverse clinical lung cancer screening program.

# **CLINICAL RELEVANCE/APPLICATION**

LungRADS and VRC achieved complementary results in a diverse urban clinical lung cancer screening program. Use of the two, in concert, may improve lung cancer prediction.

# SSC03-09 Lung MRI as a Cost-Effective Alternative to Low-Dose CT Lung Cancer Screening: A Markov Cohort Analysis

Monday, Nov. 26 11:50AM - 12:00PM Room: E451A

Awards

#### **Student Travel Stipend Award**

Participants

Bradley D. Allen, MD, Chicago, IL (Presenter) Nothing to Disclose

Mark L. Schiebler, MD, Madison, WI (Abstract Co-Author) Stockholder, Stemina Biomarker Discovery, Inc; Stockholder, HealthMyne, Inc;

Gregor Sommer, Basel, Switzerland (Abstract Co-Author) Nothing to Disclose

Hans-Ulrich Kauczor, MD, Heidelberg, Germany (*Abstract Co-Author*) Research Grant, Siemens AG Research Grant, Bayer AG Speakers Bureau, Boehringer Ingelheim GmbH Speakers Bureau, Siemens AG Speakers Bureau, Koninklijke Philips NV Speakers Bureau, Bracco Group Speakers Bureau, AstraZeneca PLC

Juergen Biederer, MD, Heidelberg, Germany (Abstract Co-Author) Nothing to Disclose

Timothy J. Kruser, MD, Chicago, IL (Abstract Co-Author) Nothing to Disclose

James C. Carr, MD, Chicago, IL (*Abstract Co-Author*) Research Grant, Astellas Group; Research support, Siemens AG; Speaker, Siemens AG; Advisory Board, Guerbet SA

Gordon Hazen, PhD, Evanston, IL (Abstract Co-Author) Nothing to Disclose

# For information about this presentation, contact:

bdallen@northwestern.edu

# PURPOSE

The purpose of this study was to evaluate the potential performance of lung MRI (MRI) vs. low dose CT (LDCT) using a Markov model of lung cancer screening. We hypothesized that MRI would be a cost-effective alternative to LDCT.

# METHOD AND MATERIALS

We converted the MISCAN Lung microsimulation of lung cancer progression into a Markov cohort model with transition probabilities based on histology/stage. Our model uses published data to specify lung cancer incidence and background non-lung cancer mortality based on gender, age and smoking burden, and survival after diagnosis by gender, histology and stage. Published LDCT screening sensitivity (Sn) and specificity (Sp) by stage/histology was used to populate the LDCT model parameters. For MRI, the Sn and Sp were based on published data of solid nodules using size and T2 contrast-to-noise ratio. Our model follows a large cohort of age-60 males with 2 packs/day smoking history for 20 years. The time-0 composition of the cohort was a mixture of well and undiagnosed cancer patients from the model when run from age 42. At each annual screening, portions of the surviving cohort experience true/false, positive/negative outcomes with true positives moving to treatment. Costs for screening LDCT (\$256), work-

up, and treatment were extracted from CMS procedure cost data and the literature. Sensitivity analysis was performed on Sn/Sp of MRI and costs of MRI. Results of interest include life-years/patient (LYs), net monetary benefit (NMB), and cost-effectiveness (C/E) of MRI relative to LDCT.

## RESULTS

LYs for MRI screening were 13.28 vs. 13.29 for LDCT. Using an acceptable cost/LY of \$100,000, MRI resulted in a net-monetary benefit (NMB) of \$3,744 over LDCT. MRI saves \$2656/patient over LDCT, while losing only 3.97 life days, for a favorable C/E ratio of \$244,189/LY. Cost ranging from \$256 to \$375 result in a favorable C/E ratio for MRI.

### CONCLUSION

Based on this simulation, MRI provides an equivalent LY benefit with cost-savings over LDCT lung cancer screening at reasonable MRI costs. This finding is driven by improved specificity of MRI for solid nodule characterization.

## **CLINICAL RELEVANCE/APPLICATION**

Markov simulation of a high-risk screening cohort shows that Lung MRI has the potential to be a cost-effective alternative to lowdose CT screening.



## SSC04

**Emergency Radiology (Thoracic, Cardiac and Vascular)** 

Monday, Nov. 26 10:30AM - 12:00PM Room: S504AB



AMA PRA Category 1 Credits ™: 1.50 ARRT Category A+ Credit: 1.75

### **Participants**

Felipe Munera, MD, Key Biscayne, FL (*Moderator*) Nothing to Disclose Ferco H. Berger, MD, Toronto, ON (*Moderator*) Nothing to Disclose

## Sub-Events

# SSC04-01 Model-Based Iterative Reconstruction on 80kV CT Pulmonary Angiography: Image Quality and Radiation Dose Saving Compared with Hybrid Iterative Reconstruction on 100Kv CT Study

Monday, Nov. 26 10:30AM - 10:40AM Room: S504AB

Participants

Andrea De Vito, MD, Milano, Italy (*Presenter*) Nothing to Disclose Davide Ippolito, MD, Monza, Italy (*Abstract Co-Author*) Nothing to Disclose Cammillo R. Talei Franzesi, Milan, Italy (*Abstract Co-Author*) Nothing to Disclose Luca Riva, MD, Monza, Italy (*Abstract Co-Author*) Nothing to Disclose Silvia Girolama Drago, Monza, Italy (*Abstract Co-Author*) Nothing to Disclose Sandro Sironi, MD, Monza, Italy (*Abstract Co-Author*) Nothing to Disclose

## For information about this presentation, contact:

A.devito@campus.unimib.it

### PURPOSE

To evaluate dose reduction and image quality of 80 kV CT pulmonary angiography (CTPA) reconstructed with model-based iterative reconstruction (IMR), and compared with 100 kV CTPA with hybrid iterative reconstruction (iDose4).

### **METHOD AND MATERIALS**

One hundred and fifty-one patients were prospectively investigated for pulmonary embolism; a study group of 76 patients underwent low-kV setting (80kV,automated mAs) CTPA study, while a control group of 75 patients underwent standard CTPA protocol (100kV; automated mAs); all patients were examined on 256 MDCT scanner (Philips iCTelite). Study Group images were reconstructed using IMR while the Control Group ones with iDose4. CTDIvol, DLP and ED were evaluated. Region of interests placed in the main pulmonary vessels evaluated vascular enhancement (HU); signal-to-noise ratio (SNR) and contrast-to-noise ratio (CNR) were calculated.

### RESULTS

Compared to iDose4-CTPA, low kV IMR-CTPA presented lower CTDIvol ( $6.41 \pm 0.84 \text{ vs} 9.68 \pm 3.5 \text{ mGy}$ ) and DLP ( $248.24 \pm 3.2 \text{ vs} 352.4 \pm 3.59 \text{ mGy} \text{ x cm}$ ), with ED of  $3.48 \pm 1.2 \text{ vs} 4.93 \pm 1.8 \text{ mSv}$ . Moreover IMR-CTPA showed higher attenuation values ( $670.91 \pm 9.09 \text{ HU} \text{ vs} 292.61 \pm 15.5 \text{ HU}$ ) and a significantly higher SNR (p<0,0001) and CNR (p<0,0001). The subjective image quality of low kV IMR-CTPA was also higher compared with iDose4-CTPA (p<0,0001).

### CONCLUSION

Low dose CT with IMR represents a feasible protocol for the diagnosis of pulmonary embolism in the emergency setting and permits to achieve excellent diagnostic images (in terms of subjective quality) with extremely low noise, and a significant reduction of the dose led to the patient (in terms of mSv) within reasonable reconstruction times (less than 120 seconds).

### **CLINICAL RELEVANCE/APPLICATION**

Low kV IMR approach allows a significant dose reduction of CTPA studies improving attenuation values, SNR and CNR in the pulmonary vessels, as compared with standard kV iDose4-CTPA.

# SSC04-02 A Proposal of a New System Score to Evaluate With Lung Ultrasound the Necessity of a Drainage Tube in Pneumothorax in Emergency Room

Monday, Nov. 26 10:40AM - 10:50AM Room: S504AB

Participants

Maria Luisa De Cicco, MD, Roma, Italy (*Presenter*) Nothing to Disclose Vittorio Miele, MD, Florence, Italy (*Abstract Co-Author*) Nothing to Disclose Vincenza Di Giacomo, Rome, Italy (*Abstract Co-Author*) Nothing to Disclose Chiara Andreoli, MD, Rome, Italy (*Abstract Co-Author*) Nothing to Disclose Stefania Ianniello, MD, Rome, Italy (*Abstract Co-Author*) Nothing to Disclose

### For information about this presentation, contact:

## stefianni66@gmail.com

### PURPOSE

Aim of this study was to evaluate the validity of a new system score and its utility in the Emergency Room to estabilish the necessity to drainage pneumothorax diagnosed by ultrasound in unstable adults major trauma.

### **METHOD AND MATERIALS**

Retrospective observational study that involved, from January 2015 to January 2018, 274 adults patients with pneumothorax, evaluated by lung ultrasound in Emergency Room during Primary Survey. All ultrasound were performed with portable ultrasound machine in Emergency Room, with patients lying on the spinal board stretcher. It was applied a system score which included the evaluation of the lung point site (parasternal =1, emiclavear =2 or axillary line=3), the presence of pleural effusion (><300 ml=1 o 0) and the position of the heart (with o without dislocation=1 o 0). Cut off estabilished to indicate the necessity of the thorax drainage was 4. All patients underwent to MDCT (gold standard) and the results compared.

## RESULTS

Among the enrolled patients with pneumothorax 184/274 had a score > 4 and the necessity of a drainage was indicated on the report. Of these in 164 the necessity was confirmed by CT, while in 20 the patients were just observed. Among the 20 'false positive to need drainage' of our retrospective review, someone had a high BMI (8), someone had subcutaneous emphysema (5), while in the other or there was an overvaluation by the US evaluation or the patients conditions improved (7).

### CONCLUSION

Our data regarding the validity of a new system score should be useful in deciding the necessity of a draining tube in major trauma unstable patients. This score would allow an early diagnosis and a promptly therapeutic decision, avoiding wasting time, essential in patients with many traumatic lesions and above all with serious pneumothorax.

## **CLINICAL RELEVANCE/APPLICATION**

Identify an useful new scoring system, helpful to estabilish the necessity to drainage pneumothorax diagnosed by ultrasound, in unstable adults major trauma

## SSC04-03 Identifying Patients with Low Cardiac Output Using Vessel Density at CTPA

Monday, Nov. 26 10:50AM - 11:00AM Room: S504AB

### Awards

## **Student Travel Stipend Award**

### Participants

Andrew D. Chang, MSc, Providence, RI (*Presenter*) Nothing to Disclose Scott Collins, RT, Providence, RI (*Abstract Co-Author*) Nothing to Disclose Derek Merck, PhD, Providence, RI (*Abstract Co-Author*) Nothing to Disclose Grayson L. Baird, PhD, Providence, RI (*Abstract Co-Author*) Nothing to Disclose Michael K. Atalay, MD, PhD, Providence, RI (*Abstract Co-Author*) Nothing to Disclose

### For information about this presentation, contact:

atalay\_99@yahoo.com

### PURPOSE

Cardiac output (CO) is an important metric that has diagnostic and prognostic value in emergency and inpatient settings. However, determining CO currently requires invasive or costly procedures such as Swan-Ganz catheterization (SGC) or cardiac MR (CMR). CT for pulmonary angiography (CTPA) is a commonly performed examination that provides a snapshot of exogenously administered contrast as it distributes through the thoracic vasculature in a manner chiefly determined by CO. We hypothesized that by measuring attenuation in different vessels we could (1) identify patients with reduced CO and, potentially, (2) quantify CO.

### **METHOD AND MATERIALS**

We retrospectively identified patients who underwent SGC or CMR within 14 days of CTPA between 1/1/2006 to 12/30/2016. Using CO values from SGC or CMR as the gold standard, patients were stratified into three groups: CO < 4 L/min (low), 4-8 L/min (normal), and over 8 L/min (high). All CT studies were performed using a standardized protocol with a fixed delay of 22 sec and an injection rate of 4 cc/s. For each patient, density (HU) was measured in the superior vena cava [SVC], main pulmonary trunk [PT], and ascending aorta [AO] on a single mid-thoracic transaxial slice. Densities and density differences were then compared with measured vales of CO.

## RESULTS

We identified 119 patients with concurrent CO measurements and CTPA studies within the study period. Compared to patients with normal CO (n=76, 63.9%), patients with low CO (n=35, 29.4%) exhibited higher attenuation in the SVC (1305 $\pm$ 846 vs 944.4 $\pm$ 556.8 HU, p=0.026) and PT (518.4 $\pm$ 149.6 vs 385.3 $\pm$ 122.4 HU, p<0.001). Adjusting for body surface area, PT-AO difference predicts low CO (OR per unit increase 1.007, 95% CI 1.004-1.010, p<0.001). ROC analysis yielded a PT-AO difference threshold of 130 HU for differentiating low from normal CO, with sensitivity and specificity of 74.3% and 87.7% (AUC 0.776, p<0.001).

## CONCLUSION

This study provides a simple approach to estimate low CO status by measuring vessel density on a single transaxial CTPA image at the level of the mid-ascending aorta. We found that the greater the attenuation difference between the PT and AO, the greater the odds of low CO, with a difference of 130 HU serving as a useful threshold distinguishing low from normal CO.

### **CLINICAL RELEVANCE/APPLICATION**

Using a standardized CTPA protocol it may be possible to confidently identify patients with reduced cardiac output.

## SSC04-04 Multi Factorial Comparative Study of Dual Source CT Scanners in Acute Pulmonary Embolism

Monday, Nov. 26 11:00AM - 11:10AM Room: S504AB

Participants Waleed Abdellatif, MD, Vancouver, BC (*Presenter*) Nothing to Disclose Savvas Nicolaou, MD, Vancouver, BC (*Abstract Co-Author*) Institutional research agreement, Siemens AG Heiko Schmiedeskamp, PhD, Malvern, PA (*Abstract Co-Author*) Employee, Siemens AG Jennifer Powell, Vancouver, BC (*Abstract Co-Author*) Nothing to Disclose

# For information about this presentation, contact:

waleed.abdellatif@vch.ca

## PURPOSE

To compare mean acquisition time, image quality and diagnostic accuracy of two dual-energy CT scanners for the evaluation of acute pulmonary embolism (PE).

## **METHOD AND MATERIALS**

Total of 50 scans on the 2nd generation dual source SOMATOM Definition Flash CT scanner (the Flash) and 49 scans on the 3rd generation dual source SOMATOM Force (the Force) were included. Scans with inadequate opacification of pulmonary artery or known chronic PE were excluded. Imaging acquisition parameters were adjusted to be the same on both the Force and the Flash. In a randomized blinded design, two radiologists independently reviewed both sets of scans in two settings (3-week interval) for image quality using a 5-point scale. The interobserver reliability and diagnostic accuracy were calculated for each reviewer. Diagnosis of acute PE was made using clinical data (acute chest pain), laboratory data (D-Dimer > 500 ug/L) and CTPA.

## RESULTS

Mean acquisition time for the Force (x= 2.81 sec, SD= 0.1) and the Flash (x= 9.7 sec, SD = 0.15) was found to be very statistically significant (P= 0.0001; 95% CI = 6.8 - 6.9) with the Force 3.4 times faster than the Flash. The mean image quality was found to be 4.47/5 and 4/5 for the Force and the Flash respectively with statistical significance (P= 0.0064 on the unpaired t-test; 95% CI = 0.80-0.13). Interobserver reliability for image quality indicates strong agreement on both, the Force (K= 0.83, p <0.005) and the Flash-generated scans (k= 0.85, p < 0.005). Acute PE was diagnosed in 17 cases on the Force and in 21 cases on the Flash. Diagnostic accuracy was 94.1% and 98.2% on the Force and 90.2% and 94.8% on the Flash for reviewers one and two respectively. Although diagnostic accuracy was higher on the Force, the difference wasn't statistically significant. Study limitations includes retrospective design and Berkson's selection bias as the Force was routinely used for emergency patients while the Flash was used for inpatients.

### CONCLUSION

Image quality is significantly higher on the Force CT scanner with significantly lower mean acquisition time and less motion artifact in comparison to the Flash.

## **CLINICAL RELEVANCE/APPLICATION**

The improved image quality and speed of the Force CT scanner with resultant less motion artifact and repeated studies could be particularly useful in emergency radiology setting with large patient volume.

## SSC04-05 Axial or Helical? CT Imaging of the Chest for Uncooperative Emergency Patients with 16-cm Wide Detector CT

Monday, Nov. 26 11:10AM - 11:20AM Room: S504AB

Participants Yanan Li, Xian, China (*Presenter*) Nothing to Disclose Jianxin Guo, Xian, China (*Abstract Co-Author*) Nothing to Disclose Tingting Qu, Xian, China (*Abstract Co-Author*) Nothing to Disclose Ganglian Fan, Xian, China (*Abstract Co-Author*) Nothing to Disclose Meiyu Wang, Xian, China (*Abstract Co-Author*) Nothing to Disclose Yang Jian, PhD, MD, Xi An, China (*Abstract Co-Author*) Nothing to Disclose

### For information about this presentation, contact:

liyanan976@163.com

### PURPOSE

To compare image quality and radiation dose between the fast-helical mode (FHM) and two-axial mode (TAM) in chest CT imaging for uncooperative emergency patients with 16-cm wide detector CT scanner.

### **METHOD AND MATERIALS**

Thirty emergency patients who were unconscious or uncooperative with the breathing instructions underwent chest CT were prospectively divided randomly into two groups: FHM Group (n=15, helical scan mode with 80mm detector coverage and pitch 0.992:1), TAM Group (n=15, axial scan mode with 160mm detector coverage, two scans). Both groups used the 0.28s rotation speed and automatic tube current modulation. All scans were performed in free-breathing. CT value, image noise and signal-to-noise ratio (SNR) were measured at each of the following locations: descending thoracic aorta, lung parenchyma and paraspinal muscle at the level of the carina. Two radiologists assessed the images for subjective image quality, motion artefacts and diagnostic confidence. The volume CT dose index (CTDIvol) and dose-length product (DLP) were evaluated from the dose reports, and effective dose was calculated. All measurements between the two groups were statistically compared.

### RESULTS

The mean total exposure time was significantly shorter for TAM group than FHM group (0.56s vs.1.12s, P<0.001). Image quality was generally better with TAM than with FHM (diagnostic confidence score, 3.87 vs. 3.47, P<0.05); However, there was no

significant difference in CT value, image noise and SNR between two groups. The DLP value was higher in FHM than TAM (123.92 $\pm$ 38.54mGy·cm vs. 94.22 $\pm$ 33.63mGy·cm, P=0.041), while CTDIvol was not significantly different. TAM group reduced the total effective radiation dose by 24% compared to FHM (1.32 $\pm$ 0.50 mSv vs. 1.73 $\pm$ 0.54mSv).

## CONCLUSION

The use of the two-axial mode further reduces the scan time in chest CT for emergency patients and ensures good image quality with 24% radiation dose reduction, compared with chest CT that uses the fast-helical scan with 80mm collimation.

## CLINICAL RELEVANCE/APPLICATION

The two-axial scan mode can be used for lung evaluation in uncooperative emergency patients in free breathing to obtain satisfactory image quality while reducing radiation dose.

## SSC04-06 Utility of 3D Post-Processing Cinematic Rendering Reconstruction Images in Acute Trauma Setting: Initial Observations

Monday, Nov. 26 11:20AM - 11:30AM Room: S504AB

Participants

Sadia R. Qamar, MBBS, Vancouver, BC (*Presenter*) University of British Columbia Hasamaster Research Agreement with Siemens Medical Health Care

Savvas Nicolaou, MD, Vancouver, BC (*Abstract Co-Author*) Institutional research agreement, Siemens AG Gordon T. Andrews, MD, Vancouver, BC (*Abstract Co-Author*) Nothing to Disclose Heiko Schmiedeskamp, PhD, Malvern, PA (*Abstract Co-Author*) Employee, Siemens AG Parisa Khoshpouri, MD, Coquitlam, BC (*Abstract Co-Author*) Nothing to Disclose Vahid Mehrnoush, Vancouver, BC (*Abstract Co-Author*) Nothing to Disclose

### For information about this presentation, contact:

raashidsadia@gmail.com

## PURPOSE

Multiple post-processing reconstruction techniques based on volumetric CT datasets are used to generate three-dimensional (3D) images to better depict complex anatomical details. Volume rendering (VR) is frequently used as a standard 3D technique, however recently an FDA-approved alternative called Cinematic Rendering (CR) is emerging with vast clinical potentials (1,2). Contrary to traditional VR reconstruction, CR utilizes a global illumination model to create high definition photo-realistic images. We describe our initial experience with CR images in the setting of acute trauma.

## METHOD AND MATERIALS

A set of polytrauma patients with ISS score >16 with simple to complex injuries presenting to Vancouver General Hospital, level 1 trauma center were evaluated. Source DICOM images using a 2nd generation 128-slice dual-source CT (Somatom Definition Flash, Siemens Healthineers, Forchheim, Germany) were used to create CR images. Cinematic Rendering software (Siemens Syngo.via Frontier) was used applying default and customized presets. CR images were assessed for image quality, depth and shape perception, delineation of osseous, vascular, soft tissue and solid organ anatomy in comparison to VR images. The images were also evaluated for their role in clinical decision making and education. Multiple trauma surgeons assessed the images using Likert scale analysis with 1 being much lower, 3 equivocal, and 5 much higher. Frequencies, percentages, mean and standard deviation were calculated.

## RESULTS

CR images were rated higher than VR images with a mean+/- SD of 4.0+/-0.8. 67 % of trauma surgeons categorized CR images as much higher for use as an education tool and 61% graded them as higher in helping with clinical decision compared to VR images.

## CONCLUSION

Our observations are one of the very few initial studies to evaluate the clinical utility of CR images. Understanding complex and challenging anatomical and pathological details are imperative for better patient management from a trauma surgeon assessment. CR provides remarkable details relative to VR reconstructions in context of complex acute trauma

## **CLINICAL RELEVANCE/APPLICATION**

Cinematic Rendering is a promising novel technique to display visually receptive 3D photorealistic high definition images with exquisite anatomical details. Formal evaluations and research is needed to assess the CR images in order to understand their clinical application in patient management.

# SSC04-07 Improving Pulmonary Embolism Detectability for Computer-Aided Detection Software Using Optimal Kev Monochromatic Images in Dual-Energy Spectral CT

Monday, Nov. 26 11:30AM - 11:40AM Room: S504AB

Participants

Ma Guangming, MMed, Xianyang City, China (*Presenter*) Nothing to Disclose Nan Yu, MD, Xian Yang, China (*Abstract Co-Author*) Nothing to Disclose Shan Dang, Xian, China (*Abstract Co-Author*) Nothing to Disclose Jing Chen, Xianyang City, China (*Abstract Co-Author*) Nothing to Disclose Yanbing Guo, Xianyang, China (*Abstract Co-Author*) Nothing to Disclose Xirong Zhang, Xianyang, China (*Abstract Co-Author*) Nothing to Disclose Chenwang Jin, Xi'an, China (*Abstract Co-Author*) Nothing to Disclose

### PURPOSE

To compare pulmonary embolism detectability using computer-aided detection (CAD) software with optimal keV monochromatic images and conventional images.

## METHOD AND MATERIALS

Retrospectively analyzed CT images of 20 patients with clinically proven pulmonary embolism (PE). These patients underwent CT pulmonary angiography (CTPA) with spectral imaging mode. The conventional images (140kVp polychromatic, group A) were reconstructed. Using the standard Gemstone Spectral Imaging (GSI) viewer on an advanced workstation (AW4.6), an optimal energy level (group B) could be automatically obtained. The images in two group were independently analyzed for detecting PE using a commercially available CAD software. Two experienced radiologists reviewed all images and recorded the number of emboli, and the results were used as the gold standard. The attenuation in the main pulmonary artery (MPA) and the embolus (in the most substantial part of the embolus) were measured. The difference in attenuation (MPA-embolus), as well as the detectability for pulmonary embolism in each case (sensitivity, false positive rate) were calculated. Data were statistically compared between the two groups.

### RESULTS

The optimal energy levels were 62.4keV. The attenuation in the MPA, difference in attenuation (MPA-embolus) for group A and B were ( $314.46\pm81.41HU$  vs.  $446.30\pm151.88HU$ ) and ( $281.89\pm73.82HU$  vs.  $404.75\pm138.74HU$ ), respectively (all p<0.001). The mean sensitivity for pulmonary embolism detection in group A was 74.63 $\pm$ 6.16%, which was lower than the 82.17 $\pm$ 4.51% in group B (t=4.26, p<0.001). The mean false positive rate in group A was 32.71 $\pm$ 4.89%, which was higher than the 13.41 $\pm$ 3.02% in group B (t=13.41, p=0.00).

## CONCLUSION

Compared with conventional images, the combination of optimal keV monochromatic images and CAD improves the diagnostic accuracy of CAD.

# **CLINICAL RELEVANCE/APPLICATION**

The combination of optimal keV monochromatic images and CAD could improve the detection rate for emboli.

# SSC04-08 Implementation of Fully Automated Computer-Aided Detection of Nodules in The Lung Bases on Emergent Abdominal CT Scans: Accuracy and Effect on Workflow

Monday, Nov. 26 11:40AM - 11:50AM Room: S504AB

Participants

Amirhossein Mozafarykhamseh, MD, Chicago, IL (*Presenter*) Grant, Siemens AG Tugce Agirlar Trabzonlu, MD, Chicago, IL (*Abstract Co-Author*) Grant, Siemens AG Pamela J. Lombardi, MD, Chicago, IL (*Abstract Co-Author*) Nothing to Disclose Rishi Agrawal, MD, Chicago, IL (*Abstract Co-Author*) Speakers Bureau, Boehringer Ingelheim GmbH Vahid Yaghmai, MD, Chicago, IL (*Abstract Co-Author*) Nothing to Disclose

### PURPOSE

To assess the value of fully automated computer-aided diagnosis (CAD) for detection of lung nodules on emergent abdominal CT studies in.

## **METHOD AND MATERIALS**

Abdominal CT scans of 50 patients in the emergency department were reviewed. A radiologist with 5 years' experience (RAD) reviewed the scans to detect pulmonary nodules in the lung bases. In order to simulate the emergency setting, time limit of 30 seconds was set in each case for RAD to review image datasets. The CAD detection performance was also evaluated in the same session by RAD. CAD nodule detection was fully automated and required no additional processing time by RAD. Fisher's exact test and T-test were used to determine the differences between the rate of detection between RAD and CAD.

## RESULTS

A total number of 54 nodules were detected by RAD in 50 patients (28 male, mean $\pm$ SD age, 51.2 $\pm$ 17.6 years). Adding the CAD increased the rate of detection by 30% (1.47 vs. 1.13 nodule/scan, P<0.05). Moreover, there was no significant difference in the rate of missed nodules per scan between CAD and RAD (0.33 nodule /scan vs. 0.25 nodule/scan), respectively. 25 out of 74 nodules detected by CAD were false positives .

## CONCLUSION

Using fully automated CAD may significantly improve the performance of the radiologist in detecting nodules located in the lung bases on abdominal CT scans obtained in the emergency department.

## **CLINICAL RELEVANCE/APPLICATION**

The role of CAD as a second reader may improve detection of lung base nodules on emergency department abdominal CT scans.

## **Honored Educators**

Presenters or authors on this event have been recognized as RSNA Honored Educators for participating in multiple qualifying educational activities. Honored Educators are invested in furthering the profession of radiology by delivering high-quality educational content in their field of study. Learn how you can become an honored educator by visiting the website at: https://www.rsna.org/Honored-Educator-Award/ Vahid Yaghmai, MD - 2012 Honored EducatorVahid Yaghmai, MD - 2015 Honored Educator

## SSC04-09 Spectrum of Radiological Manifestations of Melioidosis, Association with Risk Factors, and Its Role in Prognostication of Clinical Outcome

Monday, Nov. 26 11:50AM - 12:00PM Room: S504AB

Participants

Leena Robinson Vimala, MD, Vellore, India (Presenter) Nothing to Disclose

PURPOSE

Melioidosis being a mimicker of its more common clinical counterpart tuberculosis, is often mismanaged. The primary objective is to describe the spectrum of radiological manifestations of melioidosis. Secondary objectives are to evaluate the association between the organ involvement, known risk factors, predisposing conditions and also to predict effect on clinical outcome.

## **METHOD AND MATERIALS**

Retrospective image analysis of all culture proven cases of Burkholderia pseudomallei, between January 2011 & October 2017 was done. Demographic data, clinical characteristics, risk factors and clinical outcome were anlaysed. Unfavourable clinical outcome considered were those patients with severe disease condition requiring ICU admission for administration of ionotropes, requirement of ventilation or death.

## RESULTS

194 patients (162 males) with median age of 45 years, were included. Among the risk factors, diabetes mellitus was most common (63%), followed by alcohol abuse (28%). Table 1 demonstrates the radiological manifestation of organ/ system involvement of melioidosis. Patients with diabetes were found to have increased incidence of liver, spleen, bone and soft tissue involvement (p<0.05). Significant association of diabetes with liver, spleen and bone and soft tissue involvement seen, having odds ratios 3.213 (95% CI:1.048 - 9.855;p=0.04), 3.478 (95% CI:1.728-7;p=<0.001)&2.668 (95% CI:1.232 - 5.778;p=<0.001) respectively. Statistical significant difference was identified in the melioidosis involvement of genitourinary tract between the positive and negative TB group. 25% of patients suffered unfavourable outcome. Mortality was 11%. Using univariate binary logistic regression analysis, lung involvement was found to have 4.3 times risk for unfavourable outcome (95% CI 1.971 - 9.496; p< 0.001), whereas spleen and lymph node involvement, protected from unfavourable outcome (odds ratio being 0.202 & 0.457 respectively).

## CONCLUSION

The constellation of imaging findings could mimic disseminated tuberculosis or other pyogenic infection. Combination of organ involvement, associated superficial soft tissue involvement are imaging diagnostic clues. Knowledge about the radiological manifestations of melioidosis is essential for accurate diagnosis and management.

# **CLINICAL RELEVANCE/APPLICATION**

Present study is the largest study that has illustrated the radiological manifestations of melioidosis and its association with clinical outcome and risk factors.



### SSC05

Science Session with Keynote: Gastrointestinal (LiRADS)

Monday, Nov. 26 10:30AM - 12:00PM Room: N228



AMA PRA Category 1 Credits ™: 1.50 ARRT Category A+ Credit: 1.75

### Participants

Claude B. Sirlin, MD, San Diego, CA (*Moderator*) Research Grant, Gilead Sciences, Inc; Research Grant, General Electric Company; Research Grant, Siemens AG; Research Grant, Bayer AG; Research Grant, ACR Innovation; Research Grant, Koninklijke Philips NV; Research Grant, Celgene Corporation; Consultant, General Electric Company; Consultant, Bayer AG; Consultant, Boehringer Ingelheim GmbH; Consultant, AMRA AB; Consultant, Fulcrum Therapeutics; Consultant, IBM Corporation; Consultant, Exact Sciences Corporation; Advisory Board, AMRA AB; Advisory Board, Guerbet SA; Advisory Board, VirtualScopics, Inc; Speakers Bureau, General Electric Company; Author, Medscape, LLC; Author, Resoundant, Inc; Lab service agreement, Gilead Sciences, Inc; Lab service agreement, ICON plc; Lab service agreement, Intercept Pharmaceuticals, Inc; Lab service agreement, Shire plc; Lab service agreement, Takeda Pharmaceutical Company Limited; Lab service agreement, sanofi-aventis Group; Lab service agreement, Johnson & Johnson; Lab service agreement, NuSirt Biopharma, Inc ; Contract, Epigenomics; Contract, Arterys Inc Shahid M. Hussain, MD,PhD, Omaha, NE (*Moderator*) Nothing to Disclose

### Sub-Events

# SSC05-01 Gastrointestinal Keynote Speaker: LiRADS

Monday, Nov. 26 10:30AM - 10:40AM Room: N228

Participants

Claude B. Sirlin, MD, San Diego, CA (*Presenter*) Research Grant, Gilead Sciences, Inc; Research Grant, General Electric Company; Research Grant, Siemens AG; Research Grant, Bayer AG; Research Grant, ACR Innovation; Research Grant, Koninklijke Philips NV; Research Grant, Celgene Corporation; Consultant, General Electric Company; Consultant, Bayer AG; Consultant, Boehringer Ingelheim GmbH; Consultant, AMRA AB; Consultant, Fulcrum Therapeutics; Consultant, IBM Corporation; Consultant, Exact Sciences Corporation; Advisory Board, AMRA AB; Advisory Board, Guerbet SA; Advisory Board, VirtualScopics, Inc; Speakers Bureau, General Electric Company; Author, Medscape, LLC; Author, Resoundant, Inc; Lab service agreement, Gilead Sciences, Inc; Lab service agreement, ICON plc; Lab service agreement, Intercept Pharmaceuticals, Inc; Lab service agreement, Shire plc; Lab service agreement, Takeda Pharmaceutical Company Limited; Lab service agreement, sanofi-aventis Group; Lab service agreement, Johnson & Johnson; Lab service agreement, NuSirt Biopharma, Inc; Contract, Epigenomics; Contract, Arterys Inc

# SSC05-02 ACR Ultrasound LI-RADS: Multicenter Evaluation of Clinical Performance in HCC Screening and Surveillance

Monday, Nov. 26 10:40AM - 10:50AM Room: N228

### Awards

**Student Travel Stipend Award** 

Participants

John D. Millet, MD, Ann Arbor, MI (*Presenter*) Nothing to Disclose Katherine E. Maturen, MD, Ann Arbor, MI (*Abstract Co-Author*) Royalties, Reed Elsevier; Royalties, Wolters Kluwer nv; Consultant, Allena Pharmaceuticals, Inc; Hailey Choi, MD, San Francisco, CA (*Abstract Co-Author*) Nothing to Disclose Nirvikar Dahiya, MD, Phoenix, AZ (*Abstract Co-Author*) Nothing to Disclose

Nirvikal Daniya, MD, Phoenix, AZ (Abstract Co-Author) Nothing to Disclose Laura Parra, MD,MPH, Phoenix, AZ (Abstract Co-Author) Nothing to Disclose Paul M. Murphy II, MD, PhD, San Diego, CA (Abstract Co-Author) Nothing to Disclose Mujtaba Z. Naveed, MD, Philadelphia, PA (Abstract Co-Author) Nothing to Disclose Mary K. O'Boyle, MD, La Jolla, CA (Abstract Co-Author) Nothing to Disclose Marcelina G. Perez, MD, Menlo Park, CA (Abstract Co-Author) Nothing to Disclose Shuchi K. Rodgers, MD, Philadelphia, PA (Abstract Co-Author) Nothing to Disclose Ashish P. Wasnik, MD, Ann Arbor, MI (Abstract Co-Author) Nothing to Disclose Aya Kamaya, MD, Stanford, CA (Abstract Co-Author) Nothing to Disclose

### PURPOSE

To evaluate the clinical performance of the ACR Ultrasound Liver Reporting and Data System (US LI-RADS) Version 2017 for detecting hepatocellular carcinoma (HCC) in a population of patients at high risk for HCC.

## **METHOD AND MATERIALS**

In this retrospective, multicenter, HIPAA-compliant, IRB-approved study, patients at 5 sites had undergone screening liver ultrasound from Jan-Sep 2017 and US LI-RADS visualization scores and management categories were assigned on a clinical basis. Ultrasound reports and patient records were then retrospectively reviewed and any follow-up imaging studies and/or pathologic reports recorded. Descriptive statistics were performed.

### RESULTS

2050 patients at high risk for HCC (1078 men and 972 women; mean age 57.7 years) were included. The most common indications were cirrhosis (n=1054; 51.3%), non-cirrhotic HBV (n=555; 27.1%), and non-cirrhotic HCV (n=234; 11.4%). Among patients with cirrhosis, the most common etiologies were HCV (n=396; 19.4%), alcohol (n=194; 9.5%), and HBV (n=187; 9.2%). US LI-RADS scores had been assigned by 69 different readers with mean 19.3 years experience post-residency. US LI-RADS categories were: US-1 (Negative) in 90.4% (n=1854): US-2 (Subthreshold) in 4.6% (n=95); and US-3 (Positive) in 4.9% (n=101). Visualization scores were: A (No or minimal limitations) in 76.8% (n=1575); B (Moderate limitations) in 18.9% (n=388); and C (Severe limitations) in 4.2% (n=87). Confirmatory tests including contrast enhanced CT/MR (n=212) or histopathology (n=9) were available for 221 patients. Treating US-2 and US-3 as positive test results and LR-3, LR-4, LR-5, or LR-M imaging observations at CT/MR or tissue diagnosis of HCC as positive clinical outcomes, the sensitivity of US LI-RADS was 77.5%, specificity 58.9%, PPV 40.2%, and NPV 88.1%.

## CONCLUSION

US LI-RADS visualization scores in over 2000 patients demonstrated >95% of US screening exams were diagnostically acceptable. Approximately 90% of exams were interpreted as negative, 5% subthreshold, and 5% positive. In the subset of patients with confirmatory testing, US LI-RADS exhibited moderately high sensitivity (77.5%) and NPV (88.1%), key characteristics of a screening test.

## **CLINICAL RELEVANCE/APPLICATION**

During the first year after its release, ACR US LI-RADS was adopted into clinical practice and demonstrated promising clinical performance for HCC screening in multiple academic medical centers.

## **Honored Educators**

Presenters or authors on this event have been recognized as RSNA Honored Educators for participating in multiple qualifying educational activities. Honored Educators are invested in furthering the profession of radiology by delivering high-quality educational content in their field of study. Learn how you can become an honored educator by visiting the website at: https://www.rsna.org/Honored-Educator-Award/ Katherine E. Maturen, MD - 2014 Honored Educator

# SSC05-03 Classification of Primary Liver Cancers in Cirrhosis Using LI-RADS on Gadoxetic Acid-Enhanced MRI and Its Prognostic Implication

Monday, Nov. 26 10:50AM - 11:00AM Room: N228

Participants

Sang Hyun Choi, Seoul, Korea, Republic Of (*Presenter*) Nothing to Disclose Seung Soo Lee, MD, Seoul, Korea, Republic Of (*Abstract Co-Author*) Nothing to Disclose So Hyun Park, MD, Incheon, Korea, Republic Of (*Abstract Co-Author*) Nothing to Disclose Kang Mo Kim, Seoul, Korea, Republic Of (*Abstract Co-Author*) Nothing to Disclose Eun Sil Yu, MD, Seoul, Korea, Republic Of (*Abstract Co-Author*) Nothing to Disclose Yangsoon Park, Seoul, Korea, Republic Of (*Abstract Co-Author*) Nothing to Disclose Yong Moon Shin, Seoul, Korea, Republic Of (*Abstract Co-Author*) Nothing to Disclose Moon-Gyu Lee, MD, Seoul, Korea, Republic Of (*Abstract Co-Author*) Nothing to Disclose

## PURPOSE

This study aimed to evaluate the performance of the Liver Imaging Reporting and Data System (LI-RADS) v2017 in differentiating hepatocellular carcinoma (HCC) from intrahepatic cholangiocarcinoma (IHCC) and combined hepatocellular-cholangiocarcinoma (cHCC-CC) on gadoxetic acid-enhanced magnetic resonance imaging (MRI), and to determine its postsurgical prognostic implications.

### **METHOD AND MATERIALS**

Our institutional review board approved this study and waived the requirement for informed consent. A total of 194 patients with single primary liver cancers surgically resected (53 cHCC-CCs, 44 IHCCs, and 97 HCCs) from cirrhotic livers were evaluated on gadoxetic acid-enhanced MRI. Two independent readers analyzed each nodule and assigned a LI-RADS category. Overall survival (OS), recurrence-free survival (RFS), and their associated factors were evaluated using the Kaplan-Meier method, the log-rank test, and the Cox proportional hazard model.

### RESULTS

The sensitivity and specificity of the LR-5 category for diagnosis of HCC were 76.3% (74/97) and 84.5% (82/97), respectively; most (86.7%) false-positive diagnoses were misclassification of cHCC-CCs. In the multivariate analysis, the LI-RADS category was a significant independent factor for OS (HR=3.88; p<0.001) and RFS (HR=2.26; p=0.010). The LR-M category was associated with poorer OS and RFS than the LR-4 or LR-5 categories for all primary liver cancers (p<0.001, both), HCCs (p=0.012 and p=0.009, respectively), and cHCC-CCs (p<0.001 and p=0.002, respectively). The OS and RFS of the cHCC-CCs categorized as LR-4 or LR-5 did not significantly differ from those of HCCs (p=0.535 and p=0.074, respectively).

### CONCLUSION

LI-RADS correctly classifies most HCCs and IHCCs, whereas differentiation of cHCC-CC from HCC presents a challenge. The LI-RADS category may predict the postsurgical prognosis of primary liver cancers, independent of the pathologic diagnosis.

## **CLINICAL RELEVANCE/APPLICATION**

The LI-RADS v2017 guidelines correctly classify most HCCs and IHCCs, whereas differentiation of cHCC-CC from HCC is challenging, reducing the specificity of LI-RADS in the diagnosis of HCC. The LI-RADS category allows prediction of the postsurgical prognosis of primary liver cancers, independent of the pathologic diagnosis of the tumor.

## SSC05-04 Liver Imaging Reporting and Data System: Frequency of Category Adjustment Using Ancillary Features on CT and MRI in Clinical Practice

### Participants

# Jesse Berman, MD, Bronx, NY (Presenter) Nothing to Disclose

Claude B. Sirlin, MD, San Diego, CA (*Abstract Co-Author*) Research Grant, Gilead Sciences, Inc; Research Grant, General Electric Company; Research Grant, Siemens AG; Research Grant, Bayer AG; Research Grant, ACR Innovation; Research Grant, Koninklijke Philips NV; Research Grant, Celgene Corporation; Consultant, General Electric Company; Consultant, Bayer AG; Consultant, Boehringer Ingelheim GmbH; Consultant, AMRA AB; Consultant, Fulcrum Therapeutics; Consultant, IBM Corporation; Consultant, Exact Sciences Corporation; Advisory Board, AMRA AB; Advisory Board, Guerbet SA; Advisory Board, VirtualScopics, Inc; Speakers Bureau, General Electric Company; Author, Medscape, LLC; Author, Resoundant, Inc; Lab service agreement, Gilead Sciences, Inc; Lab service agreement, ICON plc; Lab service agreement, Intercept Pharmaceuticals, Inc; Lab service agreement, Shire plc; Lab service agreement, Takeda Pharmaceutical Company Limited; Lab service agreement, sanofi-aventis Group; Lab service agreement, Johnson & Johnson; Lab service agreement, NuSirt Biopharma, Inc; Contract, Epigenomics; Contract, Arterys Inc Victoria Chernyak, MD,MS, Bronx, NY (*Abstract Co-Author*) Nothing to Disclose

For information about this presentation, contact:

vichka17@hotmail.com

# PURPOSE

The Liver Imaging Reporting and Data System (LI-RADS, LR) uses ancillary features (AFs) to adjust the category code assigned by major features (MFs). This study assessed the frequency with which AFs are used to adjust category on CT and MRI in clinical practice.

## METHOD AND MATERIALS

All MR and CT reports issued with a standardized LI-RADS template at one tertiary care center between 3/16-3/18 were identified. For each reported LR-3, LR-4, and LR-5 observation, the presence of every MF and every AF was extracted retrospectively from the clinical report. LI-RADS categories then were assigned using the v2017 LI-RADS algorithm based on the reported MFs and AFs and following the v2017 instructions: increase category by one and up to LR-4 for >=1 AF favoring malignancy (AF-M), decrease by one with >=1 AF favoring benignity (AF-B), and no change with >=1 AF-M and >=1 AF-B. Results were summarized descriptively.

## RESULTS

314 patients (209 [66%] male, mean age 65 [ $\pm$ 10] years) were identified. They had a total of 548 observations (median size 13mm, IQR 9-20mm) including 441 (median size 13mm, IQR 9-20mm) reported on MRI and 107 (median size 15mm, IQR 10-22mm) reported on CT. Without applying AFs, 42% (232/548) of all observations were categorized LR-3, 29% (161/548) LR-4, and 28% (155/548) LR-5; 45% (198/441) of MRI observations were categorized LR-3, 28% (124/441) LR-4, and 27% (119/441) LR-5; 32% (34/107) of CT observations were categorized LR-3, 28% (36/107) LR-5. Application of AFs caused the LI-RADS category to be increased in 24% (127/524) and decreased in 4% (24/524) of all observations, increased in 28% (123/441) and decreased in 5% (22/441) of MR observation, and increased in 4% (4/107) and decreased in 2% (2/107) of CT observations. In particular, AFs caused 55% (127/232) of LR-3 observations overall, 62% (123/198) of LR-3 MRI observations, and 12% (4/34) of LR-3 CT observations to be upgraded to LR-4.

## CONCLUSION

Ancillary features can cause category adjustment in a substantial proportion of LI-RADS observations. Adjustments tend to upward, are more common in MRI than CT, and predominantly affect observations categorized LR-3 based on major features.

### **CLINICAL RELEVANCE/APPLICATION**

Ancillary features cause a substantial proportion of LR-3 observations to be upgraded to LR-4 , which is likely to affect management.

# SSC05-05 Deep Convolutional Neural Network Applied to the Liver Imaging Reporting and Data System (LI-RADS) Category Classification: A Pilot Study

Monday, Nov. 26 11:10AM - 11:20AM Room: N228

### Awards

### **Student Travel Stipend Award**

Participants

Rikiya Yamashita, MD, PhD, New York, NY (Presenter) Nothing to Disclose

Kathryn J. Fowler, MD, San Diego, CA (Abstract Co-Author) Nothing to Disclose

Cynthia S. Santillan, MD, San Diego, CA (Abstract Co-Author) Consultant, Robarts Clinical Trials, Inc

Laura P. Coombs, PhD, Reston, VA (Abstract Co-Author) Nothing to Disclose

Donald G. Mitchell, MD, Philadelphia, PA (Abstract Co-Author) Consultant, CMC Contrast AB

Mustafa R. Bashir, MD, Cary, NC (*Abstract Co-Author*) Research Grant, Siemens AG; Research Grant, General Electric Company; Research Grant, NGM Biopharmaceuticals, Inc; Research Grant, TaiwanJ Pharmaceuticals Co, Ltd; Research Grant, Madrigal Pharmaceuticals, Inc; Research Consultant, RadMD

Claude B. Sirlin, MD, San Diego, CA (*Abstract Co-Author*) Research Grant, Gilead Sciences, Inc; Research Grant, General Electric Company; Research Grant, Siemens AG; Research Grant, Bayer AG; Research Grant, ACR Innovation; Research Grant, Koninklijke Philips NV; Research Grant, Celgene Corporation; Consultant, General Electric Company; Consultant, Bayer AG; Consultant, Boehringer Ingelheim GmbH; Consultant, AMRA AB; Consultant, Fulcrum Therapeutics; Consultant, IBM Corporation; Consultant, Exact Sciences Corporation; Advisory Board, AMRA AB; Advisory Board, Guerbet SA; Advisory Board, VirtualScopics, Inc; Speakers Bureau, General Electric Company; Author, Medscape, LLC; Author, Resoundant, Inc; Lab service agreement, Gilead Sciences, Inc; Lab service agreement, ICON plc; Lab service agreement, Intercept Pharmaceuticals, Inc; Lab service agreement, Shire plc; Lab service agreement, Enanta; Lab service agreement, Virtualscopics, Inc; Lab service agreement, Alexion Pharmaceuticals, Inc; Lab service agreement, Takeda Pharmaceutical Company Limited; Lab service agreement, sanofi-aventis Group; Lab service agreement, Johnson & Johnson; Lab service agreement, NuSirt Biopharma, Inc; Contract, Epigenomics; Contract, Arterys Inc Richard Kinh Gian Do, MD, PhD, New York, NY (*Abstract Co-Author*) Consultant, Bayer AG

## For information about this presentation, contact:

### PURPOSE

To explore the performance of deep convolutional neural networks (CNN) for determining Liver Imaging Reporting and Data System (LI-RADS) category on multiphase dynamic contrast-enhanced CT and MRI.

## **METHOD AND MATERIALS**

This study used a de-identified HIPAA-compliant dataset comprised of multiphase contrast-enhanced images for 329 unique hepatic observations (168 on CT and 161 on MRI) in JPEG format with corresponding diameters and consensus categories assigned by 2 members of the LI-RADS Steering Committee using LI-RADS v2013. A radiologist manually cropped the observations, including a margin of peri-observation parenchyma. Two CNNs were applied: 1) custom-made un-pretrained CNNs with quadruple-phase images (pre, arterial, portal venous, and delayed phases), and 2) transfer learning with pretrained networks with triple-phase images (pre, arterial and delayed phases). Each method used on-the-fly data augmentation technique. Lesion diameters were included, processed through a fully-connected neural network, and concatenated with the CNN models. The dataset was randomly split into training, validation, and test set at a ratio of 70: 15: 15. Accuracy and the area under receiver operating characteristic curve (AUROC) for classifying categories LR-1/2/3 versus LR-4/5/M were calculated on the test set.

## RESULTS

Of 329 observations, 150 were LR-1/2/3 and 179 were LR-4/5/M; 229, 50, 50 observations were assigned to the training, validation, and test sets, respectively. Accuracy and the AUROC for the test set was 82% and 0.90 for transfer learning method, and 82% and 0.85 for custom-made method.

## CONCLUSION

Deep learning CNN models show promise for categorizing hepatic observations according to LI-RADS on multiphase dynamic contrast-enhanced CT and MRI.

## **CLINICAL RELEVANCE/APPLICATION**

Deep learning convolutional neural network models may provide a future platform for augmenting radiologists' interpretation of hepatic observations.

# SSC05-06 Validation of Ultrasound Liver Imaging Reporting and Data System Version 2017 in Patients at High Risk for Hepatocellular Carcinoma

Monday, Nov. 26 11:20AM - 11:30AM Room: N228

Participants

Jung Hee Son, MD, Seoul, Korea, Republic Of (*Presenter*) Nothing to Disclose Sang Hyun Choi, Seoul, Korea, Republic Of (*Abstract Co-Author*) Nothing to Disclose So Yeon Kim, MD, Seoul, Korea, Republic Of (*Abstract Co-Author*) Nothing to Disclose Jae Ho Byun, MD, Seoul, Korea, Republic Of (*Abstract Co-Author*) Nothing to Disclose Hyung Jin Won, MD, Seoul, Korea, Republic Of (*Abstract Co-Author*) Nothing to Disclose So Jung Lee, Seoul, Korea, Republic Of (*Abstract Co-Author*) Nothing to Disclose Young-Suk Lim, Seoul, Korea, Republic Of (*Abstract Co-Author*) Nothing to Disclose Moon-Gyu Lee, MD, Seoul, Korea, Republic Of (*Abstract Co-Author*) Nothing to Disclose

## PURPOSE

To evaluate diagnostic performance of the Ultrasound Liver Imaging Reporting and Data System version 2017 (US LI-RADS v2017) for diagnosing hepatocellular carcinoma (HCC) in high risk patients with liver cirrhosis and to investigate association between US visualization score and US category.

## METHOD AND MATERIALS

This study was approved by the institutional review board of our institution. A prospective surveillance study cohort included 407 cirrhosis patients at high risk for HCC who underwent US between December 2011 and March 2013. US LI-RADS category (1, 2, or 3) and US visualization score (A, B, or C) were assigned. The sensitivity and specificity for diagnosing HCC were calculated on the basis of per-patient and per-lesion, respectively, using contrast-enhanced CT, gadoxetic acid-enhanced MRI, and pathology as reference standards. The association between US visualization score and US category was evaluated using chi-squared test.

### RESULTS

Of the 429 nodule in 407 patients, 32 nodules were confirmed as HCC in 28 patients. The sensitivity and specificity of US category 3 for diagnosing HCC on per-patient analysis were 34.4% (95% confidence interval [CI], 20.3-51.8%) and 92.2% (95% CI, 89.1-94.5%), respectively, and those on per-lesion analysis were 39.3% (95% confidence interval [CI], 25.7-54.8%) and 92.9% (95% CI, 89.8-95.1%), respectively. US visualization score was significantly associated with US category (p = 0.04), i.e., 11.9% (5/42) US category 3 showed score C, whereas 29.1% (111/381) US category 1 showed score C.

## CONCLUSION

US LI-RADS v2017 category 3 demonstrated a high specificity, but a low sensitivity for diagnosing HCC in the surveillance of patients at high risk for HCC. US category assignment was significantly associated with US visualization score.

## **CLINICAL RELEVANCE/APPLICATION**

The low sensitivity of US LI-RADS category 3 might be a limitation for the diagnosis of HCC in high risk patients, and it is related to the poor US visualization score.

# ssc05-07 Accuracy of the LI-RADS v2017 Treatment Response Algorithm for Treated HCC

Monday, Nov. 26 11:30AM - 11:40AM Room: N228

Awards

## **Student Travel Stipend Award**

Participants Erin Shropshire, MD, Durham, NC (*Presenter*) Nothing to Disclose Mohammad Chaudhry, MBBS, Durham, NC (*Abstract Co-Author*) Nothing to Disclose Erol Bozdogan, MD, Sanliurfa, Turkey (*Abstract Co-Author*) Nothing to Disclose Diana Cardona, Durham, NC (*Abstract Co-Author*) Nothing to Disclose Lindsay King, MD, Durham, NC (*Abstract Co-Author*) Nothing to Disclose Gemini L. Janas, RT, Durham, NC (*Abstract Co-Author*) Nothing to Disclose Richard Kinh Gian Do, MD, PhD, New York, NY (*Abstract Co-Author*) Consultant, Bayer AG Charles Y. Kim, MD, Durham, NC (*Abstract Co-Author*) Consultant, Merit Medical Systems, Inc; Consultant, Cook Group Incorporated James S. Ronald, MD, PhD, Durham, NC (*Abstract Co-Author*) Nothing to Disclose Mustafa R. Bashir, MD, Cary, NC (*Abstract Co-Author*) Research Grant, Siemens AG; Research Grant, General Electric Company; Research Grant, NGM Biopharmaceuticals, Inc; Research Grant, TaiwanJ Pharmaceuticals Co, Ltd; Research Grant, Madrigal Pharmaceuticals, Inc; Research Consultant, RadMD

### For information about this presentation, contact:

erin.shropshire@duke.edu

### PURPOSE

To evaluate the accuracy of the LI-RADS v2017 Treatment Response algorithm for assessing viability of potential hepatocellular carcinomas that have been treated with transarterial embolization.

# METHOD AND MATERIALS

This retrospective study was approved by the Institutional Review Board and was HIPAA compliant. The requirement for informed consent was waived. Histopathology reports and imaging studies of patients who had undergone transarterial tumor embolization and subsequent liver transplantation between 2006 and 2016 were reviewed. Three radiologists independently evaluated each patient's pre- and post-embolization imaging and assessed all lesions using the LI-RADS v2017 CT/MRI (pre-embolization) and Treatment Response (LR-TR, post-embolization) algorithms, and inter-reader agreement was calculated using Fleiss' Kappa. Radiology and histopathology reports were then correlated. Lesions were categorized based on histopathologic necrosis as either completely (100%) or incompletely (<=99%) necrotic, and performance characteristics for the LR-TR viable and nonviable categories were calculated for each reader.

### RESULTS

45 patients with 64 histopathologically proven lesions were reviewed. Interreader agreement for pre-embolization category was moderate (k=0.57, 95% CI=0.45-0.71) and similar to agreement for LR-TR category (k=0.56, 95% CI=0.42-0.66). For predicting complete tumor necrosis, accuracy was moderate (0.66-0.70) and negative predictive value was very good (0.81-0.87). For predicting incomplete tumor necrosis, accuracy was moderate (0.59-0.64), and positive predictive value was very good (0.86-0.96). By consensus, 27% (17/64) of lesions were rated as LR-TR equivocal; 12 of these were incompletely necrotic.

## **CLINICAL RELEVANCE/APPLICATION**

There are currently no published data that evaluate the performance of the LI-RADS Treatment Response Algorithm for predicting degree of locoregional therapy induced necrosis in individual lesions.

# SSC05-08 Distinguishing Intrahepatic Cholangiocarcinoma from Hepatocelluar Carcinoma in Patients with and without Risks: The Evaluation of the LR-M Criteria of Contrast-Enhanced Ultrasound Liver Imaging Reporting and Data System Version 2017

Monday, Nov. 26 11:40AM - 11:50AM Room: N228

Participants

Fei Li, MD, Guangzhou, China (*Presenter*) Nothing to Disclose Jianwei Wang, Guangzhou, China (*Abstract Co-Author*) Nothing to Disclose Yini Huang, MD, Guangzhou, China (*Abstract Co-Author*) Nothing to Disclose Jing Han, MD, Guangzhou, China (*Abstract Co-Author*) Nothing to Disclose Wei Zheng, MD, Guangzhou, China (*Abstract Co-Author*) Nothing to Disclose Xueyi Zheng, Guangzhou, China (*Abstract Co-Author*) Nothing to Disclose Yun Wang, Guangzhou, China (*Abstract Co-Author*) Nothing to Disclose Jianhua Zhou, MD, Guangzhou, China (*Abstract Co-Author*) Nothing to Disclose

### For information about this presentation, contact:

lifei@sysucc.org.cn

## PURPOSE

To assess the diagnostic performance of the LR-M criteria of Contrast-Enhanced Ultrasound Liver Imaging Reporting and Data System version 2017 (CEUS-LIRADS v2017) for differentiating intrahepatic cholangiocarcinoma (ICC) from hepatocellular carcinoma (HCC) in patients with and without risks (i.e. cirrhosis or chronic hepatitis).

## METHOD AND MATERIALS

54 ICC in patients with risks and 55 ICC in patients without risks, and matched control cases of HCC with and without risks (n=59 and n=55, respectively) were enrolled. The wash-in-washout patterns of ICC and HCC lesions on CEUS were retrospectively analyzed according to the LR-M criteria of CEUS-LIRADS v2017. The diagnostic performances were assessed by receiver operating characteristic (ROC) curve analysis.

### RESULTS

Peripheral rim-like hyper-enhancement, early washout (<= 30 or 60seconds), marked washout did not differ between ICCs with and without risks, while all of these features were more common in ICCs than in HCCs (P < 0.05) no matter the risk factors. Using the LR-M criteria of CEUS-LIRADS v2017 to differentiate ICC from HCC, the area under the ROC curve (AUC), sensitivity, specificity and accuracy were 0.92, 97.25%, 87.72% and 92.38%, respectively. If onset of early washout were adjusted to <= 30 seconds and onset of marked washout were adjusted to <= 4 minutes, the specificity was significantly increased to 95.61% (P = 0.021), while the AUC, sensitivity and accuracy didn't significantly change (P > 0.05). The rate of HCCs misdiagnosed as ICCs would decrease from 12.3% to 5.3%.

## CONCLUSION

The LR-M criteria of CEUS-LIRADS v2017 showed feasibility in distinguishing ICCs from HCCs in patients with and without risks. After adjustment, specificity was significantly increased.

## **CLINICAL RELEVANCE/APPLICATION**

The LR-M criteria of CEUS-LIRADS v2017 could not only be used for distinguishing ICCs from HCC in patients with risk but also without risks. Adjustment of current criteria could reduce the rate of HCC being misdiagnosed as ICC.

# SSC05-09 ACR Ultrasound LI-RADS: Clinical Predictors of Diagnostic Adequacy for HCC Screening

Monday, Nov. 26 11:50AM - 12:00PM Room: N228

Participants

Marcelina G. Perez, MD, Menlo Park, CA (*Abstract Co-Author*) Nothing to Disclose Aya Kamaya, MD, Stanford, CA (*Abstract Co-Author*) Nothing to Disclose Hailey Choi, MD, San Francisco, CA (*Presenter*) Nothing to Disclose Nirvikar Dahiya, MD, Phoenix, AZ (*Abstract Co-Author*) Nothing to Disclose Laura Parra, MD,MPH, Phoenix, AZ (*Abstract Co-Author*) Nothing to Disclose John D. Millet, MD, Ann Arbor, MI (*Abstract Co-Author*) Nothing to Disclose Paul M. Murphy II, MD, PhD, San Diego, CA (*Abstract Co-Author*) Nothing to Disclose Mujtaba Z. Naveed, MD, Philadelphia, PA (*Abstract Co-Author*) Nothing to Disclose Shuchi K. Rodgers, MD, Philadelphia, PA (*Abstract Co-Author*) Nothing to Disclose Shuchi K. Rodgers, MD, Ann Arbor, MI (*Abstract Co-Author*) Nothing to Disclose Katherine E. Maturen, MD, Ann Arbor, MI (*Abstract Co-Author*) Nothing to Disclose Katherine E. Maturen, MD, Ann Arbor, MI (*Abstract Co-Author*) Nothing to Disclose

## For information about this presentation, contact:

kmaturen@umich.edu

### PURPOSE

Sonographic screening for hepatocellular carcinoma (HCC) may be limited by parenchymal heterogeneity and other factors. ACR Ultrasound Liver Reporting and Data System (US LI-RADS) Version 2017 uses visualization scores to reflect these limitations. The purpose of this study is to evaluate distribution and predictors of visualization scores.

## METHOD AND MATERIALS

In this retrospective, multicenter, HIPAA-compliant, IRB-approved study, patients at 5 sites had undergone screening US from Jan-Sep 2017 and US LI-RADS visualization scores were assigned on a clinical basis. Ultrasound reports and patient records were retrospectively reviewed.

## RESULTS

2050 patients at risk for HCC (1078 men and 972 women; mean age 57.7) were included. Most common indications were cirrhosis (n=1054; 51.3%), non-cirrhotic HBV (n=555; 27.1%), and non-cirrhotic HCV (n=234; 11.4%). Most common etiologies of cirrhosis were HCV (n=396; 19.4%), alcohol (n=194; 9.5%), and HBV (n=187; 9.2%). 10.3% (n=212) patients had ascites. US LI-RADS scores had been assigned by 69 different readers. 42.7% of studies were read by women and 57.3% by men, with mean 19.3 years of experience and 40.3% of clinical time on US. Visualization scores were: A (No or minimal limitations) in 76.8% (n=1575); B (Moderate limitations) in 18.9% (n=388); and C (Severe limitations) in 4.2% (n=87). Reader experience (p=.37) and clinical time on US (p=.76) were not associated with impaired visualization scores in univariate analysis. In multivariate logistic regression analysis, the clinical diagnosis of cirrhosis (OR 3.6), NASH as etiology of cirrhosis (OR 2.0), ascites (OR 1.4), and male radiologist gender (OR 1.5) were associated with moderate or severe limitations.

## CONCLUSION

US LI-RADS visualization scores in over 2000 patients demonstrated <5% of exams were severely limited and <20% were moderately limited. Clinical diagnosis of cirrhosis and NASH as etiology of cirrhosis were the strongest independent predictors of moderate to severe limitations in visualization in multivariate analysis.

# **CLINICAL RELEVANCE/APPLICATION**

Although most US screening exams for HCC are diagnostically adequate, clinical diagnosis of cirrhosis and NASH as etiology of cirrhosis are associated with limited visualization.

## **Honored Educators**

Presenters or authors on this event have been recognized as RSNA Honored Educators for participating in multiple qualifying educational activities. Honored Educators are invested in furthering the profession of radiology by delivering high-quality educational content in their field of study. Learn how you can become an honored educator by visiting the website at: https://www.rsna.org/Honored-Educator-Award/ Katherine E. Maturen, MD - 2014 Honored Educator



### SSC06

Gastrointestinal (Liver Diffuse Disease, Fibrosis)

Monday, Nov. 26 10:30AM - 12:00PM Room: N229



AMA PRA Category 1 Credits ™: 1.50 ARRT Category A+ Credit: 1.75

**FDA** Discussions may include off-label uses.

### Participants

Bachir Taouli, MD, New York, NY (*Moderator*) Research Grant, Guerbet SA; Research Grant, Bayer AG Sudhakar K. Venkatesh, MD, FRCR, Rochester, MN (*Moderator*) Nothing to Disclose Kristin K. Porter, MD, PhD, Baltimore, MD (*Moderator*) Nothing to Disclose Christoforos Stoupis, MD, Maennedorf, Switzerland (*Moderator*) Nothing to Disclose

## Sub-Events

## SSC06-01 Comparison of 2D-Shear Wave Elastography (SWE), Magnetic Resonance Elastography (MRE), and Transient Elastography (TE) for the Diagnosis of Fibrosis in Non-Alcoholic Fatty Liver Disease (NAFLD)

Monday, Nov. 26 10:30AM - 10:40AM Room: N229

Participants

Alessandro Furlan, MD, Pittsburgh, PA (*Presenter*) Book contract, Reed Elsevier; Research Grant, General Electric Company; Consultant, General Electric Company Mitchell E. Tublin, MD, Pittsburgh, PA (*Abstract Co-Author*) Nothing to Disclose Lan Yu, PhD, Pittsburgh, PA (*Abstract Co-Author*) Nothing to Disclose Amir Borhani, MD, Pittsburgh, PA (*Abstract Co-Author*) Consultant, Guerbet SA; Author, Reed Elsevier Jaideep Behari, MD, Pittsburgh, PA (*Abstract Co-Author*) Nothing to Disclose

### For information about this presentation, contact:

furlana@upmc.edu

## PURPOSE

To compare the accuracy of 2D-SWE, MRE and TE for the diagnosis of fibrosis in patients with biopsy-proven NAFLD.

# METHOD AND MATERIALS

In this IRB-approved study, 62 adult subjects (36F; 26M; age, 50±13 years; BMI, 35±7 Kg/m2) with biopsy-proven NAFLD were prospectively recruited. The distribution of fibrosis was as follow: F0=1; F1=17; F2=20; F3=15; F4=9. Subjects underwent a 2D-SWE which uses the comb-push technique (GE LOGIQ E9, GE Healthcare), MRE (2D-GRE; GE Healthcare) and TE (Fibroscan, Echosens) within one year of the biopsy. Area under the receiver operator curve (AUROC) and 95% confidence interval (CI) for the corresponding liver stiffness measurements (LSM, expressed in kPa) were calculated using as outcome significant (F>1) and advanced (F>2) fibrosis. Pairwise comparisons of AUROCs were conducted using the DeLong test. Statistical significance was set at p<.05.

### RESULTS

Valid LSM were obtained in 57/62 subjects with 2D-SWE and in 59/62 subjects with TE. MRE was completed in 59/62 cases. Valid LSM measurements for all three techniques were available in 54/62 subjects. The AUROCS (95% CI) of 2D-SWE, MRE and TE were .796 (.673-.918), .847 (.744-.950), .766 (.638-.893) for significant fibrosis respectively and .890 (.803-.976), .950 (.887-1.00), .861 (.769-.953) for advanced fibrosis respectively. Pairwise comparisons revealed no statistically significant difference for significant (2D-SWE vs. MRE, p=.43; 2D-SWE vs. TE, p=.31; MRE vs. TE, p=.05) and advanced fibrosis (2D-SWE vs. MRE, p=.34; 2D-SWE vs. TE, p=.05).

### CONCLUSION

2D-SWE, MRE and TE showed high accuracy for the diagnosis of advanced fibrosis in NAFLD with no significant difference at pairwise comparison.

### **CLINICAL RELEVANCE/APPLICATION**

2D-SWE and TE are valid alternative to MRE for the diagnosis of advanced fibrosis in patients with NAFLD.

# SSC06-02 Diagnostic Performance of Tomoelastography by Multifrequency Magnetic Resonance Elastography for Staging Hepatic Fibrosis

Monday, Nov. 26 10:40AM - 10:50AM Room: N229

Participants Rolf O. Reiter, MD, Berlin, Germany (Presenter) Nothing to Disclose Heiko Tzschatzsch, Berlin, Germany (Abstract Co-Author) Nothing to Disclose Florian Schwahofer, PhD, Berlin, Germany (Abstract Co-Author) Nothing to Disclose Matthias Haas, Berlin, Germany (Abstract Co-Author) Nothing to Disclose Christian Bayerl, MD, Berlin, Germany (Abstract Co-Author) Nothing to Disclose Marion Muche, MD, Berlin, Germany (Abstract Co-Author) Nothing to Disclose Dieter Klatt, PhD, Berlin, Germany (Abstract Co-Author) Nothing to Disclose Shreyan Majumdar, Chicago, IL (Abstract Co-Author) Nothing to Disclose Winnie A. Mar, MD, Chicago, IL (Abstract Co-Author) Nothing to Disclose Bernd K. Hamm III, MD, Berlin, Germany (Abstract Co-Author) Research Consultant, Canon Medical Systems Corporation; Stockholder, Siemens AG; Stockholder, General Electric Company; Research Grant, Canon Medical Systems Corporation; Research Grant, Koninklijke Philips NV; Research Grant, Siemens AG; Research Grant, General Electric Company; Research Grant, Elbit Imaging Ltd; Research Grant, Bayer AG; Research Grant, Guerbet SA; Research Grant, Bracco Group; Research Grant, B. Braun Melsungen AG; Research Grant, KRAUTH medical KG; Research Grant, Boston Scientific Corporation; Equipment support, Elbit Imaging Ltd; Investigator, CMC Contrast AB Jurgen Braun, PhD, Berlin, Germany (Abstract Co-Author) Nothing to Disclose Ingolf Sack, PhD, Berlin, Germany (Abstract Co-Author) Nothing to Disclose

Patrick Asbach, MD, Berlin, Germany (Abstract Co-Author) Nothing to Disclose

## For information about this presentation, contact:

rolf.reiter@charite.de

# PURPOSE

To evaluate the diagnostic accuracy and cut-off values of full field-of-view tomoelastography stiffness maps of the liver in patients with hepatic fibrosis. We investigated novel multifrequency magnetic resonance elastography (mMRE) with piezoelectric driver and tomoelastography processing pipeline.

### METHOD AND MATERIALS

In this prospective monocentre study, a total of 43 patients and 16 healthy volunteers underwent mMRE on a 1.5-Tesla MRI scanner (Magnetom Aera, Siemens Healthineers, Erlangen, Germany) using a piezoelectric driver and fast single-shot 3D wave-field acquisition at drive frequencies of 35, 40, 45, 50, 55 and 60 Hz. Acquisition parameters for each frequency were as follows: 9 slices, 8 time steps, 3 components, 256 x 256 matrix,  $3 \times 3 \times 5$  mm resolution and 2 averages. For patients, liver biopsy or definite morphological signs of cirrhosis were used as reference standard. Patients showed a wide range of chronic liver diseases including chronic hepatitis B and C, primary sclerosing cholangitis, nonalcoholic steatohepatitis and autoimmune hepatitis. Optimal cut-off values using the Youden-Index, area under the receiver-operating-characteristic-curve (AUROC), sensitivity and specificity were calculated accounting for compound multifrequency maps as well as single frequencies.

## RESULTS

Mean values of mMRE shear wave speed ( $\pm$  standard deviation) of the liver across the entire cohort for 35, 40, 45, 50, 55, 60 and 35-60 Hz were 1.60  $\pm$  0.29, 1.69  $\pm$  0.37, 1.78  $\pm$  0.43, 1.85  $\pm$  0.49, 1.88  $\pm$  0.51, 1.92  $\pm$  0.54 and 1.77  $\pm$  0.43 m/s, respectively. Tomoelastography stiffness maps showed high spatial resolution and anatomical details. E.g., 60-Hz cut-off values, AUROC values, sensitivity and specificity were as follows: fibrosis stage F>=1, 1.62 m/s, 0.92, 0.88 and 0.94; F>=2, 1.78 m/s, 0.93, 0.75 and 1.00; F>=3, 1.82 m/s, 0.97, 0.85 and 0.97; F4, 1.85 m/s, 0.98, 1.00 and 0.88.

## CONCLUSION

Tomoelastography cut-off values show an excellent diagnostic accuracy for staging hepatic fibrosis. High-resolution stiffness maps enable the display of shear wave speed-related anatomical details including multiple organs such as liver and spleen.

## **CLINICAL RELEVANCE/APPLICATION**

mMRE-based tomoelastography might reduce the need for invasive liver biopsies and indicate the distribution of fibrosis within the entire liver.

# SSC06-03 Preoperative Liver Function Reserve Assessment and Future Liver Remnant Function Prediction in HCC patients with Gd-EOB-DTPA enhanced MRI: One-Stop Process

Monday, Nov. 26 10:50AM - 11:00AM Room: N229

Participants

Mengqi Huang, MD, Guangzhou, China (*Presenter*) Nothing to Disclose Shiting Feng, MD, Guangzhou, China (*Abstract Co-Author*) Nothing to Disclose Zhi Dong, Guangzhou, China (*Abstract Co-Author*) Nothing to Disclose Ziping Li, MD, PhD, Guangzhou, China (*Abstract Co-Author*) Nothing to Disclose

## For information about this presentation, contact:

mqhuang0702@163.com

## PURPOSE

Our aim is to determine the feasibility of preoperative Gd-EOB-DTPA enhanced MRI in quantitative assessment of liver function reserve and prediction of post-hepatectomy liver function in HCC patients.

## METHOD AND MATERIALS

This study enrolled 133 HCC patients who underwent Gd-EOB-DTPA enhanced MRI and indocyanine green (ICG) tests before surgery. The liver volume(LV) and mean liver T1 relaxation time before (T1pre) and after (T1pos) contrast was measure with T1pos and LV were measured in Hepatobiliary phase (HBP) scaned 20 minutes after injection. Virtual hepatectomy was processed in 3D images with resection plan defined by multi-disciplinary team discussion and adjusted by surgery record. Remnant T1pre, T1pos and LV were measured in virtual hepatectomy. The T1 reduction rate T1% [(T1pos-T1pre)/T1pre], functional liver volume (FV=LV\*T1%), functional liver volume to weight ratio (FV/W) and T1 relaxation time to liver volume ratio (T1pos/LV) were calculated, the same as the remnant T1%, rFV, rFV/W, rT1pos/LV and rFV%. Correlations between functional parameters (T1pre, T1pos, T1%, FV, FV/W, T1pos/LV) and ICG reduction rate (ICG-R15), ALBI grade were investigated. Child-Pugh score was evaluated in postoperative day 5. The differences of remnant function reserve parameters between Child-Pugh A group and B&C group were analyzed. Multiple Logistic regression test was used to find the possible predictor for postoperative hepatic insufficient.

## RESULTS

Those function liver volume parameters T1pos, T1%, FV, FV/W, T1pos/LV (mean value: 248.4msec, 64.12%, 786.38ml, 12.75ml/Kg, 0.21msec/ml) have shown statistical significantly correlation with ICG-R15 (rho=0.275, -0.290, -0.446, -0.398, 0.438; p<0.001). In predicting preoperative ICG-R15>14%, the cut-off value of FV, FV/W and T1pos/LV were 682.8ml, 10.80ml/kg, 0.236msec/ml, with sensitivity of 73.5%, 74.4%, 81.3%, specificity of 75.0%, 75.0%, 76.9%, respectively. Preoperative measured rFV% was the only positive factor in predicting post-hepatectomy Child-Pugh B&C hepatic insufficiency with cut-off value of 0.683, sensitivity of 71.43% and specificity of 58.67%.

## CONCLUSION

Quantitative function liver volume in Gd-EOB-DTPA enhanced MRI can provide 'one-stop process' assessment of liver function reserve and prediction of post-hepatectomy liver insufficient.

## CLINICAL RELEVANCE/APPLICATION

This research provide a 'one-stop process' assessment for HCC surgical plan

# SSC06-04 Accuracy of Liver Surface Nodularity Score on CT for Staging HCV Hepatic Fibrosis: A Multi-Institutional Study

Monday, Nov. 26 11:00AM - 11:10AM Room: N229

### Participants

Andrew D. Smith, MD, PhD, Birmingham, AL (*Presenter*) President and Owner, Radiostics LLC; President and Owner, eRadioMetrics LLC; President and Owner, Liver Nodularity LLC; President and Owner, Color Enhanced Detection LLC; Patent holder Asser Abou Elkassem, Birmingham, AL (*Abstract Co-Author*) Nothing to Disclose

Seth Lirette, MS, Jackson, MS (Abstract Co-Author) Nothing to Disclose

Kelly L. Cox, DO, Atlanta, GA (Abstract Co-Author) Nothing to Disclose

Brian C. Allen, MD, Durham, NC (Abstract Co-Author) Nothing to Disclose

Erick M. Remer, MD, Cleveland, OH (Abstract Co-Author) Travel support, Bracco Group

Perry J. Pickhardt, MD, Madison, WI (*Abstract Co-Author*) Stockholder, SHINE Medical Technologies, Inc; Stockholder, Elucent Medical; Advisor, Bracco Group;

Meghan G. Lubner, MD, Madison, WI (Abstract Co-Author) Grant, Koninklijke Philips NV; Grant, Johnson & Johnson;

Claude B. Sirlin, MD, San Diego, CA (*Àbstract Co-Author*) Research Grant, Gilead Sciences, Inc; Research Grant, General Electric Company; Research Grant, Siemens AG; Research Grant, Bayer AG; Research Grant, ACR Innovation; Research Grant, Koninklijke Philips NV; Research Grant, Celgene Corporation; Consultant, General Electric Company; Consultant, Bayer AG; Consultant, Boehringer Ingelheim GmbH; Consultant, AMRA AB; Consultant, Fulcrum Therapeutics; Consultant, IBM Corporation; Consultant, Exact Sciences Corporation; Advisory Board, AMRA AB; Advisory Board, Guerbet SA; Advisory Board, VirtualScopics, Inc; Speakers Bureau, General Electric Company; Author, Medscape, LLC; Author, Resoundant, Inc; Lab service agreement, Gilead Sciences, Inc; Lab service agreement, ICON plc; Lab service agreement, Intercept Pharmaceuticals, Inc; Lab service agreement, Shire plc; Lab service agreement, Takeda Pharmaceutical Company Limited; Lab service agreement, sanofi-aventis Group; Lab service agreement, Johnson & Johnson; Lab service agreement, NuSirt Biopharma, Inc; Contract, Epigenomics; Contract, Arterys Inc

### For information about this presentation, contact:

andrewdennissmith@uabmc.edu

### PURPOSE

To assess the accuracy of the Liver Surface Nodularity (LSN) score on CT and FIB4 score for staging hepatitis C virus (HCV) hepatic fibrosis.

### **METHOD AND MATERIALS**

For this IRB-approved HIPAA-compliant retrospective multi-institutional observational study, adult patients with HCV chronic liver disease and a random liver biopsy obtained with 6 months of a liver CT were included. Participating institutions (N=5) each submitted de-identified data and liver CT images from 40 consecutive patients (N=200 total patients) centrally to a core lab. A REDCap web-based database was used to capture demographics, lab values, and the Scheuer stage of fibrosis (F0-F4) on biopsy specimens. Patients with insufficient information for Scheuer staging of fibrosis (N=3) and CT images that could not be processed (N=4) were excluded. The LSN score was measured using custom software in the final cohort (N=193), while blinded to clinical data. The patients age and serum labs (ALT, AST and platelets) were used to calculate the FIB4 score, a method for assessing liver fibrosis severity. The accuracy for differentiating the various stages of liver fibrosis using the LSN score, FIB4 score, and a combination were assessed with ROC analysis and AUC.

## RESULTS

193 patients (69 females / 124 males; mean age 54 years) had Scheuer fibrosis stage: F0-F1 (N=36), F2 (N=41), F3 (N=47), and F4 (N=67). LSN scores increased with higher stages of liver fibrosis (mean: F0-F1= $2.2\pm0.3$ , F2= $2.4\pm0.4$ , F3= $2.4\pm0.3$ , F4= $3.2\pm0.9$ ; p=0.001). For differentiating significant fibrosis (>=F2), advanced fibrosis (>=F3), and cirrhosis (>=F4), the AUCs for the LSN score were 0.88, 0.82, and 0.89, for the FIB4 score were 0.87, 0.87, and 0.91, and for both combined were 0.90, 0.87, and 0.93, respectively.

### CONCLUSION

The combination of LSN score on CT and FIB4 score was highly accurate at staging HCV hepatic fibrosis in a multi-institutional study.

# **CLINICAL RELEVANCE/APPLICATION**

The LSN score on CT and FIB4 score are easy to obtain and could be used to noninvasively and accurately stage hepatic fibrosis in patients with HCV chronic liver disease.

## **Honored Educators**

Presenters or authors on this event have been recognized as RSNA Honored Educators for participating in multiple qualifying educational activities. Honored Educators are invested in furthering the profession of radiology by delivering high-quality educational content in their field of study. Learn how you can become an honored educator by visiting the website at: https://www.rsna.org/Honored-Educator-Award/ Perry J. Pickhardt, MD - 2014 Honored EducatorPerry J. Pickhardt, MD - 2018 Honored EducatorMeghan G. Lubner, MD - 2014 Honored EducatorMeghan G. Lubner, MD - 2018 Honored Educator

## SSC06-05 Quantitative Assessment of Equilibrium Contrast-Enhanced CT to Evaluate Functional Hepatic Reserve and Liver Fibrosis

Monday, Nov. 26 11:10AM - 11:20AM Room: N229

Participants

Yasutaka Ichikawa, MD, Tsu, Japan (*Presenter*) Nothing to Disclose Motonori Nagata, MD, PhD, Tsu, Japan (*Abstract Co-Author*) Nothing to Disclose Hiroki Ikuma, MD, Ise, Japan (*Abstract Co-Author*) Nothing to Disclose Masaki Ishida, MD, PhD, Tsu, Japan (*Abstract Co-Author*) Nothing to Disclose Kakuya Kitagawa, MD, PhD, Tsu, Japan (*Abstract Co-Author*) Nothing to Disclose Hajime Sakuma, MD, Tsu, Japan (*Abstract Co-Author*) Research Grant, Fuji Pharma Co, Ltd; Research Grant, DAIICHI SANKYO Group; Research Grant, FUJIFILM Holdings Corporation; Research Grant, Siemens AG; Research Grant, Nihon Medi-Physics Co, Ltd; Speakers Bureau, Bayer AG

## PURPOSE

To evaluate hepatic extracellular volume fraction (fECV) measurement using equilibrium CT images compared with both functional hepatic reserve that is assessed with 99mTc-diethylenetriamine-pentaacetic acid-galactosyl human serum albumin (GSA) scintigraphy, and liver fibrosis that is assessed with histopathological findings.

### **METHOD AND MATERIALS**

A total of 86 patients (M/F=63/23; mean age,  $67\pm13$  years) who underwent routine dynamic liver CT and GSA scintigraphy for the clinical workup of hepatocellular carcinoma (n=74) and liver metastasis (n=12) were retrospectively studied. Absolute enhancement (in Hounsfield units) of the liver parenchyma (Eliver) and portal vein (Eblood) 3 minutes after contrast agent administration was measured on precontrast and equilibrium phase images. The fECV was calculated as the following equation: fECV(%) = Eliver x (100 - hematocrit(%)) / Eblood. Functional hepatic reserve was assessed with hepatic uptake ratio (LHL15) on GSA scintigraphy. Correlation between fECV and LHL15 was analyzed by the Spearman correlation coefficient. In 52 patients who underwent hepatectomy following the CT and GSA scintigraphy examinations, the fECV measurements were compared with the histopathological results of liver fibrosis staging ([F0-F4]: F0, absent of fibrosis; F4, severe fibrosis).

## RESULTS

The fECV measurements showed a significant correlation with LHL15 (r=-0.58, p<0.0001). With an fECV threshold of 30.0%, the sensitivity and specificity for detecting reduced functional hepatic reserve (LHL15 < 0.91) was 90.5% and 86.2%, respectively. The areas under the ROC curve (AUC) of fECV for differentiating between normal and altered LHL15 was 0.90. The fECV measurements in F4 liver (30.4 $\pm$ 4.3%) were significantly higher than that in both F0-1 (25.6 $\pm$ 2.7%, p=0.0004) and F2-3 (26.9 $\pm$ 3.1%, p=0.02), while no significant difference in fECV between F0-1 vs. F2-3 (p=0.45) was observed. With an fECV threshold of 28.8%, the sensitivity and specificity for differentiating between F0-3 and F4 was 75.0% and 77.5%, respectively. The AUC of fECV for F0-3 vs. F4 was 0.80.

## CONCLUSION

Hepatic fECV measured with equilibrium CT imaging is associated with functional hepatic reserve and severity of liver fibrosis.

## **CLINICAL RELEVANCE/APPLICATION**

Routine contrast-enhanced CT including equilibrium phase image may provide a means of assessing functional hepatic reserve and liver fibrosis.

# SSC06-06 Comparative Diagnostic Accuracy of Ultrasound Shear-Wave Elastography and Magnetic Resonance Elastography for Classifying Fibrosis Stage in Adults with Biopsy-Proven Nonalcoholic Fatty Liver Disease

Monday, Nov. 26 11:20AM - 11:30AM Room: N229

Participants

Yingzhen Zhang, MD, La Jolla, CA (*Abstract Co-Author*) Postdoctoral Research Fellowship, General Electric Company Andrew S. Boehringer, BS, La Jolla, CA (*Abstract Co-Author*) Nothing to Disclose Yali Qu, San Diego, CA (*Abstract Co-Author*) Nothing to Disclose Kang Wang, MD,PhD, San Diego, CA (*Abstract Co-Author*) Nothing to Disclose Gavin Hamilton, PhD, La Jolla, CA (*Abstract Co-Author*) Nothing to Disclose Vivian Montes, La Jolla, CA (*Abstract Co-Author*) Nothing to Disclose Ethan Sy, BS, San Diego, CA (*Abstract Co-Author*) Nothing to Disclose Claire Faulkner, San Diego, CA (*Abstract Co-Author*) Nothing to Disclose Nikolaus M. Szeverenyi, PhD, Syracuse, NY (*Abstract Co-Author*) Research Grant, General Electric Company Research Consultant, Time Medical Holdings Company Ltd Research collaboration, AMRA AB Aiguo Han, PhD, Urbana, IL (*Abstract Co-Author*) Nothing to Disclose William D. O'Brien JR, PhD, Urbana, IL (*Abstract Co-Author*) Nothing to Disclose William D. O'Brien JR, PhD, Urbana, IL (*Abstract Co-Author*) Nothing to Disclose

## Michael P. Andre, PhD, La Jolla, CA (Abstract Co-Author) Researcher, Siemens AG

Rohit Loomba, MD, MSc, La Jolla, CA (*Abstract Co-Author*) Grant, Adheron; Grant, Arora; Grant, Bristol-Myers Squibb Company; Grant, DAIICHI SANKYO Group; Grant, Galectin; Grant, Galmed Pharmaceuticals Ltd; Grant, General Electric Company; Grant, GENFIT SA; Grant, Gilead Sciences, Inc; Grant, Immuron Ltd; Grant, Intercept Pharmaceuticals, Inc; Grant, Janseen Inc; Grant, Kinemed; Grant, Madrigal Pharmaceuticals, Inc; Grant, Merck & Co, Inc; Grant, NGM Biopharmaceuticals, Inc; Grant, Promega Corporation Inc; Grant, Siemens AG; Grant, Sirius; Grant, Tobira Therapeutics, Inc

Claude B. Sirlin, MD, San Diego, CA (*Presenter*) Research Grant, Gilead Sciences, Inc; Research Grant, General Electric Company; Research Grant, Siemens AG; Research Grant, Bayer AG; Research Grant, ACR Innovation; Research Grant, Koninklijke Philips NV; Research Grant, Celgene Corporation; Consultant, General Electric Company; Consultant, Bayer AG; Consultant, Boehringer Ingelheim GmbH; Consultant, AMRA AB; Consultant, Fulcrum Therapeutics; Consultant, IBM Corporation; Consultant, Exact Sciences Corporation; Advisory Board, AMRA AB; Advisory Board, Guerbet SA; Advisory Board, VirtualScopics, Inc; Speakers Bureau, General Electric Company; Author, Medscape, LLC; Author, Resoundant, Inc; Lab service agreement, Gilead Sciences, Inc; Lab service agreement, ICON plc; Lab service agreement, Intercept Pharmaceuticals, Inc; Lab service agreement, Shire plc; Lab service agreement, Takeda Pharmaceutical Company Limited; Lab service agreement, sanofi-aventis Group; Lab service agreement, Johnson & Johnson; Lab service agreement, NuSirt Biopharma, Inc ; Contract, Epigenomics; Contract, Arterys Inc

For information about this presentation, contact:

y8zhang@ucsd.edu

## PURPOSE

There is limited data on the comparative accuracy of ultrasound (US) shear-wave elastography (SWE) and magnetic resonance elastography (MRE) for classifying fibrosis stage in nonalcoholic fatty liver disease (NAFLD). This study compares the diagnostic accuracy of SWE and MRE for classifying fibrosis stage in adults with NAFLD.

## **METHOD AND MATERIALS**

This was an IRB-approved, HIPAA-compliant, prospective study of 46 adults (mean age 52 years; 25 women; mean body mass index [BMI] 32 kg/m2) with suspected NAFLD who from May 2016 to February 2018 underwent clinical liver biopsy followed by contemporaneous MRE and SWE for research. Fibrosis stage was scored (Nonalcoholic Steatohepatitis Clinical Research Network system). Receiver operating characteristics (ROCs) were assessed for SWE and MRE classification of dichotomized fibrosis stages (fibrosis stages >=1, >=2, >=3, and = 4) and the Youden index was used to select the corresponding thresholds. DeLong test was performed to compare the areas under the ROC curves (AUCs) of MRE and SWE pairwise.

### RESULTS

Patients had the following fibrosis stages on histology: 0: 17; 1: 18; 2: 6; 3: 2; 4: 3. AUCs for SWE and MRE were 0.70 (95% confidence interval [CI], 0.55-0.85) and 0.83 (95% CI, 0.72-0.95), 0.77 (95% CI, 0.60-0.93) and 0.97 (95% CI, 0.92-1.00), 0.92 (95% CI, 0.82-1.00) and 0.93 (95% CI, 0.78-1.00), and 0.93 (95% CI, 0.84-1.00) and 1.00, for detecting fibrosis stage >=1, >=2, >=3, and =4, respectively. The differences were significant (p=0.02) for detecting fibrosis stage >=2 but not otherwise (p>=0.11). Youden-based SWE- and MRE-cutoffs for classifying stages >=1, >=2, >=3, and =4 with sensitivities/specificities were 8.67 kPa (45%/88%) and 2.29 kPa (69%/88%), 9.19 kPa (55%/89%) and 2.75 kPa (91%/97%), 8.67 kPa (100%/76%) and 4.19 kPa (80%/100%), and 9.40 kPa (100%/88%) and 5.04 kPa (100%/100%).

### CONCLUSION

In adults with suspected NAFLD, clinically indicated biopsy, and low a priori probability of advanced fibrosis, SWE showed modest accuracy for detecting stage >= 1 or >= 2 fibrosis and high accuracy for detecting advanced (stage >=3) fibrosis. MRE may be more accurate than SWE at classifying fibrosis but greater power is needed to achieve significance.

### **CLINICAL RELEVANCE/APPLICATION**

In adults with suspected NAFLD, SWE may have utility as an initial screen for advanced fibrosis. MRE may be required to reliably detect earlier stages of fibrosis.

## SSC06-07 The Optimal Measurement Number of Shear Wave Elastography (SWE) for >=F2 Liver Fibrosis Diagnosis: Percentage of Color Filling Index (PCFI) Stratification Analysis using Automated Image Quality Analysis

Monday, Nov. 26 11:30AM - 11:40AM Room: N229

Participants

Qian L<sup>i</sup>, MD, Boston, MA (*Abstract Co-Author*) Nothing to Disclose Laura Brattain, Lexington, MA (*Presenter*) Nothing to Disclose Nathaniel D. Mercaldo, Boston, MA (*Abstract Co-Author*) Nothing to Disclose Manish Dhyani, MBBS, Burlington, MA (*Abstract Co-Author*) Nothing to Disclose Melinda Chen, Cambridge, MA (*Abstract Co-Author*) Nothing to Disclose Anthony E. Samir, MD, Boston, MA (*Abstract Co-Author*) Consultant, Pfizer Inc; Consultant, General Electric Company; Consultant, PAREXEL International Corporation; Research Grant, Koninklijke Philips NV; Research Grant, Siemens AG; Research Grant, Canon Medical Systems Corporation; Research support, SuperSonic Imagine; Research support, Hitachi, Ltd

### For information about this presentation, contact:

li.qian@mgh.harvard.edu

## PURPOSE

To explore the optimal and minimum number of SWE measurements for >=F2 fibrosis considering measurement variability and diagnostic accuracy.

## METHOD AND MATERIALS

Prospectively collected adult patients who underwent SWE before non-focal liver biopsy in three years. 10 SWE measurements

were performed for each patient at the identical biopsy locations (Segment 8) by one experienced sonographer before the biopsy. Fibrosis stages were evaluate using METAVIR criteria (F0-F4). The optimal and minimum measurement number for >=F2 were analyzed: (1) for each measurement number (1-9), correlated median SWE estimates were obtained using a nested bootstrap simulation; (2) ROC curves, and the associated AUROC values, were estimated using each set of SWE measurements (e.g., 2-10 measurements); (3) steps (1) and (2) were repeated 1000 times to obtain empirical distributions of median SWE estimates, and AUC estimates. Two variation parameters were evaluated, including (1) intra-subject SWE variation (m/s): the absolute median difference between individual SWEs and median SWE, and (2) interval width difference (IWD): the width differences of AUC 95%CI between a measurement number (1-9) and 10. A subgroup of patients with >=50% PCFI images (percentage of valid SWE pixels over the entire SWE image box, a metric for SWE image quality assessment) were also selected.

## RESULTS

245 cases were enrolled (mean 48.5 $\pm$ 13.2 yr; men 109, women 136), with the fibrosis stages F0=93, F1=92, F2=27, F3=23, F4=10. The intra-subject variation of the median SWE estimate decreased from 3.12 to 0.46m/s in 1-10 measurements in overall patients (n=245), and decreased from 3.74 to 0.37 in images with >=50% PCFI (n=106). we didn't detect AUC differences between measurement numbers 1-9 and 10, but IWD, which represents the variation of diagnostic accuracy, dramatically increased when measurements number =50% group, depending on the clinicians desired precision of IWD (within 0.040 units).

### CONCLUSION

Current results demonstrated that, for >= F2 fibrosis diagnosis, the minimum SWE numbers may be reduced to 7 in overall images, and 6 when >= 50% PCFI was applied for image quality control.

## **CLINICAL RELEVANCE/APPLICATION**

Automated image quality analysis may have the potential to reduce the SWE measurements number for liver fibrosis diagnosis, thus improving the scanning process and diagnostic performance of SWE.

## SSC06-08 Hepatic Shear Wave Elastography: Correlation Between Liver Stiffness and Esophagogastric Varices

Monday, Nov. 26 11:40AM - 11:50AM Room: N229

## Participants

Vasanthakumar Venugopal, MD, New Delhi, India (*Presenter*) Nothing to Disclose Harsh Mahajan, MD, MBBS, New Delhi, India (*Abstract Co-Author*) Nothing to Disclose Rajnish K. Duggal, New Delhi, India (*Abstract Co-Author*) Nothing to Disclose Shoma M. Sharma SR, MD, New Delhi, India (*Abstract Co-Author*) Nothing to Disclose Nitin Tandon, MBBS, MD, New Delhi, India (*Abstract Co-Author*) Nothing to Disclose Vidur Mahajan, MBBS, New Delhi, India (*Abstract Co-Author*) Nothing to Disclose Murali Murugavel, PhD, New Delhi, India (*Abstract Co-Author*) Nothing to Disclose

### For information about this presentation, contact:

drvasanth@mahajanimaging.com

### PURPOSE

To evaluate the role of liver stiffness measurement (LSM) measured by shear wave elastography (SWE) in predicting the presence of esophagogastric varices (EGV) in patients with portal hypertension and to determine the correlation between the LSM and endoscopic grade of EGV.

## METHOD AND MATERIALS

This study included 331 patients with chronic liver disease being evaluated for portal hypertension and planned for esophagogastroduodenoscopy. SWE was performed in the right lobe of the liver by using a convex broadband probe on GE LOGIQ E9 ultrasound machine. The shear wave liver stiffness (in kPa) was recorded at ten locations and the median values calculated. Endoscopic findings were interpreted with reference to the presence of varices and grade of the varices. Correlation between LSM and grade of varices was analyzed with the Pearson correlation coefficient. Multiclass Receiver operating characteristic (ROC) curves were constructed, and the area under the ROC curves (AUC) was calculated to determine the discriminating power between the grades of the varices.

### RESULTS

LSM and variceal grade showed no significant correlation (R = 0.351286, P < 0001). The AUC for detection of the presence of varices was 0.7259. The AUC for differentiating between various grades of the varices was 0.6470, 0.5802, 0.6259 and 0.7692. Box plot of the LSM and grade of varices revealed no discrimination power. Hepatic shear wave stiffness was marginally useful in predicting the presence of varices. But the discriminating power of LSM among the grades of varices was poor.

### CONCLUSION

We found marginal utility of LSM in predicting the presence of EGV. However, contrary to the existing knowledge, in our study, we found no correlation between liver stiffness measurement and grade of EGV. The liver stiffness measurement is not a reliable predictor of portal hypertension.

## **CLINICAL RELEVANCE/APPLICATION**

In advanced fibrosis, liver stiffness measurements in isolation does not seem to predict the clinical severity of portal hypertension. The additional assessment of splenic stiffness should be considered.

# SSC06-09 Diagnostic Accuracy of Combination of Quantitative Point Shear Wave Elastography (pSWE) and Serum Markers for the Assessment of Fibrosis in Patients with Chronic Liver Disease Using Liver Biopsy as the Reference Standard

Monday, Nov. 26 11:50AM - 12:00PM Room: N229

Ounali Jaffer, MBBS, FRCR, London, United Kingdom (*Abstract Co-Author*) Nothing to Disclose Cheng Fang, MBBS,FRCR, London, United Kingdom (*Presenter*) Nothing to Disclose Phillip Lung, Middlesex, United Kingdom (*Abstract Co-Author*) Advisory Board, Takeda Pharmaceutical Company Limited; Speaker, Siemens AG Aarti Shah, MBBCh, MRCP, London, United Kingdom (*Abstract Co-Author*) Nothing to Disclose

Diana Bosanac, MBBS, London, United Kingdom (*Abstract Co-Author*) Nothing to Disclose

Gibran Yusuf, MBBS, London, United Kingdom (Abstract Co-Author) Speaker, Bracco Group; Speaker, Siemens AG

Suzanne Ryan, MD, London, United Kingdom (Abstract Co-Author) Nothing to Disclose

Michael Heneghan, London, United Kingdom (Abstract Co-Author) Nothing to Disclose

Kosh Agarwal, London, United Kingdom (Abstract Co-Author) Nothing to Disclose

Daniel J. Quinlan, MBBS, London, United Kingdom (Abstract Co-Author) Nothing to Disclose

Alberto Quaglia, London, United Kingdom (Abstract Co-Author) Nothing to Disclose

Paul S. Sidhu, MRCP, FRCR, London, United Kingdom (*Abstract Co-Author*) Speaker, Koninklijke Philips NV; Speaker, Bracco Group; Speaker, Hitachi, Ltd; Speaker, Siemens AG; Speaker, Samsung Electronics Co, Ltd; Advisory Board, Samsung Electronics Co, Ltd; Advisory Board, Itreas Ltd

# For information about this presentation, contact:

ChengFang@nhs.net

# PURPOSE

To evaluate individual and combined diagnostic performance of quantitative point shear wave elastography (pSWE) and serum markers for the assessment of liver fibrosis in patients with chronic liver disease.

# METHOD AND MATERIALS

This prospective study received ethics approval, and all participants provided written informed consent. Shear wave speed (SWS) using pSWE (VTQ) and serum fibrosis markers (aspartate aminotransferase-to-platelet ratio index [APRI], King's score) were measured in 169 consecutive patients with chronic liver disease (mixed aetiology). Receiver-operating characteristic (ROC) analysis were performed to evaluate the diagnostic accuracy of their individual and combined performance in predicting significant (F>=3) and severe/cirrhosis (F>=5) liver fibrosis using ISHAK histologic fibrosis stages (F0-6) as reference. Cut-off values were determined using Youden Index. Spearman's correlation coefficient between the SWS, fibrosis marker and fibrosis stage were calculated.

# RESULTS

Ishak histology stages were 0-2 (n=90, 53%), 3-4 (n=50, 30%), 5-6 (n=29, 17%). There was a good correlation between SWS, King's score, APRI and the Ishak stage (p=0.682, p=0.632 and p=0.584, respectively, P <= .001). The areas under the ROC curves (AUROC) for SWS, King's score, and APRI, were 0.86, 0.87, and 0.89 for the diagnosis of significant fibrosis (F>=3) and 0.98, 0.79, and 0.85 for the diagnosis of severe fibrosis/cirrhosis (F>=5), respectively. pSWE is superior than APRI (P=0.0005) and King's score (P=0.002) in predicting severe fibrosis/cirrhosis (F>=5), The optimum pSWE cut-off values for significant and severe fibrosis/cirrhosis were 1.22 and 1.86 m/s, respectively. The AUROC for combining the serum fibrosis marker and pSWE in diagnosing significant fibrosis were 0.93, outperforming using pSWE alone (P=0.0048).

# CONCLUSION

pSWE is superior than serum markers in predicting severe fibrosis/cirrhosis is and comparable to serum markers for significant fibrosis. Combining pSWE and serum markers improves the diagnostic accuracy in predicting significant fibrosis.

# **CLINICAL RELEVANCE/APPLICATION**

pSWE has excellent diagnostic accuracy for predicting cirrhosis. In addition, combining pSWE and serum markers significantly improve the diagnostic performance of significant fibrosis.



### SSC07

## Science Session with Keynote: Genitourinary (New Techniques for Renal Imaging)

Monday, Nov. 26 10:30AM - 12:00PM Room: S503AB



AMA PRA Category 1 Credits ™: 1.50 ARRT Category A+ Credit: 1.75

### **Participants**

John R. Leyendecker, MD, Dallas, TX (*Moderator*) Nothing to Disclose David D. Childs, MD, Clemmons, NC (*Moderator*) Nothing to Disclose

## Sub-Events

# SSC07-01 Genitourinary Keynote Speaker: Renal Mass Characterization: Quantitation, Radiomics, and Machine Learning

Monday, Nov. 26 10:30AM - 10:40AM Room: S503AB

Participants

Ivan Pedrosa, MD, Dallas, TX (Presenter) Nothing to Disclose

# SSC07-02 Utility of Google TensorFlow™ Inception Machine Learning to Discriminate Clear Cell Renal Cell Carcinoma from Oncocytoma on Multiphasic CT

Monday, Nov. 26 10:40AM - 10:50AM Room: S503AB

Participants

Heidi Coy, Los Angeles, CA (*Presenter*) Nothing to Disclose Kevin Hseih, Los Angeles, CA (*Abstract Co-Author*) Nothing to Disclose Willie Wu, Los Angeles, CA (*Abstract Co-Author*) Nothing to Disclose Fabien Scalzo, PhD, Los Angeles, CA (*Abstract Co-Author*) Nothing to Disclose Mahesh B. Nagarajan, PhD, Los Angeles, CA (*Abstract Co-Author*) Nothing to Disclose Jonathan R. Young, MD, Sacramento, CA (*Abstract Co-Author*) Nothing to Disclose Michael L. Douek, MD, MBA, Los Angeles, CA (*Abstract Co-Author*) Nothing to Disclose Steven S. Raman, MD, Santa Monica, CA (*Abstract Co-Author*) Nothing to Disclose

## For information about this presentation, contact:

hcoy@mednet.ucla.edu

### PURPOSE

Although a renal mass can have imaging features of a typical clear cell renal cell carcinoma (ccRCC) on CT, up to 30% of these are found to be benign after surgery, most commonly oncocytoma (ONC). The purpose of our study was to develop a machine learning-based renal lesion classifier using open source Google TensorFlow<sup>™</sup> Inception (TCI) Machine Learning to discriminate ccRCC from ONC on four-phase CT.

### **METHOD AND MATERIALS**

With IRB approval and HIPAA compliance, we derived a cohort of 176 patients with 195 lesions (131 patients with 125 ccRCCs; 61 patients with 49 ONC) with preoperative four phase (unenhanced (UN), corticomedullary (CM), nephrographic (NP), excretory (EX)) CT imaging. Regions of interest were drawn around the tumor on every slice in each phase to create a 3D tumor volume. To preprocess the DICOM data into a format currently supported by TCI, 3D tumor data was extracted in the x, y and z plane and converted into a red, green and blue (RGB) jpeg image using the three color channels to encode each slice. 70% of the data was used in the training set and 30% in the testing set. We investigated several approaches to convert the data into a set of 2D JPEG images that adequately represented each tumor and were used to train the final layer of the neural network model.

## RESULTS

When we analyzed 3 mid-slices of the tumor in the x, y and z plane in each post contrast phase, the EX phase had the highest accuracy in classifying both ccRCC (79.6%) and Onc (59.5%) compared to the accuracy in the CM (ccRCC=78.3%, Onc=46%) and NP (ccRCC=77.2%, Onc=46.5%) phases. The highest accuracy in classifying ccRCC was obtained by submitted all x,y and z planes in all phases as one image to TCI with an accuracy of 82.5%, however this lowered the correct classification of Onc to 52.2%.

### CONCLUSION

In this pilot study, TCI enabled independent classification of clear cell RCC from oncocytoma on a four phase MDCT with an accuracy of 82.5%.

### **CLINICAL RELEVANCE/APPLICATION**

A TCI based method if developed and validated prospectively may be an adjunct to radiologists for discrimination between clear cell RCC and Oncocytoma on multiphasic CT minimizing diagnostic uncertainty and enabling more accurate patient triage.

# ssc07-03 Differentiation of Renal Cell Carcinoma and Oncocytoma Using Machine Learning-Based MR Radiomics

Monday, Nov. 26 10:50AM - 11:00AM Room: S503AB

Participants Yijun Zhao, Changsha, China (Presenter) Nothing to Disclose Harrison X. Bai, MD, Philadelphia, PA (Abstract Co-Author) Nothing to Disclose Dhanya Mahesh, Philadelphia, PA (Abstract Co-Author) Nothing to Disclose Chang Su, New Haven, CT (Abstract Co-Author) Nothing to Disclose Ken Chang, Boston, MA (Abstract Co-Author) Nothing to Disclose Paul Zhang, MD, PhD, Philadelphia, PA (Abstract Co-Author) Nothing to Disclose Hui Liu, Changsha, China (Abstract Co-Author) Nothing to Disclose Dehong Peng, Changsha, China (Abstract Co-Author) Nothing to Disclose Mandeep S. Dagli, MD, Philadelphia, PA (Abstract Co-Author) Nothing to Disclose Terrance Gade, Philadelphia, PA (Abstract Co-Author) Nothing to Disclose Michael C. Soulen, MD, Philadelphia, PA (Abstract Co-Author) Royalties, Cambridge University Press; Consultant, Guerbet SA; Research support, Guerbet SA; Research support, BTG International Ltd; Consultant, Merit Medical Systems, Inc; Proctor, Sirtex Medical Ltd; Consultant, Terumo Corporation; Consultant, Bayer AG Zishu Zhang, MD, PhD, Ypsilanti, MI (Abstract Co-Author) Nothing to Disclose William.s Stavropoulos, Philadelphia, PA (Abstract Co-Author) Nothing to Disclose

### For information about this presentation, contact:

zhaoyj25@126.com

## PURPOSE

To build a random forest predictive model for distinguishing between renal cell carcinoma (RCC) and oncocytoma that integrates clinical, preoperative, and multimodal automated features.

### **METHOD AND MATERIALS**

Forty-one patients with histologically confirmed renal tumors (23 RCCs; 18 oncocytomas) were identified from a single institution. Two experts (HL and DP), with 23 and 10 years of experience of reading body MR respectively, blinded to the histologic diagnoses, made image diagnosis based on the preoperative MR images (T2-weighted and T1-contrast enhanced sequences). Histogram, geometric and texture features were extracted from preoperative MR images. Using a random forest algorithm, automated features were integrated with clinical data to generate a multivariate predictive model. Receiving operating characteristic curves (ROCs) and areas under the curve (AUCs) were used to assess model performance by using the Delong method for statistical comparison of ROCs.

## RESULTS

Patients with oncocytoma had higher mean age than patients with RCC ( $65.8\pm7.7$  vs.  $58.7\pm11.4$  years, p=0.022). Tumor size did not differ significantly between RCC and oncocytoma (average of  $2.3\pm0.9$  vs.  $2.5\pm1.0$ cm; p = 0.620). For each patient, 5 clinical features and 10566 automated features were included in the model. After feature reduction, 32 features remained. This included 30 T1-contrast enhanced features and 2 T2-weighted features. The tested model achieved accuracy of 80.5% (AUC = 0.80) with sensitivity of 82.6% and specificity of 77.8%. Shape Volume-Compactness (T1C), NGTDM-Busyness (T1C), GLSZM-ZSV (T1C), and Shape Volume-Volume (T2WI) were the features contributing most to the model. Compared to our model, expert 1 achieved accuracy of 63.4% (AUC = 0.59; p = 0.019) with 95.7% sensitivity and 22.2% specificity, and expert 2 achieved accuracy of 57.5% (AUC = 0.55; p = 0.005) with 65.2% sensitivity and 44.4% specificity.

## CONCLUSION

Preliminary results using machine learning algorithms demonstrated improved accuracy in differentiation of RCC and oncocytoma when compared with expert interpretation. Further validation is needed in a larger cohort.

## **CLINICAL RELEVANCE/APPLICATION**

Oncocytoma, a benign tumor, that cannot typically be distinguished from RCC based on routine clinical imaging. A machine learning based approach with high accuracy would potentially spare patients unnecessary surgery, ablation, and biopsy.

# SSC07-04 The Utility of Radiomic Features in Differentiation of Clear Cell Renal Cell Carcinoma from Non-Clear Cell Renal Cell Carcinoma: A Preliminary Study

Monday, Nov. 26 11:00AM - 11:10AM Room: S503AB

Participants Jian Wen Li, Nanjing, China (*Presenter*) Nothing to Disclose Chang Sheng Zhou, BS, Nanjing, China (*Abstract Co-Author*) Nothing to Disclose Xiuli Li, Beijing, China (*Abstract Co-Author*) Nothing to Disclose Ping Gong, Beijing, China (*Abstract Co-Author*) Nothing to Disclose Long Jiang Zhang, MD, PhD, Nanjing, China (*Abstract Co-Author*) Nothing to Disclose GM Lu, Nanjing, China (*Abstract Co-Author*) Nothing to Disclose

#### For information about this presentation, contact:

kimonlee@163.com

### PURPOSE

To investigate the ability of radiomic features derived from the corticomedullary phase images to differentiate clear cell renal cell carcinoma (RCC) from non-clear cell RCC.

### **METHOD AND MATERIALS**

This study involved 450 patients with 463 tumors histopathologically diagnosed as clear cell RCC (n=362), papillary RCC (n=54) or

chromophobe RCC (n=47), whose corticomedullary phase images were available. To conduct the study, 80% (n=371) and 20% (n=92) tumors were randomly selected as development and validation cohorts keeping the ratio of clear cell RCC to non-clear cell RCC consistent. Using the development cohort, a discriminative subset from 1023 radiomic features was selected by SVM with LASSO regularization. Receiver operating characteristic analysis was conducted to assess the predictive ability of the selected CT radiomic features in differentiation of clear cell RCC from non-clear cell RCC in the validation cohort. For contrast, a radiologist, with 6 years of experience in genitourinary imaging, was instructed to predict the subtypes (clear cell or non-clear cell RCC) of the validation cohort. The chi-square test was conducted to compare the accuracies between the SVM model and the radiologist.

## RESULTS

Our research demonstrated that the SVM model combining 15 features was strongly discriminative in differentiation of clear cell RCC from non-clear cell RCC in the validation cohort. The sensitivity, specificity, overall accuracy, and area under the curves for the SVM model in the validation cohort were 84.7% (61/72), 85% (17/20), 84.8% (78/92), and 0.905, while the sensitivity, specificity, and overall accuracy for the radiologist were 94.4% (68/72), 60% (12/20), and 86.9% (80/92). According to the chi-square test, there was no statistically significant difference between the accuracies of the SVM model and the radiologist (p=0.672).

## CONCLUSION

This study demonstrated that CT radiomic features derived from the corticomedullary phase images can aid in the differentiation of renal cell carcinoma subtypes, which is comparable to experienced radiologists.

# **CLINICAL RELEVANCE/APPLICATION**

The effective SVM model combining 15 radiomic features could help the clinical management of patients with renal cell carcinoma, especially patients with non-clear cell renal cell carcinoma.

## SSC07-05 Differentiation of Renal Lipid-Poor Angiomyolipoma from Renal Cell Carcinoma by Machine Learning Based on Whole-Tumor Texture Features of Three-Phase CT Images

Monday, Nov. 26 11:10AM - 11:20AM Room: S503AB

Participants

Enming Cui, MD, Jiangmen, China (*Presenter*) Nothing to Disclose Wansheng Long, MD, Guangdong, China (*Abstract Co-Author*) Nothing to Disclose Fan Lin, MD, Shenzhen, China (*Abstract Co-Author*) Nothing to Disclose Xiangmeng Chen, MD, Jiangmen, China (*Abstract Co-Author*) Nothing to Disclose Zhuangsheng Liu, Jiangmen, China (*Abstract Co-Author*) Nothing to Disclose

## For information about this presentation, contact:

cem2008@163.com

## PURPOSE

To determine the diagnostic performance of machine learning in the differentiation of lipid-poor angiomyolipoma (Ip-AML) from renal cell carcinoma (RCC) based on whole-tumor quantitative texture features of three-phase CT images.

# METHOD AND MATERIALS

A total of 40 patients with 41 pathologically proven Ip-AML and 95 patients with 97 pathologically proven RCCs were included by this retrospective study. All patients underwent three-phase CT study which consisted of precontrast phase (PCP), corticomedullary phase (CMP) and nephrographic phase (NP). Texture features were extracted from whole-tumor images at three-phase, single PCP, CMP and NP, respectively. Then support vector machine with recursive feature elimination method based on five-fold cross-validation (SVM-RFECV) were utilized to establish the discriminative classifiers. The performance of classifiers based on three-phase, single PCP, CMP and NP were determined and compared with each other. The performance of machine learning classifier in the differentiation of Ip-AML from RCC was compared with morphological interpretation by radiologists using Receiver operating character (ROC) analysis.

## RESULTS

43, 34, 24, 20 features subset were extracted as candidate features in three-phase, PCP, CMP and NP by Boruta package for python respectively. Among of these, 13, 24, 9 12 optimal feature subset further screened by SVM-RFECV entered to establish machine learning classifier in the differentiation of Ip-AML and RCC. The classifier base on three-phase whole tumor images achieved the best performance in discriminating Ip-AML from RCC, with the highest accuracy, area under curve (AUC), sensitivity, and specificity of 92.78%, 0.96, 92.78% and 92.78%, respectively. The performance of morphological interpretation by radiologist was inferior to machine learning classifier in differentiating Ip-AML and RCC, with lower accuracy, AUC, sensitivity and specificity of 69.57%, 0.66, 36.59% and 89.69%.

### CONCLUSION

Machine learning classifier based on whole-tumor texture features from three-phase images could reach more accurate discrimination between Ip-AML and RCC than conventional morphological interpretation.

## **CLINICAL RELEVANCE/APPLICATION**

Machine learning classifier is more powerful than morphological interpretation by radiologists and is recommended as part of a MR study prior to renal tumor removal.

# SSC07-06 Is Dual-Energy CT (DECT) Of Renal Masses Ready For Prime Time? Diagnostic Accuracy of Conventional Attenuation Change and Iodine Concentration Thresholds at Rapid-kVp-Switch DECT for Detection of Enhancement in Renal Masses

Monday, Nov. 26 11:20AM - 11:30AM Room: S503AB

Participants Nima Sadoughi, MD, Ottawa, ON (*Presenter*) Nothing to Disclose Satheesh Krishna, MD, Ottawa, ON (*Abstract Co-Author*) Nothing to Disclose Matthew D. McInnes, MD, PhD, Ottawa, ON (*Abstract Co-Author*) Nothing to Disclose Blair MacDonald, Ottawa, ON (*Abstract Co-Author*) Nothing to Disclose Nicola Schieda, MD, Ottawa, ON (*Abstract Co-Author*) Nothing to Disclose

### For information about this presentation, contact:

nschieda@toh.on.ca

## PURPOSE

Iodine concentration (i[]), measured on DECT, is an alternative to attenuation difference ( $\Delta$ HU) for diagnosis of enhancement in renal masses. Reported i[] thresholds vary and may be too high to detect enhancement in hypoenhancing papillary renal cell carcinoma (pRCC). This study re-evaluates rapid-kVp-switch DECT i[] thresholds for diagnosis of enhancement in SRMs.

## METHOD AND MATERIALS

With IRB approval, we evaluated 34 renal masses (including 9 pRCC) diagnosed histologically and 30 benign cysts with renal mass protocol rapid-kVp-switch DECT between 2015-2017. A blinded Radiologist measured i[] (mg/mL) and  $\Delta$ HU. Enhancement was defined as: 1) i[]>2 mg/mL (Marin et al., Kaza et al.) 2) i[]>1.6 mg/mL (Zarzour et al.) and 3)  $\Delta$ HU>20 HU. Diagnostic accuracy was tabulated and compared by ROC analysis.

## RESULTS

There were no differences in age, gender or size of lesions between groups (p>0.05). Using i[]>2.0 mg/mL achieved sensitivity/specificity/Area under ROC curve (AUC) of 73.3%/100%/0.87. 23.5% (8/34) pRCCs were misclassified as non-enhancing with i[] ranging from 0.7-1.6 mg/mL. Using i[]>1.2 mg/mL, sensitivity/specificity/AUC of 86.7%/100%/0.93 was achieved. 11.8% (4/34) pRCCs were misclassified as non-enhancing with i[] range from 0.7-0.9 mg/mL. Using  $\Delta$ HU>20 HU achieved sensitivity/specificity/AUC of 93.3%/94.1%/0.94. 5.9% (2/34) pRCCs were misclassified as non-enhancing and 6.7% (2/30) cysts were misdiagnosed as enhancing due to pseudoenhancement. There was no difference in AUC comparing the three methods for detecting enhancement (p>0.05), with higher false negatives encountered with i[] and false positives encounterd with  $\Delta$ HU.

## CONCLUSION

Published iodine concentration thresholds for enhancement in renal masses measured at DECT result in substantial false negative results among hypoenhancing papillary RCC, with the 1.2 mg/mL threshold outperforming 2.0 mg/mL.  $\Delta$ HU is more sensitive for detection of enhancement compared to iodine concentration but with higher false positive results due to pseudoenhancement.

# **CLINICAL RELEVANCE/APPLICATION**

 $\Delta$ HU remains a robust method to diagnose enhancement in renal masses and is more sensitive for detection of low level enhancement in papillary tumors compared to published iodine concentration values; however, DECT remains valuable for diagnosis of pseudoenhancement.

# SSC07-07 The Reality of Dual-Energy CT Iodine Quantification in High-Attenuating Renal Lesion: A Comparison to Standard Hounsfield Units Attenuation

Monday, Nov. 26 11:30AM - 11:40AM Room: S503AB

Participants

Mathias Meyer, Durham, NC (*Presenter*) Researcher, Siemens AG; Researcher, Bracco Group Federica Vernuccio, MD, Palermo, Italy (*Abstract Co-Author*) Research support, Siemens AG Christoph Schabel, MD, Durham, NC (*Abstract Co-Author*) Nothing to Disclose Fernando Gonzalez, Santiago, Chile (*Abstract Co-Author*) Nothing to Disclose Bhavik N. Patel, MD,MBA, Stanford, CA (*Abstract Co-Author*) Nothing to Disclose Rendon C. Nelson, MD, Durham, NC (*Abstract Co-Author*) Research Consultant, General Electric Company; Research Consultant, Nemoto Kyorindo Co, Ltd; Consultant, VoxelMetrix, LLC; Co-owner, VoxelMetrix, LLC; Advisory Board, Bracco Group; Advisory Board, Guerbet SA; Research Grant, Nemoto Kyorindo Co, Ltd; Speakers Bureau, Bracco Group; Royalties, Wolters Kluwer nv Daniele Marin, MD, Durham, NC (*Abstract Co-Author*) Research support, Siemens AG

### PURPOSE

To determine if dual-energy CT (DECT) derived iodine quantification allows accurate characterization of indeterminate highattenuating renal lesions, and to identify technique- and patient-related variables that may influence lesion characterization.

# METHOD AND MATERIALS

220 patients with 265 high-attenuating renal lesions (mean attenuation 54 33HU; 83 malignant lesions) were included in this retrospective IRB-approved, HIPAA-compliant study. Each patient underwent a single-energy unenhanced CT followed by nephrographic phase DECT using four different state-of-the-art DECT platforms (two rapid-kV-switching DECT [rsDECT] systems and two dual-source DECT systems [dsDECT]). Quantitative iodine concentration values and conventional enhancement ( $\Delta$ HU) were calculated for each lesion. Receiver operating characteristics area under the curve (AUC) for renal lesion characterization were determined. To calculate diagnostic accuracy, surgical resection with histological workup, biopsy, and imaging follow-up for >24 months were used to determine the final category. Receiver operation characteristics, with dedicated area under the curves (AUC) were calculated to differentiate malignant from benign renal lesions. Nominal logistic regression analysis was performed to identify technique- and patient-related variables that may influence lesion characterization.

## RESULTS

Diagnostic accuracy for lesion characterization was significantly higher using  $\Delta$ HU (AUC: 0.93 with an optimal cut-off of 20HU), compared to iodine concentration values (AUC: 0.83; p<0.0001). Optimal iodine concentration thresholds were significantly different for the rsDECT system (2.0mg/ml with AUC of 0.84) compared to the dsDECT system (1.0mg/ml with an AUC of 0.87) (p<0.0001). Using the dedicated iodine thresholds resulted in 32 false positive findings and 20 false negative findings. Lesion location relative to the dual-energy field of view, patient size and DECT platform did not demonstrate any effect on lesion characterization.

### CONCLUSION

Conventional measurements of enhancement yield statistically significant higher accuracy compared to iodine concentration measurements for the characterization of indeterminate high-attenuating renal lesions.

## **CLINICAL RELEVANCE/APPLICATION**

Conventional measurements of enhancement is statistically significantly superior to iodine concentration measurements in the characterization of indeterminate high-attenuating renal lesions.

## SSC07-08 Clinical Evaluation of Virtual Unenhanced Images from Second-Generation Dual-Energy CT Gemstone Spectral Imaging

Monday, Nov. 26 11:40AM - 11:50AM Room: S503AB

### Awards

### **Student Travel Stipend Award**

Participants

Jennifer Xiao, MD, Seattle, WA (*Presenter*) Nothing to Disclose Janet M. Busey, MS, Seattle, WA (*Abstract Co-Author*) Nothing to Disclose David A. Zamora, MS, Seattle, WA (*Abstract Co-Author*) Nothing to Disclose Achille Mileto, MD, Seattle, WA (*Abstract Co-Author*) Nothing to Disclose

## For information about this presentation, contact:

jmxiao@uw.edu

### PURPOSE

To assess virtual unenhanced (VUE) images from a second-generation dual-energy CT gemstone spectral imaging (GSI) technology and to evaluate how measured attenuation compares to that from true unenhanced (TUE) images.

# METHOD AND MATERIALS

Our single-center, retrospective study was IRB-approved and HIPAA-compliant. Fifty-seven subjects (32 men, 25 women; mean age, 65 years) underwent a contrast-enhanced CT of the abdomen on a second-generation dual-energy CT GSI technology with fast kV switching (80/140 kV) between September 2017 and March 2018 for hematuria work-up (n=42) and renal mass evaluation (n=15). TUE images were acquired in all cases in single-energy mode at 120 kV. TUE and VUE images were reconstructed at a slice thickness of 2.5 mm. Attenuation values of liver, pancreas, kidneys, adrenal glands, psoas muscle, subcutaneous fat, aorta, IVC, and main portal vein were measured on TUE and VUE images. In addition, attenuation values were obtained from 24 patients with renal mass (cystic, n=5; solid, n=19). Number of renal stones detected on TUE and VUE were also recorded. Data were analyzed using a Student paired t-test.

## RESULTS

There was no significant difference in measured attenuation between TUE and VUE images throughout the abdomen (P>.05, for all comparisons). Mean attenuation values from solid and cystic renal lesions were not significantly different (TUE: 18.4 HU and 9.8 HU vs. VUE: 18.6 HU and 8 HU; P=.76 and P=.38, respectively). We observed a significant difference in number of detected renal stones between TUE (n= 21) and VUE (n= 12) images (P=.01).

## CONCLUSION

VUE images obtained from contrast-enhanced data acquired on a second-generation dual-energy CT with GSI technology represent a good approximation of TUE images for noncontrast evaluation of abdominal organs and focal renal lesions. Nevertheless, our preliminary data indicate that a considerable number of small renal stones may not be detected.

## **CLINICAL RELEVANCE/APPLICATION**

Prospective implementation of VUE images may render opportunities for decreased radiation exposure in multi-phase abdominal CT protocols for evaluation of genitourinary pathology.

## SSC07-09 Clinical Decision Algorithm for the Evaluation of Renal Cystic Lesions Using Single-Phase Split-Filter Dual-Energy CT

Monday, Nov. 26 11:50AM - 12:00PM Room: S503AB

Participants

Aurelio Cosentino, MD, Torino, Italy (*Abstract Co-Author*) Nothing to Disclose Verena Hofmann, Basel, Switzerland (*Abstract Co-Author*) Nothing to Disclose Daniel Boll, Basel, Switzerland (*Abstract Co-Author*) Nothing to Disclose Benjamin M. Yeh, MD, San Francisco, CA (*Abstract Co-Author*) Research Grant, General Electric Company; Consultant, General Electric Company; Author with royalties, Oxford University Press; Shareholder, Nextrast, Inc; Research Grant, Koninklijike Philips NV; Research Grant, Guerbet SA; ; Matthias Benz, MD, Basel, Switzerland (*Abstract Co-Author*) Nothing to Disclose Markus M. Obmann, MD, San Francisco, CA (*Presenter*) Nothing to Disclose

## For information about this presentation, contact:

Markus.Obmann@usb.ch

## PURPOSE

To evaluate the diagnostic performance of single source split-filter dual energy CT (tbDECT) to exclude enhancement in renal cystic lesions at venous phase abdominal CT.

## METHOD AND MATERIALS

A total of n=230 simple or minimally complicated renal cysts were identified in n=51 consecutive patients who underwent both abdominal tbDECT and magnetic resonance (MR) examination; the latter was used as the 'gold standard' to classify the cysts as Bosniak I or Bosniak II. Material decomposition images were processed off of venous phase series and regions of interest (ROI) were placed within each cystic lesion, blindly to MR. For each ROI, four parameters were assessed simultaneously (Virtual Unenhanced attenuation values [HU], contrast enhancement attenuation values [HU], iodine density [mg/dl] and ROI size [cm2]) to test different approaches for lesion characterization. Renal cysts were considered as not enhancing if contrast enhancement (CM) <= 10 HU and iodine density (IOD) <= 0.5 mg/dl. The ROI was considered small if size <= 0.2 cm2.

## RESULTS

Using MR n=207 Bosniak I and n=23 Bosniak II cysts were identified. At virtual unenhanced images, 48% of the cysts were not hypodense (> 10 HU). Both CM and IOD alone gave high percentages of pseudoenhancement (false positive 47% and 33% respectively). The combination of criteria (IOD first then CM) improved specificity to 79%. Exclusion of small ROIs reduced false positives to 3%. An algorithm for the exclusion of enhancement, combining all the criteria, was created.

## CONCLUSION

The combined evaluation of multiple criteria provided by tbDECT correctly characterizes Bosniak I and II renal cysts as not enhancing, reduces false positive findings and potentially avoids unnecessary work-ups. We propose an algorithm that can be easily implemented in clinical practice.

# **CLINICAL RELEVANCE/APPLICATION**

Excluding enhancement in renal cystic lesions with 97% of specificity, applying an easy to use algorithm on single-phase dualenergy images from single source, split-filter twin-beam dual-energy CT.



### SSC08

Health Service, Policy and Research (Education Research)

Monday, Nov. 26 10:30AM - 12:00PM Room: S104A



AMA PRA Category 1 Credits ™: 1.50 ARRT Category A+ Credit: 0

### **Participants**

Aran M. Toshav, MD, New Orleans, LA (*Moderator*) Speakers Bureau, Koninklijke Philips NV Marc H. Willis, MMM,DO, Houston, TX (*Moderator*) Investor, Resonea

## Sub-Events

# SSC08-01 An Analysis of Three Years of Continuing Medical Education Exercises in the Journal 'Radiology': We Aren't Following the Rules... Even Our Own

Monday, Nov. 26 10:30AM - 10:40AM Room: S104A

Participants David J. DiSantis, MD, Jacksonville, FL (*Presenter*) Nothing to Disclose Dana E. Amiraian, MD, Jacksonville, FL (*Abstract Co-Author*) Nothing to Disclose Andres R. Ayoob, MD, Lexington, KY (*Abstract Co-Author*) Nothing to Disclose

## For information about this presentation, contact:

djdisantis@gmail.com

## PURPOSE

To analyze the multiple choice questions (MCQ) in three years of *Radiology* CME exercises with regard to: adherence to accepted MCQ question-writing tenets comportment with the journal's own 'CME Question Writing Guideline' for its authors.

## METHOD AND MATERIALS

308 multiple choice questions in *Radiology* CME exercises from 2015 through 2017 comprised the test group. They were analyzed by the three authors for: adherence to standard, validated question-writing tenets, such as those promulgated by the American Board of Radiology compliance with the 'CME Question-Writing Guideline' provided by the journal to its authors Test items that violated the question-writing tenets/guidelines were designated as flawed.

### RESULTS

Of the 308 questions, 174 (56%) contained from one to four item-writing flaws. The most frequent flaws were: an unfocused question stem a negative question stem heterogeneous answer options. The adherence to guidelines in the CME examinations varied widely, ranging from zero flawed items, to 10 of 10 flawed items. There was no pattern of improvement over the time frame of the study.

### CONCLUSION

In our specialty's most prestigious journal, more than half of the self-assessment CME questions do not follow standard, validated question-writing tenets, and do not comport with the journal's own guidelines for its authors.

## **CLINICAL RELEVANCE/APPLICATION**

Our results should prompt a relook at the process of *Radiology*'s self-assessment CME exam creation, and in particular opportunities for author training to bolster test validity.

### **Honored Educators**

Presenters or authors on this event have been recognized as RSNA Honored Educators for participating in multiple qualifying educational activities. Honored Educators are invested in furthering the profession of radiology by delivering high-quality educational content in their field of study. Learn how you can become an honored educator by visiting the website at: https://www.rsna.org/Honored-Educator-Award/ David J. DiSantis, MD - 2014 Honored Educator

# SSC08-02 A Metrics-Based Model For Allocating Research Protected Time and Salary Awards Significantly Increase Publication Productivity in an Academic Radiology Department

Monday, Nov. 26 10:40AM - 10:50AM Room: S104A

Participants

Leonid Chepelev, MD, PhD, Ottawa, ON (*Abstract Co-Author*) Nothing to Disclose Frank J. Rybicki III, MD, PhD, Ottawa, ON (*Abstract Co-Author*) Medical Director, Imagia Cybernetics Inc Nicola Schieda, MD, Ottawa, ON (*Abstract Co-Author*) Nothing to Disclose Matthew D. McInnes, MD, PhD, Ottawa, ON (*Abstract Co-Author*) Nothing to Disclose Kawan S. Rakhra, MD, Ottawa, ON (*Presenter*) Nothing to Disclose

### For information about this presentation, contact:

## krakhra@toh.ca

### PURPOSE

To determine whether a quantitative model for evaluating research productivity and distributing research salary awards with protected time increased the publication productivity of an academic radiology department.

## METHOD AND MATERIALS

A metrics based, research protected time (RPT) model awarding research salary awards with protected time was designed through a tripartite consensus process between the Departmental Academic Chair, Faculty Radiologists and Radiologist practice plan, first implemented in January 2010. A retrospective analysis was performed tabulating all unique PubMed indexed publications by Department Faculty members between January 1, 2003 and December 31, 2017 by calendar year. The annual publication productivity for the Department was compared between the non-RPT period (January 1, 2003 to December 31, 2009) and RPT-period (January 1, 2010 to December 31, 2017), in absolute numbers and also normalized to the radiologist FTE (full time equivalent) count. A sub-analysis of those faculty members who had both RPT and non-RPT status years during the period of evaluation was also performed comparing the productivity between the two statuses. Statistical analysis employed paired t-test, with level of significance set at 0.05. The proportion of publications from those in the RPT program was calculated.

### RESULTS

There was significantly greater annual departmental publication productivity in the RPT versus the non-RPT periods, in absolute numbers (75.1 vs 18.4, p=0.007) and also when normalized to FTE count (1.55 vs 0.50, p=0.004). Twenty-three faculty members were identified as having both RPT and non-RPT years during the period of evaluation. There was significantly higher mean annual publication productivity during their RPT versus their non-RPT years (5.1 vs 1.3, p=0.011). On average, 62% of annual unique publications were from faculty members with RPT, although the RPT faculty members comprised only 26% of the overall faculty membership.

## CONCLUSION

The implementation of the RPT program with funded protected time led to a significant increase in departmental publication productivity. At the individual level, faculty members' productivity was significantly greater during the years in which they received RPT.

## **CLINICAL RELEVANCE/APPLICATION**

Models of funded research time with quantitative measure of publication output should be considered in academic departments wishing to increased their publication productivity.

### **Honored Educators**

Presenters or authors on this event have been recognized as RSNA Honored Educators for participating in multiple qualifying educational activities. Honored Educators are invested in furthering the profession of radiology by delivering high-quality educational content in their field of study. Learn how you can become an honored educator by visiting the website at: https://www.rsna.org/Honored-Educator-Award/ Frank J. Rybicki III, MD, PhD - 2016 Honored Educator

## SSC08-03 Mentorship Matters: A Call for More Effective Mentorship Programs for Early-Career Radiologists

Monday, Nov. 26 10:50AM - 11:00AM Room: S104A

Participants

Amy K. Patel, MD, Boston, MA (*Presenter*) Nothing to Disclose Andrew B. Rosenkrantz, MD, New York, NY (*Abstract Co-Author*) Nothing to Disclose Katarzyna J. Macura, MD, PhD, Baltimore, MD (*Abstract Co-Author*) Author with royalties, Reed Elsevier; Research Grant, Profound Medical Inc; Research Grant, GlaxoSmithKline plc; Research Grant, Siemens AG Jay R. Parikh, MD, Houston, TX (*Abstract Co-Author*) Nothing to Disclose

For information about this presentation, contact:

amykpatel64112@gmail.com

## PURPOSE

To assess early-career radiologists' satisfaction with their professional mentorship, as well as to gain insights into the design of future mentorship programs.

## **METHOD AND MATERIALS**

A 10-question survey was distributed by email in September 2017 to a random sample of 2,000 practicing radiologists who are members of the Young and Early-Career Professionals Section (YPS), which includes radiologists who are either under age 40 or within their first 8 years of practice. The survey was designed by the ACR YPS Executive Committee and the ACR Commission for Women and Diversity. Survey questions addressed respondents' satisfaction with their current mentorship and preferences for subsequent mentorship opportunities.

#### RESULTS

Responses included 51% male, 49% female; 37% academic, 35% private practice, 14% hospital employed. 69% responded that their practice did not have a formal mentoring program. Of those with a formal mentoring program, 47% were not satisfied with the program, and an additional 21% were only somewhat satisfied. 44% of respondents reported having no mentor, and 21% had a single mentor. 78.09% responded that having a mentor would be valuable, very valuable, or extremely valuable. A mentor was described as extremely valuable by 39% of women, vs. 14% of men. Having a mentor of the same gender was described as extremely or very valuable by 44% of women vs. only 5% of men. When asked what are the most valuable characteristics of a mentor, the highest rated options were: (1) greater level of experience, (2) same subspecialty, (3) same practice type, and (4) national reputation. Respondents felt overall more strongly that mentors be able to serve as advocates for career growth outside of, rather than within, the mentee's own institution.

## CONCLUSION

Early-career radiologists commonly lacked a formal mentor or were unsatisfied with their mentor, and strongly desired greater mentorship opportunities; women radiologists more strongly expressed this desire. Radiologists generally desired an experienced mentor of a similar subspecialty and practice type who could facilitate their growth beyond the local institution.

## **CLINICAL RELEVANCE/APPLICATION**

More robust mentorship programs are needed to combat burnout, promote job satisfaction, and foster the professional development and career success of the next generation of radiologists.

### **Honored Educators**

Presenters or authors on this event have been recognized as RSNA Honored Educators for participating in multiple qualifying educational activities. Honored Educators are invested in furthering the profession of radiology by delivering high-quality educational content in their field of study. Learn how you can become an honored educator by visiting the website at: https://www.rsna.org/Honored-Educator-Award/ Katarzyna J. Macura, MD, PhD - 2012 Honored EducatorKatarzyna J. Macura, MD, PhD - 2014 Honored Educator

# SSC08-04 May I Please Speak with the Radiologist: Introducing First Year Radiology Residents to Their Consultant Role

Monday, Nov. 26 11:00AM - 11:10AM Room: S104A

Participants Karla A. Sepulveda, MD, Houston, TX (*Presenter*) Nothing to Disclose Marc H. Willis, MMM,DO, Houston, TX (*Abstract Co-Author*) Investor, Resonea

### For information about this presentation, contact:

kasepulv@bcm.edu

### PURPOSE

An education portal with case vignettes of common clinical scenarios a first year radiology resident may be consulted on was created to assist in the transition to their new role as consultants on appropriate imaging ordering. The portal emphasizes concepts of evidence based imaging utilization, patient safety and patient centered care.

### **METHOD AND MATERIALS**

A web based education portal with 20 vignettes of common clinical scenarios seen in an emergency room was created. Residents were asked to select the most appropriate imaging for the given clinical history. The questions incorporated clinical decision support technology with integrated ACR Appropriateness Criteria to provide evidence based recommendations for imaging indications. Radiation safety, IV contrast and cost questions were also included. The module ended with 2 open ended questions asking learners how they would manage clinical scenarios requiring interactions with referring clinicians, patients, and patient's family. The 12 residents participated in the pilot during their first week of residency. Following an introductory lecture highlighting concepts of high value, patient-centered care, residents took the self directed module in a virtual classroom. Residents then returned for a debrief session that included a patient discussing her perspective on radiologist communication, review of the responses to the open ended questions, and a qualitative post-assessment.

## RESULTS

The portal was well received. 90% of participants believed the module should be included in an introductory curriculum for radiology residents. 80% thought the patient centered cases and patient discussion helped them to be more aware of the patient perspective. The majority of the residents reported increased comfort level in consultation regarding appropriate imaging, IV contrast, radiation exposure, cost of imaging and patient safety following the module.

## CONCLUSION

A web based education module with integrated clinical decision support is an innovative approach to introducing first year radiology residents to their new role as consultants on high quality appropriate imaging. The portal reinforces imporant medical education concepts and encompasses multiple ACGME competencies.

## **CLINICAL RELEVANCE/APPLICATION**

High value, patient-centered care can be emphasized with incoming first year radiology residents by a web based education module with integrated clinical decision support.

# SSC08-05 The "Look Ahead" Technique: A Novel Way to Engage Medical Students in the Reading Room with Minimal Disruption to the Preceptor's Workflow

Monday, Nov. 26 11:10AM - 11:20AM Room: S104A

Participants Jennifer Huang, MD, Greensboro, NC (*Presenter*) Nothing to Disclose Brian Bingham, MD, Nashville, TN (*Abstract Co-Author*) Nothing to Disclose Martin I. Jordanov, MD, Nashville, TN (*Abstract Co-Author*) Nothing to Disclose

### For information about this presentation, contact:

j.huang002@gmail.com

### PURPOSE

Engaging medical students during a Radiology course can be challenging. We sought a way to actively engage students with live cases, allow them to interact with the PACS workstation, and experience what it is like to be a radiologist. This educational model has not been studied before.

## **METHOD AND MATERIALS**

All medical students enrolled in Diagnostic Radiology or Medical Imaging and Anatomy course at our institution between May 2016 and June 2017 were eligible. The "Look Ahead" technique is as follows: during a routine read-out, a preceptor identifies several nonurgent imaging studies and allows the students to look at the images first and make their own findings and conclusions. When ready, the students present their findings, discuss the case, and observe the preceptor generate a final report. Students were emailed a post-course survey to compare the "Look Ahead" technique with the current standard (observing a preceptor interpret imaging studies with accompanying teaching points).

### RESULTS

Thirty-four (56.7%) of 60 potential respondents completed the post-course survey. Of these 34 students, 24 (70.6%) reported at least one reading room case (mean 4.6) in which they had the opportunity to employ the technique with a mean of 2.4 unique preceptors. When compared to the current standard (0=not to 100=very interested/engaged/valuable/memorable), the 'Look Ahead' technique was associated with increased student-reported interest (92.5 vs 75.1, p<0.01), engagement (94.0 vs 70.3, p<0.01), educational value (92.5 vs 73.2, p<0.01), memorability of the case (88.5 vs 73.2, p<0.01) and of teaching points made by the preceptor (90.1 vs 76.7, p<0.01). All students agreed that compared to the current standard, the 'Look Ahead' technique increased their confidence in reviewing and interpreting imaging studies.

### CONCLUSION

The findings suggest that students benefit significantly from the 'Look Ahead' technique, with increased interest, engagement, educational value, and memorability. The potential benefits warrant further investigation on a grander scale, with greater faculty and student involvement. It would be interesting to investigate if there are any longer term effects of this technique on student performance or career choice.

## **CLINICAL RELEVANCE/APPLICATION**

The "Look Ahead" technique of medical student instruction in the radiology reading room promotes active student engagement with minimal disruption to the preceptor's workflow.

# SSC08-06 Beyond Cadaveric Dissection: Through Virtual Dissection, Radiology Adds Educational Value to Medical Undergraduate Anatomy Education

Monday, Nov. 26 11:20AM - 11:30AM Room: S104A

#### Awards

### **Trainee Research Prize - Resident**

Participants

Kathryn Darras, MD, Vancouver, BC (*Presenter*) Education Advisory Committee, Sectra AB Rebecca Spouge, Vancouver, BC (*Abstract Co-Author*) Nothing to Disclose Anique de Bruin, Maastricht, Netherlands (*Abstract Co-Author*) Nothing to Disclose Jeroen van Merrienboer, Maastricht, Netherlands (*Abstract Co-Author*) Nothing to Disclose Savvas Nicolaou, MD, Vancouver, BC (*Abstract Co-Author*) Institutional research agreement, Siemens AG Rose Hatala, Vancouver, BC (*Abstract Co-Author*) Nothing to Disclose Bruce B. Forster, MD, Vancouver, BC (*Abstract Co-Author*) Stockholder, Canada Diagnostic Centres

## PURPOSE

Virtual dissection is performed with CT scans on near life-size anatomy visualization tables, which function like touchscreen PACS workstations. Students work together to manipulate the data and perform their dissection. The purpose of this study was to develop and qualitatively assess the educational value of virtual dissection laboratories for first year medical students as well as to understand students' preferred pedagogical approaches for learning from this new technology.

### **METHOD AND MATERIALS**

Following IRB approval, all first year medical students were included in this study (n = 292). A Basic Virtual Dissection Curriculum focused on normal anatomy was offered to all students concurrently with their cadaveric laboratories and an extra-curricular Advanced Virtual Dissection Curriculum focused on pathology was offered to interested students. 36.6% of students participated in this Advanced Curriculum. Following the sessions, students were surveyed to determine their attitude toward virtual dissection and the pedagogical approaches they perceived to be the most useful for learning with this technology. Results were statistically analyzed using the Schulze method.

### RESULTS

Student response rate was 69.2% for the Basic Curriculum and 82.9% for the Advanced Curriculum. 93.1% indicated that virtual dissection was 'definitely' a valuable addition to the anatomy lab. 88.5% of respondents 'agreed' or 'strongly agreed' that virtual dissection improved their understanding of disease and 94.2% of students 'agreed' or 'strongly agreed' that it improved their understanding of the role of the radiologist in patient care. Students reported that the aortic aneurysm case was the most memorable case because the imaging made it easier to understand the pathogenesis of the disease. Students felt that small group demonstration and problem-based learning would be the best teaching approaches for this technology.

# CONCLUSION

Virtual dissection adds value to medical undergraduate anatomy teaching by increasing students' understanding of the clinical relevance of anatomy. Students' preferred pedagogical approaches for learning from this technology were small group demonstration and problem based-learning.

## **CLINICAL RELEVANCE/APPLICATION**

Virtual dissection is a new technology that can be used provide formal radiology teaching to medical students and thereby increase their awareness of the speciality.

# SSC08-07 Evidence of Gender Bias in Recommendation Letters for Women in Radiology: Are We There Yet?

# Participants

Alejandra Duarte, MD, New York, Colombia (*Abstract Co-Author*) Nothing to Disclose Jenny T. Bencardino, MD, Lake Success, NY (*Presenter*) Nothing to Disclose Christine M. Glastonbury, MBBS, San Francisco, CA (*Abstract Co-Author*) Author with royalties, Reed Elsevier Zehava S. Rosenberg, MD, New York, NY (*Abstract Co-Author*) Nothing to Disclose Mauricio Castillo, MD, Chapel Hill, NC (*Abstract Co-Author*) Nothing to Disclose

### For information about this presentation, contact:

jenny.bencardino@nyumc.org

## PURPOSE

To evaluate for gender bias language used in recommendation letters written for women trainees and faculty seeking to be hired in academic or clinical positions, promotion or professional society membership

## **METHOD AND MATERIALS**

109 letters written by 4 senior academic radiologists (1 man, 3 women) were independently assessed by 2 reviewers. The quality of the letters was scored using the University of Arizona Commission on the Status of Women (UA CSW) guidelines. Positive 1 point qualifiers included: mention of research, mention of publications, more than 1 page length, use of adjectives that emphasize accomplishments and ability, and use of adjectives that denote leadership. Negative 1 point qualifiers included the use of adjectives that evoke gender stereotypes and emphasize effort, mention personal life, and express doubt. Using these guidelines, a ranking system was created with letters classified as excellent (4-5); very good (3-4); good(2-3); fair(0-2); and poor(<0). Other positive adjectives not included in the UA CSW were recorded. Positive1 point qualifier adjectives used more than 5 times in this collection of letters were added to a revised scoring system

### RESULTS

The average score using the UA CSW guidelines was good (2.5). There was no significant difference between those letters written by the only male (56) versus female letter writers (53) (M: 2.5; W: 2.4). 81% mentioned publications while only 60% mentioned research involvement. 70% of letters contained adjectives that emphasized accomplishments and ability but only 17% used adjectives that denote leadership. In one-fifth of the letters, adjectives that denoted gender stereotype were used. When using a modified scoring system, the average score rose to very good (3.2). Again, no gender difference was noted between man (3.2) versus women (3.2) letter writers using the revised scoring system.

## CONCLUSION

In our preliminary sample, gender bias language was found in 21% of the letters written for women by senior faculty members without distinction of the writer's gender. Only 60% mentioned research and only 14% included leadership qualifiers. We encourage academic faculty to keep handy guidelines to write persuasive and gender bias-free letters for their women trainees and colleagues.

### **CLINICAL RELEVANCE/APPLICATION**

Based on preliminary results, we developed modified UA CSW guidelines that aim to help writing persuasive, gender-bias free letters for women radiologists.

## **Honored Educators**

Presenters or authors on this event have been recognized as RSNA Honored Educators for participating in multiple qualifying educational activities. Honored Educators are invested in furthering the profession of radiology by delivering high-quality educational content in their field of study. Learn how you can become an honored educator by visiting the website at: https://www.rsna.org/Honored-Educator-Award/ Jenny T. Bencardino, MD - 2014 Honored EducatorZehava S. Rosenberg, MD - 2014 Honored Educator

## SSC08-08 Appearance-Based Discrimination in Radiology Resident Selection

Monday, Nov. 26 11:40AM - 11:50AM Room: S104A

Participants

Charles M. Maxfield, MD, Durham, NC (*Presenter*) Nothing to Disclose Matthew P. Thorpe, MD, PhD, Savoy, NC (*Abstract Co-Author*) Nothing to Disclose Terry S. Desser, MD, Stanford, CA (*Abstract Co-Author*) Nothing to Disclose Darel E. Heitkamp, MD, Indianapolis, IN (*Abstract Co-Author*) Nothing to Disclose Nathan C. Hull, MD, Rochester, MN (*Abstract Co-Author*) Nothing to Disclose Lars J. Grimm, MD, Durham, NC (*Abstract Co-Author*) Editorial Advisory Board, Medscape, LLC; Educational program support, Hologic, Inc Karen S. Johnson, MD, Durham, NC (*Abstract Co-Author*) Nothing to Disclose Nicholas A. Koontz, MD, Salt Lake City, UT (*Abstract Co-Author*) Nothing to Disclose Gary W. Mlady, MD, Albuquerque, NM (*Abstract Co-Author*) Nothing to Disclose Timothy Welch, MD, Rochester, MN (*Abstract Co-Author*) Nothing to Disclose

For information about this presentation, contact:

charles.maxfield@duke.edu

### PURPOSE

To evaluate for discrimination in radiology resident selection based on the physical appearance of the applicant.

### **METHOD AND MATERIALS**

We carried out a simulated resident selection process utilizing deception of reviewers. Seventy-four core faculty (37 male and 37 female) from five academic radiology departments reviewed mock residency applications under the guise of resident application screening. Applications included demographic information and a photograph, representing a spectrum of facial attractiveness and

obesity, combined with randomized academic and supporting variables. Reviewers independently scored applications on their desirability for interview. Comparisons were made between reviewer scores and the application variables using linear mixed fixed and random effects models.

## RESULTS

Reviewers evaluated 5447 applications (mean: 74 applications per reviewer). The applicant's facial attractiveness strongly predicted reviewer rating (attractive versus unattractive,  $B = 0.30 \pm \text{standard error } 0.056$ ); neutral versus unattractive,  $B = 0.13 \pm 0.028$ ). Obesity (versus not obese) was less influential but predictive of rating ( $B = -0.14 \pm 0.024$ ). Overall, United States Medical Licensing Examination Step 1 scores were the strongest predictor of reviewer rating ( $B = 0.49 \pm 0.030$ ). Less influential but still significant predictors included preclinical class rank ( $B = 0.25 \pm 0.040$  for 1st vs. 3rd quartile), clinical clerkship grades ( $B = 0.23 \pm 0.034$  for top vs. bottom tertile), race/ethnicity ( $B = 0.25 \pm 0.059$  for black/Hispanic vs. white), and Alpha Omega Alpha membership ( $B = 0.21 \pm 0.032$ ). Using the 85th percentile of reviewer rating as a cutoff for projected interview selection, 90% of obese and facially unattractive applicants would be rejected, compared to only 76% of non-obese facially attractive applicants (p<0.01).

## CONCLUSION

Our study provides evidence of discrimination against obese and facially unattractive applicants in admissions to radiology residency programs. Notably, obesity and facial attractiveness were as influential in the selection of applicants for interview as were well-established academic factors.

## **CLINICAL RELEVANCE/APPLICATION**

Resident selection committees should invoke strategies to detect and manage appearance-based bias

## SSC08-09 Structured Tool for Screening Candidates for Academic Neuroradiology Faculty Positions

Monday, Nov. 26 11:50AM - 12:00PM Room: S104A

Participants

Maria Braileanu, MD, Atlanta, GA (*Presenter*) Nothing to Disclose Nadja Kadom, MD, Atlanta, GA (*Abstract Co-Author*) Nothing to Disclose Mark E. Mullins, MD,PhD, Atlanta, GA (*Abstract Co-Author*) Nothing to Disclose Benjamin Risk, Atlanta, GA (*Abstract Co-Author*) Nothing to Disclose Elizabeth A. Krupinski, PhD, Atlanta, GA (*Abstract Co-Author*) Nothing to Disclose Amit M. Saindane, MD, Decatur, GA (*Abstract Co-Author*) Nothing to Disclose Brent D. Weinberg, MD, PhD, Atlanta, GA (*Abstract Co-Author*) Nothing to Disclose

## PURPOSE

Interview selection of candidates for an academic radiology faculty position is variable and subject to unconscious biases, such as gender and race. The purpose of this study was to retrospectively apply a quantitative resume rubric as a screening tool to identify qualified candidates for an interview in the hiring process.

## METHOD AND MATERIALS

All resumes from 2012 to 2017 for a total of 8 neuroradiology faculty positions at our institution were collected and anonymized. One blinded reviewer scored the resumes based on categories that included: education (board certification, medical school ranking, residency ranking, fellowship years, degrees), work experience (years), extracurricular experience (leadership, societies, committees, teaching, honors, volunteerism), and research (abstracts, oral presentations, manuscripts, chapters). Maximum total score was 24 points. The relationship between 1) resume score and interview status, and 2) resume score and job offer was examined using logistic regression. Non-parametric ROC analysis based on resume score and job offer was performed using STATA. This study was IRB exempted.

## RESULTS

102 anonymized resumes were scored. The overall mean was  $13.6\pm3.8$  with a range of 5-22. A total of 17 interviews were conducted and 10 candidates were eventually offered a position. Higher resume score significantly increased the likelihood of an interview (p=0.02) but was not significantly associated with a job offer (p=0.07). The area under the curve in the ROC analysis for differentiating interview selection based on resume scoring was 0.69 (95%CI 0.56-0.82). At a cutoff of 14, the model is 82.4% sensitive, and 54.1% specific.

## CONCLUSION

We demonstrated that standardized scoring of resumes as an initial screening tool in the hiring process is feasible. A higher resume score was associated with interview selection. This tool can potentially be applied in the future to reduce unwanted bias in the hiring process as it is neutral to factors such as gender and race.

## **CLINICAL RELEVANCE/APPLICATION**

Standardized resume screening is feasible, with a higher score associated with interview selection in retrospective analysis, and may be applied in the future to reduce unwanted bias in the initial steps of the hiring process.

### **Honored Educators**

Presenters or authors on this event have been recognized as RSNA Honored Educators for participating in multiple qualifying educational activities. Honored Educators are invested in furthering the profession of radiology by delivering high-quality educational content in their field of study. Learn how you can become an honored educator by visiting the website at: https://www.rsna.org/Honored-Educator-Award/ Elizabeth A. Krupinski, PhD - 2017 Honored Educator



### SSC09

## Science Session with Keynote: Informatics (Artificial Intelligence in Radiology: Bleeding Edge)

Monday, Nov. 26 10:30AM - 12:00PM Room: E450A



AMA PRA Category 1 Credits ™: 1.50 ARRT Category A+ Credit: 1.75

**FDA** Discussions may include off-label uses.

### Participants

George L. Shih, MD, MS, New York, NY (*Moderator*) Consultant, Image Safely, Inc; Stockholder, Image Safely, Inc; Consultant, MD.ai, Inc; Stockholder, MD.ai, Inc;

Ronald M. Summers, MD, PhD, Bethesda, MD (*Moderator*) Royalties, iCAD, Inc; Royalties, Koninklijke Philips NV; Royalties, ScanMed, LLC; Research support, Ping An Insurance Company of China, Ltd; Researcher, Carestream Health, Inc; Research support, NVIDIA Corporation; ; ; ;

Safwan Halabi, MD, Stanford, CA (Moderator) Nothing to Disclose

## Sub-Events

# SSC09-01 Informatics Keynote Speaker: Bleeding Edge Medical AI

Monday, Nov. 26 10:30AM - 10:40AM Room: E450A

Participants

Ronald M. Summers, MD, PhD, Bethesda, MD (*Presenter*) Royalties, iCAD, Inc; Royalties, Koninklijke Philips NV; Royalties, ScanMed, LLC; Research support, Ping An Insurance Company of China, Ltd; Researcher, Carestream Health, Inc; Research support, NVIDIA Corporation; ;; ;

# SSC09-02 Relationship Learning and Organization of Significant Radiology Image Findings for Lesion Retrieval and Matching

Monday, Nov. 26 10:40AM - 10:50AM Room: E450A

#### Awards

### **Trainee Research Prize - Fellow**

Participants Ke Yan, Bethesda, MD (*Presenter*) Nothing to Disclose Xiaosong Wang, PhD, Bethesda, MD (*Abstract Co-Author*) Nothing to Disclose Le Lu, Bethesda, MD (*Abstract Co-Author*) Employee, NVIDIA Corporation Ling Zhang, Bethesda, MD (*Abstract Co-Author*) Nothing to Disclose Adam P. Harrison, PhD, Bethesda, MD (*Abstract Co-Author*) Nothing to Disclose Mohammad Hadi Bagheri, MD, Bethesda, MD (*Abstract Co-Author*) Nothing to Disclose Ronald M. Summers, MD,PhD, Bethesda, MD (*Abstract Co-Author*) Nothing to Disclose Ronald M. Summers, MD,PhD, Bethesda, MD (*Abstract Co-Author*) Royalties, iCAD, Inc; Royalties, Koninklijke Philips NV; Royalties, ScanMed, LLC; Research support, Ping An Insurance Company of China, Ltd; Researcher, Carestream Health, Inc; Research support, NVIDIA Corporation; ; ; ;

### For information about this presentation, contact:

yankethu@foxmail.com

### PURPOSE

Radiologists mark and measure significant image findings in their daily work to assess patients' conditions and therapy responses. These large-scale and diverse clinical annotations can be great data sources to train data-hungry algorithms (e.g. deep learning) for medical image analysis. However, they are basically unsorted and lack semantic annotations like the lesion type and location. We aim to organize and explore them by learning a deep feature embedding for each lesion. It can help us to 1) know their types and locations; 2) find similar lesions in different patients, i.e. content-based lesion retrieval; and 3) find similar lesions in the same patient, i.e. lesion matching across scans for disease tracking.

### **METHOD AND MATERIALS**

We built a large-scale and comprehensive dataset, DeepLesion, by mining the PACS. It contains 32,735 lesions from 10,594 CT studies of 4,427 patients. The lesions are quite diverse, and include e.g. lung nodules, liver lesions, adenopathy, and bone lesions. The train/val/test sets have 70%, 15%, 15% of the data split in patient level. We learn a feature embedding for each lesion that keeps the similarity relationship of the type, location, and size, i.e. lesions with similar attributes should have similar embeddings. We get the lesion types and locations by label propagation and self-supervised body-part regression. Size is directly obtained from the radiological marking. A triplet network with a sequential sampling strategy is utilized to learn the embedding. The network is a multiscale multi-crop convolutional neural network that can exploit both context and detail of the lesion images. The learned embeddings can be applied in lesion retrieval and matching by nearest neighbor searching.

### RESULTS

In the test set of DeepLesion, we achieve 91.5±0.1%, 92.8±0.0%, and 94.9±0.0% accuracy in lesion retrieval w.r.t. the lesions'

type, location, and size, respectively. The area-under-curve value for lesion matching is 95.9% in a manually labeled test set of 1313 lesions from 103 patients.

## CONCLUSION

We proposed an algorithm to learn feature embeddings for a variety of lesions to encode their type, location, and size. Experiments showed its effectiveness in lesion retrieval and matching.

## **CLINICAL RELEVANCE/APPLICATION**

The proposed algorithm can be used in content-based lesion retrieval and intra-patient lesion matching, which can help radiologists find similar lesions and track lesions in follow-up studies.

# SSC09-03 Multi-Stage Deep Disassembling Networks for Generating Bone-Only and Tissue-Only Images from Chest Radiographs

Monday, Nov. 26 10:50AM - 11:00AM Room: E450A

Participants

Jaehong Aum, Seoul, Korea, Republic Of (*Presenter*) Employee, Lunit Inc Sunggyun Park, Seoul, Korea, Republic Of (*Abstract Co-Author*) Employee, Lunit Inc Donggeun Yoo, Seoul, Korea, Republic Of (*Abstract Co-Author*) Employee, Lunit Inc Chang Min Park, MD, PhD, Seoul, Korea, Republic Of (*Abstract Co-Author*) Nothing to Disclose Eui Jin Hwang, Seoul, Korea, Republic Of (*Abstract Co-Author*) Nothing to Disclose

## For information about this presentation, contact:

sgpark@lunit.io

## CONCLUSION

Deep neural network based automatic disassembling network for CRs is demonstrated and its performance is validated by SSIM proving its potential to improve interpretability of CRs and aid pysicians for accurate diagnosis.

### Background

Dual-energy subtraction technique produces bone-only and tissue-only images to improve interpretability of chest radiographs (CRs). However, the use of this technique was limited because it requires a specialized hardware device for capturing the CRs. In order to overcome this limitation, we developed a deep disassembling networks for CRs (DDCN) which generates bone-only and tissue-only images from a normal CR.

## **Evaluation**

To develop DDCN, we collected a total of 617 CRs with both bone-only and tissue-only images, which were produced by dual energy subtraction technique. To clean the dataset, we excluded 100 cases with suboptimal image quality. Furthermore, we refined the remaining 517 cases using guided filter and non-local means filter to remove image noises. Subsequently, we randomly divided the 517 datasets into the training dataset (n=467) and validation dataset (n=50). We designed a novel two-stage deep convolutional network where the first-stage is designed for observing context of a CR and the second-stage is for producing bone-only and tissue-only images given the first-stage output. The network is constructed with residual architecture, 40 convolutions for the first-stage and 14 convolutions for the second-stage. We quantitatively measured the performance of our network using SSIM which measures the structure difference between a given ground truth image and our network-producing image. In validation dataset, the measured SSIM comparing ground truth tissue-only images and our network-producing results was 0.9678. When we limit the region of interest (ROI) as lung area, the SSIM was measured as 0.9835. In the case of bone-only image, it was 0.9877 and 0.9870 when we limit ROIs as whole image and lung area, respectively.

### Discussion

DDCN produces bone-only and tissue-only images from CRs taken by conventional X-ray device. We believe it is the first introduction of deep neural network for disassembling bone and tissue from a CR.

## SSC09-04 Non-invasive Tracking of Cancer Evolution using Deep Learning-Based Longitudinal Image Analysis

Monday, Nov. 26 11:00AM - 11:10AM Room: E450A

Participants

Yiwen Xu, PhD, Boston, MA (*Presenter*) Nothing to Disclose Ahmed Hosny, MSc, Cambridge, MA (*Abstract Co-Author*) Nothing to Disclose Thibaud Coroller, MS, Boston, MA (*Abstract Co-Author*) Nothing to Disclose Roman Zeleznik, Boston, MA (*Abstract Co-Author*) Nothing to Disclose Raymond H. Mak, MD, Boston, MA (*Abstract Co-Author*) Nothing to Disclose Hugo Aerts, PhD, Boston, MA (*Abstract Co-Author*) Stockholder, Sphera Inc

## PURPOSE

Tumors are continuously evolving biological systems, and medical imaging is uniquely poised to monitor those changes in patients, before, during, and after treatment. While it is trivial to track tumor lesions over space and time, it is much harder to develop models encompassing all the time points. Here we investigated the use of recurrent deep learning network capable of analysing time series CT images of locally advanced non-small cell lung cancer (NSCLC) patients.

## **METHOD AND MATERIALS**

Dataset A consists of 179 stage III NSCLC patients treated with definitive radiation therapy (581 scans, mean 3.2 scans per patient). This dataset was separated into independent training/tuning (n=107), and test (n=72) cohorts. Transfer learning through convolutional neural networks (CNN) merged with a recurrent neural network was trained on serial scans. Survival was analyzed for a separate test set with AUC and Kaplan Meier curves. Further pathologic response validation of the CNN model was performed on Dataset B (n=79 patients, 158 scans, 2 per patient) treated with chemoradiation followed by surgery. This cohort was used to

validate pathological tumor response and compared to performance with volume change.

## RESULTS

Enhanced performance on the test set was observed with the addition of each follow-up scan into the CNN model for 2-year survival (AUC=0.64, 0.69, 0.74, p<0.05), comporable results were demonstrated for one-year survival. The models with 3 follow-up scans showed strong stratification power for high and low risk groups of the predictions using Kaplan-Meier analysis (Log-rank, p<0.05). The hazard ratios for the one-year and 2-year survival models were 6.16 and 2.38, respectively (p<0.05). The CNN model significantly stratified pathological responders and cases of gross residual disease in Dataset B (AUC=0.65, p<0.05), with predictive results comparable to tumour volume change.

## CONCLUSION

This study demonstrates promising results using deep learning to combine patient scans at multiple time points to improve clinical survival and response predictions. Pathologic validation of this biomarker was shown on an independent validation cohort.

## **CLINICAL RELEVANCE/APPLICATION**

Tracking of cancer evolution using deep learning applied to medical imaging showed promising predictions of patient outcome and pathologic response, without the need for manual tumor contours.

# SSC09-05 Interpretation of Computed Tomography Without Reconstruction: Reading Sinograms to Detect Intracranial Hemorrhage

Monday, Nov. 26 11:10AM - 11:20AM Room: E450A

Participants

Chao Huang, PhD, Boston, MA (*Presenter*) Nothing to Disclose Hyunkwang Lee, Boston, MA (*Abstract Co-Author*) Nothing to Disclose Sehyo Yune, MD, MPH, Boston, MA (*Abstract Co-Author*) Nothing to Disclose Myeongchan Kim, MD, Boston, MA (*Abstract Co-Author*) Nothing to Disclose Synho Do, PhD, Boston, MA (*Abstract Co-Author*) Nothing to Disclose

For information about this presentation, contact:

chuang35@mgh.harvard.edu

### PURPOSE

In the current medical practice, diseases or conditions, such as intracranial hemorrhage (ICH), are usually diagnosed using reconstructed images that are generated from sophisticated reconstruction algorithms. In this study, we explore the feasibility to directly detect ICH from non-contrast head computed tomography (CT) in data domain instead of image domain by applying deep learning techniques on CT sinograms.

## METHOD AND MATERIALS

A total of 889 head CT examinations were retrieved from our institutional database, and each axial slice was annotated by 5 boardcertified neuroradiologists. The pixel values of CT images were then converted into linear attenuation coefficients, upon which the 2D parallel-beam Radon transforms were applied to generate simulated sinograms. To investigate the effects of number of projection views and detector size on ICH detection, 3 sets of sinograms were produced: '360 x 729', '120 x 240' and '40 x 80', where 'm x n' means the sinogram obtained from m projection views and n detectors. The sinograms were then randomly splitted into training (635 cases), validation (127 cases) and testing (127 cases) sets, which were used to train, validate, and evaluate a convolutional neural network (CNN) that inputs a sinogram and outputs the probability of ICH. To improve generalization, data augmentation was used for training by applying affine transformations (translation, scaling, rotation and reflection) on CT image slices followed by Radon transforms. For comparison, another CNN was built and trained with reconstructed CT images.

### RESULTS

The CNN model using CT images as inputs achieved 91.5% test accuracy on ICH detection, and the models using " $360 \times 729$ ", " $120 \times 240$ " and " $40 \times 80$ " sinograms as inputs detected ICH with 80.2%, 78.1%, and 76.7% accuracy, respectively.

## CONCLUSION

This study shows the potential of direct detection of ICH using CT raw data without image reconstruction. The results also suggest the possibility of using sparse projection views and large-size detectors without sacrificing the ICH detection accuracy, which could lower the radiation dose and equipment costs.

### **CLINICAL RELEVANCE/APPLICATION**

Direct detection of critical conditions like ICH using sinograms without image reconstruction will save the processing time that is critical in situations like emergency rooms. The potential of radiation dose and equipment cost reduction is also of interest to radiologists.

# SSC09-06 Image Annotation by Eye Tracking: Accuracy and Precision of Centerlines of Obstructed Small Bowel Segments Placed Using Eye Trackers

Monday, Nov. 26 11:20AM - 11:30AM Room: E450A

Participants

Alfredo Lucas, BSC, La Jolla, CA (Abstract Co-Author) Nothing to Disclose

Kang Wang, MD, PhD, San Diego, CA (Abstract Co-Author) Nothing to Disclose

Cynthia S. Santillan, MD, San Diego, CA (Abstract Co-Author) Consultant, Robarts Clinical Trials, Inc

Albert Hsiao, MD, PhD, La Jolla, CA (*Abstract Co-Author*) Founder, Arterys, Inc; Consultant, Arterys, Inc; Consultant, Bayer AG; Research Grant, General Electric Company;

Claude B. Sirlin, MD, San Diego, CA (*Abstract Co-Author*) Research Grant, Gilead Sciences, Inc; Research Grant, General Electric Company; Research Grant, Siemens AG; Research Grant, Bayer AG; Research Grant, ACR Innovation; Research Grant, Koninklijke

Philips NV; Research Grant, Celgene Corporation; Consultant, General Electric Company; Consultant, Bayer AG; Consultant, Boehringer Ingelheim GmbH; Consultant, AMRA AB; Consultant, Fulcrum Therapeutics; Consultant, IBM Corporation; Consultant, Exact Sciences Corporation; Advisory Board, AMRA AB; Advisory Board, Guerbet SA; Advisory Board, VirtualScopics, Inc; Speakers Bureau, General Electric Company; Author, Medscape, LLC; Author, Resoundant, Inc; Lab service agreement, Gilead Sciences, Inc; Lab service agreement, ICON plc; Lab service agreement, Intercept Pharmaceuticals, Inc; Lab service agreement, Shire plc; Lab service agreement, Enanta; Lab service agreement, Virtualscopics, Inc; Lab service agreement, Alexion Pharmaceuticals, Inc; Lab service agreement, Takeda Pharmaceutical Company Limited; Lab service agreement, sanofi-aventis Group; Lab service agreement, Johnson & Johnson; Lab service agreement, NuSirt Biopharma, Inc; Contract, Epigenomics; Contract, Arterys Inc Paul M. Murphy II, MD, PhD, San Diego, CA (*Presenter*) Nothing to Disclose

## For information about this presentation, contact:

pmmurphy@ucsd.edu

## PURPOSE

To determine the accuracy and precision of centerlines of obstructed small bowel segments placed using eye trackers.

### **METHOD AND MATERIALS**

This HIPAA-compliant IRB-approved retrospective pilot study included seven subjects diagnosed with small bowel obstruction (SBO) by CT. For each subject, an obstructed segment of bowel was chosen. Three observers then annotated the centerline of the segment with three methods: manual fiducial placement or visual fiducial placement using either a Tobii x3-120 or 4c eye tracker, which report the location on the screen at which an observer is looking. This location was mapped to 3D coordinates within the CT volume using a custom 3D Slicer module. Each annotation was repeated three times. The distance between centerlines was calculated after alignment using dynamic time warping (DTW) to account for the variable number of fiducials placed. Intra-observer DTW distance between manual and visual centerlines was calculated as measure of accuracy. Intra- and inter-observer DTW distances between centerlines placed with each method were calculated as measures of precision. One-sample t-tests were performed to assess whether mean DTW distances were less than 1.5 or 3 cm for each measure of accuracy or precision respectively.

## RESULTS

DTW distances between manual and visual centerlines ranged from  $1.1\pm0.2$  to  $1.8\pm0.2$  cm, and were significantly less than 1.5 cm for two of three observers using both visual methods (P<0.01). Intra- and inter-observer DTW distances for manual centerlines were  $0.6\pm0.1$  and  $0.8\pm0.2$  cm, and for visual centerlines ranged from  $1.0\pm0.4$  to  $1.9\pm0.6$  cm, but were less than 3.0 cm in all cases (P<0.01).

# CONCLUSION

Eye trackers may be used for visual annotation of the centerlines of obstructed small bowel segments with accuracy and precision that compare favorably to the threshold diameter of 3 cm for diagnosis of SBO on CT. Accuracy varied among observers, but precision was consistently favorable.

## **CLINICAL RELEVANCE/APPLICATION**

SBO is a common and important disease, for which machine learning tools have yet to be developed. Image annotation is a critical first step in machine learning, but manual annotation of small bowel is prohibitively time-consuming. Image annotation by eye tracking is sufficiently accurate and precise relative to the diameter of obstructed small bowel to serve as a potential first step in the development of machine learning tools that facilitate diagnosis of SBO on CT.

# SSC09-07 Big Data Interpretability: Automatically Identify Mislabeled Data in Medical Imaging Deep Learning

Monday, Nov. 26 11:30AM - 11:40AM Room: E450A

Participants Degan Hao, MS, Pittsburgh, PA (*Presenter*) Nothing to Disclose Lei Zhang, PhD, Pittsburgh, PA (*Abstract Co-Author*) Nothing to Disclose Bingjie Zheng, MD, Zhengzhou, China (*Abstract Co-Author*) Nothing to Disclose Margarita L. Zuley, MD, Pittsburgh, PA (*Abstract Co-Author*) Investigator, Hologic, Inc Ruimei Chai, Shenyang, China (*Abstract Co-Author*) Nothing to Disclose Shandong Wu, PhD, MSc, Philadelphia, PA (*Abstract Co-Author*) Nothing to Disclose

### For information about this presentation, contact:

deh95@pitt.edu

#### PURPOSE

In big data applications, data quality and variations can significantly influence performance of deep learning models. Manual labeling or natural language processing-based labeling inevitably generates some mislabeled data. We developed a dedicated method for deep learning to automatically identify potentially mislabeled data.

### **METHOD AND MATERIALS**

We proposed a novel algorithm framework using entropy loss and influence functions to measure data's relevance and correlation strengths with respect to classification performance in convolutional neural network (CNN) models. We identified a clinically-acquired digital mammographic imaging data and their BI-RADS breast density categories (a/b/c/d). Category a (fatty) and d (extremely dense) each has 350 images, while Category b (scattered fibroglandular density) and c (heterogeneously dense) each has 2,000 images. We implemented a CNN-based binary classification model on distinguishing Category a vs d and another similar model for Category b vs c. We did two experiments: 1) Before training models, we purposely flipped the labels for 10% randomly selected data in each category and used our method to identify those flipped data; and 2) We ran our method on the original unflipped data to identify those potentially mislabeled images by radiologists and evaluate the effect by using a published scheme that assesses the "correctness" of clinically-assigned BI-RADS breast density categories.

The AUC is 0.99 and 0.96 for the Category a vs d model and for the Category b vs c model, respectively. For experiment 1), our method can identify 98% of the purposely flipped data in Category a and d, and 92% in Category b and c, by automatically examining as small as only 30% of the full dataset. For experiment 2), there is 78% (or 96%) overlap in the potentially mislabeled data between those identified by our method and those specified by the "correctness" assessment method, by examining 50% (or 90%) of the full dataset.

### CONCLUSION

We developed an automated method for deep learning and demonstrated it can identify vast majority of mislabeled data in the BIRADS-based clinical breast density assessment in digital mammograms.

#### **CLINICAL RELEVANCE/APPLICATION**

Fully-automated identification of mislabeled data for deep learning can significantly improve data quality, model's performance and reliability, as well as stratified data interpretability.

### SSC09-08 Approaching Chest-CT-Level Performance on Chest X-Rays with Deep-Learning

Monday, Nov. 26 11:40AM - 11:50AM Room: E450A

Participants

Tarun Raj, Mumbai, India (*Presenter*) Employee, Qure.ai Pooja Rao, MBBS,PhD, Mumbai, India (*Abstract Co-Author*) Employee, Qure.ai Prashant Warier, PhD, Mumbai, India (*Abstract Co-Author*) Employee, Qure.ai Manoj D. Tadepalli, BEng, Mumbai, India (*Abstract Co-Author*) Employee, Qure.ai Bhargava Reddy, Mumbai, India (*Abstract Co-Author*) Employee, Qure.ai Preetham Putha, BEng, Mumbai, India (*Abstract Co-Author*) Employee, Qure.ai Justy Antony Chiramal, MBBS,MD, Mumbai, India (*Abstract Co-Author*) Research Consultant, Qure.ai

#### For information about this presentation, contact:

tarun.raj@qure.ai

### PURPOSE

To determine whether deep learning algorithms can detect abnormalities on chest X-rays (CXR) before they are visible to radiologists.

#### **METHOD AND MATERIALS**

We trained deep learning models to identify abnormal X-rays and CXR opacities using a set of 1,150,084 chest X-Rays. We used a retrospectively obtained independent set of de-identified chest X-rays from patients who had undergone a chest CT scan within 1 day (TS-1, n=187), 3 days (TS-3, n=197) and 10 days (TS-10, n=230) of the X-ray to evaluate the algorithms' ability to detect abnormalities that were not visible to the radiologist at the time of reporting on the X-ray. Natural language processing algorithms were used to establish ground truth from radiologist reports of the CT scans, on 2 parameters - 'any abnormality' and 'hyperdense abnormality (HA)' - defined as any abnormal focal or diffuse hyperdense abnormality in the lung fields including but not limited to nodule, mass, fibrosis and calcification. The CT scans were used as ground truth to evaluate the accuracy of the original CXR report and the deep learning algorithms.

#### RESULTS

Of 187 CT scans in TS-1, 153 contained an HA. 52 of these (34%) had been picked up on the original CXR by the reporting radiologist, and 63 of these (41%) were picked up by the deep learning algorithm. Of 180 abnormal scans in TS-1, 106 (59%) had been picked up as abnormal on the original CXR by the reporting radiologist, and 120 of these (67%) were picked up by the deep learning algorithm. To detect HA, this amounts to an accuracy of 0.49, sensitivity of 0.41 and specificity of 0.85 for the algorithm, versus an accuracy of 0.44, sensitivity of 0.34 and specificity of 0.91 for the original radiologist read of the chest X-ray. To detect any abnormality, the accuracy, sensitivity, and specificity are 0.67,0.67 and 0.71 respectively for the algorithm, and 0.59,0.59 and 0.71 respectively for the reporting radiologist. Similar results were observed on TS-3 and TS-10, as shown in the figure below

### CONCLUSION

Deep learning algorithms can pick up abnormalities that have been missed on chest X-rays but identified on a subsequent chest CT.

### CLINICAL RELEVANCE/APPLICATION

Using deep learning algorithms to screen chest X-rays could result in higher sensitivity at identifying abnormal scans than currently possible, with only a small corresponding increase in the number of false positives.

### ssc09-09 A Portable Automated X-Ray Imaging System and Reading Solution for Screening Lung Diseases

Monday, Nov. 26 11:50AM - 12:00PM Room: E450A

Participants Girish Srinivasan, Palatine, IL (*Presenter*) Nothing to Disclose Woo Jung Shim, Seoul, Korea, Republic Of (*Abstract Co-Author*) Nothing to Disclose Zafar Fawad, Santa Monica, CA (*Abstract Co-Author*) Nothing to Disclose Sung-Hong Park, Daejeon, Korea, Republic Of (*Abstract Co-Author*) Nothing to Disclose Huan M. Luu, BSC, Daejeon, Korea, Republic Of (*Abstract Co-Author*) Nothing to Disclose

For information about this presentation, contact:

srinivasan.girish@gmail.com

### CONCLUSION

The AXIR system allows clinicians to save time and money while providing patients with good service at any location. The AI-based

automation facilitates its use as a screening and diagnosis tool, allowing doctors to make real-time decisions with high precision and reliability. The system, in the future, may cover other anatomical regions while the AI-engine can be enhanced to diagnose broader disease indications.

### Background

A chest x-ray is a commonly used examination for screening and diagnosis of lung diseases. Artificial intelligence (AI) solutions, for automated image analysis, have been implemented as cloud-based solutions centered on hospitals with well-equipped infrastructures. However, two-thirds of the planet does not have access to radiology services due to lack of infrastructure and expertise. We have developed a portable automated X-ray imaging system and reading solution (AXIR) with embedded AI technology to solve this problem.

### Evaluation

The AXIR system comprises of a low power portable generator (3kW), a wireless detector (resolution > 4lp/mm), an image preprocessing tool, an AI-based analysis engine, and a mobile viewer. The AI engine screens images for abnormalities and displays the location. Abnormalities can further be classified as pleural effusion, cardiomegaly, opacity, infiltrate, consolidation, fibrosis, hilar enlargement, and calcification. The AI models were trained using public datasets and with images acquired using the AXIR system. The system is being validated at a poor infrastructure site handling about 1000 chest X-rays / month. The performance of the system is evaluated by measuring the accuracy, sensitivity, and specificity of diagnosis.

### Discussion

Access to diagnostic imaging services has a great impact on public health and can potentially increase, for example, early detection. AXIR's portable X-ray system with embedded AI-based analytics is a novel highly accessible medical device. In our initial test, we achieved a diagnostic accuracy of 92% with a sensitivity of 94% and specificity of 90%. At our pilot site, the system reduced the diagnosis time from an average of 3 days to less than 10 minutes and brought the patient re-visit rate down to 1% from 20%.



#### SSC10

Science Session with Keynote: Musculoskeletal (Body Composition)

Monday, Nov. 26 10:30AM - 12:00PM Room: S102CD



AMA PRA Category 1 Credits ™: 1.50 ARRT Category A+ Credit: 1.75

**FDA** Discussions may include off-label uses.

#### Participants

Ali Guermazi, MD, PhD, Boston, MA (*Moderator*) Shareholder, Boston Imaging Core Lab, LLC ; Research Consultant, Merck KGAA ; Research Consultant, sanofi-aventis Group ; Research Consultant, TissueGene, Inc; Research Consultant, OrthoTrophix, Inc; Research Consultant, AstraZeneca PLC ; Research Consultant, General Electric Company ; Research Consultant, Pfizer Inc Robert D. Boutin, MD, Davis, CA (*Moderator*) Nothing to Disclose

#### Sub-Events

### SSC10-01 Musculoskeletal Keynote Speaker: SSR 2018 Paper Award: Brown Adipose Tissue and Cancer Activity

Monday, Nov. 26 10:30AM - 10:40AM Room: S102CD

Participants

Miriam A. Bredella, MD, Boston, MA (Presenter) Nothing to Disclose

### SSC10-03 Association of DXA Markers of Sarcopenia with Inflammation and Adiposity Related Hormones in an Elderly Population: A Gender-Based Analysis

Monday, Nov. 26 10:50AM - 11:00AM Room: S102CD

Participants

Maria Pilar Aparisi Gomez, Auckland, New Zealand (Abstract Co-Author) Nothing to Disclose Aurelia Santoro, Bologna, Italy (Abstract Co-Author) Nothing to Disclose Daniele Mercatelli, PhD, Bologna, Italy (*Abstract Co-Author*) Nothing to Disclose Chiara Gasperini, Bologna, Italy (*Abstract Co-Author*) Nothing to Disclose Giulia Guidarelli, Bologna, Italy (Abstract Co-Author) Nothing to Disclose Rita Ostan, Bologna, Italy (Abstract Co-Author) Nothing to Disclose Enrico Giampieri, Bologna, Italy (Abstract Co-Author) Nothing to Disclose Cristina Fabbri, Bologna, Italy (Abstract Co-Author) Nothing to Disclose Agnes Berendsen, Wageningen, Netherlands (Abstract Co-Author) Nothing to Disclose Olga Januszko, Warsaw, Poland (Abstract Co-Author) Nothing to Disclose Amy Jennings, Norwich, United Kingdom (Abstract Co-Author) Nothing to Disclose Nathalie Meunier Meunier, Clermont-Ferrand, France (Abstract Co-Author) Nothing to Disclose Elodie Caumon, Clermont-Ferrand, France (Abstract Co-Author) Nothing to Disclose Rachel Gillings, Norfolk, United Kingdom (Abstract Co-Author) Nothing to Disclose Barbara Pietruszka, Warsaw, Poland (Abstract Co-Author) Nothing to Disclose C.P.G.M. de Groot, Wageningen, Netherlands (Abstract Co-Author) Nothing to Disclose Claudio Nicoletti, Firenze, Italy (Abstract Co-Author) Nothing to Disclose Fawzi Kadi, Orebro, Sweden (Abstract Co-Author) Nothing to Disclose Alessandro Napoli, MD, Rome, Italy (Abstract Co-Author) Nothing to Disclose Giuseppe Battista, Bologna, Italy (Abstract Co-Author) Nothing to Disclose Claudio Franceschi, Bologna, Italy (Abstract Co-Author) Nothing to Disclose Alberto Bazzocchi, MD, Bologna, Italy (Presenter) Nothing to Disclose

### For information about this presentation, contact:

abazzo@inwind.it

#### PURPOSE

Sarcopenia consists of loss of muscle mass and strength/function. As adipose tissue expands and muscle and bone tissue decrease with aging, there is a concomitant increase in proinflammatory and a reduction in anti-inflammatory factors contributory to chronic inflammation. We aimed to evaluate associations of several inflammatory markers with DXA-measured sarcopenia markers in a representative sample of European healthy adults aged 65-79 years.

### METHOD AND MATERIALS

Baseline whole-body DXA scan was performed and fresh blood samples collected in 1122 participants enrolled in the NU-AGE trial, a one-year, multicenter, randomized, single-blind, controlled trial (NCT01754012) testing the effects of a dietary intervention. Appendicular lean mass (ALMI, lean mass from arms plus legs/height2) and skeletal mass index (SMI, lean mass from arms plus legs/weight) were used as DXA markers of sarcopenia. Quantitative determination of inflammatory markers was performed by ELISA. After a log-transformation of DXA parameters the Pearson Product-Moment Correlation was applied to test the associations between body composition and inflammation markers in both genders.

#### RESULTS

In male population, a positive association was found between ALMI and albumin ( $\rho$ =0.20; p < .05) and SMI and ghrelin ( $\rho$ =0.19; p < .05). A negative association was found between ALMI and adiponectin ( $\rho$ =-0.23; p< .001), while SMI was negatively correlated with leptin ( $\rho$ =-0.70; p<.001) and C-Reactive Protein(CRP) ( $\rho$ =-0.24; p<.001). In females, ALMI was positively associated with leptin ( $\rho$ =0.19; p<.01), and CRP ( $\rho$ =0.22; p<.01). SMI was positively associated with ghrelin ( $\rho$ =0.24; p<.001), while negatively with leptin ( $\rho$ =-0.62; p<.001), CRP ( $\rho$ =-0.23; p<.001), and AGP ( $\rho$ =-0.26; p<.001).

#### CONCLUSION

Sarcopenia correlates with an increase of inflammatory status in elderly. In males and females, SMI correlates positively with ghrelin, an anti-inflammatory molecule, and negatively with pro-inflammatory markers such as leptin, CRP and AGP; while ALMI showed ambiguous associations with inflammatory markers. Thus, SMI appears to be a better predictor of inflammatory risk status in the elderly.

### CLINICAL RELEVANCE/APPLICATION

DXA-derived sarcopenia markers show a correlation with inflammatory markers useful to picture patients' risk status. SMI may predict inflammatory status better than ALMI; but further research is required.

# SSC10-04 Automated Segmentation of Thoracic Paraspinous Muscles: Pipeline for Large-Scale Data Mining on CT

Monday, Nov. 26 11:00AM - 11:10AM Room: S102CD

Participants

Leon Lenchik, MD, Winston-Salem, NC (*Presenter*) Nothing to Disclose Ryan T. Barnard, MS, Winston-Salem, NC (*Abstract Co-Author*) Nothing to Disclose Stephen B. Kritchevsky, PhD, Winston-Salem, NC (*Abstract Co-Author*) Nothing to Disclose Ashley A. Weaver, PhD, Winston Salem, NC (*Abstract Co-Author*) Nothing to Disclose Robert D. Boutin, MD, Davis, CA (*Abstract Co-Author*) Nothing to Disclose

#### For information about this presentation, contact:

llenchik@wakehealth.edu

### PURPOSE

To compare automated pipeline for thoracic paraspinous muscle segmentation with manual segmentation on chest CT examinations.

### METHOD AND MATERIALS

Atlas-based automated pipeline for thoracic paraspinous muscle segmentation was developed using open-source medical image analysis tools: Advanced Normalization Tools (ANTs), the Oxford Centre for Functional Magnetic Resonance Imaging of the Brain Software Library (FSL), and the scikit-image Python image processing library. After the correct image at T12 level was identified, the left paraspinous muscle was automatically segmented and the muscle attenuation and cross-sectional area were recorded. Ground truth was obtained using 475 non-contrast chest CT exams by manually segmenting the left paraspinous muscle at T12 level with muscle thresholds set at -29 to +150 HU (Mimics software version 19.0; Materialise, Leuven, Belgium). The CT images are heterogeneous in field of view, voxel spacing, convolution kernel, scanner manufacturer and model, reconstruction algorithm, and image quality. Dice and Jaccard similarity indices were determined.

### RESULTS

Compared to manual segmentation, the automated pipeline had a mean Dice index of 0.85 (SD=0.07) and a mean Jaccard index of 0.74 (SD=0.09). Mean accuracy error for muscle attenuation was 1.2 HU; range: 0-4.9 HU. Mean accuracy error for muscle cross-sectional area was 1.83 cm2; range: 0-9.3 cm2.

### CONCLUSION

The automated pipeline for thoracic paraspinous muscle segmentation is sufficiently accurate to allow for large-scale data mining of heterogeneous chest CT images.

### **CLINICAL RELEVANCE/APPLICATION**

Current CT image evaluation of sarcopenia requires manual segmentation, unrealistic for large datasets. The automated pipeline for sarcopenia evaluation on chest CTs could be adapted to other body regions including abdomen, pelvis, and extremities.

# SSC10-05 Assessment of Sarcopenia on Computed Tomography (CT): A Systematic Review of Technical Parameters

Monday, Nov. 26 11:10AM - 11:20AM Room: S102CD

Participants

Behrang Amini, MD, PhD, Houston, TX (*Presenter*) Nothing to Disclose Robert D. Boutin, MD, Davis, CA (*Abstract Co-Author*) Nothing to Disclose Leon Lenchik, MD, Winston-Salem, NC (*Abstract Co-Author*) Nothing to Disclose Sean P. Boyle, Sacramento, CA (*Abstract Co-Author*) Nothing to Disclose

### For information about this presentation, contact:

Bamini@mdanderson.org

#### PURPOSE

Computed tomography (CT) is being increasingly used for the assessment of sarcopenia, often by non-radiologists who may not be aware of the impact of technical parameters on muscle metrics. We sought to perform a systematic review of all relevant studies that used CT muscle measurements to assess sarcopenia to identify the differences between technical parameters used.

### METHOD AND MATERIALS

A comprehensive search of PubMed from 1983-2017 was performed to identify studies that used CT measurements of muscle to assess for sarcopenia. Review articles were excluded. The following technical parameters used to measure muscle metrics were compared: slice thickness, kVp, mAs, helical pitch, reconstruction method, and use of intravenous (IV) contrast.

#### RESULTS

From the 654 articles identified, 388 studies met the inclusion criteria for the systematic review. Slice thickness was not reported in 63% of studies. When reported, the most commonly used slice thickness was 10 mm (14%). kVp was not reported in 73% of studies. When reported, the most common kVp was 120 (19%). mAs was not reported in 75% of studies. When reported, the most common mAs values were between 200 and 300 (7%). Helical pitch and reconstruction algorithm were not reported in 98% of studies and IV contrast use was not reported in 94% of studies.

### CONCLUSION

There is a significant deficiency in reporting of CT technical parameters used for measuring muscle indices which may affect the generalizability of results in the sarcopenia literature.

### **CLINICAL RELEVANCE/APPLICATION**

Comparison between publications in the sarcopenia field is hampered by deficiency in reporting of CT technical parameters.

SSC10-06 Inter- and Intraobserver Variability of an Anatomical Landmark-Based, Manual Segmentation Method by MRI for the Assessment of Skeletal Muscle Fat Content and Area in Subjects from the General Population

Monday, Nov. 26 11:20AM - 11:30AM Room: S102CD

#### Participants

Lena Sophie Kiefer, MD, Tubingen, Germany (*Presenter*) Nothing to Disclose Jana Fabian, BSC, Tubingen, Germany (*Abstract Co-Author*) Nothing to Disclose Roberto Lorbeer, Greifswald, Germany (*Abstract Co-Author*) Nothing to Disclose Juergen Machann, MD, Tuebingen, Germany (*Abstract Co-Author*) Nothing to Disclose Corinna Storz, MD, Tubingen, Germany (*Abstract Co-Author*) Nothing to Disclose Mareen S. Kraus, MD, Tubingen, Germany (*Abstract Co-Author*) Nothing to Disclose Christopher L. Schlett, MD, MPH, Heidelberg, Germany (*Abstract Co-Author*) Nothing to Disclose Frank W. Roemer, MD, Erlangen, Germany (*Abstract Co-Author*) Officer, Boston Imaging Core Lab, LLC; Research Director, Boston Imaging Core Lab, LLC; Shareholder, Boston Imaging Core Lab, LLC Annette Peters, Neuherberg, Germany (*Abstract Co-Author*) Nothing to Disclose Konstantin Nikolaou, MD, Tuebingen, Germany (*Abstract Co-Author*) Nothing to Disclose Fabian Bamberg, MD, Tuebingen, Germany (*Abstract Co-Author*) Nothing to Disclose Konstantin Nikolaou, MD, Tuebingen, Germany (*Abstract Co-Author*) Nothing to Disclose Konstantin Nikolaou, MD, Tuebingen, Germany (*Abstract Co-Author*) Nothing to Disclose Konstantin Nikolaou, MD, Tuebingen, Germany (*Abstract Co-Author*) Nothing to Disclose Konstantin Nikolaou, MD, Tuebingen, Germany (*Abstract Co-Author*) Speakers Bureau, Bayer AG; Speakers Bureau, Siemens AG; Speaker Bureau, Bayer AG

#### For information about this presentation, contact:

lena.kiefer@med.uni-tuebingen.de

### PURPOSE

Changes in skeletal muscle composition, such as fat content and mass, may exert unique metabolic and musculoskeletal risks; however, the reproducibility of their assessment is unknown. We determined the variability of the assessment of skeletal muscle fat content and area by magnetic resonance imaging (MRI) in a population-based sample.

### METHOD AND MATERIALS

A random sample from a prospective, community-based cohort study (KORA-FF4) was included. Skeletal muscle fat content was quantified as proton-density fat-fraction (PDFF) and area as cross-sectional area (CSA) in multi-echo Dixon sequences (TR 8.90ms, six echo times, flip-angle 4°) by a standardized, anatomical landmark-based, manual skeletal muscle segmentation at level L3 vertebra by two independent observers. Reproducibility was assessed by intra-class correlation coefficients (ICC), scatter and Bland-Altman plots.

#### RESULTS

In 50 included subjects (mean age 56.1±8.8years, 60.0% males, mean BMI 28.3±5.2) 2'400 measurements were obtained. Interobserver agreement was excellent for all muscle compartments (PDFF: ICC0.99, CSA: ICC0.98) with only minor absolute and relative differences (-0.2±0.5%, 31±44.7mm2; -2.6±6.4% and 2.7±3.9%, respectively). Intra-observer reproducibility was similarly excellent (PDFF: ICC1.0, 0.0±0.4%, 0.4%; CSA: ICC1.0, 5.5±25.3mm2, 0.5%, absolute and relative differences, respectively). All agreement was independent of age, gender, BMI, body height and visceral adipose tissue (ICC0.96-1.0). Furthermore, PDFF-reproducibility was independent of CSA (ICC0.93-0.99).

### CONCLUSION

Quantification of skeletal muscle fat content and area by MRI using an anatomical landmark-based, manual skeletal muscle segmentation is highly reproducible.

### **CLINICAL RELEVANCE/APPLICATION**

An anatomical landmark-based, manual skeletal muscle segmentation provides high reproducibility of skeletal muscle fat content and area and may therefore serve as a robust proxy for myosteatosis and sarcopenia in large cohort studies.

# SSC10-07 Cortical Bone Porosity Assessment in Human Tibial and Fibular Cortex Using Ultrashort Echo Time Magnetization Transfer (UTE-MT) MRI

Participants Saeed Jerban, PhD, San Diego, CA (*Abstract Co-Author*) Nothing to Disclose Yajun Ma, San Diego, CA (*Abstract Co-Author*) Nothing to Disclose Lidi Wan, MD,MD, San Diego, CA (*Presenter*) Nothing to Disclose Adam C. Searleman, MD,PhD, San Diego, CA (*Abstract Co-Author*) Nothing to Disclose Hyungseok Jang, La Jolla, CA (*Abstract Co-Author*) Nothing to Disclose Robert Sah, La Jolla, CA (*Abstract Co-Author*) Nothing to Disclose Eric Y. Chang, MD, San Diego, CA (*Abstract Co-Author*) Nothing to Disclose Jiang Du, PhD, San Diego, CA (*Abstract Co-Author*) Nothing to Disclose

#### For information about this presentation, contact:

sjerban@ucsd.edu

### PURPOSE

To investigate the relationship between macromolecular fraction (MMF), obtained from UTE-MT modeling, and bone porosity, as measured using high-resolution micro-computed tomography ( $\mu$ CT).

### **METHOD AND MATERIALS**

Eighteen cortical bone specimens were harvested from human tibial and fibular midshafts ( $63\pm19$  and  $52\pm18$  years old). Specimens were scanned using an 8-channel knee coil on a 3T clinical scanner (MR750, GE). The UTE-MRI scans involved: A) an actual flip angle-variable TR (AFI-VTR) method, (AFI: TE=0.032, TR=20,100 ms, FA=45°; VTR: TE=0.032, TR=20 to 100 ms, FA=45°) for T1 measurement, which is a prerequisite for accurate MT modeling, and B) a 3D UTE-Cones-MT sequence (saturation pulse power=500,1000,1500°, frequency offset=2 to 50 kHz, FA=7°) for MT modelling. Field of view (FOV), matrix dimension, nominal inplane pixel size, and slice thickness were 14 cm,  $256\times256$ , 0.54 mm, and 2 mm, respectively. Afterward, specimens were scanned using a Skyscan 1076 (Kontich, Belgium)  $\mu$ CT at 9  $\mu$ m3 voxel size. Pearson's correlations were calculated between UTE-MT results and  $\mu$ CT-based measures (porosity and bone mineral density, BMD) using the data in 12 and 4 ROIs in each tibial and fibular sample, respectively. ROIs were selected at different cortical bone bands to provide an adequate range of porosity.

### RESULTS

Figures 1a-f show MMF, porosity, and BMD pixel maps for a representative tibial and fibular specimen, respectively. Regions of higher MMF corresponded to the regions of lower porosity in the porosity maps. Figures 1g-j demonstrate the correlations between MMF and  $\mu$ CT measures for tibial and fibular bone specimens, respectively. MMF presented very good correlations with  $\mu$ CT measures.

#### CONCLUSION

MMF obtained from MT modeling, as a measure for collagen content, showed very good correlations with  $\mu$ CT measures regardless of the fibular of tibial harvesting sites. This study highlighted UTE-MT MRI techniques as a useful method to assess bone porosity, which may be used in future clinical studies.

#### **CLINICAL RELEVANCE/APPLICATION**

A UTE-MRI-based technique, to estimate the collagen backbone content which correlates greatly with the bone porosity may help diagnose bone diseases earlier and more accurately.

### SSC10-08 Diagnostic Performance of Phantomless Dual-Energy CT for Volumetric Bone Mineral Density Assessment in Comparison to CT Hounsfield Unit Measurements Using Dual X-Ray Absorptiometry as Standard of Reference

Monday, Nov. 26 11:40AM - 11:50AM Room: S102CD

#### Participants

Lukas Lenga, Frankfurt, Germany (*Presenter*) Nothing to Disclose Moritz H. Albrecht, MD, Frankfurt am Main, Germany (*Abstract Co-Author*) Speaker, Siemens AG Stefan Wesarg, MS, Darmstadt, Germany (*Abstract Co-Author*) Nothing to Disclose Simon S. Martin, MD, Frankfurt, Germany (*Abstract Co-Author*) Nothing to Disclose Julian L. Wichmann, MD, Frankfurt, Germany (*Abstract Co-Author*) Speaker, General Electric Company; Speaker, Siemens AG Christian Booz, MD, Frankfurt am Main, Germany (*Abstract Co-Author*) Nothing to Disclose Marcel C. Langenbach, MD, Frankfurt, Germany (*Abstract Co-Author*) Nothing to Disclose Thomas J. Vogl, MD, PhD, Frankfurt, Germany (*Abstract Co-Author*) Nothing to Disclose Ibrahim Yel, Frankfurt, Germany (*Abstract Co-Author*) Nothing to Disclose

### For information about this presentation, contact:

boozchristian@gmail.com

### PURPOSE

To evaluate the diagnostic performance of a phantomless dual-energy computed tomography (DECT) postprocessing algorithm for volumetric bone mineral density (BMD) assessment of the lumbar spine compared to Hounsfield unit (HU) measurements.

#### **METHOD AND MATERIALS**

We retrospectively analyzed 200 lumbar vertebrae in 53 patients who had undergone third-generation dual-source DECT and dual xray absorptiometry (DXA) examinations of the lumbar spine within 7 days between March and December 2017. For volumetric BMD assessment, dedicated phantomless DECT postprocessing software which allows for freely rotatable color-coded three-dimensional visualization of trabecular BMD distribution using three-material decomposition was applied. In addition, HU measurements were performed on standard bone reconstructions by defining five trabecular regions of interest (ROI) per vertebra. Results of both approaches were compared regarding the diagnostic accuracy using the DXA T-score according to the World Health Organization as standard of reference for detecting osteoporosis.

#### RESULTS

DXA revealed a total of 92 osteoporotic lumbar vertebrae. A BMD cut-off of 92 mg/cm<sup>3</sup> at phantomless DECT yielded 98.9% sensitivity and 91.6% specificity for detecting osteoporosis; 93.3% of vertebrae below this threshold were diagnosed with osteopenia/osteoporosis according to DXA and 80.2% above showed normal BMD at DXA. A trabecular ROI attenuation cut-off of 157 HU showed 71.0% sensitivity and 66.4% specificity for osteoporosis; 73.3% of vertebrae below this threshold were diagnosed with osteopenia/osteoporosis according to DXA and 41.0% above showed normal BMD at DXA. A trabecular ROI attenuation cut-off of eotoporosis according to DXA and 41.0% above showed normal BMD at DXA. Area under the curve for detecting osteoporosis was 0.953 for phantomless DECT and 0.754 for HU-based analysis (p<0.001). Pearson product-moment correlation showed higher correlation between BMD results of phantomless DECT and DXA (r=0.848) compared to HU and DXA values (r=0.438) (p<0.001).

### CONCLUSION

A phantomless DECT postprocessing algorithm for volumetric BMD assessment of the lumbar spine is significantly superior compared to HU measurements regarding the diagnostic accuracy for detecting osteoporosis.

### **CLINICAL RELEVANCE/APPLICATION**

Opportunistic screening for osteoporosis using HU measurements on CT images as previously suggested in recent literature is less accurate than a phantomless color-coded DECT postprocessing algorithm which can be applied to routine DECT without requiring protocol changes.

### SSC10-09 Effects of Nutrition, Exercise, and Medication on Bone Microarchitecture Assessed by HR-pQCT Measurements in Long-Term HIV-Infected Individuals

Monday, Nov. 26 11:50AM - 12:00PM Room: S102CD

Participants

Sarah C. Foreman, MD, San Francisco, CA (*Presenter*) Nothing to Disclose Po-hung Wu, San Francisco, CA (*Abstract Co-Author*) Nothing to Disclose Ruby Kuang, San Francisco, CA (*Abstract Co-Author*) Nothing to Disclose Malcolm John, San Francisco, CA (*Abstract Co-Author*) Nothing to Disclose Phyllis Tien, MD, San Francisco, CA (*Abstract Co-Author*) Research Grant, Gilead Sciences, Inc Thomas M. Link, MD,PhD, San Francisco, CA (*Abstract Co-Author*) Research Grant, General Electric Company; Research Consultant, General Electric Company; Research Consultant, InSightec Ltd; Research Grant, InSightec Ltd; Royalties, Springer Nature; Consultant, Springer Nature; Research Consultant, Pfizer Inc; Roland Krug, PhD, San Francisco, CA (*Abstract Co-Author*) Nothing to Disclose Galateia J. Kazakia, PhD, San Francisco, CA (*Abstract Co-Author*) Nothing to Disclose

### PURPOSE

In long-term HIV-infected individuals, low bone density and increased fracture risk have emerged as significant comorbidities. Our aim was to assess the influence of exercise, nutrition, and medications on bone microarchitecture using high-resolution peripheral quantitative CT (HR-pQCT) in long-term HIV-infected individuals.

## METHOD AND MATERIALS

Twenty-nine HIV-infected subjects (3 postmenopausal women, 26 men) were prospectively enrolled in our study (BMI 26.1±4.3 kg/m2, age 56.9±5.6, years diagnosed with HIV 20.7±8.8). Questionnaires included the revised Community Healthy Activities Model Program for Seniors (CHAMPS), the Mini Nutritional Assessment (MNA) as well as medication assessments. Participants underwent radius and tibia HR;pQCT and laboratory evaluation. Multivariable linear regression models were used to evaluate the effects of exercise, nutritional status, tenofovir disoproxil fumarate (TDF) and protease inhibitor (PI) use on bone microarchitecture, adjusting for all demographic risk factors.

### CONCLUSION

Cortical bone in HIV-infected individuals is detrimentally affected by malnutrition, while trabecular bone is detrimentally affected by previous use of TDF in combination with a PI. In long-term HIV-infected subjects, nutritional support could potentially be more relevant for bone health compared to physical activity.

# **CLINICAL RELEVANCE/APPLICATION**

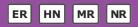
Long-term HIV-infected individuals could particularly benefit from nutritional assessment and intervention as well as avoiding use of TDF with PIs to prevent compromised bone health.



#### SSC11

### Neuroradiology/Head and Neck (Trauma Imaging: Picking Up the Pieces)

Monday, Nov. 26 10:30AM - 12:00PM Room: S402AB



AMA PRA Category 1 Credits ™: 1.50 ARRT Category A+ Credit: 1.75

#### **Participants**

C. C. Tchoyoson Lim, FRCR, MMed, Singapore, Singapore (*Moderator*) Nothing to Disclose Gaurang V. Shah, MD, Ann Arbor, MI (*Moderator*) Nothing to Disclose

# Sub-Events

### SSC11-01 Collaborative Study of CTA Utilization in Patients Presenting With Blunt Cervical or Head Injury: A Retrospective Assessment of Current Clinical Practice and Its Impact on Clinical Outcome

Monday, Nov. 26 10:30AM - 10:40AM Room: S402AB

Participants

Matylda Machnowska, MD, Toronto, ON (*Presenter*) Nothing to Disclose Aimee Chan, Toronto, ON (*Abstract Co-Author*) Nothing to Disclose Hamad Al-Sawaihey, MBChB, MPH, Toronto, ON (*Abstract Co-Author*) Nothing to Disclose David Mahmoudian, Toronto, ON (*Abstract Co-Author*) Nothing to Disclose Liying Zhang, PhD, Richmond Hill, ON (*Abstract Co-Author*) Nothing to Disclose Moira Kapral, Toronto, ON (*Abstract Co-Author*) Nothing to Disclose Jacques Lee, FRCPC, Toronto, ON (*Abstract Co-Author*) Nothing to Disclose Michael O'Keeffe, Toronto, ON (*Abstract Co-Author*) Nothing to Disclose Khaled Y. Elbanna, MBChB, FRCR, Vancouver, BC (*Abstract Co-Author*) Nothing to Disclose Leo Da Costa, MD, Toronto, ON (*Abstract Co-Author*) Nothing to Disclose Andrew McDonald, MD, Toronto, ON (*Abstract Co-Author*) Nothing to Disclose Richard Aviv, MBBCh, FRCR, Toronto, ON (*Abstract Co-Author*) Nothing to Disclose

#### PURPOSE

Blunt cerebrovascular injury (BCVI) occurs in 0.2-2.7% of blunt trauma patients, and is the cause of stroke in approximately  $\sim 2\%$  of all patients and 10-25% of young patients. BCVI patients are at highest risk of stroke within 10-72 hours following injury, with the likelihood of stroke increasing with dissection grade. The Denver screening criteria are the most commonly implemented criteria for screening BCVI. The study aims to quantify the variance of current practice at our institution from the established Denver criteria.

#### **METHOD AND MATERIALS**

A retrospective chart review was conducted on consecutive blunt trauma patients admitted to our institution from Jan 1, 2010-Dec 31, 2015. Imaging studies were reviewed by a neuroradiologist and an emergency radiologist. Patients were assessed for clinical and radiological Denver criteria, presence of dissection on CTA, medical history, treatment, and outcome.

#### RESULTS

3004 consecutive patients were included. 757 (25.2%) patients were Denver positive, but only 336 received a CTA, and nearly half with detectable dissections. Of the Denver positive patients, 54 (7.1%) patients had an in-hospital stroke (total 122 strokes), with 15 (26.8%) patients having a detectable stroke on their primary CT scan. 33 strokes were due to traumatic vessel injury; 43 were due to arterial compression; and 46 did not have a discernable cause, in part due to lack of CTA screening. Of the strokes due to dissection, 3 (9.1%) were Biffl Grade (Gr) 1; 6 (18.2%) Gr2; 12 (36.4%) Gr3; 10 (30.3%) Gr4; 2 patients had an injury in a vessel other than the carotid or vertebral. 7 patients had an arterial injury requiring neurological intervention, including intracranial ICA and ACA pseudoaneurysms. 156 (6.9%) of Denver negative patients underwent CTA, with 19 having detectable dissections. A total of 13 Denver negative patients had stroke, only 3 due to dissection: 2 Gr3 and 1 Gr4.

#### CONCLUSION

Almost 30% of Denver positive patients have a stroke earlier than the estimated 10-72 hour window, highlighting the need for early medical assessment and preventative measures. CTAs are underutilized and a considerable amount of patients have stroke as a result of lower-grade (1-2) dissections.

### **CLINICAL RELEVANCE/APPLICATION**

Early screening for arterial injury and early insitiution of antiplatelet or interventional therapy, depending on the degree of vessel injury, may help to prevent post traumatic strokes.

### SSC11-02 Brain Extraction in Susceptibility-Weighted MR Images Using Deep Learning

Monday, Nov. 26 10:40AM - 10:50AM Room: S402AB

Kevin Koschmieder, MSc, Nijmegen, Netherlands (*Presenter*) Nothing to Disclose Anke W. Van Der Eerden, MD, Nijmegen, Netherlands (*Abstract Co-Author*) Nothing to Disclose Bram Van Ginneken, PhD, Nijmegen, Netherlands (*Abstract Co-Author*) Stockholder, Thirona BV; Co-founder, Thirona BV; Research Grant, Varian Medical Systems, Inc; Research Grant, Canon Medical Systems Corporation Rashindra Manniesing, PhD, Nijmegen, Netherlands (*Abstract Co-Author*) Research funded, Canon Medical Systems Corporation

### For information about this presentation, contact:

kevin.koschmieder@radboudumc.nl

#### PURPOSE

Brain extraction methods in MRI have so far been exclusively developed for T1- and T2-weighted images. A deep neural network is presented to segment the brain tissue in susceptibility-weighted images (SWI) in healthy individuals and patients with traumatic brain injury (TBI).

### METHOD AND MATERIALS

In total, MRI scans from 33 patients with moderate to severe TBI and 18 healthy controls were collected. SWIs were acquired with 27ms TR, 20ms TE, 15° flip angle, and 0.98x0.98x1.00mm<sup>3</sup> voxel size on a 3T Siemens MRI scanner. A small scale 2D-U-Net was implemented (18 convolution layers, max. 256 features per layer) processing a volume in axial direction. The U-Net architecture allowed the model to utilize both local and contextual information. The output probability maps were thresholded and possible outliers were removed by taking the largest connected component. 20 TBI patients and 10 controls served as a test set, the remaining patients were used for training. The reference standard were brain masks obtained with SPM, a publicly available software package commonly used for brain extractions in MR neuroimaging, but not optimized for SWI sequences. These annotations were visually inspected. The results of the deep learning method were visually inspected for completeness and overall quality. Dice similarity coefficient (DCS) and the modified Hausdorff (MHD) distance were reported for the test set.

### RESULTS

The DCS was 0.98±0.002 per volume at the chosen operating point on the SPM standard and the MHD was 0.93±0.11mm per volume. It took less than 10 seconds to compute the complete 3D brain mask on a modern GPU. Overall, our method was capable of learning from a sub-optimal reference standard and extracting the brain from an SWI scan. It mimicked some of the deficiencies of the SPM brain masks, such as occasional failures in the most inferior or superior axial slices, but also mitigated others through generalization over the training set. Holes in the mask caused by contusions or hematomas were less prevalent with the 2D-U-Net than with SPM.

### CONCLUSION

The 2D-U-Net method provides fast brain extractions in MR-SWI.

### **CLINICAL RELEVANCE/APPLICATION**

SWI is the best modality to establish the extent of cerebral microbleeds in TBI. Brain extraction in SWI is the first step in the development of computer-aided systems detecting these microbleeds.

### SSC11-03 Subconcussive Head Impacts May Alter Metrics Associated with Normal Pruning in Youth and High School Football Players

Monday, Nov. 26 10:50AM - 11:00AM Room: S402AB

Participants

Gowtham Krishnan Murugesan, MS, Arlington, TX (*Presenter*) Nothing to Disclose Ryan A. Fisicaro, MD, Dallas, TX (*Abstract Co-Author*) Nothing to Disclose James M. Holcomb, BS,BA, Dallas, TX (*Abstract Co-Author*) Nothing to Disclose Elizabeth M. Davenport, PhD, Dallas, TX (*Abstract Co-Author*) Nothing to Disclose Ben Wagner, BS, Dallas, TX (*Abstract Co-Author*) Nothing to Disclose Jillian Urban, Winston- Salem, NC (*Abstract Co-Author*) Nothing to Disclose Mireille Kelley, Winston-Salem, NC (*Abstract Co-Author*) Nothing to Disclose Derek Jones, Winston-Salem, NC (*Abstract Co-Author*) Nothing to Disclose Christopher T. Whitlow, MD, PhD, Winston-Salem, NC (*Abstract Co-Author*) Nothing to Disclose Joel Stitzel, Winston-Salem, NC (*Abstract Co-Author*) Nothing to Disclose Joseph A. Maldjian, MD, Dallas, TX (*Abstract Co-Author*) Consultant, BioClinica, Inc; Consultant, Koninklijke Philips NV

### For information about this presentation, contact:

gowtham.murugesan@utsouthwestern.edu

#### PURPOSE

To determine whether exposure to repetitive subconcussive impacts affects fMRI metrics associated with normal pruning in youth and high school football players over a single season.

### METHOD AND MATERIALS

Youth and high school football players are exposed to high numbers of head impacts over the course of a season [1]. The spectral power of resting state networks typically decreases as a function of age and has been interpreted as a sign of normal Gray Matter (GM) pruning [2]. We hypothesized that a season of contact sports will alter this relationship. Specifically, there will be an increase in power of the DMN and consequent change in GM volume (GMV) associated with normal pruning.Sixty age matched players without history of developmental, neurological, or psychiatric abnormalities and no history of concussion during or prior to the season were split into high impact (HI) (24) and low impact (LI) (36) groups, respectively based on each player's risk-weighted cumulative exposure (RWEcp)[3,4]. The RWEcp represents the summed risk of concussion for each impact over the season as derived by the Head Impact Telemetry System (HITS) data [1]. High order ICA (n=60) was performed to extract independent components using the GIFT toolbox [5]. Subject specific time courses for each subject were converted into a power spectrum through power spectral decomposition. Five components of the DMN were identified and changes in the power of the network were computed as post-season minus pre-season values ( $\Delta$ PSD). Following bonferroni correction, only the anterior cingulate network

demonstrated a significant difference in  $\Delta$ PSD and was used as a mask to determine GMV using VBM8. A two-sample t-test was performed to determine significant changes in  $\Delta$ PSD and  $\Delta$ GMV between the groups.

### RESULTS

The frontal DMN (FDMN) demonstrated a significant increase in power in the HI group (p-value: 0.00018). A significant increase in GM volume was found in the same frontal regions of the DMN (p-value: 0.005) (Fig.1) for HI group.

### CONCLUSION

Our results suggests that normal GM pruning is affected in the HI group, over a single season of contact sport. Longitudinal studies are needed to understand the long-term changes in resting state networks and effects on functional brain health.

### **CLINICAL RELEVANCE/APPLICATION**

This work demonstrates that playing a season of contact sports may affect normal GM pruning in high school and youth football players

### SSC11-04 Source Space MEG Delta Waves Increase Following Concussion

Monday, Nov. 26 11:00AM - 11:10AM Room: S402AB

Participants

Elizabeth M. Davenport, PhD, Dallas, TX (*Presenter*) Nothing to Disclose Jillian Urban, Winston- Salem, NC (*Abstract Co-Author*) Nothing to Disclose Ben Wagner, BS, Dallas, TX (*Abstract Co-Author*) Nothing to Disclose Mark A. Espeland, PHD, Winston-Salem, NC (*Abstract Co-Author*) Nothing to Disclose Alexander K. Powers, MD, Winston Salem, NC (*Abstract Co-Author*) Nothing to Disclose Christopher T. Whitlow, MD, PhD, Winston-Salem, NC (*Abstract Co-Author*) Nothing to Disclose Joel Stitzel, Winston-Salem, NC (*Abstract Co-Author*) Nothing to Disclose Joseph A. Maldjian, MD, Dallas, TX (*Abstract Co-Author*) Consultant, BioClinica, Inc; Consultant, Koninklijke Philips NV

### For information about this presentation, contact:

elizabeth.davenport@utsouthwestern.edu

### PURPOSE

The purpose of this study is to determine if delta waves, measured by magnetoencephalography (MEG), increase due to a sports concussion.

### **METHOD AND MATERIALS**

From a larger study on subconcussive impacts in high school football, five players were diagnosed with a concussion during the season (mean age=16.1). Subjects followed returned-to-play protocols. Eight minutes of eyes-open, resting-state MEG data were acquired for each subject and control using a 275 channel CTF whole-head system. Football players were scanned pre-season, within 36 hours post-concussion, and post-season. Seven age and gender matched non-contact sports athletes (controls) were also recruited (mean age=16.2). Controls received baseline and follow-up scans 4 months later. Using Brainstorm, MEG data were baseline corrected, band-stop filtered (60Hz), down-sampled to 250Hz, and band-pass filtered to 1-100Hz. Eye blinks, and muscle artifacts were removed using independent component analysis. Data was source localized using a minimum norm method. The average whole-brain power of the delta frequency and total power was computed for each scan. The delta frequency power was normalized by the total power. In the concussed football players, pre-season delta power was subtracted from post-concussion delta power. For the control subjects, baseline delta power was subtracted from the 4-month follow-up scan. A t-test was performed to compare the change in delta power of controls to the change in delta power of concussed football players.

### RESULTS

The change in delta power following concussion was significantly different from controls (p=0.014). In addition to the statistical difference, delta waves visibly increased from pre-season to post-concussion (Figure 1).

### CONCLUSION

We demonstrate that a single concussion can visibly and statistically increase delta frequency power in MEG.

#### **CLINICAL RELEVANCE/APPLICATION**

Traditional imaging is typically unremarkable in concussion. This study demonstrates that MEG may be a new and useful diagnostic tool for concussion.

## ssc11-06 Longitudinal Hippocampal Subfield Volume Changes in Collegiate Football Athletes

Monday, Nov. 26 11:20AM - 11:30AM Room: S402AB

Participants

Sherveen N. Parivash, MD, Stanford, CA (*Abstract Co-Author*) Nothing to Disclose Maged Goubran, BMedSc, London, ON (*Abstract Co-Author*) Nothing to Disclose Paymon Rezaii, BS, Stanford, CA (*Abstract Co-Author*) Nothing to Disclose Dylan Wolman, MD, Santa Monica, CA (*Abstract Co-Author*) Nothing to Disclose Jitsupa Wongsripuemtet, MD, Palo Alto, CA (*Abstract Co-Author*) Nothing to Disclose Wei Bian, PhD, Stanford, CA (*Abstract Co-Author*) Nothing to Disclose Brian M. Boldt, DO, Tacoma, WA (*Abstract Co-Author*) Nothing to Disclose David B. Douglas, MD, Sacramento, CA (*Abstract Co-Author*) Nothing to Disclose Lex A. Mitchell, MD, Stanford, CA (*Abstract Co-Author*) Nothing to Disclose Jay J. Choi, MD, Honolulu, HI (*Abstract Co-Author*) Nothing to Disclose Eugene W. Wilson IV, DO, Palo Alto, CA (*Abstract Co-Author*) Nothing to Disclose Paul Yushkevich, PhD, Philadelphia, PA (*Abstract Co-Author*) Investigator, KinetiCor, Inc Mansi S. Parekh, PhD, Stanford, CA (*Abstract Co-Author*) Nothing to Disclose Jens Fiehler, Hamburg, Germany (*Abstract Co-Author*) Research Consultant, Acandis GmbH & Co KG; Research Consultant, Terumo Corporation ; Research Consultant, Johnson & Johnson; Research Consultant, Stryker Corporation; Speakers Bureau, Penumbra, Inc; Speakers Bureau, Medtronic plc

Huy M. Do, MD, Stanford, CA (Abstract Co-Author) Nothing to Disclose

Jaime S. Lopez, MD, Stanford, CA (Abstract Co-Author) Nothing to Disclose

Jarrett Rosenberg, PhD, Stanford, CA (Abstract Co-Author) Nothing to Disclose

Gerald Grant, MD, Palo Alto, CA (Abstract Co-Author) Nothing to Disclose

Max Wintermark, MD, Lausanne, Switzerland (*Abstract Co-Author*) Advisory Board, General Electric Company; Consultant, More Health; Consultant, Magnetic Insight; Consultant, Icometrix; Consultant, Nines;

Michael M. Zeineh, PhD, MD, Stanford, CA (Presenter) Research funded, General Electric Company; Consultant, Biogen Idec Inc

### PURPOSE

Collegiate football athletes are subject to repeated head impacts. The hippocampus, a structure crucial for memory, is of particular interest in the study of football. There is a lack of prospective, longitudinal data on the hippocampus in football.

### **METHOD AND MATERIALS**

A prospective cohort study was conducted over a 4-year period composed of 63 football and 34 volleyball male collegiate athletes. Automated segmentation provided hippocampal subfield volumes from whole brain axial T1 images and high-resolution coronaloblique T2 images. At baseline, these volumes were linearly regressed to compare football with volleyball. For the longitudinal data, a linear mixed-effects model assessed the interaction between sport and time.

### RESULTS

Comparing sports at baseline, the football athlete group showed a smaller subiculum volume (coefficient=-67.77, 95% CI [-120.20, -15.33], P=.012). The longitudinal interaction between sport and time demonstrated a significant decrease in total hippocampal volume in athletes who play football relative to volleyball (coefficient=-90.27, 95%CI [-177.05, -3.48], P=.041), most significantly within the CA1 hippocampal subfield (coefficient=-28.55, 95%CI [-50.94, -6.17], P=.012). This interaction within CA1 was significant even when in-study concussions were excluded (coefficient=-34.22, 95%CI [-60.79, -7.65], P=.012). Within the right CA1, this volume decrement was observed in football even in isolation from volleyball (coefficient=-22.96, 95%CI [-40.13,-5.80], P=.009).

### CONCLUSION

A prospective longitudinal evaluation comparing football and volleyball athletes showed a decrease in hippocampal volumes over time in football athletes. This longitudinal divergence was most significant in CA1, in contradistinction to baseline differences that were most significant in the downstream subiculum.

### **CLINICAL RELEVANCE/APPLICATION**

Given these observed hippocampal volume alterations, further research must be done to assess the potential relevance to cognitive function.

#### **Honored Educators**

Presenters or authors on this event have been recognized as RSNA Honored Educators for participating in multiple qualifying educational activities. Honored Educators are invested in furthering the profession of radiology by delivering high-quality educational content in their field of study. Learn how you can become an honored educator by visiting the website at: https://www.rsna.org/Honored-Educator-Award/ Max Wintermark, MD - 2018 Honored Educator

### SSC11-08 Detection of Mild Traumatic Brain Injury by Support Vector Machine Classification with Voxel-Mirrored Homotopic Connectivity: A Longitudinal Perspective

Monday, Nov. 26 11:40AM - 11:50AM Room: S402AB

#### Participants

Zhuonan Wang, Xian, China (*Presenter*) Nothing to Disclose Lijun Bai, PhD, Xian, China (*Abstract Co-Author*) Nothing to Disclose Chuanzhu Sun, Xian, China (*Abstract Co-Author*) Nothing to Disclose Shan Wang, Xi'an, China (*Abstract Co-Author*) Nothing to Disclose Yingxiang Sun, Xian, China (*Abstract Co-Author*) Nothing to Disclose Ming Zhang, Xian, China (*Abstract Co-Author*) Nothing to Disclose

#### For information about this presentation, contact:

wangzhuonan424@stu.xjtu.edu.cn

#### PURPOSE

To examine dynamic inter-hemispheric functional connectivity in mild traumatic brain injury (mTBI) patients with longitudinal observations and how machine learning can be used alongside voxel mirrored homotopic connectivity (VMHC) to accurately separate mTBI patients from healthy controls and predict the future long-term development of clinical significant cognitive impairment following mTBI.

### **METHOD AND MATERIALS**

Sixty-one patients with mTBI and forty-four age- and gender-matched subjects underwent clinical and neuropsychological evaluations with fMRI scanning. All of patients was initially evaluated within 14 days post-injury and follow-up at 6-12 months.We adopted VMHC to quantifies the functional connectivity between bilateral homotopic voxels. Next, the multivariate analysis of VMHC results was performed with linear support vector machines (SVM). The commonly affected functional brain regions were selected as the feature metrics combined with SVM to predict clinical outcome in individual patients.

Compared with healthy controls, mTBI patients showed decreased VMHC in the dorsal lateral prefrontal cortex and supplementary motor area and increased VMHC in the ventrolateral prefrontal cortex, orbitofrontal cortex and posterior cingulate cortex(P < 0.005) in sub-acute phase. In 6-12 months, decreased regions were completely disappeared while original increased regions showed continuously and extend patterns. The SVM classifier based on the sub-acute phase VMHC results yielded an accuracy rate of 82% (with a sensitivity of 88.1% and specificity of 92.9%) after 1000 permutation, which was significantly better than chance (P<0.005). Combined the sub-acute phase VMHC results with support vector regression machines, we found significant positive correlations between actual neuropsychological values and predicted values in three clinical tests (PSS, R2 = 0.83; HAMD, R2 = 0.87; FSS, R2 = 0.91).

### CONCLUSION

The VMHC results successfully revealed the time correlated functional connectivity alteration in some particular brain regions and their association with clinical outcomes. We further provided evidence that using VMHC with machine learning approache has the potential to augment diagnosis in individual patients following mTBI.

#### **CLINICAL RELEVANCE/APPLICATION**

We demonstrate relationships between inter-hemispheric functional connectivity abnormalities and predictions about individual patients' clinical outcomes.

### SSC11-09 Is a Follow-Up CT After 4 Hours Necessary for Falx and Tentorial SDH?

Monday, Nov. 26 11:50AM - 12:00PM Room: S402AB

Participants

Murat A. Oztek, MD, Seattle, WA (*Presenter*) Nothing to Disclose Wei Wu, MD, Wuhan, China (*Abstract Co-Author*) Nothing to Disclose Daniel S. Hippe, MS, Seattle, WA (*Abstract Co-Author*) Research Grant, Koninklijke Philips NV; Research Grant, General Electric Company; Research Grant, Canon Medical Systems Corporation; Research Grant, Siemens AG Richard C. Lee, Memphis, TN (*Abstract Co-Author*) Nothing to Disclose Joshua I. Rosenbaum, MD, Seattle, WA (*Abstract Co-Author*) Nothing to Disclose Charles G. Colip, MD, Seattle, WA (*Abstract Co-Author*) Nothing to Disclose William T. Yuh, MD, Seattle, WA (*Abstract Co-Author*) Nothing to Disclose

### For information about this presentation, contact:

oztekma@uw.edu

#### PURPOSE

The mandatory 4 hour follow-up CT (4Hr-CT) has been the standard for patients with traumatic intracranial hemorrhage, including Subdural Hematoma (SDH) in the Tentorium (T-SDH) and Falx (F-SDH). The purpose of this study was to assess the effectiveness of 4Hr-CT for isolated F-SDH and T-SDH in the management of traumatic intracranial hemorrhage.

### METHOD AND MATERIALS

182 consecutive cases with acute SDH treated at a major trauma center between December 2015 and March 2018 were retrospectively reviewed. Isolated F-SDH and/or T-SDH were identified in 54 patients (30%). All patients had initial and 4-HrCT. The size of the SDH was measured parallel or perpendicular to the falx or tentorium (long and short axis, respectively). The morphology of the SDH, mass effect, extent of involvement and interval change at 4-HrCT were evaluated.

#### RESULTS

All the F-SDH and T-SDH had a pancake-like configuration with the long-axis (median 38 mm) greater than the short axis (median 3 mm) by 10 fold on average (p<0.001). An interval increase along the short axis was seen in only 5 F-SDH (16%) and 7 T-SDH (19%), with a maximum change of 2 mm. Interval increases were more prominent along the long axis: 18 F-SDH (56%) and 19 T-SDH (51%), with a maximum change of 118 mm and 21 mm, respectively. F-SDH and T-SDH were contiguous in 14 out of the 18 patients with both hematomas. No patients had worsening focal neurological findings after initial diagnosis required surgical intervention or died during their hospital stay (rate 0%, 95% CI 0-6.6%).

#### CONCLUSION

Based upon our limited data, the current standard protocol of a mandatory 4-hour follow-up CT is not cost-effective in the management of patients with isolated F-SDH and/or T-SDH. These SDHs expand minimally along the short axis, if at all, without causing significant mass effect. The high incidence of continuity between co-existing F-SDH and T-SDH, characteristic anatomic structure, and deformability of the tentorium and falx may serve as a natural barrier limiting the overall growth of SDH, while providing potential space for decompression by longitudinal spread of the SDH.

### **CLINICAL RELEVANCE/APPLICATION**

The current standard protocol of a mandatory 4-hour follow-up CT for acute intracranial hemorrhage is not needed for patients with isolated Falx and/or Tentorium Subdural Hematoma.



#### SSC12

### Physics (MR: New Techniques, Systems, Evaluation)

Monday, Nov. 26 10:30AM - 12:00PM Room: N226



AMA PRA Category 1 Credits ™: 1.50 ARRT Category A+ Credit: 1.75

FDA Discussions may include off-label uses.

#### Participants

Robert E. Lenkinski, PhD, Dallas, TX (*Moderator*) Research Grant, Koninklijke Philips NV Research Consultant, Aspect Imaging Peter A. Hardy, PhD, Lexington, KY (*Moderator*) Nothing to Disclose Yi Wang, PhD, New York, NY (*Moderator*) Nothing to Disclose

#### Sub-Events

SSC12-01 Impact of Respiratory Training in Improving Image Quality: A Study Based on Free Breathing T1 Star VIBE MRI

Monday, Nov. 26 10:30AM - 10:40AM Room: N226

Participants

Ma Guangming, MMed, Xianyang City, China (*Presenter*) Nothing to Disclose Dang Shan, Xianyang, China (*Abstract Co-Author*) Nothing to Disclose Tian Qian, MMed, Xianyang City, China (*Abstract Co-Author*) Nothing to Disclose Nan Yu, MD, Xian Yang, China (*Abstract Co-Author*) Nothing to Disclose Lei Yuxin, MMed, Xianyang City, China (*Abstract Co-Author*) Nothing to Disclose Shaoyu Wang, Shanghai, China (*Abstract Co-Author*) Nothing to Disclose Chenwang Jin, Xi'an, China (*Abstract Co-Author*) Nothing to Disclose

For information about this presentation, contact:

# 416725386

### PURPOSE

Our objective was to estimate the impact of respiratory training in improving image quality of images obtained from T1 Star VIBE magnetic resonance imaging (MRI).

### METHOD AND MATERIALS

This prospective study was approved by the local ethics committee. Totally of 6 volunteers were in the study. The volunteers underwent 3 Tesla MR scanner (Siemens-Skyra) using T1 Star VIBE for two times within 24-48h. The MRI protocol (MAGNETOM 3.0T SKYRA MR scanner, Siemens healthcare, Erlangen, Germany) included a Prototyped T1-weighted 3D Star VIBE sequence(TE/TR:1.39/2.79,slice thickness 1.2mm)and T2 blade. The volunteers accepted MRI examination directly at the first scan, while they receive respiratory training before the MRI examination to make them keeping calm and breathing evenly. The observation of lung markings were used to evaluate image quality of each examination. The display of lung markings were observed in three zone (upper, middle and bottom according to the T4 and T8 vertebra level) by two experienced radiologists independently. And a 3-point system were used (3-point: no artifacts, noise, or with a little artifacts, less noise, the image quality is better; 2-point: more artifacts, more noise, image quality is acceptable; 1-point: obvious artifacts, large noise, image quality is poor.) The image quality of T1 Star VIBE MRI in two scans were compared.

#### RESULTS

All the volunteers finished MRI examination. The image quality scores of three zones(upper, middle and bottom) in first scans were  $2.5\pm0.55$ ,  $2.17\pm0.75$ ,  $1.5\pm0.55$ , and those were  $2.83\pm0.41$ ,  $2.67\pm0.52$ ,  $2.33\pm0.82$  in the second scans. The image quality scores of the lower part of the lungs had significant difference among the two groups(t=2.71, p=0.042).

#### CONCLUSION

Respiratory training could improve the image quality, especially at the bottom of the lung and increase the lesion detection rate and accuracy of diagnosis.

#### **CLINICAL RELEVANCE/APPLICATION**

Respiratory training may be used to improve the image quality of images obtained from T1 Star VIBE magnetic resonance imaging.

### ssc12-02 MRI Safety: Digital Measurement of Magnetically Induced Torque Based on ASTM F2213

Monday, Nov. 26 10:40AM - 10:50AM Room: N226

Mushtaq Musadik, Jena, Germany (*Abstract Co-Author*) Nothing to Disclose Rene Aschenbach, MD, Jena, Germany (*Abstract Co-Author*) Nothing to Disclose Florian Burckenmeyer, Jena, Germany (*Presenter*) Nothing to Disclose Ioannis Diamantis, Jena, Germany (*Abstract Co-Author*) Nothing to Disclose Niklas P. Eckardt JR, MD, Neuengonna, Germany (*Abstract Co-Author*) Nothing to Disclose Ulf K. Teichgraeber, MD, Jena, Germany (*Abstract Co-Author*) Research Consultant, W. L. Gore & Associates, Inc Research Consultant, Siemens AG Research Consultant, CeloNova BioSciences, Inc Research Consultant, General Electric Company

### CONCLUSION

Ferromagnetic stainless steel screws may exhibit large magnetically induced torque within the homogeneous magnetic field during MRI examination. For analysing of these magnetically induced torque a digital measuring device could be developed, which allows to simplify and accelerated the standard test method ASTM F2213.

#### Background

Performing MRI examinations in patients who use implantable medical devices involve safety risks both for the patient and the implant. The aim was a digital measuring device for measuring magnetically induced torque on medical implants in magnetic field center of 1.5T and 3T MR scanner.

### **Evaluation**

An MR-safe measuring platform was developed according to the standard ASTM F2213 and combined with a precision balance (PCB 1600-2, Kern & Shon GmbH, Germany). The evaluation was performed with stainless steel screws (length 24, 47 and 71 mm) and a neurostimulator (LibraXP, St. Jude Medical, USA) in the magnetic field center of a 1.5T and 3T MRI (Magnetom Avanto and Magnetom Prisma, Siemens, Germany). The torque was measured at 10-degree increments as the implant was rotated relative to the static magnetic field for all possible orientations of the object.

#### Discussion

The measured force depends on the object orientation within the static magnetic field. The neurostimulator had a torque of 1 + 1 N\*mm (maximum 3 N\*mm) for a rotation about the vertical axis, 39 + 20 Nmm (maximum 64 N\*mm) for rotation about the longitudinal axis and 40 + 20 N \* mm (maximum 64 N\*mm) ) for a rotation about the transverse axis. This corresponds to a maximum acting force of 1.28 N (mass 0.131 kg). The magnetostatic torque is proportional to the length of the test object. For the stainless steel screws, the torque is 66 + 37 N\*mm (maximum 108 N\*mm) for a length of 24 mm, 139 + 86 Nmm (maximum 247 N\*mm) for a length of 47 mm and 252 + 145 Nmm (maximum 434 N\*mm) for a length of 71 mm.

# SSC12-03 Numerical Simulation of Thermal Risk Assessment for a Compact MR Scanner

Monday, Nov. 26 10:50AM - 11:00AM Room: N226

Participants

Matthew Tarasek, PhD, Niskayuna, NY (*Abstract Co-Author*) Employee, General Electric Company Yunhong Shu, PhD, Rochester, MN (*Abstract Co-Author*) Nothing to Disclose Desmond Yeo, Niskayuna, NY (*Abstract Co-Author*) Employee, General Electric Company Ek T. Tan, MENG, Rochester, MN (*Abstract Co-Author*) Employee, General Electric Company John Huston III, MD, Rochester, MN (*Abstract Co-Author*) Stockholder, Resoundant, Inc Royalties, Resoundant, Inc Matthew A. Bernstein, PhD, Rochester, MN (*Presenter*) Former Employee, General Electric Company Thomas K. Foo, PhD, Niskayuna, NY (*Abstract Co-Author*) Employee, General Electric Company

# For information about this presentation, contact:

tarasek@ge.com

#### PURPOSE

Brain imaging on conventional MRI scanners commonly relies on a whole-body (WB) radiofrequency (RF) transmit coil to provide a uniform excitation (B1+) field. As such, patient RF power deposition may be an issue during high RF duty-cycle scanning. A recently developed compact 3T (C3T) MRI scanner with high performance gradients [1,2] has a dedicated RF transmit coil that exposes only the head region. For neuroimaging, the C3T scanner may provide lower RF power deposition compared to conventional WB scanners, thus enabling the development of advanced neuroimaging techniques.

### **METHOD AND MATERIALS**

A 16-rung high-pass birdcage head coil (127.74 MHz, 37-cm ID, driven in quadrature) was modelled using full-wave electromagnetic FDTD simulation software, Sim4Life (ZMT, Zurich, Switzerland). Simulations were performed to predict specific absorption rate (SAR) distributions using the Duke human body model as a test phantom at a landmark location of the glabella. A large-diameter standard 3T 16-rung WB birdcage coil was also modeled for comparison. Input power on the larger coil was scaled to reach the same average B1+ for the glabella slice as in the C3T, and scaled SAR maps were used as inputs to a time-dependent Penne's bioheat equation [3] thermal solver. All thermal simulations were run using 200W continuous input power for 60 minutes, with the proper scaling for the WB coil according to B1+. All material properties were set to nominal literature values [4].

### RESULTS

The following were observed as a result of the simulations of the C3T compared to whole-body MRI: (i) ~20% reduced average SAR in the head and neck region, (ii) lower ( $5.5^{\circ}$ C vs  $6.5^{\circ}$ C) peak temperature rise in the brain regions, and (iii) minimal (~0°C) temperature rise in the neck region was observed in the C3T scanner compared to the ~7°C rise in the WB MRI, due to reduced body mass exposure in the dedicated scanner.

### CONCLUSION

The C3T provides a reduction of ~20% in thermal risk over a conventional whole-body MRI due to the much smaller exposed body mass to achieve the same B1+ excitation field in the brain. This allows for improved performance from the SAR demanding applications. 1.FooT,MRM,2018 2.WeaversP,MPhys,2016 3.Pennes.JAPhys1948 4.GabrielS,PMB1996

#### **CLINICAL RELEVANCE/APPLICATION**

Advanced neuroimaging techniques require faster imaging thus creating potential for increased patient heating. Here we investigate the thermal risk of a recently developed head-only MRI scanner.

# SSC12-04 Improving Resolution, Distortion, and SNR of Clinical Diffusion Weighted Images Using Deep Learning

Monday, Nov. 26 11:00AM - 11:10AM Room: N226

Participants

Junshen Xu, Beijing, China (*Presenter*) Nothing to Disclose Nan Liu, Shanghai, China (*Abstract Co-Author*) Employee, Shanghai United Imaging Healthcare Co, Ltd Xiaodong Ma, Beijing, China (*Abstract Co-Author*) Nothing to Disclose Jun Xie, Shanghai, China (*Abstract Co-Author*) Employee, Shanghai United Imaging Healthcare Co, Ltd Guobin Li, Shanghai, China (*Abstract Co-Author*) Employee, Shanghai United Imaging Healthcare Co, Ltd Zhenkui Wang, Shanghai, China (*Abstract Co-Author*) Employee, Shanghai United Imaging Healthcare Co, Ltd Nan-Jie Gong, Houston, TX (*Abstract Co-Author*) Employee, UIH America, Inc Kui Ying, PhD, Beijing, China (*Abstract Co-Author*) Nothing to Disclose

#### PURPOSE

Diffusion weighted images (DWI) are commonly acquired with single-shot Echo-planar imaging (EPI) sequence, which is suffered from image distortion due to eddy current and B0 field inhomogeneity as well as low resolution especially in clinical settings. Multi-shot DWI has been demonstrated to outperform single-shot DWI in these aspects with optimized SNR. However, multi-shot DWI has not been widely adopted clinically due to long scan time.

#### **METHOD AND MATERIALS**

We proposed a method of generating high-quality DWI from its low-quality counterpart using fully convolutional neural network. Brain DWI data were acquired with a 3T MR system (uMR 780) using both single-shot (128\*128) and four-shots (160\*160) EPI sequences. The multi-shot EPI DWI, which has higher resolution and less distortion, served as ground truth in training process. Our dataset contains 38 pairs of single-shot and multi-shot DWI. Each pair of images were resized to 320x320 and then cropped randomly to generate 50 patches (128x128). To make full use of available data and reduce the bias, we adopted a 10-fold cross validation in experiments.

#### RESULTS

For quantitative evaluation, we calculated peak signal-to-noise ratio (PSNR) and structural similarity index (SSIM). Results showed that the proposed method gain 4.2dB in PSNR and 0.22 in SSIM compared with single-shot DWI. Additionally, perceptual results showed that our neural network can recover details and reduce distortion in single-shot DWI.

#### CONCLUSION

Results imply that we can improve resolution, SNR and reduce distortion of single-shot EPI-DWI using deep neural network, which potentially enables acquiring high quality DWI without lengthening scan time.

#### **CLINICAL RELEVANCE/APPLICATION**

This method could improve resolution, SNR and reduce distortion of clinical DW images without lengthening scan time.

### ssc12-05 Fast Field-Cycling MRI Technology: Prototype Human Scanner and First Clinical Results

Monday, Nov. 26 11:10AM - 11:20AM Room: N226

Participants

David Lurie, Aberdeen, United Kingdom (*Presenter*) Research Grant, General Electric Company Lionel M. Broche, PhD, Aberdeen, United Kingdom (*Abstract Co-Author*) Nothing to Disclose Gareth R. Davies, MSc, DPhil, Aberdeen, United Kingdom (*Abstract Co-Author*) Nothing to Disclose German Guzman Gutierrez, MD,MPH, Aberdeen, United Kingdom (*Abstract Co-Author*) Nothing to Disclose Mary J. Macleod, MBChB,PhD, Aberdeen, United Kingdom (*Abstract Co-Author*) Nothing to Disclose Peter J. Ross, PhD, Aberdeen, United Kingdom (*Abstract Co-Author*) Nothing to Disclose

#### For information about this presentation, contact:

d.lurie@abdn.ac.uk

#### PURPOSE

A prototype human-scale Fast Field-Cycling (FFC) MRI scanner has been built, allowing good quality images at ultra-low field (0.2 mT) with enhanced T1-contrast. It has been used to image the brain in patients with acute ischemic stroke.

#### **METHOD AND MATERIALS**

FFC-MRI is a new method, designed to image at ultra-low field while preserving signal-to-noise ratio (SNR) and image quality. The main field (B0) is switched between values during the pulse sequence, with polarization at the scanner's highest field, evolution (relaxation) at low field, followed by gradients, RF pulses and signal detection at high field. Our in-house-built prototype scanner has a water-cooled resistive magnet (Tesla Engineering, UK; bore 0.5 m, length 2 m) providing a maximum field of 0.2 T, with the evolution field controllable between 0.2 mT and 0.2 T; switching time between fields is 20 ms. A home-built head birdcage coil (8.5 MHz) was used. Scanner control is via a commercial console (MR Solutions, UK), running pulse sequences which include control of B0. Magnet current (up to 1950 A) is from a low-noise power supply amplifier (International Electric Company, Finland). Following research ethics committee approval, patients (N=10) with acute ischemic stroke were recruited and gave informed consent. They were scanned by FFC-MRI within 24-96 h after presentation. Duration of the FFC-MRI examination was typically 45 minutes, including setup, scout and FFC images at five evolution fields (0.2 mT to 200 mT). Patients were scanned by CT prior to FFC-MRI and some had 3 T MRI (N=2) including DWI.

#### RESULTS

The usable range of B0 during the evolution period was validated in phantoms. In scans of patients with acute ischemic stroke, T1-

weighted FFC-MRI images exhibited hyper-intense regions, with contrast increasing markedly as the evolution magnetic strength field decreased, with maximum lesion intensity at the lowest field used (0.2 mT). The infarct region seen by FFC-MRI correlated well with the appearance in CT and DWI (where appropriate) images.

### CONCLUSION

A whole-body FFC-MRI scanner was built and has been used to image the brain in patients with ischemic stroke, in the first-ever clinical demonstration of this technology.

### CLINICAL RELEVANCE/APPLICATION

FFC-MRI is a new modality which can generate diagnostic-quality images at ultra-low magnetic fields (e.g. 0.2 mT), with significantly-enhanced endogenous T1-contrast compared to conventional MRI.

### SSC12-06 Joint Cardiovascular Magnetic Resonance Image Reconstruction and Segmentation Using Deep Learning Image-to-Image Translation

Monday, Nov. 26 11:20AM - 11:30AM Room: N226

Participants

James W. Goldfarb, PhD, Roslyn, NY (*Presenter*) Nothing to Disclose Jie J. Cao, MD, Roslyn, NY (*Abstract Co-Author*) Nothing to Disclose

### PURPOSE

To develop and test a joint image reconstruction and semantic segmentation method for functional right and left ventricular cardiovascular MR imaging.

### **METHOD AND MATERIALS**

Image-to-image translation using a generative adversarial network (GAN) was implemented using PyTorch v 0.3.0, translating source radial CMR sinograms (r-theta space) to semantic segmentation of the left and right ventricles. 1700 short axis cardiac MR images were used for training (n=1400), simulation and validation(n=300). Each had expert manual segmentation of the LV and RV bloodpools. Deep learning via a U-net convolutional neural network was used for image-to-image translation (so-called 'pix2pix'), providing semantic segmentation masks of the RV and LV directly from raw CMR k-space data. The U-net Generator was trained with an adversarial loss for 100 epochs. Reconstruction/segmentation of the RV and LV was studied with undersampling factors of up to 8. The Sørensen-Dice similarity index was used to compare RV and LV masks to manual segmentation in validation data, undersampled simulations, and prospectively collected CMR radial exams (n=15).

#### RESULTS

The GAN trained quickly, providing excellent segmentation of both the LV and RV with LV Dice index=  $0.989\pm0.003$  (range: 0.975-0.996) and RV Dice Index =  $0.986\pm0.005$  (range: 0.938-0.995). Deep learning provided segmentation consistent with clinical standards, where trabeculae and papillary muscles are included inside of ventricular bloodpool segmentations. With an acceleration factor of 8, quality segmentations were maintained with slightly reduced Dice Indices: LV Dice index=  $0.961\pm0.016$  (range: 0.872 - 0.993); RV Dice index=  $0.937\pm0.023$  (range: 0.734-0.981). In-vivo prospective reconstructions using complex radial CMR data yielded similar Dice Indices.

### CONCLUSION

Image-to-image translation is a viable method for radial MR image reconstruction and provides a framework for image reconstruction, acceleration and segmentation. In this proof-of-concept study, simulations confirmed the feasibility of quantitative LV and RV imaging with image-to-image translation and prospective in vivo radial imaging yielded encouraging results with acceleration factors of up to 8.

#### **CLINICAL RELEVANCE/APPLICATION**

A deep learning approach is presented which 'translates' CMR data directly to quantitative LV and RV segmentation and eliminates the need for conventional backprojection and gridding along with manual segmentation.

### ssc12-07 Optimization of Pulse Sequence Ordering for Automated Fat and Iron Quantification

Monday, Nov. 26 11:30AM - 11:40AM Room: N226

Participants Daniel J. Margolis, MD, Los Angeles, CA (*Presenter*) Consultant, Blue Earth Diagnostics Ltd Alexander Gavlin, MD, Bronx, NY (*Abstract Co-Author*) Nothing to Disclose Andrea S. Kierans, MD, New York, NY (*Abstract Co-Author*) Nothing to Disclose

For information about this presentation, contact:

djm9016@med.cornell.edu

### PURPOSE

Commercially available pulse sequences with dedicated post-processing software can automate the creation of maps for fat and iron quantification and make them readily available on picture archiving and communication systems (PACS) workstations, obviating the need for dedicated post-processing to be performed by the radiologist. These most commonly use a gradient multi-echo Dixon technique for derivation of fat percent (or per mille, "per thousand") and R2\*, from which iron deposition can be extrapolated. However, as patients at risk for fat or iron accumulation generally also have diffuse liver disease, these scans are often combined with contrast-enhanced imaging using a hepatobiliary agent (e.g., gadoxetate disodium) with a 20-minute delayed scan in the hepatobiliary phase for improved lesion detection. This results in "down time" between the equilibration phase, generally before 5 minutes after contrast administration, and the hepatobiliary phase. It is attractive to perform as many pulse sequences as possible during this "down time," but only if they are not adversely affected by the accumulation of the contrast administration, the degree to which contrast accumulation affects signal for these acquisitions is unknown.

#### RESULTS

Twelve subjects were identified. Two were excluded as outliers (one for severe steatosis, one for iron overload). Adequate measurement of FP and R2\* was performed before and after contrast for the remaining 10 patients. The student's t-test showed no significant difference for FP (p=0.21) but a significant increase in measured R2\* after contrast (p=0.02). The control chart shows increased variability for those R2\* values acquired after contrast.

### CONCLUSION

Time is the ultimate non-renewable resource. Therefore, time optimization of magnetic resonance imaging is an important consideration for optimal utilization of resources. However, this should not sacrifice diagnostic accuracy, and thereby decrease value. This investigation of fat and iron quantification shows that fat quantification appears relatively unaffected by accumulation of a T1- and T2\*-shortening contrast agent, whereas R2\* is unreliably increased in this setting. Fat/water quantification to measure the degree of steatosis might therefore be possible in the delayed post-contrast phase, whereas quantification of iron accumulation must be done prior to contrast administration. The control chart in this case shows the opposite of the expected effect for R2\*, with an increase in variability after the intervention (contrast administration).

#### **METHODS**

The gradient multi-echo Dixon sequences were acquired before and approximately 15 minutes after administration of gadoxetate disodium (Eovist, Bayer) at 0.025 mmol/kg and 2.0 mL/sec (LiverLab q-Dixon, Siemens Healthineers, TR/TE 15.6/2.4, 4 degree flip angle, 3.5 mm slice thickness) with automated deconvolution of R2\* and fat per mille (FP) maps on the scanner and sent to PACS. All sequential patients during one month were de-identified and a region of interest at least 3 cm in diameter was drawn on a motion-free image of the right lobe, with the average value recorded. The values before and after administration of gadoxetate disodium were evaluated using paired student's t-test. A "control chart" is created showing values before and after administration of contrast.

# PDF UPLOAD

http://abstract.rsna.org/uploads/2018/18016666/18016666\_hnxa.pdf

# SSC12-08 Management of Image Artifacts on a Clinical 7T MRI Scanner

Monday, Nov. 26 11:40AM - 11:50AM Room: N226

Participants Andrew Fagan, Rochester, MN (*Presenter*) Nothing to Disclose

Kirk M. Welker, MD, Rochester, MN (*Abstract Co-Author*) Nothing to Disclose Joel P. Felmlee, PhD, Rochester, MN (*Abstract Co-Author*) Nothing to Disclose Matthew A. Frick, MD, Rochester, MN (*Abstract Co-Author*) Nothing to Disclose Kimberly K. Amrami, MD, Rochester, MN (*Abstract Co-Author*) Nothing to Disclose

#### For information about this presentation, contact:

Fagan.Andrew@mayo.edu

#### PURPOSE

In 2017, 7T MRI entered the clinical arena with a first scanner obtaining 510(k) FDA clearance for clinical brain and knee imaging. As with previous generations of 7T (research) scanners, significant image artifacts were prevalent in the images from this system, arising from the underlying physics of the interaction of the 297 MHz radiofrequency (RF) energy with the dielectric properties of tissue and also from RF coil issues. In this paper, we present the development of techniques to mitigate these artifacts.

### METHOD AND MATERIALS

Image non-uniformities arising from B1+ transmit (due to complex interference of RF waves) and B1- receive (due to RF coil receiver sensitivity problems) inhomogeneities were mitigated through the use of custom-made high permittivity dielectric pads made from a combination of CaTiO3, BaTiO3, hydroxyethyl-cellulose and D2O. Pads of differing dimensions were developed for different anatomical sites. Inter-voxel dephasing with signal drop-out due to significant magnetic susceptibility effects (e.g. at the base of the brain) was minimized through the use of localized B0 shimming techniques. Distortions arising from long echo trains were mitigated through the use of high image acquisition acceleration factors facilitated by the SNR increase at 7T. Control of receiver and transmitter bandwidths were used to minimize the in- and through-plane chemical shift artifacts.

### RESULTS

Tailored dielectric pads increased the SNR in areas of signal deficit by up to 27% and improved overall image uniformity. Clinical protocols were established for routine scanning in the brain (e.g. for seizure, tramautic brain injury, neurovascular diseases, fMRI-based surgical planning) and knee (e.g. meniscal tear, nerve visualization, cartilage repair); example images will be presented.

### CONCLUSION

7T MRI offers significant advantages over lower-field systems, arising primarily from increased SNR and image contrast possibilities. However, the successful management of image artifacts and the development of consistent diagnostic image quality across all patient cohorts is key to its integration into a routine clinical workflow.

### **CLINICAL RELEVANCE/APPLICATION**

This paper presents clinical protocols developed on a new generation of 7T MRI scanner, which successfully managed image artifacts and resulted in diagnostic image quality.

## SSC12-09 Evaluation of Deep-Learning-Based Technology for Reducing Gadolinium Dosage in Contrast-Enhanced MRI Exams

Monday, Nov. 26 11:50AM - 12:00PM Room: N226

Participants Enhao Gong, PhD, Stanford, CA (*Presenter*) Stockholder, Subtle Medical Jonathan Tamir, BSC, Berkeley, CA (*Abstract Co-Author*) Research support, General Electric Company; Stockholder, Subtle Medical, Inc John Pauly, Stanford, CA (*Abstract Co-Author*) Research support, General Electric Company Max Wintermark, MD, Lausanne, Switzerland (*Abstract Co-Author*) Advisory Board, General Electric Company; Consultant, More Health; Consultant, Magnetic Insight; Consultant, Icometrix; Consultant, Nines;

Greg Zaharchuk, MD, PhD, Stanford, CA (*Abstract Co-Author*) Research Grant, General Electric Company; Stockholder, Subtle Medical;

# For information about this presentation, contact:

enhaog@stanford.edu

### PURPOSE

Gadolinium Deposition is one of the most urgent issues facing radiology community. In this work, we further validated a Deep Learning based contrast-boost method, on 200 patients with mixed indications, and demonstrated the generalization and robustness of the deep learning based solution to reducing gadolinium dosage while maintaining diagnostic quality.

### **METHOD AND MATERIALS**

Dataset: A cohort of 200 patients were included in this study, with mixed indications and recieving clinically routine contrastenhanced MRI (CE-MRI) exams. Sequences: Pre-contrast (zero-dose), post-contrast after 10% dosage administration (low-dose) and post-contrast after 100% dosage administration (full-dose) was collected with 3D T1 IR-FSPGR sequences for each patient. Method: Different series from the same patient wer corregistered and normalized. A deep convolutional neural network (3D U-Net) was trained to learn the approximation of the full-dose CE-MRI using low-dose and zero-dose images. 5-fold cross-validation was used to generate results for evaluation. Evaluation: Quantitatve metrics (PSNR, RMSE, SSIM) were used to evaluate the improvement of the enhanced contrast using deep learning. Qualitative metrics (image quality, contrast enhancement quality) were used to evaluate the result of the DL based enhancement. A non-infereiority test was conducted to demonstrate the performance of the method and validate the capability of reducing dosage without image quality loss.

#### RESULTS

Quantitative metrics demonstrated consistent (~4dB in PSNR and 10% in SSIM) and significant (p<0.001) quality improvement of the deep learning based solution, compared with low-dose CE-MRI. Qualitative ratings showed non-significant differences between the proposed method and acquired full-dose CE-MRI images, which was also verified with the non-inferiority testing. Initial results also demonstrated the possibility of synthesizing full-dose CE-MRI images with zero-dose MR images only.

### CONCLUSION

With a large dataset, we demonstrated the DL solution can generalize well, achieving robust and significant quality improvement over the low-dose CE-MRI, using 10% or even less gadolinum dosage. It enables significantly (at least 10x) gadolinium dosage reduction without sacrificing diagnositic quality.

#### **CLINICAL RELEVANCE/APPLICATION**

Deep Learning solution is valuable in clinical radiology for fighting against gadolinium deposition.

#### **Honored Educators**

Presenters or authors on this event have been recognized as RSNA Honored Educators for participating in multiple qualifying educational activities. Honored Educators are invested in furthering the profession of radiology by delivering high-quality educational content in their field of study. Learn how you can become an honored educator by visiting the website at: https://www.rsna.org/Honored-Educator-Award/ Max Wintermark, MD - 2018 Honored Educator



### SSC13

### Physics (CT: New Systems)

Monday, Nov. 26 10:30AM - 12:00PM Room: N230B



AMA PRA Category 1 Credits ™: 1.50 ARRT Category A+ Credit: 1.75

FDA Discussions may include off-label uses.

#### Participants

Marc Kachelriess, PhD, Heidelberg, Germany (*Moderator*) Nothing to Disclose Ge Wang, PhD, troy, NY (*Moderator*) Nothing to Disclose

### Sub-Events

# SSC13-01 Dynamic Fluence Field Modulation in CT with Multiple Aperture Devices

Monday, Nov. 26 10:30AM - 10:40AM Room: N230B

Participants

Grace J. Gang, PHD, Baltimore, MD (Presenter) Nothing to Disclose

Wenying Wang, Baltimore, MD (Abstract Co-Author) Nothing to Disclose

Jeffrey H. Siewerdsen, PhD, Baltimore, MD (*Abstract Co-Author*) Research Grant, Siemens AG; Research Grant, Carestream Health, Inc; Advisory Board, Siemens AG; Advisory Board, Carestream Health, Inc; License agreement, Carestream Health, Inc; License agreement, Precision X-Ray, Inc; License agreement, Elekta AB; ; ;

Satomi Kawamoto, MD, Laurel, MD (Abstract Co-Author) Nothing to Disclose

Reuven Levinson, MSc, Haifa, Israel (Abstract Co-Author) Employee, Koninklijke Philips NV

Joseph W. Stayman, PhD, Baltimore, MD (*Abstract Co-Author*) Research Grant, Canon Medical Systems Corporation; Research Grant, Carestream Health, Inc; Research Grant, Elekta AB; Research collaboration, Fischer Medical; Research Grant, Medtronic plc; Research collaboration, Koninklijke Philips NV; Research Grant, Siemens AG

#### PURPOSE

This work reports the implementation and assessment of a novel beam filter to achieve dynamic fluence field modulation (FFM) on x-ray CT systems.

### METHOD AND MATERIALS

Multiple aperture devices (MADs) are designed and constructed with fine-scale alternating tungsten bars and air gaps to control the local transmission of x-rays. Relative motion between two MADs in sequence yields Moiré patterns permitting a wide range of fluence modulation profiles with small displacements. In physical experiments, dual MADs were combined with view-dependent mAs modulation to achieve phantom-specific FFM for different imaging objectives including, e.g., 1) a minimum mean variance objective to minimizes mean variance in filtered-backprojection reconstruction, and 2) a flat-field objective to homogenize noise in the reconstruction. Novel pre-processing approaches were developed to accommodate ray-dependent physical effects induced by the filters and to provide artifact-free reconstructions. Image quality assessments were performed for an ellipse phantom (25.8x14.1 cm) and a CatPhan sensitometry module.

#### RESULTS

The dual-MAD module is compact and yields narrow to wide fluence profiles covering 31.2° to 66.5° of the fan beam with just 0.44 mm of relative motion. The augmented pre-processing chain alleviates ring artifacts that are present in conventional gain correction methods while preserving high frequency structures in the phantom. Noise properties associated with the two imaging objectives agree with theoretical expectations, with the flat-field objective producing nearly homogeneous and isotropic noise, and with the minimum mean variance objective yielding the lowest average noise.

#### CONCLUSION

The dual MAD filter provides an effective approach to deliver dynamic FFM and image quality control for different imaging objectives and variable patient anatomies whereas traditional static bowtie filters cannot accommodate asymmetric patient cross-sections or varying patient size. The small form factor of the MAD system and the sub-mm motion requirement facilitates FFM implementation on clinical CT scanner.

### **CLINICAL RELEVANCE/APPLICATION**

The dual MAD filter facilitates dynamic FFM on diagnostic CT, which allows dose reduction and image quality control customized to the specific anatomy of the patient.

### SSC13-02 Imaging With a Full FOV Silicon-Based Spectral Photon-Counting Detector in a Clinical CT Gantry

Monday, Nov. 26 10:40AM - 10:50AM Room: N230B

#### Participants

Martin Sjolin, DPhil,MSc, Stockholm, Sweden (*Presenter*) Co-founder and employee Prismatic Sensors AB Joakim Da Silva, Stockholm, Sweden (*Abstract Co-Author*) Investor, Prismatic Sensors AB

Fredrik Gronberg, MSc, Stockholm, Sweden (*Abstract Co-Author*) Shareholder, Prismatic Sensors AB Research Consultant, Prismatic Sensors AB Staffan Holmin, MD,PhD, Stockholm, Sweden (*Abstract Co-Author*) Medical Advisor, Prismatic Sensors AB Johan Lundberg, MD,PhD, Stockholm, Sweden (*Abstract Co-Author*) Investor, Smartwise AB Hakan Almqvist, MD, Stockholm, Sweden (*Abstract Co-Author*) Nothing to Disclose Xuejin Liu, Stockholm, Sweden (*Abstract Co-Author*) Shareholder, Prismatic Sensors Cheng Xu, Stockholm, Sweden (*Abstract Co-Author*) Shareholder, Prismatic Sensors Moa Yveborg, PhD, Stockholm, Sweden (*Abstract Co-Author*) Stockholder, Prismatic Sensors AB Mats Danielsson, PhD, Stockholm, Sweden (*Abstract Co-Author*) Stockholder, Prismatic Sensors AB; Board Member, Biovica International AB; Research collaboration, General Electric Company

#### For information about this presentation, contact:

martin.sjolin@mi.physics.kth.se

### PURPOSE

A spectral photon-counting silicon edge-on detector with full field-of-view (FOV) has been mounted in a clinical CT gantry and evaluated for imaging. The aim is to demonstrate the benefit of high-resolution spectral photon-counting imaging in a clinical environment.

## METHOD AND MATERIALS

The detector is based on high-resolution edge-on silicon-strip sensors. It has 2 slices, 50 cm FOV and is mounted on a clinical GE Lightspeed VCT gantry. The sensors have 8 energy bins that are used for spectral imaging, i.e. material decomposition. The x-ray tube is operated at clinically relevant fluxes.

### RESULTS

The small detector pixels allow high-resolution imaging which will be demonstrated on anthropomorphic phantoms. High-resolution image acquisition also allows reducing the image noise for maintained spatial resolution (e.g. matching today's detector with 1mm pixels) and this effect is demonstrated for a soft-tissue imaging task. A demonstration of the spectral capability for separating materials (iodine, calcium and soft-tissue) is presented. Count-rate and pile-up are hot topics for photon-counting detectors in clinical environments. Here, the effect on the image quality when going up in the high-flux regime is demonstrated. It will be shown that the high-speed ASIC, together with the small pixels and the segmented edge-on design, is capable of handling very high count-rates without significant loss of image quality.

#### CONCLUSION

Silicon-based spectral photon-counting detectors are promising for use in high-flux clinical CT. The benefits from the higher resolution, better dose efficiency and spectral capabilities could lead to a new era in medical CT imaging.

## **CLINICAL RELEVANCE/APPLICATION**

Photon-counting spectral detectors are emerging for use in clinical CT and the potential advantages are many, including: highresolution, low-dose capability and full spectral imaging (simultaneous acquisition of more than 2 energies). Many studies have presented results from CZT-based prototype detectors, but this is to our knowledge the first full field-of-view clinical prototype of a silicon-based photon-counting detector. The benefits of silicon as a detector material include: high-resolution, spectral fidelity, count-rate resistance and manufacturability.

### SSC13-03 Using 3D Depth Camera for Precise Automatic Patient Positioning in Computed Tomography

Monday, Nov. 26 10:50AM - 11:00AM Room: N230B

Participants

Natalia Saltybaeva, PhD, Zurich, Switzerland (*Presenter*) Nothing to Disclose Bernhard Schmidt, PhD, Forchheim, Germany (*Abstract Co-Author*) Employee, Siemens AG Thomas G. Flohr, PhD, Forchheim, Germany (*Abstract Co-Author*) Employee, Siemens AG Hatem Alkadhi, MD, Zurich, Switzerland (*Abstract Co-Author*) Nothing to Disclose

### For information about this presentation, contact:

Natalia.Saltybaeva@usz.ch

### PURPOSE

The aim of this study was to evaluate the accuracy of a three-dimensional (3D) camera algorithm for automatic and individualized patient positioning based on body surface detection and to compare the results with manual positioning performed by technologists in routinely obtained chest and abdomen computed tomography (CT).

### **METHOD AND MATERIALS**

This study included data of 120 patients undergoing clinically CTs. 52 patients were scanned with CT using a table height manually selected by technologists; while other 68 were automatically positioned based on patient-specific body surface and contour detection. The ground truth table height was defined as the table height that aligns the axial center of the patient's body and the scanner isocenter. Off-centering was defined as the difference between the TGT and the table position actually used the CT. The t-test was performed to determine the significance of the differences in the vertical offset when automatic vs manual positioning was used. Chi-square test was used to check whether there was a relationship between patient size and the magnitude of off-centering.

### RESULTS

We found a significant improvement in patient centering (offset of  $5\pm3$  mm) when using the automatic positioning algorithm with the 3D camera compared to manual positioning (offset of  $19\pm10$ mm) performed by technologists (p<0.005). The absolute maximal offset was 39 mm and 43 mm for chest and abdomen CT, respectively, when patients were positioned manually, while with automatic positioning using the 3D camera the offset did not exceede15 mm. In chest CTs with manual patient positioning, the Chi-square test has shown the significant statistical correlation between the vertical offset > 20 mm and the patient size (BMI > 26 kg/m2)

(p<0.001). While in case of abdomen examinations this relationship was found to be insignificant (p=0.38).

### CONCLUSION

The study indicates that automatic patient positioning using an algorithm based on 3D patient surface detection provides better patient centering as compared to manual positioning performed by technologist.

# **CLINICAL RELEVANCE/APPLICATION**

Automatic individualized patient positioning can be successfully applied in the clinical routine for accurate patient positioning and in better radiation dose utilization.

# SSC13-04 X-ray Induced Acoustic Computed Tomography (XACT): A Novel Technique for Low-Dose, High-Resolution, CT imaging

Monday, Nov. 26 11:00AM - 11:10AM Room: N230B

Participants

Pratik Samant, BSC, Norman, OK (*Abstract Co-Author*) Nothing to Disclose Rowzat Faiz, BSC,MSc, Norman, OK (*Abstract Co-Author*) Nothing to Disclose Siqi Wang, Norman, OK (*Abstract Co-Author*) Nothing to Disclose Elijah Robertson, Norman, OK (*Abstract Co-Author*) Nothing to Disclose Luis Trevisi, Norman, OK (*Abstract Co-Author*) Nothing to Disclose Shanshan Tang, PhD, Norman, OK (*Abstract Co-Author*) Nothing to Disclose Liangzhong Xiang, PhD, Norman, OK (*Presenter*) Nothing to Disclose

#### For information about this presentation, contact:

samantp@ou.edu

#### PURPOSE

We are developing a low-dose, high resolution imaging modality, x-ray induced acoustic tomography (XACT). This novel technique can yield 3D x-ray bone density images via a single projection of a pulsed x-ray, therefore considerably lowering patient dose. In addition, XACT resolution is higher than that of conventional CT, with expected resolutions in the range of 100um.

### **METHOD AND MATERIALS**

In XACT, a pulsed x-ray beam is absorbed by a sample. The absorbed x-ray energy is converted into heat and the subsequent thermoelastic expansion results in the emission of a detectable ultrasound (US) signal. This US is a spherical wave, and so yields 3D information. The detected signal can be used to compute the x-ray absorption, and important 3D clinical information. We have constructed an XACT imaging system, which previously imaged a lead sample We have extended the imaging capability of this system to biological samples and have acquired a signal from a chicken bone. We have optimized the signal generation, detection, and image reconstruction of this system. We aim to image biological samples using XACT and a transducer array to maximize imaging speed and utility.

### RESULTS

We have obtained a signal and an image from a biological sample (chicken bone). We have also demonstrated the capability of XACT to image in vivo samples at a lower dose than that of conventional CT with higher imaging resolution. These promising results demonstrate that XACT is a viable imaging modality with high potential for clinical translation.

### CONCLUSION

The high potential for clinical translation of XACT has been demonstrated. XACT allows for the high-resolution imaging of x-ray absorption at much lower doses than conventional x-ray imaging techniques. We believe that the clinical translation of XACT is possible, and can revolutionize x-ray imaging by providing 3D information with a single projection and at lower doses than that of conventional CT.

### **CLINICAL RELEVANCE/APPLICATION**

XACT can obtain 3D x-ray absorption images via a single x-ray projection onto a sample. Therefore, the dose in XACT is substantially lower than that of conventional CT. The imaging versatility of XACT is on par with that of conventional CT, including 3D imaging capability of the breast and bone. However, XACT can perform this imaging at comparable resolutions without the need for scanning throughout the sample. This yields substantial improvement in both imaging speed and dose reduction.

### SSC13-05 Artificial Neural Network Based Prediction of Contrast Agent Injection Parameters Using Real Time Test Bolus Information

Monday, Nov. 26 11:10AM - 11:20AM Room: N230B

Participants

Pooyan Sahbaee, Malvern, PA (*Presenter*) Employee, Siemens AG Saikiran Rapaka, PhD, Princeton, NJ (*Abstract Co-Author*) Employee, Siemens AG Marly van Assen, MSc, Charleston, SC (*Abstract Co-Author*) Nothing to Disclose Puneet Sharma, Princeton, NJ (*Abstract Co-Author*) Research Director, Siemens AG Ehsan Samei, PhD, Durham, NC (*Abstract Co-Author*) Research Grant, General Electric Company; Research Grant, Siemens AG; Advisory Board, medInt Holdings, LLC; License agreement, 12 Sigma Technologies; License agreement, Gammex, Inc Katharine Grant, PhD, Rochester, MN (*Abstract Co-Author*) Employee, Siemens AG Thomas G. Flohr, PhD, Forchheim, Germany (*Abstract Co-Author*) Employee, Siemens AG

#### For information about this presentation, contact:

Pooyan.sahabee@siemens-healthineers.com

### PURPOSE

Optimization of contrast agent (CA) administration protocols is a crucial component of medical imaging to obtain diagnostic quality images. Here we aim to develop an artificial neural network (ANN) framework to predict the required contrast injection parameters to achieve a desired contrast enhancement (CE) in a given organ (kidney in this study) based on test bolus (TB) information.

#### **METHOD AND MATERIALS**

Synthetic data was used to feed and train a machine learning model to predict patient-specific CM injection protocol for a desired enhancement in different organs. Applying a validated perfusion model and tweaking the different patient-specific parameters (50 total) such as age, sex, cardiac output, and organ and vessel sizes, as well as injection protocol parameters such as iodine concentration (270, 300, 320, and 350 mg/ml), volume (100, 115, 130, and 140 ml), and injection rate (2, 3, 4, 5, and 6 ml/s), we generated 4000 CE data in kidney. TB curves were generated using the same concentrations and constant rate of 5 ml/s and volume of 10 ml. Data were split into training and test sets (split factor 0.2), and an ANN regression model was trained. For 800 given kidney peak enhancement and time to peak, injection parameters were predicted.

### RESULTS

To obtain the given CE in kidney (i.e., time-to-peak and peak enhancement) for individual patients, mean absolute percentage error in prediction of the main injection parameters, concentration, injection rate, injection time, and contrast volume were 3%, 4%, 8% and 9%, respectively. The mean error of the prediction model without including the TB information, was higher than the results reported above by maximum of 4%. Using the predicted parameters, the mean error for both time-to-peak and peak enhancement for kidney was less than 5%.

# CONCLUSION

Our results showed that, in absence of enough clinical perfusion data from different organs, by using synthetic data from a validated perfusion model, in addition to the test bolus information, we could train an AI model to offer the required CA administration parameters in order to obtain the desired CE in any targeted organ or vessel.

#### **CLINICAL RELEVANCE/APPLICATION**

This technique offers the possibility to determine patient-specific contrast material injection parameters to provide higher accuracy and consistency in the way that contrast enhanced CT examinations are performed.

### ssc13-06 Pre-Clinical Demonstration of Grating-Based Phase Contrast X-Ray Imaging for Cryoablation Therapy

Monday, Nov. 26 11:20AM - 11:30AM Room: N230B

#### Participants

Elisabeth Shanblatt, PhD, Rochester, MN (*Presenter*) Nothing to Disclose Brandon J. Nelson, BA, Rochester, MN (*Abstract Co-Author*) Nothing to Disclose Shuai Leng, PHD, Rochester, MN (*Abstract Co-Author*) License agreement, Bayer AG Christopher P. Favazza, PhD, Rochester, MN (*Abstract Co-Author*) Nothing to Disclose Aiming Lu, Rochester, MN (*Abstract Co-Author*) Nothing to Disclose Krzysztof Gorny, PhD, Rochester, MN (*Abstract Co-Author*) Nothing to Disclose Cynthia H. McCollough, PhD, Rochester, MN (*Abstract Co-Author*) Research Grant, Siemens AG

#### For information about this presentation, contact:

shanblatt.elisabeth@mayo.edu

#### PURPOSE

Cryoablation, often guided by CT or MRI, is an important tool in the treatment of cancer and other conditions. This work uses phase contrast imaging (PCI) to detect temperature changes, demonstrating cryoablation as a potential application for PCI.

### METHOD AND MATERIALS

Experiments were carried out using fresh pork loin obtained from a local grocer. The PCI system was a Talbot-Lau grating-based interferometer designed for 27 keV X-rays. Images with attenuation, phase, and dark field contrast were obtained. The first experiment tested whether temperature changes could be detected by each contrast mechanism. We imaged a porcine sample after it froze overnight in a -60°C freezer, and then again after thawing. In a second experiment, we tested if we could detect temperature changes induced by a cryoprobe. We imaged a porcine sample after forming an ice-ball with a cryoprobe (Galil Medical, IceSeed 1.5 MRI Needle). Prior to imaging, the sample was subjected to a 15 min. freeze followed by a partial thawing until the probe could be removed from the sample.

#### RESULTS

The addition of phase and dark field contrast mechanisms provided structural detail and good temperature differentiation. Histograms showing the distribution of values in the CT phase reconstruction vs. the CT attenuation reconstruction (voxel size  $54x54x54 \ \mu$ m) show a larger change in signal between the frozen and thawed pork. This result is consistent with theory: for water imaged with 27 keV photons, the change in attenuation of 54  $\mu$ m of liquid vs. frozen water is expected to be about 0.02%, whereas the change in phase is expected to be about 38%. Our data show that the mean attenuation changed by 3%, and the mean phase changed by 34%. Histograms of values from a projection image of the cryoablated pork qualitatively demonstrate that the dark field signal is more sensitive to temperature change than the attenuation signal, even for a small amount of thawing that took place over 46 min.

#### CONCLUSION

We demonstrated that PCI has potential application for temperature monitoring during cryoablation procedures. Phase and dark field contrast are very sensitive to interfaces and density changes, making them ideal for imaging temperature-sensitive processes.

### **CLINICAL RELEVANCE/APPLICATION**

Cryotherapy is used in a wide variety of treatments, and phase and dark field information can be used to sensitively monitor cryogenic and other processes during surgery.

### ssc13-07 Three-Dimensional CT Scout from Conventional Two-View Radiograph Localizers Using Deep

### Learning

Monday, Nov. 26 11:30AM - 11:40AM Room: N230B

Participants Juan Montoya, Madison, WI (*Presenter*) Nothing to Disclose Chengzhu Zhang, BS, Madison, WI (*Abstract Co-Author*) Nothing to Disclose John W. Garrett, PhD, Madison, WI (*Abstract Co-Author*) Nothing to Disclose Ke Li, PhD, Madison, WI (*Abstract Co-Author*) Nothing to Disclose Guang-Hong Chen, PhD, Madison, WI (*Abstract Co-Author*) Research funded, General Electric Company Research funded, Siemens AG

#### For information about this presentation, contact:

jcmontoya@wisc.edu

#### PURPOSE

The purpose of this work was to develop a deep learning-based image reconstruction framework to enable the reconstruction of volumetric 3D scout CT images from the conventional two-view (lateral and AP) projection scout radiographs.

### **METHOD AND MATERIALS**

751 clinically indicated chest-abdomen-pelvis (CAP) CT exams from 667 patients were retrospectively collected. Inclusion criteria were: 1. CT exams acquired with or without contrast media and 2. Either one of the following 6 scan coverages: chest-alone, abdomen-alone, pelvis-alone, chest-abdomen, abdomen-pelvis or CAP. To avoid potential data inconsistency, large patients (>50 cm lateral width) with significant truncation were excluded. CT image volumes were interpolated to a 1.0x1.0x1.0 mm3 isotropic voxel size and registered to the 2D scout radiographs using the patient positioning information in the DICOM header. A total of 163,840 CT images with 1120 radiograph localizers from 476 patients were used to train a 60-layer deep neural network which inputs the AP and lateral localizers and outputs a volumetric CT scout; 47,919 CT images with 382 radiograph localizers from 191 patients were used for testing and validation. To test the generalization error of the trained deep neural network, a Monte Carlo dose calculation of an axial CT scan was performed in three anatomical regions using both the diagnostic CT images and the 3D-scout of one subject. Gamma analysis with 10%/5mm dose-difference/distance-to-agreement criteria was performed to compare both radiation dose distributions.

### RESULTS

The average gamma indices between the diagnostic CT and the 3D-scout images were 0.33, 0.37 and 0.34 for anatomical regions in the chest, abdomen and pelvis, respectively. Similarly, the percentages of voxels with passing gamma index ( $\gamma$ <1) were 97.3%, 97.3% and 98.2% for the three anatomical regions.

### CONCLUSION

A deep learning method was developed to reconstruct volumetric scout CT images from two-view projection scout radiographs. The proposed method could enable more accurate radiation dose estimates and scanning parameter prescription prior to CT acquisition and thus potentially help overcome limitations of automatic exposure control schemes in diagnostic CT.

#### **CLINICAL RELEVANCE/APPLICATION**

The reconstruction of 3D-scouts from two-view localizers could revolutionize the prescription of radiation dose/image quality in diagnostic CT, enabling the next generation of intelligent CT scanners.

# SSC13-08 Stopping Power Ratio (SPR) Uncertainty in Pencil Beam Scanning (PBS) Proton CT (pCT) Reconstruction: Dependency on Energy Straggling and Detector Energy Resolution

Monday, Nov. 26 11:40AM - 11:50AM Room: N230B

Participants

Jun Zhou, PhD, Atlanta, GA (*Presenter*) Nothing to Disclose Xiaoqiang Li, PhD, Royal Oak, MI (*Abstract Co-Author*) Nothing to Disclose Peyman Kabolizadeh, Royal Oak, MI (*Abstract Co-Author*) Nothing to Disclose Di Yan, DSC, Royal Oak, MI (*Abstract Co-Author*) Nothing to Disclose Craig W. Stevens, MD, PhD, Tampa, FL (*Abstract Co-Author*) Nothing to Disclose Xuanfeng Ding, PHD, Royal Oak, MI (*Abstract Co-Author*) Nothing to Disclose

### For information about this presentation, contact:

zhouj995@hotmail.com

### PURPOSE

To investigate the effect of proton energy, energy straggling (ES), and detector energy resolution (DER) on the uncertainty of the SPR reconstruction in PBS pCT reconstruction.

# METHOD AND MATERIALS

A Monte-Carlo model was developed based on PBS technology to simulate the pCT acquisition. An 8cm-diameter cylinder water phantom was used in the simulation, filled with three 2-cm cylinders comprised of ICRU bone, muscle, and adipose, respectively. 180 projections were generated with 252 spots (500 protons/spot) on each projection. Spot spacing and size on the detector were 5.4mm and 6mm, respectively. Simulations were conducted w/wo energy ES fitted to real clinical 120 and 200 MeV proton beams. DER were set to 2% and 10%, in order to simulate detector uncertainty in the measurement of proton residual energy. Mean and standard deviation (STD) of SPR within the background and the three cylinders were calculated.

#### RESULTS

Total dose to the phantom was<.4mGy. The reconstructed mean RSP for both w/wo ES were the same: .995(-.5%), .968(-.2%), 1.026(-.4%), and 1.702(-1.0%) for the water, adipose, muscle, and bone, respectively. The STDs of the reconstructed RSP

were<.006 for all energies when DER=2%. With DER=10%, the STD of reconstructed RSP at 200 MeV was significantly higher(.01 vs .006, p<.05).

# CONCLUSION

As PBS pCT derives projection images from statistical analysis of PBS spots, it is not sensitive to variations in proton ES and DER up to 10%. This is the first study to demonstrate the PBS proton beams being used directly for RSP reconstruction with significantly less dependency to ES and DER. Further technology development is warranted and is in process to improve the image resolution and the RSP accuracy for small regions of interest.

### **CLINICAL RELEVANCE/APPLICATION**

Although proton radiography was first reported 5 decades ago, there is yet a commercial product to be developed given proton's multi-coulomb medium scattering, the cost of the proton CT, and furthermore the complicated single proton tracking technique used in the current passive scattering based pCT devices. In this study, we report the very first relative stopping power (RSP) reconstruction based on PBS technology and statistical processing of protons within each spot. This novel pCT acquisition and reconstruction methods could be efficient and effectively implemented into a routine clinical proton PBS machine with the capability of pre-treatment and intrafraction imaging.

### SSC13-09 Dual Source Photon-Counting-Detector CT with a Tin Filter: A Phantom Study on Iodine Quantification Accuracy and Precision

Monday, Nov. 26 11:50AM - 12:00PM Room: N230B

Participants

Ashley Tao, PhD, Rochester, MN (*Presenter*) Nothing to Disclose Richard Huang, Rochester, MN (*Abstract Co-Author*) Nothing to Disclose Shengzhen Tao, Rochester, MN (*Abstract Co-Author*) Nothing to Disclose Gregory J. Michalak, PhD, Rochester, MN (*Abstract Co-Author*) Nothing to Disclose Cynthia H. McCollough, PhD, Rochester, MN (*Abstract Co-Author*) Research Grant, Siemens AG Shuai Leng, PHD, Rochester, MN (*Abstract Co-Author*) License agreement, Bayer AG

### For information about this presentation, contact:

leng.shuai@mayo.edu

### PURPOSE

To evaluate the impact of a multi-source photon-counting-detector (PCD) CT configuration, including the use of a tin filter and increased number of energy bins, on iodine quantification.

#### **METHOD AND MATERIALS**

olllA multi-energy CT phantom (Sun Nuclear) with iodine inserts at concentrations of 0, 2, 5, 10, 15 mg/mL was scanned on a research PCD-CT system with one source/PCD array. A reference scan was performed with 140 kV, 2 energy thresholds (TL and TH) and 32 mGy CTDIvol. Various multi-source PCD configurations were emulated by performing separate scans with different tube potentials and energy thresholds. Scans were performed at tube potentials of 80, 100, 120, 140, and Sn140 kV (140 kV with a tin filter), and multiple-source configurations using all possible kV pairs were investigated. Tube current was adjusted so that the CTDIvol of each scan was half of the reference scan (16 mGy) so that the total radiation dose was matched for all scan combinations (32 mGy). For each kV pair, two scenarios were investigated: (1) dual-energy scan with only 1 energy threshold (TL) used from each detector; and (2) quad-energy scan with 2 energy thresholds used from each detector. Images were reconstructed using standard filtered backprojection. Image-based material decomposition was performed to generate iodine and water maps. Root mean square error (RMSE) was measured for all iodine inserts and for each kV and energy threshold combination.

### RESULTS

Among dual-energy configurations, 80/140 had the lowest RMSE of iodine concentration, 14.7 mg/mL, which was lower than that of reference scan using 140 kV (15.8 mg/mL). The use of a tin filter reduced the RMSE to 10.2 mg/mL. The lowest RMSE, 9.1 mg/mL, was achieved with the quad-energy configuration. Use of 4 energy thresholds (instead of 2) reduced RMSE by 20-75% for the kV pairs of 100/140 and 120/140.

### CONCLUSION

Performance of PCD-based multi-energy CT can be substantially improved using a multiple source configuration, a tin filter and multiple energy thresholds, with a 42% reduction of RMSE (15.8 to 9.1 mg/mL) in iodine quantification accuracy observed through phantom studies.

### **CLINICAL RELEVANCE/APPLICATION**

Dual-source PCD-CT with a tin filter can potentially provide better image quality, more accurate material quantification and lower dose than that of single-source PCD-CT.



#### SSC14

Science Session with Keynote: Radiation Oncology (CNS Malignancies)

Monday, Nov. 26 10:30AM - 12:00PM Room: E353A



AMA PRA Category 1 Credits ™: 1.50 ARRT Category A+ Credit: 1.75

FDA Discussions may include off-label uses.

#### Participants

Martin Colman, MD, Houston, TX (Moderator) Stockholder, Steward Health Care

John C. Grecula, MD, Columbus, OH (*Moderator*) Research Grant, Teva Pharmaceutical Industries Ltd; Research Grant, Soligenix, Inc;

#### Sub-Events

# SSC14-01 Radiation Oncology Keynote Speaker: CNS

Monday, Nov. 26 10:30AM - 10:50AM Room: E353A

Participants

Hany Soliman, Toronto, ON (Presenter) Nothing to Disclose

## SSC14-03 Fractionated Radiosurgery Compared to Single Fraction Radiosurgery in the Treatment of Unresected Large Brain Metastases: An International Meta-Analysis

Monday, Nov. 26 10:50AM - 11:00AM Room: E353A

Participants

Eric J. Lehrer, MD, New York, NY (*Presenter*) Nothing to Disclose Jennifer L. Peterson, MD, Jacksonville, FL (*Abstract Co-Author*) Nothing to Disclose Nicholas G. Zaorsky, MD, Hershey, PA (*Abstract Co-Author*) Nothing to Disclose Paul D. Brown, MD, Rochester, MN (*Abstract Co-Author*) Speaker, Wolters Kluwer nv; Data Safety Monitoring Board, Novella Clinical Veronica Chiang, MD, New Haven, CT (*Abstract Co-Author*) Nothing to Disclose Jason Sheehan, MD,PhD, Charlottesville, VA (*Abstract Co-Author*) Nothing to Disclose Arjun Sahgal, Toronto, ON (*Abstract Co-Author*) Speaker, Medtronic plc; Speaker, Elekta AB; Medical Advisory Board, Varian Medical Systems, Inc; Speaker, Accuray Incorporated; Research Grant, Elekta AB Samuel T. Chao, MD, Cleveland, OH (*Abstract Co-Author*) Speaker, Varian, Inc; Speaker, NovoCure Ltd Daniel M. Trifiletti, MD, Jacksonville, FL (*Abstract Co-Author*) Nothing to Disclose

For information about this presentation, contact:

ericjlehrer@gmail.com

### PURPOSE

SRS is commonly utilized as a definitive therapy in patients with unresected large brain metastases (BrM), as it provides excellent rates of 1-year local control (LC); however, resultant radionecrosis (RN) is a known risk. fSRS is a treatment option intended to reduce the incidence of RN and improve LC in these patients. There is a paucity of prospective data comparing these two modalities; therefore, a meta-analysis of existing retrospective and prospective studies was conducted.

#### **METHOD AND MATERIALS**

The co-primary outcome measures were incidence of RN and LC at 1 year. Large BrM were defined according to Radiation Therapy Oncology Group 90-05, where Group A: 2-3 cm diameter (4-14 cc volume) and Group B: >= 3 cm diameter (>14 cc volume). PICOS/PRISMA/MOOSE guidelines were used to select studies where patients with large BrM: (1) RN rates and/or 1-year LC were available; (2) SRS and/or fSRS were administered as treatment for unresected metastases; (3) data regarding tumor size were reported. Weighted random effects meta-analyses were used to analyze RN and 1-year LC. Fractionation and size were analyzed as moderators using analysis of variance and omnibus test where the null hypothesis was rejected for p<0.05.

#### RESULTS

A total of 17 studies conducted from 1998-2016, in 6 nations, consisting of 1,007 large BrM, met inclusion criteria. Median patient age was 62 years, median follow up was 9.5 months, and the most commonly used radiosurgery platform was Gamma Knife (9/17 studies). The range of SRS doses was 15-20 Gy, and the range of fSRS doses was 24-35 Gy in 2-5 fractions. The most common SRS dose was 18 Gy/1 fraction, and the most common fSRS dose was 27 Gy/3 fractions. Incidence of RN at 1-year for all studies was 9.2%; and was 18.2% for SRS and 6.7% for fSRS, p=0.008. 1-year LC for all studies was 79.3%; and was 74.0% for SRS and 83.4% for fSRS, p=0.20. By tumor volume, the incidence of RN in Group A was 10.5% and in Group B was 7.7%, p=0.51. 1-year LC in Group A was 86.2% and in Group B was 76.3%, p=0.07.

### CONCLUSION

Among patients with unresected large BrM treated with radiosurgery, fSRS is associated with decreased rates of RN and potentially improved 1-year LC compared to SRS.

#### **CLINICAL RELEVANCE/APPLICATION**

Fractionated stereotactic radiosurgery (fSRS) is a recent advancement in radiosurgery, although its relative safety and efficacy compared to single fraction stereotactic radiosurgery (SRS) is unknown.

# SSC14-04 The Dancing Cord: Inherent Spinal Cord Motion and Its Effect on Cord Dose in Spine Stereotactic Body Radiation Therapy

Monday, Nov. 26 11:00AM - 11:10AM Room: E353A

Participants

Murat A. Oztek, MD, Seattle, WA (*Presenter*) Nothing to Disclose Simon S. Lo, MD, Seattle, WA (*Abstract Co-Author*) Editor, Springer Nature; Mahmud Mossa-Basha, MD, Seattle, WA (*Abstract Co-Author*) Nothing to Disclose Matthew J. Nyflot, PhD, Seattle, WA (*Abstract Co-Author*) Nothing to Disclose Patricia A. Sponseller, MS,CMD, Seattle, WA (*Abstract Co-Author*) Nothing to Disclose Wei Wu, MD, Wuhan, China (*Abstract Co-Author*) Nothing to Disclose Christoph P. Hofstetter, Seattle, WA (*Abstract Co-Author*) Nothing to Disclose Rajiv Saigal, MD,PhD, Seattle, WA (*Abstract Co-Author*) Nothing to Disclose Stephen R. Bowen, PhD, Seattle, WA (*Abstract Co-Author*) Nothing to Disclose William T. Yuh, MD, Seattle, WA (*Abstract Co-Author*) Nothing to Disclose Nina A. Mayr, MD, Seattle, WA (*Abstract Co-Author*) Nothing to Disclose

#### For information about this presentation, contact:

oztekma@uw.edu

### PURPOSE

Adherence to strict dose limits is critically important in stereotactic body radiation therapy (SBRT) for spine tumors to reduce the risk of neurologic complications. Validated dose constraints have been established. However, inherent motion of the spinal cord has not yet been explored with respect to dosimetric effects in spine SBRT.

### **METHOD AND MATERIALS**

Dynamic cardiac-gated balanced fast field echo MR imaging was obtained as part of routine treatment planning imaging for VMATbased spine SBRT in 8 patients with spine tumors. Imaging and dosimetric data were analyzed in a retrospective IRB approved study. Planning CT data sets, static T2-weighted (cordstat), and each of 15 phases of the dynamic MRI images (corddyn) were coregistered. Cord deformation and motion on the dynamic imaging was compared to the static T2-weighted images, with respect to cord area, Dice coefficient, Jaccard index and excursion of the corddyn beyond the cordstat and planning organ at risk volume (PRV) margins. Dose was compared between cordstat, and corddyn. Comparisons were made using the Wilcoxon signed rank test.

#### RESULTS

The cross-sectional areas were not significantly different between cordstat and corddyn ( $0.51\pm0.12$  vs.  $0.52\pm0.13$  mm2, p=0.814), suggesting no major cord deformation. Assessing cord motion, Dice coefficient between cordstat vs. corddyn ranged from 0.70 to 0.96 (mean,  $0.85\pm0.05$ ). Jaccard index ranged from 0.54-0.92 (mean,  $0.75\pm0.08$ ). In 4 of the 8 patients, the maximal dose to corddyn exceeded that of cordstat by 1.2 - 12.8% (mean  $5.2\pm4.3\%$ ). The corddyn spatially moved outside the 1 mm PRV margin of cordstat in 4 of the 8 patients: 13% of the time in 2, and 27% of the time in 2 patients. Corddyn did not extend outside the 2 mm PRV margin of cordstat.

# CONCLUSION

The spinal cord shows inherent motion, resulting in measurable dosimetric effects which should be considered during SBRT dosimetry. A PRV margin of 2 mm surrounding the cord is suggested to account for the inherent spinal cord motion.

### **CLINICAL RELEVANCE/APPLICATION**

Accurate imaging of the spinal cord is critical to assure dose limits and prevent neurologic complications in patients receiving high-precision/high-dose stereotactic body radiation for spine tumors.

# SSC14-05 Two-Fraction Radiosurgery (9Gy x 2) is an Effective and Safe Option in the Modern Era of CNS Penetrating Systemic Therapies

Monday, Nov. 26 11:10AM - 11:20AM Room: E353A

#### Awards

### **Student Travel Stipend Award**

Participants Andrew Huang, MD, San Francisco, CA (*Presenter*) Nothing to Disclose Karen E. Huang, MS, San Francisco, CA (*Abstract Co-Author*) Nothing to Disclose Rahul Kumar, MD, San Francisco, CA (*Abstract Co-Author*) Nothing to Disclose Arun Goel, Philadelphia, PA (*Abstract Co-Author*) Nothing to Disclose Nima Harandi, San Francisco, CA (*Abstract Co-Author*) Nothing to Disclose Samuel R. Birer, MD, San Francisco, CA (*Abstract Co-Author*) Nothing to Disclose Mark C. Rounsaville, MD, San Francisco, CA (*Abstract Co-Author*) Nothing to Disclose John Lee, MD, San Francisco, CA (*Abstract Co-Author*) Nothing to Disclose Roy Abendroth, MD, San Francisco, CA (*Abstract Co-Author*) Nothing to Disclose

### For information about this presentation, contact:

huangaj@sutterhealth.org

### PURPOSE

In the era of CNS-penetrating systemic therapies, stereotactic radiosurgery (SRS) has resulted in higher intracranial control rates

as well as higher rates of radionecrosis. We sought to determine if lower biologically equivalent dose SRS, specifically 18Gy in 2 fractions (fx), can achieve adequate local control with reduced adverse events.

### METHOD AND MATERIALS

We retrospectively reviewed patients who received SRS in our department from 2014-2015. In this period, we had implemented a fractionated SRS regimen of 18Gy in 2fx for >3 simultaneously treated lesions, with all lesions typically being <2 cm which some exceptions. Median GTV-PTV expansion was 2mm (range 0-5mm). Dose was prescribed to the periphery to the 65-90% isodose line. We documented lesion location, prior radiation, volume, largest single dimension, and if symptomatic radionecrosis occurred. Cancer subtype, systemic therapies, cause of death, and performance status was included as well. Cox proportional hazards models were used to determine factors affecting local control.

#### RESULTS

From 2014-2015, we treated 242 lesions from 59 patients using stereotactic radiosurgery. Within this cohort, 126 lesions from 27 patients were treated using 18Gy in 2fx. 22 of 27 patients treated using these two fraction regimens were followed until death. The majority of lesions of the two-fraction cohort came from a melanoma primary (n=94). Ten lesions were resected before SRS. For the two fraction regimen, local control was 59% at 1-year, and 59% at 2-years. Radionecrosis occurred in 2 lesions (1.6%). The majority of lesions (n=88) were <1cc, 35 were 1-10cc in volume, and the remaining 3 were 10-98cc in volume. On multivariate analysis of the entire cohort, maximum single dimension, and prior surgical resection were independent predictors of local failure. Number of fractions was not significantly associated with local failure.

#### CONCLUSION

In our cohort, 18Gy in 2fx delivered acceptable local control with very low rates of symptomatic radionecrosis.

### **CLINICAL RELEVANCE/APPLICATION**

Lower-dose, two-fractionation radiosurgery may be appropriate for patients with high volume disease, poor performance status or patients receiving central-nervous system penetrating systemic therapies.

### SSC14-06 T2WI Histogram Analysis for Differentiating Glioblastoma from Solitary Brain Metastasis

Monday, Nov. 26 11:20AM - 11:30AM Room: E353A

Participants

Yong Zhang, DO, Zhengzhou, China (*Presenter*) Nothing to Disclose Ke Xu, Zhengzhou, China (*Abstract Co-Author*) Nothing to Disclose Jingliang Cheng, Zhengzhou, China (*Abstract Co-Author*) Nothing to Disclose Qingqing Lv, Zhengzhou, China (*Abstract Co-Author*) Nothing to Disclose

For information about this presentation, contact:

1043381896@qq.com

### PURPOSE

To study the value of T2 gray histogram analysis of differential diagnosis in glioblastoma and brain solitary metastasis.

### METHOD AND MATERIALS

A retrospective analysis was conducted by brain MRI examination and pathology diagnosis of 57 cases of glioblastoma and brain solitary metastasis in our hospital .Among them, there were 29 cases of glioblastoma(there were 17 males and 12 females ), 28 cases of astrocytoma(there were 15 males and 13 females ).Respectively, to draw the region of interest(ROI) in the T2 MR transaxial images of two groups on maximum layer of tumor level by using Mazda software and analyze the whole tumors gray histogram, performing a statistical analysis on the two sets ofparameters obtained from histograms to find out statistical significance of each parameter.The kurtosis, skewness, the first percentile, the 10th percentile and the 90th percentile were in accordance with the normal distribution. Two independent samples t-test were used to compare the differences.Mean , Variance, the 50th percentile, the 99th percentile did not fit the normal distribution, using nonparametric test, P <0.05 was statistically significant.

#### RESULTS

Through histogram analysis of 9 parameters, these 7 parameters were statistically significant (all P < 0.05), including mean , kurtosis, skewness, perc.10%, perc.50% , perc.90% and perc.99%. Among them, the sensitivity of skewness was 82.1%, the specificity was 82.8%, the area under the curve was 0.865, and the best cut-off value was 0.58.

### CONCLUSION

The T2WI gray histogram analysis is helpful for the identification of brain solitary metastasis from glioblastoma and the skewness has a high diagnostic efficiency.

#### **CLINICAL RELEVANCE/APPLICATION**

The T2WI gray histogram analysis is helpful for the identification of brain solitary metastasis from glioblastoma.

### SSC14-08 18F-FDOPA PET/MR Based Target Definition in the 3D Based Radiotherapy Treatment of Glioblastoma Multiform Patients: Early Results of a Single Institute Study

Monday, Nov. 26 11:40AM - 11:50AM Room: E353A

Awards Student Travel Stipend Award

Participants David Sipos, MSc, Kaposvar, Hungary (*Presenter*) Nothing to Disclose Zoltan Toth, Kaposvar, Hungary (*Abstract Co-Author*) Nothing to Disclose Gabor Lukacs, Kaposvar, Hungary (*Abstract Co-Author*) Nothing to Disclose Gabor Bajzik, MD, Kaposvar, Hungary (*Abstract Co-Author*) Nothing to Disclose Janaki S. Hadjiev, MD, Kaposvar, Hungary (*Abstract Co-Author*) Nothing to Disclose Imre Repa, MD, Kaposvar, Hungary (*Abstract Co-Author*) Nothing to Disclose Arpad Kovacs, Kaposvar, Hungary (*Abstract Co-Author*) Nothing to Disclose Marianna Moizs, Kabosvak, Hungary (*Abstract Co-Author*) Nothing to Disclose

# For information about this presentation, contact:

cpt.david.sipos@gmail.com

### PURPOSE

In the staging and 3D radiotherapy planning process of glioblastoma multiforme (GBM) patients conventional MRI plays important role. The 18F-F-DOPA positron emission tomography (PET) imaging utilising metabolic radiotracers for better evaluation of the affectet area by the tumor. 18F-FDOPA penetrates into the cells by a process mediated by amino acid transporters and demonstrates higher sensitivity and specificity for gliomas than traditional 18F-FDG PET and contrast enhanced MRI imaging. Our aim was to present the feasibility of this amino acid tracer in modern 3D radiotherapy planning.

### METHOD AND MATERIALS

We present a retrospective analysis of the PET/MR based planning study with 18F-FDOPA in 4 patients with histologically proven GBM. In the contouring process The native planning CT scanes were fused with the PET/MR series (T1 contrast enhanced, T2 and 18F-F-DOPA sequences). We defined 18F-F-DOPA uptake volumen (BTV-F-DOPA), the T1 contrast enhanced MRI volume (GTV-T1CE), and the volume of area covered by oedema on the T2 weighted MRI scan (CTV-oedema) in all patients. We also registered the volume BTV-F-DOPA volumes not covered by the conventional MR based target volumes.

### RESULTS

The mean 18F-F-DOPA tumor volumes was 37,1 cm3 (range 15,3-80,3; SD=29,48). The mean GTV T1 CE was 7,2 cm3 (range 2,6-13,2; SD=4,89). The mean CTV oedema volume was 57,4 cm3 (range 27,7-108,8; SD=36,49). The mean volume of the BTV-F-DOPA not covered by the CTV oedema volume was 8,6 cm3 (range 1-21; SD=9,22).

### CONCLUSION

Based on our results the tumor area defined by the amino acid tracer is not fully identical with MRI defined T2 oedema CTV. 18F-FDOPA defined BTV can modifie the definiton of the PTV, and the radiotherapy treatment.

### **CLINICAL RELEVANCE/APPLICATION**

18F-FDOPA PET/MR based target definiton in the 3D based radiotherapy treatment will provide better tumour extension characterization of patients suffering from glioblastoma multiforme.



#### SSC15

Vascular Interventional (Prostate and Uterine Embolization)

Monday, Nov. 26 10:30AM - 12:00PM Room: E352



AMA PRA Category 1 Credits ™: 1.50 ARRT Category A+ Credit: 1.75

**FDA** Discussions may include off-label uses.

#### Participants

Alexios Kelekis, MD, PhD, Athens, Greece (*Moderator*) Medical Advisory Board, BTG International Ltd; Medical Advisory Board, Merit Medical Systems, Inc; Research Grant, Mindray Medical

Thomas-Evangelos G. Vrachliotis, MD, PhD, Athens, Greece (Moderator) Nothing to Disclose

### Sub-Events

### SSC15-01 MR-Guided Focused Ultrasound Treatment for Management of Organ-Confined Intermediate Risk Prostate Cancer: Evaluation of Safety and Effectiveness

Monday, Nov. 26 10:30AM - 10:40AM Room: E352

Participants

Andrea Leonardi, MD, Roma, Italy (*Abstract Co-Author*) Nothing to Disclose Alessandro Napoli, MD, Rome, Italy (*Abstract Co-Author*) Nothing to Disclose Roberto Scipione, MD, Rome, Italy (*Abstract Co-Author*) Nothing to Disclose Fabrizio Andrani, MD, Roma, Italy (*Abstract Co-Author*) Nothing to Disclose Cristina Marrocchio, Rome, Italy (*Abstract Co-Author*) Nothing to Disclose Carlo Catalano, MD, Rome, Italy (*Abstract Co-Author*) Nothing to Disclose Hans Peter Erasmus, Rome, Italy (*Presenter*) Nothing to Disclose

### For information about this presentation, contact:

andrea.leonardi1988@gmail.com

### PURPOSE

To evaluate the safety and effectiveness of Magnetic Resonance guided Focused Ultrasound (MRgFUS) ablation in patients with organ-confined intermediate risk prostate cancer in order to postpone or eliminate the need of definitive treatment (i.e. Radical Prostatectomy or Radiation therapy).

### **METHOD AND MATERIALS**

This prospective single-arm study enrolled 19 patients, aged 50-74 years, with histologically proven organ-confined intermediate risk prostate cancer. Inclusion criteria for participation: Gleason score <= 7 (=3+4 or 4+3, no grade 5 pattern), T1-T2b, N0, M0 stage, PSA <= 20 ng/ml, lesion visible to dynamic contrast enhanced (DCE) MR imaging and no previous prostatic surgery, radiation therapy or androgen deprivation therapy. All patient underwent pre-treatment DCE (Gd-BOPTA, Bracco) MR examination (Discovery 750, GE) and MRgFUS treatment with ExAblate (InSightec). Safety of treatment was determined by evaluation of the incidence and severity of device related complications while clinical efficacy was evaluated monitoring MR imaging changes and PSA levels at 3, 6 and 12-months.

#### RESULTS

1 patient reported urinary incontinence while 2 patients referred erectile dysfunction after MRgFUS treatment. DCE MR imaging at 3, 6 and 12 months showed no recurrence/residual disease in treated patients. According to imaging, laboratory exams showed a progressive decrease of PSA level from an average value of 17,1 ng/ml before treatment to 2,2 ng/ml at 12 months follow-up. No one patient needed definitive treatment so far and can be considered free of clinically significant prostate cancer.

#### CONCLUSION

MR guided Focused Ultrasound appears as a safe and effective treatment for patients with organ-confined intermediate risk prostate cancer and can reduce the need of definitive treatment (i.e. Radical Prostatectomy or Radiation therapy).

#### **CLINICAL RELEVANCE/APPLICATION**

MRgFUS can reduce the need of surgery or radiation therapy in patient with intermediate risk prostate cancer representing a safe and effective treatment.

### SSC15-02 Magnetic Resonance-Guided Focused Ultrasound (MRgFUS) Focal Treatment of Localized Prostate Cancer: Initial Experience and Follow Up from a Multi-Center Trial

Monday, Nov. 26 10:40AM - 10:50AM Room: E352

Participants

Clare M. Tempany-Afdhal, MD, Boston, MA (Presenter) Research Grant, InSightec Ltd; Research Grant, Gilead Sciences, Inc;

Advisory Board, Profound Medical Inc; Spouse, Employee, Spring Bank Pharmaceuticals, Inc; Spouse, Director, Trio Healthcare; Spouse, Consultant, Gilead Sciences, Inc; Spouse, Consultant, Merck & Co, Inc; Spouse, Consultant, Echosens SA; Spouse, Consultant, Shinogi; Spouse, Consultant, Ligand Pharmaceuticals, Inc; Spouse, Stock options, Spring Bank Pharmaceuticals, Inc; Spouse, Stock options, Allurion; Spouse, Stock options, Trio Healthcare; ; Pejman Ghanouni, MD, PhD, Stanford, CA (*Abstract Co-Author*) Nothing to Disclose Behfar Ehdaie, New York, NY (*Abstract Co-Author*) Nothing to Disclose

Jeffrey Y. Wong, MD, Boston, MA (*Abstract Co-Author*) Nothing to Disclose

Marc H. Schiffman, MD, New York, NY (Abstract Co-Author) Nothing to Disclose

Nathan J. McDannold, PhD, Boston, MA (*Abstract Co-Author*) Nothing to Disclose

Tim McClure, Boston, MA (Abstract Co-Author) Nothing to Disclose

Lance A. Mynderse, MD, Rochester, MN (Abstract Co-Author) Investigator, NxThera, Inc

David A. Woodrum, MD, PhD, Rochester, MN (Abstract Co-Author) Consultant, Galil Medical Ltd; Consultant, Clinical Laserthermia Systems AB

Geoffrey Sonn, MD, Stanford, CA (Abstract Co-Author) Nothing to Disclose

Timothy N. Showalter, MD, Philadelphia, PA (Abstract Co-Author) Research funded, Varian Medical Systems, Inc

### For information about this presentation, contact:

ctempany-afdhal@bwh.harvard.edu

#### PURPOSE

To evaluate the initial experience, safety and feasibility of MR targeted focused ultrasound treatment of localized prostate cancer

### **METHOD AND MATERIALS**

Patients with biopsy proven prostate cancer enrolled in a prospective multi-center pivotal trial of the ExAblate 2100 prostate system. Eligibility criteria include men of 50 years or older, PSA < 20 ng/mL with either low or intermediate risk prostate cancer (Gleason Score 3+3, 3+4 or 4+3). A multi-parametric MR must confirm localized prostate cancer (Stage T1-T2) and tumor distance  $\leq$  4cm from rectal wall. All men are treated in 1.5 or 3T GEHC MR devices

#### RESULTS

38 eligible men have been enrolled and treated from 7 sites. Mean age 62.8 years, mean PSA 6.0ng/mL. Prostate MR demosntrated dominant lesions in 32 men, no lesion in 4 men and MR data was not available in 2. Pre-treatment prostate biopsy results showed Gleason 3+3 in 14, 3+4 in 19 and 4+3 in 9. All men successfully underwent MRguided FUS ablation of their focal lesion. All except one were discharged home later on the treatment day. Currently 6 men have completed follow up, 34 men are at 9 months, 27 at 12 and 12 at 18 months. There were 131 combined device or protocol related adverse events, which were Grade 1 (mild) in 117, Grade 2 (moderate) in 13 and Grade 3 (severe) in 1 (severe suprapubic pain 1 week post treatment, resolved the following day without permanent injury). Overall 77 events were procedure related, 48 were transient, 5 biopsy related and 1 device related.

### CONCLUSION

Initial experience indicates that MRgFUS appears to be both feasible and safe. Enrolling men in a trial using image-gided focal therapy in prostate cancer is feasible. Accural is ongoing in this pivotal trial.

### **CLINICAL RELEVANCE/APPLICATION**

MR guided Focused ultrasound focal prostate cancer ablation is both safe and feasible.

### SSC15-03 Uterine Artery Embolization with Gelfoam for Acquired Symptomatic Uterine Arteriovenous Shunting After Gynecologic Procedures and Obstetric Events

Monday, Nov. 26 10:50AM - 11:00AM Room: E352

Participants

Andres Camacho, MD, Boston, MA (*Presenter*) Nothing to Disclose Edward Ahn, MD, Baltimore, MD (*Abstract Co-Author*) Nothing to Disclose Johannes Boos, MD, Dusseldorf, Germany (*Abstract Co-Author*) Nothing to Disclose Quang Nguyen, MD, Brookline, MA (*Abstract Co-Author*) Nothing to Disclose Almamoon I. Justaniah, MD, Boston, MA (*Abstract Co-Author*) Nothing to Disclose Salomao Faintuch, MD, Boston, MA (*Abstract Co-Author*) Nothing to Disclose Muneeb Ahmed, MD, Boston, MA (*Abstract Co-Author*) Research Grant, General Electric Company; Stockholder, Agile Devices, Inc; Scientific Advisory Board, Agile Devices, Inc Olga R. Brook, MD, Boston, MA (*Abstract Co-Author*) Nothing to Disclose

#### For information about this presentation, contact:

obrook@bidmc.harvard.edu

#### PURPOSE

To evaluate the technical and clinical success rates and safety of bilateral uterine artery embolization (UAE) with gelfoam for symptomatic acquired uterine arteriovenous shunting presenting after obstetric or gynecologic events.

### **METHOD AND MATERIALS**

In this HIPAA-compliant, IRB approved retrospective study with a waiver of informed consent, consecutive patients of reproductive age that presented with abnormal uterine bleeding after recent gynecologic procedure or obstetric event between 01/2013 and 02/2018 at tertiary referral center were included. Bilateral uterine artery embolization was performed in all patients using gelfoam slurry. Technical success was defined as angiographic resolution of AV shunting at the end of the procedure. Clinical success was defined as cessation of bleeding, resolution of findings on subsequent imaging, or minimal estimated blood loss (<50 cc) on a subsequent dilation and curettage procedure.

### RESULTS

Eighteen patients (mean age 32.8±7.1y) were included in the study. In one patient coil embolization was used in addition to

gelfoam due to the size of the shunt. Another patient underwent a repeat UAE due to evidence of clinical and sonographic residual RPOC with subsequent technical and clinical success. Angiography demonstrated AV shunting in 18/18 (100%) with early venous drainage from the uterine arteries to internal iliac and / or gonadal veins. 7/18 (38.9%) patients underwent subsequent scheduled D&C due to remaining RPOC with EBL of  $17.9 \pm 15.6$ mL. No additional procedures were required. The technical success rate of gelfoam UAE was 17/18 (94.4%) and clinical success rate was 94.1% (16/17). There was 1/18 (5.6%) minor complication of a small groin hematoma that resolved without additional treatment and 1/18 (5.6%) asymptomatic mild pulmonary embolism (PE) detected on CT three days after a procedure, in a patient with history of PE. The average length of clinical follow-up after the UAE procedure was 18.9  $\pm$  15.9 months. 38.8% (7/18) of the patients became pregnant during the follow up.

### CONCLUSION

Uterine artery embolization with gelfoam slurry for symptomatic uterine arteriovenous shunting has a high technical and clinical success rate and low potential risk of pulmonary embolism.

### **CLINICAL RELEVANCE/APPLICATION**

Uterine artery embolization with gelfoam slurry only is successful in treating symptomatic uterine arteriovenous shunting and can be used as an alternative to permanent embolization agents.

## ssc15-04 Effect of Pelvic MRI on Clinical Management of Suspected Symptomatic Uterine Fibroids

Monday, Nov. 26 11:00AM - 11:10AM Room: E352

#### Participants

Julie C. Cronan, MD, Atlanta, GA (*Presenter*) Nothing to Disclose Mangaladevi S. Patil, MD, Atlanta, GA (*Abstract Co-Author*) Nothing to Disclose Neena A. Davisson, MD, Atlanta, GA (*Abstract Co-Author*) Nothing to Disclose Daryl T. Goldman, MD, New Orleans, LA (*Abstract Co-Author*) Nothing to Disclose Zachary Bercu, MD, Atlanta, GA (*Abstract Co-Author*) Speaker, Terumo Medical Corporation; Grant, Coulter Translational Program, Steerable Robotic Guidewire Janice M. Newsome, MD, Alexandria, VA (*Abstract Co-Author*) Nothing to Disclose Jonathan Martin, MD, Atlanta, GA (*Abstract Co-Author*) Nothing to Disclose

### For information about this presentation, contact:

jcronan@emory.edu

### PURPOSE

We aim to determine the impact of pre-procedural pelvic MRI on the clinical management and treatment of suspected symptomatic uterine fibroids.

### METHOD AND MATERIALS

An IRB-approved retrospective study of 100 patients referred to Interventional Radiology (IR) for management of suspected symptomatic uterine fibroids between 2013 and 2017 was compiled. Electronic medical records and relevant imaging in PACS were analyzed for patient age, race, gynecological evaluation including pelvic ultrasound results, as well as therapeutic plan prior to and following MRI.

### RESULTS

Of the 100 patients who underwent MRI related to IR consultation, 73 patients had previously had a pelvic US. MRI results definitively changed management in 20 patients. Of these, 4 patients had imaging characteristics concerning for malignancy, of which two had completed work-up at the time of this study with a negative endometrial biopsy and a benign teratoma, respectively. Three patients received a new diagnosis of adenomyosis, and the offered treatment plan shifted to uterine artery embolization (UAE) as adenomyosis is best treated with smaller embolic particles. An additional 13 patients were advised not to undergo uterine fibroid embolization (UFE) alone with alternatives pursued including myomectomy (n=3), myomectomy then UFE (n=1), hysterectomy (n=2), hysteroscopy with dilation and curettage (n=1), conservative management (n=1), or referral back to Gynecology prior to final decision making (n=4). An additional patient (n=1) pursued UFE despite recommendation of myomectomy vs. hysterectomy. Fibroid location and vascularity (n=9) was the most common reason for change in plan as devascularized fibroids were felt to be unlikely to respond to endovascular therapy.

### CONCLUSION

Pre-procedural evaluation of suspected symptomatic uterine fibroids differs across various clinical settings. We demonstrate a significant impact of pre-procedural MRI in the evaluation of patients: 1 in 5 patients in our small sample had a change in clinical management, and 1 in 25 demonstrated imaging findings concerning for a malignancy not previously identified by pelvic US. MRI should be incorporated into the routine work-up of patients with likely symptomatic uterine fibroids.

### **CLINICAL RELEVANCE/APPLICATION**

MRI offers invaluable information in the work-up of patients with suspected symptomatic uterine fibroids, can alter treatment planning, and can identify previously undiagnosed malignancy.

### SSC15-05 Prostate Multiparametric Magnetic Resonance May Avoid Biopsies in Patients with Elevated PSA and Surgical Indication for Prostatic Enlargement Treatment

Monday, Nov. 26 11:10AM - 11:20AM Room: E352

Participants

Fernando I. Yamauchi, MD, Sao Paulo, Brazil (*Abstract Co-Author*) Nothing to Disclose Thais Mussi, MD,PhD, Sao Paulo, Brazil (*Abstract Co-Author*) Nothing to Disclose Ronaldo H. Baroni, MD, Sao Paulo, Brazil (*Presenter*) Nothing to Disclose Gustavo C. Lemos, Sao Paulo, Brazil (*Abstract Co-Author*) Nothing to Disclose Guilherme C. Mariotti, MD, Jundiai, Brazil (*Abstract Co-Author*) Nothing to Disclose Marcelo L. Wroclawski, Sao Paulo, Brazil (*Abstract Co-Author*) Nothing to Disclose Arie Carneiro, Sao Paulo, Brazil (*Abstract Co-Author*) Nothing to Disclose Breno Amaral, Sao Paulo, Brazil (*Abstract Co-Author*) Nothing to Disclose Fernando Korkes, Sao Paulo, Brazil (*Abstract Co-Author*) Nothing to Disclose Paulo Kayano, Sao Paulo, Brazil (*Abstract Co-Author*) Nothing to Disclose

### For information about this presentation, contact:

fernando.yamauchi@einstein.br

#### PURPOSE

to evaluate the performance of mpMRI using PIRADS score on men with surgical indication for BPH and elevated PSA levels, comparing it with TRUS-guided biopsy results.

#### **METHOD AND MATERIALS**

Retrospective analysis of consecutive men with BPH and surgical candidates and concomitant elevated PSA levels (>=4ng/mL or >=2g/mL if in use of 5 alpha-reductase inhibitor), from June 2016 to August 2017. All patients were submitted to mpMRI prior to TRUS biopsy. Prostate mpMRI was done using a 1.5-T scanner (GE 350<sup>TM</sup>) without endorectal coil including high resolution T2 weighted (T2W), diffusion weighted imaging (DWI), and dynamic post-contrast enhanced sequences. Systematic 14-core biopsies were performed and in cases where mpMRI was classified as PIRADS 3 with focal lesions, PIRADS 4 or PIRADS 5, additional 2 to 3 TRUS guided targeted fragments were obtained with fusion technique. Final PIRADS score of mpMRI was compared with biopsy results and transurethral or transvesical resection (when available). Two scenarios were evaluated: first, considering only PIRADS 1 and 2 as negative and second, considering also PIRADS 3 as negative. ISUP >= 2 was was considered as csPCa.

### RESULTS

Forty men were included for final analysis, with median age of 68 years, median PSA 6.35 ng/dL and median prostatic volume 116.5 cc. Demographic data are summarized in table 1. Considering the first scenario, the sensitivity, specificity, positive (PPV) and negative (NPV) predictive values of mpMRI for any prostate cancer were 76.9%, 63%, 50%, and 85% respectively. For csPCa the sensitivity was 87.5%, specificity 59.4%, PPV 35% and NPV 95%. For the second scenario, the sensitivity, specificity, PPV and NPV of MP-MRI for any prostate cancer were 53.8%, 96.3%, 87.5%, and 81.3% respectively. For csPCa the sensitivity was 75%, specificity 93.8%, PPV 75% and NPV 93.8%.

#### CONCLUSION

Negative predictive value of mpMRI was high in patients with surgical indication for BPH and elevated PSA. Our results suggest that patients with PIRADS 1, 2 and 3 could avoid TRUS biopsies before undergoing surgical procedure.

#### **CLINICAL RELEVANCE/APPLICATION**

mpMRI may be indicated in patients with BPH and elevated PSA levels with high negative predictive value.

### SSC15-06 MRI/TRUS Fusion Guided Focal Laser Ablation for "Super-Active Surveillance" of Prostate Cancer

Monday, Nov. 26 11:20AM - 11:30AM Room: E352

#### Participants

Sheng Xu, PhD, Bethesda, MD (*Presenter*) Nothing to Disclose Baris Turkbey, MD, Bethesda, MD (*Abstract Co-Author*) Nothing to Disclose Victoria L. Anderson, MS, Bethesda, MD (*Abstract Co-Author*) Nothing to Disclose Julie Peretti, Bethesda, MD (*Abstract Co-Author*) Nothing to Disclose Charisse Garcia, RN, Bethesda, MD (*Abstract Co-Author*) Nothing to Disclose Peter Pinto, Bethesda, MD (*Abstract Co-Author*) Nothing to Disclose Peter L. Choyke, MD, Rockville, MD (*Abstract Co-Author*) Nothing to Disclose Bradford J. Wood, MD, Bethesda, MD (*Abstract Co-Author*) Researcher, Koninklijke Philips NV; Researcher, Celsion Corporation; Researcher, BTG International Ltd; Researcher, Siemens AG; Researcher, XAct Robotics; Researcher, NVIDIA Corporation; Intellectual property, Koninklijke Philips NV; Intellectual property, BTG International Ltd; Royalties, Invivo Corporation; Royalties, Koninklijke Philips NV; ; ;

#### For information about this presentation, contact:

xus2@cc.nih.gov

### PURPOSE

Prostate cancer is the most common cancer among men. Standard treatments include radiotherapy and surgery, which may lead to common side effects such as incontinence and impotence. Local focal nerve sparing treatment options often require intraoperative MRI for image guidance, with resulting limitations of cost and MR time, and requiring MR compatible equipment. MRI/TRUS fusion guided transperineal focal laser ablation may address these limitations and provide an alternative method for treating prostate cancer that might otherwise undergo active surveillance.

#### **METHOD AND MATERIALS**

A bi-plane endorectal ultrasound probe was attached to an encoded stepper which has two degrees of freedom for rotation about and translation along the probe's physical axis. At the beginning, A 3D ultrasound volume was acquired with a 2D sweep and registered to previously acquired T2w MRI. MRI/TRUS fusion was co-displayed on both transverse and longitudinal ultrasound planes. Pre-segmented MRI tumors were projected on the stepper's grid template in custom software to facilitate treatment planning. Thermocouples were placed at locations near the rectum, urethra, nerve, and bladder if needed. For each ablation, the physician picked a grid hole to insert an introducer. The software predicted the ablation zone based on the grid location and the insertion depth on longitudinal ultrasound. A side-firing laser fiber with a cooling catheter was inserted through the introducer to conduct an ablation for 2 minutes at 9-15 watts. The software estimated the residual tumor, identified regions at risk for undertreatment and planned for the next ablation. This process was iterated until the full tumor was ablated. After the procedure, a T1w contrast enhanced MRI was taken to validate tumor coverage. Seven patients with a total of 9 tumors were treated. The tumor volume was  $1.6\pm1.3cc$ . It took  $6\pm2$  ablations to treat one tumor. Post-operative MRI confirmed no residual tumor tissue following ablation. One post ablation abscess was observed in a patient without imaging evidence of residual tumor.

### CONCLUSION

MRI/TRUS fusion guided focal laser ablation is effective, safe and can serve as a low-cost option for prostate cancer treatment.

### **CLINICAL RELEVANCE/APPLICATION**

The proposed approach may provide a therapeutic option for pre-selected patients with prostate cancer who desire treatment more than active surveillance and less than full organ therapies.

### SSC15-07 Outcome of Uterine Artery Embolization for Management of Delayed Bleeding Due to Retained Placenta in Patients with Placenta Accreta

Monday, Nov. 26 11:30AM - 11:40AM Room: E352

Participants

Zhiwei Wang, MD, Beijing, China (*Presenter*) Nothing to Disclose Guorong Wang, Beijing, China (*Abstract Co-Author*) Nothing to Disclose Zheng Yu Jin, MD, Beijing, China (*Abstract Co-Author*) Nothing to Disclose

#### For information about this presentation, contact:

zhiweiwang1981@sina.com

### PURPOSE

To retrospectively evaluate the outcome of uterine artery embolization (UAE) for management of delayed bleeding due to retained placenta in patients with placenta accreta (PA).

### METHOD AND MATERIALS

A retrospective analysis of the records of all patients diagnosed with PA according to the clinical findings during delivery between January 2005 and December 2017 was performed. Twenty-eight patients were treated conservatively by leaving placenta in place and underwent UAE for bleeding subsequently. The control of hemorrhage, outcome of the placenta left in place, menses and fertility results were retrospectively reviewed.

#### RESULTS

The mean age was  $31.4\pm6.7$  years. Eight patients with massive vaginal bleeding underwent emergency UAE. The other 20 patients presented with intermittent vaginal blood loss and underwent selective UAE. The median time between delivery and UAE was 15 days. The mean retained placental volume obtained by ultrasound was  $164\pm133$  cm<sup>3</sup>. The technical success rate of embolization was 100%. Angiography revealed uterine arteriovenous malformations in two patients. Bleeding was controlled in all patients during follow-up ( $10.7\pm7.9$  months). The retained placentas were spontaneously passed vaginally or absorbed in 15 patients. Ten patients underwent curettage after UAE. Of these 10 patients, 7 retained placentas were completely removed and 3 retained placentas were partly removed and absorbed later. The other 3 retained placentas were resected for they did not decrease in size significantly after UAE. Menses returned 1-3 months after UAE in all patients and they had regular monthly cycles afterwards. And five patients delivered without complication during follow-up.

### CONCLUSION

UAE is safe and effective for management of retained placenta associated with placenta accreta.

### **CLINICAL RELEVANCE/APPLICATION**

Conservative management of the abnormal placenta, which is left inside the uterus at the time of delivery has been more and more used in clinial practice to minimize blood loss after delivery and to preserve the uterus in women with PA. UAE should be consided for subsequetly management of these patients.

### SSC15-08 The Relationship of Embolic Particle Size to Patient Outcomes in Prostate Artery Embolization for Benign Prostatic Hyperplasia: A Systematic Review and Meta-Regression

Monday, Nov. 26 11:40AM - 11:50AM Room: E352

Participants

Ruben Geevarghese, MBBS, Coventry, United Kingdom (*Presenter*) Nothing to Disclose James Harding, MRCP, FRCR, Bristol, United Kingdom (*Abstract Co-Author*) Nothing to Disclose Charles E. Hutchinson, Coventry, United Kingdom (*Abstract Co-Author*) Nothing to Disclose Caron Parsons, Coventry, United Kingdom (*Abstract Co-Author*) Nothing to Disclose

### PURPOSE

Prostate artery embolization (PAE) has been proven to be a safe, efficacious and cost-effective treatment for Benign Prostatic Hyperplasia (BPH). There has been much variation in the size of embolic particle agent used in existing studies and the degree of patient outcomes achieved. We aimed to explore the relationship of particle size to patient outcomes.

### METHOD AND MATERIALS

A systematic review of MEDLINE, PubMed and Embase was undertaken to identify all existing studies using PAE for BPH. Inclusion criteria included studies reporting a baseline and 12 month International Prostate Symptom Score (IPSS). Exclusion criteria excluded overlapping studies. Data extraction from eligible studies included the size of embolic agent and Baseline and 12 month values for: IPSS, IPSS Quality of Life, Q-max, prostate volume, prostate specific antigen and post-void residual. A weighted linear regression analysis was then used to explore the relationship between particle size and the change in the outcome measures (from baseline to 12 months).

#### RESULTS

6 non-overlapping studies were identified for data extraction. The linear regression analysis did not demonstrate a statistically significant (p<0.05) relationship of particle size with the 12 month change in patient outcome measure. However, smaller particle size and greater reductions in IPSS approached statistical significance (p=0.08).

#### CONCLUSION

Our findings suggest that there is a possible association of smaller particle size with greater reductions in IPSS. Whilst not statistically significant, these findings impress upon the need for further research on determining the optimum particle size for PAE.

### **CLINICAL RELEVANCE/APPLICATION**

Smaller embolic particle size may be associated with greater symptom severity reduction in patients undergoing PAE for BPH.

## SSC15-09 Visualization of the Different Branches of the Internal Iliac Artery Before Prostatic Artery Embolization Using Three Dimensional Contrast-Enhanced MR Angiography

Monday, Nov. 26 11:50AM - 12:00PM Room: E352

Participants

Nagy N. Naguib, MD, MSc, Frankfurt Am Main, Germany (*Presenter*) Nothing to Disclose Nour-Eldin A. Nour-Eldin, MD,PhD, Frankfurt Am Main, Germany (*Abstract Co-Author*) Nothing to Disclose Elsayed M. Elhawash, BMedSc,MS, Frankfurt Am Main, Germany (*Abstract Co-Author*) Nothing to Disclose Tatjana Gruber-Rouh, Frankfurt Am Main, Germany (*Abstract Co-Author*) Nothing to Disclose Benjamin Kaltenbach, MD, Frankfurt, Germany (*Abstract Co-Author*) Nothing to Disclose Renate M. Hammerstingl, MD, Frankfurt Am Main, Germany (*Abstract Co-Author*) Nothing to Disclose Mohammed A. Alsubhi, BMBS, Frankfurt Am Main, Germany (*Abstract Co-Author*) Nothing to Disclose Thomas J. Vogl, MD, PhD, Frankfurt, Germany (*Abstract Co-Author*) Nothing to Disclose

#### For information about this presentation, contact:

nagynnn@yahoo.com

#### PURPOSE

To evaluate the ability of Three Dimensional Contrast Enhanced MR Angiography (3D-CE-MRA) in Visualizing the branches of the Internal Iliac Artery (IIA) in males prior to prostatic artery embolization (PAE).

#### **METHOD AND MATERIALS**

Pre-embolization CE-MRA studies from 30 males (mean age 68.18 years) were retrospectively evaluated by two radiologists in consensus. Studies were done using a 3 Tesla MRI unit and 3D images were reconstructed using Syngo Vessel View Application. Studies from 2 patients were excluded (due to incomplete coverage of the pelvis). A scoring system of 3 Grades was adopted where a score of 0 means that the artery was not seen, interrupted or its origin could not be identified, a score of 1 means that the artery was faintly seen but can be traced and has no missing segments till it gives off its first branch, finally score 2 means that the artery was clearly seen.

### RESULTS

Of the studied 56 internal iliac arteries 9 different branches were evaluated. The superior gluteal artery detected in all studied arteries with a score of 2 in all of them and sensitivity 1. The inferior gluteal artery also detected in all IIA (Score 2 in all; overall sensitivity of 1). The internal pudendal detected in all IIA (Score 2 in 55, score 1 in 1; sensitivity 1). The obturator artery detected in all IIA (Score 2 in 52, score 1 in 4; sensitivity 1). The iliolumbar artery detected in all IIA (Score 2 in 53, score 1 in 3; sensitivity 1). The lateral sacral artery detected in 55 IIA (Score 2 in 49, score 1 in 6, score 0 in 1; sensitivity 0.98). The inferior vesical (prostatic) artery detected in 45 IIA (Score 2 in 26, score 1 in 19, score 0 in 11; sensitivity 0.80). The middle rectal artery detected in 21 IIA (Score 2 in 5, score 1 in 16, score 0 in 35; sensitivity 0.38). Lastly the superior vesical artery detected in 2 IIA with a score of 1 (sensitivity 0.04).

# CONCLUSION

3D-CE-MRA is a helpful non invasive tool in detecting most of the branches of the internal iliac artery in males. It can detect up to 80% of the prostatic arteries before PAE.

### **CLINICAL RELEVANCE/APPLICATION**

3D-CE-MRA is a reliable method for mapping the internal iliac artery prior to PAE which might help in reducing the procedure time.



### RCA23

### Introduction to Machine Learning and Texture Analysis for Lesion Characterization (Hands-on)

Monday, Nov. 26 12:30PM - 2:00PM Room: S401AB



AMA PRA Category 1 Credits ™: 1.50 ARRT Category A+ Credit: 1.75

FDA Discussions may include off-label uses.

#### Participants

Kevin Mader, DPhil,MSc, Basel, Switzerland (*Moderator*) Employee, 4Quant Ltd; Shareholder, 4Quant Ltd Kevin Mader, DPhil,MSc, Basel, Switzerland (*Presenter*) Employee, 4Quant Ltd; Shareholder, 4Quant Ltd Barbaros S. Erdal, PhD, Columbus, OH (*Presenter*) Nothing to Disclose Joshy Cyriac, Basel, Switzerland (*Presenter*) Nothing to Disclose

### For information about this presentation, contact:

mader@biomed.ee.ethz.ch

joshy.cyriac@usb.ch

#### **LEARNING OBJECTIVES**

1) Review the basic principles of machine learning. 2) Learn what texture analysis is and how to apply it to medical imaging. 3) Understand how to combine texture analysis and machine learning for lesion classification tasks. 4) Learn the how to visualize and analyze results. 5) Understand how to avoid common mistakes like overfitting and incorrect model selection.

### ABSTRACT

During this course, an introduction to machine learning and image texture analysis will be provided through hands on examples. Participants will use with open source as well as freely available commercial platforms in order to achieve tasks such as image feature extraction, statistical analysis, building models, and validating them. Imaging samples will include both 2D and 3D datasets from a variety of modalities (CT, PET, MR). The course will begin with a brief overview of important concepts and links to more detailed references. The concepts will then be directly applied in visual, easily understood workflows where the participants will see how the images are processed, features and textures are extracted and how publication ready statistics and models can be built and tested.



### RCB23

# A Hands-on Introduction to Using the NIH/NCI's Cancer Imaging Archive (TCIA) (Hands-on)

Monday, Nov. 26 12:30PM - 2:00PM Room: S401CD



AMA PRA Category 1 Credits ™: 1.50 ARRT Category A+ Credit: 1.75

### Participants

Justin Kirby, Rockville, MD (*Presenter*) Nothing to Disclose Lawrence R. Tarbox, PhD, Little Rock, AR (*Presenter*) Nothing to Disclose John B. Freymann, BS, Rockville, MD (*Presenter*) Nothing to Disclose Fred W. Prior, PhD, Little Rock, AR (*Presenter*) Nothing to Disclose

### LEARNING OBJECTIVES

1) Learn how to publish your research data by sharing it in TCIA. We accept a variety of 'primary' data types including radiology images, pathology images, and clinical data. Additionally researchers can submit 'analysis data' of existing primary data such as radiologist annotations, segmentations, and computer-extracted radiomic or deep learning features. 2) Review the full scope of TCIA functionality for searching, visualizing and downloading data. We provide several different ways to discover our data sets and will review each of them during the class. 3) Identify support resources that include the TCIA helpdesk, FAQs, and system documentation.

### ABSTRACT

Access to large, high quality data is essential for researchers to understand disease and precision medicine pathways, especially in cancer. However HIPAA constraints make sharing medical images outside an individual institution a complex process. The NCI's Cancer Imaging Archive (TCIA) addresses this challenge by providing hosting and de-identification services which take the burden of data sharing off researchers. TCIA now contains over 80 unique data collections of more than 30 million images. Recognizing that images alone are not enough to conduct meaningful research, most collections are linked to rich supporting data including patient outcomes, treatment information, genomic / proteomic analyses, and expert image analyses (segmentations, annotations, and radiomic / radiogenomic features). This hands-on session will teach the skills needed to fully access TCIA's existing data as well as learn how to submit new data for potential inclusion in TCIA.



#### RCC23

# Structured Reporting and the RSNA/ESR Reporting Initiative

Monday, Nov. 26 12:30PM - 2:00PM Room: S501ABC

# IN

AMA PRA Category 1 Credits  $^{\text{TM}}$ : 1.50 ARRT Category A+ Credit: 1.75

#### Participants

Marta E. Heilbrun, MD, Salt Lake City, UT (Moderator) Nothing to Disclose

### LEARNING OBJECTIVES

1) Learn how to implement structured reporting across your department to make radiology reports more consistent and improve quality. 2) Describe national and international efforts to share best-pracitce radiology report templates. 3) Explore how RSNA's reporting initiative adds value to the healthcare enterprise.

#### Sub-Events

RCC23A Successfully Implementing a Department-wide Standardized Reporting Program

Participants

David B. Larson, MD, MBA, Stanford, CA (Presenter) Grant, Siemens AG ; Grant, Koninklijke Philips NV

# LEARNING OBJECTIVES

1) Understand critical interpersonal elements to consider in implementing and managing a department-wide standardized structured report program. 2) Understand the technical challenges associated with implementing and managing a department-wide standardized structured report program.

### ABSTRACT

Modern voice recognition technology has made department-wide standardized structured reporting feasible. However, the most significant challenges often lie in the interpersonal and organizational aspects. The author will discuss his experience in implementing and maintaining department-wide standardized structured reporting programs at two academic institutions, highlighting critical steps, major pitfalls, and strategies for success. The session will focus on those who might wish to develop department-wide structured reporting programs at their own institutions.

### **Honored Educators**

Presenters or authors on this event have been recognized as RSNA Honored Educators for participating in multiple qualifying educational activities. Honored Educators are invested in furthering the profession of radiology by delivering high-quality educational content in their field of study. Learn how you can become an honored educator by visiting the website at: https://www.rsna.org/Honored-Educator-Award/ David B. Larson, MD - 2014 Honored EducatorDavid B. Larson, MD - 2018 Honored Educator

# RCC23B ESR Reporting Initiative

Participants Emanuele Neri, MD, Pisa, Italy (*Presenter*) Nothing to Disclose

# LEARNING OBJECTIVES

1) Understand the background and rationale for RSNA's reporting initiative. 2) Describe recent advances in the technologies for radiology reporting. 3) Explore how reporting can add augment radiology's value to the healthcare enterprise. 4) Envision the latest directions and opportunities for radiology reporting.

#### ABSTRACT

Since 2007, the RSNA has taken a leading role in developing tools and clinical content to help radiologists improve their reporting practices. RSNA's library of best-practice reporting templates (www.radreport.org) has seen more than 2 million views and downloads. The 'Management of Radiology Report Templates' (MRRT) profile and a DICOM standard for transmitting template-based reports into the electronic health record (EHR) have been recently developed. These standards, and a set of tools that use them, provide new opportunities for information from radiology reports to be integrated into the clnical enterprise. The 'Open Template Library' (open.radreport.org) allows any RSNA member to contribute report templates, and the open-source 'T-Rex' template editor simplifies the editing process. Through partnerships with other organizations, RSNA is seeking to improve and extend these approaches. This presentation will highlight recent advances and new directions in radiology reporting.

# RCC23C radreport.org: Publishing Your Templates

Participants

Marta E. Heilbrun, MD, Salt Lake City, UT (Presenter) Nothing to Disclose

# LEARNING OBJECTIVES

1) Understand how to share templates on open.radreport.org. 2) Know how templates from open.radreport.org are promoted to

radreport.org. 3) Describe the active collaborations with the European Society of Radiology (ESR) and other societies with the RSNA structured reporting effort.

# ABSTRACT

As a component of the RSNA structured reporting initiative a select template library was created and is available at www.radreport.org. In order to facilitate the exchange of templates and to identify best practices, a resource for hosting templates created by RSNA members and affiliated societies has been created at the www.open.radreport.org site. This presentation will walk the audience through the process for sharing templates on open.radeport.org and using the T-Rex editor to create MRRT templates. Additionally, the activities of the Template Library Advisory Panel (TLAP), a joint collaboration between the RSNA and the ESR will be described. The TLAP is responsible for promoting the crowd-sourced templates to the the select template library will be described.



### MSAS23

Global Initiatives and Relief Efforts (Sponsored by the Associated Sciences Consortium) (Interactive Session)

Monday, Nov. 26 1:30PM - 3:00PM Room: S105AB

# ОТ

AMA PRA Category 1 Credits ™: 1.50 ARRT Category A+ Credit: 1.75

#### Participants

Catherine Gunn, MBA, RT, Halifax, NS (Moderator) Nothing to Disclose

#### Sub-Events

### MSAS23A A Multidisciplinary Approach to Global Radiology Outreach: RAD-AID's Experience

Participants

Karyn A. Ledbetter, MD, Detroit, MI (Presenter) Nothing to Disclose

For information about this presentation, contact:

karynl@rad.hfh.edu

#### LEARNING OBJECTIVES

1) Describe the current state of radiology resources in the developing world. 2) Understand the history and mission of RAD-AID. 3) Discuss what makes RAD-AID a unique organization in the area of global radiology outreach. 4) Appreciate special considerations that must be made when providing imaging in underserved areas. 5) Assess future volunteer opportunities with a more thorough understanding of the complexity involved.

# MSAS23B Healthcare Aid in Africa: A Volunteer's Experience with Mercy Ships

Participants

William Creene, RT, Halifax, NS (Presenter) Nothing to Disclose

#### For information about this presentation, contact:

wcreene@gmail.com

#### LEARNING OBJECTIVES

1) Describe the medical and surgical need in developing nations. 2) Examine numerous conditions endemic to developing nations which require surgical intervention. 3) Describe the unique challenges of healthcare delivery and access in developing nations. 4) Assess the role of non-governmental organizations such as Mercy Ships in relieving the medical and surgical needs in developing nations.

# ABSTRACT

This presentation will be a synopsis of the speaker's experiences volunteering as a radiological technologist in West Africa aboard the world's largest non-governmental hospital ship, the *MV Africa Mercy*. The ship is operated by Mercy Ships, an NGO which provides free surgical care to people of developing nations. Topics will include orthopedics, maxillofacial, general surgery, and women's health. Experiences and challenges related to healthcare delivery in the developing world will be discussed. A diverse range of CT and X-ray case studies with pathology unique to the developing world will be presented.



### MSCA21

Case-based Review of the Abdomen (Interactive Session)

Monday, Nov. 26 1:30PM - 3:00PM Room: S100AB



AMA PRA Category 1 Credits ™: 1.50 ARRT Category A+ Credit: 1.75

#### Participants

Julie H. Song, MD, Providence, RI (Director) Nothing to Disclose

For information about this presentation, contact:

jsong2@lifespan.org

#### Sub-Events

MSCA21A Pediatric Abdomen

Participants Edward Y. Lee, MD, Boston, MA (*Presenter*) Nothing to Disclose

#### LEARNING OBJECTIVES

1) Discuss typical clinical presentation of pediatric patients with congenital and acquired abdominal disorders. 2) Review current imaging techniques for assessing abdominal disorders in pediatric patients. 3) Learn characteristic imaging findings to narrow the differential diagnoses of abdominal disorders in infants and children.

### MSCA21B Women's Imaging

Participants

Christine O. Menias, MD, Chicago, IL (Presenter) Nothing to Disclose

For information about this presentation, contact:

menias.christine@mayo.edu

#### LEARNING OBJECTIVES

1) Review Imaging of Gynecologic disorders in a case-based format. 2) Highlight common pitfalls and differential diagnosis in GYN. 3) Emphasize Imaging features that should not be overlooked.

#### ABSTRACT

Case based review of MR features of Gynecologic and other female pelvis disorders in a case based format

#### **Honored Educators**

Presenters or authors on this event have been recognized as RSNA Honored Educators for participating in multiple qualifying educational activities. Honored Educators are invested in furthering the profession of radiology by delivering high-quality educational content in their field of study. Learn how you can become an honored educator by visiting the website at: https://www.rsna.org/Honored-Educator-Award/ Christine O. Menias, MD - 2013 Honored EducatorChristine O. Menias, MD - 2014 Honored EducatorChristine O. Menias, MD - 2015 Honored EducatorChristine O. Menias, MD - 2016 Honored EducatorChristine O. Menias, MD - 2018 Honored Educator

# MSCA21C Abdominopelvic Emergency

Participants Michael N. Patlas, MD, FRCPC, Hamilton, ON (*Presenter*) Nothing to Disclose

#### For information about this presentation, contact:

patlas@hhsc.ca

#### LEARNING OBJECTIVES

1) To discuss common pitfalls in interpretation of challenging acute abdominal cases. 2) To review the use of different crosssectional imaging modalities in patient with acute abdomen. 3) To reduce unnecessary imaging.

# MSCA21D Abdominal Trauma

Participants Jorge A. Soto, MD, Boston, MA (*Presenter*) Royalties, Reed Elsevier Stephan W. Anderson, MD, Cambridge, MA (*Presenter*) Nothing to Disclose

#### LEARNING OBJECTIVES

1) Review Imaging of abdominal trauma in a case-based format. 2) Discuss common pitfalls and clinically relevant differential diagnosis in abdominal trauma. 3) Discuss protocol considerations to optimize diagnostic yield in abdominal trauma.

#### **Honored Educators**

Presenters or authors on this event have been recognized as RSNA Honored Educators for participating in multiple qualifying educational activities. Honored Educators are invested in furthering the profession of radiology by delivering high-quality educational content in their field of study. Learn how you can become an honored educator by visiting the website at: https://www.rsna.org/Honored-Educator-Award/ Stephan W. Anderson, MD - 2018 Honored Educator



#### MSMC23

Cardiac CT Mentored Case Review: Part III (In Conjunction with the North American Society for Cardiovascular Imaging) (Interactive Session)

Monday, Nov. 26 1:30PM - 3:00PM Room: S406A



AMA PRA Category 1 Credits ™: 1.50 ARRT Category A+ Credit: 1.75

#### **Participants**

Jill E. Jacobs, MD, New York, NY (*Director*) Nothing to Disclose Karen G. Ordovas, MD, San Francisco, CA (*Moderator*) Advisor, Arterys Inc

#### For information about this presentation, contact:

karen.ordovas@ucsf.edu

jill.jacobs@nyumc.org

### **LEARNING OBJECTIVES**

1) Identify cardiac and coronary artery anatomy. 2) Recognize cardiac disease processes, including coronary atherosclerosis, as diagnosed on CT. 3) Understand methods of cardiac CT and coronary CT angiography post-processing. 4) Understand the role of coronary artery calcium scoring. 5) Understand the role of Cardiac CTA in coronary artery pathologies including aneurysms, fistulae and other anomalies.

# Sub-Events

# MSMC23A Pulmonary Veins and Pericardial Disease

Participants

Harold I. Litt, MD, PhD, Philadelphia, PA (Presenter) Research Grant, Siemens AG ; ; ;

#### LEARNING OBJECTIVES

1) Describe normal versus anomalous pulmonary venous anatomy. 2) Understand the imaging findings of complications of ablation for atrial fibrillation. 3) Describe abnormalities of the pulmonary veins identifiable on routine CT. 4) Identify the most common pericardial abnormalities evaluated with CT.

#### MSMC23B Coronary Atherosclerosis III

Participants

Elliot K. Fishman, MD, Baltimore, MD (*Presenter*) Institutional Grant support, Siemens AG; Institutional Grant support, General Electric Company; Co-founder, HipGraphics, Inc

#### For information about this presentation, contact:

efishman@jhmi.edu

#### **LEARNING OBJECTIVES**

1) To provide a more complete understanding of cardiac CTA through a series of illustrative cases. 2) Discuss calcium scoring and its current role in a range of clinical scenarios, coronary artery anomalies, coronary artery fistulae, coronary artery aneurysms, and coronary artery challenging cases.

#### **Honored Educators**

Presenters or authors on this event have been recognized as RSNA Honored Educators for participating in multiple qualifying educational activities. Honored Educators are invested in furthering the profession of radiology by delivering high-quality educational content in their field of study. Learn how you can become an honored educator by visiting the website at: https://www.rsna.org/Honored-Educator-Award/ Elliot K. Fishman, MD - 2012 Honored EducatorElliot K. Fishman, MD - 2014 Honored EducatorElliot K. Fishman, MD - 2016 Honored EducatorElliot K. Fishman, MD - 2018 Honored Educator



### MSMI23

Molecular Imaging Symposium: Neurologic MI Applications

Monday, Nov. 26 1:30PM - 3:00PM Room: S405AB



AMA PRA Category 1 Credits ™: 1.50 ARRT Category A+ Credit: 1.75

**FDA** Discussions may include off-label uses.

#### Participants

Alexander Drzezga, MD, Cologne, Germany (*Moderator*) Consultant, Siemens AG; Consultant, Bayer AG; Consultant, General Electric Company; Consultant, Eli Lilly and Company; Consultant, The Piramal Group; Speakers Bureau, Siemens AG; Speakers Bureau, Bayer AG; Speakers Bureau, General Electric Company; Speakers Bureau, Eli Lilly and Company; Speakers Bureau, The Piramal Group Satoshi Minoshima, MD, PhD, Salt Lake City, UT (*Moderator*) Consultant, Hamamatsu Photonics KK; Research Grant, Hitachi, Ltd; Research Grant, Nihon Medi-Physics Co, Ltd;

#### Sub-Events

# MSMI23A Brain MI in Dementia

Participants

Alexander Drzezga, MD, Cologne, Germany (*Presenter*) Consultant, Siemens AG; Consultant, Bayer AG; Consultant, General Electric Company; Consultant, Eli Lilly and Company; Consultant, The Piramal Group; Speakers Bureau, Siemens AG; Speakers Bureau, Bayer AG; Speakers Bureau, General Electric Company; Speakers Bureau, Eli Lilly and Company; Speakers Bureau, The Piramal Group

# LEARNING OBJECTIVES

1) Gain overview on types of molecular neuropathology involved in the development of different forms of dementia and understand currently discussed disease concepts. 2) Learn about the currently available methods for imaging molecular pathology such as amyloid-deposition and tau-aggregation in dementia and their current status of validation. 3) Gain insights on the clinical value of the individual available methods and their combination with regard to earlier detection, more reliable diagnosis and therapy monitoring of disease.

# MSMI23B Dopaminergic Imaging in Parkinsonian Syndrome

Participants

Kirk A. Frey, MD, PhD, Ann Arbor, MI (*Presenter*) Consultant, MIM Software Inc; Stockholder, General Electric Company; Stockholder, Johnson & Johnson; Stockholder, Novo Nordisk AS; Stockholder, Bristol-Myers Squibb Company; Stockholder, Merck & Co, Inc;

# **LEARNING OBJECTIVES**

1) Understand the molecular targets available for imaging of presynaptic dopaminergic synapses. 2) Appreciate the diagnostic characteristics of dopamine transporter imaging in movement disorder syndromes. 3) Master the appropriate use settings for clinical application of dopamine transporter imaging. 4) Appreciate alternative molecular imaging approaches that may offer value in distinction between movement disorders in the future.

### MSMI23C Clinical Trials and Approval Process for New Brain MI

Participants Peter Herscovitch, MD, Bethesda, MD (*Presenter*) Nothing to Disclose

For information about this presentation, contact:

herscovitch@nih.gov

### LEARNING OBJECTIVES

Describe the U.S. Food and Drug Administration (FDA) approval process for new radiopharmaceuticals for molecular brain imaging.
 Describe the U.S. Medicare approval process for new radiopharmaceuticals for molecular brain imaging.
 Explain the features and current results of the IDEAS Study: Imaging Dementia-Evidence for Amyloid Scanning Study.
 List the evolving requirements for demonstrating the value of diagnostic imaging, with emphasis on radiopharmaceuticals for molecular brain imaging.

#### ABSTRACT

The final steps in clinical translation of molecular imaging radiopharmaceuticals for brain studies are approval by the U.S. Food and Drug Administration (FDA) for marketing and by insurance carriers for reimbursement. Given the age of patients most likely to require brain imaging studies for neurodegenerative disorders, coverage approval by the U.S. Centers for Medicare and Medicaid (CMD, 'Medicare') is crucial. This talk will discuss the FDA requirements for approval of a radiopharmaceutical, with a focus on amyloid brain imaging. It should be noted that FDA approval does not necessarily lead to Medicare approval, especially for PET agents. The CMS approval process will be outlined, including the increasing need to demonstrate the ability of PET imaging to provide improved health outcomes. CMS coverage with evidence development (CED) of PET amyloid imaging agents will be described, with a focus on the design, implementation, and current results of the Imaging Dementia-Evidence for Amyloid Scanning (IDEAS) Study. MSMI23D Machine Learning in Brain MI

Participants

Satoshi Minoshima, MD, PhD, Salt Lake City, UT (*Presenter*) Consultant, Hamamatsu Photonics KK; Research Grant, Hitachi, Ltd; Research Grant, Nihon Medi-Physics Co, Ltd;

# LEARNING OBJECTIVES

1) Gain insights on available methods of molecular imaging in dementia and their significance. 2) Gain insights in principles and value of dopaminergic imaging in Parkinsonian syndromes. 3) Gain understanding in approval processes for new brain molecular imaging tracers and ongoing clinical trials.



#### MSRO23

#### **BOOST: Head and Neck-Science Session**

Monday, Nov. 26 1:30PM - 2:30PM Room: E450A



AMA PRA Category 1 Credit ™: 1.00 ARRT Category A+ Credit: 1.00

**FDA** Discussions may include off-label uses.

#### Participants

Carryn Anderson, MD, Iowa City, IA (Moderator) Nothing to Disclose

John C. Grecula, MD, Columbus, OH (Moderator) Research Grant, Teva Pharmaceutical Industries Ltd; Research Grant, Soligenix, Inc;

#### Sub-Events

# MSR023-01 Low-Lying Lymph Node (LLLN) Involvement in Human Papillomavirus (HPV)-Associated Oropharyngeal Carcinoma (OPC)

Monday, Nov. 26 1:30PM - 1:40PM Room: E450A

#### Awards

### **Student Travel Stipend Award**

Participants

Timothy Lin, BA, Bellaire, TX (Presenter) Nothing to Disclose Hesham Elhalawani, MD, MSc, Houston, TX (Abstract Co-Author) Nothing to Disclose Baher Elgohari, MBBCh, Houston, TX (Abstract Co-Author) Nothing to Disclose James M. Debnam, MD, Houston, TX (Abstract Co-Author) Nothing to Disclose Amit Jethanandani, MPH, Houston, TX (Abstract Co-Author) Nothing to Disclose Abdallah S. Mohamed, MD, MSc, Houston, TX (Abstract Co-Author) Nothing to Disclose S. J. Frank, MD, Houston, TX (Abstract Co-Author) Board Member, C4 Imaging LLC Stockholder, C4 Imaging LLC Advisory Board, Elekta AB Erich M. Sturgis, MD, Houston, TX (Abstract Co-Author) Nothing to Disclose Jack Phan, MD, PhD, Houston, TX (Abstract Co-Author) Nothing to Disclose Jay Reddy, MD, PhD, Houston, TX (Abstract Co-Author) Nothing to Disclose Clifton D. Fuller, MD, PhD, Houston, TX (Abstract Co-Author) Research Consultant, Elekta AB; Research Grant, Elekta AB; Speaker, Elekta AB William H. Morrison, MD, Houston, TX (Abstract Co-Author) Nothing to Disclose Heath Skinner, MD, PhD, Houston, TX (Abstract Co-Author) Nothing to Disclose David I. Rosenthal, Houston, TX (Abstract Co-Author) Advisory Board, Bristol-Myers Squibb Company Advisory Board, Merck KGaA Research support, Merck KGaA Adam S. Garden, MD, Houston, TX (Abstract Co-Author) Nothing to Disclose Brandon Gunn, MD, Galveston, TX (Abstract Co-Author) Nothing to Disclose

For information about this presentation, contact:

tlin4@mdanderson.org

#### PURPOSE

To characterize the incidence/pattern of LLLN involvement in HPV-associated OPC and correlation with outcomes after radiation therapy (RT).

#### **METHOD AND MATERIALS**

We reviewed diagnostic/planning images and clinical data of an IRB-approved cohort of HPV-associated OPC patients (pts) treated with definitive RT at our institution from 2004-13. Demographics and outcomes were retrieved from the medical records. LLLN+ were defined as any radiographically involved level IV or Vb nodes. AJCC 8th edition staging was used. Actuarial outcomes were calculated using Kaplan-Meier and compared by log-rank test. One-way analysis of variance was used to compare proportions.

### RESULTS

In 796 pts, the incidence of LLLN+ was 12%, 13% in base of tongue and 10% in tonsil primaries, 10% in N1, 17% in N2, and 48% in N3. Median follow-up was 58 months (IQR: 42-77). Induction chemotherapy (IC) was used in 80% vs. 37% and concurrent in 78% vs. 65% for those with vs. without LLLN involvement, respectively. The proportion of LLLN+ patients receiving IC was 70%, 93%, and 100% for those with N1, N2, and N3 disease, respectively (p=.0034). Overall, LLLN+ was associated with worse 5-year rates for all disease control endpoints tested except freedom from distant metastasis (FDM) with a trend for OS. In patients with N1 disease, LLLN-involvement was associated with worse rates of FDM (87% vs. 94%, p=.0214); no significant differences were observed in N2 or N3 subgroups for any endpoint. In patients who received IC, LLLN+ was associated with worse 5-year local control (LC), regional control (RC), and relapse-free survival (RFS), differences ranging from 6-11% (p-value<0.004 for each). When stratified by IC and N-category, LLLN+ was associated with lower FDM rates in N1 (86% vs. 94%, p=.014) but not N2 or N3 disease.

#### CONCLUSION

Reflective of the patterns of care of those treated during this study time frame, most pts with LLLN+ received IC, which could have potentially offset any adverse correlation with subsequent distant failure. However, LLLN+ correlated with other disease control endpoints (LC, RC, and RFS), and thus could be considered a marker of regionally advanced disease in HPV-associated OPC, even for those with lower stage.

## CLINICAL RELEVANCE/APPLICATION

LLLLN involvement was associated with poorer disease control outcomes, and a potential influence of IC on subsequent distant failure is hypothesized.

# MSR023-02 Automatic Gross Tumor Volume (GTV) Delineation for Nasopharyngeal Carcinoma (NPC) Radiotherapy on Multi-modal MRI: A Deep Learning Model Trained from 1000 Patient Dataset

Monday, Nov. 26 1:40PM - 1:50PM Room: E450A

Participants

Fu Li, Guangzhou, China (*Presenter*) Nothing to Disclose Yao Lu, Guangzhou, China (*Abstract Co-Author*) Nothing to Disclose Ying Sun, Guangzhou, China (*Abstract Co-Author*) Nothing to Disclose Li Lin, Guangzhou, China (*Abstract Co-Author*) Nothing to Disclose

#### For information about this presentation, contact:

lifu5@mail.sysu.edu.cn

# PURPOSE

GTV delineation of NPC is a critical and time-consuming process during intensity modulated radiotherapy. We are developing an automatic deep learning GTV delineation approach for NPC radiotherapy on multi-model MRI.

#### **METHOD AND MATERIALS**

With IRB approval, we retrospectively collected 1012 patients who underwent intensity modulated radiotherapy for NPC from Sept. 2016 to Aug. 2017. Multi-model MRIs (T1, T1C, T1W, T2) were acquired for GTV delineation of each patient with Philips MR imaging system and covered large variations in scanning parameters. Three experienced radiotherapists manually marked the GTV contours on MRI series (1 to 2 hours per case). In this study, a modified 3D U-net deep learning network was trained to perform volume-to-volume delineation of GTV. Multi-modal MRIs were regard as different channel input of the 3D U-net and feature maps from various layers were concatenated with deep supervision to generate the output as the corresponding GTV likelihood map. Binary cross-entropy was applied as loss function for network training. To increase receptive fields and capture contextual information, two-stride convolution was used to downsample feature maps instead of maxpooling operator. Besides, clinical anatomy characteristics were explored as post-processing to protect normal tissues and further improve the model performance. We randomly split the entire data set into training (850 cases) and independent testing (162 cases). Dice coefficient (DC), average percent volume error (AVE) and average absolute volume error (AAVE) were used to compare the computed GTV results with the experts' manual results.

#### RESULTS

The average DC, AVE and AAVE on test data are  $0.79\pm0.05$ ,  $-0.09\pm0.21$ , and  $0.19\pm0.13$ , respectively. Comparing to 1-2 hours by the readers, our deep learning delineation takes less than 15 seconds per case.

#### CONCLUSION

Our results demonstrated the feasibility of deep learning approach for automatic GTV delineation of NPC during intensity modulated radiotherapy. Our automatic tool achieves good delineation quality on NPC GTV and greatly reduces the delineation time by hundred times compared to clinical doctors.

# **CLINICAL RELEVANCE/APPLICATION**

Radiotherapy is one of the efficient routine treatment for NPC and accurate delineation of GTV is a key step in radiotherapy. Our automatic tool has potential to reduce the variability between human readers as well as improve the efficiency of the whole procedure.

# MSR023-03 Using Artificial Intelligence to Predict Oropharyngeal Cancer Recurrence After Radiation Therapy

Monday, Nov. 26 1:50PM - 2:00PM Room: E450A

Participants William Su, New York, NY (*Presenter*) Nothing to Disclose Martin Kang, New York, NY (*Abstract Co-Author*) Nothing to Disclose Yading Yuan, New York, NY (*Abstract Co-Author*) Nothing to Disclose Richard L. Bakst, MD, New York, NY (*Abstract Co-Author*) Nothing to Disclose

For information about this presentation, contact:

richard.bakst@mountsinai.org

## PURPOSE

HPV derived oropharyngeal cancers are less aggressive and more radiosensitive compared to non-HPV derived oropharyngeal cancers. In the HPV era, treatment de-escalation is one of the main areas of focus for clinical trials. However, recurrences still occur in HPV derived disease and can follow unique patterns, so it is important to identify patients at high risk of recurrence and ensure that they do not receive de-intensified treatment. Artificial intelligence can be used to analyze radiomic signatures and potentially predict recurrence. This would allow for personalized treatment planning based on radiographic risk profiles. Our purpose was to demonstrate that deep learning models have the potential to assess radiographic risk factors for oropharyngeal cancer recurrence.

#### METHOD AND MATERIALS

Radiotherapy planning CT scans of 108 patients with histologically proven oropharyngeal cancer were acquired from the TCIA Head-Neck-PET-CT collection. In this collection, all patients with recurrent cancer or metastases at presentation were excluded. Of 108 cases, 44 had loco-regional or distant recurrence of cancer after definitive radiation treatment. For each patient, a volume of interest (VOI) that embraces the Gross Tumor Volume was extracted from the entire CT scan. After being preprocessed for dimension standardization and intensity normalization, the VOI was input into a VGG16 based neural network to obtain a discriminative score, which indicates an estimate of the probability of recurrence of that tumor. Receiver Operating Characteristic (ROC) analysis was used to evaluate the classification performance of the VGG-based model.

# RESULTS

By using 4-fold cross validation, the VGG-based classification model achieved an average accuracy of 0.59 and AUC of 0.60.

### CONCLUSION

Our study shows that deep learning models have potential in predicting oropharyngeal cancer recurrence. This can eventually pave the way towards individualized radiation dosage planning based on radiomic signatures. A larger, multi-institutional dataset is required to further validate the model for clinical application.

### **CLINICAL RELEVANCE/APPLICATION**

Artificial intelligence can be used to analyze radiographic features on CT simulation scans to predict recurrence risk and tailor radiation dosages in the HPV era of oropharyngeal cancers.

# MSR023-04 A Phase II, Proof-of-Concept Clinical Study of an Oral Mouth Rinse Containing Sandalwood Oil (SAO) for the Prevention of Oral and Oropharyngeal Mucositis Associated with (Chemo-) Radiation Therapy in Head and Neck Cancer Patients

Monday, Nov. 26 2:00PM - 2:10PM Room: E450A

Participants

Chul S. Ha, MD, San Antonio, TX (*Presenter*) Investigator, Santalis Pharmaceuticals, Inc Ying Li, MD, San Antonio, TX (*Abstract Co-Author*) Investigator, Santalis Pharmaceuticals, Inc Carol Jenkins, RN,MS, San Antonio, TX (*Abstract Co-Author*) Nothing to Disclose Corey Levenson, PhD, San Antonio, TX (*Abstract Co-Author*) Officer, Santalis Pharmaceuticals

## PURPOSE

Mucositis is one of the most debilitating side effects in patients treated with (chemo-) radiation therapy for head and neck cancer. This study was intended to evaluate the efficacy in alleviating mucositis, safety and tolerability of SAO (0.25% aqueous solution of an anti-inflammatory and anti-microbial essential oil from Santalum album trees).

# METHOD AND MATERIALS

Patients to be treated with (chemo-) radiation therapy (>= 60 Gy) for cancers of oral cavity/oropharynx were asked to swish and gargle for 30 seconds, and spit, with 15 ml of the SAO three times a day throughout the radiation therapy. Pain in the oral cavity/oropharynx was measured using the numerical rating pain scale (NRPS) and mucositis was graded using the RTOG scale every week. Our data were compared with historical data in table 2 (incidence of mucositis), figure 1 (mean mucositis grade) and figure 2 (mean oral pain grade) from MD Anderson Cancer Center (MDACC) (doi:10.1016/j.ijrobp.2007.01.053) and table 4 (incidence of mucositis) from Memorial Sloan Kettering Cancer Center (MSKCC) (doi:10.1016/j.ijrobp.2010.10.041).

### RESULTS

Fourteen subjects were enrolled but 6 withdrew (4 of them due to taste/smell of the rinse, 1 due to fatigue, 1 due to perceived ineffectiveness of the rinse). Among the 8 who completed the course of SAO treatment, 6 were treated with chemo-radiation and 2 with radiation only. IMRT was used for everyone. The median dose was 6,996 cGy in 33 fractions. There were no serious adverse events from SAO. The mean RTOG mucositis grades from weeks 3,6 and 9 were 1.125, 2.125 and 1.875. Two of 8 patients experienced mucositis >= 3. The corresponding mean NRPS were 3.700, 4.988 and 3.875.

#### CONCLUSION

The incidence of mucositis >= 3 were 70% from MDACC and 22% from MSKCC. Distribution of our mean NRPS and RTOG mucositis data compared favorably against figures 1 and 2 from MDACC. Though SAO was difficult to use due to poor taste/smell, it was otherwise well tolerated and appears to have enough signal to warrant further development as a potential alleviator of mucositis.

# **CLINICAL RELEVANCE/APPLICATION**

This is a proof-of-concept clinical trial for an oral mouth rinse containing Sandalwood Oil for the prevention of mucositis associated with (chemo-) radiation therapy in head and neck cancer patients. We believe our results have generated enough signal to pursue further development of this preparation.

# MSR023-05 Locoregional Patterns of Failure (POF) following Therapeutic Dose Neck Radiation Therapy (RT) for Un-Resected Anaplastic Thyroid Cancer (ATC)

Monday, Nov. 26 2:10PM - 2:20PM Room: E450A

# Awards

# **Student Travel Stipend Award**

Participants

Amit Jethanandani, MPH, Houston, TX (*Presenter*) Nothing to Disclose Mona K. Jomaa, MD,PhD, Cairo, Egypt (*Abstract Co-Author*) Nothing to Disclose Maria E. Cabanillas, Houston, TX (*Abstract Co-Author*) Research funded, Exelixis, Inc Abdallah S. Mohamed, MD, MSc, Houston, TX (*Abstract Co-Author*) Nothing to Disclose Renata Ferrarotto, MD, Houston, TX (*Abstract Co-Author*) Nothing to Disclose Mark Zafereo, MD, Houston, TX (*Abstract Co-Author*) Nothing to Disclose Adam S. Garden, MD, Houston, TX (*Abstract Co-Author*) Nothing to Disclose William H. Morrison, MD, Houston, TX (*Abstract Co-Author*) Nothing to Disclose Heath Skinner, MD, PhD, Houston, TX (*Abstract Co-Author*) Nothing to Disclose S. J. Frank, MD, Houston, TX (*Abstract Co-Author*) Board Member, C4 Imaging LLC Stockholder, C4 Imaging LLC Advisory Board, Elekta AB

Jack Phan, MD, PhD, Houston, TX (Abstract Co-Author) Nothing to Disclose

Jay Reddy, MD, PhD, Houston, TX (Abstract Co-Author) Nothing to Disclose

David I. Rosenthal, Houston, TX (Abstract Co-Author) Advisory Board, Bristol-Myers Squibb Company Advisory Board, Merck KGaA Research support, Merck KGaA

Clifton D. Fuller, MD,PhD, Houston, TX (Abstract Co-Author) Research Consultant, Elekta AB; Research Grant, Elekta AB; Speaker, Elekta AB

Brandon Gunn, MD, Galveston, TX (Abstract Co-Author) Nothing to Disclose

#### PURPOSE

Despite aggressive therapy, patients (pts) with ATC often develop locoregional progression (LRP). We aimed to identify the pattern of LRP in pts with un-resected ATC who received therapeutic doses of neck RT (>45 Gy).

### **METHOD AND MATERIALS**

An institutional ATC database was retrospectively reviewed for pts who received neck RT from 01/00-08/17. ATC pts with unresected disease were eligible if they received RT > 45 Gy at our institution and had follow-up CTs to assess for LRP. Progressive gross tumor volumes (rGTVs) were segmented on diagnostic CTs that demonstrated LRP (rCTs) and were reviewed by a head and neck radiation oncologist. rCTs were co-registered with treatment planning CTs (pCTs) using deformable image registration (VelocityAI 3.0.1). rGTVs were compared to original RT plans using a centroid-based approach. Failures were classified into 5 types based on pre-defined spatial/dosimetric criteria; A (central high dose), B (central elective dose), C (peripheral high dose), D (peripheral elective dose), and E (extraneous dose).

### RESULTS

129 ATC pts received neck RT; of these, 103 had available plans and only 73 had plans and follow-up CTs. Of the 73, pts were excluded for prior resection (n=37) or if RT dose was  $\leq$  45 Gy (n=17). Thus, 19 formed the cohort. Most (79%) were Caucasian; median age was 63.5 years; 58% were stage IVC; 95% received IMRT; and all received systemic therapy. Median RT dose was 66 Gy (IQR: 59-66); median dose per fraction was 2 Gy (IQR: 1.7-2.2). Median follow-up was 7.9 mos. Six pts (31.5%) developed LRP and 16 rGTVs were identified (6 in 1 pt, 4 in 1, 3 in 1, and 1 in 3 each). Median time to LRP was 2.3 mos (range: 0-43). Of rGTVs, 7 were local (thyroid bed) and 9 were regional (1 in the paratracheal region; 1 in base of tongue [BOT]; 3 in node levels IIa; 1 in III; 2 in IV; and 1 in paraspinal musculature [PSM]). Type A was the most common rGTV POF (56%), followed by Types E (31%; 3 nodal, 1 BOT, and 1 PSM), B and C (8% each). Actuarial locoregional control (LRC) was 73% at 6 and 12 mos. Four living patients without LRP had a median follow-up of 27.5 mos (range: 9.3-65).

# CONCLUSION

The identified POF was largely Type A and rapid (<6 mos), suggestive of a radiation resistance profile.

### **CLINICAL RELEVANCE/APPLICATION**

Rapid neck progression was avoided in most ATC pts and some exhibited durable neck control, which could allow pts to receive subsequent systemic or targeted therapies.

# MSR023-06 A Population-Based Study of the Effects of Therapy, Primary Tumor Characteristics, and Metastatic Disease Sites on Survival in Patients with Metastatic Head and Neck Cancer

Monday, Nov. 26 2:20PM - 2:30PM Room: E450A

### Awards

### **Student Travel Stipend Award**

Participants Justin Budnik, MD, Rochester, NY (*Presenter*) Nothing to Disclose Nicholas J. Denunzio, MD, PhD, Boston, MA (*Abstract Co-Author*) Nothing to Disclose Michael T. Milano, MD, PhD, Chicago, IL (*Abstract Co-Author*) Nothing to Disclose Deepinder Singh, MD, Rochester, NY (*Abstract Co-Author*) Nothing to Disclose

# PURPOSE

Data is emerging that multimodality therapy (MMT) may improve overall survival (OS) in patients with metastatic head and neck cancer (M1-HNC). We aim to investigate the effects of MMT, tumor characteristics, and sites of metastatic disease on OS in M1-HNC patients using the Surveillance, Epidemiology, and End Results (SEER) database.

#### METHOD AND MATERIALS

2,827 patients from the SEER 18 registry diagnosed with M1-HNC from 2010-2014 were analyzed. Patients coded as having metastatic disease in bone, brain, liver, and lung were identified. Kaplan-Meier analyses and Cox proportional hazards models were used to assess the impact of MMT, primary tumor characteristics, and metastatic disease sites on OS.

# RESULTS

Most patients were male (n=2,169, 76.7%), and had squamous carcinoma histology (n=2,009, 71.1%). Median age was 60 years and median OS was 10 months. Oropharynx (n=900, 31.8%) was the most common primary site. Patients coded as having metastases in lung and not in bone, brain, or liver (n=958, 33.9%) were the most common metastatic disease category. 518 patients (18.3%) received cancer-directed surgery (CDS), 1,458 patients (51.6%) received radiation (RT), and 1,690 patients (59.8%) received chemotherapy (CT). 579 patients (20.5%) received neither CDS, nor RT, nor CT (no therapy-group). With Cox regression accounting for age, sex, race, primary site, histology, grade, T stage, N stage, and metastatic sites, those who received CDS, RT, and CT (n=172, 6.1%) had the largest OS benefit (HR=0.22, 95% CI 0.17-0.28, p<0.001) compared to the no therapygroup. Patients receiving RT and CT were the most common MMT combination (n=879, 31.1%), and had improved OS (HR=0.35, 95% CI 0.30-0.40, p<0.001) compared to the no therapy-group. Primary and metastatic disease site-specific analyses showed that MMT combinations provided and OS benefit at all primary sites in the head and neck region and across metastatic sites with the exception of those coded as having metastases in bone and lung, and not in brain and liver.

# CONCLUSION

In this hypothesis-generating study MMT is associated with improved OS in patients with M1-HNC. The OS benefit persists across primary and metastatic disease sites. Prospective study of MMT in M1-HNC patients is warranted.

### **CLINICAL RELEVANCE/APPLICATION**

In this population-based, hypothesis-generating study multimodality therapy is associated with improved overall survival in patients with metastatic head and neck cancer.



#### MSRO27

#### **BOOST: Breast-Science Session with Keynote**

Monday, Nov. 26 1:30PM - 2:30PM Room: S103CD



AMA PRA Category 1 Credit ™: 1.00 ARRT Category A+ Credit: 1.00

#### Participants

Kathleen Horst, MD, Stanford, CA (*Moderator*) Nothing to Disclose Anna Shapiro, MD, Syracuse, NY (*Moderator*) Nothing to Disclose

Sub-Events

# MSR027-01 Invited Speaker:

Monday, Nov. 26 1:30PM - 1:50PM Room: S103CD

Participants Jianling Yuan, MD, PhD, Minneapolis, MN (*Presenter*) Nothing to Disclose

# MSR027-03 Where Are the RCTs? Analysis of the 2018 American Society for Radiation Oncology (ASTRO) Evidence-Based Guidelines for Radiation Therapy to the Whole Breast as Treatment for Breast Cancer

Monday, Nov. 26 1:50PM - 2:00PM Room: S103CD

Participants

Norman R. Williams, PhD, London, United Kingdom (Presenter) Travel support, Carl Zeiss AG

#### For information about this presentation, contact:

norman.williams@ucl.ac.uk

### PURPOSE

Early in 2018, the American Society for Radiation Oncology (ASTRO) produced evidence-based guidelines on five key questions for radiation therapy to the whole breast as treatment for breast cancer [Smith et al PMID: 29545124]. An analysis was made of the publications supporting these guidelines to determine how many reported level-1 evidence from randomised clinical trials (RCTs), as this is the standard applied to chemotherapy and adjuvant hormonal therapy.

#### **METHOD AND MATERIALS**

All 112 references were scrutinized, and tabulated according to level of evidence (RCT or not), year of publication, country of lead author, and which of the statements (grouped into five key questions) they addressed.

#### RESULTS

Of the 33 statements, 12 are not supported by evidence from RCTs. In a further 9 statements, data from RCTs only partly support the consensus. Therefore, 21/33 (64%) of the statements are not directly supported by evidence from RCTs. There is no evidence from RCTs to support any of the statements regarding avoiding exposure of cardiac and other normal tissue (key questions 4 and 5). Such exposure has been linked to death from ischemic heart disease [Darby et al PMID: 23484825] and lung cancer [Taylor et al PMID: 28319436]. There is evidence that the effects of a course of whole breast radiation therapy induces early ECG changes [Tuohinen et al PMID: 29599341]; biological effects can be detected after a single fraction [Woolf et al PMID: 25045612]. Such measures could be used in the design of RCTs, particularly of patients with low-risk breast cancer in whom de-escalation of breast radiation therapy (using accelerated partial breast, intra-operative, etc.) may be warranted to reduce an imbalance in the efficacy/safety profile [Franco et al PMID: 29616366].

#### CONCLUSION

The majority of the 2018 ASTRO evidence-based guidelines for use of radiation therapy in breast cancer are not based on level-1 evidence from RCTs. Trials using techniques that minimize exposure to normal tissues are urgently required.

#### **CLINICAL RELEVANCE/APPLICATION**

Clinicians and patients should be aware that current guidelines for treatment of breast cancer using radiation therapy are mostly based on sub-optimal evidence.

### MSR027-04 Clinical Outcomes and Toxicity of Proton Beam Radiation Therapy for Re-Irradiation of Locally Recurrent Breast Cancer

Monday, Nov. 26 2:00PM - 2:10PM Room: S103CD

Participants

Prashant Gabani, MD, Saint Louis, MO (*Presenter*) Nothing to Disclose Maria A. Thomas, MD, PhD, Saint Louis, MO (*Abstract Co-Author*) Nothing to Disclose Beth Bottani, CMD, Saint Louis, MO (*Abstract Co-Author*) Nothing to Disclose Jeffrey D. Bradley, MD, Saint Louis, MO (*Abstract Co-Author*) Nothing to Disclose Laura Ochoa, RN,PhD, Saint Louis, MO (*Abstract Co-Author*) Nothing to Disclose Imran Zoberi, MD, St. Louis, MO (*Abstract Co-Author*) Nothing to Disclose

# For information about this presentation, contact:

pgabani@wustl.edu

### PURPOSE

Repeat radiation therapy (RT) using x-rays for locally recurrent breast cancer results in increased short and long-term toxicity. Proton beam RT (PBRT) can minimize dose to surrounding organs thereby reducing toxicity. Here, we report the toxicity and outcomes for women who underwent re-irradiation to the chest wall for locally recurrent breast cancer using PBRT.

#### **METHOD AND MATERIALS**

A total of 16 patients with locally recurrent breast cancer who underwent re-irradiation to the chest wall with PBRT between 2014-2018 were retrospectively analyzed. For their recurrences, 6 patients underwent salvage mastectomy, 8 patients had wide local excision, and 2 patients had biopsy only. The median dose for the first RT course was 50 Gy, and for the second course, 50.4 Cobalt Gy Equivalent. The target for re-irradiation was chest wall alone in 12 patients and chest wall plus regional nodes in 4 patients. A boost was delivered in 3 (18.8%) patients. Concurrent hyperthermia was used in 10 (62.5%) patients. For systemic therapy, 4 (25%) patients received chemotherapy and 8 (50%) patients received hormone therapy. Follow up was calculated from the start of second RT course. Toxicities were based on CTCAE 4.0.

### RESULTS

The median age at diagnosis and at recurrence was 49.8 years and 60.2 years respectively. The median time between the two RT courses was 10.2 (0.7-20.2) years. The median follow up time was 10.6 (1.5-29.1) months. There were no local failures observed after re-irradiation. Only one patient developed distant metastasis and ultimately died. Grade 3-4 acute skin toxicity was observed in 5 (31.2%) patients. There were 4 (25%) patients who developed chest wall infections during or shortly (2 weeks) after re-irradiation. Grade 3-4 fibrosis was observed in only 3 (18.8%) patients. Grade 5 toxicities were not observed. Hyperpigmentation was seen in 12 (75%) patients. Other RT related toxicities such as pneumonitis, telangiectasia, rib fracture, and lymphedema occurred in 2 (12.5%), 4 (25%), 1 (6.3%), and 1 (6.3%) patients respectively.

### CONCLUSION

Re-irradiation with PBRT for recurrent breast cancer has acceptable toxicities. There was a high incidence of grade 3-4 skin toxicity and infections, however, they resolved with skin care and antibiotics. Further follow up is needed to determine long-term clinical outcomes.

# **CLINICAL RELEVANCE/APPLICATION**

PBRT can be safely used for re-irradiation of the chest wall for locally recurrent breast cancer.

# MSR027-05 Carcinosarcoma of the Breast: Treatment Patterns and Survival Outcomes

Monday, Nov. 26 2:10PM - 2:20PM Room: S103CD

### Awards

# **Trainee Research Prize - Resident**

Participants William R. Kennedy, MD, Saint Louis, MO (*Presenter*) Nothing to Disclose Prashant Gabani, MD, Saint Louis, MO (*Abstract Co-Author*) Nothing to Disclose Sahaja Acharya, MD, Saint Louis, MO (*Abstract Co-Author*) Nothing to Disclose Maria A. Thomas, MD, PhD, Saint Louis, MO (*Abstract Co-Author*) Nothing to Disclose Imran Zoberi, MD, St. Louis, MO (*Abstract Co-Author*) Nothing to Disclose

#### PURPOSE

Carcinosarcoma of the breast is a rare yet highly-aggressive tumor accounting for less than 1% of all breast cancers, for which guidance on optimal management and prognosis are sparse. The purpose of this study is to investigate population-based treatment patterns and overall survival (OS) outcomes in patients with this diagnosis.

## METHOD AND MATERIALS

We queried the National Cancer Database for patients diagnosed with carcinosarcoma (Histology 8980) of the breast. All patients included were treated with surgery, with or without chemotherapy and/or radiation therapy. Patients with metastatic disease were excluded. Kaplan-Meier analysis was used to estimate OS. Univariate and multivariate cox analyses were used to determine predictive factors of OS.

#### RESULTS

A total of 329 patients from 2004-2012 were identified. Median age at diagnosis was 58 years (range, 24-90). Patients had T1 (21%), T2 (44%), T3 (25%), or T4 disease (10%). Most patients were node-negative at diagnosis (77%). Breast conservation surgery was utilized in 33% of patients. Chemotherapy was used in 66% of patients. Less than half (44%) of patients received radiation therapy to a median dose of 50.4Gy (range 35-56 Gy), with a median 10Gy boost used in 76%. With median follow-up of 39.9 months, 3-year overall survival was 74%. Multivariate analysis revealed that T-stage, margin status, and chemotherapy use all significantly influenced OS. There was a trend towards improved survival with the use of RT (HR 0.66, 95% CI 0.43-1.01, p =0.053). The 3-yr OS was 80% in patients receiving chemotherapy vs 59% without chemotherapy. The 3-yr OS was 82% in patients receiving RT vs 66% without RT.

#### CONCLUSION

Carcinosarcoma of the breast is associated with relatively poor rates of OS. The use of chemotherapy was associated with improved OS, with a trend towards improved OS with the use of RT.

# **CLINICAL RELEVANCE/APPLICATION**

In the largest study to date investigating outcomes in carcinosarcoma of the breast, adding chemotherapy to surgery improved OS. A trend toward improved OS was also seen with adjuvant RT.

# MSR027-06 Quantitative Ultrasound Characterization of Radiation-Induced Acute Skin Toxicity in Breast Cancer Patients Receiving Radiation Therapy: A Feasibility Study

Monday, Nov. 26 2:20PM - 2:30PM Room: S103CD

Participants

Sylvia D. Tang, Johns Creek, GA (*Presenter*) Nothing to Disclose Jiwoong Jason Jeong, Atlanta, GA (*Abstract Co-Author*) Nothing to Disclose Xiaofeng Yang, PhD, Atlanta, GA (*Abstract Co-Author*) Nothing to Disclose Mylin A. Torres, MD, Atlanta, GA (*Abstract Co-Author*) Nothing to Disclose Arif N. Ali, MD, MS, Chicago, IL (*Abstract Co-Author*) Nothing to Disclose Tian Liu, PhD, Atlanta, GA (*Abstract Co-Author*) Nothing to Disclose

### PURPOSE

Despite technological advances in radiotherapy, high dose of radiation may induce acute skin toxicity in the majority of women receiving breast-cancer radiotherapy. In current clinical practice, the severity of skin toxicity is often rated by clinicians through visual inspection and physics examination, which is subjective. The purpose of this study is to investigate the feasibility of quantitative characterization of radiation-induced acute skin toxicity via ultrasound morphological and texture analysis.

### **METHOD AND MATERIALS**

Twelve patients receiving standard breast radiotherapy were enrolled in the longitudinal ultrasound study. Ultrasound B-mode images are acquired at various time points: prior to, weekly during, as well as 6 weeks and 3 months post radiotherapy. At each time point, 4 images (12, 3, 6 and 9 o'clock) were acquired on the irradiated breast and 4 mirror images were acquitted on the contralateral normal breast. To evaluate radiation-induced skin changes, we performed both morphological (area, height, perimeter and averaged skin thickness) and textural (contrast, angular second moment (ASM) and inverse difference moment (IDM)) analyses using ImageJ. Clinical assessment of skin toxicity was performed at each time point.

### RESULTS

Changes in skin thickness and texture were observed in 5 patients as early as 1 week during treatment. In 2 cases with most severe acute toxicity, the average skin thickness of irradiated breast increases more than 175% and 188% at the end of fractionated therapy in comparison to the untreated contralateral breast, while their slopes in linear regression are 0.87 and 0.70, respectively. Acute skin toxicity was observed in differences in 5 cases in the angular second moment measurements and in 4 cases of entropy analysis over the patient's temporal treatment course.

### CONCLUSION

Radiation-induced skin toxicity in breast cancer patients can be quantitatively assessed by ultrasound-based morphologic and textural characterization.

### **CLINICAL RELEVANCE/APPLICATION**

Quantitative ultrasound characterization of radiation-induced acute skin toxicity in breast cancer patients receiving radiation therapy may be of clinical relevance for the optimization of treatment protocols and potential early intervention to prevent long-term breast toxicity.



#### PS20

### **Monday Plenary Session**

Monday, Nov. 26 1:30PM - 2:45PM Room: Arie Crown Theater



AMA PRA Category 1 Credits ™: 1.25 ARRT Category A+ Credit: .75

### Participants

Vijay M. Rao, MD, Philadelphia, PA (Presenter) Nothing to Disclose

#### Sub-Events

# PS20A Presentation of Honorary Membership

Participants

Paul M. Parizel, MD, PhD, Edegem, Belgium (*Recipient*) Research Consultant, icoMetrix NV; Research Grant, Siemens AG; Research Consultant, General Electric Company; Speaker, Bracco Group; Speaker, Mallinckrodt plc Jacob Sosna, MD, Jerusalem, Israel (*Recipient*) Nothing to Disclose

# PS20B Plenary Lecture: Can Clinicians Lead Radical Redesign?

Participants

Donald M. Berwick, MD, Boston, MA (*Presenter*) Board of Directors, LumiraDx; Board of Directors, Virta Health; Board of Directors, COTA, Inc; Board Member, Google Deep Mind Health

Vijay M. Rao, MD, Philadelphia, PA (Introduction) Nothing to Disclose

### **LEARNING OBJECTIVES**

1) Discuss whether existing health care systems can achieve the "triple aim" of improved patient care, better population health, and lower cost. 2) Describe the application of radical redesign to healthcare systems. 3) Prepare to exercise leadership in achieving healthcare system evolution.



### SPPH21

# Basic Physics Lecture for the RT: Dual Energy CT Applications in Radiation Therapy

Monday, Nov. 26 1:30PM - 2:45PM Room: S402AB



AMA PRA Category 1 Credits ™: 1.25 ARRT Category A+ Credits: 1.50

#### **Participants**

Scott J. Emerson, MS, Royal Oak, MI (*Moderator*) Nothing to Disclose Jessica Miller, PhD, Madison, WI (*Presenter*) Research Grant, Siemens AG

For information about this presentation, contact:

### scott.emerson@beaumont.org

### LEARNING OBJECTIVES

1) Explain basic dual-energy CT principles. 2) Compare current dual-energy CT techniques and associated limitations. 3) Identify dual-energy CT applications in radiation therapy.

#### ABSTRACT

Nearly all patients treated with radiation therapy receive a computed tomography (CT) simulation scan for treatment planning purposes. Dual-energy CT (DECT) allows for the reconstruction of supplementary information during the CT simulation process, such as relative electron density and effective atomic number information, virtual monoenergetic images, and the differentiation of materials. The additional information gained through DECT has potential to aid in several aspects of the radiation therapy process. This course will outline the basic principles of DECT and compare different vendor solutions for acquisition of DECT images. DECT applications for radiation therapy will be discussed, including improving dose calculation accuracy, improving tumor and healthy tissue delineation, characterizing treatment response, and identifying and sparing functional healthy tissue.



#### SPPH22

# Physics Symposium: Highlights of Medical Physics Leadership Academy (MPLA) Summer School

Monday, Nov. 26 1:30PM - 5:45PM Room: S503AB



ARRT Category A+ Credit: 0 AMA PRA Category 1 Credits ™: 4.25

#### Participants

Jennifer Lynn Johnson, PHD, Houston, TX (*Presenter*) Nothing to Disclose Daniel Pavord, MS, Poughkeepsie, NY (*Presenter*) Nothing to Disclose Robert J. Pizzutiello JR, MS, Victor, NY (*Presenter*) Nothing to Disclose Michael Howard, PHD, Chattanooga, TN (*Presenter*) Nothing to Disclose

# For information about this presentation, contact:

ms\_jl\_johnson@yahoo.com

#### LEARNING OBJECTIVES

Understand the need to manage others' perceptions of medical physics. Develop awareness, knowledge and skills to create and maintain a positive influence on others to achieve desired results. Analyze the integration of leadership, management and medical physics in day-to-day practice.

#### ABSTRACT

Medical physicists are respected for their technical expertise and contributions of physics principles and applications in biology and medicine. In all work environments, however, medical physicists' technical and functional skills are not enough, especially as they advance in their career. No matter what career level, leadership and interpersonal skills are necessary. The 2016 AAPM Summer School provided a focused and hands-on environment for leadership and management skill development interwoven into the context of medical physics. Session attendees will learn a working definition of leadership and the AAPM Medical Physics Leadership Academy (MPLA) program. Session attendees will also analyze operation and human resources scenarios by way of using personal and interpersonal knowledge and skills.

#### URL

https://www.aapm.org/meetings/2016SS/default.asp

### **Active Handout:Jennifer Lynn Johnson**

http://abstract.rsna.org/uploads/2018/18002094/2018 RSNA MPLA slides comb updated SPPH22.pdf



### SPSP21

Evaluación Post-tratamiento en el Paciente Oncológico: Post Cirugía, Quimioterapia, Radioterapia, Inmunoterapia: Sesión del Colegio Interamericano de Radiología (CIR) en Espanol / Post-treatment Evaluation in the Oncological Patient: Post Surgery, Chemotherapy, Radiotherapy, Immunotherapy: Session of the Interamerican College of Radiology (CIR) in Spanish

Monday, Nov. 26 1:30PM - 3:30PM Room: E451A



AMA PRA Category 1 Credits ™: 2.00 ARRT Category A+ Credits: 2.25

FDA Discussions may include off-label uses.

#### **Participants**

Jose L. Criales, MD, Mexico City, Mexico (*Moderator*) Nothing to Disclose Jorge A. Soto, MD, Boston, MA (*Moderator*) Royalties, Reed Elsevier

# LEARNING OBJECTIVES

1) Identify the morfological and functional modifications post treatment in oncological patients / Identificar los cambios morfologicos y funcionales post tratamiento en el paciente oncológico. 2) Review potential pitfalls in the evaluation of imaging studies performed on patients who received therapy for malignant neoplasms / Revisar causas de posibles errores diagnosticos en la evaluacion de imagenes post tratamiento de neoplasias malignas. 3) Describe the most appropriate imaging tests for identification of possible recurrence of malignant tumors after therapy / Describir los estudios de imagenes mas apropiados para identificar recurrencias de tumores malignos post tratamiento

### Sub-Events

# SPSP21A Bienvenida / Welcome

Participants Jose L. Criales, MD, Mexico City, Mexico (*Presenter*) Nothing to Disclose Jorge A. Soto, MD, Boston, MA (*Presenter*) Royalties, Reed Elsevier

### LEARNING OBJECTIVES

1) Identify the morfological and functional modifications post treatment in oncological patients / Identificar los cambios morfologicos y funcionales post tratamiento en el paciente oncológico. 2) Review potential pitfalls in the evaluation of imaging studies performed on patients who received therapy for malignant neoplasms / Revisar causas de posibles errores diagnosticos en la evaluacion de imagenes post tratamiento de neoplasias malignas.3) Describe the most appropriate imaging tests for identification of possible recurrence of malignant tumors after therapy / Describir los estudios de imagenes mas apropiados para identificar recurrencias de tumores malignos post tratamiento

#### **Honored Educators**

Presenters or authors on this event have been recognized as RSNA Honored Educators for participating in multiple qualifying educational activities. Honored Educators are invested in furthering the profession of radiology by delivering high-quality educational content in their field of study. Learn how you can become an honored educator by visiting the website at: https://www.rsna.org/Honored-Educator-Award/ Jorge A. Soto, MD - 2013 Honored EducatorJorge A. Soto, MD - 2014 Honored EducatorJorge A. Soto, MD - 2015 Honored EducatorJorge A. Soto, MD - 2017 Honored EducatorJorge A. Soto, MD - 2018 Honored Educator

# SPSP21B Cáncer de Pulmón / Lung Cancer

Participants Fernando R. Gutierrez, MD, Saint Louis, MO (*Presenter*) Spouse, Stockholder, UnitedHealth Group

For information about this presentation, contact:

gutierrezf@wustl.edu

#### LEARNING OBJECTIVES

1) Be familiar with the overall incidence of lung cancer and survival curves in patients undergoing treatment. 2) Learn how new treatment options are being utilized to improve overall outcomes. 3) Understand the difference between the traditional forms of lung cancer treatment such as surgical resection, chemotherapy (adjuvant), radiation therapy and new therapies such as targeted therapy that disrupt the cancer cell ability to reproduce. 4) Be aware of how follow up imaging findings such as those of PET/CT may be different in the traditional treatment than in new forms of therapy.

# SPSP21C Linfoma / Lymphoma

Participants

Sebastian A. Rossini SR, Mar del Plata, Argentina (*Presenter*) Educational Exhibit, Baye AG; Educational Exhibit, Boehringer Ingelheim GmbH;

#### For information about this presentation, contact:

### Sebastianrossini@iradiologico.com.ar

#### LEARNING OBJECTIVES

1) Show the typical images of lymphoma. 2) Method of choice images for pre and post-treatment assessment. 3) Forms of post-treatment presentation in PET-CT. 4) Importance of the correct post-therapeutic imaging evaluation.

#### SPSP21D Melanoma / Melanoma

Participants

Guillermo Elizondo-Riojas, MD, PhD, Monterrey, Mexico (Presenter) Nothing to Disclose

#### For information about this presentation, contact:

elizondoguillermo@hotmail.com

#### LEARNING OBJECTIVES

1) Apply the most appropriate imaging examinations to patients with melanoma. 2) Understand the rationale for using a specific imaging test in the follow-up of melanoma patients. 3) Interpret the imaging findings associated with the different therapies for melanoma patients.

# SPSP21E Preguntas / Q & A

### SPSP21F Presentación del CIR / CIR Update

Participants

Henrique Carrete Jr, MD, Sao Paulo, Brazil (Presenter) Nothing to Disclose

# LEARNING OBJECTIVES

1) Present the CIR and its main educational activities.2) Address the activities of the CIR throughout the year 2018.3) Outline future directions of CIR.

#### URL

http://www.webcir.org/

# SPSP21G Tumores Neuroendocrinos / Neuroendocrine Tumors

Participants

Giancarlo Schiappacasse, MD, Las Condes, Chile (Presenter) Nothing to Disclose

# For information about this presentation, contact:

gschiappacasse@gmail.com

### LEARNING OBJECTIVES

1) Be familiar with the epidemiology, incidence and survival of neuroendocrine tumors. 2) Know the most appropriate imaging modalities (CT, MRI and PET/CT) for control and follow up. 3) Understand the different therapies such as surgical procedures, conventional chemotherapy, immunotherapy and targeted therapy.

# SPSP21H Cáncer Cervico-uterino / Cervical Cancer

Participants

Javier A. Romero, MD, Bogota, Colombia (Presenter) Speakers Bureau, Novartis AG; Speakers Bureau, Bristol-Myers Squibb Company

### LEARNING OBJECTIVES

1) Describe basic principles of cervical Cancer treatment. 2) Why using MRI in cervical Cancer. 3) MRI findings in post treatment in cervical cancer. 4) Other imaging methods for evaluating patients in post cervical Cancer Theraphy.

# SPSP21I Cáncer de Ovario / Ovarian Cancer

Participants

Alice Cristina C. Brandao Salomao, MD, Rio de Janeiro, Brazil (Presenter) Nothing to Disclose

### LEARNING OBJECTIVES

Postoperative evaluation ovarian cancer How to follow up How to perform recurrence investigation What is the recurrence pattern, typical and atypical

#### ABSTRACT

Ovarian cancer is the most aggressive gynecological cancer Its standard post treatment is remission and recurrence due to primary and secundary cytoreductive surgery, chemotherapy and immunotherapy During our presentation we aim to evaluate posttherapeutic follow-up, including screening and suspected relapse, identifying which tests should be performed. In addition, we will evaluate the pattern of recurrence, common and unusual.

### SPSP21J Preguntas / Q & A

#### SPSP21K Clausura / Closing

Participants Jose L. Criales, MD, Mexico City, Mexico (*Presenter*) Nothing to Disclose

### Jorge A. Soto, MD, Boston, MA (Presenter) Royalties, Reed Elsevier

# LEARNING OBJECTIVES

1) Identify the morfological and functional modifications post treatment in oncological patients / Identificar los cambios morfologicos y funcionales post tratamiento en el paciente oncológico. 2) Review potential pitfalls in the evaluation of imaging studies performed on patients who received therapy for malignant neoplasms / Revisar causas de posibles errores diagnosticos en la evaluacion de imagenes post tratamiento de neoplasias malignas. 3) Describe the most appropriate imaging tests for identification of possible recurrence of malignant tumors after therapy / Describir los estudios de imagenes mas apropiados para identificar recurrencias de tumores malignos post tratamiento.

# **Honored Educators**

Presenters or authors on this event have been recognized as RSNA Honored Educators for participating in multiple qualifying educational activities. Honored Educators are invested in furthering the profession of radiology by delivering high-quality educational content in their field of study. Learn how you can become an honored educator by visiting the website at: https://www.rsna.org/Honored-Educator-Award/ Jorge A. Soto, MD - 2013 Honored EducatorJorge A. Soto, MD - 2014 Honored EducatorJorge A. Soto, MD - 2015 Honored EducatorJorge A. Soto, MD - 2017 Honored EducatorJorge A. Soto, MD - 2018 Honored Educator



#### VSIO21

Interventional Oncology Series: HCC and Cholangiocarcinoma

Monday, Nov. 26 1:30PM - 6:00PM Room: S406B



AMA PRA Category 1 Credits ™: 4.00 ARRT Category A+ Credits: 5.00

**FDA** Discussions may include off-label uses.

#### Participants

Nadine Abi-Jaoudeh, MD, Orange, CA (*Moderator*) Research collaboration, Koninklijke Philips NV; Research collaboration, Teclison Cherry Pharma Inc; Research support, SillaJen, Inc

Anne M. Covey, MD, New York, NY (Moderator) Stockholder, Amgen Inc; Advisory Board, Accurate Medical

#### Sub-Events

# VSI021-01 BCLC A Tumors: Treatment with Ablation

Monday, Nov. 26 1:30PM - 1:50PM Room: S406B

Participants

Riccardo Lencioni, MD, Pisa, Italy (*Presenter*) Research Consultant, BTG International Ltd; Research Consultant, Guerbet SA; Research Consultant, Eisai Co, Ltd

Anne M. Covey, MD, New York, NY (Presenter) Stockholder, Amgen Inc; Advisory Board, Accurate Medical

For information about this presentation, contact:

riccardo.lencioni@med.unipi.it

#### LEARNING OBJECTIVES

1) Discuss the role of image-guided ablation in the multidisciplinary management of patients with early-stage HCC. 2) Understand advantages and disadvantages of the various ablation technologies used for local treatment of HCC. 3) Describe the status of clinical research investigating potential synergies between image-guided ablation and novel drugs.

# VSIO21-02 Systemic Antitumor Immunity was Augmented by Combining Radiofrequency Ablation with Anti-CTLA-4 Therapy in a Multi Subcutaneous Murine Hepatoma Model

Monday, Nov. 26 1:50PM - 2:00PM Room: S406B

Participants

Liang Zhang, MD, Shanghai, China (Presenter) Nothing to Disclose

### PURPOSE

To evaluate whether antitumor immunity is enhanced by combining radiofrequency ablation (RFA) and anti-CTLA-4 therapy, and its synergism anti-tumor effect on untreated tumors.

#### **METHOD AND MATERIALS**

Our experiments were approved by the institutional animalcare committee. 40 mice with tumor established on both side flanks were randomly divided into 4 groups: Control group (no treatment), RFA group (RFA of the right flank tumor), Anti-CTLA-4 group (anti-CTLA-4 monotherapy), Combination therapy group (RFA+Anti-CTLA-4). In each group, 8 mice were usedfor untreated tumor evaluation and survival observation, another 2 mice were sacrificed for histopathological study. Then, rechallenge test was performed to confirm whether the systematic antitumorimmunity was established by RFA+Anti-CTLA-4 therapy.

#### RESULTS

Although untreated tumor volume continued to increase untilthe end of the observation in all groups, SGRs of RFA+Anti-CTLA-4 group weresignificantly smaller than that in other groups (vs. control: p = 0.003; vs. RFA: p = 0.04; vs. Anti-CTLA-4: p = 0.10). Animals in RFA + Anti-CTLA-4 group survived significantly longer than thatin control group (p = 0.001), RFA group (p = 0.000) and Anti-CTLA-4 group (p = 0.008). The tumor metastasis free survival of RFA +Anti-CTLA-4 group was significantly longer than that in control group (p = 0.006), RFA group (p = 0.001) and Anti-CTLA-4 group (p = 0.006), RFA group (p = 0.001) and Anti-CTLA-4 group (p = 0.014). Histopathological studyshowed marked CD4 and CD8 positive lymphocyte around the tumor in mice of RFA +anti-CTLA-4 group. In rechallenge test, tumor free survival time was longer in miceof RFA+anti-CTLA-4 group than that in control group (p = 0.001) and anti-CTLA-4 group (p = 0.000).

# CONCLUSION

The present study demonstrates that RFA-induced systemicantitumor immunity was enhanced by combine use of anti-CTLA-4 therapy in a multisubcutaneous murine hepatoma model.

#### **CLINICAL RELEVANCE/APPLICATION**

This treatment regimen is apotential clinical approach to enhance systemic antitumor immunity in patientswith unresectable

multicentric HCC or multiple liver metastases.

# VSI021-03 BCLC A/B Tumors: The Role of Surgical Resection and Transplant

Monday, Nov. 26 2:00PM - 2:20PM Room: S406B

Participants Mary Maluccio, MD, Indianapolis, IN (*Presenter*) Nothing to Disclose

# VSI021-04 BCLC B/C Tumors: Arterially Directed Therapies

Monday, Nov. 26 2:20PM - 2:40PM Room: S406B

Participants

Gregory J. Nadolski II, MD, Philadelphia, PA (Presenter) Nothing to Disclose

For information about this presentation, contact:

gregory.nadolski@uphs.upenn.edu

#### LEARNING OBJECTIVES

1) Discuss differences between BCLC and Hong Kong Classification system regarding treatment recommendations. 2) Evaluate data regarding embolization for locally advanced HCC. 3) Compare differences in technique, complications, and outcomes for different embolization procedures for BCLC B/C HCC.

### VSIO21-05 Lobar versus Selective Conventional Transarterial Chemoembolization: An Interim Report of a Prospective Pharmacokinetic Study

Monday, Nov. 26 2:40PM - 2:50PM Room: S406B

Participants

Lynn J. Savic, New Haven, CT (*Presenter*) Nothing to Disclose Julius Chapiro, MD, New Haven, CT (*Abstract Co-Author*) Research Grant, Koninklijke Philips NV; Research Grant, Guerbet SA; Consultant, Guerbet SA; Consultant, Eisai Co, Ltd Teresa White, New Haven, CT (*Abstract Co-Author*) Research Grant, Guerbet SA; Eliot Funai, BS, Baltimore, MD (*Abstract Co-Author*) Research Grant, Guerbet SA; Edvin Isufi, MD, New Haven, CT (*Abstract Co-Author*) Nothing to Disclose Sophie Stark, BS, New Haven, CT (*Abstract Co-Author*) Nothing to Disclose Evan Chen, New Haven, CT (*Abstract Co-Author*) Nothing to Disclose Ping He, Baltimore, MD (*Abstract Co-Author*) Nothing to Disclose Michelle A. Rudek, PharmD,PhD, Baltimore, MD (*Abstract Co-Author*) Nothing to Disclose James S. Duncan, PhD, New Haven, CT (*Abstract Co-Author*) Nothing to Disclose Hyun S. Kim, MD, New Haven, CT (*Abstract Co-Author*) Nothing to Disclose Jeffrey S. Pollak, MD, Woodbridge, CT (*Abstract Co-Author*) Nothing to Disclose Todd Schlachter, MD, Farmington, CT (*Abstract Co-Author*) Nothing to Disclose

#### For information about this presentation, contact:

Julius.chapiro@yale.edu

## PURPOSE

To compare the pharmacokinetic (PK) profiles of doxorubicin (DOX) and its metabolite doxorubicinol (DOXOL) after conventional transarterial chemoembolization (cTACE) using lobar or segmental injection.

### **METHOD AND MATERIALS**

This interim report of an ongoing single-site, prospective trial included 22 patients with hepatocellular (n=19), cholangiocellular carcinoma (n=1), and neuroendocrine tumor metastases (n=2), who were treated with lobar (n=7) or selective (n=15) cTACE defined by catheter placement (5/2016-10/2017). cTACE utilized 50mg DOX/10mg mitomycin-C emulsified with Lipiodol followed by embospheres. Peripheral blood was sampled after cTACE (5, 10, 20, 40 min, 1, 2, 4, 24 hrs, 3-4 weeks) to measure drug concentrations by standard non-compartmental analysis. Follow-up included cross-sectional imaging and adverse events (AE) recorded 3-4 weeks post-TACE. Statistics included Pearson coefficient, Mann-Whitney, and Chi-squared test.

### RESULTS

Mean age was  $62\pm9.21$  years and 19 patients were males. HCC were BCLC stage A in 4, B in 11, and C in 4 patients. According to 3DqEASL criteria available in 20/22, complete and partial response were achieved in 1 and 6, stable and progressive disease in 8 and 5 patients, respectively. Full DOX dose was given in 17/22. DOX concentration peaks occurred earlier (median Tmax 0.25 [0.13-0.98] vs. 0.59 [0.12-1.72hrs]) and were higher after lobar than selective cTACE (mean dose normalized Cmax 4.74±3.6 vs. 3.08±3.11ng/mL/mg) and in nonresponders compared to responders (p=0.022). The DOX area under the curve was significantly larger in patients with higher enhancing tumor volume (p=0.009) or enhancing tumor burden (p=0.033) on baseline imaging. DOXOL was similar whereas DOX concentrations were higher after lobar than selective cTACE at each timepoint but without statistical significance. Both DOX and DOXOL were undetectable 3-4 weeks post-cTACE. AE were rare but occurred more often after lobar cTACE (fever, p=0.040; abdominal pain, p=0.030).

### CONCLUSION

The preliminary results of this prospective trial show a consistent trend suggesting higher systemic chemotherapy exposure and toxicity after lobar compared to selective cTACE.

### **CLINICAL RELEVANCE/APPLICATION**

If confirmed in the complete cohort, these findings may lead to a paradigm shift in intra-arterial therapy in favor of selective cTACE

as a safe and efficient treatment for liver cancer.

# VSI021-06 BCLC C Tumors: Systemic and Combination Therapies

Monday, Nov. 26 2:50PM - 3:10PM Room: S406B

Participants

Nadine Abi-Jaoudeh, MD, Orange, CA (*Presenter*) Research collaboration, Koninklijke Philips NV; Research collaboration, Teclison Cherry Pharma Inc; Research support, SillaJen, Inc

#### LEARNING OBJECTIVES

1) Identify the commonality and particularities of BCLC advanced and metastatic HCC Recognize the multiple biologic and immunotherapy available for the treatment of BCLC C HCC. 2) Learn about strategies to combine local plus systemic therapy for BCLC B and C HCC.

# VSIO21-07 Understanding Real-Time Arterial Flow Change During DEB-TACE of HCC Using Intravascular Doppler Wire

Monday, Nov. 26 3:10PM - 3:20PM Room: S406B

Participants

Ethan Y. Lin, MD, Houston, TX (*Presenter*) Nothing to Disclose Rheun-Chuan Lee, MD, Taipei, Taiwan (*Abstract Co-Author*) Nothing to Disclose Bruno C. Odisio, MD, Houston, TX (*Abstract Co-Author*) Nothing to Disclose Sanjay Gupta, MD, Houston, TX (*Abstract Co-Author*) Nothing to Disclose

### For information about this presentation, contact:

EYLin@mdanderson.org

#### PURPOSE

To evaluate the real-time hemodynamic change of tumor arterial feeder (TAF) of HCC during drug-eluting beads transarterial chemoembolization (DEB-TACE) by using an intravascular Doppler wire (IVDW) at subsegmental TAF.

### **METHOD AND MATERIALS**

This single-center prospective study included three patients with HCC submitted to DEB-TACE between June 2016 and November 2016. One vial of 100 - 300 µm DEB (Biocompatibles UK) was loaded with 75 mg doxorubicin and mixed in 40 mL 50% diluted contrast medium. A 2-French microcatheter (Asahi Intecc, Aichi, Japan) and a 0.014 inch IVDW (FloWire, Philips, Netherlands) were advanced to the level of subsegmental TAF. The arterial flow velocity was continuously monitored by IVDW during embolization procedure. The embolization procedure protocols were as follows: slow pulsatile infusion of 1mL per minute LC beads solution without contrast reflux ; embolization endpoint as contrast medium washout in 2-5 heartbeats. Average peak velocity (APV) and highest instant peak velocity (IPV-H) were analyzed.

#### RESULTS

Although the individual arterial flow varied among different patients and tumors, the IVDW measured arterial flow decreased at an early stage of the embolization procedure in all three patients. The APV decreased more than 50% of peak-trough flow difference when beads were infused in 35.7%, 10%, and 7.5% of the total infused beads amount in patient #1, #2, and #3, respectively. The IPV-H decreased more than 50% of peak-trough flow difference when beads were infused in 42.8%, 12.5%, and 17.5% of the total infused beads amount in patient #1, #2, and #3, respectively. The total infused beads amount in patient #1, #2, and #3, respectively. The contrast medium washout rate remained less than 0.5 heartbeat when objective arterial flow significantly decreased more than 50%.

#### CONCLUSION

TAF flow decreases significantly at an early stage during DEB-TACE delivery. The objective TAF flow measurement was not proportional to the contrast medium washout rate.

# CLINICAL RELEVANCE/APPLICATION

TAF flow decreased significantly at early stages of DEB-TACE delivery, potentially reducing beads penetration. A thorough investigation of TAF change could shed light on optimal DEB-TACE delivery protocol.

# VSIO21-08 Arterially Directed Therapies to Downstage/Bridge to Liver Transplant

Monday, Nov. 26 3:20PM - 3:40PM Room: S406B

Participants

Riad Salem, MD, MBA, Chicago, IL (*Presenter*) Research Consultant, BTG International Ltd; Research Grant, BTG International Ltd; Consultant, Eisai Co, Ltd; Consultant, Exelixis, Inc; Consultant, Bristol-Myers Squibb Company; Consultant, Dove; ;

### LEARNING OBJECTIVES

1) Discuss options for downstaging tumors to resection or transplantation. 2) Discuss mechaism of action of trans atreail therapies.

# VSIO21-09 Intrahepatic Cholangiocarcinoma: Treatment Approaches and Survival Trends for Surgically Ineligible Patients

Monday, Nov. 26 3:40PM - 3:50PM Room: S406B

Participants Johannes Uhlig, Goettingen, Germany (*Presenter*) Nothing to Disclose Cortlandt Sellers, New Haven, CT (*Abstract Co-Author*) Nothing to Disclose

### Hyun S. Kim, MD, New Haven, CT (Abstract Co-Author) Nothing to Disclose

# For information about this presentation, contact:

johannes.uhlig@med.uni-goettingen.de

## PURPOSE

To evaluate current treatment approaches and survival trends among surgically ineligible patients with surgically intrahepatic cholangiocarcinoma (ICC).

# METHOD AND MATERIALS

The 2004-2015 National Cancer Database was retrospectively analyzed for histopathologically proven ICC. Interventional oncology (IO) included local tissue destruction and radioembolization. Baseline variables were evaluated as predictors for treatment allocation. Overall survival was analyzed via multivariable Cox models.

### RESULTS

9,655 patients with ICC were included, of which 401 patients received IO (4.1%), 776 patients radiation oncology (RO; 8%), 4,749 patients chemotherapy (49.2%), and 3,729 patients remained untreated. Increased likelihood of treatment via interventional oncology was observed for younger male patients, those with Medicare or private insurance, higher income and education, lower comorbidities and cancer stage, and patients treated at academic centers compared to other treatment approaches (p<0.05).Interventional oncology yielded highest overall survival compared to all other treatment approaches (2-year overall survival rate: IO 41.5%; RO 28.2%; chemotherapy 17.6%; no treatment 7.2%). After multivariable adjustment for potential confounders, a statistically significant survival benefit was observed for interventional oncology versus radiation oncology (HR=0.86, p=0.02), chemotherapy (HR=0.7, p<0.001) and no treatment (HR=0.31, p<0.001). A significant interaction term between treatment year and approach was evident (p<0.01), indicating that treatment effectiveness of IO, RO and chemotherapy increased from 2004-2015.

### CONCLUSION

Treatment allocation for surgically ineligible ICC patients shows marked variation depending on socioeconomic and cancer factors. Interventional oncology demonstrated superior overall survival compared to other non-surgical treatment options. Healthcare access and utilization must be targeted to address outcome discrepancies, potentially providing interventional oncology to a broader patient population.

#### **CLINICAL RELEVANCE/APPLICATION**

For surgically ineligible ICC, interventional oncology via local tissue destruction or radioembolization offers superior overall survival compared to radiation oncology, chemotherapy and no treatment.

# VSI021-10 Y90/PVE to Facilitate Curative Resection

Monday, Nov. 26 4:10PM - 4:30PM Room: S406B

Participants

David C. Madoff, MD, New York, NY (*Presenter*) Advisory Board, RenovoRx; Consultant, General Electric Company; Consultant, Terumo Corporation; Consultant, Argon Medical Devices, Inc; Consultant, Abbott Laboratories; Consultant, Embolx, Inc

### For information about this presentation, contact:

dcm9006@med.cornell.edu

### LEARNING OBJECTIVES

1) To examine the importance of future liver remnant size determination prior to major hepatic resection for hepatocelluar carcinoma and intrahepatic cholangiocarcinoma. 2) To review the role of portal vein embolization and Y90 radiation lobectomy to hypertrophy the liver for facilitation of curative resection. 3) To assess the currently available literature to determine which procedure should be used and when.

# VSI021-11 Interventional Oncology Treatment of Cholangiocarcinoma

Monday, Nov. 26 4:30PM - 4:50PM Room: S406B

Participants

William S. Rilling, MD, Milwaukee, WI (*Presenter*) Research support, B. Braun Melsungen AG; Research support, Sirtex Medical Ltd; Research support, Siemens AG; Consultant, B. Braun Melsungen AG; Consultant, Cook Group Incorporated ; Consultant, Terumo Corporation; Advisory Board, Terumo Corporation

# VSIO21-12 Combining TACE with Adopted Iodized Oil Containing Apatinib Inhibits HCC Growth and Metastasis by Inhibiting Angiogenesis in Anoxic Environment

Monday, Nov. 26 4:50PM - 5:00PM Room: S406B

Participants

Chen Zhou, Wuhan, China (*Presenter*) Nothing to Disclose Qi Yao, Wu Han, China (*Abstract Co-Author*) Nothing to Disclose Hongsen Zhang, Wuhan, China (*Abstract Co-Author*) Nothing to Disclose Chuansheng Zheng, Wuhan, China (*Abstract Co-Author*) Nothing to Disclose Bin Xiong, Wu Han, China (*Abstract Co-Author*) Nothing to Disclose

# For information about this presentation, contact:

m201675489@hust.edu.cn

PURPOSE

To investigate the therapeutic effect of the Transcatheter arterial chemoembolization (TACE) with adopted iodized oil containing Apatinib in rabbit VX2 hepatocellular carcinoma (HCC) model. The effect and mechanism of Apatinib inhibits tube formation of human umbilical vein endothelial cells (HUVECs) will be explored as well in anoxic environment.

# METHOD AND MATERIALS

In this Animal Experiment Committee approved study, 40 New Zealand rabbit VX2 liver tumors were randomly divided into four groups and respectively treated transarterially with saline (Group NS); iodized oil containing Apatinib (Group AI); iodized oil alone (Group I); Apatinib solution (Group A). The tumor growth rates of each group were measured by enhanced CT, Microvessel density (MVD) in the adjacent tissues of implanted VX2 tumor were estimated by detecting the expression of CD34, HIF-1a and VEGF level in tumor adjacent tissues were also examined by Immunohistochemistry. And in vitro experiment, HUVECs were cultured with different concentration gradients Apatinib(0, 1, 10, 50µmol/L, 24h) in the culture medium of HepG2 with normal oxygen or hypoxia, which is manufacturing by 200µM CoCl2. CCK8 method was used to detect the effects of apatinib on HUVECs. And the PI3K-akt, RAF-mek-erk and P38MAPK pathways were detected by western blot method. The Kruskal-Wallis test, Mann-Whitney U test, and Fisher exact test were used to look for statistically significant differences between groups.

### RESULTS

The TACE procedure were successfully performed in all experimental rabbits. The observation period of 7 days after embolization, the tumor growth rate of Group AI was significantly lower than other three groups of rabbits (P=0.000<0.01). Immunohistochemistry results showed that the microvessel density(MVD) of apatinib loaded lipiodol embolization group (Group AI) was significantly lower than that of the other three groups of rabbits (P<0.01). Apatinib have a stronger inhibitory effect of tube formation of HUVECs in anoxic environment rather than in normal circumstances. Apatinib inhibits HUVECs proliferation by down-regulating the PI3K-akt, RAF-mek-erk and P38MAPK pathways.

#### CONCLUSION

Apatinib inhibits the growth of liver cancer by down-regulating the PI3K-akt, RAF-mek-erk and P38MAPK pathways, and has a stronger inhibitory effect in hypoxic environments

#### **CLINICAL RELEVANCE/APPLICATION**

Our findings may provide new treatment options and stragies for the treatment of liver cancer.

### VSI021-13 Assessing Response to Locoregional Therapies

```
Monday, Nov. 26 5:00PM - 5:20PM Room: S406B
```

### Participants

Julius Chapiro, MD, New Haven, CT (*Presenter*) Research Grant, Koninklijke Philips NV; Research Grant, Guerbet SA; Consultant, Guerbet SA; Consultant, Eisai Co, Ltd

### For information about this presentation, contact:

j.chapiro@googlemail.com

# LEARNING OBJECTIVES

1) To recapitulate and refresh knowledge of conventional tumor response criteria. 2) To learn about the most commonly used imaging-based clinical endpoints of tumor therapies (eg time-to-progression, progression-free-survival). 3) To understand the value of 3D quantitative and computer-assisted tumor analysis techniques. 4) To learn about novel machine-learning based approaches and molecular imaging techniques and decision support systems.

### ABSTRACT

This lecture will provide an overview of image analysis techniques and imaging-based endpoints for the assessment of tumor response to loco-regional therapies of liver cancer. The talk will provide an overview of the currently available response criteria (including RECIST, mRECIST, EASL, qEASL) as well as outline the challenges of assessing tumor response in light of novel pharmacotherapeutic agents available in liver cancer, including immuno-modulatory agents as well as novel molecular-targeted agents that are increasingly used in combination or sequentially with loco-regional therapies. Additionally, the talk will touch on novel molecular-imaging based techniques as well as the role of aritifical intelligence and machine learning for the assessment of the tumor microenvironment and tumor response.

### VSI021-14 Panel Discussion: Current Concepts in the Management of Intermediate-advanced HCC

Monday, Nov. 26 5:20PM - 5:35PM Room: S406B

# VSIO21-15 Tumor Board

Monday, Nov. 26 5:35PM - 6:00PM Room: S406B



#### RCA24

# Creating Patient-Specific Anatomical Models for 3D Printing and AR/VR (Hands-on)

Monday, Nov. 26 2:30PM - 4:00PM Room: S401AB

IN

AMA PRA Category 1 Credits ™: 1.50 ARRT Category A+ Credit: 1.75

# Participants

Nicole Wake, PhD, New York, NY (*Presenter*) In-kind support, Stratasys, Ltd Amy E. Alexander, MSc, Rochester, MN (*Presenter*) Nothing to Disclose Andy Christensen, BS, Littleton, CO (*Presenter*) Consultant, Integrum AB; Board Member, Integrum AB; Stockholder, Somaden LLC Peter C. Liacouras, PhD, Bethesda, MD (*Presenter*) Nothing to Disclose Jane S. Matsumoto, MD, Rochester, MN (*Presenter*) Nothing to Disclose Todd Pietila, MBA, Plymouth, MI (*Presenter*) Employee, Materialise NV

### For information about this presentation, contact:

nicole.wake@med.nyu.edu

### LEARNING OBJECTIVES

1) Classify various image post-processing and 3D modeling software programs for enabling 3D printing or AR/VR applications. 2) Explain the workflow to create patient-specific 3D anatomical models from medical images. 3) Identify and apply image segmentation techniques used to create 3D anatomical models, including thresholding, region growing, and manual editing. 4) Describe and apply image post-processing techniques and 3D design principles required to save models in appropriate file formats (i.e. STL or OBJ). 5) Interface with 3D printing software or AR/VR devices.

# ABSTRACT

Advanced image data visualization in the form of 3D printing and AR/VR continues to expand in clinical settings. In order to generate patient-specific models for 3D printing or AR/VR, image data must first be segmented and converted to virtual 3D models which represent the intended anatomy of interest. The RSNA 3D Printing Special Interest Group has adopted a position statement reflecting the FDA recommendation that FDA-cleared software is used when 3D models are created for clinical applications. This course covers the use of industry-standard FDA-cleared software (Mimics InPrint, Materialise, NV) for the design and fabrication of patient-specific 3D models. Cranio-maxillofacial and renal case examples will be shown. Once the virtual 3D models have been created, users will learn how to prepare these files for 3D printing and AR/VR. In order to aid with the hands-on course, an extensive training manual will be provided before the meeting. It is highly recommended that participants review the training manual to optimize the experience at the workstation.

### Active Handout:Nicole Wake

http://abstract.rsna.org/uploads/2018/18020316/Hands-On-Handouts RCA24.pdf



#### RCC24

# **Clinical Decision Support: From Theory to Clinical Practice**

Monday, Nov. 26 2:30PM - 4:00PM Room: S501ABC



AMA PRA Category 1 Credits ™: 1.50 ARRT Category A+ Credit: 1.75

#### Participants

Emanuele Neri, MD, Pisa, Italy (Moderator) Nothing to Disclose

#### LEARNING OBJECTIVES

1) To explore the strategy of implementation of CDS in US and Europe. 2) To report the clinical implementation and impact of CDS in a real setting. 3) To preview the future implementation of artificial intelligence in CDS.

### Sub-Events

# RCC24A How Can Radiologists Implement Decision Support Systems in Clinical Routine: ACR View

Participants Bibb Allen JR, MD, Birmingham, AL (*Presenter*) Nothing to Disclose

### LEARNING OBJECTIVES

1) Apply lessons learned from the Medicare Demonstration project to implement effective Cllinical Decision Support (CDS) programs. 2) Formuate strategies for compliance with current regulations requiring CDS.

# RCC24B How Can Radiologists Implement Decision Support Systems in Clinical Routine: ESR View

Participants

Boris Brkljacic, MD, PhD, Zagreb, Croatia (Presenter) Nothing to Disclose

For information about this presentation, contact:

boris@brkljacic.com

#### LEARNING OBJECTIVES

1) To learn about the use of imaging referral guidelines in Europe. 2) To understand the challenges of implementing a CDS for heterogeneous European countries. 3) To describe the varying experiences of implementing CDS and imaging referral guidelines in different countries.

## RCC24C Results and Lessons from Brigham and Women's Hospital

Participants

Ramin Khorasani, MD, Boston, MA (Presenter) Nothing to Disclose

# LEARNING OBJECTIVES

1) Briefly review existing federal regulations pertinent to imaging clinical decision support. 2) Discuss design, implementation and results of large scale imaging CDS intervention at Brigham and Women's Hospital. 3) Contrast results and discuss implications from CDS interventions that have and have not impacted ordering physician behavior. 4) Recommend strategies to optimize imaging CDS implementation to improve quality and enable and promote evidence-based practice.

# RCC24D Application of Machine Learning in Clinical Decision Support Systems

Participants

Tarik K. Alkasab, MD, PhD, Boston, MA (Presenter) Nothing to Disclose



### MSRO24

BOOST: Head and Neck-Case-based Multidisciplinary Review (Interactive Session)

Monday, Nov. 26 3:00PM - 4:15PM Room: E450A



AMA PRA Category 1 Credits ™: 1.25 ARRT Category A+ Credits: 1.50

### Participants

Suresh K. Mukherji, MD, Northville, MI (Presenter) Nothing to Disclose

Sung Kim, MD, New Brunswick, NJ (Presenter) Nothing to Disclose

Francis P. Worden, MD, Ann Arbor, MI (*Presenter*) Grant, Bayer AG; Grant, Eisai Co, Ltd; Grant, AstraZeneca PLC; Grant, IRX Therapeutics; Grant, Galera Therapeutics; Grant, Bristol-Myers Squibb Company; Grant, Merck & Co, Inc; Consultant, Merck & Co, Inc

Chad Zender, MD, Cleveland, OH (Presenter) Nothing to Disclose

#### LEARNING OBJECTIVES

1) Review the imaging findings of various head and neck neoplasms in the post treatment setting. 2) Discuss the benefits of various imaging modalities and the scenarios they are most useful in the post treatment setting. 3) Identify imaging findings that change treatment and management.

#### ABSTRACT

This formal is a multidisciplinary tumor board which will discuss a varity of head and neck tumors. The participants will be a Head & Neck surgeon, Radiation Oncologist, Medical Oncologist and Head & Neck Radiologist. The emphasis will be on developing a better understanding of how various imaging modalities can be used in the post treatment setting to differentiate benign post treatment radiographic changes from those that are more concerning for recurrence.



#### MSRO28

# BOOST: Breast-Case-based Multidisciplinary Review (Interactive Session)

Monday, Nov. 26 3:00PM - 4:15PM Room: S103CD



AMA PRA Category 1 Credits ™: 1.25 ARRT Category A+ Credits: 1.50

### Participants

Nora M. Hansen, MD, Chicago, IL (*Presenter*) Nothing to Disclose Bethany L. Niell, MD,PhD, Tampa, FL (*Presenter*) Nothing to Disclose Jean L. Wright, MD, Baltimore, MD (*Presenter*) Nothing to Disclose Cesar A. Santa-Maria, MD, Baltimore, MD (*Presenter*) Research funded, AstraZeneca PLC; Research funded, Pfizer Inc; Advisory Board, Polyphor

### For information about this presentation, contact:

# jwrigh71@jhmi.edu

### LEARNING OBJECTIVES

1) Describe the latest advances in breast cancer imaging before, during, and after treatment. 2) Facilitate a multidisciplinary approach to the diagnosis, management, and treatment of breast cancer.



#### SSE01

### Breast Imaging (Breast Density and Risk Assessment)

Monday, Nov. 26 3:00PM - 4:00PM Room: E451B

# BQ BR

AMA PRA Category 1 Credit ™: 1.00 ARRT Category A+ Credit: 1.00

**FDA** Discussions may include off-label uses.

#### Participants

Jennifer A. Harvey, MD, Charlottesville, VA (*Moderator*) Stockholder, Hologic, Inc; Research Grant, Volpara Health Technologies Limited; Stockholder, Volpara Health Technologies Limited;

Ioannis Sechopoulos, PhD, Atlanta, GA (*Moderator*) Research Grant, Siemens AG; Research Grant, Canon Medical Systems Corporation; Speakers Bureau, Siemens AG; Scientific Advisory Board, Fischer Medical

### Sub-Events

### SSE01-01 Surrounding Regions of Tumor in FFDM are Associated with Breast Cancer Prognostic and Proliferation Markers

Monday, Nov. 26 3:00PM - 3:10PM Room: E451B

# Awards

#### **Student Travel Stipend Award**

Participants Dooman Arefan, PhD, Pittsburgh, PA (*Presenter*) Nothing to Disclose Bingjie Zheng, MD, Zhengzhou, China (*Abstract Co-Author*) Nothing to Disclose Ruimei Chai, Shenyang, China (*Abstract Co-Author*) Nothing to Disclose Margarita L. Zuley, MD, Pittsburgh, PA (*Abstract Co-Author*) Investigator, Hologic, Inc Jules H. Sumkin, DO, Pittsburgh, PA (*Abstract Co-Author*) Research Grant, Hologic, Inc; Research Grant, General Electric Company Shandong Wu, PhD, MSc, Philadelphia, PA (*Abstract Co-Author*) Nothing to Disclose

#### For information about this presentation, contact:

wus3@upmc.edu

#### PURPOSE

Radiomic information of segmented tumors in breast images have been shown to be correlated with prediction of certain markers/surrogates for prognosis. Surrounding regions of tumor may have been affected by tumor development but its effects remain unclear for similar prediction purposes. We performed an investigation on the radiomic imaging features extracted from both tumor and surrounding regions in relation to prediction of breast cancer distant recurrence risk and tumor proliferation markers.

# METHOD AND MATERIALS

We performed an IRB-approved retrospective study on 119 ER-positive and node-negative invasive breast cancer patients diagnosed (confirmed by pathology) during 2011-2016. All patients had FFDM scans (including MLO and CC views), Oncotype DX recurrence risk scores, and proliferation markers (Ki-67) available. Breast tumor was segmented by an expert breast imaging radiologist, and a varying size (diameter) of surrounding regions outside the segmented tumor were automatically separated using automated image processing techniques. A total of 23 radiomic features were extracted respectively from tumor and its surrounding region. The logistic least absolute shrinkage and selection operator (LASSO) regression model was used to estimate the Oncotype DX risk score and Ki-67 rate, respectively, using the same set of 23 features. AUC and Pearson's correlation coefficient (r) are performance metrics.

### RESULTS

For features extracted from tumor alone, r was 27% (p<0.05) and 35% (p<0.05) for estimating Oncotype DX and Ki67, respectively, while the corresponding AUC was 0.77 (High Oncotype DX vs Intermediate and low) and 0.58 (High Ki-67 vs low Ki-67). When imaging features from the surrounding regions (6 mm outer from tumor boundary) were incorporated additionally, r increased to 34% (p<0.05) and 47% (p<0.05) for estimating Oncotype DX and Ki-67, respectively, while the AUC was 0.78 and 0.63. The LASSO-selected features included the tumor solidity, surrounding region's skewness and intensity contrast.

#### CONCLUSION

Inclusion of the surrounding regions of breast tumor in FFDM increased the performance of predicting Oncotype DX recurrence risk scores and Ki-67 proliferation rate.

#### **CLINICAL RELEVANCE/APPLICATION**

Surrounding regions of breast tumor in FFDM may provide additional quantitative information over tumors to enhance prognosis and proliferation estimation

# **Edition of ACR BI-RADS in Mammography**

Monday, Nov. 26 3:10PM - 3:20PM Room: E451B

Participants Yiming Ding, Berkeley, CA (*Presenter*) Nothing to Disclose Mian Zhong, Berkeley, CA (*Abstract Co-Author*) Nothing to Disclose Youngho Seo, PhD, San Francisco, CA (*Abstract Co-Author*) Consultant, BioLaurus, Inc Thienkhai H. Vu, MD, PhD, San Francisco, CA (*Abstract Co-Author*) Nothing to Disclose Hari Trivedi, MD, San Francisco, CA (*Abstract Co-Author*) Nothing to Disclose Dmytro Lituiev, San Francisco, CA (*Abstract Co-Author*) Nothing to Disclose Amie Y. Lee, MD, San Francisco, CA (*Abstract Co-Author*) Nothing to Disclose Dexter Hadley, San Francisco, CA (*Abstract Co-Author*) Nothing to Disclose Bonnie N. Joe, MD, PhD, San Francisco, CA (*Abstract Co-Author*) Nothing to Disclose Jae Ho Sohn, MD, San Francisco, CA (*Abstract Co-Author*) Nothing to Disclose

#### For information about this presentation, contact:

sohn87@gmail.com

### PURPOSE

The current edition of BI-RADS assigns breast density qualitatively based on potential for obscuring breast cancer, rather than a simple quantitative summation of image intensities. The aim of this study is to develop a deep learning algorithm for breast density classification based on the new BI-RADS system and then retrospectively apply them to a separate set of digital mammograms to automatically classify breast density according to BI-RADS 5th Edition.

# METHOD AND MATERIALS

A convolutional neural network with ResNet50 architecture was trained on 94,562 screening mammograms performed from 2014 to 2018 from a single institution following the current 5th edition of BI-RADS for mammography. Optimal neural network hyperparameters were selected via validation accuracy monitoring. The trained model was then applied to a hold-out test set of size 9,547 from the same institution. We then manually inspected all 13 cases in which the predicted label differed by more than 2 density labels from the ground truth. This algorithm was applied to 433,760 screening mammograms in large scale.

### RESULTS

Our deep learning model achieved high sensitivity and specificity in assigning breast density category. Breast density distribution for the training data was 7,752 (A: 8.20%), 35,656 (B: 37.71%), 40,943 (C: 43.30%), and 10,211 (D: 10.79%). The AUCs of ROC curves on the test set were 0.97, 0.93, 0.92, and 0.96, respectively for each breast density category. Error analysis revealed that among the 13 cases where breast density differed by more than 2 classes between actual and predicted labels, 7 were due to breast implants, 4 were due to incorrect ground truth labels, and 2 remained equivocal. After the model was applied to the 433,760 screening mammograms, the model-predicted breast density distribution came to be 40,109 (A, 9.25%), 151,893 (B, 35.02%), 193,283 (C, 44.56%), and 48,475 (D, 11.17%).

### CONCLUSION

Our deep learning algorithm successfully modeled the breast density classification scheme in the 5th edition BI-RADS system. This was retrospectively applied in large scale to 433,760 mammograms for further inspection.

# **CLINICAL RELEVANCE/APPLICATION**

Qualitative breast density assessment by radiologists is subject to variability. Given widespread adoption of breast density notification laws in the U.S., automated breast density assessment based on masking can improve consistency of breast density assignment particularly between categories B & C.

# SSE01-03 Using Quantitative Breast Density Analysis to Predict Interval Cancers and Node Positive Cancers in Pursuit of Improved Screening Protocols

Monday, Nov. 26 3:20PM - 3:30PM Room: E451B

Participants

Elizabeth S. Burnside, MD,MPH, Madison, WI (*Presenter*) Dr. Burnside has a research grant from Hologic Lucy M. Warren, PhD, Guildford, United Kingdom (*Abstract Co-Author*) Nothing to Disclose Louise S. Wilkinson, MBBCh,FRCR, London, United Kingdom (*Abstract Co-Author*) Nothing to Disclose Kenneth C. Young, PhD, Guildford, United Kingdom (*Abstract Co-Author*) Nothing to Disclose Jonathan Myles, London, United Kingdom (*Abstract Co-Author*) Nothing to Disclose Stephen W. Duffy, London, United Kingdom (*Abstract Co-Author*) Nothing to Disclose

#### PURPOSE

This study investigates whether quantitative breast density can predict interval cancers and node positive screen detected cancers in order to serve as a biomarker to consider more aggressive screening to improve early detection.

# METHOD AND MATERIALS

We conducted a case-control study of 1204 women drawn from the U.K. NHS Breast Screening Program aged 50-74 including 599 cases (comprising 302 screen detected cancers, 297 interval cancers; 239 node positive, 360 node negative) and 605 controls. Each woman had prior digital mammograms and 70% had unprocessed images. A radiologist assessed breast density using a visual analog scale (VAS) from 0 to 100 and BI-RADS 5th Edition density categories. Volpara software (V1.5.1) calculated fibroglandular volume (FGV) and volumetric density grade (VDG) on unprocessed images. Logistic regression determined whether the breast density measures could predict mode of detection (screen detected or interval); node-negative cancers; and node-positive cancers, all vs. controls.

#### RESULTS

ECV predicted both screen-detected (n=0.01) and interval cancers (n=0.01) compared to controls V/DC V/AS and RI-DADS

predicted both screen-detected (p<0.01) and interval cancers (p<0.01) compared to controls. VDG, VAS and DF VADS predicted interval cancers (all p<0.01) but not screen-detected cancers (p=0.16, p=0.18, p=0.46 resp.). FGV demonstrated impressive risk stratification with an age-adjusted relative risk (RR) of the 4th quartile compared to the 1st quartile of 3.7 overall, 2.8 for screen detected, and 5.3 for interval cancers. VDG also had notable risk stratification with an age-adjusted RR of 3.6 for interval cancers (Table). FGV predicted node-negative cancers as compared to controls (p<0.01) while BI-RADS, VAS, and VDG did not (p=0.07, p=0.09, and p=0.47 resp.). FGV, BI-RADS, and VDG predicted node-positive cancers (all p<0.01) while VAS did not (p=0.14).

## CONCLUSION

FGV predicts interval, screen detected, node-positive and node-negative cancers compared to controls and provides remarkable stratification the RR of interval cancers. BI-RADS and VDG predict interval and node positive cancers. VAS only predicts interval cancers. The quantitative and automated nature of FGV and VDG and notable risk stratification based on RR indicates that these variables may be promising biomarkers.

### **CLINICAL RELEVANCE/APPLICATION**

By predicting mode of detection and nodal status, FGV may be a biomarker for more intensive screening. By predicting interval cancers, BI-RADS, VAS, and VDG may act as supplementary biomarkers.

# SSE01-04 Fully-Automated Volumetric Breast Density Estimation from Digital Breast Tomosynthesis: A Case-Control Comparison to Area-Based Density Measures from Digital Mammography

Monday, Nov. 26 3:30PM - 3:40PM Room: E451B

Participants

Aimilia Gastounioti, Philadelphia, PA (*Presenter*) Nothing to Disclose Meng-Kang Hsieh, Philadelphia, PA (*Abstract Co-Author*) Nothing to Disclose Lauren Pantalone, BS, Philadelphia, PA (*Abstract Co-Author*) Nothing to Disclose Emily F. Conant, MD, Philadelphia, PA (*Abstract Co-Author*) Grant, Hologic, Inc; Consultant, Hologic, Inc; Grant, iCAD, Inc; Consultant, iCAD, Inc; Speaker, iiCME Despina Kontos, PhD, Philadelphia, PA (*Abstract Co-Author*) Nothing to Disclose

#### PURPOSE

To investigate associations between breast cancer and fully-automated volumetric density measures extracted with digital breast tomosynthesis (DBT), while also comparing to area-based density measures from digital mammography (DM).

#### METHOD AND MATERIALS

We retrospectively analyzed contralateral combo DM-DBT studies (Selenia Dimensions, Hologic Inc.) from 174 women with unilateral breast cancer and 696 controls matched to cases on age, ethnicity and screening exam date at a 4:1 ratio. The publicly available 'LIBRA' software (v1.0.4) was adapted and used to estimate absolute dense volume (DV) and volumetric percent density (VPD) from DBT, and absolute dense area (DA) and area percent density (APD) from DM images. Quantra (v2.2; Hologic Inc.) was also applied to DM images, allowing to evaluate APD as well as to infer DV and VPD via physics-based models. Associations between the different density measures and breast cancer were evaluated via logistic regression after adjustment for age, ethnicity and body mass index (BMI). Area under the curve (AUC) of the receiver operating characteristic was used to assess case-control discriminatory capacity, where model performance was compared using the DeLong's test, and odds ratios (ORs) for each of the density measures were estimated.

#### RESULTS

All density measures had a significant association with breast cancer (OR = 1.24-2.40) after adjustment for age, ethnicity and BMI. Models based on volumetric density measures had significantly (p < 0.05) larger case-control discriminatory capacity (AUC = 0.59-0.63) than models considering area density (AUC = 0.57-0.59). Maximum breast cancer association was observed for DV with slightly (p = 0.440) improved performance when extracted with DBT (AUC = 0.63) relative to DV inferred from DM (AUC = 0.61).

# CONCLUSION

Fully-automated, quantitative, volumetric evaluation of breast density from DBT is feasible and can result in larger case-control discriminatory capacity than area-based density measures from conventional planar mammography. Associations with breast cancer can potentially further improve when volumetric density evaluation is performed with the DBT reconstructed breast volume compared to physics-based models applied to DM.

### **CLINICAL RELEVANCE/APPLICATION**

Our results further elaborate important clinical implications of breast density measures estimated with DBT, which may result in improved measures of breast density in breast cancer risk assessment.

# SSE01-05 Predicting Masking Risk in Mammography

Monday, Nov. 26 3:40PM - 3:50PM Room: E451B

Participants

James G. Mainprize, PhD, Toronto, ON (*Presenter*) Institutional research agreement, General Electric Company Olivier Alonzo-Proulx, Toronto, ON (*Abstract Co-Author*) Institutional research agreement, General Electric Company James Patrie, MS, Charlottesville, VA (*Abstract Co-Author*) Nothing to Disclose Jennifer A. Harvey, MD, Charlottesville, VA (*Abstract Co-Author*) Stockholder, Hologic, Inc; Research Grant, Volpara Health Technologies Limited; Stockholder, Volpara Health Technologies Limited;

Martin J. Yaffe, PhD, Toronto, ON (*Abstract Co-Author*) Research collaboration, General Electric Company; Shareholder, Volpara Health Technologies Limited; Co-founder, Mammographic Physics Inc; Research Consultant, BHR Pharma LLC

### For information about this presentation, contact:

james.mainprize@sri.utoronto.ca

PURPOSE

Masking in mammography is the reduction of lesion conspicuity by surrounding and overlying dense tissue. Masking risk is increased in dense breasts, leading to reduced sensitivity of breast screening. We have developed a masking index that can predict the likelihood of a masked or missed cancer and could be used in a screening program to stratify women at greatest risk of masking to alternative or supplementary imaging modalities to mammography.

#### **METHOD AND MATERIALS**

The study population were cancer cases collected (2003-2013) a case-control study used to develop a breast cancer risk model incorporating density measures. Cancers were classified as screen-detected cancers (SDC) found on a screening mammogram and non-screen detected cancers (NSDC) found by clinical symptoms or other imaging. The study had ethics board approval with informed consent All SDC found on baseline images were excluded. Inclusion as NSDC required at least one prior negative screening exam within two years of diagnosis. Images were analyzed with in-house algorithms and by volumetric breast density (VBD) software. The aim in this study was to create an index that differentiated mammograms which allowed for detection (SDC) from those for causing masking or missed lesions (NSDC). To avoid the influence of the lesion itself, only the contra-lateral breast images were used.

#### RESULTS

The study included 90 NSDC cases and 186 SDC controls. Univariate masking indices based on BMI, age, BI-RADS density, VBD or mean detectability yielded areas under ROC (AUC) of 0.61, 0.65, 0.67, 0.72 and 0.75 ( $\pm$ 0.06 95% confidence) respectively. For cancers found within one year, the detectability AUC improved to 0.81.

#### CONCLUSION

Age and BMI are relatively weak predictors of masking risk whereas VBD and detectability measures have better performance. Further, adding textural measures improve predictions slightly, suggesting that the masking effects of anatomic noise and texture are informative. In future, we will validate the model in an independent population and test the result on normal mammograms to predict impact on a stratified screening program.

#### **CLINICAL RELEVANCE/APPLICATION**

A reliable masking index to predict when mammography will underperform would be a valuable tool in a stratified screening program which could be used to redirect women with highly masked mammograms to alternative or adjunct screening strategies such as tomosynthesis, MR or ultrasound.

# SSE01-06 Quantitative MRI Background Parenchymal Enhancement and Contralateral Breast Cancer Risk

Monday, Nov. 26 3:50PM - 4:00PM Room: E451B

Participants

Lei Zhang, PhD, Pittsburgh, PA (*Presenter*) Nothing to Disclose Xiaosong Chen, Shanghai, China (*Abstract Co-Author*) Nothing to Disclose Yue Liang, Shanghai, China (*Abstract Co-Author*) Nothing to Disclose Aly A. Mohamed, PhD, Pittsburgh, PA (*Abstract Co-Author*) Nothing to Disclose Yiwei Tong, Shanghai, China (*Abstract Co-Author*) Nothing to Disclose Kunwei Shen, shanghai, China (*Abstract Co-Author*) Nothing to Disclose Shandong Wu, PhD, MSc, Philadelphia, PA (*Abstract Co-Author*) Nothing to Disclose

# For information about this presentation, contact:

wus3@upmc.edu

#### PURPOSE

MRI background parenchymal enhancement (BPE) has been shown to be correlated with the risk of developing breast cancer in breast-cancer free women. History of breast cancer is a significant risk factor of contralateral breast cancer. We investigated the association between quantitative MRI BPE measures and risk of contralateral breast cancer development in a case-control setting

#### **METHOD AND MATERIALS**

A retrospective case-control (1:2 case-control ratio) study was performed using breast DCE-MRI scans from 135 newly diagnosed unilateral breast cancer patients (confirmed by pathology) from 2010-2016: 35 women had future contralateral breast cancer development after the initial breast cancer diagnosis and 70 were age- and year-of-MRI matched controls that remained breast cancer-free in the contralateral breasts after at least 1-year follow-up. The MRIs acquired at the initial diagnosis of the unilateral breast cancer were analyzed using published automated computer algorithms, generating two quantitative BPE measures computed from the first post-contrast series: the absolute BPE volume (|BPE|) and its relative amount over the whole breast volume (BPE%). Volumetric amounts of fibroglandular (dense) tissue (|FGT| and FGT%) were also automatically quantified from the MRI. Conditional logistic regression was performed to assess these BPE and FGT measures as predictors of the contralateral breast cancer development.

#### RESULTS

Average age was 52.2±13.1 (range 28-81) for cancers and 52.8±12.9 (range 28-80) for controls. 51% (or 49%) are postmenopause for cancers (or controls). Invasive other-cancer history was found in less than 10% of the patients for both cancer cases and controls. None of the |FGT|, FGT%, |BPE|, BPE% measures is statistically significant (all p>0.05) in terms of the difference between the cancer group and control group. Logistic regression showed that odds ratios of these four measures are very close to 1 with no statistical significance.

#### CONCLUSION

This pilot study showed that MRI BPE quantified in the contralateral breast of unilateral breast cancer patients is not associated with the future development of the contralateral breast cancers.

### **CLINICAL RELEVANCE/APPLICATION**

BPE may be affected bilaterally even in unilateral breast cancer patients. Contralateral breast cancer risk markers can guide

treatment selection and risk reduction, meriting further investigation.



# **Breast Imaging (Patient-Centric Care)**

Monday, Nov. 26 3:00PM - 4:00PM Room: E450B

# BR HP

AMA PRA Category 1 Credit ™: 1.00 ARRT Category A+ Credit: 1.00

# Participants

Rachel F. Brem, MD, Washington, DC (*Moderator*) Board of Directors, iCAD, Inc; Board of Directors, Dilon Technologies, Inc; Stock options, iCAD, Inc; Stockholder, Dilon Technologies, Inc; Consultant, Dilon Technologies, Inc; Consultant, ClearCut Medical Ltd; Consultant, Delphinus Medical Technologies, Inc

Priscilla J. Slanetz, MD, MPH, Belmont, MA (Moderator) Nothing to Disclose

#### Sub-Events

# SSE02-01 Communicating Mammography Results: What Method and How Quickly Do Women Want Their Screening Mammogram Results?

Monday, Nov. 26 3:00PM - 3:10PM Room: E450B

Participants Julia Staschen, BS, Richmond, VA (*Abstract Co-Author*) Nothing to Disclose Nghiem Pham, BA, Midlothian, VA (*Presenter*) Nothing to Disclose Alicia Johns, Richmond, VA (*Abstract Co-Author*) Nothing to Disclose Biren A. Shah, MD, Glen Allen, VA (*Abstract Co-Author*) Royalties, Wolters Kluwer nv; Royalties, Springer Nature

# For information about this presentation, contact:

phamn@vcu.edu

# PURPOSE

Expectations for when and how to receive results for mammograms are uncertain and the goal of this study is to explore expectations for patient care with regards to receiving mammogram results. The purpose of the study was to understand the majority preference with regards to the wait time for screening mammogram results, whether prompt communication of mammogram results was of importance to patients, whether the time frame to schedule an additional imaging follow-up appointment after an abnormal screening mammogram was of importance to patients, and how patients preferred to be given their screening mammogram results. From the survey, investigators wanted to determine whether any quality practice improvements are necessary at their academic breast imaging centers in order to improve the communication of screening mammogram results.

# RESULTS

There were 2,245 patients who participated in the survey. A majority of patients preferred to receive results on Friday (N=1,868, 85.4%). Most individuals preferred to schedule their follow up appointments soon after their initial appointment, preferring either the next day or within 1-2 days. Finally, over half of the sample preferred to be contacted via a phone call, with letter and text messaging being the next most preferred methods. The preference for receiving results on Friday was evaluated by each of the patient characteristics. The responses by the patients for preference for receiving results on Friday were significantly different by ethnicity, education, and clinic. In particular, patients of other ethnicities besides African Americans and Caucasians responded with the highest percent to receiving results on Friday and Caucasians were the least inclined to prefer to receive results on Friday. Individuals with some college and college degrees were more likely to not prefer receiving results on Friday than those with no formal education or high school graduates. The preferred time for scheduling a follow up was assessed by each of the patient characteristics. Across all the patient characteristics, patients preferred to schedule their follow up appointment the next day. Lastly, first choice of contact was examined across each of the patient characteristics. Phone call was the overwhelming choice for method of contact for all patient characteristics.

#### CONCLUSION

The findings suggest that the patient population surveyed have a preference for their wait time, which is either to wait or receive them within 24 hours. Patients preferred to receive results on Friday, and the most frequent choice for scheduling a follow up appointment was the next day. A phone call was the preferred first choice for method of contact with e-mail being the least preferred. These suggestions can help clinics and providers make changes to how they communicate their results. These findings may help to streamline results for patients who prefer a shorter wait time, and highlight the overwhelming patient preference to receive their abnormal screening mammogram results on a Friday. The findings may also suggest how to contact patients in a different way, as phone calls were the preferred method of contact. The strong preference of patients receiving their screening mammogram results more promptly should help trigger alternative methods toward improving communication between the radiologist and the patient.

#### METHODS

*Patients* The study population was patients aged 18 or older, who completed an anonymous paper survey consisting of eight questions when coming in for a routine mammogram screening. The study period lasted from September to November 2017 at two academic breast-imaging centers. *Measures* The primary objective of the study was to summarize the results from a survey examining the communication of mammography results from the patient population. The association between patient demographics

and four outcomes, preferred wait time, preferred scheduling time for a follow-up appointment, preference for receiving screening results on Friday, and preferred methods of contact was investigated. Parameters of the survey are summarized in attached Table 1. *Statistical Methods* Frequencies and percentages for clinic site, age, ethnicity, education, and insurance were calculated. Pearson chi-square analyses were conducted to determine the association between wait time preference and each patient demographic, between preferred scheduling time for follow-up appointment and each patient demographic, between preference for receiving screening results on Friday and each patient demographic, and between the first choice of method of contact and each patient demographics. SAS version 9.4 was used for all analyses.

# PDF UPLOAD

http://abstract.rsna.org/uploads/2018/18003961/18003961\_3t99.pdf

# SSE02-02 City Patterns of Screening Mammography Uptake and Disparity Across the United States

Monday, Nov. 26 3:10PM - 3:20PM Room: E450B

#### Awards

#### **Trainee Research Prize - Resident**

Participants

Eric Kim, MD, New York, NY (*Presenter*) Nothing to Disclose Linda Moy, MD, New York, NY (*Abstract Co-Author*) Nothing to Disclose Yiming Gao, MD, New York, NY (*Abstract Co-Author*) Nothing to Disclose C. A. Hartwell, BS, New York, NY (*Abstract Co-Author*) Nothing to Disclose James S. Babb, PhD, New York, NY (*Abstract Co-Author*) Nothing to Disclose Samantha L. Heller, MD, PhD, New York, NY (*Abstract Co-Author*) Nothing to Disclose

## For information about this presentation, contact:

kime18@nyumc.org

#### PURPOSE

Rural disparities in screening utilization are known to be affected by lack of access to care providers; city-level screening mammography disparity has been less well evaluated, although over 30 million adult women live in the 500 largest cities. Our purpose is therefore to evaluate disparities in screening in US cities.

#### **METHOD AND MATERIALS**

This descriptive study used public data from the 500 Cities project--500 largest cities, 103,020,808 individuals--which includes selfreported screening uptake (127,298 women ages 50-74) from the Behavioral Risk Factor Surveillance System (BRFSS). Uptake was matched with BRFSS and American Community Survey national population/economic census data variables expected to impact screening: geographic region, health insurance, median household income, obesity, race, combined preventive care services (flu, pneumococcal shots, colorectal screening), and pap smear use. Cities with incomplete data were excluded, yielding 490 cities, 34,629,163 women. Univariable and multivariable analyses were performed. All statistical tests were conducted at the two-sided 5% significance level using SAS 9.3 software (SAS Institute, Cary, NC).

# RESULTS

Mean city screening mammography utilization was 77.7% (62.8%-88.9%). Utilization was highest in New England cities (p<0.002), significantly positively correlated with pap smear (r=0.75), other preventive services (r=0.3), household income (r=0.44), %Asian race (r=0.36), weakly with %Black race (r=0.10); significantly negatively correlated with obesity (r=-0.36), poverty (r=-0.30), %White race (r=-0.29), no insurance (r=-0.27), (p<0.05 for all); not significantly correlated with population size (p=0.651). Multivariable analysis demonstrated Pap smear use, Asian race, private insurance, and geographic region to be significant independent predictors of utilization.

## CONCLUSION

Screening mammography utilization varies across large cities in the U.S. with highest uptake in New England. Although the literature focuses on rural screening disparities, disparities also exist even across large cities without physical barriers to screening.

#### **CLINICAL RELEVANCE/APPLICATION**

Mammographic screening disparities exist at the city level; identifying predictors of uptake may aid in targeting areas and populations for screening education and intervention.

# SSE02-03 Aligning Insurance Benefit Design with Patient Preference for Out-of-Pocket Cost Payments

Monday, Nov. 26 3:20PM - 3:30PM Room: E450B

Participants

Paniz Charkhchi, MD, Ann Arbor, MI (*Presenter*) Nothing to Disclose
Aaron Scherer, PhD, Iowa City, IA (*Abstract Co-Author*) Nothing to Disclose
Angela Fagerlin, Salt Lake City, UT (*Abstract Co-Author*) Nothing to Disclose
A. Mark Fendrick, MD, Ann Arbor, MI (*Abstract Co-Author*) Consultant, Abbott Laboratories; Consultant, AstraZeneca PLC; Consultant, sanofi-aventis Group; Consultant, F. Hoffmann-La Roche Ltd; Consultant, GlaxoSmithKline plc; Consultant, Merck & Co, Inc; Consultant, Neocure Group LLC; Consultant, Pfizer Inc; Consultant, POZEN Inc; Consultant, Precision Health Economics LLC;
Consultant, The TriZetto Group, Inc; Consultant, Zanzors; Speakers Bureau, Merck & Co, Inc; Speakers Bureau, Pfizer Inc;
Researcher, Abbott Laboratories; Researcher, AstraZeneca PLC; Researcher, sanofi-aventis Group; Researcher, Eli Lilly and Company; Researcher, F. Hoffmann-La Roche Ltd; Researcher, GlaxoSmithKline plc; Researcher, Merck & Co, Inc; Researcher, Novartis AG; Researcher, Pfizer Inc
Ruth C. Carlos, MD, MS, Ann Arbor, MI (*Abstract Co-Author*) Nothing to Disclose

## For information about this presentation, contact:

panizcharkhchi@gmail.com

#### PURPOSE

Alternative payment models encourage physicians to accept payment bundles. Their patients continue to pay fee-for-service (FFS) out of pocket costs, contrary to their preference for predictable out of pocket costs for a care episode. Using a hypothetical screening mammography diagnostic episode of care, we assessed patient preference for FFS vs bundled copayments (copays).

# **METHOD AND MATERIALS**

After IRB approval, we recruited a population-based cross-sectional survey of women 40-75 years old through Survey Sampling International. Participants read a hypothetical scenario describing a screening mammography episode of care where 12% of women undergoing screening needed a follow-up breast ultrasound and 2% a breast biopsy. Estimated out-of-pocket (OOP) costs for these services and the characteristics of OOP payment types (FFS and a hypothetical bundled copay) were also described. We assessed OOP payment type preference and knowledge (7 true/false items, see Fig. 1), additional test cost worry (7-point scale from not at all to very worried), likelihood of mammogram use by OOP payment type and willingness to pay (WTP) for a breast screening episode bundle.

## RESULTS

Participant (n=1,236) characteristics are described in Fig. 1. 82.9% preferred bundled copays over FFS and 70.8% answered at least half of the knowledge questions correctly. While most participants (74.5%) indicated they would get screened regardless of OOP payment type, 13.8% said they would only get screened with bundled copays and 3.4% with FFS. Sizeable percentages of participants were worried about costs associated with the ultrasound (42.0%) and biopsy (67.7%). Median WTP was \$81 (25-75IQ=\$34-\$215) for a bundle to avoid paying additional OOP for possible ultrasound or biopsy.

## CONCLUSION

Given worry over the cost over potential additional tests, participants preferred a predictable OOP cost for a breast screening episode, despite the low likelihood of additional testing. Although most participants would not defer mammography based on OOP payment type, a significant minority were more likely to screen if bundled copays were available. Insurers should consider incorporating these preferences in future benefits.

# **CLINICAL RELEVANCE/APPLICATION**

Designing insurance plans to include bundled copays may decrease financial barriers to breast cancer work-up and diagnosis after screening mammography.

# **Honored Educators**

Presenters or authors on this event have been recognized as RSNA Honored Educators for participating in multiple qualifying educational activities. Honored Educators are invested in furthering the profession of radiology by delivering high-quality educational content in their field of study. Learn how you can become an honored educator by visiting the website at: https://www.rsna.org/Honored-Educator-Award/ Ruth C. Carlos, MD, MS - 2015 Honored EducatorRuth C. Carlos, MD, MS - 2018 Honored Educator

# SSE02-04 Patient, Radiologist, and Examination Characteristics Affecting Screening Mammography Recall Rates in a Large Academic Practice

Monday, Nov. 26 3:30PM - 3:40PM Room: E450B

Participants

Catherine S. Giess, MD, Wellesley, MA (*Presenter*) Nothing to Disclose Aijia Wang, Boston, MA (*Abstract Co-Author*) Nothing to Disclose Ivan Ip, MD, MPH, Brookline, MA (*Abstract Co-Author*) Nothing to Disclose Ronilda Lacson, MD, PhD, Brookline, MA (*Abstract Co-Author*) Nothing to Disclose Sarvenaz Pourjabbar, MD, New Haven, CT (*Abstract Co-Author*) Nothing to Disclose Ramin Khorasani, MD, Boston, MA (*Abstract Co-Author*) Nothing to Disclose

#### For information about this presentation, contact:

cgiess@bwh.harvard.edu

## PURPOSE

To evaluate patient, radiologist, and examination characteristics affecting individual screening mammography recall rates in a large academic breast imaging practice.

# **METHOD AND MATERIALS**

This Institutional Review Board approved retrospective study included all screening mammography examinations in female patients interpreted by thirteen breast imaging specialists at an urban academic center and two outpatient imaging centers from 10/1/2012-5/31/2015. Patient demographics were extracted via electronic medical record. A natural language processing algorithm captured breast density, BI-RADS assessment, and current and prior screening examination findings. Radiologists' annual screening volumes, years of clinical experience, and percentage of time doing breast imaging were calculated. Risk aversion, stress from uncertainty, and malpractice concerns were derived via online survey. Univariate and multivariate analyses assessed patient, radiologist, and examination characteristics associated with likelihood of mammography recall. Pearson product-moment correlation coefficient assessed relationship between cancer detection rate and recall rate.

# RESULTS

Overall, 5,678 (9.3%) of 61,198 screening examinations were recalled. In multi-variate analysis, patient and radiologist characteristics associated with higher odds of recall included patient's age < 50 years (p<0.0001); calcification (p<0.0001), mass (p<0.0001), and higher density category (p<0.0001) on prior mammogram; baseline examination (p<0.0001); annual reading volume < 1250 screening exams (p=0.0282); and <10 years experience (p=0.0036). Radiologist's risk aversion, stress from uncertainty, malpractice concerns, or cancer detection rates were not associated with higher recall rates (r=-0.36, p=0.23).

#### CONCLUSION

In addition to patient and examination factors, screening recall variations were explained by radiologist's annual reading volume and experience. Interventions targeting radiologist factors may reduce unwarranted variation in screening recall and improve patient's care experience.

# **CLINICAL RELEVANCE/APPLICATION**

Efforts to reduce screening recall rate variability and false positive recalls might include increasing annual screening interpretive volumes and review of uncertain screening findings for less experienced radiologists by more experienced breast imaging specialists.

#### **Honored Educators**

Presenters or authors on this event have been recognized as RSNA Honored Educators for participating in multiple qualifying educational activities. Honored Educators are invested in furthering the profession of radiology by delivering high-quality educational content in their field of study. Learn how you can become an honored educator by visiting the website at: https://www.rsna.org/Honored-Educator-Award/ Catherine S. Giess, MD - 2015 Honored EducatorCatherine S. Giess, MD - 2017 Honored Educator

# SSE02-05 Preventive Care: How Comorbidities Affect Mammography Screening Rates

Monday, Nov. 26 3:40PM - 3:50PM Room: E450B

#### Awards

#### **Student Travel Stipend Award**

Participants Cindy Yuan, MD,PhD, Chicago, IL (*Presenter*) Nothing to Disclose Kirti M. Kulkarni, MD, Chicago, IL (*Abstract Co-Author*) Nothing to Disclose Brittany Z. Dashevsky, MD,DPhil, Chicago, IL (*Abstract Co-Author*) Nothing to Disclose

## PURPOSE

Here we evaluate the impact of comorbid conditions and age on screening mammography utilization.

## **METHOD AND MATERIALS**

Data was retrospectively drawn from the 2011-2015 Medical Expenditure Panel Survey, which contained 40,752 women over the age of 40. Utilization was defined as a screening mammogram within the previous one or two years, analyzed separately. A logit model was employed to evaluate correlation of comorbidities with utilization. Statistical significance was defined by a p-value <0.05 by two-sided test.

# RESULTS

Of the 36,575 women in the final sample, 45.9%, 43.6%, 3.9%, and 5.7% reported a history of hypertension (HTN), hyperlipidemia (HLD), prior heart attack (MI) and prior stroke (CVA), respectively. Among women without a comorbid condition, baseline annual mammography utilization was 47.3%. HTN and HLD were correlated with increased annual utilization [2.5 and 6.8 percentage points (pp)]. In comparison, prior MI and CVA were correlated with decreased annual utilization (-8.2 and -1.5 pp, not statistically significant in the latter). Results were similar for biennial utilization (3.0 and 7.6 pp increased utilization with HTN and HLD, respectively, and -6.5, and 0.1 pp decreased utilization for MI and CVA, respectively).

#### CONCLUSION

Screening utilization was increased in patients with HTN and HLD, and decreased in patients with prior MI and CVA. An understanding of how comorbid conditions influence screening may help better target specific populations and improve overall utilization of preventive care.

# **CLINICAL RELEVANCE/APPLICATION**

HTN and HLD, comorbidities that require regular physician visits, are correlated with increased screening. However, prior MI or CVA, are correlated with decreased screening, possibly reflecting the effect of decreased life expectancy and increased morbidity. This is especially relevant as age-based guidelines fail to take into account individual comorbidities and life expectancy.

# SSE02-06 Contrast-Enhanced Spectral Mammography (CESM) in the Screening Setting: Patient Preferences and Attitudes

Monday, Nov. 26 3:50PM - 4:00PM Room: E450B

Participants

Matthew M. Miller, MD, PhD, Charlottesville, VA (*Presenter*) Nothing to Disclose Kathy L. Repich, Charlottesville, VA (*Abstract Co-Author*) Nothing to Disclose Carrie M. Rochman, MD, Charlottesville, VA (*Abstract Co-Author*) Research Consultant, Theraclion Brandi T. Nicholson, MD, Charlottesville, VA (*Abstract Co-Author*) Nothing to Disclose Jonathan Nguyen, MD, Charlottesville, VA (*Abstract Co-Author*) Nothing to Disclose James Patrie, MS, Charlottesville, VA (*Abstract Co-Author*) Nothing to Disclose Roger T. Anderson, Charlottesville, VA (*Abstract Co-Author*) Nothing to Disclose Jennifer A. Harvey, MD, Charlottesville, VA (*Abstract Co-Author*) Stockholder, Hologic, Inc; Research Grant, Volpara Health Technologies Limited; Stockholder, Volpara Health Technologies Limited;

# For information about this presentation, contact:

matthew.miller@virginia.edu

# PURPOSE

Contrast-enhanced spectral mammography (CESM) is an emerging imaging tool that has been shown to have greater sensitivity than conventional mammography and equal sensitivity with improved specificity relative to breast MRI in the diagnostic setting. Ongoing studies are evaluating CESM performance in the screening setting, but little is known regarding whether patients would agree to its use and the associated risks in screening. Our study aims to evaluate the attitudes and concerns of patients regarding

the use of CESM in a screening setting.

# **METHOD AND MATERIALS**

In this IRB-approved HIPAA-compliant prospective study, patients with prior mammograms demonstrating heterogeneous or extremely dense breasts presenting for screening mammography were invited to complete a survey. Patients were asked to rate their perception of personal breast cancer risk compared to peers and their level of concern related to screening callbacks, radiation exposure, and contrast allergies, and then identify which factors might deter them from getting adjunct screening exams such as CESM.

# RESULTS

512 patients with dense breasts undergoing screening mammography completed surveys. While 27% of surveyed patients reported previously having been called back from screening for a diagnostic workup, a majority (63%) expressed little or no concern for callbacks leading to additional imaging or biopsy. Most patients (63%) felt it was likely or very likely that cancer could be missed on their mammogram, but only 9% had undergone adjunct screening exams in the past 3 years. The most commonly cited deterrents to undergoing adjunct screening were cost (69%), pain (35%), and concern for an increased likelihood of having a biopsy or surgery recommended (32%). When asked to select from several hypothetical adjunct screening modality choices, patients reported a strong preference (63%) for a test that is most likely to detect their cancer, even if this would require IV-line placement. Only 5% preferred a common but less sensitive test that did not require IV-line placement.

# CONCLUSION

Our study suggests that women with dense breasts may accept CESM as an adjunct screening exam and may actually prefer it over screening MRI or US given its relatively high sensitivity and low cost.

# **CLINICAL RELEVANCE/APPLICATION**

Women with dense breasts may accept CESM as an adjunct screening exam given its sensitivity and low cost.



## Cardiac (CTA: General Topics)

Monday, Nov. 26 3:00PM - 4:00PM Room: N229



AMA PRA Category 1 Credit ™: 1.00 ARRT Category A+ Credit: 1.00

FDA Discussions may include off-label uses.

#### Participants

Smita Patel, FRCR, MBBS, Ann Arbor, MI (*Moderator*) Nothing to Disclose Daniel Vargas, MD, Aurora, CO (*Moderator*) Nothing to Disclose

# Sub-Events

# SSE03-01 Association of Plasma Uric Acid and Creatinine with Coronary Artery Calcium Score

Monday, Nov. 26 3:00PM - 3:10PM Room: N229

Participants

Lei Zhang, MD, PhD, Songjiang, China (*Abstract Co-Author*) Nothing to Disclose Chen Qiao, Shanghai, China (*Abstract Co-Author*) Nothing to Disclose Han Wang, MD, PhD, Shanghai, China (*Abstract Co-Author*) Nothing to Disclose Shu Hong Fan, Shanghai, China (*Presenter*) Nothing to Disclose

For information about this presentation, contact:

zhanglei4302@hotmail.com

#### PURPOSE

The aim of this study was to conduct a statistical analysis of low-radiation-dose coronary computed tomography screening for coronary artery calcium score (CACS) to determine the correlation of the CACS with age, sex, systolic blood pressure, diastolic blood pressure, low-density lipoprotein cholesterol (LDL-C), high-density lipoprotein cholesterol (HDL-C), total cholesterol (TC), triglycerides (TG), uric acid (UA) and creatinine (Cr), as well as to investigate the predictive value of these traditional risk factors for coronary artery disease.

## **METHOD AND MATERIALS**

There were 646 patients with chest pain or suspected coronary atherosclerosis, a clinical history, smoking habit, symptoms, high blood pressure, and high blood sugar. The following biochemical parameters were assessed: LDL-C, HDL-C, TC, TG, UA, and creatinine. All patients underwent a CT scan for coronary artery calcium score analysis. The scan was then analyzed in relationship to CACS levels and the above items for all patients.

#### RESULTS

In total, 326 patients were male (59.8%), and 219 patients were female (40.2%). The average age was  $69.1 \pm 10.2$  years, and the mean CACS was  $485 \pm 814$ . Significant correlations of CACS with UA (r = 0.1518, P < 0.05) and creatinine (r = 0.2752, P < 0.05) were found. According to the multivariate Cox regression analysis, after adjusting for demographic characteristics and other serum parameters, serum UA levels (odds ratio [OR], 1.003, 95% confidence interval [CI], 1.001-1.005, p = 0.003) and creatinine levels (OR, 1.002, 95% CI, 0.999-1.005, p = 0.002) qualified as independent discriminators of the severity of coronary artery calcification.

#### CONCLUSION

We propose the need for identifying and managing UA and creatinine abnormalities to reduce excess coronary artery disease (CAD) risk. This proposal remains to be formally tested in a prospective study.

## **CLINICAL RELEVANCE/APPLICATION**

The severity of coronary artery calcification score may indicated the UA and creatinine abnormalities in the blood.

# SSE03-03 Feasibility Study of Coronary Computed Tomography Angiography in Patients with Free-Breathing Using 256-Detector CT

Monday, Nov. 26 3:20PM - 3:30PM Room: N229

Participants Zhuo Liu, Beijing, China (*Presenter*) Nothing to Disclose Nan Hong, MD, Beijing, China (*Abstract Co-Author*) Nothing to Disclose

#### For information about this presentation, contact:

liuzhuormyy@sina.cn

PURPOSE

To evaluate the feasibility of coronary computed tomography angiography (CCTA) in patients with free-breathing using 256detector CT.

# METHOD AND MATERIALS

616 patients underwent CCTA without heart rate control. 325 examinations were performed during free-breathing (group A), and the remaining 291 were performed during breath-holding(group B). The image quality scores were defined as 1 (excellent), 2 (good), 3 (adequate), and 4 (poor). 22 patients in group A and 24 in group B also underwent invasive coronary angiography (ICA) after CCTA within two weeks. The image quality score, diagnostic performance using ICA as reference, signal-to-noise ratio (SNR), and effective dose (ED) were compared between the two groups.

## RESULTS

Mean heart rate during scanning was 70.8 $\pm$ 13.8 bpm in group A and 70.7 $\pm$ 13.2 bpm in group B (P=0.950). No significant differences were observed in the quality score between breath-holding and free-breathing groups (1.10 $\pm$ 0.31 vs. 1.12 $\pm$ 0.33; P=0.647). The SNR, effective dose were not significantly different between the two groups. In a segment-based analysis, the sensitivity and specificity in the detection of coronary stenosis of more than 50% were 82.1% and 96.8%, respectively in the breath-holding group and 82.2% and 96.6%, respectively in the free-breathing group with no significant differences for these parameters between the two groups.

# CONCLUSION

CCTA for patients without heart rate control and with free-breathing using 256-detector CT showed no significant difference in image quality and diagnostic accuracy compared with patients with breath-holding.

## **CLINICAL RELEVANCE/APPLICATION**

In patients without heart rate control, CCTA can be acquired during free breathing without substantial loss of image quality when using a 256-detector CT.

# SSE03-04 Prognostic Value of Delayed Enhancement Imaging by Cardiac Computed Tomography in Predicting Major Adverse Cardiac Events in Patients with Suspected Coronary Artery Disease

Monday, Nov. 26 3:30PM - 3:40PM Room: N229

Participants

Yoshitaka Goto, MD, Tsu, Japan (*Presenter*) Nothing to Disclose Kakuya Kitagawa, MD, PhD, Tsu, Japan (*Abstract Co-Author*) Nothing to Disclose Satoshi Nakamura, MD, Tsu, Japan (*Abstract Co-Author*) Nothing to Disclose Naoki Nagasawa, RT, PhD, Tsu, Japan (*Abstract Co-Author*) Nothing to Disclose Ahmed H. Heussein, MD,MSc, Tsu, Japan (*Abstract Co-Author*) Nothing to Disclose Masafumi Takafuji, Tsu, Japan (*Abstract Co-Author*) Nothing to Disclose Hajime Sakuma, MD, Tsu, Japan (*Abstract Co-Author*) Nothing to Disclose Group; Research Grant, FUJIFILM Holdings Corporation; Research Grant, Siemens AG; Research Grant, Nihon Medi-Physics Co, Ltd; Speakers Bureau, Bayer AG

# PURPOSE

Myocardial CT delayed enhancement (CTDE) shares the same pathophysiological principle with late gadolinium enhancement MRI, and allows for infarct detection and viability assessment. However, the prognostic value of CTDE is unknown. The purpose of this study was to investigate whether the presence of delayed enhancement (DE) detected by CT is an independent predictor of major adverse cardiac events (MACEs) in patients with suspected coronary artery disease (CAD).

## **METHOD AND MATERIALS**

We studied 429 consecutive patients with suspected CAD who underwent coronary CT angiography (CTA) and CTDE. Patients with known previous myocardial infarction (MI), percutaneous coronary intervention, coronary artery bypass surgery were excluded. MACEs were defined as severe cardiac events (cardiac death, nonfatal MI, unstable angina, heart failure necessitating hospitalization) and late revascularization (>180 days after CT examination). CTA results were divided into obstructive (>=50% luminal narrowing), mild (<50%), or no CAD groups. The Cox proportional hazards model was used to investigate the relationship between conventional clinical risk factors, coronary calcium sore and coronary CTA result and MACEs.

# RESULTS

Follow-up information was obtained in 389 of the 429 patients (91%). DE was observed in 72 of the 389 patients (19%). During a median follow-up of 26 months, 24 cardiac events (2 cardiac death, 2 MI, 2 unstable angina, 6 heart failure and 12 late revascularization) were observed. When adjusted for obstructive CAD, the presence of DE maintained a significant association with risk of all cardiac events (adjusted hazard ratio, 5.9; p < 0.0001) and severe cardiac events (adjusted hazard ratio, 14.2; p = 0.0002). Kaplan-Meier curves demonstrated a significant difference in event-free survival between patients with DE and those without for severe cardiac events (log-rank test, p < 0.0001), as well as for all cardiac events (log-rank test, p < 0.0001).

#### CONCLUSION

The presence of CTDE was an independent predictor of MACEs and severe cardiac events in patients with suspected CAD among common clinical risk factors and coronary CTA findings.

#### **CLINICAL RELEVANCE/APPLICATION**

Acquisition of CTDE following coronary CTA seems to be useful since CTDE provides additional prognostic information in patients with suspected CAD.

# SSE03-05 Factors Affecting FFRCT Analysis in Routine Clinical Practice

Monday, Nov. 26 3:40PM - 3:50PM Room: N229

#### **Student Travel Stipend Award**

Participants

Jonathan Weir-McCall, MBBCh, FRCR, Vancouver, BC (*Presenter*) Speaker, Guerbet SA; Travel suppor, Guerbet SA Gianluca Pontone, MD, Milan, Italy (*Abstract Co-Author*) Speakers Bureau, General Electric Company Consultant, General Electric Company Research Consultant, HeartFlow, Inc Speakers Bureau, HeartFlow, Inc Speakers Bureau, Medtronic plc Speakers Bureau, Bayer AG

Jonathon A. Leipsic, MD, Vancouver, BC (*Abstract Co-Author*) Speakers Bureau, General Electric Company; Speakers Bureau, Edwards Lifesciences Corporation; Consultant, Heartflow, Inc; Consultant, Circle Cardiovascular Imaging Inc; Consultant, Edwards Lifesciences Corporation; Consultant, Neovasc Inc; Consultant, Samsung Electronics Co, Ltd; Consultant, Koninklijke Philips NV; Consultant, Arineta Ltd; Consultant, Pi-Cardia Ltd;

Francesca Pugliese, MD, PhD, London, United Kingdom (*Abstract Co-Author*) Nothing to Disclose Philipp Blanke, MD, Vancouver, BC (*Abstract Co-Author*) Consultant, Edwards Lifesciences Corporation Consultant, Neovasc Inc Consultant, Tendyne Holdings, Inc Consultant, Circle Cardiovascular Imaging Inc Stephanie Sellers, PhD, Vancouver, BC (*Abstract Co-Author*) Nothing to Disclose Jaydeep A. Halankar, MD, DMRD, Toronto, ON (*Abstract Co-Author*) Nothing to Disclose Jang W. Son, Vancouver, BC (*Abstract Co-Author*) Nothing to Disclose Han Y. Jin, Vancouver, BC (*Abstract Co-Author*) Nothing to Disclose

# For information about this presentation, contact:

jweirmccall@gmail.com

# PURPOSE

Reports exist of the acceptance rates of CCTA for FFRCT analysis from trials performed in academic centres, however real world data is lacking. The aim of the current study was to examine the acceptance rate, and the factors associated with rejection for FFRCT analysis.

#### **METHOD AND MATERIALS**

All clinical CCTAs referred between July 2016 and March 2018 for HeartFlow FFRCT analysis were included. Metadata from the submitted CCTAs was used to extract information on patient factors, scanner type, acquisition parameters and dose while HeartFlow FFRCT analysis data was used for quantification of aortic enhancement.

#### RESULTS

Of 10,621 CCTAs submitted, 9,524(89.7%) were accepted for FFRCT analysis. Of the 1,097 rejected: 205(18.7%) were for technical limitations of the submitted data (slice thickness/spacing >=1mm, pixel size >=0.5mm); 181(16.4%) due to the presence of stents, bypass grafts, other cardiac hardware; and 711(64.8%) for image quality. Patient factors associated with rejection were: higher heart rate (64.0(IQR 12.3) vs. 59.0(IQR 10.0) bpm, p<0.001) and heart rate variability (9.0(IQR 21.0) vs. 8.0(IQR 10.0) bpm, p<0.001). Technical factors associated with rejection were: retrospective acquisition (54% vs 31% retrospective, p<0.001), systolic phase acquisition (25% vs. 12% systolic, p<0.001), higher slice thickness (0.63(IQR 0.15) vs. 0.63(IQR 0.07) mm, p<0.001), higher pixel size (0.43(IQR 0.09) vs 0.40(IQR 20) kVp, p<0.001), lower aortic attenuation (368(IQR 147) vs. 431(IQR 167), p<0.001) and higher kVp (120(IQR 0) vs. 120(IQR 20) kVp, p<0.001). BMI (p=0.9), and image noise (p=0.07) were no different in those with accepted or rejected CCTAs. On logistic regression, heart rate, systolic image acquisition, aorta contrast, pixel spacing, and slice thickness all remained significant predictors of rejection for image analysis (p<0.001 for all).

#### CONCLUSION

Almost 20% of FFRCT rejection could be avoided by stringent post processing protocols, and a further 20% by appropriate case selection. For the remainder, utilization of CTFFR requires similar strict heart rate and contrast timing image optimization strategies required of CCTA.

#### **CLINICAL RELEVANCE/APPLICATION**

Stringent patient preparation, case selection and post processing strategies hold potential to improve the opportunity for successful utilization of FFRCT analysis.

## **Honored Educators**

Presenters or authors on this event have been recognized as RSNA Honored Educators for participating in multiple qualifying educational activities. Honored Educators are invested in furthering the profession of radiology by delivering high-quality educational content in their field of study. Learn how you can become an honored educator by visiting the website at: https://www.rsna.org/Honored-Educator-Award/ Jonathan Weir-McCall, MBBCh, FRCR - 2016 Honored EducatorJonathon A. Leipsic, MD - 2015 Honored Educator

# SSE03-06 Interaction of Endurance Sport, Coronary Atherosclerosis and Flow by Coronary Computed Tomography Angiography (CTA): Insights from 3D CFD Modelling

Monday, Nov. 26 3:50PM - 4:00PM Room: N229

Participants

Gudrun Feuchtner, MD, Innsbruck, Austria (*Presenter*) Researcher, HeartFlow, Inc Christian Langer, Innsbruck, Austria (*Abstract Co-Author*) Nothing to Disclose Christoph Beyer, Innsbruck, Austria (*Abstract Co-Author*) Nothing to Disclose Stefan Rauch, Innsbruck, Austria (*Abstract Co-Author*) Nothing to Disclose Fabian Plank, MD, Innsbruck, Austria (*Abstract Co-Author*) Nothing to Disclose

#### PURPOSE

to investigate coronary atherosclerosis and flow physiology by coronary computed tomography angiography (CTA) including 3D computational fluid dynamics (CFD) (noninvasive CT-FFR) in endurance athletes compared to inactive controls (CR)

## **METHOD AND MATERIALS**

90 subjects (ade 56.2v. 26 females) were examined with 128-dual source coronary CTA. Coronary arteries were evaluated per

segment (AHA-16-s-classification) for CAD:1) Stenosis severity (CADRADS 0-5) 2) Total plaque burden (segment involvement score, SIS) and G-score: a new indicator for non-calcified plaque burden3) High risk plaque features (LAP-HU, spotty calcification, NRS, RI) were quantified4) Coronary Fractional Flow reserve (FFR) was remodelled by CFD Study design was retrospective (matched case controlled, 45 endurance-athletes vs 45 CR)The endurance group was defined as "regular" training (cycling, running or others) for least 1h per unit and >=3 times per week. Years of training were recorded.

## RESULTS

Coronary stenosis severity (CAD RADS) score was lower in the endurance group vs CR (1.44 vs 2.1, p=0.007). Total and noncalcified plaque burden (SIS and G-score) were also sign. lower (1.8 vs 3.3; p=0.003 and 3.5 vs 6.6, p=0.002) while calcium score was trended lower only (38.9 AU vs 137.2 AU, p=0.06)HRP prev. was eminenty lower in athletes (5 vs 14 ( 2.2% vs 31.1%) p=0.02), and NRS (4 vs 7), resp.Non-calcified and total plaque burden (G-score and SIS) were strongest and significantly correlated with declining distal FFR ( RCA S4:r=-0.32 and r=-0.3; p=0.03 and p=0.02, LAD S8 r=-0.2, p=0.09 for G-score), while calcium score was not (S4:p=0.07 and S8:p=0.861, Spearman), in the entire cohort. There was no difference in distal FFR between athletes vs CR (p= 0.532, 0.203, 0.358, 0.343 ANOVA)

# CONCLUSION

Regular endurance training (min. 1 h and >=3x/week) reduces CAD burden (coronary stenosis severity, total and non-calcified plaque burden and most eminenty, high-risk plaques). Total and non-calcified plaque burden (G-score) rather than coronary calcium predicts distal coronary flow limitations in both athletes and inactives

## **CLINICAL RELEVANCE/APPLICATION**

Regular endurance training reduces CAD burden and risk, with a dominant effect on high-risk plaque. We describe a novel noncalcifying plaque burden score (G-score), which is easy- to-implement into clinical structural reporting and potentially predicts myocardial ischemia



## Cardiac (MRI: General Topics)

Monday, Nov. 26 3:00PM - 4:00PM Room: N226



AMA PRA Category 1 Credit ™: 1.00 ARRT Category A+ Credit: 1.00

FDA Discussions may include off-label uses.

#### Participants

Pamela K. Woodard, MD, Saint Louis, MO (*Moderator*) Research agreement, Siemens AG; Research, Eli Lilly and Company; Research, F. Hoffmann-La Roche Ltd; ; ; ; ; ;

Harold I. Litt, MD, PhD, Philadelphia, PA (Moderator) Research Grant, Siemens AG ; ; ;

#### Sub-Events

# SSE04-01 Convolutional Neural Network Based Guidance System for Multiplanar Cardiac MRI

Monday, Nov. 26 3:00PM - 3:10PM Room: N226

# Awards Student Travel Stipend Award

Participants Kevin Blansit, MS,BS, La Jolla, CA (*Presenter*) Nothing to Disclose Tara A. Retson, MD, PhD, San Diego, CA (*Abstract Co-Author*) Nothing to Disclose Evan Masutani, La Jolla, CA (*Abstract Co-Author*) Nothing to Disclose Naeim Bahrami, PhD, MSc, San Diego, CA (*Abstract Co-Author*) Nothing to Disclose Kang Wang, MD,PhD, San Diego, CA (*Abstract Co-Author*) Nothing to Disclose Albert Hsiao, MD,PhD, La Jolla, CA (*Abstract Co-Author*) Founder, Arterys, Inc; Consultant, Arterys, Inc; Consultant, Bayer AG; Research Grant, General Electric Company;

#### For information about this presentation, contact:

kblansit@eng.ucsd.edu

## PURPOSE

Cardiac MRI (cMRI) is the gold standard for quantitative cardiac evaluation. However, it requires specialized training and expertise to perform. To advance the accessibility and quality of cMRI, we developed a convolutional neural network (CNN) to localize key cardiac landmarks to guide plane prescription. We hypothesize that CNN-based landmark localization may generate similar imaging planes to those acquired by a dedicated cardiac technologist.

# METHOD AND MATERIALS

With HIPAA-compliance and IRB waiver of informed consent, we retrospectively collected clinical cMRIs performed at our institution from February 2012 to June 2017, including 472 short axis (SAX) and 892 long axis (LAX) cine series. Anatomic landmarks were annotated by expert radiologists. U-Net CNNs were implemented to predict the location of these structures using heatmap localization. Data was split into 80% of cases for training and 20% for testing. SAX, 4, 3, and 2 chamber planes were computed from predicted anatomic localizations. We analyzed performance of localization by calculating distances between predictions and ground truth annotation, and report mean error and standard deviations. We assessed plane prescription by calculating the angle difference between CNN-predicted planes and those acquired by the technologist. Angle bias, mean error, and standard deviations are reported for each plane orientation.

### RESULTS

From LAX images, the mean distance between annotation and predicted location was 7.70±5.90 mm for apex and 5.70±4.02 mm for the mitral valve. For SAX images, the mean distance was 11.99±7.80 mm for aortic valve, 10.20±5.65 mm for mitral valve, 12.56±5.10 mm for pulmonic valve, and 11.99±6.43 mm for tricuspid valve. For SAX stack prescription, average angle bias, mean error, and standard deviations were -7.80°, 7.80°±5.44°. For LAX prescriptions, average angle bias, mean error, and standard deviations were 5.64°, 6.65°±5.22° for 4-chamber, 10.86°, 11.95°±8.02° for 3-chamber, and 4.21°, 7.46°±7.36° for 2-chamber.

# CONCLUSION

CNN-based anatomic localization is a feasible strategy for planning cMRI imaging planes. In this study, we show that this approach can produce imaging planes similar to those chosen by dedicated cardiac technologists.

# **CLINICAL RELEVANCE/APPLICATION**

CNNs have the potential to improve the quality and accessibility of MRI, and may even benefit complex examinations like cardiac MRI, which require multiple double oblique image planes.

## SSE04-02 Deep Learning for Accelerated CMR Image Reconstruction

# Participants

Jo Schlemper, London, United Kingdom (*Presenter*) Nothing to Disclose Chen Qin, London, United Kingdom (*Abstract Co-Author*) Nothing to Disclose Jose Caballero, London, United Kingdom (*Abstract Co-Author*) Nothing to Disclose Ozan Oktay, PhD, London, United Kingdom (*Abstract Co-Author*) Nothing to Disclose Wenjia Bai, DPhil, London, United Kingdom (*Abstract Co-Author*) Nothing to Disclose Giacomo Tarroni, London, United Kingdom (*Abstract Co-Author*) Nothing to Disclose Anthony Price, London, United Kingdom (*Abstract Co-Author*) Nothing to Disclose Jo Hajnal, London, United Kingdom (*Abstract Co-Author*) Nothing to Disclose Daniel Rueckert, PhD, London, United Kingdom (*Abstract Co-Author*) Nothing to Disclose

## For information about this presentation, contact:

jo.schlemper11@imperial.ac.uk

## PURPOSE

CMR acquisition is inherently time consuming and requires multiple breath-holds, which is not only challenging for many patients, but it also makes the modality susceptible to motion artefacts. The aim of this study is to accelerate the CMR data acquisition by reducing the amount of k-space data needed for reconstructing images from undersampled data.

## **METHOD AND MATERIALS**

Fully sampled, short-axis cardiac cine MR scans from 10 volunteers were acquired. Each scan contains a single slice SSFP acquisition with 30 temporal frames, resolution of 256x256 pixels, FOV of 320x320 mm with slice thickness 10mm. The recombined single-coil images were retrospectively undersampled respecting a linear frequency/phase encode structure, while the central 8 lines in k-space were always included. Deep learning-based iterative denoising algorithms are proposed: 3D-convolutional neural network (CNN) and 2D-convolutional recurrent neural network (CRNN). The networks were trained to directly output clean image from the aliased image. The proposed methods were compared to state-of-the-art compressed sensing approaches: kt-FOCUSS and kt-SLR. The methods were evaluated using peak signal-to-noise ratio (PSNR) and reconstruction speed. We considered acceleration factors 6 and 9 and performed 3-fold cross validation.

#### RESULTS

The networks were trained within three days on GPU GeForce GTX 1080. Even from small number of training subjects one could train a network that works well on test data. For acceleration factor 6, PSNR was 32.5, 34.6, 37.2 and 37.37 dB for kt-FOCUSS, kt-SLR, CRNN and CNN respectively. For acceleration factor 9, the numbers were 29.7, 31.4, 33.3 and 34.95 dB respectively. The reconstruction speeds were 15, 450, 6 and 10 seconds respectively.

## CONCLUSION

We have proposed deep learning-based approaches for CMR image reconstruction, which both outperform current state-of-the-art both in terms of speed and reconstruction quality for single-coil, retrospective undersampling study.

#### **CLINICAL RELEVANCE/APPLICATION**

The method will be able to accelerate the CMR acquisition, which reduces burden on patients and improves image quality. In future, parallel imaging extension and implementation on scanner is expected.

# SSE04-03 Multiparametric Cardiovascular Magnetic Resonance Imaging Assessment in End Stage Renal Disease Patients with Preserved Left Ventricular Ejection Fraction

Monday, Nov. 26 3:20PM - 3:30PM Room: N226

Participants

Xuhui Zhou, MD, PhD, Shenzhen, China (*Abstract Co-Author*) Nothing to Disclose Ling Lin, MD, Leiden, Netherlands (*Presenter*) Nothing to Disclose Qiuxia Xie, Guangzhou, China (*Abstract Co-Author*) Nothing to Disclose Yang Peng, Guangzhou, China (*Abstract Co-Author*) Nothing to Disclose Hildo J. Lamb, MD, PhD, Leiden, Netherlands (*Abstract Co-Author*) Nothing to Disclose

For information about this presentation, contact:

l.lin@lumc.nl

## PURPOSE

Early detection of cardiac dysfunction in end stage renal disease (ESRD) patients is beneficial but challenging. Our study aimed to evaluate myocardial strain and tissue characteristic changes by cardiovascular magnetic resonance (CMR) imaging in ESRD patients with preserved left ventricular ejection fraction (LVEF), especially focused on those with no echocardiographic evidence of diastolic dysfunction.

# METHOD AND MATERIALS

29 ESRD patients (17 males; mean age 44±11 years) with LVEF >50% in ultrasonagraphy and 43 healthy volunteers (24 males; mean age 43±10 years) underwent CMR imaging including cine, native T1 and T2 mapping. LV function, global LV strains as well as LV myocardial native T1 and T2 of the mid-cavity slice were measured and compared between the two groups. Correlations between LVMASS and CMR parameters were analyzed. According to ASE/EACVI recommendations for the evaluation of LV diastolic function by echocardiography, ESRD group were divided into normal diastolic function subgroup (n=11) and diastolic dysfunction subgroup (n=18). CMR parameters were compared among the two subgroups and the healthy group.

#### RESULTS

Native T1 and T2 were statistically higher in ESRD group ( $1296.2\pm38.4ms$ ,  $44.0\pm2.8ms$ ) than healthy group ( $1260.1\pm51.9ms$ ,  $41.0\pm1.7ms$ ; p=0.002, p<0.001). LV Global longitudinal strain (GLS) and global circumferential strain (GCS) were statistically

impaired in ESRD group (-14.5 $\pm$ 2.9%, -16.4 $\pm$ 3.0%) compared with the healthy group (-16.5 $\pm$ 2.2%, -18.2 $\pm$ 2.5%; p=0.002, 0.008). Increased LVMASS was strongly associated with impaired LV GLS and GCS (r= 0.72, 0.73; p<0.001) in ESRD group. In subgroup with normal diastolic function, T2 (43.2 $\pm$ 1.5ms) and LV GLS (-14.3 $\pm$ 3.0%) were statistically different from those in the healthy group (p=0.002, 0.008), while native T1 and LV GCS were similar with those in the healthy group.

# CONCLUSION

ESRD patients with preserved LVEF demonstrated higher myocardial native T1, T2, and impaired LV GLS and GCS compared with healthy people. Myocardial edema and decreased myocardial compliance might exist in ESRD patients with preserved LVEF and normal diastolic function, as indicated by higher T2 and impaired LV GLS.

## **CLINICAL RELEVANCE/APPLICATION**

Early stage of myocardial fibrosis, edema and decreased myocardial compliance might exist in ESRD patients with preserved LVEF, even when their diastolic function is normal on echocardiography.

# SSE04-04 Subharmonic Aided Pressure Estimation (SHAPE) for Obtaining Intra-Cardiac Pressures Noninvasively in Real-Time: Preliminary Results

Monday, Nov. 26 3:30PM - 3:40PM Room: N226

#### Participants

Cara Esposito, Philadelphia, PA (Abstract Co-Author) Nothing to Disclose Jaydev K. Dave, PHD, Philadelphia, PA (Presenter) Research Grant, Koninklijke Philips NV; Equipment support, Lantheus Medical Imaging, Inc; Equipment support, General Electric Company Flemming Forsberg, PhD, Philadelphia, PA (Abstract Co-Author) Research Grant, Canon Medical Systems Corporation; Research Grant, General Electric Company; Research Grant, Siemens AG; Research Grant, Lantheus Medical Imaging, Inc Maureen McDonald, MBA, Philadelphia, PA (Abstract Co-Author) Nothing to Disclose Priscilla Machado, MD, Philadelphia, PA (Abstract Co-Author) Nothing to Disclose Kris Dickie, Burnaby, BC (Abstract Co-Author) Employee, Clarius Mobile Health Corp Ira S. Cohen, Philadelphia, PA (Abstract Co-Author) Nothing to Disclose Praveen Mehrotra, MD, Philadelphia, PA (Abstract Co-Author) Nothing to Disclose Michael Savage, MD, Philadelphia, PA (Abstract Co-Author) Nothing to Disclose David Fischman, Philadelphia, PA (Abstract Co-Author) Nothing to Disclose Nicholas J. Ruggiero II, MD, Philadelphia, PA (Abstract Co-Author) Nothing to Disclose Paul Walinsky, MD, Philadelphia, PA (Abstract Co-Author) Nothing to Disclose Andrew Boyle, Philadelphia, PA (Abstract Co-Author) Nothing to Disclose Eron Sturm, Philadelphia, PA (Abstract Co-Author) Nothing to Disclose Marguerite Davis, Philadelphia, PA (Abstract Co-Author) Nothing to Disclose

# For information about this presentation, contact:

jaydev.dave@jefferson.edu

# PURPOSE

Subharmonic aided pressure estimation (SHAPE) utilizes subharmonic signals from ultrasound contrast agents for pressure estimation. The purpose of this work was to evaluate the efficacy of intra-cardiac SHAPE using Definity (Lantheus Medical Imaging) and Sonazoid (GE Healthcare) microbubbles in patients scheduled for cardiac catheterization procedures.

#### **METHOD AND MATERIALS**

Patients scheduled for left and/or right heart catheterization procedures were recruited into this IRB-approved study. During the catheterization procedure, 15 patients received an infusion of Definity (2 activated vials mixed in 50 mL saline; 4-10 mL per minute) and 3 patients received a co-infusion of Sonazoid (infusion rate (mL/hour) = 0.18 x body weight in kg) and saline (120 mL/hour). During contrast infusion, the patients were scanned using a customized interface developed on a SonixTablet scanner (BK Ultrasound; interface developed using C/C++ and cross-platform Qt libraries (The Qt Company)) to determine optimum incident acoustic output (IAO; from a set of 16 pre-configured acoustic outputs coded from 0 or minimum to 15 or maximum) eliciting ambient pressure sensitive growth phase subharmonics for SHAPE, on a per-patient basis. Previously determined optimal parameters for Definity (ftransmit: 3.0 MHz; a chirp down pulse) and Sonazoid (ftransmit: 2.5 MHz; square wave pulse) were used for data acquisition. Correlation coefficient between the SHAPE and pressure catheter data was computed using MATLAB (2016A, The MathWorks, Inc.).

## RESULTS

The IAO's at which the best correlation coefficient obtained between the SHAPE and pressure catheter data varied on a perpatient basis from coded values of 3 to 15 (patient BMI range: 22.7-64.6). Data with Definity infusion showed that the correlation coefficient between SHAPE and pressure catheter for the left ventricle (LV) was  $-0.8 \pm 0.03$  (mean  $\pm$  standard deviation; n = 10) and for the right ventricle (RV) was  $-0.8 \pm 0.08$  (n = 12). Data with Sonazoid infusion showed the correlation coefficient between SHAPE and pressure catheter for the LV was  $-0.8 \pm 0.04$  (n = 2) and the RV was -0.8 (n = 1).

## CONCLUSION

Preliminary results indicate a good correlation (correlation coefficient range: -0.7 to -0.9) between SHAPE and pressure-catheter based intra-cardiac pressures.

#### **CLINICAL RELEVANCE/APPLICATION**

Intra-cardiac SHAPE may become an effective noninvasive alternative to cardiac catheterization procedures.

# SSE04-05 Transient Ischemic Dilation and Coronary Artery Disease Burden in Cardiac MRI

Monday, Nov. 26 3:40PM - 3:50PM Room: N226

# For information about this presentation, contact:

jmyan@mcw.edu

# PURPOSE

Transient Ischemic Dilation (TID) is a well-established finding in nuclear myocardial perfusion imaging (MPI) and is a marker for coronary artery disease (CAD) severity. Stress perfusion cardiac MRI (CMR) offers significantly improved spatial and temporal resolution relative to MPI and allow for direct measurement of the LV wall cavity dimensions. Despite these advantages, CMR-derived TID ratios are not well established and thus not utilized in the clinical setting for CAD severity. The aim of this study was to confirm whether TID occurs during stress perfusion CMR and define a TID ratio that predict the presence and severity of CAD.

# **METHOD AND MATERIALS**

Patients who underwent a complete stress CMR from 2012-2016 were included in the study. Imaging studies were analyzed and stress and rest left ventricular (LV) area at three myocardial cross-sections, basal, mid, and apex, was recorded. Coronary angiographic data for all patients with this information available was reviewed. TID ratio was calculated as the LV cavity area minus papillary muscles at stress versus rest. Global TID ratio was calculated by taking the mean of the segments (basal, mid, and apex) for each patient. Patients were classified into High Risk group if angiography results show >= 70% stenosis in the proximal LAD, >= 70% stenosis in the Left Main, >=90% lesion in more than 2 major vessels, or prior CABG with >=70% graft lesion. Unpaired t-test was used to compare mean values of High Risk and Low Risk groups and a ROC analysis was performed to determine the global TID ratio that differentiated patients with High Risk CAD versus Low Risk CAD.

#### RESULTS

One hundred forty three patients underwent stress CMR. Fourteen patients met criteria for High Risk CAD on coronary angiography, while the remainder had either negative stress or positive stress with low risk CAD. Mean Global TID ratio for high risk group was 1.18 vs 0.98 in the low risk group (p = 0.004). AUC in the ROC analysis was 0.734 (p=0.004). Associated criterion maximizing specificity revealed global TID ratio > 1.16 with a sensitivity of 57% and specificity of 85%.

#### CONCLUSION

Significant dilation in the LV area at stress occurs when severe CAD is present compared to rest.

## CLINICAL RELEVANCE/APPLICATION

A global stress to rest ratio of 1.16 in cardiac stress MRI may provide an additional marker for identifying high-risk multi-vessel CAD.

# SSE04-06 Is Cardiac MR Indispensable for Assessing the Cardiac Mass?: Based on the Review of 10-Years of Hospital Records

Monday, Nov. 26 3:50PM - 4:00PM Room: N226

Participants

Ji Eun Park, Seongnam, Korea, Republic Of (*Presenter*) Nothing to Disclose Eun Ju Chun, MD, PhD, Seongnam-Si, Korea, Republic Of (*Abstract Co-Author*) Nothing to Disclose Jeong A Kim, MD, Goyangsi, Korea, Republic Of (*Abstract Co-Author*) Nothing to Disclose Jin Young Yoo, MD, Cheongju, Korea, Republic Of (*Abstract Co-Author*) Nothing to Disclose Yeonyee E Yoon, Sengnam, Korea, Republic Of (*Abstract Co-Author*) Nothing to Disclose

# PURPOSE

Although cardiac magnetic resonance (MR) is useful for assessing cardiac mass, it has limited to use as the first modality because of high cost and long scan times. Therefore, we aimed to evaluate how MR is effective in assessing the cardiac mass based on the review of 10-years of hospital records.

# METHOD AND MATERIALS

We hypothesized that cardiac mass is firstly detected with echocardiography, and further evaluated with CT and MR. On the basis of echocardiography from 2008 to 2017 in single tertiary hospital, we searched patients with cardiac mass using ICD code and keywords. Cardiac mass was classified by the location (intracardiac, valve and extracardiac) and evaluated the transferred ratio to next modality (CT or MR) from echocardiography according to mass location. Finally, we evaluated why the clinician performed MR and how successful that goal was achieved.

#### RESULTS

In a total of 718 adults (390 males,  $62.6\pm18.7$  years) with cardiac mass (282 intracardiac mass, 262 valve mass, 174 extracardiac mass) which detected on echocardiography, 406 patients (56.5%) were performed CT. Among them, CT performed ratio is highest for extracardiac mass (92.0%) followed by intracardiac mass (66.0%) and valve mass (22.9%), sequentially. MR was performed in 64 patients (8.9%); 16 patients with directly performed MR, 48 patients were performed MR after CT. Role of MR in assessing the cardiac mass was as follows; tissue characterization (n=36), differentiation of thrombus from tumor (n=15) and detection of invasiveness (n=25). After MR, the successful rate which met the goals of MR was highest for detection of invasiveness (92.0%), followed by differentiation of thrombus (80.0%) and tissue characterization (61.1%).

# CONCLUSION

Valve mass may be sufficient with echocardiography, and extracardiac mass requires CT to assess the extent. CMR is useful for determine invasiveness and differentiate thrombus from tumor than tissue characteristics

# **CLINICAL RELEVANCE/APPLICATION**

From this review of our data, the efficacy of CMR for assessing cardiac mass might be higher to determine the invasiveness and differentiate the thrombus from tumor than to detect tissue characteristics.



## Chest (Airway Disease)

Monday, Nov. 26 3:00PM - 4:00PM Room: N230B



AMA PRA Category 1 Credit ™: 1.00 ARRT Category A+ Credit: 1.00

FDA Discussions may include off-label uses.

#### Participants

Yoshiharu Ohno, MD, PhD, Kobe, Japan (*Moderator*) Research Grant, Canon Medical Systems Corporation; Research Grant, Koninklijke Philips NV; Research Grant, Bayer AG; Research Grant, DAIICHI SANKYO Group; Research Grant, Fuji Pharma Co, Ltd; Research Grant, Guerbet SA;

Matthew J. DeVries, MD, Omaha, NE (Moderator) Nothing to Disclose

## Sub-Events

# SSE05-01 Generation-Based Airway Remodeling in Smokers with Normal-Looking CT: After Normalization to Control Inter-Subject Variability

Monday, Nov. 26 3:00PM - 3:10PM Room: N230B

Participants

Kum Ju Chae, MD, Jeonju, Korea, Republic Of (*Presenter*) Nothing to Disclose Gong Yong Jin, MD, PhD, Jeonju, Korea, Republic Of (*Abstract Co-Author*) Nothing to Disclose Jiwoong Choi, PhD, Seoul, Korea, Republic Of (*Abstract Co-Author*) Nothing to Disclose Chang Hyun Lee, MD, PhD, Seoul, Korea, Republic Of (*Abstract Co-Author*) Nothing to Disclose Sanghun Choi, Daegu, Korea, Republic Of (*Abstract Co-Author*) Nothing to Disclose Ching-Long Lin, PhD, Iowa City, IA (*Abstract Co-Author*) Nothing to Disclose Eric A. Hoffman, PhD, Iowa City, IA (*Abstract Co-Author*) Founder, VIDA Diagnostics, Inc; Shareholder, VIDA Diagnostics, Inc; Advisory Board, Siemens AG

#### For information about this presentation, contact:

para2727@gmail.com

## PURPOSE

As the quantitative airway analysis has been evolved, the effect of smoking has been established. However, the generation-based smoking effect where inter-subject variabilities are normalized is rarely known. The purpose of this study is to evaluate a prediction model of airway parameters, and further to investigate generation-based structural and functional airway alterations in smokers with the derived normalization scheme.

#### **METHOD AND MATERIALS**

68 smokers and 174 nonsmokers with inspiratory/expiratory CT findings, and normal pulmonary function tests were included in the study. VIDA Apollo software (Coralville, IA) was used for the airway size analysis. To control inter-subject variability, multiple linear regressions of tracheal wall thickness (WT), diameter (D), and luminal area (LA) were used for the normalization of airway parameters considering the effects of age, sex and height. Using this scheme, each airway parameter was normalized by individual predicted values, and normalized WT (WT\*), D (D\*), LA (LA\*) from the 1st to 8th generation of each lobe were compared between smokers and non-smokers.

#### RESULTS

LA\* and D\* decreased and WT\* increased in the smokers after normalization (p<0.05), which was not observed before normalization. The wall thickness of the segmental airways in smokers was not changed between inspiration and expiration (WT\*ins-WT\*exp= 0.01±0.01), whereas that in non-smokers was thicker at expiration than inspiration (-0.02±0.01). Besides, airways at the 3rd generation showed significant wall thickening in smokers than nonsmokers (p=0.003).

#### CONCLUSION

Quantitative CT assessment using a normalization scheme suggest that smoking may induce airway wall thickening and reduce changes of wall thickening during respiration, which means a decrease in airway wall compliance. Generation-based analysis showed that the 3rd generation is most affected by smoking.

## **CLINICAL RELEVANCE/APPLICATION**

When it comes to the effect of smoking, it is important to perform normalization and focus on wall thickening of segmental airways.

# SSE05-02 Enhanced Evaluation of Tracheomalacia with Use of Cyclic Ultra-low Dose Dynamic Expiratory CT

Monday, Nov. 26 3:10PM - 3:20PM Room: N230B

#### **Student Travel Stipend Award**

Participants Seung Y. Lee, MD, Manhasset, NY (*Presenter*) Nothing to Disclose Eran Ben-Levi, MD, Lake success, NY (*Abstract Co-Author*) Nothing to Disclose Navid Rahmani, MD, Manhasset, NY (*Abstract Co-Author*) Nothing to Disclose Amar B. Shah, MD, New York, NY (*Abstract Co-Author*) Nothing to Disclose Rakesh D. Shah, MD, Manhasset, NY (*Abstract Co-Author*) Nothing to Disclose Stuart L. Cohen, MD, manhasset, NY (*Abstract Co-Author*) Nothing to Disclose

## For information about this presentation, contact:

slee55@northwell.edu

# PURPOSE

The percent tracheal area narrowing (%TN) between paired inspiration CT and dynamic expiratory CT (DECT) is used to diagnose and grade tracheomalacia (TM). At our institution this is done clinically with the maximum %TN on either of two consecutive ultra low dose DECTs (mDECT). This study aims to evaluate the implications of mDECT vs. single DECT in TM diagnosis and grading.

## METHOD AND MATERIALS

CT studies for evaluation of TM from 2017 performed at a single imaging site were retrospectively evaluated. CT protocol of one routine inspiratory chest CT and two consecutive ULD (100 kVp, fixed mA 10) DECT. The %TN for each DECT was obtained by comparing the greatest percent tracheal narrowing on anatomically matched expiration and inspiration CT, measured independently for DECT 1 and 2. Tracheal area was measured manually delineating the luminal contour of the trachea with the free-hand PACS ROI tool on 2.5 mm axial slices by a thoracic fellowship trained radiologist. The presence of TM (>70 %TN) and its severity (negative <70%, mild 70-80%, moderate 80-90%, severe >90%) were assessed. The mean %TN, percent of patients with TM diagnosis, and distribution of TM severity between DECT1, DECT2 and mDECT were analyzed using paired 2-tailed t-test, 2-tailed binomial proportions test, and chi-squared test, respectively.

#### RESULTS

184 patients (41% male) with mean age of 64 were analyzed. Mean radiation dose for each DECT phase was 0.07 mSv with all studies deemed diagnostic. mDECT demonstrated 57 mean %TN, 10% greater than DECT1 and 6% greater than DECT2 (each p<0.001), with DECT2 9% greater mean %TN than DECT1 (p<0.05). 40% Percentage of patients with TM diagnosis with mDECT (40%) was 10% greater than DECT1 or 2 (each 30%, p<0.05). mDECT (109 negative, 31 mild, 24 moderate, and 20 severe) had significantly greater number of patients diagnosed with TM with a significantly more severe distribution of disease than DECT1 (128, 27, 21, 12) or DECT2 (127, 21, 21, 15), (each p<0.05) without significant differences between DECT1 and 2.

# CONCLUSION

For CT evaluation of TM, mDECT demonstrated low patient radiation dose with an increase in mean %TN, a higher rate of TM diagnosis and a more severe distribution of disease than a single DECT phase alone.

## **CLINICAL RELEVANCE/APPLICATION**

CT evaluation of TM with two ultra low dose DECTs should be considered to diagnose and grade TM.

# SSE05-04 Correlation of CT Small Airway Measurement with Clinical and Inflammation Factors in Asthma Patients

Monday, Nov. 26 3:30PM - 3:40PM Room: N230B

Participants Meijiao Li, MD, Beijing, China (*Presenter*) Nothing to Disclose Wei Guo, Beijing, China (*Abstract Co-Author*) Nothing to Disclose Huishu Yuan, Beijing, China (*Abstract Co-Author*) Nothing to Disclose

# For information about this presentation, contact:

newgljyk@163.com

#### PURPOSE

To evaluate the correlation of CT small airway measurement with clinical and inflammatory indicators in Asthma Patients.

## **METHOD AND MATERIALS**

20 patients with asthma were enrolled, all received spiral CT, pulmonary function test, serum leptin, IgE and TGF-B1, induced sputum cytology and MMP-9. Asthma Control Test (ACT) and smoking condition were recorded. At the end of 6th generation airway, adjusted by body surface area, Luminal diameter(LD), luminal area(Ai), wall thickness(WT) and wall area%(WA%)were measured. Inter-observer repeatability was estimated by intra-class correlation coefficients(ICC). Comparison of the CT airway indexes between groups of onset age<=12yrs and>12yrs, ACT well/partly controlled and poorly controlled, with and without smoking history, induced sputum Eos%<3% and >=3% were made. Correlations between CT airway measurements with clinical and inflammatory indicators were determined.

# RESULTS

The ICC of LD, Ai , WT and WA% was 0.813, 0.923, 0.850, 0.958. In asthma patients, both LD and Ai were significantly lower in groups of onset age <=12yrs, patients with smoking history and induced sputum Eos%>=3% than corresponding groups(LD, t=-2.760, -2.459, -3.935, Ai, t=-2.851, -2.267, -4.492, all P<0.05). WA% was significantly higher in groups of induced sputum Eos%>=3% than the corresponding group(t=2.448, P<0.05). LD and Ai had negative correlation with course of disease and induced sputum Eos%(LD, r=-0.512, -0.841, Ai, r=-0.489,-0.841, all P<0.05), and positive correlation with FEV1/FVC and serum leptin(LD, r=0.669, 0.533, Ai, r=0.681,0.552, all P<0.05). Ai also showed positive correlation with FEV1%(r=0.452, P<0.05). WT and WA% were significantly negative correlated with FEV1/FVC and FEV1%(WT, r=-0.621, -0.483, WA%, r=-0.729, -0.548, all P<0.05). WA% also showed positive correlation with serum IgE and induced sputum MMP-9(r=0.509, 0.636, all P<0.05).

## CONCLUSION

CT airway indexes were found partially associated with asthma onset age, course of disease, smoking condition, serum leptin and IgE, induced sputum Eos% and MMP-9,. CT airway indexes showed correlation with FEV1/FVC and FEV1%.

# **CLINICAL RELEVANCE/APPLICATION**

CT indexes of small airway were found associated with asthma onset age, course of disease, smoking condition, serum leptin and IgE, induced sputum Eos% and MMP-9, as well as FEV1/FVC and FEV1%.

#### SSE05-05 A Comparative Study of Performance Between Radiographers and Machine Learning Model (MLM) for **Airway Measurement**

Monday, Nov. 26 3:40PM - 3:50PM Room: N230B

#### Participants

Hee J. Park, MS, Seoul, Korea, Republic Of (Presenter) Nothing to Disclose Sang Min Lee, MD, Seoul, Korea, Republic Of (Abstract Co-Author) Nothing to Disclose Hyungi Seo, Seoul, Korea, Republic Of (Abstract Co-Author) Employee, Coreline Soft, Co Ltd Mi Jeong Song, Seoul, Korea, Republic Of (Abstract Co-Author) Nothing to Disclose Jahee Gu, Seoul, Korea, Republic Of (Abstract Co-Author) Nothing to Disclose Ilsang Woo, MS , Seoul, Korea, Republic Of (Abstract Co-Author) Nothing to Disclose Jongha Park, Seoul, Korea, Republic Of (Abstract Co-Author) Nothing to Disclose Joon Beom Seo, MD, PhD, Seoul, Korea, Republic Of (Abstract Co-Author) Nothing to Disclose Namkug Kim, PhD, Seoul, Korea, Republic Of (Abstract Co-Author) Stockholder, Coreline Soft, Co Ltd Sang Young Oh, MD, Seoul, Korea, Republic Of (Abstract Co-Author) Nothing to Disclose Sang Min Lee, MD, Seoul, Korea, Republic Of (Abstract Co-Author) Nothing to Disclose Hye Jeon Hwang, MD, PhD, Seoul, Korea, Republic Of (Abstract Co-Author) Nothing to Disclose

#### PURPOSE

The purpose of this study is to compare the performance between radiographers and machine learning model of analyzing airway.

# **METHOD AND MATERIALS**

Total 182 patients' thin slice CT data of KOLD cohort was used and their all airway branches were semi-automatically segmented by AView software (Coreline Soft, Co., Ltd, South Korea). 46,436 airway axial images were used to train MLM using DenseNet 201 that we changed the last DenseLayer to binary classification. All airway axial images were colored using integral-based half-band method and they were labeled as accept or reject to clarify and precise airway results. In randomly selected 50 axial images, accuracy was compared among two radiographers with 4-year experience on airway measurement and MLM. Cohen's Kappa was used to assess the inter-observers agreement and elapsed time was measured. T-test, in addition, was performed to compare airway results on 182 patients of KOLD cohort between one blinded radiographer and MLM.

# RESULTS

The ROC analysis of the test data sets showed 0.92 of area under curve. In the 50 randomly selected airway axial images, Sensitivity, specificity of MLM were 0.96, 0.88 and its accuracy was 0.92. In radiographers, respectively, 0.86, 0.7 and 0.78 were shown (Cohen's kappa = 0.62). Elapsed time between two control groups, two radiographers and MLM, showed statistically significant difference (190.3 and 1.8 seconds, p < 0.05). The mean airway pi-10 and wall area percent showed no statistically significant difference (radiographer,  $4.12 \pm 0.89$  mm,  $66.43 \pm 7.56$  %; MLM,  $4.15 \pm 0.88$  mm,  $66.66 \pm 7.35$  %, p > 0.05, respectively).

# CONCLUSION

Trained MLM showed no differences comparing with skilled radiographers in the results of airway measurement with short elapsed time. Consequentially, MLM measures all airway branches fully automatically without expert interactions, if airway segmentation well performed.

# **CLINICAL RELEVANCE/APPLICATION**

The airway is considered as an imperative index of lung. Fully automatic airway measurement of whole branch would be more efficient for imaging biomarker in COPD patients.

#### SSE05-06 Catheter-Based Endobronchial Navigation with a Novel Cone Beam CT Airway Segmentation Platform to Reach Peripheral Lung in a Swine Model Without Bronchoscopy

Monday, Nov. 26 3:50PM - 4:00PM Room: N230B

Participants

Quirina M. de Ruiter, PhD, Bethesda, MD (Presenter) Former Employee, Koninklijke Philips NV; ; John W. Karanian, PhD, Laurel, MD (Abstract Co-Author) Nothing to Disclose Stephanie Schampaert, Best, Netherlands (Abstract Co-Author) Employee, Koninklijke Philips NV Martijn Van Der Bom, MSC, Andover, MA (Abstract Co-Author) Employee, Koninklijke Philips NV Joseph Fontana, Bethesda, MD (Abstract Co-Author) Nothing to Disclose Bradford J. Wood, MD, Bethesda, MD (Abstract Co-Author) Researcher, Koninklijke Philips NV; Researcher, Celsion Corporation; Researcher, BTG International Ltd; Researcher, Siemens AG; Researcher, XAct Robotics; Researcher, NVIDIA Corporation; Intellectual property, Koninklijke Philips NV; Intellectual property, BTG International Ltd; Royalties, Invivo Corporation; Royalties, Koninklijke Philips NV; ; Alessandro G. Radaelli, PHD, MS, Best, Netherlands (Abstract Co-Author) Employee, Koninklijke Philips NV William van der Sterren, MSc, Best, Netherlands (Abstract Co-Author) Employee, Koninklijke Philips NV Juan Esparza-Trujillo, Bethesda, MD (Abstract Co-Author) Nothing to Disclose Ivane Bakhutashvili, Bethesda, MD (Abstract Co-Author) Nothing to Disclose William F. Pritchard JR, MD, PhD, Bethesda, MD (Abstract Co-Author) Research collaboration, Koninklijke Philips NV; Research collaboration, Biocompatibles International plc; Research collaboration, BTG International Ltd; Research collaboration, Siemens AG; Research collaboration, Act Robotics; Research collaboration, W. L. Gore & Associates, Inc; Research collaboration, Celsion

# Corporation

# PURPOSE

To investigate the feasibility of catheter-based endobronchial navigation to peripheral lung without a bronchoscope using a novel Cone Beam CT (CBCT) image-guidance prototype in a swine model.

# METHOD AND MATERIALS

All animal procedures were approved by the Animal Care and Use Committee. Swine (n=3) were placed under general anesthesia. Thoracic CBCT (FD20, Philips Healthcare) was imported into a workstation with prototype software (Philips) that provides for 3D airway segmentation, manual identification of targets and 3D navigation guidance superimposed on fluoroscopic imaging. Peripheral targets (bronchial subsegments) were identified. Catheter-based endobronchial navigation to targets was performed with 4 and 5 Fr catheters (Cook Medical) with varying shapes (e.g., C2, multipurpose, DAV) over 0.035' hydrophilic vascular guidewires of various curves and stiffness (Terumo). The primary endpoint was successful navigation of a catheter into a bronchial target. Success was assessed by catheter position on multiple X-ray images at preplanned C-arm angles and CBCT.

#### RESULTS

Catheter-based navigation to primarily 3rd and 4th order airway segments was successful in 11/13 tasks in the first two swine. Failure to navigate guidewires to distal targets occurred when the guide wire or catheter tip was too stiff with poor maneuverability or had a sub-optimal shape for the airway geometry. With optimization of device selection and imaging settings, catheter-based navigation to even more complex 4th and 5th order segments targets was successful in 8/11 tasks; navigation failures occurred due to suboptimal catheter or wire shape or stiffness for the target (n = 2) or suboptimal imaging settings (n=1). In these cases, operator adherence to predefined fluoroscopic imaging protocols also restricted identification of malposition and adjustments that might otherwise occur.

# CONCLUSION

Catheter-based endobronchial navigation without a bronchoscope is feasible with CBCT 3D segmentation and image-guidance combined with fluoroscopy. Catheter and wire design, including size, shape and physical properties, are important predictors of navigation success, especially for more peripheral airway tasks.

## **CLINICAL RELEVANCE/APPLICATION**

CBCT airway segmentation and guidance software may advance endobronchial catheter-based approaches for lung diagnostics and treatments beyond the reach of a bronchoscope. Catheter and wire selection impacts procedural success.



# Science Session with Keynote: Emergency Radiology (Forensic and Musculoskeletal Imaging)

Monday, Nov. 26 3:00PM - 4:00PM Room: E353A



AMA PRA Category 1 Credit ™: 1.00 ARRT Category A+ Credit: 1.00

## **Participants**

Scott D. Steenburg, MD, Zionsville, IN (*Moderator*) Research collaboration, IBM Corporation Martin L. Gunn, MBChB, Seattle, WA (*Moderator*) Research Grant, Koninklijke Philips NV; Royalties, Cambridge University Press; Spouse, Consultant, Reed Elsevier; Spouse, Consultant, athenahealth, Inc

#### Sub-Events

# SSE06-01 Emergency Radiology Keynote Speaker: Post-Mortem CT for Trauma

Monday, Nov. 26 3:00PM - 3:20PM Room: E353A

Participants

Scott D. Steenburg, MD, Zionsville, IN (Presenter) Research collaboration, IBM Corporation

# SSE06-03 Evaluation of Organ Density Values in Postmortem Computed Tomography (PMCT) in Correlation with Radiological Alteration Index (RAI) as Possible Surrogate for Postmortal Alteration in Human Cadavers

Monday, Nov. 26 3:20PM - 3:30PM Room: E353A

Participants

Judith Boven, Dusseldorf, Germany (*Presenter*) Nothing to Disclose Johannes Boos, MD, Dusseldorf, Germany (*Abstract Co-Author*) Nothing to Disclose Rotem S. Lanzman, MD, Duesseldorf, Germany (*Abstract Co-Author*) Nothing to Disclose Patric Kroepil, MD, Duesseldorf, Germany (*Abstract Co-Author*) Nothing to Disclose Christoph K. Thomas, MD, Dusseldorf, Germany (*Abstract Co-Author*) Nothing to Disclose Gerald Antoch, MD, Duesseldorf, Germany (*Abstract Co-Author*) Nothing to Disclose Joel Aissa, MD, Duesseldorf, Germany (*Abstract Co-Author*) Nothing to Disclose

# For information about this presentation, contact:

Judith.boeven@med.uni-duesseldorf.de

#### PURPOSE

We evaluated the correlation between organic parenchymal density in Hounsfield Units (HU) with the radiological alteration index (RAI) level as surrogate for postmortal alteration in postmortem computed tomography (PMCT).

# METHOD AND MATERIALS

We retrospectively included 14 human cadavers (6 females, 8 males) undergoing whole body PMCT. RAI was assessed in 7 localizations reflecting the presence of gas. Based on the total RAI-score cadavers were divided into three groups. [Group 1: low RAI (total score: 0-30); Group 2: medium RAI (total score: 30-60) and Group 3: high RAI (total score: 60-100)]. Density values (HU) were measured in 8 different localizations (1. frontal lobe, 2. basal-ganglia, 3. myocardium, 4. pectoral muscle, 5. liver, 6. left kidney, 7. m. iliopsoas, 8. first lumbar vertebral body[L1]). Correlation between density values and RAI was tested.

#### RESULTS

7 cadavers were included in group 1 with a mean RAI-score of 8.9±9.8,4 cadavers in group 2 with a mean RAI-score of 36.5±6.7 and 3 cadavers in group 3 with a mean RAI-score of 83.7±14.8. Density measurements showed no significant difference between the three groups for all anatomic landmarks (frontal lobe: group 1: 43.4±6.5 HU vs. group 2: 46.1±5.8 HU vs. group 3: 46.4±6.4 HU; basal-ganglia: 43.7±5.3 vs. 41.8±4.8 vs. 44.7±6.8 HU; myocardium: 49.4±9.7 vs. 44.7±8.3 vs. 45.9±8.6 HU; pectoral muscle: 52.9±7.2 vs. 47,0±8.1 vs. 50.8±14.3; liver: 61.5±10.4 vs. 76.1±12.0 vs. 64.1±9.6; left kidney: 49.1±9.5 vs. 43.9±10.7 vs. 35.6±9.8; m. iliopsoas: 48.7±9.2 vs. 51.4±10.3 vs. 55.1±9.8; L1: 169.8±40.5 vs.165.8±46.8 vs. 141.9±30.0; p> 0.05 for all). There was no significant correlation between density measurements and RAI.

# CONCLUSION

There was no correlation between RAI and density measurements in 8 evaluated organs irrespective of the patients' RAI index.

# **CLINICAL RELEVANCE/APPLICATION**

CT organ density measurements cannot be reliably used to assess decay in postmortem CT.

# SSE06-04 Diagnostic Value and Forensic Relevance of a Novel 3D-Reconstructions Method (Cinematic Rendering) in Postmortem Computed Tomography (PMCT)

# Participants

Judith Boven, Dusseldorf, Germany (*Presenter*) Nothing to Disclose Johannes Boos, MD, Dusseldorf, Germany (*Abstract Co-Author*) Nothing to Disclose Rotem S. Lanzman, MD, Duesseldorf, Germany (*Abstract Co-Author*) Nothing to Disclose Patric Kroepil, MD, Duesseldorf, Germany (*Abstract Co-Author*) Nothing to Disclose Gerald Antoch, MD, Duesseldorf, Germany (*Abstract Co-Author*) Nothing to Disclose Joel Aissa, MD, Duesseldorf, Germany (*Abstract Co-Author*) Nothing to Disclose

# For information about this presentation, contact:

judith.boeven@med.uni-duesseldorf.de

#### PURPOSE

To evaluate the radiologic performance and forensic relevance of novel photorealistic 3D reconstructions (Cinematic Rendering) of traumatic injuries in comparison to conventional postmortem computed tomography (PMCT).

# METHOD AND MATERIALS

22 human cadavers undergoing whole body PMCT on 3 different CT-scanners (Definition Flash, Edge and AS+, Siemens, Germany) after traumatic death were retrospectively analyzed. A total of 38 pathologies were reconstructed with 3D Cinematic Rendering mode and conventional multiplanar CT in all 3 dimensions (bone and soft tissue window). 3D reconstructions of pathologies were performed with the preset gallery settings 'Patient Marking CT VRT' and 'Myocardium dark'.Two forensic pathologists evaluated the images according to their expressiveness and judicial relevance on a five-level scale (1: high expressiveness; 5: low expressiveness) and decided whether Cinematic Rendering reconstructions are suitable for judicial reviews or not. Two radiologists analyzed all images due to the detection rate of pathologies in both, Cinematic Rendering reconstructions and PMCT.

#### RESULTS

Forensic estimation: Mean value expressiveness of Cinematic rendering reconstructions: forensic Reader 1:  $2.4\pm1.1$  (range:1-5); forensic Reader 2:  $1.9\pm1.2$  (range: 1-5); total:  $2.1\pm1.2$  (range:1-5). Mean value expressiveness of conventional PMCT: forensic Reader 1:  $4.1\pm1.1$  (range: 2-5); forensic Reader 2:  $3.7\pm1.1$  (range: 1-5); total:  $3.9\pm1.1$  (range: 1-5). Concerning forensic interpretation and demonstration aspects results showed that Cinematic Rendering reconstructions were significantly more expressive than conventional PMCT images (p<0.05). Regarding the radiologic detection rate of all pathologies the evaluation of both radiologists lead to no significant difference between 3D reconstructions and original CT slices for all pathologies.

# CONCLUSION

Cinematic Rendering reconstructions are more helpful for forensic pathologists than standard PMCT images. Concerning the detection of pathologies by radiologists, there is no significant difference between PMCT and Cinematic Rendering reconstructions. Essentially, Cinematic Rendering is suitable for demonstration and detection of relevant findings.

#### **CLINICAL RELEVANCE/APPLICATION**

Cinematic Rendering is a good method for visualizing pathologies, e.g. fractures or soft tissue injuries in judicial reviews and helps forensic pathologists correlate the findings with autopsy results.

# SSE06-05 Utilizing the Broken Circle Sign: A New Method for Detecting a Hill-Sachs Lesion on an Internal Rotation Shoulder Radiograph

Monday, Nov. 26 3:40PM - 3:50PM Room: E353A

Participants

Sarah M. Yu, BS, Columbus, OH (*Presenter*) Nothing to Disclose Trent Rink, MD, Columbus, OH (*Abstract Co-Author*) Nothing to Disclose Kevin Liu, BS, Columbus, OH (*Abstract Co-Author*) Nothing to Disclose Keith Carver, MD, Columbus, OH (*Abstract Co-Author*) Nothing to Disclose Jason D. Lather, MD, Columbus, OH (*Abstract Co-Author*) Nothing to Disclose Jason E. Payne, MD, Columbus, OH (*Abstract Co-Author*) Nothing to Disclose Alan Rogers, MD, Columbus, OH (*Abstract Co-Author*) Nothing to Disclose Barbaros S. Erdal, PhD, Columbus, OH (*Abstract Co-Author*) Nothing to Disclose Joseph S. Yu, MD, Columbus, OH (*Abstract Co-Author*) Nothing to Disclose

# For information about this presentation, contact:

joseph.yu@osumc.edu

#### PURPOSE

A Hill-Sachs (HS) lesion is a potential indicator of shoulder joint instability. Diagnosis is based on a flat or concave defect in the superior aspect of the humeral head on an internal rotation (IR) radiograph but the finding is often subtle. The purpose of this study was to describe a new method designed to increase the sensitivity for HS lesions.

#### **METHOD AND MATERIALS**

A retrospective search for patients who sustained a prior dislocation, were evaluated with x-rays, and had a HS lesion on MRI was performed for a 10-yr period. In Part 1, only the AP IR x-ray was utilized and these were randomized with controls. Three readers were asked to independently score all x-rays with 'yes' if they detected a HS lesion or 'no' if they did not or were unsure. One month later, the readers were taught the Broken Circle Sign, and re-scored the x-rays using the new technique. In Part 2, 15 MRI-confirmed cases of HS lesions that were missed on initial review were mixed with normal x-rays and shown to 17 residents individually before and after teaching the new method. A paired t-test was used to evaluate the differences in sensitivity, specificity, accuracy, positive predictive value (PPV) and negative predictive value (NPV).

A total of 256 patients met the selection criteria (199 men, 57 women; age range: 15-82 yrs, mean: 31.2 yrs). There were 127 right and 129 left shoulders. In Part 1, sensitivity for all 3 readers increased by an average of 20.6% (54.1% to 74.7%; p<0.02), accuracy increased by an average of 7.4% (69.1% to 76.5%; p<0.05), and NPV increased by an average of 10.8% (62.4% to 73.3%; p<0.005). In Part 2, sensitivity for the residents increased by an average of 20.4% (54.1% to 74.5%; p<0.001), accuracy increased by an average of 14.6% (65.1% to 79.7%; p<0.0001), and NPV increased by an average of 15.3% (41.6% to 56.9%;p<0.001) independent of their level of training. Only 2 residents did not improve due to high initial scores in sensitivity and accuracy.

# CONCLUSION

The Broken Circle Sign is a simple tool that helps to increase the conspicuity of a Hill-Sachs lesion on internal rotation shoulder radiographs. It appears to increase the sensitivity, accuracy, and NPV at all levels of training.

# **CLINICAL RELEVANCE/APPLICATION**

The Hill-Sachs lesion occasionally is a difficult diagnosis to make on radiographs. The Broken Circle Sign is a simple method that can aid in increasing the diagnostic acumen for this abnormality.

# SSE06-06 Radiology "Forensics": Determination of Age and Gender from Chest X-Rays Using Deep Learning

Monday, Nov. 26 3:50PM - 4:00PM Room: E353A

Participants

Paul H. Yi, MD, Baltimore, MD (*Presenter*) Nothing to Disclose
Tae Kyung Kim, Baltimore, MD (*Abstract Co-Author*) Nothing to Disclose
Jinchi Wei, Baltimore, MD (*Abstract Co-Author*) Nothing to Disclose
Ji Won Shin, Baltimore, MD (*Abstract Co-Author*) Nothing to Disclose
Tae Soo Kim, Baltimore, MD (*Abstract Co-Author*) Nothing to Disclose
Gregory D. Hager, PhD, MSc, Baltimore, MD (*Abstract Co-Author*) Nothing to Disclose
Gregory D. Hager, PhD, MSc, Baltimore, MD (*Abstract Co-Author*) Nothing to Disclose
Ferdinand K. Hui, MD, Richmond, VA (*Abstract Co-Author*) Nothing to Disclose
Ferdinand K. Hui, MD, Richmond, VA (*Abstract Co-Author*) Speakers Bureau, Terumo Corporation Speakers Bureau, Penumbra, Inc
Stockholder, Blockade Medical Inc
Cheng Ting Lin, MD, Baltimore, MD (*Abstract Co-Author*) Nothing to Disclose

For information about this presentation, contact:

#### pyi10@jhmi.edu

## PURPOSE

To develop and test the performance of deep convolutional neural networks (DCNNs) for the automated detection of 1) age and 2) gender on chest radiographs (CXRs).

#### **METHOD AND MATERIALS**

We obtained 112,120 frontal CXRs from the NIH ChestX-ray14 database performed in 48,780 females (44%) and 63,340 males (56%) ranging from 1 to 95 years old; amongst 5941 pediatric CXRs (5%), 2546 (43%) were female (p=0.3). The entire dataset was split into training (70%), validation (10%), and test (20%) datasets and used to train, validate, and test the ResNet-18 DCNN pretrained on ImageNet for: 1) determination of gender (using both entire dataset and only pediatric CXRs); 2) determination of age <18 years old or >=18 years old (using entire dataset); and 3) determination of age <11 years old or 11-18 years old (using only pediatric CXRs). During each training epoch, each image was augmented via random rotations, cropping, and flipping. We also tested the DCNNs on an external dataset of 662 CXRs performed in adults and children from China. Receiver operating characteristic (ROC) curves with area under the curve (AUC) and standard diagnostic measures (e.g, accuracy) were used to evaluate DCNN test performance with AUCs statistically compared between DCNNs.

## RESULTS

The DCNNs trained to determine gender on the entire dataset and pediatric CXRs only had AUC of 1.0 and 0.91, respectively (p<0.0001) and accuracy of 98% and 83%, respectively. The DCNNs trained to determine age <18 years old or >=18 years old and <11 years old or 11-18 years old had AUCs of 0.99 and 0.96 (p<0.0001), respectively, with accuracy of 98% and 89%, respectively. On the external dataset, the DCNNs achieved AUC of 0.98 for gender (p=0.01) and 0.91 for determining age < or >=18 years old (p<0.001), with accuracy of 94% and 97%, respectively.

## CONCLUSION

DCNNs can accurately predict gender from CXRs, as well as distinguish between adult and pediatric patients, in both American and Chinese populations, and between pre-pubescent and pubescent children in American populations. The ability to glean demographic information from CXRs may aid forensic investigations, as well as help identify novel anatomic landmarks for gender and age.

#### **CLINICAL RELEVANCE/APPLICATION**

Deep convolutional neural networks can accurately infer gender and age from chest radiographs from American and Chinese populations, which may be a useful tool in "forensic" radiology.



# **Gastrointestinal (Advanced Liver Ultrasound Techniques)**

Monday, Nov. 26 3:00PM - 4:00PM Room: S402AB



AMA PRA Category 1 Credit ™: 1.00 ARRT Category A+ Credit: 1.00

FDA Discussions may include off-label uses.

#### Participants

Michael S. Gee, MD, PhD, Boston, MA (Moderator) Nothing to Disclose

Mark E. Lockhart, MD, Birmingham, AL (*Moderator*) Author, Oxford University Press; Author, JayPee Brothers Publishers; Editor, John Wiley & Sons, Inc; Deputy Editor, Journal of Ultrasound in Medicine

#### Sub-Events

# SSE07-02 The Value of Portal Vein Pulsatility for Diagnosis of High Risk Nonalcoholic Steatohepatitis

Monday, Nov. 26 3:10PM - 3:20PM Room: S402AB

# Awards

**Trainee Research Prize - Fellow** 

Participants Masoud Baikpour, MD, Boston, MA (*Presenter*) Nothing to Disclose Arinc Ozturk, MD, Boston, MA (*Abstract Co-Author*) Nothing to Disclose Manish Dhyani, MBBS, Burlington, MA (*Abstract Co-Author*) Nothing to Disclose Nathaniel D. Mercaldo, Boston, MA (*Abstract Co-Author*) Nothing to Disclose Joseph R. Grajo, MD, Tampa, FL (*Abstract Co-Author*) Nothing to Disclose Anthony E. Samir, MD, Boston, MA (*Abstract Co-Author*) Nothing to Disclose Anthony E. Samir, MD, Boston, MA (*Abstract Co-Author*) Consultant, Pfizer Inc; Consultant, General Electric Company; Consultant, PAREXEL International Corporation; Research Grant, Koninklijke Philips NV; Research Grant, Siemens AG; Research Grant, Canon Medical Systems Corporation; Research Grant, General Electric Company; Research Grant, Samsung Electronics Co, Ltd; Research Grant, Analogic Corporation; Research support, SuperSonic Imagine; Research support, Hitachi, Ltd

# For information about this presentation, contact:

mbaikpour@mgh.harvard.edu

# PURPOSE

To determine the value of portal vein pulsatility for diagnosis of high risk nonalcoholic steatohepatitis (NASH).

# METHOD AND MATERIALS

This IRB-approved HIPAA-compliant study included 123 consecutive subjects (54 males and 69 females, average age of 50.3±12.2 years) with a biopsy proven diagnosis of Nonalcoholic Fatty Liver Disease (NAFLD) who had undergone Duplex Doppler ultrasound assessment of their main portal vein within 1 year prior or after their liver biopsy, from January 2014 to February 2018. We reviewed the Doppler ultrasound images of these patients, used the spectral waveform to measure the maximum (Vmax) and minimum (Vmin) velocity of blood in their portal veins, and calculated the Venous Pulsatility Index (VPI) defined as (Vmax-Vmin)/Vmax. Area under the receiver operating characteristic curve (AUC) was measured to determine the value of this index for diagnosis of high risk NASH (hrNASH), which is defined as a NASH stage of equal or greater than F2 based on the extent of fibrosis on liver biopsy.

## RESULTS

Of 123 study subjects, 33 (26.8%) had hrNASH. These patients had a significantly lower VPI than the other 90 subjects ( $0.19\pm0.08$  vs.  $0.32\pm0.11$ ; p<0.001). The AUC of VPI for diagnosis of hrNASH was calculated to be 0.838 (95%CI: 0.757-0.920). Subgroup analysis in subjects whose Doppler ultrasound assessment was performed within 6 months of liver biopsy yielded a similar hrNASH diagnosis AUC of 0.830 (95%CI: 0.735-0.925). VPI analysis was demonstrated to be superior to commonly used hrNASH diagnosis serum tests in this cohort.

# CONCLUSION

VPI analysis may be a useful non-invasive tool for hrNASH diagnosis.

## **CLINICAL RELEVANCE/APPLICATION**

VPI analysis may be useful for high risk NASH diagnosis, which is important for liver-specific mortality NAFLD risk assessment.

# SSE07-03 Viscoelasticity Measurement Using Shear Wave Elastography for the Evaluation of Allograft Rejection after Liver Transplantation

Monday, Nov. 26 3:20PM - 3:30PM Room: S402AB

Dong Ho Lee, MD, Seoul, Korea, Republic Of (*Presenter*) Nothing to Disclose Jae Young Lee, MD, PhD, Seoul, Korea, Republic Of (*Abstract Co-Author*) Nothing to Disclose Jae Seok Bae, MD, Seoul, Korea, Republic Of (*Abstract Co-Author*) Nothing to Disclose

For information about this presentation, contact:

dhlee.rad@gmail.com

## PURPOSE

To evaluate whether viscoelasticity measurement using shear wave elastography could help detect acute cellular rejection of allograft after liver transplantation

# METHOD AND MATERIALS

Between Jan 2018 and March 2018, we prospectively enrolled 33 patients who underwent liver transplantation. Ultrasound (US) examination of allograft liver using shear wave elastography was done for all of 33 patients, and stiffness value (kilopascal, kPa) as well as shear wave dispersion slope ([m/s]/kHz) of allograft liver were measured and recorded. Percutaneous liver biopsy was performed to diagnose acute cellular rejection histopathologically using 18G automating cutting needle immediate after US evaluation. Relationship between US parameters obtained from shear wave elastography and presence of acute cellular rejection on histopathologic examination was evaluated using Mann-Whitney U test and receiver operating characteristic analysis.

## RESULTS

Allograft liver stiffness value as well as shear wave dispersion slope were successfully measured in all of 33 patients. Acute cellular rejection was diagnosed in 12 patients out of 33 patients (12/33, 36.4%) on histopathologic examination. Mean allograft liver stiffness value was  $8.04 \pm 2.33$  kPa in 12 patients with acute cellular rejection, and was not significantly different from that of 7.07  $\pm$  3.62 kPa in 21 patients without acute cellular rejection (P=0.082). However, mean shear wave dispersion slope of allograft liver was 15.03  $\pm$  2.85 [m/s]/kHz in 12 patients with acute cellular rejection, and significantly higher than that of 11.81  $\pm$  4.10 [m/s]/kHz in 21 patients without (P=0.004). The area under the curve for the prediction of acute cellular rejection in allograft liver was 0.802 (P<0.001, 95% confidence interval; 0.626-0.919) for shear wave dispersion slope with a sensitivity of 100% (12/12) and specificity of 57.1% (12/21) when the cut-off value was set at 11.5 [m/s]/kHz.

#### CONCLUSION

Shear wave dispersion slope obtained from shear wave elastography could have a potential to predict the presence of acute cellular rejection in allograft liver after transplantation, and could help make decision regarding the treatment plan for liver transplantation recipients.

# **CLINICAL RELEVANCE/APPLICATION**

Shear wave dispersion slope obtained from shear wave elastography could help make decision regarding the treatment plan for liver transplantation recipients.

# SSE07-04 Role of Contrast-Enhanced Ultrasound for the Post-Treatment Evaluation of Hepatocellular Carcinoma

Monday, Nov. 26 3:30PM - 3:40PM Room: S402AB

Participants

Daniel Ohngemach, MD, Manhasset, NY (*Presenter*) Nothing to Disclose Rebecca Schickman, MD, Bronx, NY (*Abstract Co-Author*) Nothing to Disclose Fahim Hashmi, MD, Manhasset, NY (*Abstract Co-Author*) Nothing to Disclose Gregory M. Grimaldi, MD, Manhasset, NY (*Abstract Co-Author*) Nothing to Disclose Craig R. Greben, MD, Great Neck, NY (*Abstract Co-Author*) Consultant, Vascular Solutions, Inc License agreement, Vascular Solutions, Inc John S. Pellerito, MD, Manhasset, NY (*Abstract Co-Author*) Research Grant, General Electric Company

#### For information about this presentation, contact:

dohngemach@northwell.edu

# PURPOSE

Minimally-invasive treatments for hepatocellular carcinoma (HCC) continue to rise in popularity. Monitoring treated lesions for residual tumor has been accomplished by contrast-enhanced CT or MR (CEMR); however, there is growing interest in the use of contrast-enhanced ultrasound (CEUS) to monitor treatment response following thermo-ablation and embolization of hepatocellular carcinoma. We sought to compare post-treatment findings at CEUS with findings at CEMR to evaluate the efficacy of monitoring treatment response with CEUS.

## **METHOD AND MATERIALS**

We reviewed CEUS examinations performed for evaluation of hepatomas treated by thermo-ablation and/or embolization from April 2017 through March 2018. A positive CEUS or CEMR was defined as residual enhancing tumor within the treatment bed. CEUS examinations were compared with CEMR after treatment but before any further intervention on that lesion.

## RESULTS

We identified 28 lesions in 24 patients that underwent CEUS for post-treatment evaluation. 22 lesions (79%) had CEMR for comparison. Mean time between CEMR and CEUS was 37.8 days (range: 0-112 d). CEUS identified enhancing tumor in 86.7% (13/15) lesions with positive CEMR, and did not demonstrate enhancement in any of 100% (5/5) of lesions with negative CEMR. While CEUS did not detect any CEMR-occult disease, it did confirm presence of enhancing tumor in 2 lesions with indeterminate CEMR. Finally, CEUS confirmed absence of tumor in a lesion characterized as negative at noncontrast MR, but which could not be confirmed by CEMR due to contraindication to gadolinium. Overall, CEUS had a 90% (18/20) agreement rate with diagnostically confirmed lesions on CEMR.

CEUS demonstrated high agreement rate with CEMR in our study population of ablated and embolized hepatic lesions. There were several cases for which contrast-enhanced ultrasound outperformed MRI or enabled evaluation in patients who could not undergo contrast-enhanced MR. These results suggest an ongoing role for CEUS as an adjunct to cross-sectional imaging in the monitoring of HCC following ablation or embolization.

# **CLINICAL RELEVANCE/APPLICATION**

Contrast-enhanced ultrasound may potentially add value in the evaluation of treated hepatic lesions, particularly in patients with contraindications to contrast-enhanced MR or in whom MRI findings are inconclusive.

# SSE07-05 A Comparative Study of Shear Wave Elastography Measurement on Liver's Right Lobe and Left Lobe for diagnosis of Chronic Liver Disease using Liver Biopsy as 'Gold Standard'

Monday, Nov. 26 3:40PM - 3:50PM Room: S402AB

Participants

Ilias Gatos, MSc, PhD, Rion, Greece (*Abstract Co-Author*) Nothing to Disclose Athanasios Angelakis, PhD, Athens, Greece (*Abstract Co-Author*) Nothing to Disclose Pavlos Zoumpoulis, MD, PhD, Athens, Greece (*Presenter*) Nothing to Disclose

#### For information about this presentation, contact:

ath.angelakis@gmail.com

#### PURPOSE

Chronic Liver Disease (CLD) is one of the major causes of death nowadays and the major cause of Hepatocellular Carcinoma development. Therefore, accurate diagnosis regarding CLD progress is very important. Although Liver Biopsy (LB) is considered as 'Gold Standard' for diagnosis, several non-invasive methods have emerged in order to avoid LB complications. Standard SWE examination protocol involves measurements on the Right Lobe (RL), but this is not always feasible since on CLD we observe liver's RL shrinkage and liver's Left Lobe (LL) widening. On the other hand, an alternative measurement on LL can be performed but has not been yet evaluated. The aim of this study is to compare the performance of SWE on liver's RL and LL in CLD diagnosis using LB as 'Gold Standard'.

#### **METHOD AND MATERIALS**

163 subjects, 56 normal (F0) and 107 with CLD (F1-F4), were included in the study. a B-Mode and Color/Power Doppler examination was performed on each patient. SWE measurements were performed on the RL and LL of each patient. SWE measurements on each lobe were compared to LB results that were classified according to the Metavir Classification System for fibrosis (F0-F4). Receiver Operating Characteristic analysis was then performed on each set of SWE measurements (RL and LL) to obtain best cut-off stiffness values.

# RESULTS

ROC analysis was performed for each lobe (RL/LL) showing: AccuracyRL/AccuracyLL = 0.9448/0.9264 for F=F4, AccuracyRL/AccuracyLL = 0.9448/0.9509 for F>=F3, AccuracyRL/AccuracyLL = 0.9571/0.9387 for F>=F2, and AccuracyRL/AccuracyLL = 0.8589/0.8957 for F>=F1. Best cut-off stiffness values calculated for each lobe (RL/LL) compared to Metavir fibrosis stages were: F=F4: 11.8/10.6 kPa, F>=F3: 9.7/9.8 kPa, F>=F2: 8.3/8.1 kPa, F>=F1: 6.3/5.9 kPa respectively.

# CONCLUSION

This study shows that SWE measurements on the LL, when feasible, are reliable in CLD diagnosis and can be used alternatively when measurements on the RL are not possible.

# **CLINICAL RELEVANCE/APPLICATION**

This study shows that SWE measurements on the LL, when feasible, are reliable in CLD diagnosis and can be used alternatively when measurements on the RL are not possible.

# SSE07-06 SHI CEUS Signals in the Hepatic Vein are an Indirect Sign of Pathophysiology Changes Caused by Portal Hypertension

Monday, Nov. 26 3:50PM - 4:00PM Room: S402AB

Participants

Priscilla Machado, MD, Philadelphia, PA (Presenter) Nothing to Disclose Ipshita Gupta, MS, Philadelphia, PA (Abstract Co-Author) Nothing to Disclose Maria Stanczak, MS, Philadelphia, PA (Abstract Co-Author) Nothing to Disclose Corinne Wessner, Philadelphia, PA (Abstract Co-Author) Nothing to Disclose Sriharsha Gummadi, MD, Philadelphia, PA (Abstract Co-Author) Nothing to Disclose Colette Shaw, MBBCh, Philadelphia, PA (Abstract Co-Author) Nothing to Disclose Susan Shamimi-Noori, MD, Philadelphia, PA (Abstract Co-Author) Nothing to Disclose Susan M. Schultz, Philadelphia, PA (Abstract Co-Author) Nothing to Disclose Michael C. Soulen, MD, Philadelphia, PA (Abstract Co-Author) Royalties, Cambridge University Press; Consultant, Guerbet SA; Research support, Guerbet SA; Research support, BTG International Ltd; Consultant, Merit Medical Systems, Inc; Proctor, Sirtex Medical Ltd; Consultant, Terumo Corporation; Consultant, Bayer AG Chandra Sehgal, PhD, Philadelphia, PA (Abstract Co-Author) Nothing to Disclose John R. Eisenbrey, PhD, Philadelphia, PA (Abstract Co-Author) Support, General Electric Company Support, Lantheus Medical Imaging, Inc Flemming Forsberg, PhD, Philadelphia, PA (Abstract Co-Author) Research Grant, Canon Medical Systems Corporation; Research Grant, General Electric Company; Research Grant, Siemens AG; Research Grant, Lantheus Medical Imaging, Inc

# For information about this presentation, contact:

## PURPOSE

To determine if the presence of SHI signals inside the hepatic vein can be used as an indirect qualitative sign of portal hypertension.

# METHOD AND MATERIALS

Eighty-seven patients that were part of an IRB and FDA approved portal hypertension study underwent a subharmonic imaging (SHI) contrast US (CEUS) examination of their portal and hepatic veins using a modified Logiq 9 scanner (GE, Milwaukee, WI) with a 4C probe. SHI is a new CEUS imaging technique where the receive frequency is half of the fundamental (1.25 and 2.5 MHz, respectively) resulting in better tissue suppression. Images were acquired after infusion of the US contrast agent Sonazoid (GE Healthcare, Oslo, Norway) at a rate of 1.44 $\mu$ L of microbubbles/kg/hour and analyzed for the presence or absence of SHI signals in the hepatic vein; based on the assumption that in portal hypertensive patients SHI signals would be seen in the hepatic vein. These findings were compared to the hepatic venous pressure gradient (HVPG; i.e., the gold standard) obtained by transjugular liver biopsy as part of the subject's standard of care.

## RESULTS

Out of the 87 cases, 10 cases were excluded, 5 cases because the HVPG values were clinically discordant and 5 cases because the ROI used was close to the IVC junction causing the physiologic reflux from the IVC to not permit a clear evaluation of the hepatic vein SHI signal. From the 77 patients that could have their data analyzed, 44 had increased HVPG values corresponding to subclinical and clinical portal hypertension (>5 and 10 mmHg, respectively) and 33 patients had normal HVPG values (< 5mmHg). Qualitative assessments of the digital clips acquired during the examinations showed that in all of the 44 cases with increased HVPG values a SHI signal was seen in the hepatic vein and from the 33 cases with normal HVPG values, 30 cases had no SHI signal in the hepatic vein. The overall accuracy was 96% (74/77) with a sensitivity of 100% (44/44) and specificity of 91% (30/33).

#### CONCLUSION

The presence of SHI signal inside the hepatic vein can be used as a qualitative indirect sign for portal hypertension.

# **CLINICAL RELEVANCE/APPLICATION**

SHI CEUS evaluation of the hepatic vein is a non-invasive and safe method that can be used in as a new initial, qualitative sign of portal hypertension.



# Gastrointestinal (Hepatocellular Carcinoma Imaging)

Monday, Nov. 26 3:00PM - 4:00PM Room: S404AB

# GI OI

AMA PRA Category 1 Credit ™: 1.00 ARRT Category A+ Credit: 1.00

## **Participants**

Rajan T. Gupta, MD, Durham, NC (*Moderator*) Consultant, Bayer AG; Speakers Bureau, Bayer AG; Consultant, Invivo Corporation Jeong Min Lee, MD, Seoul, Korea, Republic Of (*Moderator*) Grant, Bayer AG Grant, General Electric Company Grant, Koninklijke Philips NV Grant, STARmed Co, Ltd Grant, RF Medical Co, Ltd Grant, Samsung Electronics Co, Ltd Grant, Guerbet SA

#### Sub-Events

# SSE08-01 Imaging of Hepatocellular Carcinoma: A Preliminary International Survey

Monday, Nov. 26 3:00PM - 3:10PM Room: S404AB

Participants

An Tang, MD, Montreal, QC (*Presenter*) Research Consultant, Imagia Cybernetics Inc; Speaker, Siemens AG; Speaker, Eli Lilly and Company

Karma Abukasm, Montreal, QC (Abstract Co-Author) Nothing to Disclose

Bin Song, MD, Chengdu, China (Abstract Co-Author) Nothing to Disclose

Jin Wang, MD, Guangzhou, China (Abstract Co-Author) Nothing to Disclose

Andrew M. Wai, MBBS, MMedSc, Kowloon, Hong Kong (Abstract Co-Author) Nothing to Disclose

Mathilde Wagner, MD, PhD, Paris, France (Abstract Co-Author) Consultant, Canon Medical Systems Corporation

Christoph F. Dietrich, MD, Bad Mergentheim, Germany (Abstract Co-Author) Nothing to Disclose

Giuseppe Brancatelli, MD, Palermo, Italy (*Abstract Co-Author*) Speaker, Bayer AG; Speaker, Guerbet SA; Advisory Committee, Guerbet SA

Kazuhiko Ueda, MD, Tokyo, Japan (Abstract Co-Author) Nothing to Disclose

Jin-Young Choi, Seoul, Korea, Republic Of (Abstract Co-Author) Nothing to Disclose

Guilherme M. Cunha, MD, Rio de Janeiro, Brazil (Abstract Co-Author) Nothing to Disclose

Diego A. Aguirre, MD, Bogota, Colombia (Abstract Co-Author) Nothing to Disclose

Claude B. Sirlin, MD, San Diego, CA (*Abstract Co-Author*) Research Grant, Gilead Sciences, Inc; Research Grant, General Electric Company; Research Grant, Siemens AG; Research Grant, Bayer AG; Research Grant, ACR Innovation; Research Grant, Koninklijke Philips NV; Research Grant, Celgene Corporation; Consultant, General Electric Company; Consultant, Bayer AG; Consultant, Boehringer Ingelheim GmbH; Consultant, AMRA AB; Consultant, Fulcrum Therapeutics; Consultant, IBM Corporation; Consultant, Exact Sciences Corporation; Advisory Board, AMRA AB; Advisory Board, Guerbet SA; Advisory Board, VirtualScopics, Inc; Speakers Bureau, General Electric Company; Author, Medscape, LLC; Author, Resoundant, Inc; Lab service agreement, Gilead Sciences, Inc; Lab service agreement, ICON plc; Lab service agreement, Intercept Pharmaceuticals, Inc; Lab service agreement, Shire plc; Lab service agreement, Takeda Pharmaceutical Company Limited; Lab service agreement, sanofi-aventis Group; Lab service agreement, Johnson & Johnson; Lab service agreement, NuSirt Biopharma, Inc; Contract, Epigenomics; Contract, Arterys Inc

#### For information about this presentation, contact:

an.tang@umontreal.ca

## PURPOSE

To describe 2018 international current practices in imaging-based surveillance, diagnosis, staging, and treatment response assessment for hepatocellular carcinoma (HCC).

# METHOD AND MATERIALS

Institutional review board exemption was granted for this survey-based study. An electronic survey was sent to members of the LI-RADS International Working Group (94 liver imaging experts from 27 countries and 5 continents) and 40 additional abdominal radiologists identified by survey authors. The 42-item survey captured data on respondents' demographics and liver imaging expertise; local imaging practices for HCC screening, surveillance, diagnosis, staging, and treatment response assessment; and personal use of HCC diagnostic imaging systems.

#### RESULTS

Of 90 respondents (response rate, 55%), 21% were from Asia, 31% from Europe, 8% from North America, 36% from South America, and 4% from Australasia. Similar proportions of respondents were in academic (47%) and private or mixed practice (53%). Median respondents' experience was 16 years (interquartile range, 8-24 years). Noncontrast ultrasound was the most common modality for HCC screening and surveillance (89%). Multiphase computed tomography and MRI were used for HCC diagnosis by 96% and 83% of respondents, respectively. Biopsy was most commonly performed for lesions considered probably or definitely malignant but not meeting definitive HCC imaging criteria for HCC (89%). Extracellular contrast agents (72%) were the most commonly used MRI contrast agents and Lumason<sup>™</sup>/SonoVue<sup>™</sup> (64%) the most commonly used CEUS contrast agent. A majority (95%) of respondents use ancillary in addition to major imaging features for liver lesions assessment. The use of HCC diagnostic imaging systems for HCC varied by region. Response Evaluation Criteria In Solid Tumors (RECIST) or mRECIST were most the common criteria for assessing HCC treatment response (53%). Usage of diagnostic systems varied from 0-81% depending on the system and region. Overall, the most commonly used diagnostic systems were LI-RADS (64%), AASLD (33%), and EASL-EORTC (30%).

# CONCLUSION

HCC imaging diagnostic systems vary geographically. Efforts to unify these diagnostic systems should rely on larger surveys to identify and address regional differences and potential barriers to adoption.

# CLINICAL RELEVANCE/APPLICATION

Regional differences in imaging practices should be taken into account in developing a unified system for imaging of HCC.

## **Honored Educators**

Presenters or authors on this event have been recognized as RSNA Honored Educators for participating in multiple qualifying educational activities. Honored Educators are invested in furthering the profession of radiology by delivering high-quality educational content in their field of study. Learn how you can become an honored educator by visiting the website at: https://www.rsna.org/Honored-Educator-Award/ An Tang, MD - 2018 Honored Educator

# SSE08-02 Add the Value of Gd-EOB-DTPA-Enhanced MRI in Characterizing Cirrhotic Nodules with Atypical Enhancement on CT Enhanced Images: Implications for CT/MRI LI-RADS V2017 Characterization of Hepatocellular Carcinoma

Monday, Nov. 26 3:10PM - 3:20PM Room: S404AB

Participants Jinkui Li, Lanzhou, China (*Presenter*) Nothing to Disclose Junqiang Lei, Lanzhou, China (*Abstract Co-Author*) Nothing to Disclose Zhao Liu, Lanzhou, China (*Abstract Co-Author*) Nothing to Disclose Yongsheng Xu, Lanzhou, China (*Abstract Co-Author*) Nothing to Disclose Hai-Feng Liu II, Lanzhou, China (*Abstract Co-Author*) Nothing to Disclose

# PURPOSE

To evaluate the value of Gd-EOB-DTPA-enhanced magnetic resonance imaging (MRI) in characterizing atypically enhanced nodules in high-risk patients detected on CT enhanced images for the detection of hepatocellular carcinoma (HCC) in reference to the CT/MRI LI-RADS v2017 classification system.

# METHOD AND MATERIALS

Data of 43 patients consecutive patients with 50 atypical nodules seen on enhanced CT images who further underwent Gd-EOB-DTPA MRI between January 2016 and June 2017 were retrospectively analyzed. CT and MRI examination interval were range 1 to 52 days. Two experienced radiologist assigned LI-RADS scores with a blind method. The diagnostic accuracy of CT/MRI LI-RADS v2017 was assessed by comparing with pathological or clinical diagnosis, which as s reference standard.

# RESULTS

Excellent agreement between readers were reached with CT (K=0.806, P<0.001) and MRI (K=0.852, P<0.001), respectively. MRI can show more major and ancillary features than CT significantly (P<0.05). With LR-4, LR-5 regarded as HCC, the accuracy of CT and MRI in diagnosing HCC by comparing with the reference standard was 86.67% and 90.9%, respectively. There is no significant differences in statistic (P>0.05). However, 17 HCC lesions categorized as LR-3 with CT were classified as LR-4 or LR-5 with MRI, and 1 benign lesion was classified as LR-3 with CT and LR-2 with MRI.

# CONCLUSION

With LI-RADS, Gd-EOB-DTPA MRI is more sensitive than CT for diagnosing HCC by providing more information. Thus, Gd-EOB-DTPA MRI can improve the accuracy for detecting HCC of atypical enhanced nodules on CT.

# **CLINICAL RELEVANCE/APPLICATION**

Gd-EOB-DTPA MRI can improve the accuracy for detecting HCC of atypical enhanced nodules on CT with LI-RADS.

# SSE08-03 Impact on Liver Imaging Reporting and Data System Categorization and Tumor Staging of the 2018 Change in the American Association for the Study of Liver Diseases Criteria for HCC

Monday, Nov. 26 3:20PM - 3:30PM Room: S404AB

Participants

Jesse Berman, MD, Bronx, NY (Abstract Co-Author) Nothing to Disclose

Kate Fruitman, Bronx, NY (Abstract Co-Author) Nothing to Disclose

Claude B. Sirlin, MD, San Diego, CA (*Abstract Co-Author*) Research Grant, Gilead Sciences, Inc; Research Grant, General Electric Company; Research Grant, Siemens AG; Research Grant, Bayer AG; Research Grant, ACR Innovation; Research Grant, Koninklijke Philips NV; Research Grant, Celgene Corporation; Consultant, General Electric Company; Consultant, Bayer AG; Consultant, Boehringer Ingelheim GmbH; Consultant, AMRA AB; Consultant, Fulcrum Therapeutics; Consultant, IBM Corporation; Consultant, Exact Sciences Corporation; Advisory Board, AMRA AB; Advisory Board, Guerbet SA; Advisory Board, VirtualScopics, Inc; Speakers Bureau, General Electric Company; Author, Medscape, LLC; Author, Resoundant, Inc; Lab service agreement, Gilead Sciences, Inc; Lab service agreement, ICON plc; Lab service agreement, Intercept Pharmaceuticals, Inc; Lab service agreement, Shire plc; Lab service agreement, Enanta; Lab service agreement, Virtualscopics, Inc; Lab service agreement, Alexion Pharmaceuticals, Inc; Lab service agreement, Takeda Pharmaceutical Company Limited; Lab service agreement, sanofi-aventis Group; Lab service agreement, Johnson & Johnson; Lab service agreement, NuSirt Biopharma, Inc ; Contract, Epigenomics; Contract, Arterys Inc Milana Flusberg, MD, Bronx, NY (*Abstract Co-Author*) Nothing to Disclose Victoria Chernyak, MD,MS, Bronx, NY (*Presenter*) Nothing to Disclose

# For information about this presentation, contact:

#### PURPOSE

The American Association for the Study of Liver Diseases (AASLD) in 2018 changed one of its criteria for the diagnosis of hepatocellular carcinoma (HCC). Previously, the AASLD counted 10-19 mm observations with arterial phase hyperenhancement (APHE) and "washout" (WO) as HCC only if they were visible at antecedent surveillance ultrasound (US). The latest AASLD guidance removed the requirement for US visibility so that all 10-19 mm observations with APHE and WO would count as HCC, regardless of US visibility. The aim of this study is to determine the impact on LI-RADS categorization and HCC staging if LI-RADS adopts the new AASLD criterion, causing a subset of LR-4 observations to be recategorized LR-5.

## **METHOD AND MATERIALS**

All MRI and CT reports issued using a standardized LI-RADS template at one tertiary care center between 4/15-3/18 were identified. For each reported LR-3, LR-4, or LR-5 observation, the presence of each major feature (size, APHE, WO, 'capsule', threshold growth [TG]) and antecedent US visibility was extracted from the reports retrospectively. All observations were assigned a LI-RADS v2017 category based on the extracted features. Observations categorized LR-4 using v2017 were then recategorized by adopting the new AASLD criterion (modified LI-RADS). Patients were assigned a radiologic tumor stage (T-stage) based on the number and size of observations categorized LR-5, first using v2017 LI-RADS and then using modified LI-RADS.

# RESULTS

Of the 672 reported observations in 411 patients reviewed for this study, 187 observations (28%) in 149 patients were categorized LR-4 using v2017 LI-RADS (median size 13 mm, IQR 10-19 mm). Of 187 LR-4 observations, 78 (42%) had APHE and WO only, without US visibility, 'capsule', or TG; these were re-categorized LR-5 using modified LI-RADS. 57 of 67 (85%) patients with re-categorized observations had a change in radiologic T-stage: 68% (39/57) from stage 0 to 1, 12% (7/57) from stage 0 to 2, 5% (3/57) from stage 1 to 2, 12% (7/57) from stage 2 to 3, and 2% (1/57) from stage 2 to 4a.

#### CONCLUSION

The proposed AASLD guideline change will cause 42% of LR-4 observations to be categorized LR-5 and 85% of affected patients to have an increase in radiologic T-stage.

## **CLINICAL RELEVANCE/APPLICATION**

The revised AASLD criteria will cause substantial upgrading of observation and upstaging of patients; further studies are needed to assess how these changes affect accuracy and outcome.

# SSE08-04 Comparison of Diagnostic Performance of Non-Contrast MRI and Abbreviated MRI in Initially Diagnosed Hepatocellular Carcinoma Patients: A Simulation Study of Surveillance for Hepatocellular Carcinomas

Monday, Nov. 26 3:30PM - 3:40PM Room: S404AB

Participants

Sun young Whang, Seoul, Korea, Republic Of (*Presenter*) Nothing to Disclose Joon-Il Choi, Seoul, Korea, Republic Of (*Abstract Co-Author*) Nothing to Disclose Moon Hyung Choi, MD, Seoul, Korea, Republic Of (*Abstract Co-Author*) Nothing to Disclose Young Joon Lee, MD, Seoul, Korea, Republic Of (*Abstract Co-Author*) Nothing to Disclose Sung Eun Rha, MD, Seoul, Korea, Republic Of (*Abstract Co-Author*) Nothing to Disclose

For information about this presentation, contact:

dumkycji@gmail.com

# PURPOSE

To compare the diagnostic performance of non-contrast MRI and abbreviated MRI using gadoxetic acid for detecting hepatocellular carcinoma (HCC) in initially diagnosed, early stage HCC patients

# **METHOD AND MATERIALS**

We identified 142 consecutive, initially diagnosed HCC patients within Milan criteria, who performed liver MRI between 2015 and 2016. For the control group, we enrolled 158 consecutive patients without HCC but had risk factors (liver cirrhosis, chronic hepatitis B or C) of HCC, who also performed liver MRI in the same period. Total number of HCCs was 177 and the number of HCCs smaller than 2 cm and 2 cm <= were 92 and 85, respectively. Two radiologists independently reviewed two MRI sets; non-contrast set and abbreviated set. Non-contrast set consists of T2 FSE/ssFSE with fat saturation, T1 in- and out-of-phase image, non-contrast 3D GRE T1 images, DWI (with b-value 500s/mm2) and ADC map. Abbreviated set consists of T2 FSE/ssFSE with fat saturation, 3D GRE T1 images at hepatobiliary phase 20 minutes after gadoxetic acid injection, DWI and ADC map. Both readers recorded the presence, size and location of HCCs.

#### RESULTS

In per-patient analysis, sensitivity of reader 1 of non-contrast and abbreviated set were 90.8% and 89.8%, respectively. Specificity of non-contrast and abbreviated set were 92.7% and 92.3%, respectively. For reader 2, sensitivity of both sets were 87.4% and 87.5%, and specificity were 90.3% and 91.7%, respectively. When comparing two image sets, there was no statistical difference in both readers (p=0.65 and 0.86 for reader 1 and 2, respectively, using MeNemar test). Kappa statistics showed excellent inter-observer agreement (0.86 for non-contrast and 0.84 for abbreviated set). In per-tumor analyses, sensitivity of reader 1 for non-contrast and abbreviated set were 81.9% and 83.1%, respectively. For reader 2, per-tumor sensitivity for both sets were 80.8% and 83.6%, respectively.

## CONCLUSION

Non-contrast and abbreviated MRI using gadoxetic acid showed comparable diagnosing performance for detecting HCCs in early stage HCC patients.

#### **CLINICAL RELEVANCE/APPLICATION**

Ultrasonography is not sensitive enough for the surveillance of patients with very high risk of HCCs. Non-contrast MRI is cheaper

than abbreviated MRI using gadoxetic acid and can avoid the repeated usage of contrast media which can be accumulated in human brain. Non-contrast liver MRI can be a potential candidate for a surveillance tool of HCC.

# SSE08-05 CT Findings on Hepatocellular Carcinoma in Patients with Hepatitis C Showing a Sustained Virologic Response after Interferon-Free Therapy: Comparison with that in Patients with Interferon-Based Therapy

Monday, Nov. 26 3:40PM - 3:50PM Room: S404AB

Participants

Motonori Akagi, MD, Hiroshima, Japan (*Presenter*) Nothing to Disclose Yuko Nakamura, MD, Hiroshima, Japan (*Abstract Co-Author*) Nothing to Disclose Keigo Narita, Hiroshima, Japan (*Abstract Co-Author*) Nothing to Disclose Yukiko Honda, MD, Hiroshima, Japan (*Abstract Co-Author*) Nothing to Disclose Toru Higaki, PhD, Hiroshima, Japan (*Abstract Co-Author*) Nothing to Disclose Kazuo Awai, MD, Hiroshima, Japan (*Abstract Co-Author*) Nothing to Disclose Kazuo Awai, MD, Hiroshima, Japan (*Abstract Co-Author*) Research Grant, Canon Medical Systems Corporation; Research Grant, Hitachi, Ltd; Research Grant, Fujitsu Limited; Research Grant, Bayer AG; Research Grant, DAIICHI SANKYO Group; Research Grant, Eisai Co, Ltd; Medical Advisory Board, General Electric Company; ; Makoto Iida, Hiroshima, Japan (*Abstract Co-Author*) Nothing to Disclose

## PURPOSE

Hepatitis-C virus (HCV) infection is a common cause of chronic hepatitis and can lead to hepatocarcinogenesis. Antiviral therapy with interferon (IFN) can reduce the incidence of hepatocarcinogenesis especially in patients with a sustained virologic response (SVR). New direct-acting antiviral agents (DAA), approved in several countries for the treatment of chronic HCV infection, have markedly increased the SVR rate. However, it remains controversial whether IFN-free therapy such as DAA reduces hepatocarcinogenesis as same as IFN-based therapy. We compared the CT findings of hepatocellular carcinoma (HCC) in patients with HCV infection who manifested SVR after IFN-free and IFN-based therapy.

## METHOD AND MATERIALS

We divided 43 patients with surgically resected solitary HCC that developed after achieving SVR for HCV infection into 2 groups. Group A (n=30) had received IFN-based- and group B (n=13) IFN-free therapy. We compared the patient- and the HCC characteristics (size and histological grade), serum tumor markers, and the tumor-liver contrast (TLC: difference in the CT value between the hepatic parenchyma and HCC) on arterial- and equilibrium-phase at dynamic CT scans between two groups using the Fisher exact- and the Mann-Whitney's U test.

## RESULTS

There were no significant inter-group differences with respect to the patient- and the HCC characteristics and serum tumor markers. In the equilibrium phase, TLC was significantly higher in group B than group A (median 16.1 vs 9.2 Hounsfield units, p<0.01). In the arterial phase there was no significant difference in TLC between the two groups (p=0.17).

## CONCLUSION

The CT features of HCC in patients who achieved SVR after treatment with IFN-free or IFN-based therapy were different.

#### **CLINICAL RELEVANCE/APPLICATION**

Differences in the CT imaging features of HCC that developed after achieving SVR in patients treated with IFN-based- or IFN-free therapy may suggest differences in the biological characteristics of their tumors.

# SSE08-06 Negative Results at US-Guided Biopsy of Focal Liver Lesions: Conservative or Aggressive Management?

Monday, Nov. 26 3:50PM - 4:00PM Room: S404AB

# Participants

Federica Vernuccio, MD, Palermo, Italy (*Presenter*) Research support, Siemens AG Michael D. Rosenberg, MD, Durham, NC (*Abstract Co-Author*) Nothing to Disclose Mathias Meyer, Durham, NC (*Abstract Co-Author*) Researcher, Siemens AG; Researcher, Bracco Group Kingshuk Choudhury, PhD, Durham, NC (*Abstract Co-Author*) Nothing to Disclose Rendon C. Nelson, MD, Durham, NC (*Abstract Co-Author*) Research Consultant, General Electric Company; Research Consultant, Nemoto Kyorindo Co, Ltd; Consultant, VoxelMetrix, LLC; Co-owner, VoxelMetrix, LLC; Advisory Board, Bracco Group; Advisory Board, Guerbet SA; Research Grant, Nemoto Kyorindo Co, Ltd; Speakers Bureau, Bracco Group; Royalties, Wolters Kluwer nv Daniele Marin, MD, Durham, NC (*Abstract Co-Author*) Research support, Siemens AG

# For information about this presentation, contact:

federicavernuccio@gmail.com

#### PURPOSE

In patients with suspicious malignant liver lesions, the management of a negative result at biopsy is challenging. Our purpose was to investigate patient- and procedure-related variables affecting the false-negative (FN) results of US-guided biopsy of focal liver lesions, and to develop a patient-specific predictive model for the management of negative biopsy results.

# METHOD AND MATERIALS

In this retrospective IRB-approved, HIPAA-compliant study, we included 389 patients (mean age 62 years  $\pm$  12.1; 175 men, 214 women) who had undergone US-guided liver biopsy of suspicious malignant liver lesions between 2013-2015. A total of 405 lesions (mean diameter: 3.8 cm  $\pm$ 2.7) were analyzed. We collected multiple patient- and procedure- related variables, including gender, age, body mass index, history of malignancy, cirrhosis, lesion size and location and sample acquisition technique. By comparing pathology reports of biopsy and the reference standard (further histology or imaging follow-up>1 year), the results were categorized as true-positive (TP), true negative (TN), and FN. Diagnostic accuracy and diagnostic yield were measured. Univariate and multivariate analysis was performed to evaluate variables affecting FN results. Statistical significance was set at p<0.05. A

patient-specific predictive model of FN results based on decision tree was fit.

# RESULTS

Diagnostic accuracy and diagnostic yield of US-guided liver biopsy were 93.8% (380 of 405) and 89.4% (362 of 405), respectively. The FN rate was 6.5% (25 of 387). Predictive variable of a FN result at univariate analysis included body mass index, lesion size and sample acquisition technique. The only independent predictors at multivariate analysis was patient age. By taking into account lesion size and location in combination with patient age and history of previous malignancy, we developed a decision tree model predictive of FN results with confidence up to 100%.

## CONCLUSION

FN results are rare but not negligible at US-guided liver biopsy. Independent predictors of FN results are difficult to identify. Our decision tree predictive model suggests that patient age, history of malignancy, lesion size and location may predict FN results with high confidence.

# **CLINICAL RELEVANCE/APPLICATION**

We developed a decision tree predictive model that allows to identify US-guided liver biopsy results with high probability of being false-negative, and thus could support personalized management.



Gastrointestinal (Advanced Imaging Texture Analysis)

Monday, Nov. 26 3:00PM - 4:00PM Room: S404CD



AMA PRA Category 1 Credit ™: 1.00 ARRT Category A+ Credit: 1.00

FDA Discussions may include off-label uses.

## Participants

Daniele Marin, MD, Durham, NC (*Moderator*) Research support, Siemens AG Alvin C. Silva, MD, Scottsdale, AZ (*Moderator*) Nothing to Disclose

# Sub-Events

# SSE09-01 Contrast-Enhanced MR Imaging Based 3D Texture Analysis as a Potential Tool for Preoperative Prediction of Microvascular Invasion in Hepatocellular Carcinoma

Monday, Nov. 26 3:00PM - 3:10PM Room: S404CD

Participants Yongjian Zhu, Beijing, China (*Presenter*) Nothing to Disclose Xiaohong Ma Jr, MD, PhD, Beijing, China (*Abstract Co-Author*) Nothing to Disclose Xinming Zhao, Beijing, China (*Abstract Co-Author*) Nothing to Disclose Xin Li, Shanghai, China (*Abstract Co-Author*) Nothing to Disclose

For information about this presentation, contact:

zhuyj04@126.com

#### PURPOSE

To investigate the value of contrast enhanced MR imaging (CE-MRI) texture analysis in preoperative predicting the microvascular invasion (MVI) status of hepatocellular carcinoma (HCC).

# **METHOD AND MATERIALS**

A retrospective study of 142 pathologically confirmed cases were conducted. Studies were divided into two cohort: the training cohort (n=99) and validation cohort (n=43), including MVI positive group (n=53) and MVI negative group (n=89) based on pathology. 58 textural parameters were extracted in two cohort using baseline MRI on both arterial phase (AP) and portal phase (PP) by a 3D method. The clinical-radiological features were also included. Univariate logistic regression identified potentially predictive parameters, which were entered into the multivariate logistic regression to build the texture model and the combined model together with clinical features to predict development of MVI.

## RESULTS

In the clinical features, significant difference was found in max tumor diameter (MTD) (P=0.002), tumor differentiation (P=0.026) and AFP (P=0.025) between the two groups in training cohort. Four MR texture features in AP and five in PP were used to build the texture model. The combined model in AP showed a better diagnostic performance than PP using ROC analysis in validation cohort, with area under the curve (AUC) 0.794 vs. 0.706, sensitivity 0.812 vs. 0.750 and specificity 0.852 vs. 0.704.

#### CONCLUSION

The CE-MRI 3D texture analysis can predict MVI of HCC preoperatively and noninvasively, and AP image showed better predictive efficiency than in PP image. Combined model with clinical-radiological features could improve MVI prediction ability to some extent.

# **CLINICAL RELEVANCE/APPLICATION**

Preliminary studies had shown that MVI was a risk factor for the overall survival and recurrence rates of HCC patients. However, there was no accepted method for predicting MVI preoperativeIn this study, 3D CE-MRI texture analysis was used together with clinical-radiological features to build model to predict the MVI status in a training cohort preoperatively. A validation cohort was set to validating the model efficiency and stability. After multivariate logistic regression, our result revealed that the combined model in arterial phase showed a good performance to predicting MVI with AUC of 0.810. This is of great clinical significance for the surgical decision-making and treatment after surgery to avoid recurrence.

# SSE09-02 Machine Learning Models for Prediction of Hepatocellular Carcinoma Response to Transcatheter Arterial Chemoembolization based on Baseline CT Image Texture Analysis and clinical Staging Data

Monday, Nov. 26 3:10PM - 3:20PM Room: S404CD

Participants

Ali Morshid, MD, Houston, TX (*Abstract Co-Author*) Nothing to Disclose Ahmed M. Khalaf, MD, Houston, TX (*Abstract Co-Author*) Nothing to Disclose Justin Yu, BA, Houston, TX (*Abstract Co-Author*) Nothing to Disclose

## For information about this presentation, contact:

KMElsayes@mdanderson.org

## PURPOSE

The purpose of this work is to develop a fully automated algorithm that uses pre-therapeutic quantitative image features and clinical data as inputs to predict HCC response to TACE.

# METHOD AND MATERIALS

TACE outcome information on 113 HCCs in 105 patients receiving first-line treatment with TACE was obtained from a database. An automated segmentation program was developed using fully convolutional neural networks and random forest classification methods to parse out each HCC. The Dice similarity coefficient was calculated to compare the automated segmentation accuracy with that of a manually validated process. A boruta feature selection algorithm was used for data reduction for the quantitative image features considered. The response of HCC to TACE was predicted using a second random forest classifier with the inputs; 1) Barcelona clinic liver cancer (BCLC) stage alone 2) quantitative image features alone 3) BCLC stage plus quantitative image features. The primary clinical endpoint was time to progression (TTP) based on follow-up CT radiological criteria (mRECIST). TTP cutoff of 14 weeks was used to stratify patients as follows; TTP >= 14 wks as TACE susceptible and would benefit from further TACE sessions, TTP < 14 wks as TACE refractory and would be better suited for a change of treatment strategy.

# RESULTS

The automated segmentation model had a Dice similarity coefficient scores at baseline of  $0.65 \pm 0.048$  and  $0.64 \pm 0.081$  for viable and necrotic tissue, respectively. The model's response prediction accuracy rate was 73.2% using a combination of the BCLC stage and quantitative image features (P-value= 0.0096, 95% CI=0.64-0.8, SN=0.83, SP=0.55) versus 62.9% using the BCLC stage alone. Shape image features of the viable, necrotic and background liver were the dominant features correlated to the TTP as selected by the Boruta method and were used to predict the outcome.

#### CONCLUSION

This preliminary study demonstrates the feasibility of improving the accuracy of predicting treatment response of HCC to TACE therapy using quantitative imaging feature obtained prior to therapy. The approach is likely to provide useful information for assisting in patient selection for the continuation of TACE therapy versus changing treatment strategy.

# **CLINICAL RELEVANCE/APPLICATION**

TACE is recommended for unresectable BCLC stage B HCC. Tumor response to first TACE session affects the treatment strategy.

#### **Honored Educators**

Presenters or authors on this event have been recognized as RSNA Honored Educators for participating in multiple qualifying educational activities. Honored Educators are invested in furthering the profession of radiology by delivering high-quality educational content in their field of study. Learn how you can become an honored educator by visiting the website at: https://www.rsna.org/Honored-Educator-Award/ Khaled M. Elsayes, MD - 2014 Honored EducatorKhaled M. Elsayes, MD - 2017 Honored EducatorKhaled M. Elsayes, MD - 2018 Honored Educator

# SSE09-03 CT-Textural Analysis for Discrimination Between Chronic Lymphocytic Leukemia (CLL) and CLL Transformed into Diffuse Large B-Cell Lymphoma (Richter's Syndrome)

Monday, Nov. 26 3:20PM - 3:30PM Room: S404CD

Participants

Christian P. Reinert, MD, Tuebingen, Germany (Presenter) Nothing to Disclose

Johannes Hofmann, Tuebingen, Germany (Abstract Co-Author) Nothing to Disclose

Konstantin Nikolaou, MD, Tuebingen, Germany (Abstract Co-Author) Advisory Panel, Siemens AG; Speakers Bureau, Siemens AG; Speaker Bureau, Bayer AG

Marius Horger, MD, Tuebingen, Germany (Abstract Co-Author) Nothing to Disclose

For information about this presentation, contact:

Christian.Reinert@med.uni-tuebingen.de

#### PURPOSE

To find CT-texture analysis (CTTA) features for discrimination between chronic lymphocytic leukemia (CLL) including indolent and aggressive subtypes and diffuse large B cell lymphoma (DLBCL) caused by transformation (Richter's syndrome).

# **METHOD AND MATERIALS**

We retrospectively identified 52 patients with indolent (26/52) or aggressive CLL (8/52) and DLBCL caused by Richter's syndrome (18/52) who underwent contrast-enhanced CT (CECT) between 03/2011 and 05/2017 using a standardized protocol (120 kV, 200-250 mAs, thin-collimation, weight-adapted i.v. contrast media in portal-venous phase). ROIs were set in the main lymphoma masses as large as possible avoiding partial volume averaging. CTTA evaluation included heterogeneity, intensity, average, deviation, skewness, entropy of co-occurrence matrix, number non-uniformity grey-level dependence matrix (NGLDM), mean contrast neighborhood grey-tone difference matrix (NGTDM) and entropy NGLDM. For each CTTA parameter the respective mean, entropy and uniformity were calculated. For final calculation a medium filter was used. We first grouped all CLLs and compared them with DLBCL and secondly compared both the indolent and aggressive CLL subtypes separately with DLBCL.

## RESULTS

CTTA-values between the entire CLL-group and DLBCL significantly differed with respect to entropy (P<.002), uniformity of heterogeneity (P<.008), mean intensity (P<.0001), mean average (P<.007), entropy of co-occurrence matrix (P<.012) and number

non-uniformity (P<.03). Indolent CLLs significantly differed from DLBCL in terms of entropy (P<.007), uniformity of heterogeneity (P<.018), mean intensity (P<.001), mean average (P<.004) whereas aggressive CLLs were significantly different from DLBCL in terms of entropy (P<.03), uniformity of heterogeneity (P<.02), mean intensity (P<.02) and mean entropy of co-occurrence matrix (P<.04).

# CONCLUSION

CTTA features significantly differ in subjects with CLL compared to DLBCL caused by Richter's syndrome and could therefore be implemented in the routine evaluation of patients suspected of CLL transformation into a DLBCL. Differences in CTTA-features represent ultrastructural characteristics like tissue heterogeneity and contrast-induced attenuation.

# **CLINICAL RELEVANCE/APPLICATION**

Differentiation between CLL and DLBCL caused by Richter's syndrome has major therapeutic and prognostic implications.

# SSE09-04 Correlation Between Whole-Tumor CT Texture Analysis and Pathological Findings in Resected Primary Colon Cancer: Preliminary Results

Monday, Nov. 26 3:30PM - 3:40PM Room: S404CD

Participants Fabio Lombardo, MD, Verona, Italy (*Presenter*) Nothing to Disclose Gabriele Corradi, Verona, Italy (*Abstract Co-Author*) Nothing to Disclose Matteo Bonatti, MD, Bolzano, Italy (*Abstract Co-Author*) Nothing to Disclose Giacomo Avesani, MD, Bolzano, Italy (*Abstract Co-Author*) Nothing to Disclose Francesca Fornasa, MD, Lavagno, Italy (*Abstract Co-Author*) Nothing to Disclose

# For information about this presentation, contact:

fabio.lombardo@me.com

# PURPOSE

to correlate tumor heterogeneity by using whole-tumor CT texture analysis with pathological findings in primary colon cancer.

# METHOD AND MATERIALS

IRB-approved retrospective study; need for informed consent was waived. Thirty patients with resected primary colon cancer were included (21M, 9F; mean age 75y). Thirty-nine first, second and higher order texture features were obtained from preoperative CT portal-venous phase images using a dedicated software (LifEX, www.lifexsoft.org). The results were compared with 10 histopathological features from the specimen (histology, tumor grade, growth pattern, T status, N status, presence of ulceration, percentage of necrosis, presence of vascular and lymphatic invasion, presence of free nodules).

#### RESULTS

tumor histology, tumor grade, growth pattern, T and N status were significantly correlated with 20 different Grey-Level Cooccurrence Matrix (GLCM), Grey-Level Run-Length Matrix (GLRLM), Grey-Level Zone-Length Matrix (GLZLM) and Neighborhood Grey-Level Different Matrix (NGLDM) parameters (Mann-Whitney test; p<0.05). No differences were found between first order texture features and the considered pathological findings (p=ns).

# CONCLUSION

CT second and higher order texture features correlate with tumor biology and with T/N status at pathology.

## **CLINICAL RELEVANCE/APPLICATION**

Second and higher order texture features are a new promising tool for preoperative characterization of colon cancer.

# SSE09-05 Performance of 3T-MRI-Derived Texture Analysis in Rectal Cancer: Predicting Tumoral Response to Therapy

Monday, Nov. 26 3:40PM - 3:50PM Room: S404CD

# Participants

Marta Zerunian, MD, Latina, Italy (*Presenter*) Nothing to Disclose Davide Bellini, MD, Latina, Italy (*Abstract Co-Author*) Nothing to Disclose Damiano Caruso, MD, Rome, Italy (*Abstract Co-Author*) Nothing to Disclose Domenico De Santis, MD, Charleston, SC (*Abstract Co-Author*) Nothing to Disclose Nicola Panvini, MD, Latina, Italy (*Abstract Co-Author*) Nothing to Disclose Andrea Laghi, MD, Rome, Italy (*Abstract Co-Author*) Nothing to Disclose

For information about this presentation, contact:

marta.zerunian@gmail.com

#### PURPOSE

To determine the performance of texture analysis(TA) in predicting tumoral response to therapy in patients with rectal cancer.

# METHOD AND MATERIALS

Forty consecutive patients with clinical suspicion of rectal cancer were prospectively enrolled and had undergone 3T-MRI examination pre- and post- chemo-radiotherapy(CRT). All patients underwent total mesorectal excision 6-8 weeks after the end of CRT. The gross specimens were analyzed by an expert gastrointestinal pathologist and the histological results were considered the reference standard. A region-of-interest was manually drawn around the largest tumour area on a single axial oblique T2-w slice. Slices were analyzed with a dedicated software(TextRad) and the following first order statistical TA parameters were computed: Skewness, Kurtosis, Entropy, and Mean Value of Positive Pixels[MPP]). Non-parametric Mann-Whitney U test was used to compare

TA parameters and the response rate among complete responders(CR), partial responders(PR), and non-responders(NR) before and after CRT. Receiver operating characteristic curves(ROC) were used to assess the discriminatory power of TA parameters to predict complete response to CRT.

# RESULTS

Thirteen patients(32,5%) showed CR, twenty-two patients(55%) showed PR and five patients(12,5%) were classified as NR. After CRT, CR showed significant reduction of Entropy( $6.17 \pm 0.54$  vs  $6.49 \pm 0.43$ ), Kurtosis( $0.72 \pm 1.05$  vs  $2.60 \pm 2.01$ ) and MPP(306.33  $\pm$  168.97 vs 414.24  $\pm$  219.26); all P <= 0.002. After CRT, PR/NR showed significant reduction of Entropy( $6.47 \pm 0.57$  vs  $6.70 \pm 0.50$ ) and Skewness( $0.53 \pm 0.75$  vs  $0.35 \pm 0.67$ ); all P <= 0.029. After CRT, CR showed significant lower Kurtosis( $0.33 \pm 0.65$ ) and MPP(262.19  $\pm$  135.28), compared to PR/NR(Kurtosis:  $1.87 \pm 1.85$ ; MPP:  $357.54 \pm 155.07$ ); all P <= 0.042.Entropy was the only TA parameter showing significance in the predicting CR(AUC 0.64 [95% CI: 0.57 - 0.71]), P < 0.001 with the best cut-off value of >= 6.68, with a sensitivity of 76.9% and a specificity of 38.46% in predicting CR.

# CONCLUSION

Among TA parameters Entropy might be a good predictor of tumor response showing the best AUC in ROC curves with good sensitivity and specificity. Kurtosis and MPP showed a significant decrease in patients with CR.

# **CLINICAL RELEVANCE/APPLICATION**

TA parameters derived from T2 images such as Kurtosis, Skewness and Entropy might potentially play an important role as imaging biomarkers of tumoral response to CRT in patients with rectal cancer.

# SSE09-06 Texture Analysis of Pancreas MRI: Utility for Differentiating Pancreatic Head Cancer from Mass-Forming Chronic Pancreatitis at the Pancreatic Head

Monday, Nov. 26 3:50PM - 4:00PM Room: S404CD

Participants

Lei Chu, MSc, Chengdu, China (*Presenter*) Nothing to Disclose Rongbo Liu, MD, Sichuan, China (*Abstract Co-Author*) Nothing to Disclose Xin Li, Shanghai, China (*Abstract Co-Author*) Nothing to Disclose

#### For information about this presentation, contact:

celotus@foxmail.com

## PURPOSE

To investigate Haralick texture analysis of pancreatic head mass MRI for differentiating pancreatic head cancer(PHC) from massforming chronic pancreatitis at the pancreatic head.

## **METHOD AND MATERIALS**

58 PHC patients, 23 mass-forming chronic pancreatitis patients prior to pancreatoduodenectomy or biopsy and 30 healthy controls undergoing MRI were included. Whole-lesion volumes of interests were placed on T2WI, pre- and post-contrast T1WI, which based on pathological information. Histogram-based parameters and textural features extracted from VOIs were analyzed using generalized estimating equations. The resulting data were processed with Kruskal-Wallis test and binary logistic regression models. Diagnostic accuracy was assessed by area under the receiver operating characteristic curves.

## RESULTS

For pre-contrast T1WI, significant differences were observed for 26 matrixes. At binary logistic regression, among the 17 matrixes (AUCs>0.8), significant independent predictors of PHC were Quantile95, Compactness1 with a combined AUC of 0.953 (P=0.000). Combining these two matrixes achieved sensitivity of 89.7% and specificity of 89.7%. On post-contrast T1WI, significant differences were observed for thirty-nine matrixes. At binary logistic regression, among the 18 matrixes (AUCs>0.8), significant independent predictors of PHC were RelativeDeviation, Uniformity, and Compactness1, with a combined AUC of 0.948 (P<0.0001). Combining these three matrixes achieved sensitivity of 86.2% and specificity of 84.9%. PHC has the highest degree of compactness, followed by chronic pancreatitis, and the lowest normal pancreas. PHC shows higher Relative Deviation and lower uniformity than chronic pancreatitis and normal pancreatic tissue. However, chronic pancreatitis and normal pancreas did not differ between these two matrixes. For T2WI significant differences were observed for Skewness, Haralick Correlation, and Inverse Difference Moment, but the AUCs of these parameters were not greater than 0.8.

## CONCLUSION

Texture metrics obtained on various MRI sequences, post- contrast T1WI provided the highest, and T2WI the lowest performance for differentiating pancreatic head mass. Several Haralick-based texture features appear useful for distinguishing chronic inflammatory mass from PHC.

# **CLINICAL RELEVANCE/APPLICATION**

Several Haralick-based texture features appear useful for distinguishing chronic inflammatory mass at the pancreatic head and PHC.



# Gastrointestinal (General Abdominal Oncology)

Monday, Nov. 26 3:00PM - 4:00PM Room: S403A



AMA PRA Category 1 Credit ™: 1.00 ARRT Category A+ Credit: 1.00

# Participants

Jessica B. Robbins, MD, Madison, WI (*Moderator*) Nothing to Disclose Lauren F. Alexander, MD, Jacksonville, FL (*Moderator*) Spouse, Stockholder, Abbott Laboratories; Spouse, Stockholder, AbbVie Inc; Spouse, Stockholder, General Electric Company

## Sub-Events

# SSE10-01 18F-FDG PET/MRI versus PET/CT in Staging of Gastro-Esophageal Junction Cancer

Monday, Nov. 26 3:00PM - 3:10PM Room: S403A

Participants

Bert-Ram Sah, MD, London, United Kingdom (*Presenter*) Nothing to Disclose Serena Baiocco, Bologna, Italy (*Abstract Co-Author*) Nothing to Disclose Andrew Mallia, London, United Kingdom (*Abstract Co-Author*) Nothing to Disclose Christian Kelly-Morland, FRCR,MBBS, London, United Kingdom (*Abstract Co-Author*) Nothing to Disclose James Stirling, Middlesex, United Kingdom (*Abstract Co-Author*) Nothing to Disclose Sami Jeljeli, BSc, London, United Kingdom (*Abstract Co-Author*) Nothing to Disclose Alessandro Bevilacqua, PhD,MSc, Bologna, Italy (*Abstract Co-Author*) Nothing to Disclose Gary Cook, MD, FRCR, London, United Kingdom (*Abstract Co-Author*) Research support, General Electric Company Research support, Alliance Medical Limited Research support, Siemens AG Research Consultant, Blue Earth Diagnostics Ltd Speakers Bureau, Bayer AG Vicky J. Goh, MBBCh, London, United Kingdom (*Abstract Co-Author*) Research Grant, Siemens AG Speaker, Siemens AG

## PURPOSE

To compare F-18-Fluorodeoxyglucose (FDG)-positron-emission-tomography/magnetic-resonance-imaging (PET/MRI) and PET/computed-tomography (PET/CT) in staging of gastro-esophageal junction (GEJ) cancer.

# METHOD AND MATERIALS

Following IRB approval and informed consent, 24 patients with histologically proven GEJ cancer were prospectively recruited; 4 patients were excluded for technical reasons (19 male, 1 female; mean 68.3+/-9.1 years). Patients were injected with 326+/-28 MBq FDG intravenously for the clinical PET/CT. Uptake time was 60 minutes. PET/MRI was acquired directly after the PET/CT. 2 experienced radiologists and nuclear physicians reviewed the images and defined the PET/MRI-TNM stage in consensus. PET/CT NM-stage was defined for clinical routine. Standard of reference was the multidisciplinary team meeting (MDT) stage, which was defined by contrast enhanced CT+/-endoscopic ultrasonography (EUS) and PET/CT. Sensitivity (SE), Specificity (SP), positive predictive value (NPV) and accuracy (AC) were calculated. McNemar test was performed to assess differences between different modalities.

# RESULTS

For PET/MRI T-stage was concordant with MDT stage in 14 (70%) of 20 patients. Differences in T-stages between PET/MRI and MDT were statistically significant (p=0.03) (Table 1). In our cohort, PET/MRI upstaged three T3 primary lesions as T4 and correctly assigned two T4 lesions. Both PET/MRI and PET/CT agreed in N-and M-staging in all patients. Differences in N-stage between hybrid modalities and MDT were significant (p=0.03) (6 of 20 patients) (Table 2). SE, SP, PPV, NPV and AC for detection of lymph node metastases were 94%, 100%, 100%, 67% and 95% for both imaging modalities.

# CONCLUSION

PET/MRI and PET/CT performed similarly in N and M staging. PET/MRI has advantages over PET/CT in providing additional T-stage.

# **CLINICAL RELEVANCE/APPLICATION**

PET/MRI might be used for staging of patients with GEJ cancer in the future.

# SSE10-02 Arterial Enhancement Patterns on MR imaging as Preoperative Prognostic Markers of Intrahepatic Mass-forming Cholangiocarcinoma

Monday, Nov. 26 3:10PM - 3:20PM Room: S403A

Participants

Ji Hye Min, MD, PhD, Daejeon, Korea, Republic Of (*Presenter*) Nothing to Disclose Young Kon Kim, MD, PhD, Seoul, Korea, Republic Of (*Abstract Co-Author*) Nothing to Disclose Seo-Youn Choi, MD, Bucheon, Korea, Republic Of (*Abstract Co-Author*) Nothing to Disclose Tae Wook Kang, MD, Seoul, Korea, Republic Of (*Abstract Co-Author*) Nothing to Disclose Soon Jin Lee, MD, Toronto, ON (*Abstract Co-Author*) Nothing to Disclose Jeong Eun Lee, Daejeon, Korea, Republic Of (*Abstract Co-Author*) Nothing to Disclose

# For information about this presentation, contact:

minjh1123@gmail.com

# PURPOSE

This study aimed to evaluate the prognostic factors of intrahepatic mass-forming cholangiocarcinoma (IMCC) and to determine the relationship between the magnetic resonance imaging (MRI) features of IMCC including arterial enhancement pattern, the clinicopathologic factors, and the clinical outcomes.

#### **METHOD AND MATERIALS**

The institutional review board approved this retrospective study. The need for informed patient consent was waived. This stud included 134 patients who underwent curative hepatic resection and preoperative MRI for IMCCs (median size: 4.5 cm). The MRIs were reviewed for the IMCCs, which were classified according to the arterial enhancement pattern (diffuse hypoenhancement vs. peripheral rim enhancement vs. diffuse hyperenhancement). We performed survival analysis according to preoperative and postoperative clinicopathologic factors as well as imaging findings.

# RESULTS

In multivariate analysis, the CA 19-9 level (P = 0.010), tumor size (P = 0.001), tumor number (P = 0.008), tumor differentiation (P = 0.036), vascular invasion (P < 0.001), and arterial enhancement pattern (P < 0.001) were significant prognostic factors for overall survival (OS). The CA 19-9 level (P = 0.013), tumor size (P = 0.018), T classification (P = 0.013), necrosis (P = 0.019), and arterial enhancement pattern (P = 0.005) were significant prognostic factors for recurrence-free survival (RFS). There were significant differences in clinicopathologic features among the three arterial enhancement groups. The OS and RFS of the diffuse hyperenhancement group were significantly better than those of the peripheral rim or diffuse hypoenhancement group (P < 0.001).

#### CONCLUSION

The arterial enhancement pattern on MRI, along with the CA 19-9 level and tumor size may be a useful prognostic marker in the preoperative evaluation of patients with IMCC.

# **CLINICAL RELEVANCE/APPLICATION**

The arterial enhancement patterns on MRI are the potential prognostic marker in the preoperative evaluation of patients with IMCC. Patients with IMCC with diffuse hyperenhancement had significantly better clinical outcomes than those with peripheral rim enhancement or diffuse hypoenhancement.

# SSE10-03 Clinical Value of Single-Source, Dual-Energy Spectral CT Imaging in Differentiating Small Liver Cyst from Micro-Metastatic Lesion

Monday, Nov. 26 3:20PM - 3:30PM Room: S403A

Participants

Xinying Li, Dalian, China (*Presenter*) Nothing to Disclose Ailian Liu, MD, Dalian, China (*Abstract Co-Author*) Nothing to Disclose Yue Lv, Dalian, China (*Abstract Co-Author*) Nothing to Disclose Wang Nan, Dalian, China (*Abstract Co-Author*) Nothing to Disclose Anliang Chen, Dalian, China (*Abstract Co-Author*) Nothing to Disclose Fengming Tao, Dalian, China (*Abstract Co-Author*) Nothing to Disclose Jianying Li, Beijing, China (*Abstract Co-Author*) Employee, General Electric Company

#### For information about this presentation, contact:

lixinying0121@163.com

## PURPOSE

To evaluate the value of single-source, dual-energy CT in the differential diagnosis of small liver cysts from micro-metastatic lesions.

# METHOD AND MATERIALS

From January 2014 to Oct 2016, 30 patients with 55 liver lesions underwent spectral CT scans. The lesions were divided into two groups: group A (micro-metastatic) and group B (small liver cysts) (all lesions were diagnosed by medical history and follow-up). The mean CT value of the 40-140keV monochromatic images, iodine (water) concentration and effective atomic number (eff-Z) for the lesions were measured on an AW 4.5 workstation The slope of the spectral curve (K) was measured in the two groups and were statistically compared. Receiver operating characteristic (ROC) curves were constructed to evaluate the effectiveness of each parameter.

#### RESULTS

The consistency of measurements between the observers was rated very well (ICC>0.75). In the unenhanced CT phase, there was no difference in all measurements between the 2 lesion groups (P>0.05). The CT values of the 40-70keV images in group A were significantly higher than those in group B in all three contrast-enhanced phases (P<0.05). Using the CT value of 79.06HU as a threshold for the 40keV images, one obtained an area-under-curve (AUC) for ROC study of 0.802 with sensitivity of 87.5% and specificity of 61.3% for differentiating small liver cysts from micro-metastatic lesions. The iodine concentration, eff-Z and K measurements were different between the two lesion groups only in the arterial phase (P<0.05) (AUC=0.747, 0.765, 0.753). Through combining the CT value at 40keV, iodine concentration, eff-Z and K values in the arterial phase, we could obtain an pooled sensitivity of 90.3%, specificity of 66.7% with a pooled AUC of0.856.

# CONCLUSION

Single-source dual-energy CT provides multiple parameters for relatively high diagnostic accuracy in differentiating small liver cysts from micro-metastatic lesions.

#### **CLINICAL RELEVANCE/APPLICATION**

Single-source dual-energy CT has good clinical value in differentiating small liver cyst from micro-metastatic lesion.

# SSE10-04 Volumetric Measurement of Split and Merged Target Lymph Nodes on CT in Clinical Trials, Compared with RECIST Version 1.1

Monday, Nov. 26 3:30PM - 3:40PM Room: S403A

Participants

Ahmad Shafiei, MD, Bethesda, MD (*Presenter*) Nothing to Disclose Mohammad Hadi Bagheri, MD, Bethesda, MD (*Abstract Co-Author*) Nothing to Disclose Faraz Farhadi, Bethesda, MD (*Abstract Co-Author*) Nothing to Disclose Anna K. Paschall, BS, Bethesda, MD (*Abstract Co-Author*) Nothing to Disclose Andrea B. Apolo, MD, Bethesda, MD (*Abstract Co-Author*) Nothing to Disclose Les R. Folio, MPH,DO, Bethesda, MD (*Abstract Co-Author*) Institutional research agreement, Carestream Health, Inc Elizabeth C. Jones, MD, Bethesda, MD (*Abstract Co-Author*) Nothing to Disclose Ronald M. Summers, MD,PhD, Bethesda, MD (*Abstract Co-Author*) Nothing to Disclose Ronald M. Summers, MD,PhD, Bethesda, MD (*Abstract Co-Author*) Royalties, iCAD, Inc; Royalties, Koninklijke Philips NV; Royalties, ScanMed, LLC; Research support, Ping An Insurance Company of China, Ltd; Researcher, Carestream Health, Inc; Research support, NVIDIA Corporation; ; ; ;

# For information about this presentation, contact:

ahmad.shafiei@nih.gov

#### PURPOSE

To investigate the volumetric changes of split or merged target lymph node on CT scans compared with Response Evaluation Criteria in Solid Tumors (RECIST) version 1.1 measurements.

## **METHOD AND MATERIALS**

Target lymph nodes (short axis diameter >= 1.5 cm) that separated from a conglomerate node (split node) or merged with other nodes (merged node) were retrospectively examined at multiple time points in a cohort of 182 patients with cancers enrolled in clinical trials. Each target node was measured in PACS (Carestream Health) based on RECIST 1.1 before and after splitting or merging, and percent size change was calculated. Volumetric changes of the nodes were also calculated using Vitrea Enterprise Suite V:6.8.0, with percent change recorded as the ground truth. RECIST and volumetric measurements were compared using a t-test. Our cohort was categorized into 3 groups: a conglomerate node splits, one target node merge with other nodes (one-target merged), and two neighboring target nodes merge (two-target merged) as RECIST allows a maximum of two target lymph nodes per patient.

# RESULTS

Our cohort consisted of 20 split nodes and 30 merged nodes (19 were 1-target merged, and 11 were 2-target merged). A significant difference (p<0.001) was seen in all groups between RECIST and volumetric measurements. Mean percent change in size of split nodes was +1% range -48% to +52%) by RECIST and -66% (range from -98% to -13%) by volumetric method. Mean percent change in size of one-target merged nodes was 65% (range 29% to 107%) by RECIST and 210% (range 15% to 607%) by volumetric method. Mean percent change in size of two-target merged nodes was -15% (ranging from -31% to -4%) by RECIST and 110% (ranging from 15% to 234%) two-target merged. While volumetric measurements indicated a decrease in size of all split nodes, RECIST measurements indicated an increase in size in 60% of cases. In merged nodes, volumetric measurements indicated an increase in size for both merged groups, while RECIST measurement showed a decrease in size in all 2-target merged nodes (11 of 11).

## CONCLUSION

RECIST 1.1 may not accurately represent the volumetric increase or decrease in size of target lymph nodes during merging or splitting events.

# **CLINICAL RELEVANCE/APPLICATION**

Volumetric analysis of split and merged lymph nodes indicates a need for revision of target lymph node measurement methodologies of RECIST version 1.1.

# SSE10-05 Is There a Direct Correlation Between Microvascular Wall Structure and K-Trans Values Obtained from Perfusion-CT Measurements in Lymphomas?

Monday, Nov. 26 3:40PM - 3:50PM Room: S403A

Participants

Christopher Kloth, Ulm, Germany (*Presenter*) Nothing to Disclose Petra Fallier-Becker, Tuebingen, Germany (*Abstract Co-Author*) Nothing to Disclose Hans Bosmuller, Tubingen, Germany (*Abstract Co-Author*) Nothing to Disclose Wolfgang M. Thaiss, MD, Tuebingen, Germany (*Abstract Co-Author*) Nothing to Disclose Alexander Sauter, Basel, Switzerland (*Abstract Co-Author*) Nothing to Disclose Heike Preibsch, Tuebingen, Germany (*Abstract Co-Author*) Nothing to Disclose Konstantin Nikolaou, MD, Tuebingen, Germany (*Abstract Co-Author*) Nothing to Disclose Konstantin Nikolaou, MD, Tuebingen, Germany (*Abstract Co-Author*) Nothing to Disclose Speaker Bureau, Bayer AG Jan Fritz, MD, Baltimore, MD (*Abstract Co-Author*) Research Grant, Siemens AG; Scientific Advisor, Siemens AG; Scientific Advisor, Alexion Pharmaceuticals, Inc; Speaker, Siemens AG Meinrad J. Beer, MD, Ulm, Germany (*Abstract Co-Author*) Nothing to Disclose

Marius Horger, MD, Tuebingen, Germany (Abstract Co-Author) Nothing to Disclose

# For information about this presentation, contact:

Christopher.Kloth@uniklinik-ulm.de

## PURPOSE

To test the hypothesis that ultrastructural wall abnormalities of lymphoma vessels correlate with CT perfusion kinetics.

## METHOD AND MATERIALS

Our local institutional review board approved this prospective study. Between February 2013 and June 2016, we included 23 consecutive subjects with newly diagnosed lymphoma, who were referred for CT-guided biopsy (6 female, 17 male; mean age, 60.61±12.43years; range, 28-74 years) and additionally agreed to undergo perfusion-CT of the target lymphoma tissues. Perfusion-CT was obtained for 40 seconds using 80 kV, 120 mAs, 64 x 0.6 mm collimation, 6.9 cm z-axis coverage, and 26 volume measurements. Mean and maximum k-trans (ml/100ml/min), blood flow (BF; ml/100ml/min) and blood volume (BV) were quantified using the deconvolution and the maximum slope + Patlak calculation models. Immunohistiochemical staining was performed for microvessel density (MVD) quantification (vessels/m2) and electron microscopy was used to determine the presence or absence of tight junctions, endothelial fenestration, basement membrane, pericytes and for measurement of extracellular matrix thickness

## RESULTS

Extracellular matrix thickness as well as the presence/absence of tight junctions, basal lamina and pericytes did not correlate with CT perfusion parameters. Endothelial fenestrations correlated significantly with mean BFdeconvolution (p=0.047, r=0.418), and additionally was significantly associated with higher mean BVdeconvolution (p<0.005). Mean k-transPatlak correlated strong with mean k-transdeconvolution (r=0.939, p=0.001), and both correlated with mean BFdeconvolution (p=0.001, r=0.748), max BFdeconvolution (p=0.028, r=0.564), mean BVdeconvolution (p=0.001, r=0.752) and max BVdeconvolution (p=0.001, r=0.771). MDV correlated with max k-transdeconvolution(r=0.564, p=0.023).

### CONCLUSION

K-trans values of perfusion CT do not correlate with ultrastructural microvessel features, whereas endothelial fenestrations correlate with increase intra-tumoral blood volumes.

## **CLINICAL RELEVANCE/APPLICATION**

Numerous imaging studies have been conducted with the aim of non-invasively quantify tumor vascularization and vessel wall leakiness. However, to the best of our knowledge, an association between electron microscopy-based ultrastructural vessel wall features and PCT kinetics of lymphoma has not been investigated. Therefore, we tested the hypothesis that ultrastructural wall abnormalities of lymphoma vessels correlate with PCT kinetics.

# SSE10-06 Nationwide, Longitudinal Trends in CT Colonography Usage: Cross Sectional Survey Results from the 2010 and 2015 National Health Interview Survey

Monday, Nov. 26 3:50PM - 4:00PM Room: S403A

Participants

Anand K. Narayan, MD, PhD, Boston, MA (Presenter) Nothing to Disclose

Diego Lopez, Boston, MA (Abstract Co-Author) Nothing to Disclose

Avinash R. Kambadakone, MD, Boston, MA (Abstract Co-Author) Nothing to Disclose

Peter F. Hahn, MD,PhD, Belmont, MA (*Abstract Co-Author*) Stockholder, Abbott Laboratories; Stockholder, Medtronic plc; Stockholder, CVS Caremark Corporation; Stockholder, Kimberly-Clark Corporation; Stockholder, LANDAUER, Inc; Spouse, Stockholder, Medtronic plc; Spouse, Stockholder, Gilead Sciences, Inc; Spouse, Bondholder, Bristol-Myers Squibb Company; Spouse, Bondholder, Johnson & Johnson

Debra A. Gervais, MD, Boston, MA (Abstract Co-Author) Nothing to Disclose

For information about this presentation, contact:

aknarayan@mgh.harvard.edu

# PURPOSE

Colorectal cancer screening reduces mortality however screening rates have plateaued. Prior studies have found that giving patients choices between different screening tests improves adherence. CT colonography is an emerging minimally invasive screening test that demonstrates high sensitivity for colonic polyps(>1 cm). With increasing health insurance coverage, there are limited national, population-based estimates of CT colonography utilization over time. Our purpose was to estimate longitudinal utilization of CT colonography among eligible participants using nationally representative cross sectional survey data.

# METHOD AND MATERIALS

We used nationally representative cross sectional survey data from 2010 and 2015 National Health Interview Surveys including information about CT colonography usage. 2010 response rate was 77% and 2015 response rate was 80%. Participants between ages 50-75 without histories of colon cancer were included. Logistic regression analyses were used to evaluate longitudinal changes in the proportion of eligible individuals undergoing CT colonography, adjusted for potential confounders and stratified by type of health insurance and age category. Analyses were conducted taking into account complex survey design elements (adjusted weights, strata and sampling units).

## RESULTS

8,965 survey respondents in 2010 and 12,721 survey respondents in 2015 were included. 1.2% reported usage of CT colonography in 2010 and 0.9% reported usage of CT colonography in 2015, a statistically significant decrease (Adjusted OR 0.92, 95% CI 0.86 - 0.99). Optical colonoscopy usage increased from 57.9 to 63.6% (Adjusted OR 1.04, 95% CI 1.02 - 1.06). In our stratified analyses, patients with private health insurance(p = 0.35), patients below 65 (not Medicare eligible)(p = 0.07) and patients who had heard of CT colonography(p = 0.28), did not experience changes in CT colonography usage. Overall awareness of CT colonography decreased from 20.5% to 15.9%, a statistically significant decrease (Adjusted OR 0.94, 95% CI 0.92 - 0.96).

## CONCLUSION

Despite increasing overall usage of optical colonoscopy from 2010 to 2015, CT colonography awareness ( $\sim$ 16%) and utilization ( $\sim$ 1%) remained low.

## **CLINICAL RELEVANCE/APPLICATION**

Improved public awareness and coverage expansion to Medicare age populations will promote increased CT colonography utilization and improvements in overall colorectal cancer screening.

# **Honored Educators**

Presenters or authors on this event have been recognized as RSNA Honored Educators for participating in multiple qualifying educational activities. Honored Educators are invested in furthering the profession of radiology by delivering high-quality educational content in their field of study. Learn how you can become an honored educator by visiting the website at: https://www.rsna.org/Honored-Educator-Award/ Debra A. Gervais, MD - 2012 Honored Educator



# Genitourinary (Imaging of Renal Stones)

Monday, Nov. 26 3:00PM - 4:00PM Room: S102CD



AMA PRA Category 1 Credit ™: 1.00 ARRT Category A+ Credit: 1.00

**FDA** Discussions may include off-label uses.

# Participants

Mitchell E. Tublin, MD, Pittsburgh, PA (Moderator) Nothing to Disclose

## Sub-Events

# SSE11-01 Three Dimensional Texture Analysis with Machine Learning Provides Incremental Predictive Information for Successful Shock Wave Lithotripsy in Patients with Kidney Stones

Monday, Nov. 26 3:00PM - 3:10PM Room: S102CD

Participants

Manoj Mannil, Zurich, Switzerland (*Presenter*) Nothing to Disclose Jochen von Spiczak, MD,MSc, Zurich, Switzerland (*Abstract Co-Author*) Nothing to Disclose Christian Fankhauser, Zurich, Switzerland (*Abstract Co-Author*) Nothing to Disclose Thomas Hermanns, Zurich, Switzerland (*Abstract Co-Author*) Nothing to Disclose Hatem Alkadhi, MD, Zurich, Switzerland (*Abstract Co-Author*) Nothing to Disclose

## PURPOSE

To determine the predictive value of three-dimensional texture analysis (3D-TA) in computed tomography (CT) images for successful shock wave lithotripsy (SWL) in patients with kidney stones.

## **METHOD AND MATERIALS**

Patients with pre and postoperative CT scans, previously untreated kidney stones and a stone diameter of 5-20 mm were included. A total of 224 3D-TA features of each kidney stone, including the attenuation measured in Hounsfield Units (HU), and the clinical variables body mass index (BMI), initial stone size, and skin-to-stone distance (SSD) were analyzed using five commonly used machine learning models. The data set was split in a ratio of 2/3 for model derivation and 1/3 for validation. Machine learning-based predictions for SWL success in the validation cohort were evaluated calculating sensitivity, specificity, and the area-under-the-curve (AUC).

## RESULTS

For SWL success the three clinical variables BMI, initial stone size and SSD showed AUCs of 0.68, 0.58 and 0.63 respectively and no predictive information for HU could be noted. By use of a RandomForest classifier using three 3D-TA features an AUC of 0.79 could be observed. By combining 3D-TA features and clinical variables, the discriminatory accuracy improved further with an AUC of 0.85 for 3D-TA features and SSD, an AUC of 0.8 for 3D-TA features and BMI and an AUC of 0.81 for 3D-TA and stone size.

# CONCLUSION

Our in-vivo study indicates the potential of 3DTA of urinary stone CT enabling the prediction of successful stone disintegration with SWL with high accuracy.

## **CLINICAL RELEVANCE/APPLICATION**

Selected 3D-TA features provide incremental predictive value for successful SWL, which allows stratifying patients with symptomatic kidney stones to either primary SWL or Ureterorenoscopy.

# SSE11-02 Usefulness of Computer Aided Detection of Urinary Stones in Computed Tomography Kidney Ureter Bladder using Convolutional Neural Networks: Preliminary Study

Monday, Nov. 26 3:10PM - 3:20PM Room: S102CD

Participants

Sung Bin Park, MD, Seoul, Korea, Republic Of (*Presenter*) Nothing to Disclose Hyun Jeong Park, Seoul, Korea, Republic Of (*Abstract Co-Author*) Nothing to Disclose Eun Sun Lee, MD, PhD, Seoul, Korea, Republic Of (*Abstract Co-Author*) Nothing to Disclose Jong Beum Lee, Seoul, Korea, Republic Of (*Abstract Co-Author*) Nothing to Disclose Byung Ihn Choi, MD, PhD, Seoul, Korea, Republic Of (*Abstract Co-Author*) Nothing to Disclose

#### For information about this presentation, contact:

pksungbin@paran.com

Computed tomography kidney ureter bladder (CTKUB) is the method of choice for diagnosing urinary stones. The purpose of this study is to develop a computer aided detection (CAD) algorithm for identifying a urinary stone in thin slice CTKUB.

# METHOD AND MATERIALS

Thin slices (3 mm) CTKUB (120 kVp and 150 mAs) in patients with suspicious of stone disease were included in the study. The labeling of urinary stones or not in CTKUB as reference standard was performed by an expert radiologist. 5,268 urinary stones and 4,980 non-urinary stones on CTKUB images were evaluated for training dataset. 551 urinary stones and 528 non-urinary stones on CTKUB images were evaluated for validation dataset. The convolutional neural network was consisted of 8 convolution layers, 9 fully connected layers and softmax classifier. The diagnostic performance of CAD algorithm for identifying a urinary stone from combination of three different image planes (axial, coronal and sagittal) in thin slice CTKUB using convolutional neural network was analyzed.

## RESULTS

In training dataset, the performance was almost perfect. In validation dataset, the CAD algorithm was classified all 551 urinary stones as stones. It was also classified 528 non-urinary stones as 527 non-urinary stones and 1 urinary stone. The sensitivity, specificity, accuracy, positive predictive value and negative predictive value of CAD algorithm were 100%, 99.8%, 99.9%, 99.8% and 100%, respectively.

#### CONCLUSION

CAD algorithm in thin slice CTKUB using convolutional neural network can have high diagnostic performance for urinary stone detection. Prospective further studies involving more participants and focusing on the factors affecting clinical practice such as stone size, location (ureter, kidney) are needed.

## **CLINICAL RELEVANCE/APPLICATION**

In view of its high accuracy, we believe CAD algorithm in thin slice CTKUB using convolutional neural network can be used as an initial examination in patients with suspicious of stone disease.

# SSE11-03 Efficacy of Single-Source Rapid kV-Switching Dual-Energy CT for Characterization of Non-Uric Acid Renal Stones: A Prospective Ex-Vivo Study Using Anthropomorphic Phantom

Monday, Nov. 26 3:20PM - 3:30PM Room: S102CD

#### Awards

## **Student Travel Stipend Award**

Participants Roberto Cannella, MD, Pittsburgh, PA (*Presenter*) Nothing to Disclose Mohammed Shahait, Pittsburgh, PA (*Abstract Co-Author*) Nothing to Disclose Alessandro Furlan, MD, Pittsburgh, PA (*Abstract Co-Author*) Book contract, Reed Elsevier; Research Grant, General Electric Company; Consultant, General Electric Company Joel D. Bigley, Pittsburgh, PA (*Abstract Co-Author*) Nothing to Disclose Timothy Averch, Pittsburgh, PA (*Abstract Co-Author*) Nothing to Disclose Amir Borhani, MD, Pittsburgh, PA (*Abstract Co-Author*) Consultant, Guerbet SA; Author, Reed Elsevier

## For information about this presentation, contact:

rob.cannella89@gmail.com

# PURPOSE

To investigate the accuracy of rapid kV-switching single-source dual-energy computer tomography for prediction of classes of nonuric acid stones.

## **METHOD AND MATERIALS**

Non-uric-acid renal stones retrieved via percutaneous nephrolithotomy were prospectively collected between January 2017 and February 2018 in a single institution. Only stones >5mm and with pure composition (i.e. >80% composed of one element) were studied. Stone composition was determined using Fourier Transform Infrared Spectroscopy. The stones were scanned in 32 cm-wide anthropomorphic whole body phantom in a location mimicking the kidneys. Image acquisition was performed using a single-source rapid-kVp switching CT scanner. The effective atomic number (Zeff) and the attenuation (HU) at 40 kev, 70 kev, and 140 kev virtual monochromatic sets of images were extracted by placing a ROI at the largest cross-sectional areas. Ratios between the attenuations at different energy levels were calculated. Mean values of different stone classes were compared using ANOVA and student t-test. Difference between the actual class of stone and the predicted class of stone based on vendor-recommended Zeff thresholds were assessed. A p-value <0.05 was considered statistically significant. Receiver operating curves (ROC) and area under curve (AUC) with 95% confidence intervals were calculated to assess the efficacy of each parameter.

#### RESULTS

The final study sample included 31 stones from 31 patients consisting of 2 (6%) struvite, 4 (13%) cysteine and 25 (81%) calciumbased pure stones. The mean size of the stones was  $9.9 \pm 2.4$  mm. The mean Zeff of the stones was  $12.0\pm0.41$  for calcium-based,  $10.1 \pm 0.14$  for struvite, and  $9.9 \pm 0.57$  for cysteine stones which were statistically different (p<0.001). In 16 cases (51.6%), there was discrepancy between the actual stone class and the predicted class based on vendor-recommended thresholds. Zeff had the best efficacy for differentiation of different stone classes. The calculated AUC was for 0.947 for Zeff; 0.833 for HU40; 0.880 for HU70 and 0.893 for HU140.

# CONCLUSION

Zeff has superior performance to HU and attenuation ratios for differentiation of different classes of non-uric-acid stones.

## **CLINICAL RELEVANCE/APPLICATION**

Non-invasive determination of composition of urinary stone has important clinical implication in guiding the decision making algorithm

for stone treatment.

# SSE11-04 Dual-Energy Spectral CT Characterization of Urinary Calculi In Vivo

Monday, Nov. 26 3:30PM - 3:40PM Room: S102CD

Participants Xiaohu Li, MD, Hefei, China (*Presenter*) Nothing to Disclose Yongqiang Yu, MD, Hefei, China (*Abstract Co-Author*) Nothing to Disclose Jianying Li, Beijing, China (*Abstract Co-Author*) Employee, General Electric Company

# PURPOSE

To explore the feasibility of using dual-energy energy spectral CT to determine the components of urinary calculi in vivo

# METHOD AND MATERIALS

Fifty-seven cases of patients with urinary calculi were included in the present eighty-nine stones, with GSI (gemstone spectral imaging) scan using AW4.6 workstation for image analysis indexes:GSI scan mode (Effective atomic number), the material (Materia Density) calcium water ratio (calcium water ratio, CWR),50keV and 70keV single energy CT value. The differences of 4 indexes were compared. According the infrared spectrum analysis results as the reference standard. Compared with spectrum diagnosis ,we can conclude that sensitivity, specificity and positive predictive value, negative predictive value of pure uric acid stones, pure non-uric acid stones, stones mixed . Retrospective study of involving 24 cases of single component calculi (11 pieces of uric acid stones, 9 pieces of calcium oxalate, 3 pieces of calcium phosphate stones ) and 53 cases of mixed stones.Stones were respectively measuring the effective atomic number, CWR, 50ke V, 70keV single energy CT value and we can compare the indexes of different groups with the one way anova.

# RESULTS

The infrared spectrum analysis results as the reference standard, the sensitivity for analysis pure uric acid calculi, pure non-uric acid stones and mixed stones were 100%, 91.7%, 97.0%, respectively; with specificity of 100%, 97.4%, 95.7%, respectively; with the positive predictive value of 100%, 84.6% 98.5% respectively and the negative predictive value were 100%, 98.7%, 91.7%, respectively.

## **CLINICAL RELEVANCE/APPLICATION**

It is useful to reduce the occurrence of complications if we can make a definite diagnosis of stone composition before surgery.

# SSE11-05 Role of Single Source Dual Energy CT in Evaluation of Chemical Composition of Urinary Tract Calculi

## Monday, Nov. 26 3:40PM - 3:50PM Room: S102CD

Participants

CHANDRESH O. KARNAVAT, Mumbai, India (*Abstract Co-Author*) Nothing to Disclose Niravkumar K. Kadavani, MBBS, Mumbai, India (*Presenter*) Nothing to Disclose Ritu M. Kakkar, MBBS, DMRD, Mumbai, India (*Abstract Co-Author*) Nothing to Disclose Shrinivas B. Desai, MD, Mumbai, India (*Abstract Co-Author*) Nothing to Disclose

# For information about this presentation, contact:

chand.k.13@gmail.com

# PURPOSE

To evaluate the diagnostic accuracy of Single Source Dual Energy CT in characterisation of renal stones with biochemical analysis as reference

# METHOD AND MATERIALS

This was a prospective study carried out at a tertiary care centre for a period of 3 years using Gemstone Spectral Imaging in single source dual energy CT scanner- GE Discovery CT750 HD. A total of 70 patients with renal calculi who underwent single source dual energy CT and subsequent surgery were included in the study. Both high and low energy data sets are acquired simultaneously for axial and helical acquisitions at the full 50 cm field of view. Dual-energy data were processed by the GSI general protocol on the CT workstation (Advantage Windows, version 4.2; GE Healthcare). A region of interest (ROI) was applied over the renal stone viewed on the bone window settings occupying approximately 50% of the stone area on axial images. Using GSI software effective atomic number of the ROI area Z (Zeff) was calculated and stones were characterised. Post surgery biochemical analyses of these stones were sent to a common laboratory. All results of dual energy CT were compared to the biochemical analysis by applying kappa statistics

# RESULTS

Out of 70 patients, 43 were male and rest were female. The age group of patients ranged from 25 to 70 years (mean 47 years). Out of 48 calcium oxalate stones on dual energy CT, 47 were calcium oxalate and one was mixed. Out of 12 struvite stones on dual energy CT, 10 were struvite and 2 were mixed. Single cysteine stone detected on dual energy CT was found to be mixed stone on biochemistry. All 7 ammonium urate stones on dual energy were found to be same on biochemistry. Single mixed stone detected on dual energy CT showed similar result on biochemistry. Weighted kappa was found to be 0.835 which indicates very good agreement between two different diagnostic tests

# CONCLUSION

Single Source Dual energy CT scan has a role in accurately assessing the chemical composition of the urinary tract calculi

# **CLINICAL RELEVANCE/APPLICATION**

Chemical composition of the urinary tract calculi using Single Source Dual Energy CT has significant impact on medical management of patient with stone disease

# SSE11-06 Comparison of CT-Index and Effective Z Analysis for Characterization of Urinary Stones with Dual-Energy CT: A Phantom Study

Monday, Nov. 26 3:50PM - 4:00PM Room: S102CD

# Participants

Felice A. Burn, MD, Aarau, Switzerland (*Presenter*) Nothing to Disclose Daniel Mueller, Zurich, Switzerland (*Abstract Co-Author*) Nothing to Disclose Sebastian T. Schindera, MD, Aarau, Switzerland (*Abstract Co-Author*) Nothing to Disclose

## For information about this presentation, contact:

felice.burn@ksa.ch

# PURPOSE

To assess the accuracy of CT-index and effective Z value (atomic number) derived from dual-energy CT for differentiation of uric acid from non-uric acid stones and to further characterize the subgroup of non-uric acid stones.

## **METHOD AND MATERIALS**

Total of 64 urinary stones from humans (32 uric acid and 32 non-uric acid stones with subgroups of oxalate, struvite, brushite and apatite) were included in the study. The stones were placed in an anthropomorphic CT-phantom (diameter, 30 cm). All stones underwent an x-ray diffraction analysis representing the gold standard and they had a high purity and homogeneity of at least 90% in their compositions. The phantom was scanned on a 360-slice MDCT scanner (Aquilion ONE Vision, Canon Medical) with a dual-energy mode using tube voltages of 135 and 80 kVp. The acquired datasets were automatically segmented and postprocessed with commercially available software. The CT-index and the effective Z, which was derived from raw data-based dual-energy analysis, was assessed. A statistical receiver operating characteristics (ROC) analysis and multivarable discrimination analysis was performed.

## RESULTS

The differentiation of uric acid stones from non-uric acid stones were significant, using the CT-index (p < 0.001) and the effective Z value (p < 0.01). The use of the effective Z and CT-index allow further separation in subcategories as uric acid, oxalat, apatit, brushit and struvit stones (Figure 1), whereas this separation is less accurate than for the differentiation of uric acid from non-uric acid stones. If the CT-index and the effective Z values were taken both in consideration a subgroup analysis shows. If the CT-index and the effective Z values were taken both in consideration a subgroup analysis shows more powerful options in differentiation.

# CONCLUSION

CT-index and effective Z values, derived from dual-energy CT, allow very accurate differentiation of uric acid from non-uric acid stones. The differentiation of non-uric acid subgroups is not very reliable for both parameters separately. However, the combinations of both parameters in the evaluation of subgroups can improve the separation of non-uric acid stones.

# **CLINICAL RELEVANCE/APPLICATION**

Improved characterization of renal stone compositions with dual-energy CT using CT index and effective Z value in combination has a direct impact on the clinical management and therefor may improve patient outcome and may reduce treatment costs.



# Science Session with Keynote: Genitourinary (Adrenal Imaging)

Monday, Nov. 26 3:00PM - 4:00PM Room: S103AB

# CT GU

AMA PRA Category 1 Credit ™: 1.00 ARRT Category A+ Credit: 1.00

# Participants

Elaine M. Caoili, MD, MS, Ann Arbor, MI (*Moderator*) Nothing to Disclose Hebert Alberto Vargas, MD, Cambridge, United Kingdom (*Moderator*) Nothing to Disclose

# Sub-Events

# SSE12-01 Genitourinary Keynote Speaker: Imaging of the Adrenal Glands-What More Do We Need to Know?

Monday, Nov. 26 3:00PM - 3:10PM Room: S103AB

Participants Michael T. Corwin, MD, Sacramento, CA (*Presenter*) Nothing to Disclose

# SSE12-02 The Diagnostic Value of Modified Dixon Fat Quantification Technique in the Evaluation of Adrenal Masses

Monday, Nov. 26 3:10PM - 3:20PM Room: S103AB

Participants

Andreas Feist, Bonn, Germany (*Presenter*) Nothing to Disclose Leonie Kramer, Bonn, Germany (*Abstract Co-Author*) Nothing to Disclose Daniel Kuetting, MD, Bonn, Germany (*Abstract Co-Author*) Nothing to Disclose Frederic Carsten Schmeel, Bonn, Germany (*Abstract Co-Author*) Nothing to Disclose Hans H. Schild, MD, Bonn, Germany (*Abstract Co-Author*) Nothing to Disclose Guido M. Kukuk, MD, Bonn, Germany (*Abstract Co-Author*) Nothing to Disclose

## PURPOSE

To evaluate the diagnostic value of six-echo modified Dixon (mDixon) fat quantification techniques in the differentiation between benign and malignant adrenal masses.

## **METHOD AND MATERIALS**

All dedicated upper abdominal MRI examinations including proton density fat fraction (PDFF) maps of the year 2015 (n=535) were re-evaluated for the presence of adrenal incidentalomas. PDFF values acquired by placing one single ROI were compared to adrenal signal intensity index (ASII, [(signal intensity on in-phase imaging - signal intensity on opposed-phase imaging) / (signal intensity on in-phase imaging)]  $\times$  100%) and adrenal-to-spleen chemical-shift ratio (ASR, ([(signal intensity of lesion on opposed-phase imaging - signal intensity of spleen on opposed-phase imaging) / (signal intensity of lesion on in-phase imaging - signal intensity of spleen on opposed-phase imaging)]-1)  $\times$  100%) for all lesions by two independent readers. All lesions were interpreted in the clinical context including -if available- histological results, interdisciplinary tumor board decisions and follow-up examinations.

## RESULTS

Fifty-five patients with 70 lesions were identified. 47 lesions (67.1%) were finally diagnosed as adenomas, 23 lesions (32.9%) were confirmed adrenal metastases. Applying PDFF maps a fat fraction of at least 8.3% was 100% sensitive and 91.7% specific for the diagnosis of adrenal adenoma (AUC: 0.996). A fat fraction of at least 12.25% showed a sensitivity of 91.5% and specificity of 100% in detecting adenomas ruling out all possible malignant adrenal masses. PDFF measurements were significantly more observer independent than calculations of ASII and ASR (p < 0.05).

## CONCLUSION

Six-echo mDixon fat quantification technique provides a robust, fast and highly observer independent tool for the distinction between benign and malignant adrenal masses.

# **CLINICAL RELEVANCE/APPLICATION**

Providing a high diagnostic accuracy and superior inter-rater variability compared to ASII and ASR PDFF maps might replace the established indices in the evaluation of adrenal masses.

# SSE12-03 Adrenal Nodules Greater Than 10 Hounsfield Units (HU) on Non-Contrast CT: Still Indeterminate?

Monday, Nov. 26 3:20PM - 3:30PM Room: S103AB

Awards Student Travel Stipend Award

Participants

Zi Jun Wu, MD, Seattle, WA (*Presenter*) Nothing to Disclose Carolyn L. Wang, MD, Seattle, WA (*Abstract Co-Author*) Nothing to Disclose Daniel S. Hippe, MS, Seattle, WA (*Abstract Co-Author*) Research Grant, Koninklijke Philips NV; Research Grant, General Electric Company; Research Grant, Canon Medical Systems Corporation; Research Grant, Siemens AG Erik Soloff, MD, Seattle, WA (*Abstract Co-Author*) Nothing to Disclose Man Zhang, MD,PhD, Ann Arbor, MI (*Abstract Co-Author*) Nothing to Disclose Larson Hsu, MD, Buffalo, NY (*Abstract Co-Author*) Nothing to Disclose Toshimasa J. Clark, MD, Denver, CO (*Abstract Co-Author*) Nothing to Disclose

## For information about this presentation, contact:

wangcl@uw.edu

## PURPOSE

To determine if a Gaussian-based algorithm (GA) analysis with and without noise correction can help characterize indeterminate adrenal nodules (> 10HU) on non-contrast CT as lipid poor adenomas.

# **METHOD AND MATERIALS**

IRB-approved, HIPAA-compliant retrospective study evaluated adrenal nodules greater than 1 cm on non-contrast CT using the GA based region of interest histogram analysis with and without noise correction (normalization of mAs, kVp, and slice thickness to published data). Two independent readers evaluated the nodules and were blinded to final pathology. Lesions were characterized as malignant if pathology proven by biopsy or surgical resection or likely benign due to pathology or imaging features (stability > 1 year, adrenal CT washout, MRI signal loss, or negative FDG PET/CT with a FDG positive primary). Inter-reader agreement was assessed using intraclass correlation coefficient (ICC). Sensitivity, specificity and area under the curve (AUC) were derived.

# RESULTS

There were 91 adrenal nodules in 83 patients that averaged 2.6 cm in size ( $\pm$ 1.9 cm). 33 nodules were pathologically confirmed metastases most commonly lung cancer: average size 1.7  $\pm$  0.7 cm, mean attenuation 23.8  $\pm$  8.8 HU. 58 nodules were presumed to be adenomas based on imaging characteristics: average size 3.9  $\pm$  2.6 cm, mean attenuation 32.2  $\pm$  8.2 HU. Inter-reader agreement was excellent (ICC > 0.8) for multiple variables, including nodule size, mean attenuation, SD of attenuation, and G-index. The noise-corrected GA had significantly higher specificity (85% vs. 59%, p<0.001) and lower sensitivity (38% vs. 58%, p<0.001) for identifying adenoma than the uncorrected GA. The AUC for the corrected GA-index was 0.74, which was statistically improved compared to uncorrected GA-index (0.52, p=0.04) while being similar to the mean attenuation (0.78, p=0.1) and size (0.81, p=0.3).

## CONCLUSION

A Gaussian-based algorithm based on histogram analysis can discriminate between lipid-poor adrenal adenomas and non-adenomas, although it performed no better than an alternative mean attenuation cutoff.

# **CLINICAL RELEVANCE/APPLICATION**

Noise correction Gaussian based algorithm can be used to assess indeterminate adrenal nodules >10HU with high specificity, however further workup may still be needed in patients with a history of cancer.

# SSE12-04 Correlation Between Subclinical Hypercortisolism and Adrenal Volumetry in Patients with Incidental Adrenal Adenoma

Monday, Nov. 26 3:30PM - 3:40PM Room: S103AB

Participants

Nicolas Mertens Folch, Santiago, Chile (*Presenter*) Nothing to Disclose Roberto I. Olmos, MD, Santiago, Chile (*Abstract Co-Author*) Nothing to Disclose Rene Baudrand, Santiago, Chile (*Abstract Co-Author*) Nothing to Disclose Alvaro Huete Garin, MD, Santiago, Chile (*Abstract Co-Author*) Nothing to Disclose

# PURPOSE

To correlate lesion and contralateral adrenal gland volume (CLAV) measurements in asymptomatic patients with incidental adrenal adenoma (IAA) found on computed tomography (CT) with the presence of subclinical hypercortisolism (SCH).

## **METHOD AND MATERIALS**

50 consecutive subjects with IAA were prospectively enrolled after obtaining informed consent between August 2016 and January 2018 according to local scientific ethics committee guidelines. Dexamethasone suppression test and ACTH quantification in peripheral blood was performed in all patients to diagnose SCH. All subjects underwent an adrenal protocol CT with iodinated intravenous contrast and lesion was confirmed as adenoma using known diagnostic criteria (non contrast density < 10 HU, relative washout > 40%, absolute washout > 60%). Volume of the IAA and the CLAV was calculated with Osirix® viewer software by 2 reviewers, with reproducibility evaluated using Bland-Altman analysis. Mann-Whitney U test was used for statistical correlation. Receiver operating characteristic (ROC) curves were obtained to determine the discrimination capabilities of each variable.

#### RESULTS

Subjects included had a mean age of 57.2 years, 82% (n=41) were female. 12 subjects (24%) from the group were diagnosed with SCH. Patients with SCH had larger IAA volumes (p<0.0001) and lower CLAV (p=0.005) than those without SCH. The Bland-Altman analysis showed acceptable inter-reader measurement agreement and moderate dispersion of the results, especially at higher IAA and CLAV volumes, with a mean difference of 0.09 cm3, 95% CI [-1.4, 1.58] for IAA volume and a mean difference of 0.42 cm3, 95% CI [-2.69, 3.53] for CLAV. Area under the ROC curve (AUC) for IAA volume and CLAV was 0.936, 95% CI [0.869, 1] and 0.822, 95% CI [0.668, 0.976] respectively.

# CONCLUSION

IAA volume and CLAV appear to be useful and reproducible tools predicting the presence of SCH in asymptomatic patients with IAA.

Endocrinologic work-up may be advised for patients with IAA and volumetric markers suggesting SCH.

# SSE12-05 Hollowed Adrenal Gland Sign in Patients of Septic Shock: Incidence, CT Appearance and Prognosis

Monday, Nov. 26 3:40PM - 3:50PM Room: S103AB

Participants Yang Peng, Guangzhou, China (*Presenter*) Nothing to Disclose Qiuxia Xie, Guangzhou, China (*Abstract Co-Author*) Nothing to Disclose Jian Guan, MD, Guangzhou, China (*Abstract Co-Author*) Nothing to Disclose Fan Zhang, Guangzhou, China (*Abstract Co-Author*) Nothing to Disclose Xuhui Zhou, MD, PhD, Shenzhen, China (*Abstract Co-Author*) Nothing to Disclose

#### For information about this presentation, contact:

usefulkey0077@hotmail.com

## PURPOSE

To investigate the incidence, CT appearance and prognosis of hollowed adrenal gland sign in septic shock patients.

## **METHOD AND MATERIALS**

From January 2014 to May 2017, there were181 patients with septic shock in ICU (mean 60.7 years; range 19-89 years; 112 males, 69 females). All the patients received dual-phase enhanced CT scan in one week after diagnosis. CT findings and clinical records were reviewed retrospectively. When patients showed diffuse enlargement of bilateral adrenal glands on CT, and in arterial phase the central area of adrenal gland showed much lower attenuation while in venous phase the central "hollowed" area showed further enhancement and was similar to the peripheral area, they were defined as hollowed adrenal gland sign positive. Single factor analysis was performed.

## RESULTS

59 patients showed hollowed adrenal gland sign (32.6%, 59/181) as positive group, while the remain 122 patients were negative. Total mortality rates of positive group and negative group were 81.3% (48/59) and 49.1% (60/122), respectively. According to the primary diseases causing septic shock, patients in both groups were divided into 4 subgroups (intestinal diseases, biliary and pancreatic diseases, postoperative infection and others). The mortality rates of 4 subgroups in positive group were 75.0% (12/16), 66.7% (10/15), 91.7% (22/24), and 100% (4/4), respectively. And the mortality rates of 4 subgroups in negative group were 43.8% (14/32), 28.6% (8/28), 64.3% (27/42) and 55.0% (11/20), respectively. There were significant difference of total mortality rates and mortality rates of matching subgroups between two groups (P<0.01). Single factor analysis of variance showed that the hollowed adrenal gland sign was an independent factor to predict a poor prognosis (death) for septic shock patients.

# CONCLUSION

Hollowed adrenal gland sign is common on CT in septic shock patients and predicts a poor prognosis.

#### **CLINICAL RELEVANCE/APPLICATION**

Hollowed adrenal gland sign is a typical CT appearance of septic shock patient with relative adrenal insufficiency, and appears to be an independent adverse prognostic factor.

## SSE12-06 Adrenal Incidentalomas: A New Risk Factor for Overall Mortality?

Monday, Nov. 26 3:50PM - 4:00PM Room: S103AB

# Awards

#### **Trainee Research Prize - Medical Student**

Participants Michio Taya, MD, Seattle, WA (*Presenter*) Nothing to Disclose Viktoriya Paroder, MD,PhD, Bronx, NY (*Abstract Co-Author*) Nothing to Disclose Eran Bellin, Bronx, NY (*Abstract Co-Author*) Nothing to Disclose Linda B. Haramati, MD, MS, Bronx, NY (*Abstract Co-Author*) Spouse, Board Member, Kryon Systems Ltd

For information about this presentation, contact:

michio.taya@gmail.com

## PURPOSE

To determine the mortality risk of adrenal incidentaloma on abdominal CT.

# METHOD AND MATERIALS

Retrospective cohort study at a multicenter academic medical center. Cohort was identified from patients with newly detected adrenal incidentaloma on CT abdomen report; the primary outcome was all-cause mortality. Study population was derived from patients >=18 years with CT abdomen within 24 hours of emergency department presentation 1/1/05-12/31/09 without history of adrenal disease, adrenal lab testing, or cancer. Incidentaloma cohort was identified by database query of CT reports, followed by manual review to exclude misclassifications. Confirmed incidentaloma cohort was matched to 'no nodule' controls at 3:1 on age  $\pm 1$  year and exam date  $\pm 3$  months. Mortality was ascertained by database query for in-hospital deaths and supplemented with National Death Index query for those lost to follow-up. Survival analysis performed with Kaplan-Meier curves and Cox proportional hazards model examining the effect of adrenal incidentaloma on all-cause mortality.

# RESULTS

Initial query yielded a population of 42,575 adults with CT abdomen, mean age 50  $\pm$ 19 years, 63% women. 969 (2.3%) patients had confirmed adrenal incidentalomas and were matched with 2,907 controls. These 3,876 individuals entered survival analysis with 31,182 total person-years follow-up, median follow-up 8.8 years (IQR 6.0-10.6) in the incidentaloma cohort and 9.0 years (IQR 7.1-

10.7) in the no nodule cohort. Mortality was 36.4% (353/969) in the incidentaloma cohort and 31.6% (919/2907) in the no nodule cohort for a rate difference of 7.6 deaths/1000 person-years (95% CI 2.1-13.0; p=0.005). Adrenal incidentaloma presence was associated with an unadjusted 19% increased risk of death (HR 1.19; 95% CI 1.05-1.36) and a 14% increased risk of death when adjusted for age, sex, race, and other significant predictors including diabetes (HR 1.14; 95% CI 1.01-1.29).

# CONCLUSION

Incidentally discovered adrenal nodules are associated with a significant though small increased risk of all-cause mortality.

# **CLINICAL RELEVANCE/APPLICATION**

The clinical significance of adrenal incidentalomas remain understudied; results of the present study suggest that incidentalomas may not be as harmless as previously thought.



# Health Service, Policy and Research (Trends and Utilization)

Monday, Nov. 26 3:00PM - 4:00PM Room: S403B

# HP

AMA PRA Category 1 Credit ™: 1.00 ARRT Category A+ Credit: 0

## **Participants**

David C. Levin, MD, Philadelphia, PA (*Moderator*) Consultant, HealthHelp, LLC; Board Member, Outpatient Imaging Affiliates, LLC Jonathan James, BMBS, Nottingham, United Kingdom (*Moderator*) Nothing to Disclose

# Sub-Events

# SSE13-01 The Impact of a Program to Manage the Utilization of Advanced Diagnostic Imaging in Accord with Appropriateness Criteria: The Multi-Year Experience of Multiple States

Monday, Nov. 26 3:00PM - 3:10PM Room: S403B

Participants

Mark D. Hiatt, MD, Draper, UT (*Abstract Co-Author*) Vice President, Guardant Health; Board Member, RadSite Kevin D. Hiatt, MD, Winston-Salem, NC (*Presenter*) Nothing to Disclose

## For information about this presentation, contact:

mhiatt@guardanthealth.com

# PURPOSE

In the context of recent concerns about inappropriate utilization of advanced diagnostic imaging (ADI) and the associated deleterious effects of excessive radiation exposure, a radiology benefit manager implemented a program to assist a multi-state health insurance plan manage the use of outpatient ADI, encouraging the withdrawal of inappropriate requests or change to a more appropriate modality (such as ultrasound or MRI in lieu of CT, when indicated). This study investigated the impact of this program.

## **METHOD AND MATERIALS**

A utilization management program was instituted in the middle of 2009 in 2 states in the U.S., and in the middle of 2011 in 2 additional states, to manage the utilization of CT, MRI, PET, and cardiac nuclear medicine (CNM) in accord with appropriateness criteria for the 1.6 million commercial and Medicare members of a health insurance plan. Utilization for each modality was monitored via claims data for 1 year prior to implementation and during the program (through the end of 2015) and expressed in terms of units per 1,000 members (UPK).

# RESULTS

Across all 4 states after implementation, utilization declined from 60.1 to 52.0 UPK for CT (-14%), 63.7 to 55.6 for MRI (-13%), 2.2 to 1.9 for PET (-15%), and 7.2 to 3.4 for CNM (-53%) in the commercial population and from 277.2 to 226.8 for CT (-18%), 152.5 to 132.4 for MRI (-13%), and 48.3 to 27.2 for CNM (-44%) in the Medicare population, but increased from 10.9 to 11.5 for PET (+5%) in the Medicare population.

## CONCLUSION

After program implementation, utilization declined for all studied modalities in all states for all populations except for PET in the Medicare population.

# **CLINICAL RELEVANCE/APPLICATION**

The imposition of appropriateness criteria in the ordering process through a radiology benefit management program may significantly alter the utilization of ADI for the modalities managed.

# ssE13-02 Exploring CMS Quality Measure #405 for Small Incidental Abdominal Lesions

#### Monday, Nov. 26 3:10PM - 3:20PM Room: S403B

Participants

Bari Dane, MD, New York, NY (*Presenter*) Nothing to Disclose Andrew B. Rosenkrantz, MD, New York, NY (*Abstract Co-Author*) Nothing to Disclose

## For information about this presentation, contact:

bari.dane@nyumc.org

## PURPOSE

One measure that CMS has adopted to evaluate and adjust Medicare payments for radiologists under the Merit-Based Incentive Payment System is measure #405, relating to appropriate follow-up imaging recommendations for incidental abdominal lesions. Measure #405 reflects the fraction of incidental <=0.5 cm liver, <1 cm cystic renal, and <=1 cm adrenal lesions detected on CT,

MRI, or ultrasound, for which radiologists recommend follow-up imaging (lesions excluded in presence of malignancy or other medical reason). A rate of 0% indicates perfect performance. We assessed outcomes of lesions encompassed by CMS quality measure #405.

# **METHOD AND MATERIALS**

1,000 consecutive incidental lesions fulfilling measure #405 criteria were identified. Reports were reviewed for follow-up recommendations. Subsequent imaging, whether or not performed specifically for index lesion follow-up, was assessed for size increase or evidence of lesion malignancy.

## RESULTS

The final cohort included 378 ultrasound, 313 CT, and 311 MRI exams, demonstrating 150 liver, 738 renal, and 112 adrenal lesions. Follow-up imaging was recommended in 3% (33) of patients, including 55% (18) of ultrasound exams. Follow-up imaging was obtained in 58% (19) of the 33 recommended cases, compared with at least one subsequent exam in 52% of lesions without a recommendation (p=0.560). Subsequent cross-sectional imaging occurred for a total of 517/1000 cases (>=6 months follow-up in 428 cases; >=1 year in 358). On subsequent imaging, one renal cyst detected on ultrasound showed low-level enhancement on MRI, and three simple renal cysts demonstrated slight size increase; no other lesion in the cohort showed a size increase or evidence of malignancy. No follow-up was recommended for any of these 4 lesions on the baseline exam.

## CONCLUSION

Small incidental lesions encompassed by CMS quality measure #405 (most commonly renal cysts on ultrasound) have an extremely minimal risk of being clinically important. Radiologists' recommendations for follow-up did not seem to drive subsequent imaging rates nor detection of the very rare potentially relevant outcome for such lesions. The findings support the measures aim of avoiding follow-up recommendation for these lesions.

## **CLINICAL RELEVANCE/APPLICATION**

The findings support CMS measure #405 that avoids follow-up recommendations for small incidental abdominal lesions. Radiologists should consider using the measure to optimize their MIPS performance.

## SSE13-03 Vertebral Fracture Assessment (VFA) Utilization, 2005-2016: A COARDRI Study

Monday, Nov. 26 3:20PM - 3:30PM Room: S403B

Participants

Robert J. Ward, MD, Boston, MA (*Presenter*) Nothing to Disclose Richard Duszak JR, MD, Atlanta, GA (*Abstract Co-Author*) Nothing to Disclose Danny Hughes, PhD, Reston, VA (*Abstract Co-Author*) Nothing to Disclose Hansel J. Otero, MD, Philadelphia, PA (*Abstract Co-Author*) Nothing to Disclose Leon Lenchik, MD, Winston-Salem, NC (*Abstract Co-Author*) Nothing to Disclose

For information about this presentation, contact:

robert.ward@tufts.edu

# PURPOSE

To characterize utilization of VFA since 2005 with emphasis on the impact of the 2007 DXA reimbursement cut.

# METHOD AND MATERIALS

Data was derived from the CMS Medicare Part B Physicians/Supplier Procedure Summary Master Files from 2005 through 2016. Codes 76077, 77082, and 77085 were utilized.

## RESULTS

1.713,443 VFA procedures were evaluated from 2005 to 2016. Over that period of time non radiologists billed 74.9% of the studies, 23.0% were billed by radiologists, and 2.1% were unknown. The overall trend in utilization over this period mirrors DXA utilization with decreased utilization (-44.8%) for non-imagers since the 2007 DXA reimbursement cut. Likewise, trending increases in radiologist utilization (+30.6) is noted over the same period. As VFA is performed concurrently with DXA we corrected for DXA trends by utilizing a VFA/DXA ratio. Non-radiologists demonstrated a increasing trend of VFA cases relative to DXA over 2005 to 2016 increasing from 5.8% to 9.2% in 2016. Radiologists in comparison ranged from 1.7% in 2005 to 2.7%. The top 5 specialties for utilization over the period are as follows: Internal Medicine (25.1%), Radiology (21.7%), Rheumatology (17.9%), Family Practice (10.1%), and Endocrinology (9.3%).

## CONCLUSION

VFA trends somewhat mirror utilization of DXA since 2005 demonstrating decreasing volumes for most non imaging specialties and increasing volumes for radiology. From 2005 a small absolute increase in DXA study volume relative to VFA is identified.

# CLINICAL RELEVANCE/APPLICATION

VFA utilization demonstrates a trend of shifting volumes from non-radiologists to radiologists. VFA aids in the detection of vertebral fractures, (osteoporosis) in patients who may not qualify for treatment based solely on DXA derived BMD/T-scores. It is of growing importance for radiologists to become familiar with VFA indications, reporting standards, and significance in the detection and treatment of osteoporosis.

# SSE13-04 Show Me The Money: Practice Patterns of the Top 50 Highest Medicare-Reimbursed Diagnostic Radiologists

Monday, Nov. 26 3:30PM - 3:40PM Room: S403B

Participants Paul H. Yi, MD, Baltimore, MD (*Presenter*) Nothing to Disclose John F. Swietlik, MD, Milwaukee, WI (*Abstract Co-Author*) Nothing to Disclose Nathan Y. Kim, MD, Madison, WI (*Abstract Co-Author*) Nothing to Disclose Ferdinand K. Hui, MD, Richmond, VA (*Abstract Co-Author*) Speakers Bureau, Terumo Corporation Speakers Bureau, Penumbra, Inc Stockholder, Blockade Medical Inc

## For information about this presentation, contact:

pyi10@jhmi.edu

## PURPOSE

With the advent of universal health care in the USA, demand for radiological services continue to rise while health care reimbursements decline. The purpose of this study was to examine the 50 diagnostic radiologists who received the most Medicare reimbursements in 2014 and their practice patterns to glean potential solutions for financial viability.

## METHOD AND MATERIALS

The Medicare Provider Utilization and Payment Database was queried for the 50 diagnostic radiologists who received the most Medicare reimbursements in 2014. The following were recorded for these radiologists: total reimbursements, total number of patients treated, and distribution of reimbursements amongst types of services rendered. Chi-Squared tests were used to compare reimbursements between radiologists from different US regions.

#### RESULTS

In 2014, the top 50 Medicare-reimbursed radiologists were paid an average of \$1,958,011 (range, \$1,247,255 to \$5,146,999) for treating an average of 2524 patients (range, 137 to 11,460) and average payment per patient of \$3018 (range, \$121 to \$14,084). 40% of reimbursements came from procedures, 31% from imaging tests, 10% from radiation oncology procedures, and 19% from other services. 80% of radiologists focused the majority of their services to one type of service (e.g., primarily imaging studies), with the remaining 20% having a more balanced mix of imaging studies and procedures. There were even distributions of these radiologists from the Northeast (14; 28%), West (15; 30%), and South (18; 35%) with fewer from the Midwest (3; 6%), although all regions had an average total reimbursement of at least \$1,900,000 (p>0.05).

#### CONCLUSION

Even amidst decreasing reimbursements, some radiologists are maintaining very high levels of Medicare payment. Although fewer of these highly-reimbursed radiologists are from the Midwest, overall reimbursements are similar between regions. How these radiologists achieve high levels of reimbursement vary, with most focusing on one service type, e.g., primarily procedures, suggesting that a focused practice may improve overall productivity. Radiologists should be reassured that it is possible to maintain high reimbursement levels in today's healthcare market.

## **CLINICAL RELEVANCE/APPLICATION**

Amidst decreasing reimbursements, some radiologists are able to maintain very high levels of Medicare payment at an average of nearly \$2 million.

# SSE13-05 How Specialized are Radiologists Who Are Reading MRI Studies of the Brain?

Monday, Nov. 26 3:40PM - 3:50PM Room: S403B

#### Awards

## **Student Travel Stipend Award**

Participants Evan D. Calabrese, MD, PhD, San Francisco, CA (*Presenter*) Nothing to Disclose Brian Trinh, MD, San Francisco, CA (*Abstract Co-Author*) Nothing to Disclose Thienkhai H. Vu, MD, PhD, San Francisco, CA (*Abstract Co-Author*) Nothing to Disclose Howard P. Forman, MD, New Haven, CT (*Abstract Co-Author*) Nothing to Disclose Brian Haas, MD, San Francisco, CA (*Abstract Co-Author*) Nothing to Disclose

## For information about this presentation, contact:

evan.calabrese@ucsf.edu

# PURPOSE

To assess the degree of specialization in radiologists who are interpreting MRI studies of the brain.

## **METHOD AND MATERIALS**

The IRB approved this study under exempt review. We accessed the Medicare Physician and Other Supplier Public Use File for calendar year 2015. We searched for all radiologists who interpreted MRI of the brain, neck, and spine (i.e. neuro MRI). Radiologists were sorted by the number of MRI studies interpreted and by percent of fee-for-service Medicare (FFSM) claims derived from interpretation of the associated CPT codes. Based upon the distribution of percent claims from neuro MRI, we sought to identify a group of radiologists who read the fewest numbers of neuro MRI, termed "low volume readers," and the associated percent of all FFSM MREx that are interpreted by these low volume readers. The database was queried with Python. Statistical analysis was performed with Python and Excel.

#### RESULTS

A total of 13,694 radiologists interpreted 4,066,887 neuro MRIs. Of the radiologists reading FFSM neuro MRI, the average number of studies read was 297 (10th-90th percentile, 46-690) and the average percent of claims dollars arising from neuro MRI was 23% (10th-90th percentile, 6%-56%). The distribution in numbers of MRI interpreted and in percent of claims dollars arising from neuro MRI is shown in Figure 1. Based upon the distributions of radiologist volume and percent revenue from neuro MRI, the threshold for low volume readers was set at 97 FFSM neuro MRI examinations. There were 3,674 radiologists in the low volume group (27% of radiologists interpreting neuro MRI), and these radiologists were responsible for interpreting 207,8144 of 4,066,887 neuro MRI (5% of all neuro MRI).

# CONCLUSION

There are large numbers of radiologists who read small numbers of neuro MRI per year. Approximately 27% of radiologists interpreting neuro MRI read fewer than 97 neuro MRI per year, which corresponds to 5% of all neuro MRI studies being interpreted by a low volume radiologist. The composition of this low volume radiologist group, and whether there is a relationship between volume of neuro MRI interpreted and quality of those interpretations, are unknown; these questions should be further studied.

# **CLINICAL RELEVANCE/APPLICATION**

We describe a method for assessing degree of specialization of the radiology workforce. The methods can be used to assess either individual radiology practices, or regional or national samples.

# SSE13-06 Qualitative and Quantitative Analysis of Radiologists' Workload in an Academic Hospital Department

Monday, Nov. 26 3:50PM - 4:00PM Room: S403B

Participants

Ulrike Streit, MD, Goettingen, Germany (*Presenter*) Nothing to Disclose Joachim Lotz, MD, Gottingen, Germany (*Abstract Co-Author*) Nothing to Disclose Ali Seif Amir Hosseini, MD, Goettingen, Germany (*Abstract Co-Author*) Nothing to Disclose

# For information about this presentation, contact:

Ulrike.Streit@med.uni-goettingen.de

## PURPOSE

The role of today's hospital-based radiologists goes far beyond interpretation-related tasks. This observational study defines these types of activities, as well as quantifies the type of value-adding interactions radiologists experience on a daily basis with referring departments and other health personnel. The purpose of this study is to evaluate the quality and quantity of these value-adding non-image interpretation tasks in the daily routine of hospital-based resident and attending radiologists.

# RESULTS

Five main categories of responsibilities for NITs were identified including teaching and education, clinical decision support, management and organizing, patient care, and other. For both cross-sectional imaging units, CT and MRI, NITs constituted 50% of the workday for attending radiologists and 48% for resident radiologists. Subcategories revealed heterogeneous results for attendings and residents for each category: teaching and education (14% / 18%), management and organizing (17% / 6%), patient care (7% / 25%), clinical decision support (44% / 24%), and other (18% / 27%).

# CONCLUSION

NITs consumed a significant portion of a radiologist's workday, therefore, number of examinations performed is not a reliable surrogate for the daily workload of hospital-based radiologists especially in the cross-sectional imaging units. Though time consuming these non-image interpretation tasks contribute to the already perceived evolving role of a modern radiologist towards central figures in the process of managing patients and patient information, fulfilling a critical role, which surpasses image interpretation-related tasks towards a more integrative and consultative role. These findings will help to further define the changing role of the radiologist to other physicians, non-medical personnel, hospital administrators, as well as policy makers.

## METHODS

A prospective, observational study was performed in the department of radiology of a German university hospital. Two experienced radiologists performed a two months observation of the entire medical staff. The observers followed the subject radiologists throughout the workday, recording activities using a time and motion methodology. An evaluation matrix was developed to characterize and quantify image interpretation tasks (IITs) and non-image interpretation tasks (NITs) for resident and attending radiologists.

## PDF UPLOAD

http://abstract.rsna.org/uploads/2018/18019421/18019421\_s1ez.pdf



# Informatics (Artificial Intelligence in Radiology: More Cutting-Edge Deep Learning)

Monday, Nov. 26 3:00PM - 4:00PM Room: E353C



AMA PRA Category 1 Credit ™: 1.00 ARRT Category A+ Credit: 1.00

FDA Discussions may include off-label uses.

## Participants

Norio Nakata, MD, Tokyo, Japan (*Moderator*) Nothing to Disclose Nabile M. Safdar, MD, Milton, GA (*Moderator*) Nothing to Disclose Safwan Halabi, MD, Stanford, CA (*Moderator*) Nothing to Disclose Alexandre Cadrin-Chenevert, MD, St Charles Borromee, QC (*Moderator*) Nothing to Disclose

## Sub-Events

# SSE14-01 Machine Learning Fully Automatic Analysis of Vertebrae Trabecular Bone Mineral Density in 10,000 CTs: Groundwork for Opportunistic Osteoporosis Screening

Monday, Nov. 26 3:00PM - 3:10PM Room: E353C

Participants

Thomas J. Re, MD, Princeton, NJ (*Presenter*) Consultant, Siemens AG Bogdan Georgescu, PhD, Princeton, NJ (*Abstract Co-Author*) Employee, Siemens AG Guillaume J. Chabin, MS, Princeton, NJ (*Abstract Co-Author*) Employee, Siemens AG Sasa Grbic, Princeton, NJ (*Abstract Co-Author*) Employee, Siemens AG Dorin Comaniciu, PhD, Princeton, NJ (*Abstract Co-Author*) Employee, Siemens AG

# For information about this presentation, contact:

sasa.grbic@siemens-healthineers.com

# CONCLUSION

ML technology can be exploited to perform large-scale investigations of CT-tBMD on this and other large cohorts as groundwork for developing CT-based osteoporosis screening.

# Background

Opportunistically CT measured vertebral trabecular bone mineral density (CT-tBMD) has been proposed as a possible alternative to DEXA measurements for assessing osteoporosis in cases where a body CT is performed for other motives (trauma, surgery, oncology, COPD, etc). Such an application will require better understanding of CT-tBMD ranges in health and pathology. Previous works, using traditional semi-automatic quantization methods, have been of limited cohort size. Recent developments in machine learning (ML) applied to analyze medical imaging data have increased robustness and accuracy enabling accurate automated segmentation of anatomic structures. We applied a ML pipeline to a large public cohort containing CT and correlated clinical data (COPDgene.org) to demonstrate the viability of using such technology for large-scale tBMD studies.

## **Evaluation**

Deep Reinforcement Learning and Adversarial Deep Image-to-Image ML networks were trained with 4560 manually segmented vertebrae from 380 CTs. A pipeline incorporating this network and 5% erosion algorithm, for trabecular bone isolation, was developed. It showed a 4.5% prediction error when tested on another 834 manually segmented vertebrae. The pipeline was applied to 9554 chest CTs from the COPDGene cohort and correlated to available corresponding clinical data. Results demonstrate a downward trend of BMD with age with slightly more rapid decline in later years for women than men. The data demonstrated significantly lower BMD in subjects diagnosed with osteoporosis, with history of compression or hip fracture (p-values<0.01). Processing time was 5.9 sec per series on a 3 GPU workstation.

#### Discussion

These findings agree with previous ones obtained by traditional semi-automatic techniques on smaller cohorts. Novelty in this work is the use of an ML based and fully automatic pipeline which provides precision and scalability and permits rapid application to the current and other large cohorts.

# SSE14-02 Towards Hierarchical Optimization of Pretrained Deep Learning Models for Tuberculosis Screening in Chest Radiograph

Monday, Nov. 26 3:10PM - 3:20PM Room: E353C

Participants

Jeonghwan Gwak, Seoul, Korea, Republic Of (*Abstract Co-Author*) Nothing to Disclose Chang Min Park, MD, PhD, Seoul, Korea, Republic Of (*Abstract Co-Author*) Nothing to Disclose Jae Won Choi, MD, Seoul, Korea, Republic Of (*Presenter*) Nothing to Disclose Hyungjin Kim, MD, Seoul, Korea, Republic Of (*Abstract Co-Author*) Nothing to Disclose Eui Jin Hwang, Seoul, Korea, Republic Of (*Abstract Co-Author*) Nothing to Disclose Jin Mo Goo, MD, PhD, Seoul, Korea, Republic Of (*Abstract Co-Author*) Research Grant, Samsung Electronics Co, Ltd; Research Grant, Lunit Inc

## For information about this presentation, contact:

james.han.gwak@gmail.com

# CONCLUSION

We verified that hierarchical optimization process could assist to optimize the pretrained deep learning models by developing and incorporating hierarchical and structured feature information.

## Background

Tuberculosis (TB) is a chronic infectious disease and thus early screening is critical in alleviating its transmission and reducing reproductive rate. While there are a few researches for the given task in chest radiograph through developing new deep learning models and simply using fixed pretrained models, there are very rare researches on further optimizing pretrained models to improve the performance.

# Evaluation

We focused on optimizing pretrained models using hierarchical optimization process using iterative adaptive fixation and release operations and parallel model building. Based on the implications of high-level abstractions, lower layers in pretrained models will have more general feature information (e.g., edges) and upper layers keep domain-specific feature information (e.g., object parts or objects). The optimization is done by making a parallel pool consisting of 10 instances of a pretrained deep learning model and by bypassing through fixation/release of convolution layers with slightly perturbed feature information and then fine-tuning is repeatedly done until the gradient changes become negligible. Finally, the winner will be selected as the best model. We used 7,000 normal patients' chest radiograph images, and 7,000 TB patients' images for training using the hierarchical optimization. As the pretrained models, we used GoogLeNet, ResNet-152 and Inception-ResNet-V2. For validation and test, we used two independent datasets each consisting of 300 normal patients' images and 150 TB patients' images. Results showed that the area under the receiver operating characteristics curves (AUCs) of GoogLeNet, ResNet-152 and Inception-ResNet-V2 were 0.97, 0.99 and 0.99, respectively. For comparison, the AUCs of the models without such optimization process obtained 0.89, 0.93, 0.92, respectively.

## Discussion

We proposed a method of optimizing pretrained deep learning models in a hierachical manner. Further study is required to deal with class-imbalanced dataset issues.

# SSE14-03 Understanding Deep Learning: Insights from a Classifier Trained to Predict Contrast Enhanced Phase from Abdominal CT Imaging

Monday, Nov. 26 3:20PM - 3:30PM Room: E353C

Participants

Kenneth Philbrick, Rochester, MN (*Presenter*) Nothing to Disclose Zeynettin Akkus, PhD, Rochester, MN (*Abstract Co-Author*) Nothing to Disclose Timothy L. Kline, PhD, Rochester, MN (*Abstract Co-Author*) Nothing to Disclose Panagiotis Korfiatis, PhD, Rochester, MN (*Abstract Co-Author*) Nothing to Disclose Naoki Takahashi, MD, Rochester, MN (*Abstract Co-Author*) Nothing to Disclose Bradley J. Erickson, MD, PhD, Rochester, MN (*Abstract Co-Author*) Stockholder, OneMedNet Corporation; Stockholder, VoiceIt Technologies, LLC; Stockholder, FlowSigma;

For information about this presentation, contact:

Philbrick.Kenneth@mayo.edu

# CONCLUSION

The data that we report here demonstrates that voxel level visualizations provide powerful insight into the precise anatomical regions of imaging which activate a network. Investigating the anatomical structures identified in these maps may provide key insight for systems (e.g., tumor) where well performing deep learning models exist but defining radiological signatures are unknown.

## Background

The imaging features identified by deep learning classifiers are difficult to describe directly. Deep learning classifiers learn to identify images by optimizing a series of non-linear functions to activate on texture and shapes. The effect of this, is that for a given multilayer network, multiple visually different inputs can act to strongly activate a network's output. Multiple techniques (attention maps, grad-cam maps, saliency maps, guided backpropagation maps, and saliency-attention maps) have been purported to provide insight as to the specific imaging features identified by a deep learning model. We directly investigated the utility of these methods in a radiology context.

## **Evaluation**

Typical organ enhancement patterns that follow vascular contrast agent administration are well understood. We leveraged this and developed a deep learning classifier to identify contrast enhanced renal scan phase from whole slice CT data. The classifier exceeded 90% accuracy on the test set. We utilized this classifier to explore the utility of attention maps, grad-cam maps, saliency maps, guided backpropagation maps, and saliency-attention maps to identify the imaging features our model utilized to predict scan phase.

## Discussion

Saliency maps and guided back propagation maps identify voxels in input imaging which promote model prediction. For most scans these visualizations identified similar anatomical regions which directly reflect renal scan phase (renal: cortex, medulla, artery, vein, aorta, and vene cava). Attention maps, grad-cam maps, and saliency-attention maps illustrate layer activations and indirectly identified the anatomy responsible for these activations. As a whole, these maps indicated that the kidneys were responsible classification but could not clearly localize the features.

#### **Honored Educators**

Presenters or authors on this event have been recognized as RSNA Honored Educators for participating in multiple qualifying educational activities. Honored Educators are invested in furthering the profession of radiology by delivering high-quality educational content in their field of study. Learn how you can become an honored educator by visiting the website at: https://www.rsna.org/Honored-Educator-Award/ Naoki Takahashi, MD - 2012 Honored Educator

# SSE14-04 Multi-Class Deep Learning for Classification of Thoracic Radiographs to Enable Accurate and Efficient Workflow

Monday, Nov. 26 3:30PM - 3:40PM Room: E353C

## Participants

Jennie S. Crosby, BS, Chicago, IL (Presenter) Nothing to Disclose

Thomas J. Rhines, Chicago, IL (Abstract Co-Author) Nothing to Disclose

Feng Li, MD, PhD, Chicago, IL (Abstract Co-Author) Nothing to Disclose

Heber MacMahon, MD, Chicago, IL (*Abstract Co-Author*) Consultant, Riverain Technologies, LLC Stockholder, Hologic, Inc Royalties, UCTech Research support, Koninklijke Philips NV Consultant, General Electric Company

Maryellen L. Giger, PhD, Chicago, IL (*Abstract Co-Author*) Stockholder, Hologic, Inc; Shareholder, Quantitative Insights, Inc; Shareholder, QView Medical, Inc; Co-founder, Quantitative Insights, Inc; Royalties, Hologic, Inc; Royalties, General Electric Company; Royalties, MEDIAN Technologies; Royalties, Riverain Technologies, LLC; Royalties, Mitsubishi Corporation; Royalties, Canon Medical Systems Corporation

## For information about this presentation, contact:

jenniea@uchicago.edu

# PURPOSE

DICOM header information is frequently used to classify image types within the clinical radiological workflow, however, if a header contains incorrect or missing fields, it cannot be reliably used for classification. To expedite image transfer and interpretation, we trained a convolutional neural network in the task of classifying chest radiographs into 4 categories: AP/PA images, lateral images, soft tissue images and bone images (for dual energy studies).

## **METHOD AND MATERIALS**

Our research included 5669 clinical thoracic radiographs. One set of 1911 radiographs, acquired Feb. 2006 to Feb. 2017, was manually sorted into the four categories. The manually sorted set consisted of 818 AP/PA images, 419 lateral images, 389 soft tissue images, and 285 bone images. Classifying the images using DICOM header information alone left 38% unclassified. Using TensorFlow (Google, 2015), an AlexNet architecture network was trained from scratch, in which 1242 images (65%) were used for training, 382 images (20%) for validation, and 287 images (15%) for testing. Next, the trained network was applied to an independent set of 3758 additional images yielding 68 (1.8%) images misclassified, 65% of which were soft tissue and AP/PA images.

## RESULTS

The network classified Images with a high accuracy (98.19%). An important task for clinical workflow is the distinction between an AP/PA and its associated lateral view to ensure correct organization of the imaging sequence as well as appropriate image processing and CAD application. The AUC for distinguishing between AP/PA and lateral was 0.9998  $\pm$  0.0002. Other results included AUC=0.9979  $\pm$  0.0005 in distinguishing between soft tissue and AP/PA images and AUC=1 in distinguishing between soft tissue and bone images. In addition to high performance, the rapid classification of images could be applied in a hospital setting without disruption of clinical workflow. The model was trained in 5 min and classified 3758 images in 3 min. By comparison, an experienced human sorter took about 11.6 hours to classify the test set.

## CONCLUSION

A trained convolutional neural network can classify different radiographic projections from the same study, most notably AP/PA vs. lateral, with high speed and accuracy.

## **CLINICAL RELEVANCE/APPLICATION**

A trained neural network can be used in a clinical setting to quickly and accurately classify radiographs by image type to ensure correct organization of the study sequence.

# SSE14-05 Deep-Learning Renal Segmentation for Fully Automated Radiation Dose Estimation in Radionuclide Therapy

Monday, Nov. 26 3:40PM - 3:50PM Room: E353C

Participants

Price Jackson, PhD, Melbourne, Australia (*Presenter*) Nothing to Disclose Nicholas Hardcastle, PHD, St Leonards, Australia (*Abstract Co-Author*) Nothing to Disclose Noel Dawe, Parkville, Australia (*Abstract Co-Author*) Nothing to Disclose Michael S. Hofman, MBBS, East Melbourne, Australia (*Abstract Co-Author*) Nothing to Disclose Tomas Kron, PHD, East Melbourne, Australia (*Abstract Co-Author*) Nothing to Disclose Rodney Hicks, MBBS, East Melbourne, Australia (*Abstract Co-Author*) Nothing to Disclose

# For information about this presentation, contact:

Price.Jackson@petermac.org

## PURPOSE

Convolutional neural networks have been shown to be powerful tools to assist with object detection and, like a human observer, may be trained based on a relatively small cohort of reference subjects. Rapid, accurate organ recognition in medical imaging permits a variety of new quantitative diagnostic techniques. In the case of therapy with targeted radionuclides, it may permit comprehensive radiation dose analysis in a manner that would often be prohibitively time-consuming using conventional methods.

# **METHOD AND MATERIALS**

An automated image segmentation tool was developed based on 3-dimensional convolutional neural networks to detect right and left kidney contours on low-dose, non-contrast CT images. The model training set involved 89 manually-contoured cases and was then tested on a cohort of 24 patients receiving therapy with 177Lu-PSMA-617 for metastatic prostate cancer. Automatically generated contours were compared with those drawn by expert and assessed for similarity based on dice score, mean distance-to-agreement and total segmented volume. Further, the contours were applied to voxel dose maps computed from post-treatment quantitative SPECT imaging and renal dose estimates using automated and manual means were evaluated for statistical bias.

## RESULTS

Neural network segmentation was able to identify right and left kidneys in all patients with a high degree of accuracy. Mean dice score was  $0.91\pm0.05$  and  $0.86\pm0.18$  for right and left kidneys, respectively, with associated mean distances-to-agreement of  $2.0\pm1.0$  and  $4.0\pm7.5$  millimetres. The system was integrated into the hospital image database, returning contours for a selected study in approximately 90 seconds. Poor performance was observed in 3 patients with cystic kidneys of which only few were included in the training data. Mean radiation absorbed dose based on automated contours was within 4.0% of that computed with manual segmentation.

# CONCLUSION

Automated contouring using convolutional neural networks shows promise in providing quantitative assessment of functional SPECT and PET images; in this case demonstrating comparable accuracy for radiation dose interpretation in radionuclide therapy relative to a human observer.

# **CLINICAL RELEVANCE/APPLICATION**

The primary application of this research is quantitative diagnosis and improved nuclear medicine treatment personalisation.

# SSE14-06 Using Active Learning and Domain Adaptation to Train a 3D-Unet for Liver Segmentation at a High Volume Liver Transplant Center

Monday, Nov. 26 3:50PM - 4:00PM Room: E353C

Participants

Brett Marinelli, MD,MS, New York, NY (*Abstract Co-Author*) Nothing to Disclose Michael Martini, BA, New York, NY (*Abstract Co-Author*) Nothing to Disclose Martin Kang, New York, NY (*Abstract Co-Author*) Nothing to Disclose Anthony Costa, PhD, New York, NY (*Abstract Co-Author*) Nothing to Disclose Eric K. Oermann, MD, New York, NY (*Abstract Co-Author*) Nothing to Disclose Ivan Jambor, MD,PhD, Turku, Finland (*Presenter*) Speakers Bureau, Koninklijke Phillips NV

For information about this presentation, contact:

brett.marinelli@gmail.com

# PURPOSE

To demonstrate the ability of a deep learning model to automatically assess liver volume utilizing publicly available data and active learning that successfully transfers to an external cohort at a high volume transplant center.

# **METHOD AND MATERIALS**

131 CTs and liver segmentations were used from the MICCAI Grand Challenge LiTS dataset. 257 clinically acquired CTs (CACs) were collected from an institution's PACs where liver volumetry was recorded. CACs are from between 1/2014 - 12/2016 and include145 pre-transplant evaluations (56%), 159 cirrhotics (62%), 92 hepatocellular carcinoma cases (36%), and 18 prospective living liver transplant donors (7.0%). A preprocessing pipeline standardized all images to 128x128x128 voxels. As a benchmark, a 3D-UNet convolutional neural network (CNN) was trained on an 80/20 train/validation split of the LiTS dataset. Then, a 3D-UNet was fit to a training set composed of the LiTS dataset augmented by six copies of five CACs in an active learning framework. A semi-automatic GrowCut method was used for segmentation of active learning cases with Slicer3D. The CAC dataset excluding active learning scans was used as the comparative test set. Dice similarity validation scores were recorded. Successful volume measurement was defined as a difference within 200cc. Median and 1st-3rd interquartile range (IQR) were reported for both tested models. A paired student's t-test compared performance before and after implementation of active learning.

# RESULTS

The benchmark model demonstrated a 0.90 Dice on the LiTS validation set, successful volume measurements in 139/257 livers and median absolute difference of 180 mL (IQR 80-311 mL) in the test set. The active learning approach demonstrated a 0.84 Dice on the LiTS validation cohort, successful volume measurements in 150/252 livers and a median absolute difference of 160 mL (IQR 67-313mL). The active learning approach yielded superior results (P=0.04).

## CONCLUSION

Combining active learning and domain adaptation for liver segmentation can significantly improve model performance at capturing liver volumes utilizing publicly available datasets while deploying the model at a high volume liver transplant center.

## **CLINICAL RELEVANCE/APPLICATION**

We describe methods that use a deep learning model for automatically assessing liver volume with publicly available data and active learning that successfully transfers to an external cohort at a high volume transplant center.



# Musculoskeletal (Upper Extremity)

Monday, Nov. 26 3:00PM - 4:00PM Room: N228



AMA PRA Category 1 Credit ™: 1.00 ARRT Category A+ Credit: 1.00

## Participants

Ambrose J. Huang, MD, New York, NY (*Moderator*) Nothing to Disclose Connie Y. Chang, MD, Boston, MA (*Moderator*) Nothing to Disclose

# Sub-Events

# SSE15-01 Dynamic MRI of the Midcarpal Compartment in 20 Seconds: Normal Motion Pattern Analysis and Reader Reliability

Monday, Nov. 26 3:00PM - 3:10PM Room: N228

Participants

Stephen S. Henrichon, MD, Sacramento, CA (*Presenter*) Nothing to Disclose Brent Foster, Sacramento, CA (*Abstract Co-Author*) Nothing to Disclose Calvin B. Shaw, MD, Sunnyvale, CA (*Abstract Co-Author*) Nothing to Disclose Christopher Bayne, Sacramento, CA (*Abstract Co-Author*) Nothing to Disclose Robert M. Szabo, MD,MPH, Sacramento, CA (*Abstract Co-Author*) Research Grant, Medartis AG Abhijit J. Chaudhari, PhD, Sacramento, CA (*Abstract Co-Author*) Nothing to Disclose Robert D. Boutin, MD, Davis, CA (*Abstract Co-Author*) Nothing to Disclose

# For information about this presentation, contact:

rdboutin@ucdavis.edu

## PURPOSE

To describe the normal motion pattern of the scaphotrapezial joint (STJ) and capitate-triquetrum interval (CTI) during active radial and ulnar deviation of the wrist during dynamic MRI, and to determine the observer performance of measurements in asymptomatic volunteers.

## **METHOD AND MATERIALS**

In this prospective study, real-time 3T MRI examinations were performed in 35 wrists (19 asymptomatic volunteers; age mean: 30.5 yrs [range: 20-55]; M/F:10/9). Using a radial fast-GRE coronal sequence with 315 ms temporal resolution and a total acquisition time of ~ 20 seconds, 60 images were acquired during continuous imaging of the moving wrist through the full range of motion from radial to ulnar deviation. Two independent readers measured 1) the transverse translation of the trapezium at the STJ and 2) the CTI. A two-sample Kolmogorov-Smirnov goodness-of-fit hypothesis test was performed to evaluate the relationship between these measurements with laterality (right vs. left), sex, lunate type, and wrist kinematic pattern (row vs. column kinematics). Intra-observer and inter-observer correlation coefficients were determined.

## RESULTS

Translation of the trapezium at the STJ in neutral, radial, and ulnar deviation averaged  $0.3\pm0.8$  mm,  $1.9\pm1.2$  mm, and  $-0.4\pm1.0$  mm, respectively. There was no significant difference in trapezium translation with wrist laterality, sex, lunate type, or wrist kinematic pattern. The CTI in neutral, radial, and ulnar deviation averaged  $5.3\pm1.4$  mm,  $3.6\pm1.1$  mm, and  $6.0\pm1.4$  mm, respectively. The mean CTI was greater in men than women in the neutral position only (p=0.019). The mean CTI was increased in wrists with type II lunates during radial (p=0.001) and ulnar deviation (p=0.014). There was no difference in CTI with wrist laterality or wrist kinematic pattern. Mean intraobserver and interobserver correlation coefficient was 0.79 and 0.77, respectively.

# CONCLUSION

Using dynamic MRI, this study provides a normal range of expected STJ and CTI measurements in asymptomatic wrists. Dynamic MRI with a short acquisition time may be used as a supplement to conventional static MRI in the diagnostic evaluation of the midcarpal compartment.

## **CLINICAL RELEVANCE/APPLICATION**

Understanding midcarpal motion patterns is a key step in efforts to establish an accurate diagnosis and promote optimized treatment regimes including nonoperative rehabilitation and surgical planning.

# SSE15-02 Distal Radioulnar Joint MR Arthrography for Diagnosing Foveal Tear of Triangular Fibrocartilage: Comparison of MR imaging and MR Arthrography with Arthroscopic Correlation

Monday, Nov. 26 3:10PM - 3:20PM Room: N228

Kyung-Sik Ahn, MD, Seoul, Korea, Republic Of (*Abstract Co-Author*) Nothing to Disclose Chang Ho Kang, MD, Seoul, Korea, Republic Of (*Abstract Co-Author*) Nothing to Disclose Suk-Joo Hong, MD, Rochester, MN (*Abstract Co-Author*) Nothing to Disclose Baek Hyun Kim, MD, Ansan, Korea, Republic Of (*Abstract Co-Author*) Nothing to Disclose Euddeum Shim, Ansan, Korea, Republic Of (*Abstract Co-Author*) Nothing to Disclose

# PURPOSE

To evaluate the value of distal radioulnar joint (DRUJ) MR arthrography for diagnosing foveal tear of triangular fibrocartilage (TFC).

## **METHOD AND MATERIALS**

A total of 83 patients (54 men, 29 women; mean age, 32.7 years) who underwent DRUJ MR arthrography and arthroscopy were retrospectively reviewed. MR protocol includes pre-injection T2- and T1-weighted coronal images and post-injection T2-weighted coronal and T1-weighted fat suppressed coronal, sagittal, and axial images. Two radiologists graded the foveal lamina of the TFC as normal, partial tear, or complete tear after the review of pre-injection image sets and post-injection image sets separately. Diagnostic performance of MR imaging and MR arthrography was assessed based on the arthroscopic findings and compared by using McNemar test.

#### RESULTS

On arthroscopy, 71 of 83 patients had foveal tear of TFC; 51 cases were isolated foveal tear and 20 cases were combined foveal and styloid tear. On the review of MR images, the sensitivity, specificity, and accuracy for diagnosing foveal tear were 62.0%, 41.7%, and 59.0%. In MR arthrography, the values were 94.4%, 41.7%, and 86.7%, respectively. Sensitivity was significantly higher in DRUJ MR arthrography (P < .001).

#### CONCLUSION

DRUJ MR arthrography increase the accuracy for diagnosing foveal tear of TFC compared to standard MR imaging. The benefit of pre-injection images was minimal in diagnosing foveal tear of TFC.

#### **CLINICAL RELEVANCE/APPLICATION**

DRUJ MR arthrography increase the accuracy for diagnosing foveal tear of TFC compared to standard MR imaging.

# SSE15-03 Bennett Lesions in Overhead Throwers and Associated Shoulder Abnormalities on MRI

Monday, Nov. 26 3:20PM - 3:30PM Room: N228

Participants

Jenika Karcich, MD, New York, NY (*Presenter*) Nothing to Disclose Jonathan K. Kazam, MD, New York, NY (*Abstract Co-Author*) Nothing to Disclose Michael J. Rasiej, MD, New York, NY (*Abstract Co-Author*) Nothing to Disclose Tony T. Wong, MD, New York, NY (*Abstract Co-Author*) Nothing to Disclose

## For information about this presentation, contact:

jek9125@nyp.org

## PURPOSE

To determine if the presence of a Bennett lesion in overhead throwers is associated with additional shoulder abnormalities on MRI.

## **METHOD AND MATERIALS**

An IRB approved retrospective review of our database from 1/2012 to 4/2018 identified 35 overhead throwers with a Bennett lesion on MRI. An additional control group consisting of 35 overhead throwers without a Bennett lesion were matched for age, level of play (professional vs. non-professional), and type of study (arthrogram vs. non-arthrogram). Each study was assessed independently by 2 MSK fellowship trained radiologists. The sizes of the Bennett lesions were measured. Each MRI was assessed for the presence of a labral tear, posterior glenoid cartilage deficiency, humeral head notching/cysts, and posterior supraspinatus/infraspinatus tendon fraying or tear. Discrepancies were adjudicated by a third MSK fellowship trained radiologist. Statistical analysis was performed with a chi-squared test.

### RESULTS

Average Bennett lesion volume in a professional vs. non-professional overhead thrower: 708 mm3 vs. 545 mm3 (p=0.43). Total Bennett lesions resected: 6% (2/35) Associated MRI abnormalities in Bennett vs. Non-Bennett overhead throwers: SLAP tear: 51% vs. 31% (p = 0.09) Posterior labral tear: 51% vs. 31% (p=0.09) Anteroinferior labral tear: 26% vs. 17% (p=0.38) Posterior glenoid cartilage abnormality (fissure, delamination, partial/full thickness): 23% vs. 3% (p = 0.01) Humeral head notching/cysts: 77% vs. 63% (p = 0.19) Articular surface rotator cuff fraying/tear: 26% vs. 17% (p = 0.38)

## CONCLUSION

Overhead throwers with Bennett lesions have an increased frequency of posterior glenoid cartilage abnormalities, but not labral tears or findings of internal impingement.

# CLINICAL RELEVANCE/APPLICATION

The presence of a Bennett lesion in an overhead thrower warrants close examination for an adjacent posterior glenoid cartilage abnormality.

# SSE15-04 Comparison Between High-Resolution Isotropic Three-Dimensional Cube FS PD and Conventional Two-Dimensional FS PD MR Images of the TFCC at 3 Tesla

Yanmei Qi, Gansu, China (*Presenter*) Nothing to Disclose Sheng Zhou, Lanzhou, China (*Abstract Co-Author*) Nothing to Disclose Xiaofei Chen, BA, Lanzhou, China (*Abstract Co-Author*) Nothing to Disclose Yuan Wang, Lanzhou, China (*Abstract Co-Author*) Nothing to Disclose Fu Wen Dong, Lan Zhou, China (*Abstract Co-Author*) Nothing to Disclose

## For information about this presentation, contact:

1424125302@qq.com

## PURPOSE

To compare a newly developed high-resolution isotropic 3D Cube FS PD sequence with conventional high-resolution sequences in assessing TFCC of the wrist in term of image quality and diagnostic performance.

## **METHOD AND MATERIALS**

12 volunteers were enrolled in the study with an average age 22.7 years (range 22-27 years). All the sequences were carried out on all volunteers at 3.0T MR scanner (Signa HDxt, GE Healthcare, Milwaukee, WI) and a Wrist Array coil. Each imaging was performed with 2D PD FS(coronal,axial and sagittal:TR=2900ms,,TE=32.0ms,Matrix=320×256, FOV=10×7cm2, Slicethickness =2.0mm,gap=0.3mm,NEX=2,acquisition,time=99s)and 3D isotropic PD FS (coronal:TR=1400ms, TE=36.4,Matrix=256×256, FOV=10×9cm2, Slicethickness=0.4mm, gap=-0.2mm, NEX=0.5, acquisition time=279s).Delineation of anatomic structures of the wrist, amount of artifact, effect of fat suppression, image blur, and overall quality were qualitatively evaluated using the 5-point scoring system(5: excellent, 4: good,3: satisfactory, 2: poor, and 1: nonidentified.Signal-to-noise-ratios (SNR) of each structure and contrast-to-noise ratios(CNR)between structures of the TFCC were quantitatively measured using vendor supplied software (AW4.6work station, GE).

# RESULTS

The 2D MRI demonstrated higher scores than 3D in anatomic structure of the SL ligament(P=0.043), the LT ligament(P=0.022), cartilage(P=0.043), artifact(p=0.007) and image blur(p=0.015). However, there were no statistical significance between 2D and 3D MRI in disc and overall quality. Higher SNR values were found for in the 2D sequence  $(6.32\pm3.32)$  than the 3D(4.20±1.66), The corresponding CNR values were( $4.87\pm3.10$ ) for the 2D and( $3.45\pm1.97$ ) for the 3D.To better control for voxel size, we also measured the SNR and CNR values in the reconstructed 2-mm images from original 3D isotropic images and obtained similar values as in the 2D ( $5.86\pm3.05$  and  $3.01\pm0.86$ , respectively), indicating that reconstruction with larger slice thickness improved SNR and CNR.

# CONCLUSION

Although, Isotropic 3D Cube FS PD sequence may enhance standard wrist MRI by increased visualization of multiplanar and post processing capabilities, however, the 3D Cube image quality was lower.

# **CLINICAL RELEVANCE/APPLICATION**

With regard to clinical applications, 3D Cube image of the wrist has almost equal potential to 2D MRI.

# SSE15-05 Correlation Between Fat Fraction, Cross Sectional Area of Rotator Cuff and Muscle Strength: Using MRI DIXON Sequence and Biodex Isokinetic Test

Monday, Nov. 26 3:40PM - 3:50PM Room: N228

Participants

Sung Tae Hwang, Seoul, Korea, Republic Of (*Presenter*) Nothing to Disclose Chang Ho Kang, MD, Seoul, Korea, Republic Of (*Abstract Co-Author*) Nothing to Disclose Kyung-Sik Ahn, MD, Seoul, Korea, Republic Of (*Abstract Co-Author*) Nothing to Disclose Woong-Kyo Jeong, MD, Seoul, Korea, Republic Of (*Abstract Co-Author*) Nothing to Disclose Suk-Joo Hong, MD, Rochester, MN (*Abstract Co-Author*) Nothing to Disclose Baek Hyun Kim, MD, Ansan, Korea, Republic Of (*Abstract Co-Author*) Nothing to Disclose Euddeum Shim, Ansan, Korea, Republic Of (*Abstract Co-Author*) Nothing to Disclose

# PURPOSE

To evaluate the correlation between fat fraction (FF), cross sectional area (CSA) of rotator cuff and muscle strength using T2weighted Dixon Spin-Echo Fat image and biodex isokinetic test.

## **METHOD AND MATERIALS**

37 patients (13 men, 24 women; age range, 45-78 years) undergoing shoulder MR imaging with concomitant biodex isokinetic test were enrolled in this study. Quantitative fat analysis and CSA measurement of rotator cuff (supraspinatus [SS], infraspinatus [IS], teres minor [TM]) in the image plane of scapular Y-shape were performed by one musculoskeletal radiologist using a post-processing software (Syngo via, Siemens healthineers, Erlangen, Germany) for T2-weighted Dixon Spin-Echo fat image. Multivariate regression and multiple linear regression analysis were used to investigate the relationship between 4 biodex isokinetic test parameters (peak torque [PT], peak torque/body weight [BW], torque at 30° [T30], total work [TW]) for 8 shoulder movements (60°, 180° flexion [FL] and extension [EX], 60°, 180° internal rotation [IR] and external rotation [ER]) and FF and CSA of the rotator cuff.

## RESULTS

Multiple linear regression analysis shows significant correlation between CSA of SS and T30, TW of 180° ER; PT, T30, TW of 60° IR; PT, T30, TW of 180° IR, and between CSA of IS and T30 of 60° IR; PT, BW, TW of 180° ER (all p <= 0.04). A significant correlation between FF of IS with all parameters of 180° IR and 180° ER, and between CSA of IS with all parameters of 180° IR was found on multivariate regression analysis (all p <= 0.04). FF of TM was significantly associated with PT, T30, TW of 60° IR (p <= 0.03). There was no significant correlation between CSA and FF of rotator cuff and parameters of FL and EX, whereas age and sex were significantly associated with parameters of FL and EX, as well as with some parameters of ER and IR (all p <= 0.05).

# CONCLUSION

CSA and FF of SS and IS measured on T2-weighted Dixon Spin-Echo Fat image correlated with the strength of shoulder movements, especially IR and ER. Therefore, the strength of rotator cuff could be more elaborately evaluated by measuring both FF and CSA of the muscles.

# **CLINICAL RELEVANCE/APPLICATION**

CSA measurements and fat quantification using DIXON have the potential to become an important clinical resource when evaluating the muscles of the rotator cuff.

# SSE15-06 Intra and Inter Observer Variability among Different Methods of Measuring Carpal Collapse

Monday, Nov. 26 3:50PM - 4:00PM Room: N228

#### Awards

**Student Travel Stipend Award** 

#### Participants

Muhil Kannan, MD, Coimbatore, India (*Presenter*) Nothing to Disclose Sumit Agrawal, MS, Katmandu, Nepal (*Abstract Co-Author*) Nothing to Disclose Tarun Chabra, Coimbatore, India (*Abstract Co-Author*) Nothing to Disclose Praveen Bhardwaj, MS, Coimbatore, India (*Abstract Co-Author*) Nothing to Disclose Pushpa Bhari Thippeswamy, MD, MBBS, Coimbatore, India (*Abstract Co-Author*) Nothing to Disclose Anupama N. V., MBBS, FRCR, Coimbatore, India (*Abstract Co-Author*) Nothing to Disclose Raja Sabapathy S, MS, Coimbatore, India (*Abstract Co-Author*) Nothing to Disclose

## For information about this presentation, contact:

dr.muhil@gmail@gmail.com

# PURPOSE

To find out that the method with least intraobserver and interobserver variability among different methods used for determining carpal collapse.

# METHOD AND MATERIALS

Retrospective radiographic evaluation of 50 normal wrist PA radiographs were done by 3 observers, measuring normitative values of Carpal height ratio (CHR), Revised Carpal Height Ratio (RCH ratio), Capitate radius (CR index). 1) Carpal Height Ratio (CHR) measured by carpal height divided by the length of 3rd metacarpal. 2) Revised Carpal Height Ratio (RCH ratio) measured by dividing the carpal height by the length of capitate. 3) Capitate radius (CR index) measured by closest distance between the distal edge of radius and the proximal edge of capitate. The measurements were repeated after one month by all the observers. Data was collected and statistical analysis was done by using SPSS 21 version. Data from all the observers were was described in descriptive terms with mean and standard deviation. For intra observer variability, correlation coefficient was calculated for every individual observer. For inter observer variability intraclass correlation coefficient was calculated and presented with r and p value.

## RESULTS

Total of 50 normal wrist PA radiographs (17 females and 33 males) were studied between the age 13 to 71 years with mean age of 37.52 years. The mean range of values in our study for CHR was  $0.49 \pm .03$ to  $.51 \pm .03$ ; RCHR  $1.51 \pm .077$  to  $1.57 \pm .059$  and CRI  $0.972 \pm .09$  to  $1.06 \pm .12$ . The r value was close to 0.91 and p value was <0.001 in all the three observers in CR Index meaning that the intra observer variability was least in CR Index. For the inter observer variability Intra Class Coefficient of 0.9 indicates that the CR Index has the least variability. RCH Ratio has the maximum variability in both inter and intra observer comparisions

## CONCLUSION

We conclude that CR Index is the best method to measure carpal collapse in terms of reproducibility of the results.

## **CLINICAL RELEVANCE/APPLICATION**

With regard to intra and inter observervariability, CR Index was most reliable measurement for carpal collapse, as only one measurement is taken in CR index and the measurement points are well defined.



# **Musculoskeletal (Metal Artifact Reduction Techniques)**

Monday, Nov. 26 3:00PM - 4:00PM Room: N227B



AMA PRA Category 1 Credit ™: 1.00 ARRT Category A+ Credit: 1.00

**FDA** Discussions may include off-label uses.

#### Participants

Christian W. Pfirrmann, MD, MBA, Forch, Switzerland (*Moderator*) Nothing to Disclose Luca Maria Sconfienza, MD, PhD, Milano, Italy (*Moderator*) Travel support, Bracco Group; Travel support, Esaote SpA; Travel support, ABIOGEN PHARMA SpA; Speakers Bureau, Fidia Pharma Group SpA

#### Sub-Events

# SSE16-01 Metal Artifact Reduction MRI of Patients with Painful Hip Arthroplasty Implants: Fully Sampled SEMAC versus Vastly Undersampled Compressed Sensing SEMAC

Monday, Nov. 26 3:00PM - 3:10PM Room: N227B

Participants

Benjamin Fritz, MD, Zurich, Switzerland (*Presenter*) Nothing to Disclose Robert Sterling, Baltimore, MD (*Abstract Co-Author*) Nothing to Disclose Mathias Nittka, PhD, Erlangen, Germany (*Abstract Co-Author*) Employee, Siemens AG Reto Sutter, MD, Zurich, Switzerland (*Abstract Co-Author*) Nothing to Disclose Jan Fritz, MD, Baltimore, MD (*Abstract Co-Author*) Research Grant, Siemens AG; Scientific Advisor, Siemens AG; Scientific Advisor, Alexion Pharmaceuticals, Inc; Speaker, Siemens AG

# For information about this presentation, contact:

benjamin.fritz@balgrist.ch

# PURPOSE

To compare fully sampled slice-encoding for metal artifact correction (SEMAC) and vastly undersampled compresses sensing-(CS)-SEMAC sequences for metal artifact reduction MRI in patients with total hip arthroplasty (THA).

# METHOD AND MATERIALS

Following internal review board approval and informed consent, 30 patients with pain and dysfunction following THA underwent prospectively 1.5 T MRI, including coronal intermediated-weighted (IW)- and short tau inversion recovery (STIR) SEMAC (22:39 min) and CS-SEMAC (9:55 min) pulse sequences with otherwise identical parameters. Following anonymization and randomization, two fellowship-trained musculoskeletal radiologists independently evaluated the datasets. Outcome variables included image quality parameters, bone implant interface visibility, overall reader satisfaction, detection rate of abnormalities of the hip joint. Statistical analysis included kappa statistics and paired rank sum tests. P-values <= 0.05 were considered significant.

#### RESULTS

The inter-observer agreements were at least adequate for all categories (kappa > 0.58). There was no significant difference for the technical parameters, including motion (p = 0.69), blur (p = 0.37), noise (p = 0.06), metal artifact reduction (p = 0.46), tissue contrast (p = 0.81), and fat-suppression (p > 0.99). The visibility of bone implant interface of the acetabular and femoral component was rated on average as "good" indicting minimal impairment with preservation of all structural details without significant differences between SEMAC and CS-SEMAC (p = 0.51). The overall reader satisfaction was "good" for both SEMAC and CS-SEMAC (p=0.85). For SEMAC versus CS-SEMAC, readers found an average of 18 versus 18 osteolyses (p = 0.87), 15 versus 17 cases of synovitis (p = 0.38), 23 versus 21 peritorchanteric fluid accumulations (p = 0.55) and 23 versus 19 abductor tendon tears (p = 0.34), respectively.

## CONCLUSION

In patients with painful hip arthroplasty implants, fully sampled and vastly undersampled SEMAC pulse sequences produce similar image quality and afford similar detection rates of abnormalities.

#### **CLINICAL RELEVANCE/APPLICATION**

The vastly undersampled CS-SEMAC technique allows for 55% faster MRI of THA implants, thereby preserving the detection rates of abnormalities, when compared to fully sampled SEMAC technique.

# SSE16-02 SEMAC-VAT MR Imaging at 1.5 T in Patients with Pedicle Screw Fixation: Is It Superior to Standard MR Imaging for the Detection of Postoperative Complications?

Chankue Park, Yangsan, Korea, Republic Of (*Presenter*) Nothing to Disclose Eugene Lee, Seongnam-Si, Korea, Republic Of (*Abstract Co-Author*) Nothing to Disclose Yusuhn Kang, MD, Seoul, Korea, Republic Of (*Abstract Co-Author*) Nothing to Disclose Joon Woo Lee, MD, PhD, Sungnamsi, Korea, Republic Of (*Abstract Co-Author*) Nothing to Disclose Joong Mo Ahn, MD, PhD, Pittsburgh, PA (*Abstract Co-Author*) Nothing to Disclose Heung Sik Kang, Gyeonggi-Do, Korea, Republic Of (*Abstract Co-Author*) Nothing to Disclose

# PURPOSE

To compare the Slice-encoding metal artifact correction (SEMAC)-View-angle tilting (VAT) sequence with the standard turbo-spin echo (TSE) MR sequence for image quality, visibility of periprosthetic structures, and diagnostic confidence for detection of postoperative complications in patients with pedicle screw fixation at 1.5 T.

## **METHOD AND MATERIALS**

Seventy patients with pedicle screw fixation between the thoracic vertebrae and the sacrum were included. SEMAC-VAT imaging were compared with standard TSE images. The MR imaging were retrospectively evaluated by two radiologists for SNR (signal-to-noise ratio) of anatomical structures and size of artifacts, visibility of periprosthetic anatomical structures, and diagnostic confidence for detection of postoperative complications. Paired t-tests and Wilcoxon signed-rank tests were used for comparisons, and intra-class correlation and kappa values were used for inter-observer agreement.

## RESULTS

For all anatomical structures, the signal-to-noise ratio was significantly lower for SEMAC-VAT than for TSE images (p < 0.001). SEMAC-VAT images demonstrated effective artifact reduction compared to TSE images (p < 0.001). The visibility of most periprosthetic anatomical structures, and diagnostic confidence for detection of postoperative complications, were better for SEMAC-VAT than for TSE imaging (p < 0.001). For the spinal canal, however, TSE was better (p < 0.001).

## CONCLUSION

MR images with SEMAC-VAT can significantly reduce metal artifact, providing improved delineation of periprosthetic anatomical structures and diagnostic confidence for detection of postoperative complication compared with standard TSE images. For the spinal canal, however, TSE was better.

## **CLINICAL RELEVANCE/APPLICATION**

Taking into account the results of our own, we propose the following guidelines for performing SEMAC-VAT image on patients with pedicle screw fixation.

# SSE16-03 Metal Artifact Reduction on Photon-Counting-Detector CT Using Tin Filtration and Detection of High-Energy Photons

Monday, Nov. 26 3:20PM - 3:30PM Room: N227B

## Awards

## **Student Travel Stipend Award**

Participants

David J. Bartlett, MD, Rochester, MN (*Presenter*) Nothing to Disclose Amy L. Kotsenas, MD, Rochester, MN (*Abstract Co-Author*) Nothing to Disclose Felix E. Diehn, MD, Rochester, MN (*Abstract Co-Author*) Nothing to Disclose Katrina N. Glazebrook, MBChB, Rochester, MN (*Abstract Co-Author*) Nothing to Disclose Wei Zhou, PhD, Rochester, MN (*Abstract Co-Author*) Nothing to Disclose Joel G. Fletcher, MD, Rochester, MN (*Abstract Co-Author*) Grant, Siemens AG; Consultant, Medtronic plc; ; Jayse Weaver, Rochester, MN (*Abstract Co-Author*) Nothing to Disclose Shuai Leng, PHD, Rochester, MN (*Abstract Co-Author*) Nothing to Disclose Shuai Leng, PHD, Rochester, MN (*Abstract Co-Author*) Nothing to Disclose Rickey E. Carter, PhD, Jacksonville, FL (*Abstract Co-Author*) Nothing to Disclose

## For information about this presentation, contact:

bartlett.david@mayo.edu

## PURPOSE

To evaluate the use of photon-counting-detector CT with tin filtration (PCD-CT Sn) to improve diagnosis in patients with orthopedic metal implants.

# **METHOD AND MATERIALS**

Adult patients with orthopedic metal implants underwent CT using commercial energy-integrating-detector CT (EID-CT) followed by PCD-CT Sn (140 kV, 0.4 mm Sn, energy thresholds of 25 and 75 keV). EID-CT and PCT-CT Sn Bin 2 (75 - 140 keV) 2-mm images were reconstructed. Three radiologists blindly evaluated images in a side-by-side fashion, comparing predefined anatomic structures using a 6-point scale (0 = critical structures totally obscured to 5 = anatomic recognition with high confidence in diagnosis). Preference for PCD-CT Sn was assessed using a 5 point scale (-2= decline in confidence; 0= no difference; +2= improvement in diagnostic confidence). The effect of artifact on the ability to make a diagnosis was also graded (1= artifact has no/minimal effect to 3= artifact impedes diagnosis), with quantitative analysis measuring the width of most prominent artifact at the axial plane. Statistical analysis was performed using the Wilcoxon signed rank test, where p<0.05 was considered statistically significant.

## RESULTS

20 patients with orthopedic metal implants were included in the study, with hardware in the spine in 12 patients, shoulder in 3, and extremities in 5. The mean overall visualization scores of the cortex, trabeculae, and implant-trabecular interface were significantly better for PCT-CT Sn (4.4. vs. 3.3, p<0.0001). For spinal hardware, PCD-CT Sn showed improved image quality score for the central canal (3.3 v 0.9, p<0.0001), with similar findings for neural foramina. The mean overall preference score for PCT-CT Sn was +1.6  $\pm$  0.7 compared to EID (p<.0001), indicating improved diagnostic confidence. The effects of metal artifact on diagnosis were

less at PCD-CT Sn (1.9 v 2.6, p<0.0001), and the width of the metal artifact was substantially reduced (from 1.1  $\pm$  1.4 cm to 0.5  $\pm$  0.5 cm, p<0.0001).

# CONCLUSION

Selection of high-energy photons using a Sn filter and PCD-CT bin 2 images markedly improves visualization of key anatomic structures and improves diagnostic confidence by reducing the size of metal-related artifacts.

## **CLINICAL RELEVANCE/APPLICATION**

PCD-CT with tin filtration and reconstruction of images obtained using high-energy photons provides additional critical diagnostic information compared to commercial EID-CT systems to patients with metal implants.

# SSE16-04 Utility of CT Metal Artifact Reduction Algorithms for Intervertebral Devices: Experimental Study in Ex Vivo Bovine Coccyx Using Micro-CT as the Reference Standard

Monday, Nov. 26 3:30PM - 3:40PM Room: N227B

Participants

Miyuki Takasu, MD, Hiroshima, Japan (*Presenter*) Nothing to Disclose Kazuyoshi Nakanishi, Hiroshima, Japan (*Abstract Co-Author*) Nothing to Disclose Chikako Fujioka, RT, Hiroshima, Japan (*Abstract Co-Author*) Nothing to Disclose Shota Kondo, Hiroshima, Japan (*Abstract Co-Author*) Nothing to Disclose Tomoyo Fuji, Hiroshima, Japan (*Abstract Co-Author*) Nothing to Disclose Masao Kiguchi, RT, Hiroshima, Japan (*Abstract Co-Author*) Nothing to Disclose Chihiro Tani, MD, Hiroshima, Japan (*Abstract Co-Author*) Nothing to Disclose Kazuo Awai, MD, Hiroshima, Japan (*Abstract Co-Author*) Nothing to Disclose Kazuo Awai, MD, Hiroshima, Japan (*Abstract Co-Author*) Nothing to Disclose Kazuo Awai, MD, Hiroshima, Japan (*Abstract Co-Author*) Nothing to Disclose Kazuo Awai, MD, Hiroshima, Japan (*Abstract Co-Author*) Research Grant, Canon Medical Systems Corporation; Research Grant, Hitachi, Ltd; Research Grant, Fujitsu Limited; Research Grant, Bayer AG; Research Grant, DAIICHI SANKYO Group; Research Grant, Eisai Co, Ltd; Medical Advisory Board, General Electric Company; ;

# PURPOSE

The accuracy of radiological assessments of bony fusion following spinal fusion is affected by radiographic interference from metallic components of the intervertebral devices. Therefore, this study evaluated the utility of dedicated CT metal artifact reduction algorithms (SEMAR and MAR) for measuring trabecular bone microarchitecture in a comparison using micro-CT as the gold standard.

# **METHOD AND MATERIALS**

Twenty bovine coccyges with and without titanium or poly-ether-ether-ketone (PEEK) interbody devices were scanned by ultrahigh resolution MDCT (Aquilion Precision, SEMAR), 256-MDCT (Revolution CT, MAR), and micro-CT as the gold standard. The quality of the MDCT images was evaluated in terms of the visibility of trabecular bone using a 3-point Likert scale. Trabecular thickness (Tb.Th), trabecular number (Tb.N), trabecular separation (Tb.Sp), fractal dimension (FD), and volumetric bone mineral density (vBMD) of the same 10-mm-thick portion of coccyx including a metal artifact were obtained for MDCTs and micro-CT. Relationships between MDCT- and micro-CT-derived trabecular bone indices were compared.

# RESULTS

The mean reduction in the width of the artifact was 48.7% for SEMAR/titanium, 20.6% for SEMAR/PEEK, 15.8% for MAR/titanium, and 18.9% for MAR/PEEK. The image quality analysis revealed that the artifact was removed from the trabecular bone space in 72.7% of the SEMAR/titanium images and 18.2% of the images obtained using the three other combinations. FD, Tb.Th, Tb.Sp, and vBMD measured by ultra-high resolution MDCT were found to be significantly correlated with micro-CT values ( $\rho$ =0.486~0.499, p= <0.001~0.05) while no significant correlation was observed between 256-MDCT- and micro-CT values. For coccyx with titanium, the correlations of Tb.Th, Tb.Sp, and vBMD with micro-CT values were improved by SEMAR ( $\rho$ =0.491~0.489, p=<0.001~0.05). For coccyx with PEEK, correlations of FD, Tb.Sp, and vBMD with micro-CT values were improved by SEMAR ( $\rho$ =0.502~0.525, p= <0.001~0.05).

# CONCLUSION

SEMAR combined with ultra-high resolution MDCT objectively and subjectively decreases metal artifacts when compared to 256-MDCT with MAR. Correlations of trabecular indices and vBMD with micro-CT values were improved with SEMAR.

## **CLINICAL RELEVANCE/APPLICATION**

Trabecular bone architecture can be assessed using ultra-high resolution MDCT with a metal artifact reduction algorithm, suggesting that it is possible to evaluate bony fusion after spinal fusion.

# SSE16-05 Combined Iterative Metal Artifact Reduction Reconstruction and Virtual Monoenergetic Extrapolation at Higher Photon Energies in CT Imaging of Ankle Arthroplasty Implants

Monday, Nov. 26 3:40PM - 3:50PM Room: N227B

## Awards

## Student Travel Stipend Award

Participants

Iman Khodarahmi, MD, PhD, Baltimore, MD (*Presenter*) Nothing to Disclose Reham R. Haroun, MD, Salt Lake City, UT (*Abstract Co-Author*) Nothing to Disclose George S.K. Fung, PhD, Ellicott City, MD (*Abstract Co-Author*) Employee, Siemens AG Matthew K. Fuld, PhD, Malvern, PA (*Abstract Co-Author*) Employee, Siemens AG Elliot K. Fishman, MD, Baltimore, MD (*Abstract Co-Author*) Institutional Grant support, Siemens AG; Institutional Grant support, General Electric Company; Co-founder, HipGraphics, Inc Jan Fritz, MD, Baltimore, MD (*Abstract Co-Author*) Research Grant, Siemens AG; Scientific Advisor, Siemens AG; Scientific Advisor, Alexion Pharmaceuticals, Inc; Speaker, Siemens AG

For information about this presentation, contact:

## PURPOSE

To compare the effects of combined virtual monoenergetic extrapolation (VME) and iterative metal artifact reduction (iMAR) at higher photon energies on low and high-density metal artifacts and overall image quality.

## **METHOD AND MATERIALS**

Six total ankle arthroplasties were implanted into human cadaveric ankles and underwent computed tomography with a dual-source scanner at tube voltages of 80 and tin-filtered 150 kVp to produce mixed 120 kVp equivalent polychromatic images. Image datasets were created with six protocols including polychromatic weighted filtered back projection (WFBP), polychromatic iMAR, monoenergetic WFBP at 150 and 190 keV, and monoenergetic iMAR at 150 and 190 keV. High- and low-density artifacts were separately quantified with a threshold-based MATLAB script. After anonymization and randomization, two observers independently ranked the datasets for overall image quality. A conservative p-value of less than 0.001 was considered significant for all statistical analyses.

## RESULTS

Least amount of high-density artifacts were visualized with iMAR 190 keV and iMAR 150 keV (all p-values < 0.001), whereas polychromatic iMAR was the most effective method of mitigating low-density streaks (p-values < 0.001). For both low and high-density artifacts, polychromatic iMAR acquisition was superior to WFBP 150 keV and WFBP 190 keV (p-values < 0.001). Readers ranked the overall image quality of polychromatic iMAR images highest on sharp kernel reconstructions (p-values < 0.001). Similarly, on soft tissue kernel reconstructions, the polychromatic iMAR images were ranked the highest with a statistically significant difference over other techniques (p-values < 0.001), except for iMAR 150 keV (p = 0.356).

## CONCLUSION

iMAR with polychromatic spectra and VME result in fewer metal artifacts and better image quality than WFBP with polychromatic spectra and VME. The combination of iMAR and VME at higher photon energies results in mixed effects on implant-induced metal artifacts, including decreasing high-density artifacts and increasing low-density artifacts, which in combination may not improve image quality for a particular implant when compared to polychromatic iMAR images at lower photon energies.

# **CLINICAL RELEVANCE/APPLICATION**

Combined iMAR and VME at higher photon energies results in mixed effects on metal-related artifacts, which overall may not improve image quality for a particular implant.

## **Honored Educators**

Presenters or authors on this event have been recognized as RSNA Honored Educators for participating in multiple qualifying educational activities. Honored Educators are invested in furthering the profession of radiology by delivering high-quality educational content in their field of study. Learn how you can become an honored educator by visiting the website at: https://www.rsna.org/Honored-Educator-Award/ Elliot K. Fishman, MD - 2012 Honored EducatorElliot K. Fishman, MD - 2014 Honored EducatorElliot K. Fishman, MD - 2016 Honored EducatorElliot K. Fishman, MD - 2018 Honored Educator

# SSE16-06 Improved Visualization of Juxtaprosthetic Tissue Using Metal Artifact Reduction MRI: Experimental and Clinical Optimization of Compressed Sensing SEMAC

Monday, Nov. 26 3:50PM - 4:00PM Room: N227B

Participants

Pia M. Jungmann, MD, Zurich, Switzerland (*Presenter*) Nothing to Disclose Susanne Bensler, Zurich, Switzerland (*Abstract Co-Author*) Nothing to Disclose Patrick Zingg, MD, Zurich, Switzerland (*Abstract Co-Author*) Nothing to Disclose Benjamin Fritz, MD, Zurich, Switzerland (*Abstract Co-Author*) Nothing to Disclose Christian W. Pfirrmann, MD, MBA, Forch, Switzerland (*Abstract Co-Author*) Nothing to Disclose Reto Sutter, MD, Zurich, Switzerland (*Abstract Co-Author*) Nothing to Disclose

#### PURPOSE

To identify an optimal imaging protocol for metal artifact reduced MRI by application of different post-processing parameters in compressed sensing slice-encoding for metal artifact correction (CS-SEMAC).

## **METHOD AND MATERIALS**

In an experimental setup, a total hip arthroplasty (THA) embedded in gadolinium containing agarose was scanned at 1.5T. Pulse sequences included coronal STIR, T1w and T2w CS-SEMAC sequences. All pulse sequences were acquired with 11, 19 and 27 sliceencoding steps (SES). Post-processing was performed with variations of the parameters (i) number of iterations (5, 10, 20, 30, 50) and (ii) normalization factor (0.0005, 0.001, 0.002, 0.003, 0.005). Following, identical STIR, T1w and T2w pulse sequences with 11 and 19 SES were acquired in patients with THA. Semi-quantitative outcome measures were assessed on a five-point scale (1=best, 5=worst). The overall best image quality was determined. Statistical analyses included descriptive statistics, t-tests, multivariate regression models and partial Spearman correlations.

## RESULTS

Scan times varied between 2:24 and 8:49 minutes. Reconstruction times varied between 3:14 and 85:00 minutes. Artifact reduction was optimal with an intermediate normalization factor (0.001) and improved with higher SES and iterations. Iterations >20 did not improve artifact reduction or image quality further. Ripple artifacts increased with higher SES and iterations. A normalization factor of 0.001 or 0.002 was best for reduction of blurring, while the soft tissue contrast was better and the distortion of soft tissue was less severe with lower normalization factors. Overall best soft tissue image quality was found for STIR and T1w images with 19 SES, 10 iterations and a normalization factor of 0.001 and for T2w images with 11 SES, 10 iterations and a normalization factor of 0.0005.

# CONCLUSION

For the advanced acceleration and reconstruction algorithms of CS-SEMAC, optimal SES, iterations and normalization factors could

be identified. 19 SES and 20 iterations were sufficient for optimal artifact reduction, enabling an imaging protocol with clinically feasible acquisition and reconstruction times.

# CLINICAL RELEVANCE/APPLICATION

Identified optimal CS-SEMAC MRI parameters may be applied in clinical practice and allow for improved evaluation of juxtaprosthetic tissue in patients with THA due to excellent artifact reduction.



# Nuclear Medicine (Central Nervous System Nuclear Imaging)

Monday, Nov. 26 3:00PM - 4:00PM Room: S505AB

# NR NM

AMA PRA Category 1 Credit ™: 1.00 ARRT Category A+ Credit: 1.00

**FDA** Discussions may include off-label uses.

## Participants

Amir H. Khandani, MD, Chapel Hill, NC (*Moderator*) Consultant, Progenics Pharmaceuticals, Inc; Consultant, F. Hoffmann-La Roche Ltd;

Yonglin Pu, MD, PhD, Chicago, IL (Moderator) Nothing to Disclose

## Sub-Events

# SSE17-01 18F-Fluciclovine PET Evaluation of Recurrent High-Grade Glioma

Monday, Nov. 26 3:00PM - 3:10PM Room: S505AB

Participants

Akinyemi A. Akintayo, MD, Atlanta, GA (Presenter) Nothing to Disclose

Ephraim E. Parent, MD,PhD, Ponta Vedra Beach, FL (*Abstract Co-Author*) Research support, Blue Earth Diagnostics Ltd; Research support, Advanced Accelerator Applications SA

Marc D. Benayoun, MD, PhD, Atlanta, GA (Abstract Co-Author) Nothing to Disclose

Ijeoma Ibeanu, MD, MPH, Atlanta, GA (Abstract Co-Author) Nothing to Disclose

Jeffrey Olson, PHD, Atlanta, GA (Abstract Co-Author) Nothing to Disclose

Constantinos G. Hadjipanayis, MD, PhD, Atlanta, GA (Abstract Co-Author) Nothing to Disclose

Daniel J. Brat, MD, PhD, Atlanta, GA (Abstract Co-Author) Nothing to Disclose

Vikram Adhikarla, PhD, Atlanta, GA (Abstract Co-Author) Nothing to Disclose

Jonathon Nye, PhD, Atlanta, GA (Abstract Co-Author) Consultant, Lantheus Medical Imaging, Inc

David M. Schuster, MD, Decatur, GA (*Abstract Co-Author*) Institutional Research Grant, Nihon Medi-Physics Co, Ltd; Institutional Research Grant, Blue Earth Diagnostics Ltd; Institutional Research Grant, Advanced Accelerator Applications SA; Consultant, Syncona Ltd; ; ;

Mark M. Goodman, PhD, Atlanta, GA (Abstract Co-Author) Royalties, Nihon Medi-Physics Co, Ltd

For information about this presentation, contact:

akinyemi.akintayo@emory.edu

## PURPOSE

18F-Fluciclovine has shown promise in the detection and diagnosis of high-grade gliomas (HGG) due to minimal uptake in normal brain parenchyma and increased uptake in neoplastic tissue. The goal of this study is to evaluate 18F-fluciclovine PET uptake in patients with suspected recurrent HGG previously treated with chemotherapy and/or radiotherapy and correlate with overall survival.

# METHOD AND MATERIALS

Nine patients with suspected recurrent HGG (WHO grade III, IV) previously treated with surgical resection followed by either chemotherapy and/or radiotherapy underwent dynamic 18F-fluciclovine brain PET. Average 18F-fluciclovine dose was  $10.5 \pm 0.41$  mCi (390  $\pm$  15 MBq). Semi-quantitative PET analysis (SUVmax, SUVmean) was performed for each lesion identified on standard of care MRI and compared to normal brain parenchyma and venous blood at all time points to obtain time activity curves. Metabolic tumor volume of each lesion was measured at each time point using a threshold of 1.6\* normal brain parenchyma. True recurrence was confirmed with histopathological confirmation in 5 patients and subsequent serial MRI examinations.

## RESULTS

18F-Fluciclovine uptake greater than background was visually identified in 6 of 9 patients. Average SUVmax and SUVmean of identifiable lesions were 5.7±1.2 and 1.4±0.5 at 60 minutes respectively. Average SUVmax and SUVmean for normal brain uptake were 1.8±0.6 and 0.5±0.2 respectively. Range of glioma SUVmax/normal SUVmean was 32.5 - 6.6 with an average ratio of 15.1±10.4. 18F-Fluciclovine PET identified a new distinct local metastasis in a patient that was confirmed on subsequent MRI examinations. Recurrent gliomas that were not visually identified by 18F-fluciclovine PET had an average SUVmax of 2.1±0.6 with a glioma SUVmax/normal SUVmean time of survival from the 18F-fluciclovine PET with identifiable recurrent HGG was 14.9 months vs 24.1 months for those lesions not visually identified on PET.

## CONCLUSION

18F-fluciclovine PET/CT is a promising diagnostic tool for identifying recurrent HGG and may be a valuable tool for survival prognostication although more work is needed to verify these results.

# **CLINICAL RELEVANCE/APPLICATION**

18F-fluciclovine PET/CT is a promising diagnostic tool for identifying recurrent HGG and may be a valuable tool for survival

# SSE17-02 PET-MR Imaging Biomarkers Improving Differential Diagnosis Between Progression and Radionecrosis of Brain Tumors

Monday, Nov. 26 3:10PM - 3:20PM Room: S505AB

Participants

Nadya Pyatigorskaya, MA, Paris, France (*Presenter*) Nothing to Disclose Marc Bertaux, Paris, France (*Abstract Co-Author*) Nothing to Disclose Brian Sgard, Paris, France (*Abstract Co-Author*) Nothing to Disclose Lydia Yahia-Cherif, Paris, France (*Abstract Co-Author*) Nothing to Disclose Damien P. Galanaud, MD, PhD, Paris, France (*Abstract Co-Author*) Research Consultant, Olea Medical Marie-Odile Habert, MD, Paris, France (*Abstract Co-Author*) Nothing to Disclose Marine Soret, Paris, France (*Abstract Co-Author*) Nothing to Disclose Didier Dormont, MD, Paris, France (*Abstract Co-Author*) Nothing to Disclose Aurelie Kas, Paris, France (*Abstract Co-Author*) Nothing to Disclose

# For information about this presentation, contact:

nadya.pyatigorskaya@gmail.com

#### PURPOSE

Follow-up under treatment of patients with high grade glioma is essential, the MRI being the modality of choice. However, anatomical MRI may not be always reliable after radiation or chemotherapy. Advanced MRI techniques as well as PET were proposed for improving the diagnostic accuracy, that remains still moderate and variable across studies. Our purpose was to evaluate the diagnostic accuracy of PET-MRI for differential diagnosis between tumor progression and radionecrosis.

#### **METHOD AND MATERIALS**

Between December 2015 and September 2017, patients followed for primary malignant brain tumors underwent FDOPA PET-MRI. The acquisitions were performed with a 3T PET-MR system (SIGNA, GE Healthcare). The MRI acquisition included SE 3D T1-weighted images without and after contrast injection, 3D FLAIR imaging, DWI, pseudo-continuous arterial spin labeling (pCASL) and dynamic susceptibility-contrast (DSC) perfusion. The SUVmax, SUVmean, and SUVpeak were measured in each lesion with Volume of Interest (VOI). A region of interest was drawn in each lesion and the mean rADC, rCBV, and rCBF for both DSC and pCASL perfusion were calculated. In addition, the visual analysis was performed.

## RESULTS

Forty-four patients were included. ROC analysis showed good discrimination between progression and radionecrosis with a good diagnostic accuracy for SUVmax (0.82), for SUVpeak (0.9) and for ASL rCBF (0.86). It was fair for rADC (0.63) and rCBV (0.75). A logistic regression model found among predictor variables, the combination of these SUVpeak and pCASL rCBF variables improved sensitivity (0.94), specificity (0.83), the AUC (0.97, 95% CI=[0.93,0.99]) and the accuracy (0.94). Visual analysis allowed a diagnostic accuracy of 0.77 for PET reading only, of 0.89 for PET reading with morphological MRI and of 0.98 for PET-MRI combined reading.

## CONCLUSION

We have observed an increase in diagnostic accuracy for combined analysis of PET and MRI biomarkers for both qualititative and qualitative biomarkers, SUVpeak and pCASL rCBF being the most significant quantitative biomarkers. Combined PET-MR imaging allows to increase the diagnostic accuracy for differential diagnosis between tumor progression and radionecrosis in neuro-oncology.

#### **CLINICAL RELEVANCE/APPLICATION**

The combined analysis of imaging morphological, functional and metabolic markers on PET-MRI is helpful in differential diagnosis between tumor progression and radionecrosis in neuro-oncology.

# SSE17-03 Detection of Abnormal Brain FDG-PET Images With Deep Learning

Monday, Nov. 26 3:20PM - 3:30PM Room: S505AB

Participants

Tomomi Nobashi, MD,PhD, Palo Alto, CA (*Abstract Co-Author*) Nothing to Disclose Claudia Zacharias, MD, Seattle, WA (*Abstract Co-Author*) Nothing to Disclose Andrei Iagaru, MD, Emerald Hills, CA (*Abstract Co-Author*) Research Grant, General Electric Company Guido A. Davidzon, MD, Stanford, CA (*Abstract Co-Author*) Nothing to Disclose Heying Duan, Stanford, CA (*Presenter*) Nothing to Disclose

# PURPOSE

FDG-PET/CT is widely used in routine clinical practice and its utilization is projected to increase. The brain is often included as part of the study; however, due to its background physiological FDG uptake, the sensitivity for abnormality detection in this region is usually low. By utilizing a deep learning algorithm to aid radiologists detect abnormalities, clinical management and outcomes could be improved. The aim of this study was to evaluate the ability of a new deep learning framework to discern between normal and abnormal FDG uptake in the brain.

# METHOD AND MATERIALS

285 FDG-PETs acquired between 2007 and 2017 were retrospectively reviewed. A deep learning framework was trained using 110 normal and 110 abnormal brain studies, including 10 studies for testing in each category. The remaining 36 normal and 29 abnormal studies were used for validation of the resulting inference model and its sensitivity and specificity were analyzed. DICOM studies were anonymized, appropriately windowed and converted into portable network graphics format. A network architecture that uses a time distributed 2D convolutional neural network with 100 epochs was generated. A classification was performed based on the probability of an individual FDG-PET scan being normal or abnormal. Various models were derived.

## RESULTS

Accuracy and loss function of the optimal trained model were calculated at 0.761 and 0.462, respectively. Receiver operating characteristic (ROC) curve demonstrated an area under the curve of 0.832 (Figure 1). According to ROC curve, the optimal probability threshold to detect abnormal Brain FDG-PET scans was 0.661. Validation test characteristics resulted in sensitivity of 80.6% and specificity of 75.9%.

# CONCLUSION

Preliminary results of a novel deep learning model showed promising capability in detecting brain abnormalities on FDG-PET images which could aid radiologists and improve clinical outcomes.

# **CLINICAL RELEVANCE/APPLICATION**

Improving detection of brain FDG-PET abnormalities in daily clinical practice with the aid of a deep learning method that could help improve clinical management and outcomes.

# SSE17-04 Posterior Cortical Variant Alzheimer's Disease and Lew Body Dementia: Similarities and Differences on FDG PET Scan

Monday, Nov. 26 3:30PM - 3:40PM Room: S505AB

Participants

Ritu Verma, New Delhi, India (*Presenter*) Nothing to Disclose Rajeev Ranjan, New Delhi, India (*Abstract Co-Author*) Nothing to Disclose Harsh Mahajan, MD, MBBS, New Delhi, India (*Abstract Co-Author*) Nothing to Disclose Vidur Mahajan, MBBS, New Delhi, India (*Abstract Co-Author*) Nothing to Disclose Vanshika Gupta, New Delhi, India (*Abstract Co-Author*) Nothing to Disclose Ethel S. Belho, New Delhi, India (*Abstract Co-Author*) Nothing to Disclose Nikhil Seniaray, New Delhi, India (*Abstract Co-Author*) Nothing to Disclose Ankur Pruthi, New Delhi, India (*Abstract Co-Author*) Nothing to Disclose

# For information about this presentation, contact:

vidur@mahajanimaging.com

## PURPOSE

Posterior cortical atrophy (PCA) is a form of dementia considered to be an atypical variant of Alzheimer's disease (AD) and Dementia with Lewy bodies (DLB) is a type of posterior dementia characterized by fluctuating levels of cognition, changes in behavior, visual hallucinations with accompanying extrapyamidal motor symptoms. We attempt to identify specific core areas on FDG PET imaging which are common to both and also establish the differences which may be helpful to differentiating the two.

# **METHOD AND MATERIALS**

We retrospectively analysed of 30 patients with clinically suspected posterior dementia. All the subjects underwent F-18 FDG PET CT scan of the brain and the studies were analyzed both qualitatively (visually) and semi-quantitatively. The subjects had undergone dopamine transporter imaging with Tc 99 m TRODAT 1 on a prior date. The subjects were divided into possible PCA with TRODAT scan normal (n=10) and possible DLB with abnormal (n=20). The FDG uptake patterns were recorded and areas of cortical hypometabolism in the cerebral cortex that were two standard deviations from the mean were considered as abnormal.

# RESULTS

All the subjects had an abnormal pattern of F-18 FDG uptake on PET scan, both on visual inspection and semiquantitative analysis. Bilateral parieto-occipital hypometabolism was consistently found in all the subjects. Hypometabolism in precuneus, posterior cingulate and the cortex around the angular gyrus was present in all the subjects of PCA with relative sparing of the medial occipital cortices. DLB subjects showed variable degrees of involvement of the medial occipital cortices with relative sparing of posterior cingulate and precuneus.

# CONCLUSION

FDG PET scan can act as a non-invasive diagnostic modality in differentiating the two posterior cortical dementias despite significant clinical and imaging overlap.

# CLINICAL RELEVANCE/APPLICATION

We present features based on which FDG-PET can be used to diagnose and differentiate Posterior Cortical Atrophy (PCA) and Dementia with Lewy Bodies (DLB) in the clinical practice.

# SSE17-05 Correlation of 4´-[methyl-11C]-thiothymidine Uptake with Human Nucleoside Transporter and Thymidine Kinase-1 Expressions in Patients with Newly Diagnosed Gliomas

## Monday, Nov. 26 3:40PM - 3:50PM Room: S505AB

Participants

Yasukage Takami, Mikicho, Japan (*Presenter*) Nothing to Disclose Yuka Yamamoto, MD, PhD, Kagawa, Japan (*Abstract Co-Author*) Nothing to Disclose Masaki Ueno, Mikicho, Japan (*Abstract Co-Author*) Nothing to Disclose Yoichi Chiba, Mikicho, Japan (*Abstract Co-Author*) Nothing to Disclose Takashi Norikane, Kita-gun, Japan (*Abstract Co-Author*) Nothing to Disclose Tetsuhiro Hatakeyama, Kagawa, Japan (*Abstract Co-Author*) Nothing to Disclose Keisuke Miyake, Mikicho, Japan (*Abstract Co-Author*) Nothing to Disclose Jun Toyohara, Tokyo, Japan (*Abstract Co-Author*) Nothing to Disclose Yoshihiro Nishiyama, MD, Kagawa, Japan (*Abstract Co-Author*) Nothing to Disclose We examined expressions of four human nucleoside transporters including: human equilibrative nucleoside transporters (hENT1 and hENT2); and human concentrative nucleoside transporters (hCNT1 and hCNT3), and thymidine kinase-1 (TK1), the key enzyme in 4'-[methyl-11C]-thiothymidine (4DST) phosphorylation, to elucidate the mechanism of 4DST uptake in patients with newly diagnosed gliomas.

# **METHOD AND MATERIALS**

A total of 19 patients with newly diagnosed gliomas were examined with 4DST PET. Tumor lesions were identified as areas of focally increased uptake, exceeding that of normal brain background. For semi-quantitative analysis, tumor-to-contralateral normal brain tissue (T/N) ratio was determined by dividing the maximal standardized uptake value (SUV) for tumor by that of the mean SUV for reference tissue. The expressions of hENT1, hENT2, hCNT1, hCNT3, and TK1 in tumor specimens were examined by immunohistochemistry and compared with 4DST T/N ratio.

## RESULTS

All but two gliomas showed focally increased 4DST uptake. All but one grade II glioma that was not visualized with 4DST PET showed hENT1 staining. Of the gliomas, hENT2 and hCNT3 staining was observed in 11 and 16 gliomas, respectively. No hCNT1 staining was observed in any of the gliomas. All but two gliomas that were not visualized with 4DST PET showed TK1 staining. A significant correlation was observed between T/N ratio and hENT1 score (r = 0.75, p < 0.001). There was no significant correlation between T/N ratio and TK1 score. There was a significant strong correlation between T/N ratio and TK1 score (r = 0.92, p < 0.001). It is likely that expression of TK1 might be more important than expression of hENT1 for uptake of 4DST.

# CONCLUSION

Results of this preliminary study indicate that expressions of hENT1 and TK1 appear to be important determinants of 4DST uptake in newly diagnosed gliomas.

# **CLINICAL RELEVANCE/APPLICATION**

Expressions of hENT1 and TK1 appear to be important determinants of 4DST uptake in newly diagnosed gliomas.

# SSE17-06 A Novel Clustering Approach in Brain Tumors Using Dynamic 18F-FET PET/MRI

Monday, Nov. 26 3:50PM - 4:00PM Room: S505AB

# Participants

Cristina Campi, PhD, Padova, Italy (*Abstract Co-Author*) Nothing to Disclose Stefano De Marchi, Padova, Italy (*Abstract Co-Author*) Nothing to Disclose Mariagiulia Anglani, Padova, Italy (*Abstract Co-Author*) Nothing to Disclose Valentina Bodanza, Padova, Italy (*Abstract Co-Author*) Nothing to Disclose Giancarlo Gorgoni, Negrar, Italy (*Abstract Co-Author*) Nothing to Disclose Matteo Salgarello, Vicenza, Italy (*Abstract Co-Author*) Nothing to Disclose Giuseppe Lombardi, Padova, Italy (*Abstract Co-Author*) Nothing to Disclose Franco Bui, MD, Padova, Italy (*Abstract Co-Author*) Nothing to Disclose Diego Cecchin, MD, Padova, Italy (*Presenter*) Nothing to Disclose

## For information about this presentation, contact:

diego.cecchin@unipd.it

# PURPOSE

Purpose of the present study is to present a user-independent, quantitative approach to easily classify brain areas on the base of uptake temporal evolution using dynamic 18F-FET PET/MRI.

# **METHOD AND MATERIALS**

O-(2-18F-fluoroethyl)-L-tyrosine (18F-FET) PET/MRI performed at out Institution in brain tumors were retrospectively analyzed using a clustering technique in order to differentiate areas using uptake dynamics: time activity curves (TACs) were considered for each voxel in the brain volume and an unsupervised clustering algorithm was applied. This algorithm provides as output an automatic grouping of TACs and hence of voxels they are associated to. Therefore, it is possible to create parametric images, representing the different behavior over time of the tissues.

## RESULTS

We were able to automatically identify brain areas grouped by dynamic similarities using 18F-FET uptake and produce parametric images (see Figure 1, panel (a)) and associated mean time-activity curves obtained averaging the TACs of voxels belonging to the same group (see Figure 1, panel (b)).

## CONCLUSION

The proposed approach allows to exploit dynamic 18F-FET PET data: the automatic nature of the method removes the userdependent ROI drawing step, the clustered data can be further analyzed to extract representative features of the average TACs and intuitive parametric images are produced. Moreover the method could be easily employed with other tracers.

## **CLINICAL RELEVANCE/APPLICATION**

Validation of the method against pathological data is ongoing and seems to provide encouraging results. The method could then be used to plan areas for radiotherapy clustering areas with similar dynamic characteristics.



# Neuroradiology/Head and Neck (Thyroid and Parathyroid Imaging)

Monday, Nov. 26 3:00PM - 4:00PM Room: E351



AMA PRA Category 1 Credit ™: 1.00 ARRT Category A+ Credit: 1.00

#### Participants

Christine M. Glastonbury, MBBS, San Francisco, CA (*Moderator*) Author with royalties, Reed Elsevier Paul M. Bunch, MD, Winston-Salem, NC (*Moderator*) Nothing to Disclose

## Sub-Events

# SSE18-01 Thyroid Nodules on Ultrasound: Effect of Computer-Aided Diagnosis (CAD) on Radiologists' Performance with a Large Clinical Diagnostic Population

Monday, Nov. 26 3:00PM - 3:10PM Room: E351

Participants Feng Han MD PhD

Feng Han, MD,PhD, Guangzhou, China (*Presenter*) Nothing to Disclose Xiao Luo, Guangzhou, China (*Abstract Co-Author*) Nothing to Disclose Min Xu, Guangzhou, China (*Abstract Co-Author*) Nothing to Disclose An-Hua Li, MD, Guangzhou, China (*Abstract Co-Author*) Nothing to Disclose

## For information about this presentation, contact:

hanfeng@sysucc.org.cn

# PURPOSE

To evaluate the effect of computer-aided diagnosis (CAD) on different level radiologists' performance for discriminating malignant from benign thyroid nodules on US images.

## METHOD AND MATERIALS

From January 2013 to December 2017, thyroid nodules with decisive diagnosis on the basis of pathologic results were consecutively enrolled. The observer study was conducted with four experienced radiologists and four radiology fellows, all of whom analyzed the thyroid nodules using 2017 ACR TIRADS first without and subsequently with CAD software. The performance of each observer without and with the CAD was assessed by measuring the area under the receiver operating characteristics curve (Az), sensitivity, specificity, PPV and NPV. To quantify the changes in clinical management decisions with the CAD aid, we computed for each radiologist the number of malignant and benign nodules for which the clinical management decision was changed. Concordance between observers in classing the thyroid nodules was measured in without and with CAD conditions.

# RESULTS

In total, 1065 thyroid nodules from 1035 patients were included; 382 (35.87%) were benign and 683 (64.13%) were malignant. Use of the CAD resulted in an improvement of the average performance of the 8 observers, as measured by means of a statistically significant increase in Az value (0.840-0.853; p < .000), sensitivity (86.44%-87.52%; p < .000) and inter-observer agreements(0.744-0.769; p < .05) A statistically significant difference was not found in the specificity without and with the computer aid (38.74%-38.55%; p = .20). On the basis of TI-RADS assessments, it was estimated that with CAD, each observer, on average, correctly recommended 1.02% (7/683) of additional biopsies and also increased 0.37% (1.4/382) of unnecessary biopsies.

## CONCLUSION

Computer-aided diagnosis can help radiologists improve their sensitivity in detection of thyroid malignancies and also increased the rate of unnecessary biopsies.

## **CLINICAL RELEVANCE/APPLICATION**

To aid diagnosis for inexperienced radiologists and decrease workload

# SSE18-02 Comparision of Morphology and Enhancement Characteristics of Ectopic and Eutopic Parathyroid Adenomas.

Monday, Nov. 26 3:10PM - 3:20PM Room: E351

Participants

Harika Tirumani, MBBS, MD, Little Rock, AR (*Presenter*) Nothing to Disclose Rohan Samant, MD, Little Rock, AR (*Abstract Co-Author*) Nothing to Disclose Raghu H. Ramakrishnaiah, MBBS, FRCR, Little Rock, AR (*Abstract Co-Author*) Nothing to Disclose Jennifer L. McCarty, MD, Houston, TX (*Abstract Co-Author*) Nothing to Disclose Stephen J. Geppert, MD, Little Rock, AR (*Abstract Co-Author*) Nothing to Disclose Rudy L. Van Hemert JR, MD, Little Rock, AR (*Abstract Co-Author*) Nothing to Disclose Edgardo J. Angtuaco, MD, Little Rock, AR (*Abstract Co-Author*) Nothing to Disclose

# For information about this presentation, contact:

htirumani@uams.edu

## PURPOSE

4D-CT is a novel technique for pre-surgical localization of parathyroid adenomas (PA). PA can be eutopic or ectopic. Detection of ectopic PA is crucial for surgical success especially if patient has multigland disease with both eutopic and ectopic PA. Purpose of our study is to determine the differences in morphology and enhancement characteristics between eutopic and ectopicPA which will help in increasing the confidence of radiologist for suggesting high probability.

# **METHOD AND MATERIALS**

This is an IRB approved retrospective study of 232 patients with surgically proven PA who underwent 4D CT imaging for pre surgical localization of PA between 2014 and 2017. All 4D CT scans were performed with initial noncontrast followed by 30 sec and 90 sec postcontrast images on 64 slice MDCT scanner. Contrast washout ratios (CWR) were calculated by measuring Hounsfield units (HU) of PA on the noncontrast, 30 second post contrast early arterial exam (30A) and on the 90 second post contrast delayed exam (90D). CWR =  $[100 \times (HU \text{ on } 30A - HU \text{ on } 90D)/HU \text{ on } 30A]$ .

## RESULTS

Out of 232 patients, 186 patients - 1 gland, 37 patients - 2 gland, 6 patients - 3 gland and 3 patients - 4 gland adenomas constituting a total of 290 radiologically diagnosed lesions. Out of these, 25 (6M, 17F) PA were in ectopic and 265 (37M, 228F) PA were eutopic. Out of 290 radiologically reported lesions, 242 lesions (21 Ectopic and 221 Eutopic) matched to the adenomas found on surgery and pathology constituting to 242 radiological-surgical-pathology matched lesions. 48 lesions were false positive, which did not correlate with the location on surgical pathology. Morphological characteristics like shape, size, heterogeneity were studied and compared between eutopic and ectopic adenomas. Enhancement characteristics of eutopic and ectopic adenomas were compared and were categorized at 10% washout intervals, for example: 1-10%, 11-20% and so on.

## CONCLUSION

1. 217 out of 265 eutopic adenomas and 20 out of 25 ectopic adenomas demonstrated contrast washout ratios between 31%-80% and did not demonstrate significant difference in washout characteristics. 2. Size and shape of ectopic PA did not show significant influence on washout characteristics. 3. Measurement of contrast enhancement and washout dynamics is limited in lesions with large cystic areas.

# **CLINICAL RELEVANCE/APPLICATION**

Detection of ectopic PA is crucial for surgical success especially in the setting of multigland disease.

# SSE18-03 The Assessment of Cervical Lymph Node Metastasis from Thyroid Cancers: A Quantitative Analysis on Multiphasic CT

Monday, Nov. 26 3:20PM - 3:30PM Room: E351

## Participants

Aysegul Gursoy Coruh, MD, ANKARA, Turkey (*Presenter*) Nothing to Disclose Caglar Uzun, Ankara, Turkey (*Abstract Co-Author*) Nothing to Disclose Melahat Kul, Ankara, Turkey (*Abstract Co-Author*) Nothing to Disclose Zehra Akkaya, Ankara, Turkey (*Abstract Co-Author*) Nothing to Disclose Kursat Gokcan, Ankara, Turkey (*Abstract Co-Author*) Nothing to Disclose Atilla Elhan, Ankara, Turkey (*Abstract Co-Author*) Nothing to Disclose

## For information about this presentation, contact:

draysegulgursoy@gmail.com

## PURPOSE

Purpose: The purpose of this study was to evaluate the diagnostic performance of multiphasic CT in the discrimination of metastatic lymph nodes of papillary (PTC) and medullary (MTC) thyroid cancers from non-metastatic ones with the use of quantitative parameters.

## **METHOD AND MATERIALS**

Materials-methods: This study enrolled 62 pathologically proven metastatic and 62 benign lymph nodes from 23 thyroid cancer patients (19 PTC and 4 MTC). Multiphasic CT was utilized by using non-enhanced, arterial (25-second delay) and venous (80second delay) phases. Two readers independently measured mean tissue attenuation values (MAV) of metastatic and benign lymph nodes. The relative wash in and wash out percentages were calculated and were defined as: arterial MAV-nonenhanced MAV/nonenhanced MAV, venous MAV- arterial MAV/arterial MAVx100; respectively.

## RESULTS

Results: The difference in MAV between metastatic and benign lymph nodes for the PTC were maximum in the arterial phase (p<0.001). The arterial phase showed the highest diagnostic performance compared with other phases for the PTC (AUC±SE:0.98±0.01; %95 CI: 0.96-1). A cutoff value of 97.5 HU for the arterial phase had a sensitivity of 96.3% (%95 CI: 87.5-99%) and specificity of 94.4% (%95 CI: 84.8-98.1%), positive predictive value (PPV) of 97.2% and negative predictive value (NPV) of 92.6% in the discrimination of metastatic lymph nodes from PTC (p<0.001). Metastatic lymph nodes from MTC showed progressive enhancement compared to benign lymph nodes and the venous phase showed the highest diagnostic performance in discrimination between metastatic and benign lymph nodes (p<0.05). A MAV cutoff of 112.5 HU in the venous phase predicted metastatic lymph nodes from MTC with a sensitivity of 87.5%, specificity of 75%, (p=0.015).

# CONCLUSION

The detection of metastatic lymph nodes from thyroid cancers can be achievable with the use of quantitative parameters in

multiphasic CT. Metastatic lymph nodes from PTC show strong uptake of contrast in the arterial phase and wash out of contrast in the venous phase. Whereas, metastatic lymph nodes from MTC show progressive enhancement in the venous phase.

# **CLINICAL RELEVANCE/APPLICATION**

Determination of metastatic lymph nodes is an important problem in thyroid cancers. Complete resection of the primary disease and metastases is the one of the important factor in the survival.

# SSE18-04 Retrospective Analysis of Thyroid Ultrasound Recommendations Using Thyroid Imaging Reporting and Data System (TI-RADS) Scoring

Monday, Nov. 26 3:30PM - 3:40PM Room: E351

## Awards

# **Student Travel Stipend Award**

Participants

Charles E. Runyan III, MD, Phoenix, AZ (*Presenter*) Nothing to Disclose Alexia Tatem, BS, Cave Creek, AZ (*Abstract Co-Author*) Nothing to Disclose Samantha Matz, DO, Phoenix, AZ (*Abstract Co-Author*) Nothing to Disclose Albert Roh, MD, Phoenix, AZ (*Abstract Co-Author*) Nothing to Disclose Mary J. Connell, MD, Phoenix, AZ (*Abstract Co-Author*) Nothing to Disclose

## PURPOSE

Breast Imaging, Reporting, and Data System (BI-RADS) has been used to standardize mammogram reports and recommendations; Thyroid Imaging, Reporting, and Data System (TI-RADS) seeks to do the same. We compared our institution's prior biopsy recommendations on ultrasound reports to what the recommendations would have been using TI-RADS.

## **METHOD AND MATERIALS**

Our study was a retrospective review of 449 thyroid nodules which were assessed by ultrasound and subsequently biopsied. We collected the description of the lesion and the original recommendations from the radiology report. Pathology results were collected. Three radiologists then performed blinded and independent evaluations of each exam; a TI-RADS score was assigned to each thyroid nodule. Recommendations based on TI-RADS were compared with prior recommendations and biopsy results.

## RESULTS

449 thyroid nodules were identified by review of biopsies. Had we implemented TI-RADS, we would have recommended 102 fewer biopsies (23%). No nodules for which a biopsy was initially recommended but not recommended by TI-RADS criteria demonstrated a clinically significant malignancy at biopsy. Incidental foci of papillary carcinoma found within benign follicular nodules less than 0.5cm were considered not clinically relevant, as studies have shown that 5-30% of autopsies have found occult papillary carcinoma in patients who died of unrelated causes. Our positive predictive value before implementing TI-RADS was 8.2%. Utilizing TI-RADS, our positive predictive value is 10.5%, a ~25% difference.

# CONCLUSION

There was a decrease in the number of thyroid biopsies that would have been recommended when using TI-RADS. We demonstrated a 23% decrease in the number of recommended biopsies without decreasing our ability to identify clinically significant malignancies. Findings suggest that implementing TI-RADS will decrease the number of negative biopsies performed, which will decrease patient risk and worry as well as save the health system from the cost of these additional procedures. Our study is limited by only selecting patients who underwent biopsy. Due to our inclusion criteria, we did not assess for any missed malignancies in nodules presumed to be benign on prior ultrasound reports.

# **CLINICAL RELEVANCE/APPLICATION**

Use of TI-RADS for thyroid nodule biopsy recommendations can greatly reduce the number of biopsies recommended without missing a clinically significant malignancy.

# SSE18-05 Machine Learning Optimization of 4D-CT and 99m-Technetium Sestamibi for Preoperative Localization in Patients with Primary Hyperparathyroidism

Monday, Nov. 26 3:40PM - 3:50PM Room: E351

Participants

Laurent Dercle, MD, New York, NY (*Presenter*) Nothing to Disclose Yu-Kwang Donovan Tay, MD, New York, NY (*Abstract Co-Author*) Nothing to Disclose Gaia Tabacco, MD, New York, NY (*Abstract Co-Author*) Nothing to Disclose Prachi Dubey, MD, NY, NY (*Abstract Co-Author*) Nothing to Disclose Gul Moonis, MD, New York, NY (*Abstract Co-Author*) Nothing to Disclose Randy Yeh, MD, New York, NY (*Abstract Co-Author*) Nothing to Disclose

## For information about this presentation, contact:

ry2210@cumc.columbia.edu

# PURPOSE

The purpose of this study is to apply machine learning to 4D-CT and 99mTechnetium sestamibi (MIBI) for preoperative localization of hyperfunctioning parathyroid glands in patients with primary hyperparathyroidism (PHPT). Our aim is to develop a model and decision tree algorithm to maximize diagnostic accuracy.

## **METHOD AND MATERIALS**

A retrospective study of 400 patients who underwent combined imaging protocol of 4D-CT and MIBI SPECT/CT and subsequent parathyroidectomy was performed. Four parathyroid glands were assumed for each patient (n=1600). Reference standard was surgical pathology. Both 4D-CT and MIBI were interpreted by two nuclear radiologists. Using machine learning, a random-forest tree

algorithm using 3-fold cross validation was trained and validated to predict the probability of a parathyroid gland as positive hyperfunctioning gland on pathology (adenoma or hyperplasia). A total of 17 variables were used, including 4 clinical, 10 biological, and 3 imaging variables. Imaging variables included 4D-CT, MIBI, and combined 4D-CT+MIBI.

# RESULTS

Of 1600 parathyroid glands, 521 were abnormal on surgical pathology. The model output was probability of a gland as positive on pathology. The final model selected variables of combined 4D-CT+MIBI and preoperative serum PTH and Calcium crossproduct (PTH\*Ca). The AUC of the model was 0.99 (95 CI: .984-.996) and outperformed AUC of radiologist interpretation of 4D-CT and MIBI, alone and in combination. When both 4D-CT and MIBI are positive, the probability of a true positive is 97% (n=305) and when either test is positive, the probability is 75% (n=164). When both tests are negative, the gland is a true negative in 96% of cases if PTH\*Ca is > 1232 (n=333), 92% of cases if PTH\*Ca>675 and <1232 (n=563) and 81% of cases if PTH\*Ca<675 (n=297).

## CONCLUSION

Diagnostic accuracy of preoperative 4D-CT and MIBI is improved with machine learning compared with radiologist interpretation. A decision tree algorithm simplified into three variables selected by machine learning can provide probability of correct classification of each parathyroid gland as normal or abnormal and guide the surgeon to pursue minimally invasive parathyroidectomy or 4-gland exploration.

# **CLINICAL RELEVANCE/APPLICATION**

Machine learning-derived model and decision tree algorithm can improve diagnostic accuracy of preoperative localization of 4D-CT and 99mTechnetium Sestamibi for patients with primary hyperparathyroidism.

# SSE18-06 Utility of Ultrasound Elastography (Acoustic Radiation Force Impulse Imaging) in the Diagnosis of Parathyroid Adenoma in Correlation with Sestamibi Scan

Monday, Nov. 26 3:50PM - 4:00PM Room: E351

Participants

Sooraj Prasannakumar, MBBS, Chennai, India (*Presenter*) Nothing to Disclose Sudhakar H. K., DMRD, MD, Chennai, India (*Abstract Co-Author*) Nothing to Disclose Meera K., DMRD, MD, Chennai, India (*Abstract Co-Author*) Nothing to Disclose Jayasudha Sambedu, MBBS,DMRD, Chennai, India (*Abstract Co-Author*) Nothing to Disclose Sandhya Gh JR, MBBS, Chennai, India (*Abstract Co-Author*) Nothing to Disclose Ajai R. Kattoju, MBBS, Chennai, India (*Abstract Co-Author*) Nothing to Disclose

## For information about this presentation, contact:

spsoorajp@gmail.com

# PURPOSE

In this study we consider applying the technique of ARFI with Virtual Touch Quantification (a type of quantitative elastography) in diagnosis of parathyroid adenomas(most common cause of primary hyperparathyroidism), to prospectively assess whether this technique can increase the diagnostic value of ultrasound approaching nearer to or more than the sensitivity and specificity of sestamibi scan.

# METHOD AND MATERIALS

This was a prospective observational study conducted in the department of radiodiagnosis of our institution from October 2016 to December 2017. The study population consisted of 36 patients(n=36) with clinical suspicion of primary hyperparathyroidism with positive Sestamibi scan for parathyroid adenoma irrespective of ultrasound results(done prior to the Sestamibi scan). The parathyroid adenoma was first identified by grey scale imaging features and then a region of interest for elastography was placed within the lesion and the stiffness of the lesion using ARFI-VTQ values were obtained. Five successful measurements were taken for ARFI -VTQ(measured in meters per second) and the median value was calculated.

# RESULTS

Ultrasound elastography was performed on all the 36 cases of adenomas and the median ARFI-VTQ values were calculated. The mean ARFI values of the corresponding adjacent thyroid tissue were also calculated. The mean ARFI-VTQ values of adenomas was  $(1.72\pm0.45m/s)$ . The mean ARFI-VTQ values of normal thyroid tissue was  $(2.66\pm0.38m/s)$ . There was a statistically significant difference between the two variables with [p <0.0001]. The study shows a consistently low elastography values for adenomas than adjacent thyroid tissue and other lesions which mimic adenomas like lymph nodes. Thus ultrasound along with ARFI-VTQ values has high accuracy in diagnosing adenomas.

# CONCLUSION

Ultrasound elastography(withARFI-VTQ) is an excellent tool which enhances the diagnostic value of ultrasound in parathyroid adenomas when used along with B-mode ultrasound and doppler.

## **CLINICAL RELEVANCE/APPLICATION**

In clinically diagnosed patients of hyperparathyroidism ultrasound ARFI-VTQ can be applied as a solitary imaging modality(in place of sestamibi), since it is an excellent diagnostic imaging tool in the diagnosis of normally located parathyroid adenomas with high accuracy.



# Neuroradiology (Epilepsy Imaging)

Monday, Nov. 26 3:00PM - 4:00PM Room: E352



AMA PRA Category 1 Credit ™: 1.00 ARRT Category A+ Credit: 1.00

**FDA** Discussions may include off-label uses.

#### Participants

Diana M. Gomez-Hassan, MD, PhD, Ann Arbor, MI (*Moderator*) Nothing to Disclose Alexander M. McKinney IV, MD, Minneapolis, MN (*Moderator*) CEO, VEEV, Inc

#### Sub-Events

# SSE19-01 7T MRI of Hippocampal Internal Architecture in Medial Temporal Lobe Epilepsy Compared with that in 3T MRI

Monday, Nov. 26 3:00PM - 3:10PM Room: E352

Participants

Yiwei Zhang, BS, Beijing, China (*Presenter*) Nothing to Disclose Hui You, Beijing, China (*Abstract Co-Author*) Nothing to Disclose Wanchen Dou, Beijing, China (*Abstract Co-Author*) Nothing to Disclose Yuelei Lv, Beijing, China (*Abstract Co-Author*) Nothing to Disclose Bo Hou, BA, Beijing, China (*Abstract Co-Author*) Nothing to Disclose Weiyu Mao, Beijing, China (*Abstract Co-Author*) Nothing to Disclose Feng Feng, MD, Beijing, China (*Abstract Co-Author*) Nothing to Disclose Lin Shi, BS, Hong Kong, China (*Abstract Co-Author*) Nothing to Disclose Zhentao Zuo, Beijing, China (*Abstract Co-Author*) Nothing to Disclose

## For information about this presentation, contact:

1556222529@qq.com

## PURPOSE

Asymmetry of hippocampal internal architecture (HIA) clarity has been regarded as a sign of hippocampal sclerosis (HS). The aim of this work was to compare HIA in patients with medial temporal lobe epilepsy (MTLE) in 3T and 7T MRI in lateralizing epileptic side and its relationship with postoperative seizure outcome

## **METHOD AND MATERIALS**

39 patients with MTLE were recruited, and MRI at 3 T and 7T were obtained respectively (GE Discovery MR750 3T and Siemens Investigational Device 7T) for semi-quantitative assessment of the HIA by visual scoring system (Ver Hoef et al., 2013). The values of the average HIA scores of 3T and 7T MRI in the epileptogenic and non-epileptogenic hippocampi were compared with Kruskal-Wallis H test. Pair-wise differences between groups were evaluated with Mann-Whitney U test. A logistic regression model examined the utility of average HIA asymmetry score in lateralizing seizure onset determined by video-EEG. 25 patients underwent amygdalohippocampectomy and received postoperative follow up. The relationship between HIA and postoperative seizure freedom was investigated

## RESULTS

HIA scores of the epileptogenic hippocampi were lower than that of non-epileptogenic hippocampi either in 3TMRI (P=0.0166) or 7TMRI (P=0.0014). The HIA scores of either side of hippocampi in 7T MRI were higher than that of 3T MRI (Contralateral P < 0,0001, Ipsilateral P=0.0002). Logistic regression analysis showed that the HIA asymmetry score either in 3T MRI or 7T MRI was the strong predictor of epileptic laterality (3T MRI: B = 1.504, P = 0.033; 7T MRI: B = 1.705, P = 0.019). However, there were no significant differences in HIA asymmetry score between patients rendered seizure free (ILAE 1) compared to those continuing to experience seizures (ILAE 2-5) either in 3T MRI or 7T MRI.

# CONCLUSION

7T MRI was relatively superior to 3TMRI in displaying the subtle hippocampal internal architecture for its higher HIA scores. HIA asymmetry is a significant predictor in lateralizing epileptic side of MTLE patients either in 3T MRI or 7T MRI, but not in the surgical outcomes of the patients

## **CLINICAL RELEVANCE/APPLICATION**

The superiority of 7T MRI in presenting subtle hippocampal internal architecture may help lateralize epileptic side of temporal lobe epilepsy on early side or without evident hippocampal sclerosis in 3T MRI

## SSE19-02 Detecting Mesial Temporal Sclerosis on 3D T1 Weighted MRIs Using Deep Learning

Participants Richard J. Gorniak, MD, Philadelphia, PA (*Presenter*) Consultant, BioClinica, Inc; Consultant, Medtronic plc Adam E. Flanders, MD, Philadelphia, PA (*Abstract Co-Author*) Nothing to Disclose Paras Lakhani, MD, Philadelphia, PA (*Abstract Co-Author*) Nothing to Disclose Joseph Tracy, PhD, Philadelphia, PA (*Abstract Co-Author*) Nothing to Disclose Michael Sperling, Philadelphia, PA (*Abstract Co-Author*) Nothing to Disclose

For information about this presentation, contact:

richard.gorniak@jefferson.edu

# PURPOSE

Mesial temporal sclerosis (MTS) is a common cause of surgically treatable epilepsy in adults. MTS is frequently, but not always, detectable on MRI. The purpose of this project was to determine if deep learning using a convolutional neural network can be used to detect MTS on MRI.

### **METHOD AND MATERIALS**

Anonymized volumetric T1 weighted MRIs were retrospectively obtained from 88 normal controls and 119 patients with a clinical and EEG consensus diagnosis of MTS. Of the MTS patients, 39 were read as no MTS on MRI and 80 were read as having MTS during routine clinical interpretation. These studies were divided into training(173), validation (17) and test(17) groups each with a similar distribution of MRI types. The images were bias corrected and the hippocampi were segmented using FSL(Analysis Group, FMRIB, Oxford, UK). The hippocamal segmentations were used to construct bounding boxes around each hippocampus which was utilized during model training. Using TensorFlow, a 3D convolutional neural network modeled after the VGG architecture was constructed and trained to predict normal vs MTS and to locate a bounding box around each hippocampus.

#### RESULTS

During training, the maximum accuracy achieved on the validation set was 100%. Using the model weights from that epoch, an accuracy of 88% was achieved on the test set with a sensitivity of 89% and a specificity of 88%. For comparison, the sensitivity of the human interpretation for detection of MTS in this cohort of patients with clinical and EEG consensus diagnosis of MTS was 67%.

### CONCLUSION

On this small sample, deep learning methods show potential utility for automating the detection of MTS on MRI, warranting further investigation.

# **CLINICAL RELEVANCE/APPLICATION**

Deep learning has the potential to aid in detecting MTS in epilepsy patients

# SSE19-03 In Vivo Measurements of GABA and Glutamate-Glutamine in Nocturnal Frontal Lobe Epilepsy

Monday, Nov. 26 3:20PM - 3:30PM Room: E352

Participants

Weina Wang, Chengdu, China (*Presenter*) Nothing to Disclose Xiaorui Su, Chengdu, China (*Abstract Co-Author*) Nothing to Disclose Huaiqiang Sun, Chengdu, China (*Abstract Co-Author*) Nothing to Disclose Simin Zhang, Chendu, China (*Abstract Co-Author*) Nothing to Disclose Qiyong Gong, MD, PhD, Chengdu, China (*Abstract Co-Author*) Nothing to Disclose Qiang Yue, Chengdu, China (*Abstract Co-Author*) Nothing to Disclose

#### PURPOSE

Nocturnal frontal lobe epilepsy (NFLE) is a focal epilepsy with seizures arising mainly during sleep and characterized by violent limb movement or tonic-dystonic postures. The major inhibitory and excitatory neurotransmitters,  $\gamma$ -aminobutyric acid (GABA) and glutamate, respectively, are implicated in the pathophysiology of NFLE. This study aimed to compare the measurements of GABA, and glutamate-glutamine (Glx) levels in NFLE subjects.

#### **METHOD AND MATERIALS**

Study participants were recruited at the seizure disorders outpatient clinic from November 2013 to July 2017. T1-weighted images were acquired and reconstructed for the spectral voxels using a 3T system. Proton magnetic resonance spectroscopy was used to measure GABA and Glx levels in the bilateral dorsolateral prefrontal cortex (DLPFC) regions with a voxel size of  $4.0 \times 2.0 \times 1.5$  cm3. Figure 1 illustrates voxels position. Spectra were analyzed using 'Gannet'. The GABA and Glx levels were expressed in 'institutional units' as ratios of peak areas relative to the Cr signal. Only spectra with a relative fitting error generated by GannetFit below 15%, and FWHM below11 Hz were included.

### RESULTS

Demographic information is provided in table 1. Thirty-nine subjects with NFLE and 63 controls participated in this study with wellmatched for age and gender. As shown in Figure 2, Glx level in the right DLPFC region was higher in NFLE compared with controls (P=0.020). We did not find any GABA level alterations in the current study. In NFLE patients there was significant positive correlations between illness duration and right DLPFC glx level (R2=0.514, P=0.05).

### CONCLUSION

In patients with seizures characterized by complex motor behaviors, the region of seizure onset may involve the DLPFC. In line with our finding, elevations in Glx were also observed in idiopathic generalized epilepsy, which may imply increased neuronal excitability. A significant positive correlation was found in NFLE subjects between Glx levels and illness duration, indicating that the longer illness duration may due to severer hyperactivity. These findings are interpreted in terms of a pathophysiological model of NFLE in which excitatory neurotransmission abundance in right DLPFC could lead to hyperexcitability and, potentially seizures-related neuronal dysfunction. (dealing with MRS) 'MRS exam in possible focus region is recommended in epilepsy patients.'

# SSE19-04 White Matter Regional Based Analysis Using Diffusion Tensor Tractography in Patients with Temporal Lobe Epilepsy and Correlation with Patient Outcomes

Monday, Nov. 26 3:30PM - 3:40PM Room: E352

Participants

Mahdi Alizadeh, Philadelphia, PA (*Presenter*) Nothing to Disclose Lauren Kozlowski, Philadelphia, PA (*Abstract Co-Author*) Nothing to Disclose Jennifer Muller, MS,BS, Philadelphia, PA (*Abstract Co-Author*) Nothing to Disclose Feroze B. Mohamed, PhD, Philadelphia, PA (*Abstract Co-Author*) Nothing to Disclose Ashwini Sharan, MD, Philadelphia, PA (*Abstract Co-Author*) Nothing to Disclose Chengyuan Wu, Philadelphia, PA (*Abstract Co-Author*) Nothing to Disclose

### PURPOSE

In this study, we aim to evaluate the use of diffusion tensor tractography (DTT) as a predictive model of temporal lobe epilepsy (TLE) and correlate their clinical significance with respect to postsurgical outcome. Automated regional based white matter analysis was used to compare the tract density in two groups of TLE patients: responders and non-responders to the surgical treatments.

### METHOD AND MATERIALS

A total of 19 patients with TLE underwent either a craniotomy anterior temporal lobectomy (ATL) or a Selective Laser Amygdalohippocampectomy (SLAH) and were imaged using 3.0T Philips Achieva MR scanner. DTI images were acquired axially in the same anatomical location prescribed for the T1-weighted images. The raw data set of the diffusion volumes were first corrected for eddy current distortions and motion artifacts. Track density imaging (TDI) of 68 white matter parcels were generated using fiber orientation distribution (FOD) based deterministic fiber tracking and compared between responders (10) and non-responders (n=9) to the surgical treatments.

# RESULTS

looking at tract density of white matter parcels, significant increases have been observed in five distinct white matter parcels (Table 1) in non-responders. These regions are included ipsilateral lingual (p=0.04), ipsilateral temporal pole (p=0.007), ipsilateral pars opercularis (p=0.03), ipsilateral inferior parietal (p=0.04) and contralateral frontal pole (p=0.04).

# CONCLUSION

The significant decreases exhibited in tractography on the ipsilateral hemisphere as the pathological process are likely attributed to direct effects of the sclerotic disease such as the ipsilateral temporal pole in TLE patients [9]. These findings may also be attributed to extensions of the disease process/disruptions in connections to adjacent structures, for instance, the ipsilateral lingual gyrus which joins the parahippocampal gyrus and is a continuation of the tentorial surface of the temporal lobe.

# **CLINICAL RELEVANCE/APPLICATION**

These results may have the potential to be developed into imaging prognostic markers of postoperative outcomes and provide new insights for why some patients with TLE continue to experience postoperative seizures if pathological/clinical correlates are further confirmed. On the contrary, arears predicting unfavorable postsurgical outcome were distinct, suggesting different configuration of epileptogenic networks between responders and non-responders.

# SSE19-05 Assessment of ASL Perfusion MRI as an Imaging Biomarker in Seizure: Imaging Timing and Perfusion Pattern Analysis

Monday, Nov. 26 3:40PM - 3:50PM Room: E352

Participants

Jungbin Lee, MD, Seoul, Korea, Republic Of (*Presenter*) Nothing to Disclose Aleum Lee, MD, Bucheon-Si, Korea, Republic Of (*Abstract Co-Author*) Nothing to Disclose

#### For information about this presentation, contact:

noiese@icloud.com

### PURPOSE

The aim of the study is to identify time-related perfusion change after seizure by ASL-PWI, and to evaluate additional values of ASL-PWI in seizure patients.

# METHOD AND MATERIALS

The ASL-PWI and EEG were performed on 61 patients who suspected seizures. The electronic medical records of the patients were reviewed to record the time intervals between seizure and MR imaging, seizure semiology, multiplexity and suspected seizure etiology. And we analyzed perfusion abnormality on ASL-PWI in each patient by pattern of perfusion maps (increase/decrease) and location of the abnormality. Then the concordance of location which showed abnormality between ASL-PWI and EEG was scored from 0 to 4 and compared ASL-PWI findings with conventional MRI findings.

#### RESULTS

The time interval between seizure attack and ASL-PWI ranged from  $0.5 \sim 121.5$  hrs (mean period, 31.6 hr). 5 patients (8.2%) were performed MR imaging shorter than 6 hours, 9 (14.8%) were 6-12 hours, 27 (29.5%) were 6-24 hours and 29 (47.5%) were longer than 24 hours. There was a negative linear correlation between time interval and concordance of location with statistically significant (p=0.040). In single seizure group, the first hypoperfusion was 13 hours and the last hyperperfusion was 26 hours. Delayed hyperperfusion (>24hrs) seems to be related with multiple seizures. In normal routine MRI group, 56.8% (21/37) showed abnormal ASL-PWI results. In abnormal routine MRI group, 29.1% (7/24) showed perilesional perfusion change.

### CONCLUSION

ASL-PWI findings after seizure, although are time-dependent and challenging to analysis, but since abnormal perfusion findings on ASL-PWI is observed in many seizure patients and have added values, ASL-PWI is recommended in a routine seizure protocol

# **CLINICAL RELEVANCE/APPLICATION**

By adding ASL-PWI in seizure protocol, the accuracy of the seizure diagnosis can be improved and the estimation of epileptogenic foci can be assisted.

# SSE19-06 Interhemispheric White Matter Asymmetries Are Distinctly Affected in Left and Right Medial Temporal Lobe Epilepsy with Hippocampal Sclerosis

Monday, Nov. 26 3:50PM - 4:00PM Room: E352

Participants Xu Zhao, Wuhan, China (*Presenter*) Nothing to Disclose Zhiqiang Zhou, MD,MD, Wuhan, China (*Abstract Co-Author*) Nothing to Disclose Ying Xiong, Wuhan, China (*Abstract Co-Author*) Nothing to Disclose Wenzhen Zhu, MD, PhD, Wuhan, China (*Abstract Co-Author*) Nothing to Disclose

# For information about this presentation, contact:

zhaoxu96@163.com

# PURPOSE

Many past studies reported the asymmetrical structural and/or functional changes of mesial temporal lobe epilepsy (MTLE), that is, the abnormalities in the ipsilateral were more obvious than the contralateral hemisphere in both left MTLE (LMTLE) and right MTLE (RMTLE). However, none of these studies compared the left hemisphere to right hemisphere directly and the asymmetry traits of MTLE remain largely unconfirmed. Thus, this study aims to investigate the white matter microstructure asymmetries of MTLE by compare the two hemispheres directly.

# METHOD AND MATERIALS

25 MTLE patients with unilateral hippocampal sclerosis (HS) (LMTLE-HS group, n=13; RMTLE-HS group, n=12) and 26 health controls (HC) were enrolled. Diffusion tensor imaging (DTI) data were analyzed by tract-based spatial statistics (TBSS) to test the hemispheric differences across the entire white matter skeleton. We also conducted two-sample paired t-test for 21 paired-ROIs parceled on the basis of ICBM-DTI-81 white-matter labels atlas of bilateral hemispheres. An asymmetry index (AI) was calculated using the formula AI=100\*[Right-Left]/[(Right+Left)/2] to further quantify the differences between the left and right paired-ROIs mentioned above.

# RESULTS

The asymmetries across a large number of white matter skeletons were significantly reduced in LMTLE-HS group and RMTLE-HS group compared to HC. ROI-based quantitative analysis of FA/MD showed the asymmetry traits of fornix (FORX), cingulum (hippocampus), cingulum (cingulus gyrus), uncinate fasciculus (UF), superior longitudinal fasciculus (SLF) and superior fronto-occipital fasciculus (SFOF) were disappeared in LMTLE-HS and/or RMTLE-HS group. Apart from that, the intergroup analysis of AI revealed no significant difference between LMTLE-HS group and HC, but some differences were showed when compared RMTLE-HS with LMTLE-HS or RMTLE-HS with HC.

# CONCLUSION

The asymmetry traits of MTLE patients were reduced compared to HC. The AI between LMTLE-HS and HS did not show any significant difference indicated that LMTLE-HS might impair the two hemispheres equally. The differences of AI between RMTLE-HS and LMTLE-HS indicated that they might have different mechanisms.

# **CLINICAL RELEVANCE/APPLICATION**

The different asymmetry traits among LMTLE-HS, RMTLE-HS and HC may be able to differentiate LMTLE-HS from RMTLE-HS and thus may be useful for locating side of seizure lesions in MTLE patients.



#### SSE20

# Neuroradiology (Young Brain, Old Brain)

Monday, Nov. 26 3:00PM - 4:00PM Room: E350

# NR

AMA PRA Category 1 Credit ™: 1.00 ARRT Category A+ Credit: 1.00

### Participants

Margaret N. Chapman, MD, Boston, MA (*Moderator*) Nothing to Disclose Leo J. Wolansky, MD, Farmington, CT (*Moderator*) Institutional Grant, Guerbet SA

# Sub-Events

# SSE20-01 Neuroimaging Evidence of Structural and Functional Brain Plasticity After Sight Onset Late in Childhood

Monday, Nov. 26 3:00PM - 3:10PM Room: E350

Participants

Tapan Gandhi, New Delhi, India (*Abstract Co-Author*) Nothing to Disclose Ming Meng, Guangzhou, China (*Abstract Co-Author*) Nothing to Disclose Lotfi Merabet, Boston, MA (*Abstract Co-Author*) Nothing to Disclose Bas Rokers, Madison, WI (*Abstract Co-Author*) Nothing to Disclose Pawan Sinha, Cambridge, MA (*Presenter*) Nothing to Disclose Harsh Mahajan, MD, MBBS, New Delhi, India (*Abstract Co-Author*) Nothing to Disclose Vidur Mahajan, MBBS, New Delhi, India (*Abstract Co-Author*) Nothing to Disclose

# For information about this presentation, contact:

vidur@mahajanimaging.com

### PURPOSE

Direct data from human subjects on the validity of the "critical period" of brain development and the permanent detrimental impact of sensory deprivation during this period is lacking. We present evidence for neural plasticity in congenitally blind children following sight restoration.

# METHOD AND MATERIALS

Pre- and post-treatment scans of 15 participants (8 to 24 years) who had been treated for bilateral congenital blindness were done on a 3.0T MRI (750w, GE Healthcare) using a 32 channel brain coil. A high-resolution T1-weighted fast spoiled gradient echo anatomical scan was acquired for each participant. To measure blood oxygen level dependent (BOLD) contrast, 35 slices parallel to the AC/PC were acquired using standard T2 weighted gradient-echo echoplanar imaging. A diffusion-weighted scan (40 direction + 5 b0; 74.4 ms TE; 13.7s TR; 2x0.86x0.86 mm3; FOV: 256 x 256 x 72; b = 1000 nm/s2) was performed for diffusion tensor tractography.

#### RESULTS

Using functional connectivity analyses, we find marked changes in the functional organization of the visual cortex. There is a significant enhancement of cortical decorrelation as a function of time following sight onset. The fusiform facial area (FFA) and occipital facial area (OFA) develop rapidly. Structural imaging demonstrates increase in both volume and thickness of grey matter compared to controls, especially in the fusiform. Analysis of the optic tract in the same participants revealed no change in mean diffusivity (MD) and fractional anisotropy (FA) during the post-treatment period, while the FA of the optic radiation decreased steeply over 2 years.

### CONCLUSION

Contrary to our expectation of limited neural plasticity late in the developmental timeline, we find strong evidence of brain malleability using both functional and structural imaging. Our findings help explain the behaviourally observed gains in visual proficiency congenitally blind individuals exhibit as a function of time after sight restoring surgery.

# **CLINICAL RELEVANCE/APPLICATION**

Our study presents evidence for brain plasticity and hence opens up treatment avenues for conditions such as late-diagnosed congenital blindness.

# SSE20-02 Evolution of Brain Dynamics in the First 2 Years of Life

Monday, Nov. 26 3:10PM - 3:20PM Room: E350

Participants Xuyun Wen, Chapel Hill, NC (*Presenter*) Nothing to Disclose Han Zhang, Chapel Hill, NC (*Abstract Co-Author*) Nothing to Disclose Weili Lin, PhD, Chapel Hill, NC (*Abstract Co-Author*) Nothing to Disclose Dinggang Shen, Chapel Hill, NC (Abstract Co-Author) Nothing to Disclose

# PURPOSE

Brain is a dynamic system with its state varying all the time. Increasing evidences have indicated that the brain dynamics may evolve in early development and contribute to the cognitive development. This study uses resting-state fMRI and dynamic graph analysis to delineate how such dynamics develop in the first 2 years of life.

# **METHOD AND MATERIALS**

Seventy-two normal infants at 0-, 1- and 2-years old were recruited. After data preprocessing, we extracted regional mean BOLD time series (140 TRs) from 116 pre-defined regions based on AAL atlas and constructed a temporal adjacency network by treating each TR as a node and the similarity (measured by inverse Euclidean distance) in brain states between two different TRs as an edge. Here, each brain state is a momentary (single TR) pattern of the BOLD activities at the 116 brain regions. We performed a subject-level clustering on the temporal adjacency network to divide the brain states into several groups. For each group, we generated a representative state by averaging all time series with the same state. To identify the common states in age groups, we used a second-level clustering over the subject-level state network, where nodes are identified as brain states of the subjects and edges are the similarity between pairs of brain states.

### RESULTS

We observed three major brain states that frequently occurred across almost all ages (see histograms in Fig.1). We found these three states could be one-to-one matched across age groups. The first state displays high activities in the sensorimotor cortex, while the second state shows high activities in the visual cortex. In the third state, high activities in the higher-order cognition-related areas are prominent. The first state is highly consistent across all age groups. The second state has a higher similarity between 0- and 1-year-old. For the third state, the later two age groups are much more similar.

### CONCLUSION

In closing, three common brain states were identified from 0- to 2-years-old, but showing different similarities across age groups. Such state-level differences may be due to the brain evolution in the first 2 years of life to support the development of the cognitive function.

# **CLINICAL RELEVANCE/APPLICATION**

This study is helpful to better understand the infancy normal neurodevelopment and provides a baseline for the disease diagnosis in early ages.

# SSE20-03 Evaluating Normal Fetal Brain Development in 25-39 Weeks Gestational Age Using IVIM-DWI: A Preliminary Study

Monday, Nov. 26 3:20PM - 3:30PM Room: E350

Participants

Yuan Xiao, Xi'an, China (*Presenter*) Nothing to Disclose Yue Cui, Xi'an, China (*Abstract Co-Author*) Nothing to Disclose Hu Yuchuan, Xi'an, China (*Abstract Co-Author*) Nothing to Disclose Yu Mei, Xi'an, China (*Abstract Co-Author*) Nothing to Disclose Wang Shaoyu, Shanghai, China (*Abstract Co-Author*) Nothing to Disclose Li Yanyan, Xi'an, China (*Abstract Co-Author*) Nothing to Disclose Jie Zhang, Xian, China (*Abstract Co-Author*) Nothing to Disclose Chen Ping, Xi'an, China (*Abstract Co-Author*) Nothing to Disclose Jin Liu, Xi'an, China (*Abstract Co-Author*) Nothing to Disclose Siaocheng Wei, Beijing, China (*Abstract Co-Author*) Nothing to Disclose Wang, Xi'an, China (*Abstract Co-Author*) Nothing to Disclose Xiaocheng Wei, Beijing, China (*Abstract Co-Author*) Nothing to Disclose Du Pang, Xi'an, China (*Abstract Co-Author*) Nothing to Disclose Zhongqiang Shi, Xi an, China (*Abstract Co-Author*) Nothing to Disclose Cui Guangbin, Xi'an, China (*Abstract Co-Author*) Nothing to Disclose

### For information about this presentation, contact:

yuan19841016@163.com

### PURPOSE

To evaluate the age-related normal changes of water diffusivity and perfusion in the fetal brain using intravoxel incoherent motion diffusion weighted imaging (IVIM-DWI).

# METHOD AND MATERIALS

This study was approved by the local Ethics Committee and informed consents were obtained. Seventy nine normal singleton fetuses between 25-39 weeks of gestation were scanned without sedation of healthy pregnant women. The multi-b DWI with 9 b-values (0 - 800 sec/mm2) was performed using a 1.5-Tesla MR scanner. Pure diffusion coefficient (D), pseudo-diffusion coefficient (D\*) and perfusion fraction (f) values were measured in white matter (frontal, parietal, temporal and occipital lobe), cerebral hemisphere (CH), thalamus (TH), basal ganglia region (BGR) and pons using an IVIM model. D, D\* and f values were compared among different brain regions with one-way ANOVA. Correlation between IVIM parameters and gestational age (GA) was assessed with quadratic polynomial regression.

### RESULTS

Statistical difference in D and f values were found among the different right brain regions (D values, F = 96.644, P < 0.0001; f values, F = 105.598, P < 0.0001). Mean D values in supratentorial deep white matter areas were higher than those in other regions (P < 0.0001). There were significant negative correlation between GA and D values in CH, BGR, TH and pons (CH, R2 = 0.49, p < 0.0001; BGR, R2 = 0.33, P < 0.0001; TH, R2 = 0.12, p = 0.0014; pons, R2 = 0.22, p < 0.0001). D values in supratentorial regions gradually increased before 29th GA and then decreased. The f values in the pons were positively related with GA (R 2 = 0.23, p = 0.0325). The f value was higher at 32-36 GA in other brain regions.

### CONCLUSION

These results suggested that IVIM-DWI parameters is promising in evaluating the fetal brain development.

### CLINICAL RELEVANCE/APPLICATION

# no

# SSE20-04 Associations Between Age-Related Neuropathology and Magnetic Susceptibility of the Human Brain

Monday, Nov. 26 3:30PM - 3:40PM Room: E350

Participants

Arnold M. Evia Jr, PhD, Chicago, IL (*Presenter*) Nothing to Disclose Ashish A. Tamhane, MS, Chicago, IL (*Abstract Co-Author*) Nothing to Disclose Aikaterini Kotrotsou, PhD, MEng, Houston, TX (*Abstract Co-Author*) Nothing to Disclose Robert Dawe, PhD, Chicago, IL (*Abstract Co-Author*) Nothing to Disclose Sue Leurgans, Chicago, IL (*Abstract Co-Author*) Nothing to Disclose Julie A. Schneider, MD, Chicago, IL (*Abstract Co-Author*) Nothing to Disclose David A. Bennett, MD, Chicago, IL (*Abstract Co-Author*) Nothing to Disclose Konstantinos Arfanakis, PhD, Chicago, IL (*Abstract Co-Author*) Nothing to Disclose

# For information about this presentation, contact:

arfanakis@iit.edu

# PURPOSE

Studies suggest that quantitative susceptibility mapping (QSM) may be sensitive to brain changes related to Alzheimer's disease (AD) and vascular dementia. However, these studies are typically performed with clinical diagnosis, and are susceptible to contributions from unidentified pathology. In contrast, measuring the underlying neuropathology through histology allows for an accurate assessment of neuropathologic burden. Therefore, this work investigated the associations of magnetic susceptibility with multiple age-related neuropathologies by combining ex-vivo QSM and histology in a large community cohort of older adults.

### **METHOD AND MATERIALS**

Postmortem cerebral hemispheres were obtained from 223 participants of two longitudinal cohort studies of aging. Each hemisphere was imaged on a 3T MR scanner with 3D gradient-echo and 2D spin-echo sequences. Ex-vivo magnetic susceptibility maps were generated using the MEDI toolbox and spatially transferred to a template constructed by applying the "unbiased atlas construction via group-wise DRAMMS registration" tool to the spin-echo data. A board-certified neuropathologist, who was blinded to age and clinical diagnoses, evaluated each hemisphere for neurodegenerative and vascular pathologies: AD, Lewy bodies, hippocampal sclerosis (HS), TDP-43, arteriolosclerosis, atherosclerosis, cerebral amyloid angiopathy, gross and microscopic infarcts. Voxelwise linear regression of the participants' magnetic susceptibility values was conducted with the neuropathologies and demographics as independent variables. Statistical significance was achieved at p<0.05 for the FDR-adjusted p-values.

### RESULTS

Significant associations were discovered between magnetic susceptibility and measures of AD, HS, arteriolosclerosis, gross and microscopic infarcts.

### CONCLUSION

This work demonstrated that magnetic susceptibility shifts linked to age-related neuropathologies can be detected by QSM. Both neurodegenerative and vascular pathologies were linked to magnetic susceptibility. These findings are expected to translate well to in-vivo QSM, as it was recently shown that ex-vivo magnetic susceptibility can be linked to in-vivo magnetic susceptibility for this work's experimental setup.

# **CLINICAL RELEVANCE/APPLICATION**

Quantitative susceptibility mapping can detect brain changes linked to age-related neuropathology, and may be a valuable diagnostic tool for age-related brain diseases.

# SSE20-06 Whole Brain Structural Health in Relation to Cardiovascular Risk Factors: An Evaluation Using the Brain Atrophy and Lesion Index

Monday, Nov. 26 3:50PM - 4:00PM Room: E350

Participants Tao Gu, MD, PhD, Beijing, China (*Presenter*) Nothing to Disclose Min Chen, MD, PhD, Beijing, China (*Abstract Co-Author*) Nothing to Disclose Xiaowei Song, PhD,MSc, Surrey, BC (*Abstract Co-Author*) Nothing to Disclose

### For information about this presentation, contact:

gutao001@hotmail.com

# PURPOSE

Multiple structural changes on MRI in the brain can have interactive and additive impacts on aging and dementia. These changes can be collectively assessed using a semi-quantitative brain atrophy and lesion index (BALI). Previous studies have been focused on using the BALI to understand brain health of older adults, while it is not known how age and cardiovascular risk factors affect the accumulation of these various changes. In the present study, we address the question using a sample containing younger and middle-aged adults.

### **METHOD AND MATERIALS**

Data of 239 subjects (men=71%; age range=20-80 years) who underwent regular health check and a routine anatomical MRI

examination in Beijing Hospital of China were analyzed. Basic demographics and traditional cardiovascular risk factors (CVRF) of the subjects were reviewed. A BALI score was generated for each subject by evaluating T2 weighted MRI at 1.5T and 3T. Mean difference in BALI total and subcategory scores between subjects of difference age and CVRF conditions were examined using t-test and ANOVA, while associations between the BALI score and age or CVFR was evaluated by correlation and regression analyses.

### RESULTS

Over 89% of these subjects had at least one CVRF, while respectively 29%, 18%, 11%, 1% had two to five CVRFs. On average, older subjects had more CVRF. The BALI total score and subcategory scores were closely related to age (r's=0.41-0.69, p's<0.001). The BALI total and the categorical scores differed significantly by the number of CVRF (t's=4.16-14.83, p's<0.05). Subjects with a higher BALI score were more likely to be associated with at least one CVRF (X2's=6.9-43.9, p's<0.05). Multivariate analyses adjusting for various possible confounders demonstrated a strong impact of the CVRF on whole structural brain health as evaluated using BALI (Odds Ratio = 1.676, 95% CI=1.207-2.325), especially hypertension (OR=2.455, 95% CI=1.126-5.353), independent of the effect of age.

# CONCLUSION

The accumulation of deficits in brain structure can start at a younger age. Cardiovascular risk factors play a key role in affecting such accumulation. The data emphasize the importance of early control of cardiovascular risk factors on promoting brain health in aging-and dementia.

# **CLINICAL RELEVANCE/APPLICATION**

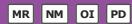
understand the relationship between age and whole brain structural health and how cardiovascular risk factors affect the accumulation of deficits in the brain over time using BALI



#### SSE21

# Pediatrics (Oncology and Nuclear Medicine)

Monday, Nov. 26 3:00PM - 4:00PM Room: E353B



AMA PRA Category 1 Credit ™: 1.00 ARRT Category A+ Credit: 1.00

**FDA** Discussions may include off-label uses.

#### Participants

Heike E. Daldrup-Link, MD, Palo Alto, CA (*Moderator*) Nothing to Disclose Ethan A. Smith, MD, Cincinnati, OH (*Moderator*) Travel support, Koninklijke Philips NV

# Sub-Events

# SSE21-01 Whole-Body Magnetic Resonance Imaging in Newly Diagnosed Langerhans Cell Histiocytosis Patients: Lesion Detectability and Risk Stratification

Monday, Nov. 26 3:00PM - 3:10PM Room: E353B

Participants

Jisun Hwang, MD, Seoul, Korea, Republic Of (*Presenter*) Nothing to Disclose Hee Mang Yoon, MD, Seoul, Korea, Republic Of (*Abstract Co-Author*) Nothing to Disclose Jeong Rye Kim, MD, Cheonan, Korea, Republic Of (*Abstract Co-Author*) Nothing to Disclose Ah Young Jung, MD, Seoul, Korea, Republic Of (*Abstract Co-Author*) Nothing to Disclose Young Ah Cho, MD,PhD, Seoul, Korea, Republic Of (*Abstract Co-Author*) Nothing to Disclose Jin Seong Lee, MD, Seoul, Korea, Republic Of (*Abstract Co-Author*) Nothing to Disclose

### For information about this presentation, contact:

espoirhm@gmail.com

# PURPOSE

To compare lesion detectability and the accuracy of risk stratification of skeletal survey, bone scan, and whole-body magnetic resonance imaging (WB-MRI) in patients with newly-diagnosed Langerhans cell histiocytosis (LCH).

# METHOD AND MATERIALS

Patients who presented with newly-diagnosed LCH and who underwent skeletal survey, bone scan, and WB-MRI (n=46) between June 2011 and April 2017 were retrospectively included. The sensitivity and mean number of false-positives per patient in the three whole-body imaging modalities (skeletal survey, bone scan, and WB-MRI) were assessed. Risk stratification was performed in each patient for each whole-body imaging modality. The reference standard for LCH lesions was histopathologic findings or clinical and imaging follow-up. The ability to detect LCH lesions and the accuracy of the initial risk stratification were compared between the three whole-body imaging modalities.

### RESULTS

WB-MRI had significantly higher sensitivity (99.0%; 95% confidence interval [CI], 93.2-99.9%) than skeletal survey (56.6%; 95% CI, 46.7-66.0%; p<0.0001) and bone scan (38.4%; 95% CI, 29.4-48.3%; p<0.0001) in the detection of LCH lesions, and there were no significant differences in the number of false-positives per patient (p>0.017 for all comparisons). WB-MRI tended to have higher accuracy for the risk stratification than skeletal survey and bone scan (concordance rate of 0.98, 0.91, and 0.83, respectively), although the differences between imaging modalities were not statistically significant (overall p-value 0.066).

### CONCLUSION

WB-MRI had higher detectability for LCH lesions than skeletal survey and bone scan, while the three whole-body imaging modalities had comparable accuracy in the initial risk stratification of LCH.

# **CLINICAL RELEVANCE/APPLICATION**

WB-MRI might serve as a primary imaging modality for risk stratification in patients with initially diagnosed LCH.

# SSE21-02 The Complementary Role of Early Interim PET Semi-Quantitative Metrics to Lugano Criteria in Predicting Treatment Response in Children with Hodgkin Lymphoma

Monday, Nov. 26 3:10PM - 3:20PM Room: E353B

# Awards

Student Travel Stipend Award

Participants Eman E. Marie, MD, MSc, Toronto, ON (*Presenter*) Nothing to Disclose Amer Shammas, MD, Toronto, ON (*Abstract Co-Author*) Nothing to Disclose

# For information about this presentation, contact:

eezzatmarie@gmail.com

### PURPOSE

To evaluate if adding iPET semiquantitative metrics to Lugano criteria will increase its predictability for response to therapy.

### METHOD AND MATERIALS

112 children with newly diagnosed Hodgkin lymphoma between January 1, 2007 and January 1, 2017 underwent PET before treatment, after 2 cycles, and at the end of first line treatment. The diagnostic test accuracy of semi-quantitative metrics results were compared to Lugano criteria for assessment of treatment response at iPET time point to predict the final response to treatment. The standard of reference for treatment response was based on clinical assessment, imaging results at end of first line of treatment, and histopathological confirmation of residual masses. The group of patients with positive iPET as per Lugano criteria had been re-classified into positive and negative iPET as per semiquantitative metrics cut offs.

### RESULTS

Using the Lugano criteria, 41 patients were positive and 71 were negative at iPET with accuracy of 70 %. Using semi-quantitative metrics, the number of positive cases decreased to 34 cases with a higher accuracy of 75%. On further analysis of the 41 positive iPET patients detected by Lugano classification, the number of positive cases decreased to 23 after applying our proposed cut offs for each of the semi-quantitative metrics. Thus, 18 patients were reclassified as good responders according to semiquantitative analysis.

# CONCLUSION

Semiquantitative metrics proved to be more accurate than Lugano criteria in prediction of treatment response at interim timepoint. Patients with positive iPET results according to Lugano classification may require additional evaluation using semi-quantitative metrics that classify the patients into groups with different outcomes. Larger prospective cohort and longer duration follow up is needed to support our claim.

# CLINICAL RELEVANCE/APPLICATION

Therapeutic protocols for Hodgkin lymphoma have recently employed a response adapted approach with de-escalation of therapy for those patients with adequate interim response to avoid late effects of therapy. Definitions of adequate response have tended to be conservative to avoid undertreatment for a disease with excellent cure rates. The addition of semi-quantitative analysis may be helpful in therapy planning by identifying a larger pool of patients that may be eligible for de-escalation compared to the Lugano criteria.

# SSE21-03 Value of Superb Microvascular Imaging in Biopsy Site Selection of Pediatric Solid Tumor

Monday, Nov. 26 3:20PM - 3:30PM Room: E353B

Participants

Yaqing Chen, PhD, Shanghai, China (*Presenter*) Nothing to Disclose Yunkai Zhu, MD, Shanghai, China (*Abstract Co-Author*) Nothing to Disclose Jun Jiang, Shanghai, China (*Abstract Co-Author*) Nothing to Disclose Shengli Gu, Shanghai, China (*Abstract Co-Author*) Nothing to Disclose Wenbin Guan, Shanghai, China (*Abstract Co-Author*) Nothing to Disclose

For information about this presentation, contact:

joychen1266@126.com

### PURPOSE

To investigate the value of superb microvascular imaging (SMI) in biopsy site selection in children with solid tumor.

# METHOD AND MATERIALS

A total of 48 children with solid tumors scheduled for biopsy were recruited in this retrospective study with mean age  $4.58\pm3.62y$  (0.08-15y). All patients underwent CDFI/ CDE and SMI to image tumor vascularity using Adler criteria for biopsy site selection. Ultrasound guided biopsy was performed targeting hyper-vascularity region on SMI within 3 days following ultrasound evaluation. Another 35 patients with mean age  $5.6\pm3.2y$  (1.6-15y) underwent CDFI/ CDE targeted biopsy between July 2012 and March 2015 were served as historical control. The sample adequacy of these two groups was compared retrospectively.

### RESULTS

The Adler grade of 48 solid tumors using CDFI/ CDE was as follows: 2 tumors with grade 0 (4.2%, 2/48); 16 with grade I (33.3%, 16/48) and 14 with grade III(29.2%, 14/48). By applying SMI technology, no tumor was scored with grade 0, one patient with grade I (2.1%, 1/48), 8 with grade II (16.7%, 8/48) and 39 with grade III (81.3%, 39/48). SMI was more sensitive in imaging tumor vascularity than CDFI/ CDE (P<0.001). The pathologic diagnosis was confirmed in all 48 tumors evaluated with SMI technology with sample adequacy of 100% (48/48). In comparison, the pathologic diagnosis was confirmed in 31 tumors in control group with sample adequacy of 88.6% (31/35, P=0.025). The biopsy was sampled in necrosis regions in 4 tumors in control group, and the final pathologic diagnosis was then confirmed by further surgery.

# CONCLUSION

By increasing micro vessel display, SMI technology provides a practical solution to the problem of biopsy site selection in children with solid tumor. The biopsy site selected by SMI can avoid sampling necrosis or fibrotic regions and thus improve sample adequacy.

#### **CLINICAL RELEVANCE/APPLICATION**

For children with unresectable solid tumor, biopsy pathology is the standard approach for further treatment decision. The biopsy guided by SMI can avoid sampling necrosis or fibrotic regions, and thus reduce false negative results.

# SSE21-04 Does Ferumoxytol Detect Joint Infiltration of Pediatric Cancer Patients?

Monday, Nov. 26 3:30PM - 3:40PM Room: E353B

Participants

Ashok Joseph Theruvath, MD, Mainz, CA (*Presenter*) Nothing to Disclose Anuj Pareek, MD, Aarhus C, Denmark (*Abstract Co-Author*) Nothing to Disclose Anne M. Muehe, MD, Stanford, CA (*Abstract Co-Author*) Nothing to Disclose Sheri Spunt, Palo Alto, CA (*Abstract Co-Author*) Nothing to Disclose Heike E. Daldrup-Link, MD, Palo Alto, CA (*Abstract Co-Author*) Nothing to Disclose

For information about this presentation, contact:

atheruva@stanford.edu

### PURPOSE

During our MR imaging evaluations of pediatric cancer patients with the iron oxide nanoparticle compound ferumoxytol (Feraheme), we observed a surprising marked T1-enhancement of the joint effusion in some patients and not others. The purpose of this study was to elucidate the underlying pathological mechanisms that lead to the observed ferumoxytol-induced indirect arthrography effect.

### **METHOD AND MATERIALS**

We retrospectively identified 13 pediatric cancer patients and young adults (mean age  $17.1 \pm 4.1$ , 8 males, 5 females) with bone sarcomas (n=12) and desmoid tumor (n=1) who had undergone MRI scans at 1 hour (n=8), 24 hours (n=6) or 48-120 hours (n=1) after intravenous injection of ferumoxytol at a dose of 5 mg Fe/kg body weight. The patients received a whole-body MRI with T1-weighted LAVA sequences, followed by a local MRI with T1-SE, T2-FSE and LAVA sequences. 6 of the 13 patients had also received a gadobutrol (Gadavist)-enhanced MRI. 8 of the 13 tumors were resected and underwent surgical and/or histopathological evaluation of joint invasion. The signal-to-noise ratio (SNR) of tumors with and without joint invasion was compared using a t-test and a p<0.05.

### RESULTS

At 1 hour after ferumoxytol infusion, we did not observe enhancement of joint effusions and no significant difference in SNR (p>0.05), regardless of tumor infiltration status. At >24 hours post-contrast, four patients showed significantly increased SNR values (p=0.002) of the effusion compared to muscle as an internal standard on T1-weighted images. Two of these patients were diagnosed with joint infiltration histologically while two others who did not undergo resection showed signs of joint infiltration on imaging. The other three > 24-hour scans did not show significant enhancement of the effusion and showed no joint infiltration on histology. Standard gadobutrol-enhanced MR images did not show this differential signal effect.

### CONCLUSION

This pilot study suggests that ferumoxytol leak into a joint effusion might serve as an indirect indicator for joint infiltration in pediatric cancer patients. Further studies have to prove this finding in a larger cohort of patients.

### **CLINICAL RELEVANCE/APPLICATION**

Ferumoxytol-enhanced MRI can detect joint infiltration in pediatric cancer patients.

# SSE21-05 Ferumoxytol Does Not Impact SUV Values on PET/MR Scans

Monday, Nov. 26 3:40PM - 3:50PM Room: E353B

Awards

# **Student Travel Stipend Award**

Participants Anne M. Muehe, MD, Stanford, CA (*Presenter*) Nothing to Disclose Ashok Joseph Theruvath, MD, Mainz, CA (*Abstract Co-Author*) Nothing to Disclose Ketan Yerneni, Stanford, CA (*Abstract Co-Author*) Nothing to Disclose Praveen Gulaka, PhD, Stanford, CA (*Abstract Co-Author*) Nothing to Disclose Avnesh S. Thakor, MBBCHIR, PhD, Menlo Park, CA (*Abstract Co-Author*) Nothing to Disclose Heike E. Daldrup-Link, MD, Palo Alto, CA (*Abstract Co-Author*) Nothing to Disclose

### PURPOSE

Accurate measurement of standardized uptake values (SUV) of tumors and normal organs in positron emission tomography (PET) is crucial for treatment response assessment of pediatric cancer patients. The iron oxide nanoparticle compound ferumoxytol can be used "off label" as a contrast agent for integrated PET/MR scans. However, ferumoxytol accumulation in the reticuloendethelial system (RES) could affect MR-based attenuation corrections of PET data. The purpose of our study was to compare SUV values of normal organs on ferumoxytol-enhanced and unenhanced 18F-FDG PET/MR scans.

### **METHOD AND MATERIALS**

In this IRB approved prospective study, 16 children (2-18 years) with malignant tumors underwent 18F-FDG PET/MR scans (dose 3 MBq/kg) before chemotherapy with (n=8) or without (n=8) intravenous injection of ferumoxytol (5 mg Fe/kg). Patients who received ferumoxytol were age- and sex-matched with patients who received unenhanced scans. MR attenuation correction was obtained by a four-point Dixon LAVA sequence accounting for fat, air, water, and soft tissue (TR 4.2 ms, TE 1.1, 1.7, 2.3 ms, FA 5). Anatomical correlation was obtained with a high-resolution LAVA (TR 4.4 ms, TE 1.1, 1.7, 2.2 ms, FA 15). For SUV mean values of normal organs three dimensional spherical region of interests were placed with MIM software over specified regions of the brain,

parotid gland, larynx, mediastinal blood pool, thymus, myocardium, liver, spleen, bone marrow, kidney and muscle and compared with a t-test.

# RESULTS

The SUV mean values of patients with and without ferumoxytol-enhanced PET/MR scans were for brain (6.5 vs 6.4, p=0.96), parotid gland (1.3 vs 1.5, p=0.49), larynx (1.4 vs 1.6, p=0.14), mediastinal blood pool (1.4 vs 1.2, p=0.33), thymus (2.0 vs 2.0, p=0.76), myocardium (1.8 vs 1.7, p=0.44), liver (1.4 vs 1.6, p=0.67), spleen (1.7 vs 1.7, p=0.92), bone marrow (1.5 vs 1.8, p=0.12), kidney (2.0 vs 1.7, p=0.34), and muscle (0.5 vs 0.7, p=0.23). None of the organs or tissues showed a statistical significant difference.

# CONCLUSION

Ferumoxytol at a dose of 5 mg Fe/kg has no impact on the SUV mean values of normal organs on PET/MR.

## **CLINICAL RELEVANCE/APPLICATION**

Ferumoxytol can be used as a contrast agent in pediatric whole body PET/MR scans without impacting the SUV values of normal tissues.

# SSE21-06 Voxel-Based Volumetric Analysis of Cortical Asymmetry in Glucose Metabolism in the Developing Human Brain

Monday, Nov. 26 3:50PM - 4:00PM Room: E353B

### Awards

### **Student Travel Stipend Award**

Participants

Ajay Kumar, MD, PhD, Detroit, MI (*Presenter*) Nothing to Disclose V Pilli, Detroit, MI (*Abstract Co-Author*) Nothing to Disclose Jeong-Won Jeong, PhD, Detroit, MI (*Abstract Co-Author*) Nothing to Disclose Praneetha Konka, MBBS, Detroit, MI (*Abstract Co-Author*) Nothing to Disclose Harry T. Chugani, MD, Bloomfield Hills, MI (*Abstract Co-Author*) Nothing to Disclose Csaba Juhasz, Detroit, MI (*Abstract Co-Author*) Nothing to Disclose

### For information about this presentation, contact:

ajay@pet.wayne.edu

# PURPOSE

Clinical interpretation of cerebral positron emission tomography with 2-deoxy-2[F-18] fluoro-D-glucose (FDG-PET) images often relies on evaluation of regional asymmetries. This study was designed to establish age-related variations in regional cortical glucose metabolism asymmetries in the developing human brain.

### **METHOD AND MATERIALS**

FDG-PET scans of 58 children (age 1-18 years) were selected from a tertiary care single center pediatric PET database. All children had a history of epilepsy, normal MRI, and normal pattern of PET glucose metabolism on careful visual evaluation. PET images were analyzed objectively by statistical parametric mapping with the use of age-specific FDG-PET templates. Regional FDG uptake was measured in 35 cortical regions in both hemispheres using an automated anatomical labeling atlas, and left-to-right metabolic ratios of homotopic regions were correlated with age, gender, and epilepsy variables.

### RESULTS

Regional cortical glucose metabolism was mostly symmetric in young children and became increasingly asymmetric in older subjects. Specifically, several frontal cortical regions showed an age-related increase of left>right asymmetries, while right>left asymmetries emerged in posterior cortex (including portions of the occipital, parietal and temporal lobe) in older children. Similar trends were seen in a subgroup of 39 children with known right-handedness. Age-related correlations of regional metabolic asymmetries showed no robust gender differences and were not affected by epilepsy variables.

# CONCLUSION

These data demonstrate a region-specific emergence of cortical metabolic asymmetries between age 1-18 years, with left>right asymmetry in frontal and right>left asymmetry in posterior regions. These findings can facilitate correct interpretation of cortical regional asymmetries on pediatric FDG-PET images across a wide age range.

# **CLINICAL RELEVANCE/APPLICATION**

Our findings will help in understanding the regional neurometabolic evolution and its relationship with neurocognitive development and its impairment in various neurological conditions.



### SSE22

# **Physics (CT: QA and Protocols)**

Monday, Nov. 26 3:00PM - 4:00PM Room: S504AB



AMA PRA Category 1 Credit ARRT Category A+ Credit: 1.00

### Participants

Frank N. Ranallo, PhD, Madison, WI (*Moderator*) Grant, General Electric Company Bob Liu, PhD, Boston, MA (*Moderator*) Nothing to Disclose

# Sub-Events

# SSE22-01 Improving Computed Tomography (CT) Scanning Practices in the Era of Automation

Monday, Nov. 26 3:00PM - 3:10PM Room: S504AB

Participants

Usman Mahmood, MS, New York, NY (*Abstract Co-Author*) Nothing to Disclose Rommel DeOcampo, New York, NY (*Abstract Co-Author*) Nothing to Disclose Edward Fung, PHD, New York, NY (*Abstract Co-Author*) Nothing to Disclose Rhonda Best, New York, NY (*Abstract Co-Author*) Nothing to Disclose Heeralall R. Mohabir, RT, New York, NY (*Abstract Co-Author*) Nothing to Disclose Lawrence T. Dauer, PhD, New York, NY (*Abstract Co-Author*) Nothing to Disclose Yusuf E. Erdi, DSc, New York, NY (*Abstract Co-Author*) Nothing to Disclose Jimmy Chin, New York, NY (*Abstract Co-Author*) Nothing to Disclose Dustin Lynch, MS, New York, NY (*Abstract Co-Author*) Nothing to Disclose Lorenzo Mannelli, MD, PhD, New York, NY (*Abstract Co-Author*) Nothing to Disclose Marc J. Gollub, MD, New York, NY (*Presenter*) Nothing to Disclose

### CONCLUSION

This study showed widespread vertical off-centering across all sites and for all CT protocols. The effectiveness of individualized training of technologists is demonstrated by the significant (p < 0.0001) reduction in cases where patients were placed vertically off-center, as compared to the insignificant reduction following the classroom style annual training.

### Background

Due to technological innovations, many aspects of CT systems have become automated to optimize patient dose and image quality. However, for some CT vendors, patient centering, which is critical for the proper performance of automatic exposure control, still remains a manual task. We sought to assess the frequency of patient vertical off-centering across the institution. We also investigated the effectiveness of methods used to re-educate technologists on optimal CT imaging practices.

### **Evaluation**

Using a commercially available automated dose monitoring system (ADMS) (Dose Watch, GE), CT scan acquisition data for all protocols was collected from 12 CT scanners beginning in January 2017. The scanners were located at the main cancer hospital (n=3) and at 6 affiliated outpatient locations (OPL)(n=9). Data on vertical centering within the CT gantry were sorted by scanner location and operator. Comparisons of vertical off-centering were made across all locations. Re-education about optimal CT imaging practices was performed with each technologist at 1 OPL. The staff at the main cancer hospital and 6 other OPL received classroom-style annual training on optimal CT imaging practices.

#### Discussion

During the 2nd quarter of 2017, out of a total of n = 22708 patients, 50.5% percent of patients (n=11469) undergoing CT scans were positioned vertically off-center by a range of -11.8 cm to 10.9 cm, with a median (interquartile range) of 0.818 cm (-0.491 to 2.13 cm). Of these, 34.9% (n=7921) were scanned at OPLs. After individualized re-education with technologists at one OPL, patient vertical off-centering at that site decreased by 31.8% in the 3rd quarter. For all other locations where a classroom style annual training was delivered, a reduction of 1% in vertical off-centering was observed.

# SSE22-02 Optimizing CT Image Characteristics Using a Large Data Set from Annual Medical Physics Performance Evaluations

Monday, Nov. 26 3:10PM - 3:20PM Room: S504AB

Participants

Christopher Smitherman, MS, Staten Island, NY (*Presenter*) Nothing to Disclose David W. Jordan, PhD, Cleveland, OH (*Abstract Co-Author*) Nothing to Disclose Thomas Petrone, PhD, Staten Island, NY (*Abstract Co-Author*) President, Petrone Associates William Moloney, MS, Brooklyn, NY (*Abstract Co-Author*) Nothing to Disclose

For information about this presentation, contact:

### PURPOSE

This work determines typical image reconstruction and display settings for CT imaging and compares them to the reference values published by the AAPM.

# METHOD AND MATERIALS

Scan protocol parameters were collected from reports of 100 annual CT scanner medical physics surveys in two states for adult head and abdomen and pediatric head and abdomen protocols per the ACR accreditation procedures. Data collection spanned academic and community hospitals and freestanding imaging centers; the data set includes pooled data collected by academic and consulting medical physicists. Reconstruction kernel/algorithm, image thickness, and image interval were tabulated for four protocols for all scanners; subgroups were analyzed to compare scanner manufacturers and different types of imaging facilities. Values were compared to reference protocols published by AAPM and recommended and required parameters given in the ACR CT Accreditation Clinical Image Quality Guide.

### RESULTS

Protocols for CT scanners at ACR-accredited facilities adhered to the maximum slice width values specified by the ACR accreditation program. There was variability in adherence to AAPM-recommended reference parameters, ranging from 80% agreement for adult head protocols to 44% agreement for pediatric abdomen protocols. There was wide variation in the chosen reconstruction algorithm; subgroups were used to compare protocols within each manufacturer since direct comparison between different manufacturers' proprietary algorithms was not possible within the scope of this work.

### CONCLUSION

There is substantial variation in image reconstruction parameters among ACR-accredited CT facilities that conform to ACR requirements. These parameters impact key image quality characteristics and radiation doses used for imaging, so appropriate choices are crucial to achieving optimization of imaging. Further work is needed to understand the nature of the deviation between the data collected at clinical sites and the AAPM reference protocols; while the AAPM protocols were published relatively recently, it is not clear whether the standard practice reflects changes that run ahead of updates to the AAPM protocols or whether the community is lagging in adopting the AAPM recommendations.

# **CLINICAL RELEVANCE/APPLICATION**

This work validates reference CT protocols against protocols used in real imaging departments. Deviations from reference protocol can be used in troubleshooting image quality.

# SSE22-03 CT Resolution, Noise, and Dose Reference Levels Across a Multi-Center Patient Population

Monday, Nov. 26 3:20PM - 3:30PM Room: S504AB

#### Participants

Taylor Smith, Durham, NC (*Presenter*) Nothing to Disclose Francesco Ria, DMP, Durham, NC (*Abstract Co-Author*) Nothing to Disclose John Heil, BA, King of Prussia, PA (*Abstract Co-Author*) CEO and Chairman, Imalogix Ehsan Samei, PhD, Durham, NC (*Abstract Co-Author*) Research Grant, General Electric Company; Research Grant, Siemens AG; Advisory Board, medInt Holdings, LLC; License agreement, 12 Sigma Technologies; License agreement, Gammex, Inc

# For information about this presentation, contact:

taylor.smith@duke.edu

# PURPOSE

The diagnostic reference level (DRL) is useful as a first-order tool to compare radiation exposures of one's imaging clinic against those of one's peers in computed tomography. Ria et al. have advocated for the addition of a Noise Reference Level (NRL), Noise Reference Range (NRR), a Dose Reference Level (DoRL) and a Dose Reference Range (DoRR) as a means of extending the first steps of optimization of clinical operation to image quality in addition to radiation exposure (ICRP 135). In this work, we investigate and establish another reference level, for the case of resolution, called the Resolution Reference Level (RRL) and Resolution Reference Range (RRR).

### **METHOD AND MATERIALS**

Over 10000 anonymized scans were sampled from 109 institutions in the United States which represented 13 large (estim. > 36,000 scans/yr), 32 medium (6000 - 36,000), 64 small (< 6000) imaging centers. CTDIvol, Noise and resolution (MTF) were measured for chest and abdominopelvic (AP) helical single-acquisitions of the trunk (extremity/head scans, multiple reconstructions excluded). Noise was taken as a modified version of the Global Noise Level measured in air. MTFs were measured from the air-skin interface. Patients were binned by their effective diameter. DoRL, NRL, and RRLs were measured for each size bin. Reference Levels for each were defined as the median values. Reference Ranges were defined as interquartile intervals.

#### RESULTS

Measurements of the f50 MTF in AP exams in all sizes had RRR lower bounds from 0.33 - 0.42 mm-1. The RRR upper bounds for these exams ranged from 0.38 - 0.46 mm-1. In chest exams these ranges were from 0.39 - 0.42 mm-1 and 0.45 - 0.46 mm-1 respectively. The lower bound of DoRR in the AP exams in all sizes ranged from 5.3 - 11.2 mGy. The upper bounds of DoRR ranged from 7.4 - 16.5 mGy. In chest exams these lower and upper bounds of the DoRR ranged from 5.4 - 11.5 mGy and 7.5 - 14.4 mGy.

# CONCLUSION

An extension to the reference level methodology has been proposed. With this new RRL and RRR, and existing NRL, NRR, DoRL, and DoRR, a clinic can begin to make holistic decisions regarding population-based imaging-protocol adjustments with consideration to dose, noise, and resolution.

### **CLINICAL RELEVANCE/APPLICATION**

This work extends the notion of NRL to the assessment of resolution. It represents a more generalizable sampling, with more vendors and kernels, and an order of magnitude increase in population.

# SSE22-04 Image Quality Metric Extraction Based on Machine Learning Techniques for Clinical CT Protocol Optimization

Monday, Nov. 26 3:30PM - 3:40PM Room: S504AB

# Participants

Zhye Yin, Niskayuna, NY (*Abstract Co-Author*) Employee, General Electric Company Rajesh Langoju, Bangalore, India (*Abstract Co-Author*) Nothing to Disclose Xin Wang, PhD, Niskayuna, NY (*Abstract Co-Author*) Employee, General Electric Company Bruno De Man, PhD, Niskayuna, NY (*Abstract Co-Author*) Employee, General Electric Company Jean-Baptiste Thibault, PhD, Brookfield, WI (*Presenter*) Employee, General Electric Company

### For information about this presentation, contact:

yin@research.ge.com

### PURPOSE

To extract standard image quality metrics (image noise and spatial resolution) directly from clinical CT images using machine learning techniques. This capability is desired to guide optimization and customization of clinical protocols to achieve desired diagnostic image quality and clinical task performance.

### **METHOD AND MATERIALS**

For training and testing of the machine learning networks, we acquire a series of clinical datasets and use post-processing techniques to generate datasets with various noise levels and various spatial resolution levels. We use the full-width-at-half-maximum (FWHM) of the point spread function (PSF) as spatial resolution metric and the standard deviation of the noise as image noise metric. 9 cardiac acquisitions with 224 images are post-processed to create various (5) levels of blurring, resulting in a combined training and test set of 10,080 images. We use both feature-based machine learning techniques and deep convolution neural networks (CNN) to execute supervised learning to estimate traditional analytic IQ metrics such as noise and spatial resolution. For example, to demonstrate the feasibility of the framework, we selected and implemented random forest regression approach for the supervised learning task. 7 features are extracted from the raw image and 8 features are extracted from the edge map. We extend this framework to deep convolution neural network (CNN) based machine learning method using Keras

#### RESULTS

Mean and standard deviation of estimation error is (0.0003mm, 0.0352mm) where true FWHM was emulated at [0.66mm, 1.174mm]. The figure below shows two example results: (a) an emulated image with a FWHM of 0.77 mm and the corresponding estimated FWHM has an error of 1.6%; (b) an emulated image with a FWHM of 1.02 mm and the corresponding estimated FWHM has an error of 4.7%.

#### CONCLUSION

It is feasible to extract image quality directly from clinical images. Both feature-based machine learning techniques and deep learning techniques are implemented and evaluated. Preliminary results show an accurate estimation of image quality with average errors of 3%.

# **CLINICAL RELEVANCE/APPLICATION**

IQ estimation directly from clinical images is a critical enabler to guide optimization and customization of clinical protocols to achieve desired diagnostic image quality and clinical task performance.

# SSE22-05 Predicting Major CT Scanner Failures Using Routine Quality Control Data

Monday, Nov. 26 3:40PM - 3:50PM Room: S504AB

Participants

Rose Al Helo Jr, MS, Cleveland, OH (*Presenter*) Nothing to Disclose Atallah Baydoun, MD, Cleveland, OH (*Abstract Co-Author*) Nothing to Disclose David W. Jordan, PhD, Cleveland, OH (*Abstract Co-Author*) Nothing to Disclose

## For information about this presentation, contact:

Rose.Alhelo@uhhospitals.org

# PURPOSE

Data collected for daily equipment quality control (QC) on computed tomography (CT) scanners contain patterns that may predict near term failure of major scanner components. Such defects are usually time consuming and hamper significantly the clinical workflow. The purpose of this study is to identify, from determinable QC parameters, the key performance values that can predict scanner hardware failure.

# **METHOD AND MATERIALS**

Our retrospective review included 37 CT scanners from four different manufacturers. Available QC data for all CT scanners included the daily records of mean and standard deviation (SD) of the CT number (HU) using the manufacturer's factory water phantom and a custom scan protocol. Data was stored in a cloud-based compliance solution and monitored using statistical process control according to our institution protocol. We identified two identical clinical CT units that had tube replacement within the last year. We collected the SD values over three month period before and after the replacement date. We then calculated the mean SD values before and after the repair for both units. We also determined pre- and post-repair cumulative SD and cumulative SD error relatively to each scanner mean SD.

### RESULTS

The mean SD of the CT numbers (HU) before and after the tube replacement for CT1 were respectively 5.75 and 5.33 (Ratio=1.078) and for CT2 5.92 and 5.48 (Ratio=1.080). Pre-repair cumulative SD and cumulative SD error for CT1 were 517 and 745% and for CT2 538.9 and 842%. Post-repair cumulative SD and cumulative SD error for CT1 were 463.5 and 271% and for CT2

460.5 and 277%. The pre- and post-repair cumulative SD and SD error satisfy a linear model curve that correlates the QC measurements with the tube defect of both CT units.

# CONCLUSION

Daily scanner HU noise values are insufficient to anticipate a major defect. However, a three-month cumulative SD and SD error above 500 and 700% respectively can predict failure of the tube component. Future studies are needed to highlight the possible use of such observed trends to predict impending failures. Thus, collection of data in an electronic database for a large scanner fleet would allow early intervention ultimately improving patient care.

### **CLINICAL RELEVANCE/APPLICATION**

To our knowledge, this study is the first to introduce the cumulative SD and cumulative SD error as a predictive tool of a major CT performance failure.

# SSE22-06 Realism and Potential of Population-Based Virtual Clinical Trials in Computed Tomography: Are We There Yet?

Monday, Nov. 26 3:50PM - 4:00PM Room: S504AB

# Participants

Ehsan Abadi, Durham, NC (*Presenter*) Nothing to Disclose William P. Segars, PhD, Durham, NC (*Abstract Co-Author*) Nothing to Disclose Brian Harrawood, MS, Durham, NC (*Abstract Co-Author*) Nothing to Disclose Shobhit Sharma, BEng,MSc, Durham, NC (*Abstract Co-Author*) Nothing to Disclose Anuj Kapadia, PHD, Durham, NC (*Abstract Co-Author*) Nothing to Disclose Ehsan Samei, PhD, Durham, NC (*Abstract Co-Author*) Nothing to Disclose Ehsan Samei, PhD, Durham, NC (*Abstract Co-Author*) Research Grant, General Electric Company; Research Grant, Siemens AG; Advisory Board, medInt Holdings, LLC; License agreement, 12 Sigma Technologies; License agreement, Gammex, Inc

### PURPOSE

Medical imaging systems are currently evaluated using either physical phantoms or patient images, both with limitations. Physical phantoms are generally simplistic, not representative of a human population, and thus limited to fully reflect task-based or patient-specific assessments. Patient images are ground truth-limited, expensive, and ethically unattainable in repetitive studies. Virtual clinical trial (VCT), defined as conducting clinical experiments using realistic simulations, can overcome these challenges. This work aimed to develop a comprehensive package to conduct realistic VCT using realistic human models with known ground truth and representative CT imaging conditions.

# METHOD AND MATERIALS

A realistic VCT requires two main toolsets: computational anthropomorphic phantoms and scanner simulators. We developed a series of high-resolution phantoms including highly detailed intra-organ anatomies. We also developed a rapid, realistic, and scanner-specific CT simulator to image the phantoms. Our simulator included geometry and physics (spectrum and bowtie filter) of commercial scanners, axial/helical trajectories, focal spot wobbling, poly/monochromacity, noise and detector response characteristics, scatter, tube current modulation, beam hardening correction, and a commercial processing box for scanner-specific reconstructions. Two pilot VCTs were performed: characterizing noise across reconstruction algorithms, and quantifying information loss as a function of beam collimation and pitch values.

### RESULTS

Our simulator produced CT images with NPS, MTF, and HU values close to real CT scans of same physical phantoms, under different acquisition settings and reconstruction kernels. The pilot VCT showed that iterative images have non-stationary noise texture with higher noise magnitude in the edges.

# CONCLUSION

We developed a package that conducts VCTs in the context of CT imaging and demonstrated its applicability in clinical studies where those studies need realistic heterogeneous models and repetitive measurements and therefore unattainable using physical phantoms or patient images. Our tool enables the imaging scientists and clinicians to explore and optimize the imaging systems more comprehensively.

### **CLINICAL RELEVANCE/APPLICATION**

A realistic virtual clinical trial enables the medical imaging community to conduct clinically-relevant experiments that are impossible to perform using patient images or physical phantoms.



#### SSE23

### Physics (Breast X-Ray Imaging)

Monday, Nov. 26 3:00PM - 4:00PM Room: S502AB



AMA PRA Category 1 Credit ™: 1.00 ARRT Category A+ Credit: 1.00

**FDA** Discussions may include off-label uses.

### Participants

Srinivasan Vedantham, PhD, Tucson, AZ (*Moderator*) Research collaboration, Koning Corporation Hilde Bosmans, PhD, Leuven, Belgium (*Moderator*) Co-founder, Qaelum NV Research Grant, Siemens AG

# Sub-Events

# SSE23-01 Radiation Dose Reduction in Digital Breast Tomosynthesis (DBT) by Means of Neural Network Convolution (NNC) Deep Learning

Monday, Nov. 26 3:00PM - 3:10PM Room: S502AB

Participants

Junchi Liu, MS, Chicago, IL (Abstract Submitter) Nothing to Disclose

Amin Zarshenas, MSc, Chicago, IL (Abstract Co-Author) Nothing to Disclose

Syed Ammar Qadir, Chicago, IL (Abstract Co-Author) Nothing to Disclose

Limin Yang, MD, PhD, Iowa City, IA (Abstract Co-Author) Nothing to Disclose

Laurie L. Fajardo, MD, MBA, Park City, UT (*Abstract Co-Author*) Consultant, Hologic, Inc; Consultant, Siemens AG; Consultant, FUJIFILM Holdings Corporation;

Kenji Suzuki, PhD, Chicago, IL (*Presenter*) Royalties, General Electric Company; Royalties, Hologic, Inc; Royalties, MEDIAN Technologies; Royalties, Riverain Technologies, LLC; Royalties, Canon Medical Systems Corporation; Royalties, Mitsubishi Corporation; Royalties, AlgoMedica, Inc

### For information about this presentation, contact:

jliu118@hawk.iit.edu

### PURPOSE

To reduce cumulative radiation exposure and lifetime risks for radiation-induced cancer from breast cancer screening, we developed novel NNC deep learning for radiation dose reduction in DBT.

### **METHOD AND MATERIALS**

Our original NNC deep learning employed patched-based neural network regression in a convolutional manner to convert lower-dose (LD) to higher-dose (HD) tomosynthesis images. We trained NNC with quarter-dose (25% of the standard dose: 12mAs at 32kVp) raw-projection images and corresponding "teaching" higher-dose (HD) images (200% of the standard dose: 99mAs at 32kVp) of a breast cadaver phantom acquired with a DBT system (Selenia Dimensions, Hologic). Once trained, NNC no longer requires HD images. It converts new LD images to images that look like HD images; thus the term "virtual" HD (VHD) images. We reconstructed tomosynthesis slices on a research DBT system. To determine a dose reduction rate, we acquired 4 studies of another test phantom at 4 different doses (1.35, 2.7, 4.04, and 5.39mGy entrance dose). Structural SIMilarity(SSIM) index was used to evaluate the image quality. For further testing, we collected half-dose (50% of the standard dose: 32±14 mAs at 33±5 kVp) and full-dose (100% of the standard dose: 68±23mAs at 33±5kvp) images of 51 clinical cases with the DBT system at Univ. of Iowa Hospitals & Clinics. We evaluated resulting images in a blinded observer study with 35 breast radiologists to rate and distinguish blinded VHD and real full-dose DBT images.

# RESULTS

NNC converted quarter-dose images (1.35mGy; SSIM: 0.88) of the testing cadaver phantom to VHD images with image quality (SSIM:0.97) equivalent to 119% dose images (6.41mGy), achieving 79% dose reduction. In our blinded observer study, 21(60%) of 35 breast radiologists either preferred VHD images over real full-dose images or could not distinguish between the two. The difference in image quality between the two was not statistically significant (P=0.37). The time required to process each study was 0.48 sec. on a GPU (GTX Titan Z, Nvidia).

### CONCLUSION

Blinded observer study with 35 radiologists demonstrated that VHD images converted by our deep-learning technology were equivalent to full-dose DBT images. Our cadaver phantom experiment demonstrated 79% dose reduction.

### **CLINICAL RELEVANCE/APPLICATION**

Substantial radiation dose reduction would benefit patients by reducing the lifetime risk of radiation-induced cancer from DBT screening.

Participants

Martin J. Yaffe, PhD, Toronto, ON (*Presenter*) Research collaboration, General Electric Company; Shareholder, Volpara Health Technologies Limited; Co-founder, Mammographic Physics Inc; Research Consultant, BHR Pharma LLC

Etta D. Pisano, MD, Charleston, SC (*Abstract Co-Author*) Researcher, Freenome Holdings Inc; Researcher, Real Imaging Ltd; Researcher, Therapixel; Researcher, DeepHealth, Inc; Researcher, ToDos

Aili K. Maki, BEng, Toronto, ON (Abstract Co-Author) Research collaboration, General Electric Company; Contractor, Mammographic Physics, Inc

James G. Mainprize, PhD, Toronto, ON (*Abstract Co-Author*) Institutional research agreement, General Electric Company Gordon Mawdsley, BS, Toronto, ON (*Abstract Co-Author*) Director, Medical Physics Incorporated Research collaboration, General Electric Company

Sam Shen, Toronto, ON (Abstract Co-Author) Employee, Mammographic Physics Inc; Research collaboration, General Electric Company

Ruth C. Carlos, MD, MS, Ann Arbor, MI (Abstract Co-Author) Nothing to Disclose

Kathy D. Miller, MD, Indianapolis, IN (Abstract Co-Author) Nothing to Disclose

Christopher E. Comstock, MD, New York, NY (Abstract Co-Author) Nothing to Disclose

# For information about this presentation, contact:

martin.yaffe@sri.utoronto.ca

### PURPOSE

To describe and provide preliminary results from a remote-monitoring QC program developed to provide assessment of quality and rapid feedback in a screening trial. The program is being used in the randomized TMIST trial of screening with breast tomosynthesis versus digital mammography. TMIST is expected to include 125 sites in the US and Canada and will recruit 164,986 women who will be imaged up to 5 times over 4 years.

# METHOD AND MATERIALS

The QC program is based on imaging of phantoms by the technologist at each site and digital transmission to a central analysis server. Phantoms assess signal and noise properties, artifacts, spatial resolution and geometric fidelity of the imaging system. The analysis is performed automatically with results made available to technologists on a password protected web site. Technical information from the DICOM header, stripped of personal identifiers, from every clinical image is available for analysis of doses, exposure factors and compression parameters..

# RESULTS

As of April 2018, initial QC data from 87 units at the first 29 TMIST sites were available, including de-identified screening mammogram header data from 60 units at the first 25 sites. The most frequent technical problems were due to electronic interference, dustlike artifacts and the compression force being reported in the header as '0. Problems were also noted due to duplication of image submission from the same individual as separate cases and noncompliance with the QC protocol. In addition, it was noted that digital detectors were occasionally replaced without technical documentation. This was accompanied by changes in signal-to-noise performance. Based on 881 examinations, the mean dose (CC + MLO) was 4.2 mGy for 2D digital mammograms and 8.2 mGy for tomosynthesis. The presentation will report on results up to November, 2018.

# CONCLUSION

Use of a centralized remote data collection QC system reduces technologist labor at the site and reduces subjectivity in testing. This approach enables consistent analysis and rapid reporting of QC results.

# **CLINICAL RELEVANCE/APPLICATION**

Sensitivity and specificity of breast cancer detection depend critically on the technical image quality. The credibility of the results from the TMIST trial requires that the image quality of both modalities is verified. In addition, experience from this trial will provide data to help define the essential elements of the standard QC program for tomosynthesis.

### **Honored Educators**

Presenters or authors on this event have been recognized as RSNA Honored Educators for participating in multiple qualifying educational activities. Honored Educators are invested in furthering the profession of radiology by delivering high-quality educational content in their field of study. Learn how you can become an honored educator by visiting the website at: https://www.rsna.org/Honored-Educator-Award/ Ruth C. Carlos, MD, MS - 2015 Honored EducatorRuth C. Carlos, MD, MS - 2018 Honored Educator

# SSE23-03 Visual Grading Characteristics Analysis of Propagation-Based X-Ray Phase Contrast Mammography

Monday, Nov. 26 3:20PM - 3:30PM Room: S502AB

Participants

Seyedamir Tavakoli Taba, Sydney, Australia (*Abstract Co-Author*) Nothing to Disclose Sarah J. Lewis, PhD,MEd, Sydney, Australia (*Abstract Co-Author*) Nothing to Disclose Patrycja Baran, Parkville, Australia (*Abstract Co-Author*) Nothing to Disclose Matthew Dimmock, Clayton, Australia (*Abstract Co-Author*) Nothing to Disclose Mikkaela McCormack, Heidelberg, Australia (*Abstract Co-Author*) Nothing to Disclose Sheridan Mayo, Clayton, Australia (*Abstract Co-Author*) Nothing to Disclose Sheridan Mayo, Clayton, Australia (*Abstract Co-Author*) Nothing to Disclose Yakov Nesterets, Clayton, Australia (*Abstract Co-Author*) Nothing to Disclose Christopher Hall, Clayton, Australia (*Abstract Co-Author*) Nothing to Disclose Jane Fox, Clayton, Australia (*Abstract Co-Author*) Nothing to Disclose Zdenka Prodanovic, Clayton, Australia (*Abstract Co-Author*) Nothing to Disclose Darren Lockie, FRANZCR, Southbank, Australia (*Abstract Co-Author*) Nothing to Disclose Daniel Hausermann, Clayton, Australia (*Abstract Co-Author*) Nothing to Disclose Giuliana Tromba, PhD, Trieste, Italy (*Abstract Co-Author*) Nothing to Disclose

### For information about this presentation, contact:

amir.tavakoli@sydney.edu.au

### PURPOSE

While all current x-ray based breast imaging modalities rely on minimal differences in soft tissue x-ray attenuation (absorption contrast), phase-contrast imaging has the capacity to also visualise variations in x-ray refraction (phase contrast). For x-ray energies typically used in breast imaging, the phase contrast can be substantially larger than the absorption contrast, presenting an opportunity to improve soft tissue visualisation especially in mammographically dense breasts. The goal of this study was to evaluate the radiological quality of images produced by the x-ray propagation-based phase-contrast computed tomography (PB-CT) technique at two different x-ray energies in comparison to absorption-based CT images collected at the same radiation dose (4 mGy).

# METHOD AND MATERIALS

Twenty-seven synchrotron-based CT images of a full-size breast mastectomy specimen were reconstructed. Nine images were absorption-based CT at 32 KeV, nine images were PB-CT at 32 KeV and nine were PB-CT at 38 KeV. A group of breast specialist radiologists and medical imaging experts compared the radiological quality of the three sets of images based on various image quality criteria. Visual grading characteristics (VGC) analysis was conducted and VGC curves were obtained. The area under the VGC curve (0<=AUCVGC<=1) was calculated as the measure of the difference in image quality between two compared sets of images.

### RESULTS

The results show that the radiological quality ratings of PB-CT 32 KeV images were significantly higher than absorption-based CT images (AUCVGC=0.879, p<=.001) and PB-CT 38 KeV images (AUCVGC=0.795, p<=.001). The image quality ratings were not significantly different between PB-CT 38 KeV images and absorption-based CT images (AUCVGC=0.567, p=.076).

#### CONCLUSION

Phase-contrast PB-CT mammography can be used to produce images with substantially higher radiological quality compared to conventional absorption-based images, but this advantage appears to be dependent on beam energy. The results from this study should provide a strong basis for future experimental and clinical protocols for further optimisation of this novel and promising approach to breast imaging.

# **CLINICAL RELEVANCE/APPLICATION**

PB-CT of the breast is expected to deliver improved image quality compared to current x-ray modalities and become a viable method for early diagnosis of breast cancer in the future.

# SSE23-04 Evaluation of American College of Radiology (ACR) Mammography Accreditation Phantom Image Quality of a Grid-Less and Software-Based Scatter Correction Technology

Monday, Nov. 26 3:30PM - 3:40PM Room: S502AB

Participants

Anzi Zhao, MS, Cleveland, OH (*Presenter*) Nothing to Disclose Katie Hulme, MS, Cleveland, OH (*Abstract Co-Author*) Nothing to Disclose

### PURPOSE

To evaluate the quality of ACR mammography accreditation phantom images acquired with a grid-less and software-based scatter correction technology - Progressive Reconstruction Intelligently Minimizing Exposure (PRIME).

### **METHOD AND MATERIALS**

3 Siemens Mammomat Inspiration units with PRIME were utilized in this study. The same ACR phantom was imaged on all units. 20 2D phantom images were acquired on each unit using a phototimed technique (W/Rh, 28kVp, AEC segmentation off, dose level 'normal', exam tag 'QC RAW'), of which 10 were acquired with grid in position and 10 were acquired with PRIME. Mode of acquisition was varied in a random order. 10 additional PRIME images were acquired on one unit with a resolution test pattern to assess spatial resolution. Contrast-to-noise ratio (CNR), signal-to-noise ratio (SNR), and standard deviation (SD) of phantom images were evaluated using the method in Siemens quality control manual. Incident air kerma and average glandular dose (AGD) were measured and calculated for each exposure. A total of 60 phantom images were scored by 4 qualified medical physicists and 2 experienced mammography technologists on a diagnostic workstation in clinical viewing conditions, and using ACR phantom evaluation guidelines with demographics hidden.

# RESULTS

With PRIME, all images failed CNR criteria (>=2) with significantly lower CNR and higher SD than grid-based images by as much as 43% and 23%, respectively; SNR was reduced by 2-4%; spatial resolution was unaffected at 7 mm/lp; AGD was reduced by up to 16%. Visual scoring by 6 viewers resulted in no significant difference between the two types of images. Minor degradation on average score of masses on PRIME images compared to grid-based images (4.1 vs 4.2) was noted on one unit. All viewers agreed on the notable difference in image appearance and noise texture when PRIME was employed.

### CONCLUSION

PRIME didn't penalize ACR phantom scoring, although there was a significant degradation of CNR on PRIME images because of the increased noise. The clinical implications of differences in noise texture warrant further investigation. Although PRIME offers moderate dose savings, clinicians should still be aware of potential effects on image appearance.

#### **CLINICAL RELEVANCE/APPLICATION**

DDIME technology corrects coattor radiation and anables and loss full field digital mammaranhy at lower nations average alandular

PRIME technology corrects scatter radiation and enables grid-less full new digital manifold appropriat lower patient average glandular dose, with comparable image quality.

# SSE23-05 Mammographic Compression Variability Increased after Removing Real-Time Pressure Indicator

Monday, Nov. 26 3:40PM - 3:50PM Room: S502AB

Participants

Monique G. van Lier, MSc, Amsterdam, Netherlands (*Presenter*) Employee, SigmaScreening BV Jerry E. De Groot, PhD, Amsterdam, Netherlands (*Abstract Co-Author*) Employee, SigmaScreening BV Woutjan Branderhorst, PhD, Amsterdam, Netherlands (*Abstract Co-Author*) Employee, SigmaScreening BV Laura J. Schijf, MD, Amsterdam, Netherlands (*Abstract Co-Author*) Nothing to Disclose Cornelis A. Grimbergen, PhD, Amsterdam, Netherlands (*Abstract Co-Author*) Founder, SigmaScreening BV Employee, SigmaScreening BV Board Member, SigmaScreening BV Patent holder, SigmaScreening BV Gerard J. den Heeten, MD,PhD, Nijmegen, Netherlands (*Abstract Co-Author*) Founder, SigmaScreening BV; Scientific Advisor, SigmaScreening BV; Patent Holder, SigmaScreening BV; Stock options, Volpara Health Technologies Limited; Medical Advisory Board, Volpara Health Technologies Limited

For information about this presentation, contact:

m.g.vanlier@amc.nl

### CONCLUSION

When replacing a paddle with a pressure indicator, in a group of technicians familiar with the indicator, by a conventional paddle, the variability increased significantly leading to more unfavorable over- and under-compression.

### Background

A certain level of breast flattening in mammography is needed to obtain a high quality image. Generally accepted and quantifiable standards do not exists. Recent studies show that the level of compression pressure at exposure influences screening performance. Attempts are made to standardize the compression procedure by introducing pressure-based compression using a paddle equipped with a real-time pressure indicator. We aimed to study the impact on compression practice when replacing the pressure-based paddle with a conventional paddle without pressure indication in group experienced technicians.

### **Evaluation**

Mammographic compression pressure was retrospectively obtained from mammographic images (VolparaAnalytics) and evaluated in two datasets from the same radiology department with the same technician team. The first dataset (4 years, n=11.561 compressions) was collected when using a compression paddle equipped with a real-time pressure indicator aiming for a 10kPa (75mmHg) compression pressure. The second dataset (3 months, n=1331 compressions) was collected 4 months after the mammography system with pressure indicator was replaced by a system without pressure indicator. The average compression pressure and variance significantly (P<0.001) increased from 11.23  $\pm$  0.04 kPa to 11.60  $\pm$  0.14 kPa (mean  $\pm$  SEM) after removal of the pressure indicator. The proportion of compressions in the pressure range 5-15 kPa decreased from 87.4% to 77.9%. The proportion of high pressures (>15kPa) almost doubled (11.0% to 18.8%) and low pressures (<5kPa) more than doubled (1.6% to 3.3%).

# Discussion

When removing the pressure indicator, the initially low variability is increasing rapidly, indicating that an indicator is needed to remain high compression reproducibility. An increase in over- and under-compression can ultimately lead to decreased mammographic performance.

# SSE23-06 Development of Low Dose Digital Mammography Platform by Image Reconstruction Using Deep Learning Algorithm: A Preliminary Study

Monday, Nov. 26 3:50PM - 4:00PM Room: S502AB

Participants

Su Min Ha, MD, Seoul, Korea, Republic Of (*Presenter*) Nothing to Disclose Eunhee Kang, Daejon, Korea, Republic Of (*Abstract Co-Author*) Nothing to Disclose Jong Chul Ye, PhD, Daejon, Korea, Republic Of (*Abstract Co-Author*) Nothing to Disclose Hak Hee Kim, MD, Seoul, Korea, Republic Of (*Abstract Co-Author*) Nothing to Disclose

### PURPOSE

To investigate whether low dose mammography can be reconstructed to standard dose mammography using the new deep learning algorithm.

# METHOD AND MATERIALS

14 specimens from 14 patients who underwent total mastectomy for primary breast cancer were included. Specimen mammograms were obtained with standard routine dose and reduced sequential doses; 80% of routine dose, 60%, 40%, 20% and 10%. The proposed de-noising method is designed based on semi-supervised learning with cycle consistency loss. Most of the mammography has Automatic Exposure Control (AEC) system which chooses an appropriate current X-ray source. The routine dose and 20% dose level images were selected as training dataset. Since the noise levels between two images are different and unavoidable slight mismatch due to potential deformation between multiple acquisitions, we developed the semi-supervised learning using cyclic consistency. We trained two generators (network G and F) and two discriminators (network Dx and Dy). Since we had 14 datasets, we performed cross-validation. Last, image quality of reconstructed low dose image was compared with the standard full dose image and was qualitatively rates as follows; 1= poor, 2= fair, 3= equal, 4=better.

#### RESULTS

As more radiation dose was decreased, noise was increased and contrast resolution was decreased accordingly. However, in the reconstructed images, noise was decreased and contrast resolution was rather improved. Overall, when we evaluated the lesions according to Breast imaging-reporting and data system lexicon, and with consideration of underlying breast parenchyma density,

the reduced dose of 20% cut-off of standard full dose showed no significant difference in image quality compared with standard dose mammography.

# CONCLUSION

The image quality of reconstructed low dose mammography using the new deep learning algorithm is comparable with standard dose mammography until dose reduction cut-off 20% of standard full dose. Therefore, the radiation dose of mammography could be considerably reduced using this deep learning algorithm.

# **CLINICAL RELEVANCE/APPLICATION**

Image reconstruction using the new deep learning algorithm is effective in dose reduction of mammography, especially in young women with high risk who are routinely examined with mammography for screening.



### SSE24

# Physics (MR: Diffusion and Susceptibility Imaging)

Monday, Nov. 26 3:00PM - 4:00PM Room: S504CD



AMA PRA Category 1 Credit ™: 1.00 ARRT Category A+ Credit: 1.00

FDA Discussions may include off-label uses.

### Participants

Hui Mao, PhD, Atlanta, GA (*Moderator*) Nothing to Disclose Timothy J. Carroll, PhD, Chicago, IL (*Moderator*) Nothing to Disclose

# Sub-Events

# SSE24-01 A Preliminary Study of Incoherent Motion Diffusion Weighted Imaging (IVIM) in the Curative Effect Evaluation of Diabetic Nephropathy

Monday, Nov. 26 3:00PM - 3:10PM Room: S504CD

Participants

Zhang Xirong, MMed, Xianyang City, China (*Presenter*) Nothing to Disclose Jing Chen, Xianyang City, China (*Abstract Co-Author*) Nothing to Disclose Ma Junchao, Xianyang, China (*Abstract Co-Author*) Nothing to Disclose Guangming Ma, Xianyang, China (*Abstract Co-Author*) Nothing to Disclose Changyi Guo, PhD, Xi'an, China (*Abstract Co-Author*) Nothing to Disclose He Taiping, MMed, Xian Yang City, China (*Abstract Co-Author*) Nothing to Disclose Shaoyu Wang, Shanghai, China (*Abstract Co-Author*) Nothing to Disclose Ming Zhang, Xian, China (*Abstract Co-Author*) Nothing to Disclose Wei Wang, MD, Xi'an, China (*Abstract Co-Author*) Nothing to Disclose

### For information about this presentation, contact:

113124329@qq.com

### PURPOSE

To investigate the change of IVIM quantitative parameters before and after clinical treatment of patients with diabetic nephropathy, and objectively evaluate the clinical therapeutic effects of patients with diabetic nephropathy.

# METHOD AND MATERIALS

20 patients(average age 56.60±9.38)with diabetic nephropathy who were diagnosed with diabetic nephropathy and received systemic hospitalization were selected. The clinical symptoms of the patients after treatment were significantly improved. The IVIM(b=0,50,100,150,200,400,600,800sec/mm<sup>2</sup>) and Diffusion weighted imaging(DWI,b=50,800 sec/mm<sup>2</sup>) sequence were obtained on a 3T scanner(Skyra, Siemens Healthineers). A total of 12 regions of interest were mapped in the cortex and medulla region of the upper pole, the renal hilum and the lower pole of the kidneys, and the results were averaged to obtain the measurement results.ADC map was automatically generated on the Siemens MRWP workstation after DWI sequence executed. IVIM parameters(ADC,D,f, and D\* values) were generated by using a prototype software body diffusion toolbox(Siemens healthineers).Paired-sample t-test was used to compare changes in renal cortex and medulla ADC, D, f, and D\* values before and after treatment in patients with diabetic nephropathy.

#### RESULTS

Compared to pre-treatment, ADC, D, f, and D\* values of both kidney and medulla in patients with diabetic nephropathy were significantly higher (p < 0.0001) (Figure 1,Table 1).

### CONCLUSION

IVIM is feasible for the evaluation of the efficacy of diabetic nephropathy, and it is helpful for the monitoring of clinical efficacy.

# **CLINICAL RELEVANCE/APPLICATION**

IVIM responds to changes in the microstructure of the tissue, more scientific and objective assessment of clinical efficacy of diabetic nephropathy, with potential clinical application value.

# SSE24-02 Diffusion-Weighted Imaging and Diffusion Kurtosis Imaging in the Diagnosis of Prostate Cancer: A Preliminary Retrospective Study

Monday, Nov. 26 3:10PM - 3:20PM Room: S504CD

Participants Guodong Jing, Shanghai, China (*Presenter*) Nothing to Disclose Xu Yan, Shanghai, China (*Abstract Co-Author*) Nothing to Disclose Luguang Chen, Shanghai, China (*Abstract Co-Author*) Nothing to Disclose Jian Wang, MD, Shanghai, China (*Abstract Co-Author*) Nothing to Disclose Caixia Fu, Shenzhen, China (*Abstract Co-Author*) Employee, Siemens AG Li Wang, Shanghai, China (*Abstract Co-Author*) Nothing to Disclose Jianping Lu, MD, Shanghai, China (*Abstract Co-Author*) Nothing to Disclose

#### For information about this presentation, contact:

147966863@qq.com

#### PURPOSE

This study explored and compared the value of DKI with DWI in distinguishing prostate cancer from non-cancer tissues and compared their performances in the peripheral zone and the central lobe.

### **METHOD AND MATERIALS**

A retrospective review was performed in 212 consecutive patients who underwent examination on a clinical 3T MR scanner , and all patients were confirmed by pathology. A multi-b DWI sequence was performed with the following parameters: TR/TE = 5100/89ms, FOV = 280x224 mm2, scan, slice thickness = 4mm, slice number = 20, bandwidth = 1755Hz/Px, iPAT factor = 2, b-values =0, 500, 1000, 1500, 2000 mm2/s, scan time = 4min10s. Mean kurtosis (MK), mean diffusivity (MD) derived from DKI and apparent diffusion coefficient (ADC) derived from conventional DWI were calculated and analyzed by using an in-house-developed software based on MATLAB (Mathworks, Natick MA). The diagnostic accuracy of MK, MD and ADC values was evaluated with sensitivity, specificity, and area under receiver operating characteristic (ROC) curve (AUC). Student's t-test and ROC curves were used for statistical analysis.

#### RESULTS

There was a significant difference between non-cancerous tissues in the peripheral zone and central lobe (P <0.001) for MK, MD and ADC; while these parameters show no significant difference between prostate cancers in the peripheral zone and the central lobe (p>0.05). For the peripheral zone, MK, MD and ADC had sensitivities of 0.980, 0.983, 0.993, specificities of 0.994, 0.988, 0.993, and AUCs of 0.9996, 0.9993, 0.9998 when using cutoff values of 0.701, 1.693x10-3mm2/s, and 1.141x10-3mm2/s, respectively. While for the central lobe, the diagnostic performance of MK, MD and ADC dropped and got sensitivities of 0.785, 0.843, 0.855, specificities of 0.983, 0.978, 0.981, and AUCs of 0.9430, 0.9571, 0.9569, when the cut-off points were 0.829, 1.527x10-3mm2/s, 0.997x10-3mm2/s, respectively.

### CONCLUSION

DKI and DWI may depict microstructure changes of prostate cancer, and can potentially provide quantitative information for the prostate tissue and have similar good diagnostic performance to distinguish prostate cancer from non-cancer tissues. the diagnosis values in the peripheral zone were slightly better than in the central lobe.

# **CLINICAL RELEVANCE/APPLICATION**

DKI and DWI both could be used in clinical for distinguishing prostate cancer from non-cancer tissues, and would lead to a substantial improvement in the diagnosis of prostate cancer.

# SSE24-03 The Susceptibility of Thrombus in Middle Cerebral Artery Predicts Prognosis by Quantitative Susceptibility Mapping

Monday, Nov. 26 3:20PM - 3:30PM Room: S504CD

Participants

Meizhu Zheng, Tianjin, China (*Presenter*) Nothing to Disclose Qingyuan Yang, Tianjin, China (*Abstract Co-Author*) Nothing to Disclose Xiudi Lu, Tianjin, China (*Abstract Co-Author*) Nothing to Disclose Shuang Xia, MD, Tianjin, China (*Abstract Co-Author*) Nothing to Disclose

#### For information about this presentation, contact:

zhengmeizhu163@163.com

### CONCLUSION

The susceptibility remained consistent regardless the location, thrombus length and onset time, which indicated that the thrombus composition was similar when detected on SWI. Susceptibility, thrombus length and CBS could predict clinical severity and short-term clinical prognosis.

### Background

The quantitative susceptibility mapping(QSM) is used to evaluate susceptibility, length of thrombus and clot burden score (CBS) in the middle cerebral arterial.

#### **Evaluation**

To explore the relationship between thrombus and cerebral infarction and to early clinically prognose patients with acute cerebral infarction by QSM. We analyzed the data of 73 patients with acute cerebral infarction who had unilateral middle cerebral arterial occlusion on time of flight magnetic resonance angiography (TOF-MRA), and had the corresponding susceptibility vessel sign (SVS) on susceptibility weighted imaging (SWI). Susceptibility, length of CBS were evaluated based on QSM. The relationships between susceptibility and thrombus length, CBS, DWI-ASPECTS, admission and discharge National Institutes of Health stroke scale (NIHSS) were analyzed. The susceptibility among different locations and different segments of the thrombi did not achieve statistically difference(All p>0.05). The susceptibility and length were negatively correlated with DWI-ASPECTS (R2=0.045,0.186, p=0.034,0.000) and positively correlated with admission NIHSS(R2=0.058,0.067, p=0.014,0.015). The susceptibility was positively correlated with discharge NIHSS(R2=0.096, p=0.036). CBS was negatively correlated with thrombus length, admission and discharged NIHSS (R2=0.177,0.133,0.042, p=0.000,0.006,0.019) and positively correlated with DWI-ASPECTS(R2=0.107, p=0.002).

There were two main findings in this study. First, all the susceptibility remained consistent regardless of the different segments, locations and onset time. Second, susceptibility, length of thrombus and CBS correlated to the extent of cerebral infarction, and they could all independently predict clinical severity and short-term clinical prognosis apart from the effect of length of MCA thrombus to the discharge NIHSS.

# SSE24-04 Optimization and Clinical Evaluation of Wave-CAIPI Susceptibility-Weighted Imaging (SWI) for Detection of Intracranial Hemorrhage

Monday, Nov. 26 3:30PM - 3:40PM Room: S504CD

### Awards

# Student Travel Stipend Award

Participants

John Conklin, MD, MSc, Boston, MA (*Abstract Co-Author*) Nothing to Disclose Steve Cauley, PhD, Charlestown, MA (*Abstract Co-Author*) Nothing to Disclose Kawin Setsompop, Charlestown, MA (*Abstract Co-Author*) Nothing to Disclose Bruce R. Rosen, MD, PhD, Charlestown, MA (*Abstract Co-Author*) Nothing to Disclose Ramon G. Gonzalez, MD, PhD, Boston, MA (*Abstract Co-Author*) Nothing to Disclose Pamela W. Schaefer, MD, Boston, MA (*Abstract Co-Author*) Nothing to Disclose Otto Rapalino, MD, Boston, MA (*Abstract Co-Author*) Nothing to Disclose Susie Y. Huang, MD, PhD, Boston, MA (*Presenter*) Research Grant - Siemens Healthineers John Kirsch, PhD, Charlestown, MA (*Abstract Co-Author*) Nothing to Disclose

# For information about this presentation, contact:

jconklin1@mgh.harvard.edu

# PURPOSE

To characterize image quality and accuracy of highly accelerated Wave-CAIPI SWI compared to standard 3D SWI and 2D gradientecho (GRE) for detection of intracranial hemorrhage.

### **METHOD AND MATERIALS**

*Optimization:* Wave-CAIPI SWI was evaluated on a 3T Prisma MR scanner (Siemens, Erlangen) using 6-fold (acquisition time TA=1.5 min) and 9-fold (TA=1 min) acceleration on commercially available 20-channel and 32-channel RF coils. SNR was evaluated as a function of acceleration factor and head position in a healthy subject using the multiple acquisition method (NEX=10). *Clinical evaluation:* Wave-CAIPI SWI was prospectively compared to standard 3D SWI (TA=4.5 min) or 2D GRE (TA=2.3 min) for 63 consecutive patients undergoing clinical brain MRI. Two radiologists evaluated all images for the presence of hemorrhage, number of hemorrhagic foci, motion artifacts, and subjective image quality.

#### RESULTS

Adequate SNR (>30) was achieved in the central brain using 9-fold acceleration on the 32-channel coil and 6-fold acceleration on the 20-channel coil. Wave-CAIPI SWI was compared to standard SWI for 33 patients and 2D GRE for 30 patients. Inter-rater reliability was almost perfect for presence of hemorrhage ( $\kappa$ =0.92) and number of hemorrhages ( $\kappa$ =0.89), substantial for motion artifact ( $\kappa$ =0.69), and modest for subjective image quality ( $\kappa$ =0.50). Motion artifacts in Wave-CAIPI SWI were less severe than standard SWI (p<0.01). Wave-CAIPI and standard SWI provided 100% agreement for presence of hemorrhage (13 of 33 patients). In two cases, additional hemorrhagic foci were detected on Wave-CAIPI SWI which were obscured by motion on the standard SWI. Wave-CAIPI SWI identified presence of hemorrhage in 13 of 30 patients compared to 11 of 30 patients for 2D GRE. In 6 cases, additional hemorrhagic foci were identified on Wave-CAIPI SWI that were not seen on the 2D GRE sequence. Subjective image quality was higher for Wave-CAIPI SWI than 2D GRE (p<0.01), and was not significantly different between Wave-CAIPI and standard SWI.

### CONCLUSION

A 1 minute Wave-CAIPI SWI acquisition is comparable to a 4.5 minute resolution-matched standard SWI sequence and superior to a 2.3 minute 2D GRE sequence for detection of intracranial hemorrhage.

### **CLINICAL RELEVANCE/APPLICATION**

Wave-CAIPI SWI may be useful to shorten clinical brain MR protocols, especially in motion prone populations. Acceleration should balance scan time with acceptable SNR for a given hardware configuration.

# SSE24-05 5D Relaxation-Diffusion Tensor Correlation MRI for Model-Free Quantification of Microscopic Heterogeneity of Brain Tissue

Monday, Nov. 26 3:40PM - 3:50PM Room: S504CD

Participants

Daniel Topgaard, Lund, Sweden (*Presenter*) Stockholder, Random Walk Imaging AB Joao P. de Almeida Martins, Lund, Sweden (*Abstract Co-Author*) Employee, Random Walk Imaging AB Chantal Tax, Cardiff, United Kingdom (*Abstract Co-Author*) Nothing to Disclose Filip Szczepankiewicz, PhD, Boston, MA (*Abstract Co-Author*) Employee, Random Walk Imaging AB Maxime Chamberland, Cardiff, United Kingdom (*Abstract Co-Author*) Nothing to Disclose Greta Eklund, Lund, Sweden (*Abstract Co-Author*) Employee, Random Walk Imaging AB Karin M. Bryske, PhD, Lund, Sweden (*Abstract Co-Author*) Employee, Random Walk Imaging AB Derek Jones, Cardiff, United Kingdom (*Abstract Co-Author*) Nothing to Disclose Carl Fredrik Westin, PhD, Boston, MA (*Abstract Co-Author*) Nothing to Disclose

### For information about this presentation, contact:

daniel.topgaard@fkem1.lu.se

PURPOSE

Conventional quantitative MRI yields voxel-average relaxation rates and diffusion tensors that are difficult to interpret in terms of chemical composition and microstructure whenever the voxels contain more than one tissue type such as white matter (WM), gray matter (GM), cerebrospinal fluid (CSF), and tumor. Here we introduce a method to quantify per-voxel heterogeneity as joint relaxation and diffusion tensor distributions.

### METHOD AND MATERIALS

We propose a data acquisition protocol and inversion procedure to estimate nonparametric 5D joint distributions with the dimensions transverse relaxation rate R2, isotropic diffusivity, normalized diffusion anisotropy, and diffusion tensor orientation (two dimensions). A healthy volunteer was scanned on a Siemens Prisma 3T system using a diffusion-weighted EPI sequence customized for variable echo times and tensor-valued diffusion encoding, giving a 5D acquisition space with dimensions directly corresponding to the ones of the sought-for distributions. A total of 852 images were acquired at 2x2x6 millimeter spatial resolution, 110x110 matrix size, 11 slices, and a total scan time of 45 min without using simultaneous multislice. Per-voxel distributions were obtained by unconstrained Monte Carlo inversion including uncertainty estimation.

### RESULTS

Voxels containing pure WM, GM, or CSF give nearly single-mode distributions (WM: high R2, low diffusivity, high anisotropy; GM: high R2, low diffusivity, low anisotropy; CSF: low R2, high diffusivity, low anisotropy), while voxels with binary mixtures yield the corresponding bimodal distributions. Component-resolved maps of signal amplitude, R2, diffusivity, anisotropy, and orientation for the WM, GM, and CSF fractions are obtained by binning and parameter calculation in the 5D distribution space.

### CONCLUSION

Our image acquisition protocol and model-free data inversion procedure yields per-voxel quantification of distinct tissue types without relying on assumptions about the number or properties of the individual components.

### **CLINICAL RELEVANCE/APPLICATION**

The new method is expected to be useful for pathological conditions associated with sub-voxel tissue heterogeneity, e.g. tumor infiltration in surrounding brain tissue or replacement of myelin with free water.

# SSE24-06 Susceptibility Artifact on Diffusion-Weighted Imaging for 3T Prostate MR: Effect of Rectal Gel on Image Quality

Monday, Nov. 26 3:50PM - 4:00PM Room: S504CD

Participants

Abdul-Rahman Abualruz, MD, Winston Salem, NC (*Presenter*) Nothing to Disclose Jao J. Ou, MD,PhD, Winston-Salem, NC (*Abstract Co-Author*) Nothing to Disclose David D. Childs, MD, Clemmons, NC (*Abstract Co-Author*) Nothing to Disclose John T. McCarty, DO, Winston-Salem, NC (*Abstract Co-Author*) Nothing to Disclose Joshua M. Similuk, DO, Winston Salem, NC (*Abstract Co-Author*) Nothing to Disclose

## For information about this presentation, contact:

dchilds@wakehealth.edu

### CONCLUSION

Our preliminary data suggests that for patients undergoing 3T surface coil prostate MR, instilling rectal gel can successfully decrease susceptibility artifact from excess gas, resulting in improved visualization of the PZ and increased diagnostic confidence.

### Background

While use of 3T surface coil examinations has led to increased patient comfort for prostate MR, elimination of the endorectal coil has resulted in new challenges. Susceptibility artifact from rectal gas can significantly limit visualization of the peripheral zone (PZ) on diffusion-weighted (DWI) images, potentially risking the detection of clinically significant cancers. Few studies have evaluated strategies to reduce this artifact, so we have piloted a method of instilling rectal gel in an attempt to displace excess gas.

#### **Evaluation**

We introduced a new workflow for real-time monitoring of prostate MR studies. If a marked amount of rectal gas or DWI susceptibility artifact was noted, 60 mL of ultrasound gel was administered per rectum, and images repeated. Between July 2017 and February 2018, 149 evaluations were performed at our institution, of which 26 cases with both pre- and post-gel DWI series were identified for retrospective analysis. Two subspecialty abdominal radiologists assigned 5-point scale values to assess the amount of PZ visualized (1=low, 5=high), PZ distortion by susceptibility artifact (1=low, 5=high), degree of rectal distention (1=none, 5=high), and overall diagnostic confidence (1=none, 5=without limitation). Both paired t-test and Wilcoxon rank-sum tests were performed to assess the effectiveness of the intervention. Rectal gas volumetry was also performed with segmentation of the estimated intraluminal space on T2-weighted images from the level of the prostatic base to the anorectal junction.

#### Discussion

PZ visualization and overall diagnostic confidence were increased for both readers to a statistically significant level (p<0.05). A corresponding decrease in perception of gas volume and decreased PZ distortion was also achieved to a statistically significant level (p<0.05). The administration of gel on average decreased rectal gas volume by 2-fold. Gel injection was well tolerated by all patients.



#### SSE25

Science Session with Keynote: Radiation Oncology (Gynecologic Cancers)

Monday, Nov. 26 3:00PM - 4:00PM Room: S104B



AMA PRA Category 1 Credit ™: 1.00 ARRT Category A+ Credit: 1.00

**FDA** Discussions may include off-label uses.

### Participants

Tracy M. Sherertz, MD, San Francisco, CA (*Moderator*) Nothing to Disclose Jianling Yuan, MD, PhD, Minneapolis, MN (*Moderator*) Nothing to Disclose

# Sub-Events

# SSE25-03 The Value of K-trans in DCE-MRI in the Diagnosis of Pathological Grade of Cervical Cancer

Monday, Nov. 26 3:20PM - 3:30PM Room: S104B

Participants

Miao Niu, Dalian, China (*Abstract Co-Author*) Nothing to Disclose Ailian Liu, MD, Dalian, China (*Abstract Co-Author*) Nothing to Disclose Shifeng Tian, Dalian, China (*Abstract Co-Author*) Nothing to Disclose Wang Nan, Dalian, China (*Abstract Co-Author*) Nothing to Disclose Ying Zhao Jr, Dalian, China (*Abstract Co-Author*) Nothing to Disclose Yue Lv, Dalian, China (*Presenter*) Nothing to Disclose

### PURPOSE

The value of Ktrans in DCE-MRI in the diagnosis of pathological grade of cervical cancer

### **METHOD AND MATERIALS**

Retrospective analysis of 19 patients with poorly differentiated and 15 moderately well-differentiated cervical cancers who were confirmed by surgery and pathology from September 2015 to February 2017 and preoperatively performed 1.5T MRT1WI, T2WI, DCE-MRI, DWI, and other MR examinations. DCE-MRI images were analyzed and measured by two observers using the GenIQ software on the ADW4.6 workstation. The consistency of the data was evaluated by using ICC. An independent sample t test was used to compare the difference in Ktrans values in DCE-MRI between poorly differentiated and moderately differentiated cervical cancers. The ROC curve was used to analyze the Ktrans value to identify the diagnostic efficiency of poorly differentiated and moderately differentiated.

### RESULTS

The parameters measured by the two observers were in good agreement (ICC values >0.75). The Ktrans value of the poorly differentiated group was greater than the moderately high differentiated group  $(0.70\pm0.21 \text{ vs } 0.52\pm0.20)$ , and the difference was statistically significant (P<0.05). The Ktrans value >=0.68 is a diagnostic threshold for the diagnosis of poorly differentiated and moderately differentiated, corresponding sensitivity and specificity of 52.6% and 81.2%, and AUC is 0.717.

### CONCLUSION

The value of Ktrans in DCE-MRI has a certain value in the differential diagnosis of poorly differentiated and moderately differentiated cervical cancer.

### **CLINICAL RELEVANCE/APPLICATION**

The prognosis of poorly differentiated and moderately differentiated cervical cancer is completely different, and differential diagnosis is extremely important.

# SSE25-04 Radiologic Assessment of Inguinal Lymph Nodes in Pelvic Malignancies

Monday, Nov. 26 3:30PM - 3:40PM Room: S104B

# Awards

# Student Travel Stipend Award

Participants

Soumon Rudra, MD, St. Louis, MO (*Presenter*) Nothing to Disclose Dominique Fuser, MD, Saint Louis, MO (*Abstract Co-Author*) Nothing to Disclose Margery Gang, Saint Louis, MO (*Abstract Co-Author*) Nothing to Disclose Caressa Hui, BS, Saint Louis, MO (*Abstract Co-Author*) Nothing to Disclose Yuan J. Rao, MD, Saint Louis, MO (*Abstract Co-Author*) Nothing to Disclose Todd DeWees, Saint Louis, MO (*Abstract Co-Author*) Nothing to Disclose Julie K. Schwarz, MD, PhD, Saint Louis, MO (*Abstract Co-Author*) Nothing to Disclose Perry W. Grigsby, MD, Saint Louis, MO (*Abstract Co-Author*) Speaker, Siemens AG

# For information about this presentation, contact:

smarkovina@wustl.edu

# PURPOSE

Metastatic involvement of inguinal lymph nodes can alter radiation therapy (RT) planning for pelvic tumors. 18F-FDG PET/CT can identify metastatic nodes; however, inguinal nodes are commonly abnormal due to non-malignant processes such as infection or inflammation, complicating interpretation. We evaluated quantitative PET metrics to improve identification of metastatic inguinal nodes in patients with pelvic tumors compared to standard clinical interpretation.

### **METHOD AND MATERIALS**

We identified 36 patients with vulvar cancer, 4 with vaginal cancer, and 14 with anal cancer who underwent 18F-FDG PET/CT prior to pathologic evaluation of inguinal nodes. For each groin evaluated pathologically, we analyzed the following values on the node with highest FDG uptake: maximum, peak and mean standardized uptake values (SUVmax, SUVpeak, SUVmean, respectively), total lesion glycolysis (TLG) and metabolic tumor volume (MTV). SUVmean, TLG and MTV were determined for volumes defined by thresholds of 42% and 50% of SUVmax, and for SUV >= 2.5. CT images were used to measure volume, short and long axes of each lymph node. Multivariate logistic regression identified predictive metrics for pathologic positive nodes and generated a probabilistic model. The AUCs of ROC curves for the model were compared to the standard clinical interpretation from the diagnostic report using adjacent pairwise differences.

# RESULTS

Of 54 patients identified, 75 groins were evaluated pathologically resulting in 75 nodes for analysis (35 were positive for malignancy). Logistic regression identified SUVmean (50% threshold) and short axis length as most predictive for metastatic nodes. The model was better able to predict pathologic involvement compared to standard clinical interpretation (AUC: 0.91 [95%CI: 0.84 - 0.97] vs 0.80 [95%CI: 0.71 - 0.90], P<0.01).

### CONCLUSION

18F-FDG PET/CT diagnostic accuracy for metastatic inguinal nodes in pelvic tumors may be improved with use of quantitative PET metrics and warrants further validation. Improving prediction of metastatic nodes can aid with appropriate selection of patients for pathologic node evaluation and guide RT volumes and doses.

### **CLINICAL RELEVANCE/APPLICATION**

18F-FDG PET/CT accuracy for inguinal metastases may be improved with quantitative metrics for patients with pelvic malignancies and aid with radiation treatment planning.

# SSE25-05 Assessment of MR Compatibility of Novel Needle Placement Template and Collets for Intraperitoneal Interstitial Gynecological Brachytherapy Application

Monday, Nov. 26 3:40PM - 3:50PM Room: S104B

Participants

Christopher J. Tien, PhD, New Haven, CT (*Abstract Co-Author*) Nothing to Disclose Marie Hausner, RT, New Haven, CT (*Abstract Co-Author*) Nothing to Disclose Zhe Chen, PhD, New Haven, CT (*Abstract Co-Author*) Nothing to Disclose Matthew Hoerner, PhD, New Haven, CT (*Abstract Co-Author*) Nothing to Disclose Holly Lincoln, MS, New Haven, CT (*Presenter*) Nothing to Disclose

# For information about this presentation, contact:

christopher.tien@yale.edu

### PURPOSE

A supplemental template kit was obtained to aid intraperitoneal needle implant geometry for MR-guided interstitial cervical brachytherapy. This product is in final stages of FDA approval and has not yet received MR-conditional designation. Therefore, our institution independently evaluated the MR compatibility using ASTM International guidelines and report our results.

### **METHOD AND MATERIALS**

The supplemental kit consisted of the template (made of PEEK material with 40 6-Fr diameter holes) and 25 titanium collets. In the proposed clinical kit, the template and collets would be added to existing equipment including the cylindrical obdurator, tandem, and PEEK needles, which have been deemed MR-conditional previously. The planned fully-assembled applicator set is shown in Figure 1. A 3.0 T magnet was used to represent the most challenging MR environment as our institutional policy for MR-guided treatment planning is 1.5 T. Magnetically-induced effects of displacement force and torque were evaluated using ASTM F2052-15 and F2213-06 standard test methods, respectively. RadioFrequency (RF)-induced heating was evaluated using ASTM F2182-11a standard test methods. Final assessment for MR-conditional status was defined using ASTM F2503 requirements.

### RESULTS

For the template and collets, the mean measured displacement was undetectable, there was no observed translation, no observed deflection, and no observed torque when placed at the strongest point of the magnet. Neither template nor collets were deemed candidates for RF-induced heating. The template was exempted based on its composition of 100% PEEK material. The collets were exempted as literature has repeatedly shown that devices smaller than one-tenth of the electromagnetic field (i.e. 5 cm for 1.5 T and 2.4 cm for 3.0 T) will not have a measurable rise in temperature.

### CONCLUSION

ASTM International standards and guidelines were newly-acquired equipment. Standard test methods showed absence of any movement or torque, and complied with exemptions for RF-induced heating tests. Following ASTM F2503 guidelines, the equipment

is MR-conditional for 3 T, and thus is MR-conditional for 1.5 T.

# **CLINICAL RELEVANCE/APPLICATION**

Novel brachytherapy applicator designed for MR-guided radiation therapy was tested internally by our institution to ensure MR compatibility and was deemed MR-conditional.

# SSE25-06 3D MRI-Based Brachytherapy for Cervical Cancer: Can Dose Escalation Improve Survival?

Monday, Nov. 26 3:50PM - 4:00PM Room: S104B

# Awards

## **Student Travel Stipend Award**

Participants Zachary D. Horne, MD, Pittsburgh, PA (*Presenter*) Nothing to Disclose Ronny Kalash, Pittsburgh, PA (*Abstract Co-Author*) Nothing to Disclose Sushil Beriwal, MD, Wexford, PA (*Abstract Co-Author*) Consultant, Varian Medical Systems, Inc

# PURPOSE

Brachytherapy is an essential component of the treatment of locally advanced cervical cancer; recent GEC-ESTRO guidelines recommend that the dose to 90% (D90) of the high-risk clinical target volume (HRCTV) be at least 85Gy with even higher doses recommended to improve outcomes

# METHOD AND MATERIALS

A retrospective review of brachytherapy plans delivered at a single institution were evaluated for dose parameters and local control following treatment. The HRCTV D90 was retrieved from all plans. Survival was defined as the interval between last brachytherapy fraction to time of death or last follow up. Significance of tumor parameters on survival was evaluated with uni- and multivariable Cox regression analysis.

## RESULTS

A total of 250 women underwent high dose-rate brachytherapy for cervical cancer between 2007 and 2017 with evaluable dosimetry. Median follow up was 27.5 months. The median prescribed dose was 27.5Gy/5fx with a median HRCTV D90 of 83.9Gy (IQR: 81.9-85.7Gy), HRCTV volume of 31cc (IQR: 25.9-39.9cc), and treatment time of 7.3 weeks. Overall survival at 2 and 5 years was 84.9% and 72.4%. Factors which correlated with survival included age, initial tumor size, HRCTV D90, treatment time and HRCTV volume. On multivariable analysis, only HRCTV volume (HR 1.039 [95%CI 1.017-1.062], p=0.001), prolonged treatment time (HR 1.439 [HR 1.176-1.762], p<0.001), initial tumor size (HR 1.184 [95%CI 1.010-1.389], p=0.037), and age (HR 1.038 [95%CI 1.016-1.060], p<0.001) correlated with survival. HRCTV D90 approached significance with a higher D90 per Gy: HR 0.901 [95%CI 0.808-1.005], p=0.061. Survival at 2 and 5 years for women with tumors 31cc and less at the time of BT were 91.6% and 78.5% vs 78.3% and 66.0% for women with tumors greater than 31cc (p=0.026).

### CONCLUSION

Survival is excellent with MRI-based planning in the entire cohort of patients. Our data suggests that adverse factors such as adenocarcinoma histology, large tumor, and poor response to chemoradiation cannot be overcome with dose escalation. The prospective EMBRACE II trial will further help us clarify the impact of dose escalation in poor responders.

### **CLINICAL RELEVANCE/APPLICATION**

This suggests that different methods of therapeutic intervention are required for high-risk and poor-responding cervical cancer patients.



#### SSE26

### Vascular Interventional (Education)

Monday, Nov. 26 3:00PM - 4:00PM Room: S104A



AMA PRA Category 1 Credit ™: 1.00 ARRT Category A+ Credit: .25

### Participants

Nikunj R. Chauhan, MD, Cleveland, OH (*Moderator*) Nothing to Disclose Sarah B. White, MD,MS, Philadelphia, PA (*Moderator*) Research support, Guerbet SA; Research support, Siemens AG; Consultant, Guerbet SA; Consultant, BSC; Consultant, Cook Group Incorporated

#### Sub-Events

# SSE26-01 Has Black Trainee Representation Improved in Interventional Radiology Fellowship from 1995 to 2015? A Comparative Study with Other Related Fields

Monday, Nov. 26 3:00PM - 3:10PM Room: S104A

Participants

Paul H. Yi, MD, Baltimore, MD (*Presenter*) Nothing to Disclose William Barge, Peoria, IL (*Abstract Co-Author*) Nothing to Disclose Won Kyu Choi, BS, Baltimore, MD (*Abstract Co-Author*) Nothing to Disclose Ferdinand K. Hui, MD, Richmond, VA (*Abstract Co-Author*) Speakers Bureau, Terumo Corporation Speakers Bureau, Penumbra, Inc Stockholder, Blockade Medical Inc

### For information about this presentation, contact:

pyi10@jhmi.edu

# PURPOSE

Prior studies have shown underrepresentation of people of African-American descent within multiple medical specialties. Interventional Radiology (IR) has traditionally been a white male-predominate field and it is unknown if race diversity in IR has improved over time. The purpose of this study was to analyze trends in representation of black trainees in IR in comparison with other related fields over the past 20 years.

### **METHOD AND MATERIALS**

We reviewed data from the American Association of Medical Colleges reported in annual issues on medical education in JAMA for the years 1995-2015. We assessed the percentages of black trainees in IR fellowships and other training programs, including Diagnostic Radiology residency, Radiation Oncology residency, Pediatric Radiology fellowship, and Neuroradiology Fellowship, as well of Residents from all specialties. Changes in the percentages of black residents/fellows from 1995 to 2015 were calculated for each group using Chi-Square tests.

#### RESULTS

From 1995 to 2015, the percentage of black trianees in IR fellowship increased from 0% to 4% (p=0.03). Similarly, from 1995 to 2015, the percentage of black trainees in every other training program studied increased significantly; for example, black representation in residency (all specialties) improved from 5% to 6% (p<0.0001) [Image 1]. In 2015, IR had no significant difference in black trainee representation compared to the other training programs studied.

# CONCLUSION

Although the percentage of black trainees in IR fellowship has significantly increased over the past 20 years and is commensurate with the general residency population, black trainees are under-represented compared to the general USA population (18%). We recommend increased recruitment efforts towards black trainees at different levels of training both during and after medical school to improve the diversity within IR and other fields.

### **CLINICAL RELEVANCE/APPLICATION**

Although the percentage of black trainees in IR fellowship has significantly increased over the past 20 years, black trainees are under-represented compared to the general USA population.

# SSE26-02 An Analysis of the Patient Population Seen in a Newly Established Interventional Radiology Ambulatory Clinic

Monday, Nov. 26 3:10PM - 3:20PM Room: S104A

Participants Andrew J. Gunn, MD, Birmingham, AL (*Abstract Co-Author*) Nothing to Disclose Joel M. Raborn, MD, Birmingham, AL (*Presenter*) Nothing to Disclose William M. Parkhurst, MD, Birmingham, AL (*Abstract Co-Author*) Nothing to Disclose Timothy S. Tatum, MD, Birmingham, AL (*Abstract Co-Author*) Nothing to Disclose Anand R. Patel, MD, Birmingham, AL (*Abstract Co-Author*) Nothing to Disclose Benjamin L. Triche, MD, Birmingham, AL (*Abstract Co-Author*) Nothing to Disclose Aliaksei Salei, MD, Birmingham, AL (*Abstract Co-Author*) Nothing to Disclose Souheil Saddekni, MD, Birmingham, AL (*Abstract Co-Author*) Consultant, Abbott Laboratories Ahmed K. Abdel Aal, MD, PhD, Birmingham, AL (*Abstract Co-Author*) Consultant, Abbott Laboratories; Consultant, Baxter International Inc; Consultant, C. R. Bard, Inc; Consultant, Boston Scientific Corporation; Consultant, W. L. Gore & Associates, Inc; Consultant, Sirtex Medical Ltd

### For information about this presentation, contact:

agunn@uabmc.edu

# PURPOSE

To analyze the types of patients seen in a newly established interventional radiology (IR) ambulatory clinic with an assessment of changes in that population over the clinic's first eight months of existence.

### **METHOD AND MATERIALS**

A retrospective review of the clinic appointments that occurred in the first eight months was performed. Patient demographics, diagnosis, type of IR procedure for which they were being seen, and the type of visit (i.e new vs. return patient) were collected. Data points from the first four months (group 1) and second four months (group 2) of the clinic were analyzed separately to assess for any changes over time. A p value of <= 0.05 was considered statistically significant.

# RESULTS

There were a total of 1,489 clinic visits in the first eight months (739 males; 750 females; mean age: 57.3 years). Overall, the three most common diagnoses were hepatocellular carcinoma (HCC) (14.3%, n=214), abscess (9.8%, n=146), and oropharyngeal cancer (8%, n=119). HCC, abscess, and oropharyngeal cancer were the three most common diagnoses for both groups 1 and 2 without a significant difference between groups. The three most common procedures performed on patients overall were chest port (24.9%, n=371), gastrostomy/gastrojejunostomy (20.6%, n=307), and chemoembolization (15.4%, n=229). Chest ports, gastrostomy/gastrojejunostomy, and chemoembolization were the three most common types of procedures performed on these patients in both groups 1 and 2 without any significant difference between the groups. There was also no significant difference between the groups for any other procedures performed, including: primary biliary drainage, IVC filter placement/retrieval, abscess drainage, uterine fibroid embolization, radioembolization, renal cryoablation, liver ablation, TIPS, kyphoplasty/vertebroplasty, or percutaneous sclerotherapy. Overall, 283 visits (19%) were "new" patient appointments. There was no significant difference between the groups in number of new patients seen (group 1: 18.4%, group 2: 19.4%; p=0.6).

# CONCLUSION

IR sees a wide variety of patients in ambulatory clinic but the population did not change significantly during the sampling period.

# **CLINICAL RELEVANCE/APPLICATION**

Ambulatory clinics can help IR establish itself as a clinical service. Information about the types of patients seen in these clinics can inform quality improvement and practice-building initiatives.

# SSE26-03 Trends in Imaging Guidance for Percutaneous Procedures in the Medicare Population, 2007-2016

Monday, Nov. 26 3:20PM - 3:30PM Room: S104A

Participants

Ali B. Syed, MD, Philadelphia, PA (Presenter) Nothing to Disclose

David C. Levin, MD, Philadelphia, PA (*Abstract Co-Author*) Consultant, HealthHelp, LLC; Board Member, Outpatient Imaging Affiliates, LLC

Laurence Parker, PhD, Philadelphia, PA (*Abstract Co-Author*) Nothing to Disclose Vijay M. Rao, MD, Philadelphia, PA (*Abstract Co-Author*) Nothing to Disclose

### For information about this presentation, contact:

ali.b.syed@jefferson.edu

### PURPOSE

Imaging guidance has driven the rapid growth of percutaneous procedures. Our purpose was to assess utilization trends in imaging guidance for percutaneous procedures in recent years.

### **METHOD AND MATERIALS**

The nationwide Medicare Part B databases for 2004-2016 were utilized. We selected the current procedural terminology (CPT) codes for CT, ultrasound (US), fluoroscopy (FL), and MRI guided procedures. CT, MRI, and FL codes were first introduced in 2007. The database provides volumes for each code. Medicare specialty codes were used to identify the specialty of the billing provider. Trend lines were plotted for total volume per year as well as for radiology and other major specialties per year. Because these databases represent a full population, sample statistics are not required.

### RESULTS

US is the most common imaging modality used for guidance, followed by FL, then CT, and lastly MRI. Total volume of US guided procedures increased steadily from 864,008 in 2007 to 2,144,285 in 2016 (+148%). Orthopedic surgeons perform the highest proportion of US procedures (20% - mostly joint injections and aspirations), followed by anesthesia (19%) and then radiologists (9%). FL guidance has increased from 150,165 in 2007 to 495,273 in 2016 (+230%). Radiologists perform the highest proportion of these procedures (26%) among the individual specialties. CT guidance has remained relatively constant from 2007-2016 (196,473 to 204,063), with radiologists performing 98% of these procedures. MRI guidance volumes were very low, with radiologists performing 44%, followed by urologists at 39%. Total imaging-based guidance procedures (all modalities) increased from 1,220,749 in 2007 to 2,847,651 in 2016 (+133%).

### CONCLUSION

Image guidance for procedures has grown since 2007. Radiologists perform more image-guided procedures than any other single specialty, although their overall share is only 19%. Ultrasound is the modality of choice for most procedures, accounting for over 75% of the image guidance for percutaneous procedures performed in 2016. Other specialties have increased their share of image-guided procedures since 2007, particularly of procedures with US and FL guidance.

# **CLINICAL RELEVANCE/APPLICATION**

Radiologists perform the greatest proportion of image guided procedures, predominantly with US guidance, although other specialties have increased their usage of image guidance in recent years.

# SSE26-04 Show Me the Money: Comparison of Political Action Committee Funding and Physician Compensation

Monday, Nov. 26 3:30PM - 3:40PM Room: S104A

Participants

Junjian Huang, MD, Philadelphia, PA (*Presenter*) Nothing to Disclose M. Brett Hyatt, DO, Oklahoma City, OK (*Abstract Co-Author*) Nothing to Disclose Mario Cedillo, MD, New York, NY (*Abstract Co-Author*) Nothing to Disclose Stephen Belmustakov, Baltimore, MD (*Abstract Co-Author*) Nothing to Disclose Mina S. Makary, MD, Columbus, OH (*Abstract Co-Author*) Nothing to Disclose Bo Liu, MD, Maitland, FL (*Abstract Co-Author*) Nothing to Disclose Haiying Yu, MD,PhD, Detroit, MI (*Abstract Co-Author*) Nothing to Disclose Karan N. Patel, MD, Detroit, MI (*Abstract Co-Author*) Nothing to Disclose

### For information about this presentation, contact:

junjian.huang@uphs.upenn.edu

### PURPOSE

To compare physician compensation of specialties with a political action committee (PAC) to those who do not.

### **METHOD AND MATERIALS**

Physician specialties were identified through the AAMC 2015 physician workforce survey as well as the Medscape 2017 physician compensation report. Compensation data was collected via Medscape compensation surveys from the years of 2011-2017, American Medical Group Association (AMGA), Pinnacle Group, and Doximity. All PAC related data was collected via opensecrets.org. Statistics were performed with SPSS (IBM).

### RESULTS

A total of 31 physician specialties were included in the analysis. Nearly 90% (n=28) had a PAC,10% (n=3) did not. Averages of the following were calculated for each specialty from 2010-2016: physician compensation, PAC donation, and PAC expenditure. Average PAC donation and PAC expenditure per capita was also calculated. A direct linear correlation was found between average PAC donation and average PAC expenditure for all the physician specialties (R2 of 0.999). Specialties with a PAC demonstrated higher average compensation than those without a PAC (\$328,700 vs. \$211,500) with a mean difference of \$117,000 (p=0.04). SIR has one of the most underfunded PACs. For comparison, vascular surgery PAC contributions is 1.5x that of SIR's and cardiology PAC boasts a 9x financial advantage over our own.

# CONCLUSION

Advocacy is not just about compensation but the reality is that being paid what you deserve is important. Our analysis reveals that over the past decade, specialties with higher physician compensation tend to have larger, more well funded PACs. A well funded PAC allows for more PAC expenditure which grants better access to members of Congress. Considering IR has recently separated from diagnostic radiology, which boasts one of the most robust PACs on our list, the impact of having an underfunded political action committee is unknown but worrisome considering our direct competitors (cardiology and vascular surgery) dwarf us in comparison. Policy drives practice, if we are to be true competitors then awareness and support of our PAC is critical.

### **CLINICAL RELEVANCE/APPLICATION**

Political awareness and activisim is critical to the success of a specialty and those with political action committees lobbying on their behalf earn substantially more than those who do not.

# SSE26-05 Training by the Numbers: A Survey-Based Analysis of the Number of Positions Available in New Interventional Radiology Training Pathways

Monday, Nov. 26 3:40PM - 3:50PM Room: S104A

### Awards

**Student Travel Stipend Award** 

Participants Jung H. Yun, Closter, NJ (*Presenter*) Nothing to Disclose David J. Maldow, MD , Jericho, NY (*Abstract Co-Author*) Nothing to Disclose Rakesh S. Ahuja, MD, Philadelphia, PA (*Abstract Co-Author*) Nothing to Disclose Faraz Khan, MD, Pittsford, NY (*Abstract Co-Author*) Nothing to Disclose Andrew J. Gunn, MD, Birmingham, AL (*Abstract Co-Author*) Nothing to Disclose Jason C. Hoffmann, MD, Mineola, NY (*Abstract Co-Author*) Speakers Bureau, Merit Medical Systems, Inc; ;

### For information about this presentation, contact:

Jason.Hoffmann@nyulangone.org

# PURPOSE

The number and types of training pathways in interventional radiology (IR) have undergone a fundamental change, yet little is

known about the number of Independent IR (IndIR) positions relative to the number of positions in the Early Specialization in IR (ESIR) pathway. Thus, we investigate whether the number of available ESIR positions is aligned with the number of IIR positions.

# METHOD AND MATERIALS

A three-question survey was conducted over e-mail and telephone to residency program directors and coordinators (Figure). Data collected included the number of ESIR, IntIR (Integrated IR), and IndIR positions, and number of current IR fellows accepted per year. Information was also obtained from publicly available databases on the SIR, ACGME, and ERAS websites. Analysis of results was performed using Microsoft Excel (Microsoft, Redmond, VA).

### RESULTS

Ninety-nine of 113 ESIR programs (87.6% response rate) reported a total of 176 approved ESIR positions. Based on this average of 1.78 positions per program, the actual number of ESIR positions in the U.S. is likely more than 200. While 111 fellowship programs in the U.S. currently offer a total of 331 positions, current new training pathways include 77 IntIR programs and 48 IndIR programs with 150 and 133 positions, respectively. As the Integrated IR programs matched at 100% in the same time frame, thus have no open positions, this leaves substantially more ESIR positions that must feed into Independent IR training programs than are currently available.

### CONCLUSION

A substantial discrepancy currently exists with IR training pathways, as the number of available ESIR positions far outnumbers the available Independent IR pathway positions.

# **CLINICAL RELEVANCE/APPLICATION**

Given that the Integrated IR Residency was the most competitive match in 2018 (100% of positions filled with more than 250 applicants not matching into IR), it is expected that the ESIR program will become increasingly utilized. However, if the number of ESIR positions far outnumbers the Independent IR residency positions, these trainees will be expecting to train in IR but may not find out until the end of their PGY-4 year (and after other specialties have matched) that they have no advanced training position.

### SSE26-06 Fundamentals of Interventional Radiology Skills Training: The FIRST Curriculum

Monday, Nov. 26 3:50PM - 4:00PM Room: S104A

Participants

Brian M. Currie, MD, Philadelphia, PA (*Presenter*) Nothing to Disclose Shaun McLaughlin, MD, Philadelphia, PA (*Abstract Co-Author*) Nothing to Disclose Stephen J. Hunt, MD,PhD, Philadelphia, PA (*Abstract Co-Author*) Consultant, Amgen Inc; Consultant, BTG International Ltd Terence P. Gade, MD, PhD, New York, NY (*Abstract Co-Author*) Research Grant, Guerbet SA Scott O. Trerotola, MD, Philadelphia, PA (*Abstract Co-Author*) Royalties, Cook Group Incorporated Royalties, Teleflex Incorporated Consultant, C. R. Bard, Inc Consultant, Medical Components, Inc Consultant, B. Braun Melsungen AG Consultant, Teleflex Incorporated Gregory J. Nadolski II, MD, Philadelphia, PA (*Abstract Co-Author*) Nothing to Disclose

Jonas W. Redmond, MD, Philadelphia, PA (*Abstract Co-Author*) Nothing to Disclose

# For information about this presentation, contact:

brian.currie@uphs.upenn.edu

### PURPOSE

There has been a paradigm shift in medical education, transitioning from an apprenticeship model to one centered on more directed skills training. There is a unique opportunity to embrace this changing landscape of medical education via usage of simulation-based training for interventional radiology. This is a preliminary study examining the efficacy of modules to be utilized in a forthcoming curriculum entitled, The Fundamentals of Interventional Radiology Skills Training (FIRST).

### **METHOD AND MATERIALS**

A procedural checklist was generated from a core task analysis of two attendings performing each skill: venous access, biopsy, and interventional suturing. This checklist was then used to teach first year diagnostic radiology residents (n=7). A jugular venous access phantom was formed in realistic polycarbonate molds with a mixture of gelatin (7.4% by weight) and sugar-free psyllium fiber (4.6% by weight) combined with silicone tubing. This same gelatin and psyllium fiber mixture was also used for an ultrasound-guided liver biopsy phantom, with several targets at variable depths. Ultrasound (US) was performed with a portable GE VScan Dual Probe device. A high-fidelity suturing pad was also constructed from platinum-catalyzed silicone gels reinforced with power mesh. Pre- and post-session surveys utilizing a Likert scale were administered to quantify effectiveness of the teaching session with regard to (i) ability to perform skills and (ii) knowledge of procedural steps and equipment. Statistical analysis was performed using Mann-Whitney U Test.

# RESULTS

On the pre-session survey, 100% of residents reported being uncomfortable with IR procedures. After the session, 100% of residents agreed simulation-based education would be invaluable prior to IR rotations. Compared to pre-session responses, there were significant differences in ability to perform a dermal stitch and drain knot (p=0.0023 for both), describe the steps in US-guided biopsy (p<0.001), and identify vascular access components (p=0.0017).

# CONCLUSION

These preliminary data demonstrate efficacy of dedicated IR skills teaching sessions and simulation using constructed phantoms. Our experience will inform future module development, including use of 3D printed vessels and a fluoroscopic trainer.

# **CLINICAL RELEVANCE/APPLICATION**

A standardized simulation-based curriculum would be indespensible to IR trainee education to enable deliberate practice in a risk-free environment.



### MSAS24

Commitment to Safety: Providing Effective & Efficient Imaging Services (Sponsored by the Associated Sciences Consortium) (Interactive Session)

Monday, Nov. 26 3:30PM - 5:00PM Room: S105AB



AMA PRA Category 1 Credits ™: 1.50 ARRT Category A+ Credit: 1.75

#### **Participants**

Craig St George, ARRT, RT, Albuquerque, NM (*Moderator*) Nothing to Disclose Jody Erickson, RT, BS, Jacksonville, FL (*Presenter*) Nothing to Disclose Andre Brown, ARRT, MA, Jacksonville, FL (*Presenter*) Nothing to Disclose Andrew Bowman, MD, PhD, Jacksonville, FL (*Presenter*) Nothing to Disclose Adam Rubin, ARRT, RT, Jacksonville, FL (*Presenter*) Nothing to Disclose

### For information about this presentation, contact:

bowman.andrew@mayo.edu

### LEARNING OBJECTIVES

1) Understand the concept behind the Commitment to Safety process and how it was developed. 2) Identify how Commitment to Safety could be used to improve the work environment. 3) Define goals that could be accomplished through the Commitment to Safety process. 4) Understand how to begin Commitment to Safety initiative. 5) Know how to use results of a Commitment to Safety project to improve a work unit.



### MSCA22

### Case-based Review of the Abdomen (Interactive Session)

Monday, Nov. 26 3:30PM - 5:00PM Room: S100AB



AMA PRA Category 1 Credits ™: 1.50 ARRT Category A+ Credit: 1.75

#### Participants

Julie H. Song, MD, Providence, RI (Director) Nothing to Disclose

### For information about this presentation, contact:

jsong2@lifespan.org

#### Sub-Events

# MSCA22A Gastrointestinal Tract

Participants Jay P. Heiken, MD, Rochester, MN (*Presenter*) Patent agreement, Guerbet SA; Patent agreement, Bayer AG

For information about this presentation, contact:

heiken.jay@mayo.edu

#### LEARNING OBJECTIVES

1) Identify the imaging features of select benign and malignant diseases of the gastrointestinal tract. 2) Discuss the role of CT, MR and fluoroscopy in evaluating diseases of the gastrointestinal tract.

# MSCA22B Hepatobiliary Tract

Participants Karen S. Lee, MD, Boston, MA (*Presenter*) Nothing to Disclose

For information about this presentation, contact:

kslee@bidmc.harvard.edu

### LEARNING OBJECTIVES

1) Identify key typical imaging findings of select hepatic lesions. 2) Develop a differential diagnosis of benign and malignant hepatic lesions based on specific MRI features. 3) Examine the imaging features of diffuse biliary disease processes.

# MSCA22C Genitourinary Imaging

Participants Julie H. Song, MD, Providence, RI (*Presenter*) Nothing to Disclose

# For information about this presentation, contact:

jsong2@lifespan.org

### **LEARNING OBJECTIVES**

1) Improve knowledge base to recognize, analyze, and diagnose select pathology of genitourinary tract. 2) Learn to avoid pitfalls and misdiagnoses of genitourinary tract pathology.

# MSCA22D Abdominal Complications of Oncologic Therapy

Participants Kumaresan Sandrasegaran, MD, Phoenix, AZ (*Presenter*) Nothing to Disclose

### For information about this presentation, contact:

ksandras@iupui.edu

### LEARNING OBJECTIVES

1) To understand how the newer targeted biological agents (mabs and nibs) work on cancer cells at membrane receptors, in cytoplasmic signaling pathways or in the nucleus. 2) To learn the side effects of antiangiogenic drugs which may mimic tumor progression. 3) To learn the types of immune therapies, including immune checkpoint drugs, and the pitfalls in interpretation of post treatment imaging studies.

### ABSTRACT

In the last 20 years over hundred taraeted hiological agents have been discovered. These are monoclonal antihodies (mahs) or

small molecule inhibiters (nibs) that inhibit tyrosine kinase activity. These drug works at the cell membrane, in the cytoplasmic signaling pathways, such as RAS-RAF pathway, or in DNA replication or transcription in the nucleus. They are different to conventional chemotherapy drugs in that they typically do not cause necrosis. The range of side effects seen on post treatment scans is also different and may mimic tumor progression or post-surgical complications. Another set of drugs act on the immune system, predominantly T lymphocytes, to activate immune cells to destroy cancer cells. These include immune checkpoint drugs, immune vaccines, and oncolytic viruses. They have a unique set of side effects which may be confusing to the unwary radiologist. These drugs usually cause initial increase in tumor size due to the immune response and newer systems of response assessment, such as immune RECIST, need to be used.

### **Honored Educators**

Presenters or authors on this event have been recognized as RSNA Honored Educators for participating in multiple qualifying educational activities. Honored Educators are invested in furthering the profession of radiology by delivering high-quality educational content in their field of study. Learn how you can become an honored educator by visiting the website at: https://www.rsna.org/Honored-Educator-Award/ Kumaresan Sandrasegaran, MD - 2013 Honored EducatorKumaresan Sandrasegaran, MD - 2014 Honored EducatorKumaresan Sandrasegaran, MD - 2016 Honored EducatorKumaresan Sandrasegaran, MD - 2018 Honored Educator



### MSMC24

Cardiac CT Mentored Case Review: Part IV (In Conjunction with the North American Society for Cardiovascular Imaging) (Interactive Session)

Monday, Nov. 26 3:30PM - 5:30PM Room: S406A



AMA PRA Category 1 Credits ™: 2.00 ARRT Category A+ Credits: 2.25

### Participants

Jill E. Jacobs, MD, New York, NY (Director) Nothing to Disclose

Stefan L. Zimmerman, MD, Ellicott City, MD (*Moderator*) Project consultant, Siemens Healthcare; Research grant, American Heart Association;

### LEARNING OBJECTIVES

1) Understand the clinical indications for retrospective ECG gated cardiac CT. 2) Illustrate methods to assess myocardial function from cine cardiac CT images. 3) Illustrate methods to assess normal and abnormal valvular function from cine cardiac CT images.

### Sub-Events

# MSMC24A Coronary Atherosclerosis and Bypass Grafts

Participants

Gregory Kicska, MD, PhD, Seattle, WA (Presenter) Nothing to Disclose

# LEARNING OBJECTIVES

1) Recognizing anatomic subsets coronary artery bypass. 2) Technical considerations when imaging a bypass graft.3) Stenosis and aneurysms in vein grafts.4) Patterns of stenosis in internal mammary grafts.5) Evaluating a bypass patient before reoperation.

# ABSTRACT

Cardiac CT is often used to evaluate coronary bypass graft function. To accurately interpret these images, the Imager needs to be familiar with the patterns of stenosis, aneurysms or other complications associated with different bypass types. In addition to assessing function and need for intervention, CT can identify patients with unique risks associated with reoperation.

# MSMC24B Congenital Heart Disease

Participants Carlo N. De Cecco, MD, PhD, Atlanta, GA (*Presenter*) Research Grant, Siemens AG

# For information about this presentation, contact:

carlo.dececco@emory.edu

# LEARNING OBJECTIVES

1) Recognize the most common congenital heart disease (CHD) findings found in adults with unsuspected CHD. 2) Recognize and understand findings of CHD in patients with known CHD and the findings which may trigger surgical intervention. 3) Recognize the CT findings of commonly performed surgical procedures for palliation of CHD. 4) Develop an organized pattern for search and reporting of CHD findings. 5) Understand why CT is chosen as the advanced imaging modality over MR.

# ABSTRACT

Adults with congenital heart disease (CHD) now outnumber children with CHD two to one. Thisphenomenon is due to the success of surgical palliation and medical management of patients with even themost severe forms of CHD. Surgical intervention is often performed at the time of diagnosis and in patients with residual hemodynamic lesions is often required throughout life. Though echocardiography is typically the initial imaging modality of choice, diagnosis and imagingsurveillance of complex hemodynamic and anatomic CHD lesions is now most often accomplished with CT and MR. CT and CTA imaging techniques may be used to show detailed anatomic and functional images of the heart, postoperative changes and long term consequences of CHD. An organized, reproducible approach to identify cardiac anatomy of CHD lesions and surgical palliationshould be adopted in order to accurately and thoroughly describe findings.

# MSMC24C Coronary Artery Disease and Incidental Non-cardiac Findings

Participants

Diana Litmanovich, MD, Haifa, Israel (Presenter) Nothing to Disclose

# LEARNING OBJECTIVES

1) Recognizing non-cardiac and non-coronary anatomic structures that can be seen on cardiac CT. 2) Become familiar with possible non-cardiac and non-coronary pathological findings that could be seen on cardiac CT. 3) Review the suggested work-up for patients with incidentally found non-cardiac and non-coronary pathologies on cardiac CTA.

ABSTRACT Cardiac CT often includes information about surrounding structures such as lungs, meidastinum, airways, pleura, liver and bones. To accurately interpret the scan and not to overlook the possible non-cardiac pathologies, familiarity with potential incidental findings is required. Clinical importance and severity of incidental findings varies, thus currently existing algorithms for incidental findings on cardiac CT are helpful for further work-up.



### MSMI24

Molecular Imaging Symposium: MI Case-based Discussion

Monday, Nov. 26 3:30PM - 5:00PM Room: S405AB



AMA PRA Category 1 Credits ™: 1.50 ARRT Category A+ Credit: 1.75

### Participants

Munir Ghesani, MD, New York, NY (*Moderator*) Nothing to Disclose Hubert J. Vesselle, MD, PhD, Seattle, WA (*Moderator*) Consultant, MIM Software Inc

## ABSTRACT

Molecular imaging is increasingly being utilized in the initial staging as well as in the follow up of various disease conditions. In addition, several new imaging tracers are either recently approved by FDA. As a result, this modality, while clinically useful, is becoming increasingly complex.

## Sub-Events

## MSMI24A Assessing Tumor Therapeutic Response with FDG PET and CT: Practical Aspects

Participants

Hubert J. Vesselle, MD, PhD, Seattle, WA (Presenter) Consultant, MIM Software Inc

## LEARNING OBJECTIVES

1) Use the case-based approach to illustrate utility of molecular imaging in clinical applications and demonstrate how to avoid false positive interpretations.

## MSMI24B What You See May Not Be What You Think

Participants

Munir Ghesani, MD, New York, NY (Presenter) Nothing to Disclose

## LEARNING OBJECTIVES

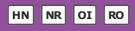
1) Recognize that molecular imaging in general is a very sensitive modality but its specificity is relatively lower. 2) Recognize that the specificity can be improved by various measures, such as obtaining detailed patient information, multimodality correlation with recently performed imaging studies and careful comparison with prior imaging studies. 3) Recognize that improved specificity will improve overall patient care by avoiding unnecessary procedures and treatments resulting from false positive interpretations. It will also help in building referring physicians' confidence in the molecular imaging modality.



### MSRO29

## **BOOST: Head and Neck-eContouring**

Monday, Nov. 26 4:30PM - 5:30PM Room: S104B



AMA PRA Category 1 Credit <sup>™</sup>: 1.00 ARRT Category A+ Credit: 1.00

## Participants

Suresh K. Mukherji, MD, Northville, MI (*Presenter*) Nothing to Disclose Sung Kim, MD, New Brunswick, NJ (*Presenter*) Nothing to Disclose

## LEARNING OBJECTIVES

1) Demonstrate how Radiation Oncologists contour head & necks prior to delivering radiation therapy. 2) Review the concepts of GTV, CTV & PTV. 3) Allow participants to contour the tumors and compare this with our experts.

### ABSTRACT

This e-contouring session is an interactive session that allows the attendees to contour head and neck tumors and compare their results with the expert. We will also review the important of imaging for idenfying tumor mapping and tumor spread.



#### RCA25

## Image to 3D Prints: How 3D Printing Works (Hands-on)

Monday, Nov. 26 4:30PM - 6:00PM Room: S401AB

# IN

AMA PRA Category 1 Credits ™: 1.50 ARRT Category A+ Credit: 1.75

## Participants

Beth A. Ripley, MD, PhD, Seattle, WA (*Presenter*) Nothing to Disclose Tatiana Kelil, MD, San Francisco, CA (*Presenter*) Nothing to Disclose Dmitry Levin, Seattle, WA (*Presenter*) Nothing to Disclose Anish Ghodadra, MD, New Haven, CT (*Presenter*) Advisory Board, axial3D Limited

## For information about this presentation, contact:

beth.ripley2@va.gov

## LEARNING OBJECTIVES

1) Describe optimal CT and MRI protocols for 3D printing. 2) Explain basic software requirements for converting DICOM images to 3D-printable .STL (standard tessellation language) files. 3) Recognize some common 3D printing artifacts. 4) Apply basic 3D printed model post-processing techniques learned during the session, including UV curing and support material removal.

#### **Honored Educators**

Presenters or authors on this event have been recognized as RSNA Honored Educators for participating in multiple qualifying educational activities. Honored Educators are invested in furthering the profession of radiology by delivering high-quality educational content in their field of study. Learn how you can become an honored educator by visiting the website at: https://www.rsna.org/Honored-Educator-Award/ Tatiana Kelil, MD - 2017 Honored Educator



### RCB25

## Intro to Statistics with R (Hands-on)

Monday, Nov. 26 4:30PM - 6:00PM Room: S401CD



AMA PRA Category 1 Credits ™: 1.50 ARRT Category A+ Credit: 1.75

## Participants

James E. Schmitt, MD, PhD, Philadelphia, PA (*Moderator*) Nothing to Disclose James E. Schmitt, MD, PhD, Philadelphia, PA (*Presenter*) Nothing to Disclose Nathan M. Cross, MD, MS, Seattle, WA (*Presenter*) Nothing to Disclose David Gutman, MD, Philadelphia, PA (*Presenter*) Nothing to Disclose

## **LEARNING OBJECTIVES**

1) Install and launch the R software package. Understand how to search for and download external packages to extend R's functionality. 2) Load data from external files such as txt, csv, and xlsx. 3) Perform basic mathematical operations and utilize data structures to manipulate data. 4) Use loops to perform more complex operations over the data, including true/false logic. 5) Understand the basics of creating plots and histograms. 6) Perform common statistical tests including correlation, Chi-square, and ANOVA.



## RCC25

## Medical 3D Printing Operations and Applications I

Monday, Nov. 26 4:30PM - 6:00PM Room: S501ABC



AMA PRA Category 1 Credits ™: 1.50 ARRT Category A+ Credit: 1.75

#### Participants

Adnan M. Sheikh, MD, Ottawa, ON (*Moderator*) Nothing to Disclose Frank J. Rybicki III, MD, PhD, Ottawa, ON (*Moderator*) Medical Director, Imagia Cybernetics Inc

## For information about this presentation, contact:

frybicki@toh.ca

## **LEARNING OBJECTIVES**

Dr. Rybicki will moderate this session and synethize input from the speakers regarding the operations and applications of medical 3D printing and anatomic modeling.

## ABSTRACT

Not applicable (moderator).

## Sub-Events

## RCC25A Establishing a Radiology-based 3D Medical Printing Practice

Participants

William J. Weadock, MD, Ann Arbor, MI (Presenter) Owner, Weadock Software, LLC

## **LEARNING OBJECTIVES**

1) Describe the process of creating a 3D printed model using DICOM images. 2) List the common musculoskeletal applications of 3D printing.

## RCC25B Key Technologies for Medical 3D Printing: Applications and Experiences

Participants

Sang Joon Park, PhD, Seoul, Korea, Republic Of (Presenter) Nothing to Disclose

## RCC25C 3D Printing for Renal Sparing Surgery 3D

Participants

Bernard F. King JR, MD, Rochester, MN (Presenter) Nothing to Disclose

## RCC25D Medical 3D Printing for MSK Applications

Participants

Adnan M. Sheikh, MD, Ottawa, ON (Presenter) Nothing to Disclose

## RCC25E FDA Current Practices and Regulations: 3D Printed Patient-Specific Anatomic Models

Participants

Nooshin Kiarashi, PhD, Silver Spring, MD (Presenter) Nothing to Disclose

#### **LEARNING OBJECTIVES**

- Overview of FDA Guidance Document: Technical Considerations for Additive Manufactured Medical Devices - Design -Manufacturing - Testing - 3D Printed Patient-specific Anatomic Models - What is considered diagnostic use of these models? -What is regulated? The models, the 3D printers, or the software? - What information is required for FDA clearance? - Who should apply for FDA clearance?



### SPDL21

## Chest and Abdomen (Case-based Competition)

Monday, Nov. 26 4:30PM - 6:00PM Room: E451B



AMA PRA Category 1 Credits ™: 1.50 ARRT Category A+ Credit: 1.75

## Participants

Paul J. Chang, MD, Chicago, IL (*Presenter*) Co-founder, Koninklijke Philips NV; Researcher, Koninklijke Philips NV; Researcher, Bayer AG; Advisory Board, Aidoc Ltd; Advisory Board, EnvoyAI; Advisory Board, Inference Analytics Neety Panu, MD, FRCPC, Ottawa, ON (*Presenter*) Nothing to Disclose Ashley Altman, MD, Chicago, IL (*Presenter*) Nothing to Disclose

## LEARNING OBJECTIVES

1) Be introduced to a series of radiology case studies via an interactive team game approach designed to encourage 'active' consumption of educational content. 2) Use their mobile wireless device (tablet, phone, laptop) to electronically respond to various imaging case challenges; participants will be able to monitor their individual and team performance in real time. 3) Receive a personalized self-assessment report via email that will review the case material presented during the session, along with individual and team performance. This interactive session will use RSNA Diagnosis Live<sup>™</sup>. Please bring your charged mobile wireless device (phone, tablet or laptop) to participate.

## ABSTRACT

The extremely popular audience participation educational experience, Diagnosis Live!, is an expert-moderated session featuring a series of interactive case studies that will challenge radiologists' diagnostic skills and knowledge. The session features a lively, fast-paced game format: participants will be automatically assigned to teams who will then use their personal mobile devices to test their knowledge in a fast-paced session that will be both educational and entertaining. After the session, attendees will receive a personalized self-assessment report via email that will review the case material presented during the session, along with individual and team performance.



Special Interest Session: Quantitative Imaging Applications in Screening, Treatment Selection, and Treatment Assessment - The Need for Standardization in the Era of Personalized Medicine

Monday, Nov. 26 4:30PM - 6:00PM Room: S504AB



AMA PRA Category 1 Credits ™: 1.50 ARRT Category A+ Credit: 1.75

**FDA** Discussions may include off-label uses.

### Participants

Edward F. Jackson, PhD, Madison, WI (Moderator) Nothing to Disclose

### LEARNING OBJECTIVES

1) Appreciate the opportunities and advantages of quantitative imaging biomarkers in clincal research and clinical practice, particularly in the era of precision medicine.

#### ABSTRACT

Quantitative imaging should undoubtedly be an enabler of the practice of precision medicine. Applications include patient screening, optimal treatment selection, and treatment assessment (both short term for potential adaptive therapy and long term for surveillance). To fully achieve the goal of enabling precision medicine, however, quantitative imaging measurands must be standardized at each step in the imaging and data analysis chain. This is the primary goal of the RSNA Quantitative Imaging Biomarkers Alliance (QIBA®), which has as its mission to 'improve the value and practicality of quantitative imaging biomarkers by reducing variability across devices, sites, patients, and time'. This session will highlight initiatives of QIBA and other quantitative imaging efforts, such as the NCI Quantitative Imaging Network (QIN), that seek to translate quantitative imaging measures from academic centers of excellence to clinical trial applications to patient care in the era of precision medicine.

### Sub-Events

## SPSI21A Quantitative Imaging Applications in Lung Cancer Screening

Participants

James L. Mulshine, MD, Chicago, IL (Presenter) Nothing to Disclose

## SPSI21B Quantitative Imaging Applications for Therapy Selection

Participants

David A. Mankoff, MD, PhD, Philadelphia, PA (*Presenter*) Speaker, Koninklijke Philips NV; Consultant, General Electric Company; Advisory Board, RefleXion Medical Inc; Consultant, Blue Earth Diagnostics Ltd; Research Funded, Siemens AG; Advisory Board, ImaginAb, Inc; Spouse, Owner, Trevarx

#### For information about this presentation, contact:

david.mankoff@uphs.upenn.edu

## LEARNING OBJECTIVES

1) List clinical and biologic questions molecular imaging can address relevant to drug treatment selection. 2) List current applications of molecular imaging to therapy guidance. 3) Describe future applications and ongoing trials applying molecular imaging as a quantitative biomarker to guide targeted treatments.

### ABSTRACT

This talk will review quantitatvie molecular imaging as a cancer imaigng biomarker to guide therpaeutic decision making and evaluate the efficacy of treatment, focusing largeyl on current and emerging PET methods.

#### **Honored Educators**

Presenters or authors on this event have been recognized as RSNA Honored Educators for participating in multiple qualifying educational activities. Honored Educators are invested in furthering the profession of radiology by delivering high-quality educational content in their field of study. Learn how you can become an honored educator by visiting the website at: https://www.rsna.org/Honored-Educator-Award/ David A. Mankoff, MD, PhD - 2013 Honored EducatorDavid A. Mankoff, MD, PhD - 2018 Honored Educator

## SPSI21C Quantitative Imaging Applications for Treatment Assessment and Adaptive Therapy

Participants

Clifton D. Fuller, MD, PhD, Houston, TX (Presenter) Research Consultant, Elekta AB; Research Grant, Elekta AB; Speaker, Elekta AB

## SPSI21D Quantitative Imaging Applications - The Importance of Study Design

### Participants

Nancy A. Obuchowski, PhD, Cleveland, OH (*Presenter*) Research Consultant, Siemens AG; Research Consultant, QT Ultrasound Labs; Research Consultant, Elucid Bioimaging Inc; Research Consultant, FUJIFILM Holdings Corporation

## LEARNING OBJECTIVES

1) Understand the effects of ignoring quantitative imaging biomarker (QIB) measurement error on clinical trials. 2) Recognize how the known technical performance of a QIB can be used to improve clinical trial study design.

## ABSTRACT

Quantitative imaging biomarkers (QIBs) have increasingly become part of clinical trials both to qualify the QIB (e.g. as integrated biomarkers to assess association with patient outcome) and utilize the QIB (e.g. as integral biomarkers to determine study eligibility and monitor therapy effects). The measurement error associated with QIBs is often overlooked in trial design planning, yet it affects study power and how the QIB measurements should be interpreted. We examine the impact of typical QIB measurement error on a variety of study designs and provide recommendations for how to use the known technical performance of a QIB for improving study planning.

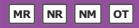
### URL

Bio: https://my.clevelandclinic.org/staff/25-nancy-obuchowski#research-publications



## Special Interest Session: Imaging Cognition 2018: Addiction

Monday, Nov. 26 4:30PM - 6:00PM Room: E353C



AMA PRA Category 1 Credits ™: 1.50 ARRT Category A+ Credit: 1.75

#### Participants

David B. Hackney, MD, Boston, MA (*Moderator*) Nothing to Disclose Jody L. Tanabe, MD, Aurora, CO (*Moderator*) Nothing to Disclose

### Sub-Events

## SPSI22A Addiction in America 2018

Participants Diana M. Martinez, MD, New York, NY (*Presenter*) Nothing to Disclose

## SPSI22B PET as a Tool in Investigating Addiction

Participants Diana M. Martinez, MD, New York, NY (*Presenter*) Nothing to Disclose

For information about this presentation, contact:

dm437@cumc.columbia.edu

## **LEARNING OBJECTIVES**

Learn the basis of PET neurochemical imaging.
 Learn the association between dopamine signaling and drug seeking behavior.
 Understand the correlation between striatal dopamine signaling and treatment response.
 Understand the status of dopamine imaging across different types of addictions.
 Understand the theory behind addiction as a habitual behavior and its imaging correlates.

#### ABSTRACT

The involvement of dopamine in addiction has its origins in studies investigating reward and reinforced behavior. Much of this research has been explored in the human brain using Positron Emission Tomography (PET) imaging of striatal dopamine transmission. These studies show that addiction is associated with a decrease in dopamine D2/3 receptors and a decrease in pre-synaptic dopamine release, and that this decrease occurs across different types of addiction, including cocaine, alcohol, and heroin dependence. However, these imaging studies also show that, in cocaine abuse, blunted dopamine transmission is predictive of cocaine seeking behavior. Low D2/3 receptor binding and low dopamine release are associated with the choice to self-administer cocaine over alternative reinforcers, which can be viewed as a failure to shift between competing rewards. It is striking that addiction to different substances of abuse are accompanied by the same alteration in neurobiology, independent of their primary impact on the dopaminergic system. Moreover, similar alterations of the dopaminergic transmission and D2-like receptor system have been described in psychiatric diseases other than addiction. Although these psychiatric disorders differ in their phenomenology, they share a common deficit in reward-related behavior, particularly with respect to impulsivity and motivation. This presentation will describe the animal and human studies that link alterations in dopamine transmission represent the neurobiological underpinnings that facilitate impulsivity and undermine motivation, rather than the only the consequences of addiction itself, will be discussed.

## SPSI22C fMRI in Addiction

Participants Jody L. Tanabe, MD, Aurora, CO (*Presenter*) Nothing to Disclose

## LEARNING OBJECTIVES

1) Describe the neural circuit associated with cravings in addictions. 2) Name 3 interventions shown to modulate craving and the "craving circuit.' 3) Identify 3 metrics that would be needed to implement an fMRI craving marker into addiction management.

## SPSI22D MRS in Craving with a Focus on Alcoholism

Participants

John D. Port, MD, PhD, Rochester, MN (Presenter) Research Consultant, Biomedical Systems; Research Consultant, Neuronetics

## LEARNING OBJECTIVES

1) Describe the theoretical reward circuitry of the human brain. 2) Explain how the reward circuitry homeostasis is altered in the setting of addiction/alcoholism. 3) Discuss current MR spectroscopy findings in alcoholism/craving.

## ABSTRACT

The human brain has a complex reward system that impacts much of human behavior. Over the last 60 years, numerous brain

regions have been identified in humans and other animals that together explain the different aspects of behavior and reward. The cortico-basal ganglia-thalamo-cortical loop is perhaps the best known model of the human reward system, but many other areas participate in reward. Addiction is the process whereby a drug (alcohol, cocaine, etc) alters the homeostasis of the reward system in a predictable way, thus creating addictive behaviors that are difficult to manage and reverse. This talk will first introduce the current best model of the human reward system homeostasis is disrupted in addiction, using alcoholism as an example. Finally, I will review the MR spectroscopic studies of alcoholism from the perspective of this altered reward system homeostasis, exploring the metabolic abnormalities in craving.

## SPSI22E Panel Discussion

Participants

David B. Hackney, MD, Boston, MA (*Moderator*) Nothing to Disclose Jody L. Tanabe, MD, Aurora, CO (*Moderator*) Nothing to Disclose



Special Interest Session: High-value MRI: Updates from the February 2018 ISMRM-RSNA Co-provided Workshop

Monday, Nov. 26 4:30PM - 6:00PM Room: E450B



AMA PRA Category 1 Credits ™: 1.50 ARRT Category A+ Credit: 1.75

**FDA** Discussions may include off-label uses.

#### **Participants**

Clare M. Tempany-Afdhal, MD, Boston, MA (*Moderator*) Research Grant, InSightec Ltd; Research Grant, Gilead Sciences, Inc; Advisory Board, Profound Medical Inc; Spouse, Employee, Spring Bank Pharmaceuticals, Inc; Spouse, Director, Trio Healthcare; Spouse, Consultant, Gilead Sciences, Inc; Spouse, Consultant, Merck & Co, Inc; Spouse, Consultant, Echosens SA; Spouse, Consultant, Shinogi; Spouse, Consultant, Ligand Pharmaceuticals, Inc; Spouse, Stock options, Spring Bank Pharmaceuticals, Inc; Spouse, Stock options, Allurion; Spouse, Stock options, Trio Healthcare; ;

### For information about this presentation, contact:

ctempany@bwh.harvard.edu

## LEARNING OBJECTIVES

To inform on a path to value with clinical MRI and MR guided interventions in Prostate cancer

## Sub-Events

## SPSI23A High-value MRI: Paths Forward from the ISMRM-RSNA Workshop

Participants

James G. Pipe, PhD, Rochester, MN (Presenter) Research Grant, Koninklijke Philips NV

#### For information about this presentation, contact:

pipe.james@mayo.edu

## **LEARNING OBJECTIVES**

1) To learn how to increase the value in their own practice or research. 2) To understand the breadth of activity in value-oriented development in imaging.

#### ABSTRACT

In February 2018, RSNA and ISMRM co-provided a workshop on High Value MRI. The overarching themes presented at this workshop will be reviewed, illustrating several areas of activities, for researchers and practitioners in clinically focused MRI, that can be both achievable and impactful in increasing the Value of MRI moving forward.

## SPSI23B Demonstrating Value of Neuro MR through Comparative Effectiveness Research

Participants

Yoshimi Anzai, MD, Salt Lake City, UT (Presenter) Nothing to Disclose

For information about this presentation, contact:

yoshimi.anzai@hsc.utah.edu

## LEARNING OBJECTIVES

1) To learn how to measure the downstream effect of neuro MR imaging to patients' management. 2) To demonstrate the impact of the neuro MR imaging on the downstream cost.

#### **Honored Educators**

Presenters or authors on this event have been recognized as RSNA Honored Educators for participating in multiple qualifying educational activities. Honored Educators are invested in furthering the profession of radiology by delivering high-quality educational content in their field of study. Learn how you can become an honored educator by visiting the website at: https://www.rsna.org/Honored-Educator-Award/ Yoshimi Anzai, MD - 2014 Honored Educator

## SPSI23C Demonstrating High-value Prostate Cancer Diagnosis with MR from Protocol Development and PI-RADS to Cost-effectiveness

Participants

Clare M. Tempany-Afdhal, MD, Boston, MA (*Presenter*) Research Grant, InSightec Ltd; Research Grant, Gilead Sciences, Inc; Advisory Board, Profound Medical Inc; Spouse, Employee, Spring Bank Pharmaceuticals, Inc; Spouse, Director, Trio Healthcare; Spouse, Consultant, Gilead Sciences, Inc; Spouse, Consultant, Merck & Co, Inc; Spouse, Consultant, Echosens SA; Spouse,

Consultant, Shinogi; Spouse, Consultant, Ligand Pharmaceuticals, Inc; Spouse, Stock options, Spring Bank Pharmaceuticals, Inc; Spouse, Stock options, Allurion; Spouse, Stock options, Trio Healthcare; ;

## LEARNING OBJECTIVES

1) To review the current state of the art of prostate cancer diagnostics. 2) To understand the added- value of mpMRI for detection, diagnosis and biopsy sampling. 3) To review the results of current cost-effectiveness studies.

## ABSTRACT

Technological advances in 5 areas-MR techniques, clinical innovations, interventional MRI, new prostate biopsy approaches and cost effectiveness studies- will be reviewed to provide background understanding of the science and added value of MRI behind current innovations in prostate cancer diagnosis.

### URL

www.ncigt.org

## SPSI23D High-value MRI: Hope for Busy Radiology Departments Around the World

Participants Bhavya Rehani, MD, San Francisco, CA (*Presenter*) Nothing to Disclose

For information about this presentation, contact:

bhavya.rehani@ucsf.edu

## LEARNING OBJECTIVES

1) Discuss High Value MRI and Implications for Busy Radiology Departments Worldwide.



## Special Interest Session: Demystifying Machine Learning and Artificial Intelligence for the Radiologist

Monday, Nov. 26 4:30PM - 6:00PM Room: E451A



AMA PRA Category 1 Credits ™: 1.50 ARRT Category A+ Credit: 1.75

#### **Participants**

Safwan Halabi, MD, Stanford, CA (*Moderator*) Nothing to Disclose Ruth C. Carlos, MD, MS, Ann Arbor, MI (*Moderator*) Nothing to Disclose

### **LEARNING OBJECTIVES**

1) Practical introduction to machine learning and artificial intelligence including allaying fears of joblessness among radiologists while providing potential scenarios of what being a radiologist in the era of artificial intelligence might entail. 2) Describe cutting-edge examples of research and clinical applications of AI and machine learning in imaging, using the High Impact Clinical Trials (HICT) format of research presentation followed by a topic discussant. 3) Discuss the future applications of machine learning and artificial intelligence.

#### ABSTRACT

The application of machine learning and artificial intelligence in medicine, and especially radiology, has caught the attention of physicians, researchers and the global tech industry. While some radiologists worry their jobs will be taken over by software, others are optimistic that this technology will make image interpretation faster, more accurate and pertinent. Coupling the increasing amounts of data radiologists have to interpret with decreasing reimbursement, artificial intelligence software has the potential to reinvent the entire radiology practice from exam ordering to diagnosis. What distinguishes this special interest session is the combination that addresses the current concerns of radiologists, presents leading edge research and provides insight into the impact of current technology on future practice.

#### Sub-Events

SPSI24A The Lowdown: Introduction to Machine Learning and Artificial Intelligence (Or Machines Will Not Take Our Jobs)

Participants

Bradley J. Erickson, MD, PhD, Rochester, MN (*Presenter*) Stockholder, OneMedNet Corporation; Stockholder, VoiceIt Technologies, LLC; Stockholder, FlowSigma;

## LEARNING OBJECTIVES

View learning objectives under main course title.

## SPSI24B The Reality: Current Application of Machine Learning and Artificial Intelligence in Clinical Radiology and Research

Participants

Jayashree Kalpathy-Cramer, MS, PhD, Charlestown, MA (*Presenter*) Consultant, Infotech Software Solution Kristen W. Yeom, MD, Palo Alto, CA (*Presenter*) Nothing to Disclose Bhavik N. Patel, MD, MBA, Stanford, CA (*Presenter*) Nothing to Disclose

For information about this presentation, contact:

kalpathy@nmr.mgh.harvard.edu

## LEARNING OBJECTIVES

View learning objectives under main course title.

## SPSI24C The Fantasy: Future Applications of Machine Learning and Artificial Intelligence in Radiology and Radiogenomics

Participants

Bradley J. Erickson, MD, PhD, Rochester, MN (*Presenter*) Stockholder, OneMedNet Corporation; Stockholder, VoiceIt Technologies, LLC; Stockholder, FlowSigma;

### For information about this presentation, contact:

bje@mayo.edu

#### **LEARNING OBJECTIVES**

View learning objectives under main course title.

SPSI24D Q&A



Special Interest Session: Academy for Radiology and Biomedical Imaging Research Imaging Shark Tank Session

Monday, Nov. 26 4:30PM - 6:00PM Room: S502AB

# OT RS

AMA PRA Category 1 Credits ™: 1.50 ARRT Category A+ Credit: 0

## LEARNING OBJECTIVES

The Academy's Imaging Shark Tank session primary goal is to educate imaging investigators about how best to present translational research and technology development ideas to industry and alternate non-governmental funding sources. This session will present a panel of experts in IP, venture capital and industry, who will hear from lucky investigators pitch their idea to the audience and in turn receive feedback from both the panel and audience. A truly interactive and fun session!

### Sub-Events

## SPSI25A Creating a Form for Venture Funding Pitches

Participants Renee L. Cruea, Washington, DC (*Presenter*) Nothing to Disclose Ronald L. Arenson, MD, San Francisco, CA (*Presenter*) Scientific Advisory Board, Imagion Biosystems

## LEARNING OBJECTIVES

View learning objectives under main course title.

## SPSI25B The Pitch Teams

Participants

Jesse L. Courtier, MD, San Francisco, CA (*Presenter*) Founder, HoloSurg3D, Inc; Consultant, HoloSurg3D, Inc Benjamin A. Laguna, MD, San Francisco, CA (*Presenter*) Nothing to Disclose Sandip Biswal, MD, Stanford, CA (*Presenter*) Research Grant, General Electric Company; Michelle James, MD, Sacramento, CA (*Presenter*) Nothing to Disclose Srini Tridandapani, MD,PhD, Decatur, GA (*Presenter*) Co-founder, CameRad Technologies, LLC; Spouse, Co-founder, CameRad Technologies, LLC;

## SPSI25C Shark Tank Panel

Participants Scott A. Penner, JD, San Diego, CA (*Presenter*) Nothing to Disclose Jacob A. Stolk, PhD,MBA, Waukesha, WI (*Presenter*) Employee, General Electric Company Ronald L. Arenson, MD, San Francisco, CA (*Presenter*) Scientific Advisory Board, Imagion Biosystems Sean Kendall, Chicago, IL (*Presenter*) Investor, Healthcare & Biotech Companies

## SPSI25D Discussion



### Special Interest Session: High Impact Clinical Trials

Monday, Nov. 26 4:30PM - 6:00PM Room: N229

# OT RS

CME credit is not available for this session. ARRT Category A Credit: 1.75

**FDA** Discussions may include off-label uses.

#### **Participants**

Udo Hoffmann, MD, Boston, MA (*Moderator*) Institutional Research Grant, Kowa Company, Ltd; Institutional Research Grant, Abbott Laboratories; Institutional Research Grant, HeartFlow, Inc; Institutional Research Grant, AstraZeneca PLC

## Sub-Events

## SPSI26A Efficacy and Safety of Transdermal, Sublingual, and Oral Nitroglycerin Administration for Coronary CT Angiography: Results of a Prospective Randomized Trial

### Participants

Dominik Fleischmann, MD, Stanford, CA (*Presenter*) Research Grant, Siemens AG Jan-Erik Scholtz, MD, Boston, MA (*Presenter*) Nothing to Disclose Vinit Baliyan, MBBS, MD, Boston, MA (*Abstract Co-Author*) Nothing to Disclose Sandeep S. Hedgire, MD, Boston, MA (*Abstract Co-Author*) Nothing to Disclose Nathaniel D. Mercaldo, Boston, MA (*Abstract Co-Author*) Nothing to Disclose Theodore T. Pierce, MD, Boston, MA (*Abstract Co-Author*) Nothing to Disclose Gabriela Spilberg, MD, Brookline, MA (*Abstract Co-Author*) Nothing to Disclose Katherine Stockton, Boston, MA (*Abstract Co-Author*) Nothing to Disclose Frederic R. McNulty Jr, RT, Boston, MA (*Abstract Co-Author*) Nothing to Disclose Frederick R. McNulty Jr, RT, Boston, MA (*Abstract Co-Author*) Nothing to Disclose Udo Hoffmann, MD, Boston, MA (*Abstract Co-Author*) Nothing to Disclose Grant, Abbott Laboratories; Institutional Research Grant, HeartFlow, Inc; Institutional Research Grant, AstraZeneca PLC Brian B. Ghoshhajra, MD, Waban, MA (*Abstract Co-Author*) Research Grant, Siemens Healthcare USA;

#### For information about this presentation, contact:

janerikscholtz@gmail.com

#### PURPOSE

Nitroglycerin increases vessel diameter and is used prior to coronary CT angiography (CTA) to improve coronary artery assessment. Our aim was to compare oral, sublingual and transdermal nitroglycerin administration for coronary vasodilation and safety.

### **METHOD AND MATERIALS**

This prospective, single center, randomized controlled study included 198 subjects who were scheduled for elective coronary CTA and randomized to one of three NTG (0.8 mg) delivery methods: patch (transdermal, n=66), tablet (sublingual, n=66) or spray (oral, n=66). NTG was given after non-contrast acquisition and 5 minutes (sublingual, oral) or at least 45 minutes (transdermal) before CTA. We compared diameters measured in short axis before and after NTG at 7 pre-defined locations in proximal, mid and distal coronary artery segments by using mixed-effect linear regression model. We assessed vital parameter before and after NTG administration and side effects of drug administration.

#### RESULTS

The studied population had a mean age of  $58.1\pm12.6$  years, 91/198 [46.0%] were females, and an average BMI of  $28.7\pm5.6$  kg/m<sup>2</sup>. On average, coronary diameters in CTA were 115.2% (95% CI: 114.0-116.4), 115.0% (113.8-116.1) and 116.3% (115.1-117.5) of baseline in tablets, spray and patches, respectively, without statistically significant differences (p >= 0.20; Figure, left). Regardless of NTG delivery route, NTG had highest vasodilation effect in distal coronary segments (125.6, 124.2-126.9) compared to proximal (111.7, 110.8-112.5) and mid coronary segments (116.4, 115.5-117.2) (Figure, right). 30 (15.2%) patients reported transient headache (tablet, n=12; spray=4; patch=14; p=0.03 [spray vs patch, p=0.02]) with a median intensity of 3 on a 10-point scale (0=no headache, 10=worst headache) (interquartile range: 2-5; tablet=3[3-6], spray=2[2-5], patch=3[2-5], p=0.02 [Tablet vs Patch, p=0.004). Heart rate increased on average by  $4.3\pm11.0$  bpm without significant difference between drug delivery routes (p=0.56). Systolic blood pressure decreased significantly more in tablets ( $13.6\pm13.0$  mmHg) vs. patches ( $7.0\pm17.8$  mmHg, p=0.008).

#### CONCLUSION

NTG can be administered safely oral, sublingual or transdermal with similar vasodilatory effect on coronary arteries prior to coronary CTA.

## **CLINICAL RELEVANCE/APPLICATION**

Transdermal nitroglycerin administration by patch prior to coronary CTA can be seen as a safe alternative to tablets and spray with similar vasodilatory effect on coronary arteries.

## FIGURE

http://abstract.rsna.org/uploads/2018/18014875/18014875\_vyt2.jpg

### **Honored Educators**

Presenters or authors on this event have been recognized as RSNA Honored Educators for participating in multiple qualifying educational activities. Honored Educators are invested in furthering the profession of radiology by delivering high-guality educational content in their field of study. Learn how you can become an honored educator by visiting the website at: https://www.rsna.org/Honored-Educator-Award/ Udo Hoffmann, MD - 2015 Honored Educator

#### SPSI26B Optoacoustic Imaging (OA) is Helpful in Predicting Breast Cancer Molecular Subtypes

Participants

Linda Moy, MD, New York, NY (Presenter) Nothing to Disclose

Basak E. Dogan, MD, Dallas, TX (Presenter) Nothing to Disclose

Gisela D. Menezes, San Antonio, TX (Abstract Co-Author) Researcher, UTHSCSA; Medical Director, Seno Medical Instruments, Inc Erin I. Neuschler, MD, Chicago, IL (Abstract Co-Author) Research Grant, Seno Medical Instruments, Inc; Speaker, Northwest Imaging Forums, Inc; ; ;

Reni S. Butler, MD, Madison, CT (Abstract Co-Author) Nothing to Disclose

A. Thomas Stavros, MD, San Antonio, TX (Abstract Co-Author) Advisor, Devicor Medical Products, Inc Advisor, General Electric Company Advisor, SonoCine, Inc Owner, Ikonopedia, LLC Medical Director, Seno Medical Instruments, Inc

Philip T. Lavin, PhD, Framingham, MA (Abstract Co-Author) Research Consultant, Seno Medical Instruments, Inc

Roger Aitchison, Longmont, CO (Abstract Co-Author) Nothing to Disclose Pamela M. Otto, MD, San Antonio, TX (Abstract Co-Author) Consultant, Seno Medical Instruments, Inc Investigator, Seno Medical Instruments, Inc Speaker, World Class CME F. L. Tucker, MD, Wirtza, VA (*Abstract Co-Author*) Nothing to Disclose

Stephen Grobmyer, MD, Cleveland, OH (Abstract Co-Author) Travel support, Seno Medical Instruments, Inc Research support, Mitaka USA, Inc Research support, Provista Diagnostics, Inc

## For information about this presentation, contact:

basak.dogan@utsouthwestern.edu

basak.dogan@utsouthwestern.edu

### PURPOSE

To investigate the potential role of functional optoacoustic imaging-derived hemoglobin de-oxygenation and angiogenesis feature scoring combined with conventional gray-scale US (OA/US) in non-invasively diagnosing breast cancer molecular subtypes.

## **METHOD AND MATERIALS**

In a IRB approved, 16-center multi-institutional study, 2105 women with a suspicious breast mass underwent pre-biopsy OA/US using Imagio<sup>™</sup> breast imaging system between 12/2012-09/2015. Lesions revealing invasive breast cancer at needle biopsy were retrospectively reviewed. Seven blinded readers scored the internal (OAINT) and external (OAEXT) OA/US features of identified cancers. The ratio of total internal to total external OA/US feature scores (RInt/Ext) was derived. Tumor hormone receptor (ER and PR), and HER-2neu status, and available ki-67(%) labeling index were derived from pathology specimens. Analysis of individual OA/US feature scores and tumor molecular subtypes of Luminal A (LumA), Luminal B (LumB), Triple-negative (TRN) and HER2 amplified (HER2+) was performed using ANOVA.

## RESULTS

Of 653 invasive cancers, 537 (82.2%) were ER+, 111 (17%) ER-negative, while in 5(0.8%) ER was missing. ER+ cancers had significantly higher OAEXT (p=0.0004), with lower OAINT (p<0.05), and RInt/Ext (p<0.0001) compared to ER-negative ones. Of 532 patients with available pathologic molecular subtype, 186(35.0%) were LumA, 244(45.9%) LumB, 79(14.8%) TRN and 23(4.3%) were HER2+. OAEXT was lower in TRN compared to LumA (p<0.0001), whereas OAINT were lower in LumA compared to TRN(p=0.031). The mean RInt/Ext was significantly higher in TRN (1.7, SD  $\pm$  0.7) compared to LumB (1.3, SD  $\pm$ 0.5) and LuminalA  $(1.2, SD \pm 0.5)$  subtypes (p<0.0001), but not significantly different from HER2 (1.5, SD ±0.6). RInt/Ext helped distinguish LumA vs LumB (p=0.044), LumA vs HER2+ (p=0.0286), LumA vs TNBC (p<0.0001), LumB vs TNBC (p<0.0001) while LumB vs HER2+ was not significant (p=0.1866). HER2+vs TNBC (p=0.1597) did not reach statistical significance.

## CONCLUSION

Functional OA/US features can help non-invasively distinguish breast cancer molecular subtypes, showing promise as a clinical prognostic tool that can facilitate management decisions.

## **CLINICAL RELEVANCE/APPLICATION**

OA/US imaging phenotypes can help serve as molecular surrogates that contribute to the diagnosis and prognosis of breast cancer.

#### SPSI26C Safety and Tolerability of High-Specific-Activity I-131 MIBG (AZEDRA®) in Patients with Iobenguane Scan Positive Cancers: A Pooled Analysis Across AZEDRA Clinical Studies

Participants

Richard L. Wahl, MD, Saint Louis, MO (Presenter) Research Consultant, Nihon Medi-Physics Co, Ltd; Contract, WhiteRabbit.AI Inc Miguel Pampaloni, MD, San Francisco, CA (Abstract Co-Author) Nothing to Disclose

Daniel Pryma, MD, Philadelphia, PA (Abstract Co-Author) Research Grant, Siemens AG; Research Grant, 511 Pharma; Research Grant, Progenics Pharmaceuticals, Inc; Research Consultant, Progenics Pharmaceuticals, Inc; Research Consultant, 511 Pharma; Research Consultant, Actinium Pharmaceuticals, Inc; Research Consultant, Nordic Nanovector ASA

Bennett B. Chin, MD, Durham, NC (Abstract Co-Author) Scientific Advisory Board, Progenics Pharmaceuticals, Inc

Richard B. Noto, MD, Providence, RI (Abstract Co-Author) Consultant, Progenics Pharmaceuticals, Inc;

Joseph S. Dillon, Iowa City, IA (Abstract Co-Author) Research Grant, Progenics Pharmaceuticals, Inc; Research Grant, Lexicon Pharmaceuticals, Inc

Stephanie M. Perkins, MD, Saint Louis, MO (Abstract Co-Author) Nothing to Disclose Lilja B. Solnes, MD, Baltimore, MD (Abstract Co-Author) Nothing to Disclose

Lale Kostakoglu, MD, MPH, New York, NY (*Abstract Co-Author*) Research Consultant, F. Hoffmann-La Roche Ltd Aldo N. Serafini, MD, Miami, FL (*Abstract Co-Author*) Research Consultant, Progenics Pharmaceuticals, Inc Katherine K. Matthay, MD, San Francisco, CA (*Abstract Co-Author*) Nothing to Disclose Jessica Jensen, New York, NY (*Abstract Co-Author*) Employee, Progenics Pharmaceuticals, Inc Tess Lin, New York, NY (*Abstract Co-Author*) Employee, Progenics Pharmaceuticals, Inc Stuart Apfel, New York, NY (*Abstract Co-Author*) Employee, Progenics Pharmaceuticals, Inc Theresa White, New York, NY (*Abstract Co-Author*) Employee, Progenics Pharmaceuticals, Inc Nancy Stambler, Tarrytown, NY (*Abstract Co-Author*) Employee, Progenics Pharmaceuticals, Inc Vincent DiPippo, New York, NY (*Abstract Co-Author*) Employee, Progenics Pharmaceuticals, Inc Syed M. Mahmood, MD, New York, NY (*Abstract Co-Author*) Employee, Progenics Pharmaceuticals, Inc Vivien Wong, New York, NY (*Abstract Co-Author*) Employee, Progenics Pharmaceuticals, Inc Syed M. Mahmood, MD, New York, NY (*Abstract Co-Author*) Employee, Progenics Pharmaceuticals, Inc Syed M. Mahmood, MD, New York, NY (*Abstract Co-Author*) Employee, Progenics Pharmaceuticals, Inc Camilo Jimenez, Houston, TX (*Abstract Co-Author*) Employee, Progenics Pharmaceuticals, Inc Sohail Chaudhry, MD,PhD, Dallas, TX (*Presenter*) Consultant, Progenics Pharmaceuticals, Inc.

#### For information about this presentation, contact:

smahmood@progenics.com

#### PURPOSE

There is an unmet medical need for the treatment of iobenguane scan positive cancers, and especially in patients with advanced pheochromocytoma/paraganglioma (PPGL). High-specific-activity I- 131 meta-iodobenzylguanidine (HSA I-131 MIBG, AZEDRA®) is the first and only radioactive therapeutic agent approved for the treatment of adult and pediatric patients 12 years and older with iobenguane scan positive, unresectable, locally advanced or metastatic PPGL who require systemic anticancer therapy. Conventional I-131 meta-iodobenzylguanidine (MIBG) therapy has been associated with hematological toxicity in nearly all treated subjects, and up to a 15% incidence of severe acute hypertension including hypertensive crises and tachycardia during or immediately after the infusion. The purpose of this pooled analysis is to characterize the safety and tolerability of HSA I-131 MIBG.

## **METHOD AND MATERIALS**

Data from four HSA I-131 MIBG open-label, Phase I and phase II studies (NCT00339131; NCT00458952; NCT00874614; NCT00659984) were pooled for safety analysis with a data cutoff of March 10, 2017. A literature review was conducted on the safety of conventional I-131 MIBG. Demographic and baseline characteristics will be presented with descriptive statistics for continuous variables, and frequencies/percentages for categorical variables. Adverse event (AE) data will be described by disease indication, age, gender, race, treatment with prior conventional I-131 MIBG, number of HSA I-131 MIBG doses, vital signs, electrocardiogram (ECG), laboratory values, reasons for treatment or study discontinuation, and long-term AEs.

#### RESULTS

The pooled safety population included 118 patients (age range: 3-76 years) who received any dose of HSA I-131 MIBG. Few AEs showed a clear association with age. The incidence of most AEs was similar regardless of gender or race. The incidence of AEs was comparatively higher after the second therapeutic dose; however, the incidences of most serious AEs (SAEs) were similar after each therapeutic dose. No clinically significant trend was seen in ECG changes from baseline. 21 patients (18%) experienced hypertensive events of which treatment-related hypertension/increased blood pressure was reported in 7 (5.9%) patients and treatment-related tachycardia was reported in 6 (5.1%) subjects. Within 48 hours of therapeutic dosing, only one possibly related mild increase in blood pressure was reported as an AE; other changes in blood pressure were not deemed clinically significant by the investigators in this time period. The most common reason for discontinuation was occurrence of an AE(s) (n=11, 9.3%), followed by receiving another anticancer therapy (n=8, 6.8%) and progressive disease (n=7, 5.9%). Thirty-four (28.8%) deaths were reported, two of which (myelodysplastic syndrome and acute myeloid leukemia) were related to late radiation toxicity attributed to HSA I-131 MIBG.

## CONCLUSION

HSA I-131 MIBG was safe and well-tolerated across patients with iobenguane scan positive cancers. As with other similar radioactive therapeutic agents, HSA I-131 MIBG is associated with a predictable pattern of AEs. No serious treatment-related hypertensive events were observed suggesting that HSA I-131 MIBG would be less likely than conventional I-131 MIBG (with a 15% reported rate of severe hypertensive events) to cause acute or subacute severe hypertensive events. With proactive toxicity management, health care practitioners can ensure maximum treatment benefit and mitigate unnecessary treatment discontinuation.

### **Honored Educators**

Presenters or authors on this event have been recognized as RSNA Honored Educators for participating in multiple qualifying educational activities. Honored Educators are invested in furthering the profession of radiology by delivering high-quality educational content in their field of study. Learn how you can become an honored educator by visiting the website at: https://www.rsna.org/Honored-Educator-Award/ Lale Kostakoglu, MD, MPH - 2012 Honored Educator



Special Interest Session: Integrated Diagnostics-Combining Genomics, Pathology and Radiology: The Future Now

Monday, Nov. 26 4:30PM - 6:00PM Room: N226



AMA PRA Category 1 Credits ™: 1.50 ARRT Category A+ Credit: 1.75

**FDA** Discussions may include off-label uses.

#### **Participants**

Pablo R. Ros, MD, PhD, Cleveland, OH (*Presenter*) Nothing to Disclose R. Nick Bryan, MD, PhD, Austin, TX (*Presenter*) Stockholder, Galileo CDS, Inc Officer, Galileo CDS, Inc Jacob J. Visser, MD, PhD, Rotterdam, Netherlands (*Presenter*) Nothing to Disclose

For information about this presentation, contact:

nick.bryan@austin.utexas.edu

Pablo.Ros@UHhospitals.org

## LEARNING OBJECTIVES

1) To become familiar with the concept of Integrated Diagnosis, which combines Radiology, Pathology and Genomics into an innovative diagnostic tool. 2) To understand how the current computational revolution provides the technological basis for the cross-disciplinary implementation of Integrated Diagnosis. 3) To share the early experiences of established Integrated Diagnosis organizations in Academic Medical Centers and Medical Schools.

#### ABSTRACT

Making medicine more personalized and precise will entail increasing emphasis on, and precision in, diagnostics. Diagnoses however, depend on multiple components that include not only imaging, but also clinical observations, pathology, laboratory, and genomic tests. Biomarkers, including quantitative imaging markers and generic radiomics platforms in combination with deep learning algorithms contribute to the concept of data driven medicine allowing the optimal integration of information from different sources. To date, however, there is too little coordination between the medical specialties responsible for ordering and performing diagnostic tests, nor is there enough consideration as to the optimal order of tests. 'Integrated diagnostics': the convergence of imaging, pathology and laboratory tests with advanced information technology (IT) is the solution for bridging this gap. At Erasmus MC in Rotterdam, the organizational structures are optimal for the implementation of this concept: all diagnostic specialties are gathered in the division 'Diagnostics and Advice' and agreements with referring physicians are performed jointly. However, there is major resistance from the side of clinicians who rarely commit to acknowledged protocols. The potential of integrated diagnostics for disease prediction, diagnosis, and therapy monitoring and the barriers to its optimal implementation will be demonstrated in the specific case study at Erasmus MC.